THORPEX
A World Weather Research Programme

Second THORPEX International Science Symposium (STISS)

Landshut, Germany

4 – 8 December 2006

Programme & Extended Abstracts

WMO/TD No. 1355 WWRP/THORPEX No. 7

THORPEX Programme Office World Meteorological Organization

Collage of images on the cover – in cyclonic order:

top left:	aerial view of the historic centre of Landshut between *Burg Trausnitz* (castle) and river Isar
bottom left:	modern entrance to the conference venue, the city-owned *Stadtsäle Bernlochner* (yellow dot)
bottom right:	three Landshut landmarks: cathedral *St. Martin*, *Burg Trausnitz*, *Stadtsäle Bernlochner*
top right:	December time Christmas market in the *Freyung* quarter, close to *St. Jodok* church (blue dot)

STISS sponsors:

The planning and conduct of the Second THORPEX International Science Symposium (STISS) was generously supported by contributions in money and in kind by

WMO	World Meteorological Organization, Geneva, CH
GEO	Group of Earth Observations, Geneva, CH
CRAY	Cray Inc., Seattle, USA
intel	Intel GmbH Munich, Feldkirchen, D

DLR-IPA	Deutsches Zentrum für Luft- und Raumfahrt, Institut für Physik der Atmosphäre, D
DWD-GB FE	Deutscher Wetterdienst, Geschäftsbereich Forschung und Entwicklung, D
FZK-IMK	Forschungszentrum Karlruhe, Institut für Meteorologie und Klimaforschung, D
JGU-IPA	Johannes Gutenberg-Universität Mainz, Institut für Physik der Atmosphäre, D
LMU-MIM	Ludwig-Maximilians-Universität, Meteorologisches Institut, München, D
UKA-IMK	Universität Karlsruhe, Institut für Meteorologie und Klimaforschung, D

This volume was produced for WWRP/THORPEX at the Institut für Physik der Atmosphäre (IPA) of Deutsches Zentrum für Luft- und Raumfahrt e.V. (DLR), Oberpfaffenhofen, D-82234 Weßling, Germany.

Editing & layout: Hans Volkert Compilation & annotation: Jana Freund Printing & binding: Karl-Heinz Koos

FOREWORD

THORPEX: A Global Atmospheric Research Programme is an international research and development programme responding to the weather related challenges of the 21st century to accelerate improvements in the accuracy of 1-day to 2-week high impact weather forecasts for the benefit of society, the economy and the environment. THORPEX research topics include: global-to-regional influences on the evolution and predictability of weather systems; global observing system design and demonstration; targeting and assimilation of observations; societal, economic and environmental benefits of improved forecasts. The programme establishes an organizational framework that addresses weather research and forecast problems whose solutions will be accelerated through international collaboration among academic institutions, operational forecast centres and users of forecast products.

Science symposia provide an important method to establish new cooperation and to further existing cooperation. They provide occasions for the exchange of new ideas and techniques between staff and students from universities, research laboratories, and meteorological services. In December 2004 the international THORPEX community gathered for the First THORPEX International Science Symposium in Montreal, Canada. Formal proceedings were published after the event as publication WWRP/THORPEX No. 6 (cf. inside back cover). Late in 2005 the offer from the German meteorological community was accepted to host the Second THORPEX International Science Symposium (STISS) in Landshut near Munich in southern Germany.

The city of Landshut looks back to a history of some 800 years. It is the capital of the district *Niederbayern* (Lower Bavaria), gives home to 58,000 inhabitants and lies as close to Munich International Airport as the centre of Munich. The old town between the river *Isar* and the former ducal residence *Burg Trausnitz* on the river's high bank constitutes one of Germany's finest ensembles of houses in the 15th century late gothic style. In 1475 Landshut witnessed the weeklong festivities on the occasion of the wedding between the Bavarian Duke *Georg der Reiche* (the rich) and the Polish princess *Hedwig*. In commemoration the citizens of Landshut perform the wedding procession every four years during weekends in the summer, again in 2009. We take Landshut's international spirit from more than half a millennium ago as a good *omen* for the success of STISS.

The response to the call for papers was overwhelming. The programme committee structured the submitted contributions in two different, but equally important classes: short oral presentations to the plenary and poster presentations for in-depth discussions with interested conference participants during extended poster sessions. All contributors were given the possibility to submit a two-page extended abstract four weeks before the conference in order to aid individual selections during the symposium. Nearly 140 Extended Abstracts were received and are collected here together with the STISS programme. It is hoped that this volume serves the intended purpose during the symposium and that it will help to conserve some of its spirit in the tradition of WMO sponsored conference volumes during the Global Atmospheric Research Programme (GARP). For cost reasons the figures are printed in black-and-white; colour versions are available from the STISS website under http://www.pa.op.dlr.de/stiss/proceedings.html .

In conclusion we express our gratitude to all contributors to this volume for adhering well to dates and guidelines (cf. p.276), to our colleagues on the organisation and programme committees for all their efforts to set up a balanced programme and to stage the event, and to our sponsors from industry, international agencies and meteorologically oriented German institutions for their confidence and support.

November 2006

David Burridge George Craig Hans Volkert Heini Wernli

Second Thorpex International Science Symposium (STISS)

Structure of sessions and overview timetable

Time	*Monday 4 Dec. 2006*	*Tuesday 5 Dec. 2006*	*Wednesday 6 Dec. 2006*	*Thursday 7 Dec. 2006*	*Friday 8 Dec. 2006*
09:00 – 10:30	**Opening Session**	**Overviews: Links**	**TIGGE-B**	**SERA-B**	**PDP-D**
	Coffee	*Coffee*	*Coffee*	*Coffee*	*Coffee*
11.00 - 12.30	**DAOS-A**	**SERA-A**	**DAOS-B**	**PDP-C**	**SERA-C**
	Lunch	*Lunch*	*Lunch* & guided City tour	*Lunch*	Disc+Closure *Lunch*
14:00 - 15:00	**TIGGE-A**	**OS-A**		**DAOS-C**	
15.00 – 16:30	Coffee & **Poster-I** DAOS-1, PDP-1, SERA-1, TIGGE-1	Coffee & **Poster-II** DAOS-2, OS-1, PDP-2, SERA-2 TIGGE-2	**Overviews: Campaigns I**	Coffee & **Poster-III** DAOS-3, OS-2, PDP-3, SERA-3	
16:30 – 18:00	**PDP-A**	**PDP-B**	*Coffee* **Overviews: Campaigns II**	**OS-B**	
19.30 - 21.30	***ICEBREAKER***		***DINNER***		
22.30					

Note:

STISS is structured in Overview Sessions and five larger groups along the themes of the THORPEX working groups:

1. **Predictability and Dynamic Processes (PDP)**
2. **Observing System (OS)**
3. **Data Assimilation and Observing Strategies (DAOS)**
4. **Societal and Economic Research and Applications (SERA)**
5. **THORPEX Interactive Grand Global Ensemble (TIGGE)**

According to the number of submitted papers these latter sessions are spread out over several days to facilitate inter-group understanding, i.e. TIGGE-A/B (Mon. to Wed.), OS-A/B (Tue. to Thu.), DAOS-A/B/C, (Mon. to Thu.), SERA-A/B/C (Tue. to Fri.) and PDP-A/B/C/D (Mon. to Fri.).

The poster contributions for each working group are divided analogously in 2 or 3 numbered groups. They will be explained by the authors in one of the 3 mid-afternoon poster sessions, but are on display for the entire conference to obtain optimal visibility.

The programme also serves as table of contents for the 2-page Extended Abstracts
(these are available for all contributions for which a page number is given)

as of 16 November 2006

Part A) Sequence of events and oral presentations

Sunday, 03 December 2006		
17:00-19:00		Registration

Monday, 04 December 2006		
08:00-09:00	***page***	Registration (continued)
Opening session		***"THORPEX on the road"*** *chair: Hans Volkert*
09:00-09:20		- Welcome to Landshut - *Michel* ***Béland*** (WMO-CAS and Meteo. Service, Dorval, CAN): THORPEX at the cross roads: Where do we go from here?
	002	- *Gerhard* ***Adrian*** (DWD, Offenbach, D): The relevance of THORPEX for meteorology in Germany
09:20-09:40	***004***	*David* ***Burridge*** (WMO, THORPEX-IPO, Geneva, INT): THORPEX, an element of the WMO World Weather Research Programme
09:40-10:00	***006***	*Huw* ***Davies*** (ETH, Zurich, CH): THORPEX: A protean project
10:00-10:20	***008***	*Mel* ***Shapiro*** (NOAA & NCAR, Boulder, USA): Will THORPEX science benefit humanity?
10:20-10:30		*Datong* ***Zhao*** (GEO secretariat, Geneva, INT): GEO and GEOSS: Understand trends, forecast changes and support informed decisions
10:30-11:00		**Coffee**
Session: DAOS-A		***"Modelling adaptive observations"*** *Chair: Philippe Bougeault*
11:00-11:30		*Carla* ***Cardinali*** (ECMWF, Reading, INT)*:* Towards an adaptive observation network: Monitoring the observation impact on the forecast (keynote)
11:30-11:45		*Michiko* ***Masutani*** (NOAA, Camp Springs, USA): Observing system simulation experiments at NCEP and JCSDA
11:45-12:00	***010***	*Neill* ***Bowler*** (MetOffice, Exeter, UK), *Mylne*, *Arribas* and *Robinson*: Performance of the local ETKF in the Met Office global ensemble
12:00-12:15	***012***	*Alexis* ***Doerenbecher*** (Meteo France, Toulouse, F)*:* Adaptive observation in the Atlantic and the Mediterranean region
12:15-12:30	***014***	*Yoshiaki* ***Takeuchi*** (JMA, Tokyo, Japan), Yamaguchi, Iriguchi, Nakazawa: Observing system experiments using a singular vector method for a 2004 DOTSTAR case
12:30-14:00		**Lunch**
Session: TIGGE-A		***"Multimodel ensembles"*** *Chair: Melvyn Shapiro*
14:00-14:30	***016***	*Philippe* ***Bougeault*** (ECMWF, Reading, INT): The THORPEX Interactive Grand Global Ensemble (TIGGE): Concept and current status (keynote)
14:30-14:45	***018***	*Richard* ***Swinbank*** (MetOffice, Exeter, UK)*:* Medium-range ensemble forecasts at the MetOffice
14:45-15:00	***020***	*Mio* ***Matsueda*** (Tsukuba University, Japan), *Kyouda*, *Tanaka* & *Tsuyuki*: Daily forecast skill of multi-center grand ensemble
15:00-16:30		**Refreshments and Poster session** ***"DAOS-1, PDP-1, SERA-1, TIGGE-1"***

Monday, 04 December 2006 (continued)		
Session: PDP-A		***"Tropical weather systems and interaction with extratropics"*** *Chair: Huw Davies*
	page	
16:30-16:45	***022***	*Frederic* ***Vitart*** (ECMWF, Reading, INT) and *Barkmeijer*: Organized tropical convection and weather prediction on sub-seasonal time scales (short keynote)
16:45-17:00		*Naoko* ***Kitabatake*** (JMA, Tsukuba, Japan), *Majumdar* & *Sarah* ***Jones***: Predictability of tropical cyclones and of their extratropical transition (short keynote)
17:00-17:15	***024***	*Patrick* ***Harr*** (NRL, Monterey, USA) and *Jones*: The impact of extratropical transition on the downstream midlatitude predictability (short keynote)
17:15-17:30	***026***	*Peter* ***Knippertz*** (Mainz University, D) and *Jones*: AMMA and aspects of tropical-extratropical interactions (short keynote)
17:30-17:45	***028***	*Manoel* ***Gan*** (INPE, São José dos Campos, Brazil), *Dal Piva* and *B. Rao*: Catarina cyclone: a hurricane-like cyclone over south Atlantic
17:45-18:00	***030***	*Harry* ***Weber-Philipp*** (Munich University, D): On the determination of tropical-cyclone size and intensity parameters
19:30-21:30		***I C E B R E A K E R***

Tuesday, 05 December 2006		
Overview Session		***"THORPEX: Programmatic Links"*** *Chair: David Burridge*
09:00-09:30		*Brian* ***Hoskins*** (University Reading, UK) and *Gilbert* ***Brunet*** (Met. Res. Division, Dorval, CAN): The weather-climate interface (keynote)
09:30-10:00		*Paul* ***Kovacs*** (ICLR, University of Western Ontario, CAN): Building resilient communities (keynote)
10:00-10:30	***032***	*David* ***Rogers*** (WMO, Geneva, INT): Health forecasting in Africa (keynote)
10:30-11:00		**Coffee**
Session: SERA-A		***"Verification, Water, Traffic"*** *Chair: Ulrich Schumann*
11:00-11:15	***034***	*Barbara* ***Brown*** (NCAR, Boulder, USA): Moving toward user-relevant verification
11:15-11:30	***036***	*Tim* ***Hewson*** (MetOffice, Exeter, UK): New approaches to verifying forecasts of hazardous weather
11:30-11:45	***038***	*Warren* ***Tennant*** (South African Weather Serv., Pretoria, South Africa): Bias-correction methods applied to NCEP-EPS output
11:45-12:00	***040***	*Andy* ***Morse*** (Liverpool University; UK) and *Foamouhoue*: Towards seamless ensemble forecasts and the potential for alleviation of high impact weather for users in Africa
12:00-12:15	***042***	*Thomas* ***Gerz*** (DLR-IPA, Oberpfaffenhofen, D) *and Theusner:* Weather for cockpit and tower: The benefit of an improved weather information system for aviation
12:15-12:30		*Azmat* ***Hayat*** (Pakistan Meteo. Dept., Islamabad, Pakistan): Economic and societal impacts of very high impacts forecasts in developing countries and user concerns: Pakistan perspective
12:30-14:00		**Lunch**

Tuesday, 05 December 2006 (continued)		
Session: OS-A	***page***	***"Ground-based observing systems"*** *Chair: Neil Gordon*
14:00-14:30	***044***	*Roger* ***Wakimoto*** (NCAR, Boulder, USA): Ground-based and airborne observational needs for THORPEX (keyno.)
14:30-14:45	***046***	*Oleg* ***Pokrovsky*** (Main Geophys. Observ., St. Petersburg, Russia): Recent changes in atmospheric circulation regimes over northern Eurasia and suggestions to redesign the RAOB network
14:45-15:00		*Hal* ***Cole*** (NCAR, Boulder, USA): Driftsonde measurements during AMMA
15:00-16:30		**Refreshments and Poster session** ***"DAOS-2, OS-1, PDP-2, SERA-2, TIGGE-2"***
Session: PDP-B		***"Dynamical processes in the extratropics"*** *Chair: Sarah Jones*
16:30-16:45		*Gudrun.* ***Magnusdottir*** *(Univ. of California, Irvine, USA):* The role of Rossby wave dynamics in predictability (short keynote)
16:45-17:00		*Cornelia* ***Schwierz*** (Leeds University, UK): Atmospheric blocking, low-frequency variability and their rôle in predictability (short keynote)
17:00-17:15		*Heini* ***Wernli*** (Mainz University, D): The impact of moist processes on dynamical processes and predictability in the extra-tropics (short keynote)
17:15-17:30		*Olivier* ***Talagrand*** (LMD, Paris, F)*:* Ensemble prediction (short keynote)
17:30-17:45	***048***	*Rich* ***Moore*** (ETH Zurich, CH) and *Montgomery*: Finite amplitude threshold behavior of diabatic Rossby vortex formation
17:45-18:00	***050***	*Olivier* ***Rivière*** (LMD, Paris, F), *Lapeyre* and *Talagrand:* Influence of large-scale precipitation on the predictability of baroclinic systems
18:30-20:00		**Side meetings** of working groups (e.g. **DAOS**, **PDP**, **TIGGE**) – check onsite announcements

Wednesday, 06 December 2006		
Session: TIGGE-B	***page***	***"Operational ensembles"*** *Chair: Takeshi Enomoto*
09:00-09:30		*Zoltan* ***Toth*** (NOAA, Camp Springs, USA), *Lefaivre,Lobato,Wilson et al.*: The north American ensemble forecast system: An operational multi-center forecast system (keynote)
09:30-09:45	***052***	*Laurence* ***Wilson*** (EC, Dorval, CAN), *Beauregard, Cui, Zhu, Toth et al.*: Calibration and post-processing methods to combine ensembles from multiple sources: The NAEFS experience
09:45-10:00	***054***	*Mathias* ***Rotach*** (Meteo Swiss, Zurich, CH) and *Arpagaus*: Demonstration of probabilistic hydrological and atmospheric simulation of flood events in the Alpine region (D-PHASE)
10:00-10:15	***056***	*Michael* ***Denhard*** (DWD, Offenbach, D) and *Trepte*: Calibration of the European regional multi-model ensemble SRNWP-PEPS
10:15-10:30		*Ken* ***Mylne*** (MetOffice, Exeter, UK): Multi-model ensemble forecasts of windstorms: Eurorisk PREVIEW
10:30-11:00		**Coffee**

Wednesday, 06 December 2006 (continued)		
Session: DAOS-B	***page***	***"Fundamentals"*** *Chair: Florence Rabier*
11:00-11:15		*Pierre* ***Gauthier*** (Env.Canada, Dorval, CAN): Objectives of the THORPEX working group on data assimilation and observing strategies for high impact weather forecast improvements
11:15-11:45		*Michael* ***Ghil*** (LMD, Paris, F): Dynamical systems, sequential estimation and parameter estimation (keynote)
11:45-12:00	***058***	*Martin* ***Ehrendorfer*** (Innsbruck University, A) and *Errico*: An intermediate-complexity model for data assimilation
12:00-12:15		*Jeffrey* ***Whitaker*** (NOAA, Boulder, USA) and *Hamill:* A comparison between an operational 3D-VAR and an experimental data assimilation system
12:15-12:30	***060***	*Andy* ***Lawrence*** (ECMWF, Reading, INT), *Leutbecher* and *Palmer*: Does the global observing system possess a 'satellite Achilles heel'?
12:30-15:00		**Lunch** & guided city tour
Overview Session I		***"THORPEX: Future field campaigns"*** *Chair: Mamina Kamara*
15:00-15:15		*Thor-Erik* ***Nordeng*** (NMI, Oslo, N) and *Jon-Egill* ***Kristiansson***: The International Polar Year (IPY) – THORPEX cluster
15:15-15:30	***062***	*Gudrun Nina* ***Petersen*** (University of East Anglia, Norwich, UK), *Renfrew*, *Moore*, *Olafsson* and *Kristjansson*: The Greenland flow distortion experiment
15:30-15:45		*David* ***Parsons*** (NCAR, Boulder, USA) *and Patrick* ***Harr*** (NRL, USA) *:* THORPEX Pacific Asia Regional campaign (TPARC): American perspective
15:45-16:00	***064***	*Tetsuo* ***Nakazawa*** (JMA, Tsukuba, Japan): THORPEX Pacific Asian Regional campaign (TPARC): Asian perspective
16:00-16:25	***066***	*Neil* ***Gordon*** (Met. Service, Wellington, New Zealand) and *Kamal* ***Puri*** (Bureau of Meteorology, Melbourne, AUS): Southern Hemisphere perspective of THORPEX (keynote)
16:25-16:50		**Coffee**
Overview Session II		***"THORPEX: More campaigns"*** *Chair: Rebecca Morss*
16:50-17:15	***068***	*Mitch* ***Moncrieff*** (NCAR, Boulder, USA) and *Duane* ***Waliser*** (NASA, Pasadena, USA): The challenge of organized tropical convection in the THORPEX era (keynote)
17:15-17:30	***070***	*Ernest* ***Afiesimama*** (Nigerian Meteorol.Agency, Lagos, Nigeria), *Jones, Parsons, Rabier, Thorncroft, Toth:* High Impact weather prediction and predictability for the west African Monsoon: Introduction to the joint AMMA-THORPEX working group
17:30-17:45	***072***	*Andreas* ***Behrendt*** (Hohenheim University, Stuttgart, D)*, Wulfmeyer*, *Kottmeier*, *Corsmeier*, *Hagen*, *Craig* and *Bauer*: The Convective and Orographically-induced Precipitation Study (COPS) 2007 and its links to THORPEX
17:45-18:00	***074***	*Véronique* ***Ducrocq*** (Météo France, Toulouse F), *Drobinski* et xxvii al.: Hydrological cycle in the Mediterrean Experiment (HyMEx): Towards a major field experiment between 2009 and 2012
19:30-22:30		**D I N N E R**

Thursday, 07 December 2006		
Session: SERA-B		***"The future: For society and economy"*** *Chair: Linda Anderson-Berry*
	page	
09:00-09:30		*Eve* ***Gruntfest*** (NCAR, Boulder, USA): Integrating social science to improve the effectiveness of forecasting and the benefits of research: Implementing the change in meteorology and in meteorologists (keynote)
09:30-09:45	***076***	*Céline* ***Lutoff*** (UMR PACTE, Grenoble University, F) and *Ruin:* Vulnerability to flash floods: The problem of mobile people and decision-making in crisis situations
09:45-10:00	***078***	*Mamina* ***Kamara*** (Météo. Nat. Senegal, Dakar, Senegal)*:* Assistance of the marine weather for artisanal and industrial fishing
10:00-10:15		*Rebecca* ***Morss*** (NCAR, Boulder, USA) *Lazo, Chapman, Brown* et al.: Estimating the value of current and improved weather forecast
10:15-10:30		*Julie* ***Demuth*** (NCAR, Boulder, USA): Weather and society: Developing the next generation of weather researchers and users
10:30-11:00		**Coffee**
Session: PDP-C		***"Extratropical transition and subseasonal variability"*** *Chair: Warren Tennant*
11:00-11:15	***080***	*Doris* ***Anwender*** (FZK-IMK & Karlsruhe Univ., D), *Leutbecher*, *Jones* & *Harr*: Sensitivity of ensemble forecasts of extratropical transition to initial perturbations targeted on the tropical cyclone
11:15-11:30	***082***	*Christopher* ***Davis*** (NCAR, Boulder, USA), *Jones* and *Riemer*: WRF simulation and diagnosis of the extratropical transitions of Irene (2005)
11:30-11:45		*Michael* ***Morgan*** (Wisconsin University, Madison, USA): An adjoint-derived forecast sensitivity study of hurricane track and extratropical transition
11:45-12:00	***084***	*Takeshi* ***Enomoto*** (JAMSTEC, Yokohama, Japan), *Yamane* & *Miyoshi*: Simulations of the intra-seasonal oscillation in the tropics with ensemble techniques
12:00-12:15	***086***	*Hai* ***Lin*** (Env.Canada, Dorval, CA), *Brunet* and *Derome*: Intraseasonal variability in a dry atmospheric model
12:15-12:30	***088***	*Thomas* ***Spengler*** (ETH Zurich, CH), *Schwierz* and *Davies*: Sub-tropical synoptic-scale forcing of extra-tropical flow: Diagnostic analyses and model simulations
12:30-12:45	***090***	*Xuefeng* ***Cui*** (Liverpool University, UK), *Messager* and *Morse*: Westafrica weather forecasting in AMMA-UK: A frist case study
12:45-14:00		**Lunch**
Session: DAOS-C		***"Impact of observations"*** *Chair: Carla Cardinali*
14:00-14:15	***092***	*Rolf* ***Langland*** (NRL, Monterey, USA), *Baker*, *Pauley*, *Hogan, Pauley, Xu* and Ruston: Observation impact monitoring with a data assimilation adjoint
14:15-14:30		*Martin* ***Weissmann*** (DLR-IPA, O'hofen, D), *Cardinali, Dörnbrack et.al.:* Impact of airborne Doppler lidar measurements on ECMWF forecasts
14:30-14:45	***094***	*Elana* ***Fertig*** (Maryland University, College Park, USA), *Aravéquia* et al.: Assessing the local ensemble transform Kalman filter and its assimilation of AIRS observations
14:45-15:00	***096***	*Fatima* ***Karbou*** (Météo France, Toulouse, F), *Gérard*, *Rabier*: Impact of estimated land emissivities from satellite microwave observations in the 4D-var system at Météo-France
15:00-16:30		**Refreshments and Poster session** ***"DAOS-3, OS-2, PDP-3, SERA-3"***

Thursday, 07 December 2006 (continued)		
Session: OS-B	***page***	***"Space-based observing systems"*** *Chair: Chris Velden*
16:30-17:00		*John* ***LeMarshall*** (JCSDA, Camp Springs, USA): Satellite observing system needs and challenges as they relate to THORPEX's overarching goal of forecast improvements (keynote)
17:00-17:15	***100***	*Roger* ***Saunders*** (MetOffice, Exeter, UK) and *English*: Exploitation of satellite data for NWP
17:15-17:30		*James* ***Purdom*** (CIRA, Fort Collins, USA) and *John* ***LeMarshall***: THORPEX and the satellite system of the future: Toward optimum utilization
17:30-17:45	***102***	*Christoph* ***Kiemle*** (DLR-IPA, O'hofen, D), *Flentje, Dörnbrack, Fix, Ehret:* Towards more accurate water vapour observations: Airborne Lidar measurement examples and characteristics
17:45-18:00	***104***	*Paul* ***Ingmann*** (ESTEC, Noordwijk, INT), *Straume*, *Lajas* et al.: ADM-Aeolus: ESA's Doppler wind Lidar mission
18:30-20:00		**Side meetings** of working groups (e.g. **OS**, **EuroTHORPEX**) – check onsite announcements

Friday, 08 December 2006		
Session: PDP-D		***"Subtropics and theory"*** *Chair: Detlev Majewski*
09:00-09:15	***106***	*Klaus* ***Weickmann*** (NOAA, Boulder, USA), *Berry* and *Sardeshmukh*: The strong jet stream over the north Pacific in Nov-Dec 2005
09:15-09:30		*Ahmed* ***Yousef*** (EMA, Cairo, Egypt): Forecasting for dust storms over north Africa and Arab lands using the Egypt numerical dust model
09:30-09:45		*Jianhua* ***Sun*** (IAP, Beijing, China): An analysis of heavy rainfall in Mei-yu front using the intensive observation data during CHeRES 2002
09:45-10:00	***108***	*Didier* ***Ricard*** (Météo France, Toulouse, F), *Arbogast, Crépin* and *Joly*: The intense jet stream of December 1999: An outcome of tropical-extratropical transition?
10:00-10:15	***110***	*Joseph* ***Egger*** (Munich University, D) and *Hoinka:* What do we learn from piecewise potential vorticity inversion?
10:15-10:30	***112***	*Dmitry* ***Sonechkin*** (RAS, Moscow, Russia): A revision of the Lorenz chaoticity paradigm and its consequence for the extended-range weather forecasting problem
10:30-11:00		**Coffee**
Session: SERA-C		***"Weather: Science for society"*** *Chair: Tetsuo Nakazawa*
11:00-11:30		*Linda* ***Anderson-Berry*** (Bureau of Meteorology, Melbourne, AUS): Describing and understanding the socio-economic 'value' of significant weather forecast products and services (keynote)
11:30-11:45	***114***	*Hans* ***Volkert*** (DLR-IPA, Oberpfaffenhofen, D): Evolution in global weather research: From GARP to THORPEX
11:45-12:00	***116***	*Ricardo* ***Prieto-Gonzalez*** (IMTA, Jiutepec, Mexico), *Mundo*, *Caballero*: The effects of intense weather system over the Chiapas state of Mexico
12:00-12:15	***118***	*Brian* ***Mills*** (Env.Canada and Waterloo University, CAN), *Morss*, *Lazo*, *Brooks, Brown* and *Ganderton:* A societal and economic research and applications agenda for the north American THORPEX programme
12:15-12:30	***120***	*Detlev* ***Majewski*** (DWD, Offenbach, D): Transfer of regional NWP capabilities to developing countries: The HRM of the Deutscher Wetterdienst
12:30-13:00		**General discussion and adjourn** *Chair: George Craig*

Part B) **Poster blocks**

All posters are on display for the entire week. Authors are asked to be ready for discussions at the appropriate poster times on Monday, Tuesday and Thursday afternoon.

Poster block: DAOS-1 „Adaptive observations" ***page***

Poster block: DAOS-2 „Fundamentals"

Poster block: DAOS-3 „Experience" ***page***

Poster block: OS-1 „Ground-based observing systems“ ***page***

Poster block: OS-2 „Space-based observing system“

Poster block: PDP-1 „Tropical and seasonal interactions" page

Poster block: PDP-2 „Dynamical processes" page

Part A

Extended abstracts of

Oral presentations

The order is chronologically as in the programme

THE RELEVANCE OF THORPEX FOR METEOROLOGY IN GERMANY

Gerhard Adrian
Deutscher Wetterdienst, Kaiserleistraße 42, 63067 Offenbach, Germany
E-mail: gerhard.adrian@dwd.de

1. SOCIETAL ASPECTS OF WEATHER RESEARCH AND WEATHER FORECASTING

Vulnerability is often defined as the product of risk and possible damage. The development of societies and national economies in many areas leads to concentrations of values causing increasing possible damage due to severe weather events and thereby increasing vulnerability. Climate change is an additional thread of increasing risks. Therefore the vulnerability of societies and national economies against severe weather events is increasing not only caused by climate change. Because weather forecasting is one important source of information required for the management of weather sensible systems improvements of weather forecasting by weather research is one important strategy to reduce the vulnerability of society and national economy against severe weather events and to mitigate effects of climate change. Therefore research on weather forecasting, the World Weather Research Programme and THORPEX is important for all societies.

2. FRAMEWORK OF ATMOSPHERIC RESEARCH IN GERMANY

Atmospheric research in Germany is supported by very different organisations reflecting the federal structure of the German government. We have university institutes in the German states (“Länder”) responsible both for research and education; we have the research institutes of the Leibniz society shared by the German states and the federal government, the national research institutes of the Helmholtz society and the institutes of the Max-Planck Society. The latter might be the most independent institutes mainly doing basic research. Research of Deutscher Wetterdienst (DWD) as the German national meteorological service is focused on supporting its own operational services. Main activities of DWD are the development of numerical weather prediction systems for short range and very short range weather prediction complementing the activities of the European Centre for Medium range Weather Forecasting (ECMWF), and tools for interpretation of NWP-products and now casting. DWD is well integrated in the European Meteorological Infrastructure. However we have not been successful in integrating German research institutes satisfactorily in this system.

3. THORPEX AS A FOCUS FOR ATMOSPHERIC RESEARCH

All these different institutions get their funds from different sources of budget and have different tasks in science and education causing unavoidably different interests and duties. Coordination of interests between these institutions has become a difficult task. Sometimes European and international collaboration seem to be easier to organise than the collaboration between German institutions. However the scientific objectives of THORPEX are so attractive to all of them that it will help to focus all the different interests on weather research and will help to improve the weather research infrastructure in Germany. Contributions from DWD, German university institutes and one Helmholtz-institute to this conference show that THORPEX has successfully started a self organisation process which will help to acquire additional support for joined and valuable contributions from German institutions to the aims of THORPEX in the near future.

THORPEX, an element of the WMO World Weather Research Programme

David Burridge

World Meteorological Organization, THORPEX International Programme Office

1 Background

THORPEX is a key component of the WMO Natural Disaster Reduction and Mitigation Programme. It will contribute to WMO's goal to halve the number of deaths due to natural disasters of meteorological, hydrological and climatic origin over the next 15 years. In order to further reduce and mitigate the results of weather-related disasters it is crucial to improve the accuracy of high-impact weather forecasts. High-impact weather is defined by its effect on society, the economy and the environment.

Under the auspices of THORPEX, regional and global projects and experiments are carried out to

- Improve forecast skill by advancing the knowledge of global-to-regional influences on the initiation, evolution and predictability of weather systems
- target satellite and in situ observations to design the strategy for interactive forecasting and observation, thus contributing to the evolution of the WMO Global Observing System (GOS), a core component of the Global Earth Observation System of Systems (GEOSS)
- develop data assimilation to create and evaluate systems for the assimilation of targeted observations from satellites and in situ measurements
- accelerate improvements in the accuracy of numerical weather prediction and to test and demonstrate the effectiveness of a global multinational multi-model multi-analysis ensemble forecasting system
- demonstrate societal and economic benefits of improved forecasts, by improving decision-support tools, which utilize advanced forecasting products to benefit directly social and economic sectors

The THORPEX International Science Plan, (www.wmo.int/thorpex/mission.html) has been developed and the plan was published in November 2003. An ICSC Group of Experts developed the THORPEX International Research Implementation Plan (TIP) and following its approval, in December 2004, the ICSC agreed to proceed with the implementation of the TIP. The TIP is available at www.wmo.int/thorpex.

Regional THORPEX Committees, aligned with WMO regional associations, coordinate activities of regional groups of nations. Currently, there are Regional Committees for North America (2002), Asia (2003), Europe (2003) and the Southern Hemisphere (2006).

The THORPEX International Programme Office (IPO) at the WMO Secretariat in Geneva directs, coordinates and monitors activities between various elements of the programme. The THORPEX (IPO) and the international programme activities are supported through voluntary contributions of the governments of the WMO Members participating in THORPEX, including donations to the THORPEX Trust Fund established by WMO.

2 Global Interactive Forecast Systems

THORPEX will contribute to the development of a future global interactive forecasting system, which would generate numerical probabilistic products, available to all nations - developed or developing. At the heart of THORPEX is the research needed for the design and demonstration of a global interactive forecasting system that allows information to flow interactively between forecast users, numerical forecast models, data assimilation systems and observations. Such a system can also be adapted to allow the observing system, observations, assimilation and the model to be configured to maximize forecast skills for specific societal and economic uses. The THORPEX design of the strategy for interactive forecasting and targeted observations will contribute to the evolution of the WMO Global Observing System (GOS), a core component of the Global Earth Observation System of Systems (GEOSS).

2.1 Regional Campaigns - ATReC

The first regional campaign carried out under the auspices of THORPEX, the Atlantic regional Campaign (ATReC), tested the hypothesis that short term forecast errors over Europe and the Eastern seaboard of the USA can be reduced by targeting extra observations over sensitive areas determined each day by the forecast flow patterns using NWP techniques. The field campaign took place in the autumn of 2003. It was the first attempt at real time adaptive control of a full set of operational observing systems (in an international context) in addition to the deployment of research aircraft. The ATReC was an example of quasi-operational targeting of observations that involved considerable planning and good collaboration between operational forecasters, observation providers and research scientists which contained many examples of good practice. This experience will be taken into consideration in the planning of other THORPEX activities.

2.2 Regional Plans – future campaigns and experiments

The Asian, European and North American Regional Committees are developing plans for regional campaigns in 2007 and 2008.

THORPEX Pacific Asian Regional Campaign (TPARC) 2008

The concept of a THORPEX Pacific Asian Regional Campaign (PARC) 2008 is being developed as a result of a workshop held in Seattle in June 2005 and the subsequent continuing dialogue between the NARC and the ARC. The proposed campaign is planned for the second half of 2008 and in this case would coincide with the IPY and with campaign to take additional measurements in support of the Beijing Summer Olympics (including Asian measurements in the vicinity of typhoons and perhaps over the Asian continent) and may continue into the November-December time-frame to study tropical cyclone tracks, extra-tropical transitions, tropical warm-pool physics and down-stream propagation.

European TReC (ETReC)

Several major research activities relating to summertime high impact weather are planned for the year 2007, most importantly the WWRP forecast demonstration project occurring as part of MAP, and the international field experiment COPS. The European Region Committee are proposing to initiate ETReC 2007, to support these programs, link them and leverage their efforts to contribute to THORPEX scientific goals.

3 TIGGE - the THORPEX Interactive Grand Global Ensemble

Many evolving weather situations may be characterized as low probability/high risk; that is, the event is unlikely, but the consequences of occurrence may be catastrophic in terms of loss of life, property damage, loss of revenue, cost of compensation and operating costs. Decision making in this category of events is most difficult, stretching the capabilities of the tools and the decision makers. The recent shift in the weather forecasting community towards probabilistic forecasts offers a solution. By characterizing the probability of a particular weather event, we can now provide more specific information on the likely outcomes. For this information to be useful, it must become an integral part of decision support tools.

The TIGGE, the THORPEX Interactive Grand Global Ensemble, is a major element of the WMO's programme to accelerate the improvements in the accuracy of 1-day to 2-week high-impact weather forecasts. The key objectives of TIGGE are:

- An enhanced collaboration on development of ensemble prediction, internationally and between operational centres and universities
- New methods of combining ensembles from different sources and of correcting for systematic errors (biases, spread over-/under-estimation)
- A deeper understanding of the contribution of observation, initial and model uncertainties to forecast error
- Real-time support for demonstration projects and field experiments
- Societal applications leading to increased benefits to society

It is now highly likely that routine access to data bases (located at the CMA, ECMWF and NCAR) of global forecasts from 10 forecasting centres will be possible in January 2007.

4 Partnerships for research and development

A key element of the THORPEX strategy is to develop working partnerships with other programmes and considerable efforts have been made over the last 12 months to develop collaboration as follows.

With the WCRP:

- A joint project has been initiated to develop unified approaches to the development of ultra-high resolution global systems for weather prediction and climate simulation
- Collaboration in tropical meteorology including tropical convection - a successful joint workshop on the MJO was held in March 2006
- TIGGE and Task Force on Seasonal Prediction (TFSP) – given the similar technical issues (data, archiving, policy) there is a potential for "seamless" days-seasons prediction systems

With GEOSS – involvement in four main GEO tasks:

HEALTH	To improve predictability of major health hazards in W. Africa
WEATHER	Further develop TIGGE and societal applications
AGRICULTURE	Help improve the predictability of food supplies in Africa
ENERGY	Demonstration project to improve energy management techniques

These tasks represent a very important and wide-ranging contribution from THORPEX to the GEO initiative and they will also mandate assistance and support from the GEOSS to THORPEX for their successful completion.

THORPEX: A PROTEAN PROGRAMME

Huw C. Davies

Institute for Atmospheric & Climate Science, ETH, Zürich, Switzerland
E-mail: *huw.davies@env.ethz.ch*

Abstract: THORPEX constitutes an unprecedented opportunity for academic and operationally-orientated atmospheric scientists to jointly address one of the major challenges currently confronting the scientific community. The challenge of enhancing our predictive capabilities of the chaotic large-scale atmospheric flow in a meaningful and beneficial way is intellectually stimulating, technological demanding, and societally and economically relevant. Success will hinge upon the successful conduct of well-founded purpose-driven research that will focus upon and exemplify the above characteristics.

1. INTRODUCTION

The scientific rationale for and the ingredients of the THORPEX programme is set out in the programme's research and implementation plans (Shapiro and Thorpe, 2004; Rodgers et al 2005). In effect THORPEX is designed to build upon the current and foreseen research capabilities, serve as a focus for future activity, help identify the major challenges, and provide an organizational framework that bridges the realms of fundamental research, operational forecasting, and forecast application.

The programme itself is geared to making advances across a broad front that includes extending the range of skilful weather forecasts to time-scales of value in decision-making by using ensemble forecast techniques; developing accurate and timely weather warnings designed *ab initio* to be user-useful whilst contributing to mitigating the effects of weather-related natural hazards. Achievement of these goals is to be underpinned by the four THORPEX sub-programmes :– Predictability and Dynamical Processes (PDP); Observing Systems (OS); Data Assimilation and Observing Strategies (DAOS); and Societal and Economic Research and Applications (SERA).

In the next two sections we highlight aspects of the sub-programmes's core challenges and point to their inter-dependence (see also Davies, 2006).

2. THE SUB-PROGRAMMES

The PDP sub-programme includes consideration of the role of Rossby wave dynamics in predictability; the strategy and goals and dynamics of ensemble prediction; the impact of moist processes upon tropical and extratropical development and predictabilit; predictability of tropical cyclones; tropical-extra-tropical interaction, extratropical transition and downstream development; and prediction on sub-seasonal time scales and blocking.

The OS sub-programme will major on the development, testing and deployment of in-situ sensors, field demonstrations of prototype remote sensing systems, and the provision of observing-system characteristics, as well as providing management support for field campaigns. The companion DAOS sub-programme focuses on the refinement of data-assimilation techniques by incorporating improved use of observations and devising adaptive techniques, and evaluating and further developing targeting strategies.

Finally the SERA sub-programme's broad ranging remit includes developing tools to assess the potential benefits of (deterministic and ensemble) predictions for a wide range of users, developing and supporting demonstration projects to explore and highlight these benefits, and aligning their activities with that of the other sub-programmes particularly PDP.

In effect the themes outlined above encompass a major portion of the currently perceived challenges in weather prediction. Moreover the combination of quality basic research allied to social and economic relevance is central to the emerging relationship between science and society, and THORPEX is an exemplar of this new relationship.

3. AN ILLUSTRATIVE EXAMPLE

Here an overtly inadequate, but hopefully helpful, straw-man example is provided of some of the questions, ingredients and interactions that THORPEX will need to address, incorporate and exemplify to attain its goals. The example's essence is shown in Fig.1 which depicts the "forecast-analysis" difference between the 72 hour forecast and the corresponding analysis of the ECMWF forecasting suite for the potential vorticity (PV) field on the 320K surface for the 10th Oct. 2001.

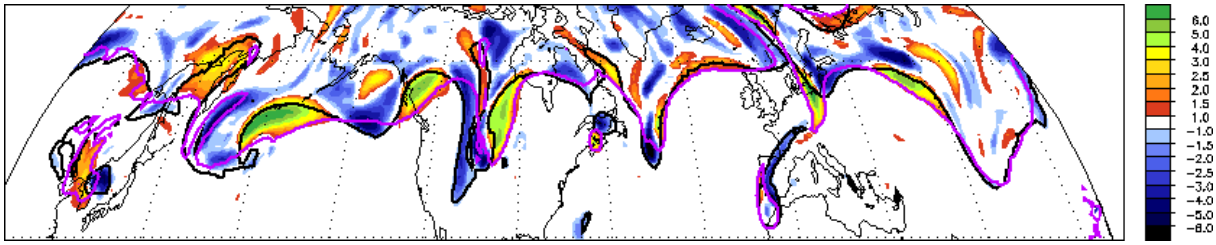

Figure 1. "Forecast-Analysis" difference for the 72hrs forecast to 10 Oct. 2001 based upon the ECMWF IFS T511 model. The difference field is that for PV on the 320K surface and the field is colour shaded. Likewise the black and purple contour lines denote the 2pvu isolines on this isentropic surface for respectively the analysis and the forecast.

The existence of such a difference prompts a sequence of questions that relate to the four THORPEX sub-programmes. These include:

(i) Is the difference pattern typical, and does it persist in today's upgraded prediction suites ? *(PDP & DAOS issue)*

(ii) Is the difference dynamically significant and/or operationally important? *(PDP & SERA issue)*

(iii) Is the analysis field itself likely to be inadequate? *(OS & DAOS issue)*

(iv) How does the difference relate to and is it encompassed within the spread of the accompanying ensemble predictions? *(PDP & DAOS issue)*

(v) Is it possible to diagnose the cause of the difference and proceed to rectify the mismatch of forecast and analysis?

For (i) there are firm indications that the difference pattern is indeed typical, and that it is evident in today's NWP suites. For (ii) the difference can be deemed dynamically significant because it relates directly to the location of the jet stream that in turn exerts a major influence upon surface weather, and also operationally important because the flow's large-amplitude wave pattern is often a precursor of severe extra-tropical weather events. For (iii) there are indications that the analysis field itself might deficient since a misplacement of the jet's location and/or a significant misrepresentation of the jet's lateral scale and amplitude is not unusual, and that in turn implies major finite-amplitude deviations away from the 'true' state. For (iv) note that the form of the two 2 pvu isolines resembles the output of ensemble predictions (c.f. the standard 500 hPa spaghetti diagrams), and moreover their structure is consistent with a significant under-estimation of the amplitude and/or phase of the prevailing Rossby wave pattern on the extra-tropical wave guide (sic. jet stream).

It follows that comprehensive consideration of Question (v) would entail :- ensuring the adequate use of the available measurements and examining strategies for the selective flow-dependent enhancement of measurements (OS); refining data assimilation techniques to accord with the existence of highly structured predictively-sensitive flow features (DAOS); devising diagnostic techniques to determine the dynamical nature and possible origin of the differences, and assessing the implications for ensemble prediction of the existence of major finite-amplitude errors in the specification of the initial field (PDP); and finally there is the subtle task of evaluating the possible pay-back that alleviating the foregoing deviations would have upon the forecast accuracy and the effective ensemble spread, and then translating that it into quantifying the realizable benefit for users (PDP and SERA).

4. END NOTE

The term *protean* is linked both to the Greek word *protos* signifying primary importance and to the Greek mythological figure *Proteus* whose attributes included being able to assume diverse forms and provide valid predictions to those who grappled successfully with him. It appears appropriate to refer to THORPEX as a protean programme.

Acknowledgements: *It is a pleasure to acknowledge the collaboration and support of Marco Didone and Sandro Buss in the development of the research related to the material presented in Section 3.*

REFERENCES

Davies, H.C., 2006: Large-scale weather systems: A future research priority. Adv. Atmos. Sci., **23,** (in press).

Rogers D.P., M. Beland, P. Bougeault, J. Caughey, Chen Dehui, P. Courtier, E. Manaenkova, M. Miller, K. Mylne, T. Nakazawa, D. Parsons, J. Purdom, K. Puri, D. Richardson, M. Shapiro, A.Thorpe, Z. Toth, 2005: THORPEX International Research Implementation Plan. WMO/TD- No.1258. 96pp

Shapiro, M.A. and A.J. Thorpe, 2004: THORPEX International Science Plan, Version III. WMO TD-No. 1246, 51pp

WILL THORPEX SCIENCE BENEFIT HUMANITY?

M. A. Shapiro[1]
[1] NOAA/Office of Weather and Air Quality, Boulder CO, USA
E-mail: *mshapiro@ucar.edu*

Abstract: This contribution presents examples of global-to-regional influences on high-impact weather events and their prediction, with an emphasis on the potential benefit of THORPEX research to humanity.

Keywords – *THORPEX, Socioeconomic impacts, high-impact weather forecasts*

1. INTRODUCTION

We stand at the threshold of accelerating advances in the skill of weather prediction and in its use and benefits to society. This opportunity has arisen out of recent achievements in monitoring, assessing and predicting weather hazards and the utilization of this information by natural-hazard mitigation managers, socio-economic decision makers, environmental policy makers and global societies. These achievements represent some of the most significant scientific, technological and societal accomplishments of the 20th century. Yet despite the notable improvements in weather prediction skill over a broad range of space and time scales, there remains an urgent necessity to accelerate further improvements to realize a higher level of societal, economic and environmental benefit. This necessity is driven by the heightened awareness of the increasing vulnerability of global societies and the physical-geochemical-biological environment to hazardous weather, climate variability and change.

The past quarter century has witnessed a notable increase in predictive skill, especially when viewed in terms of improvements in meteorological metrics such as 500hPa anomaly correlation, Fig.1. In contrast, there has been a lesser rate of progress toward: i) translating the great wealth of weather forecast information into user-relevant verification metrics to assist beneficial decisions for specific socioeconomic sectors (e.g., health; food security; energy); ii) the quantitative assessment of the use and value of weather information to global societies. Progress toward identifying, prioritising and responding to the urgent need for accelerated advances in weather forecast systems and their associated user/sector relevant derivatives demands greater collaboration between the physical and societal science communities.

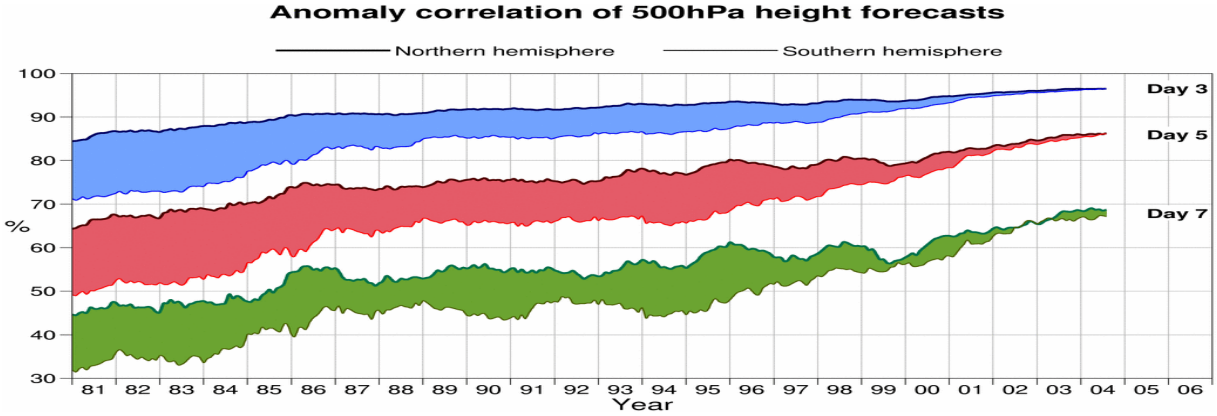

Figure 1. Evolution of forecast skill for the northern and southern hemispheres: 1980-2004. Anomaly-correlation coefficients of 3, 5, and 7-day ECMWF 500-mb height forecasts for the extratropical northern and southern hemispheres, plotted in the form of running means for the period of January 1980-August 2004. Shading shows differences in scores between hemispheres at the forecast ranges indicated (from Simmons and Hollingsworth, *et al*. 2002).

2. THE USE AND VALUE OF WEATHER INFORMATION

Weather forecasts provide timely information about atmospheric conditions that affect society, economy and the natural environment. Skillful forecasts allow society to mitigate the consequences of high-impact weather and to respond efficiently to day-to-day weather. Many applications of weather forecasts involve translating predicted meteorological parameters (e.g., wind speed; temperature; precipitation) at specific spatial and temporal scales into socioeconomic attributes of the natural or human environment, such as: energy demand; transportation efficiency; demands on health services; water resources; pest infestations; wildfire; air quality.

The impact of weather information on societal and economic activities is a consequence of several elements: i) ***content*****:** relevance of product information to the users; ii) ***distribution***: product dissemination on spatial and temporal scales sufficient for action; iii) ***communication*****:** product formats that users can comprehend and interpret; iv*)* ***recognition*****:** recognition by users that the information has value; v) ***respons*****e:** actions taken by users in response to the information. These elements are links along a chain of action. If any one link is broken, then the impact and the value of the forecast information will be diminished. THORPEX socioeconomic research and applications (SERA) will: i) identify weaknesses in the above links; ii) contribute to the development and application of existing and new methods that enhance the societal, economic and environmental use and value of weather information; iii) participate in establishing socioeconomic priorities for accelerating advances in weather, climate and Earth-system prediction.

3. A GLOBAL-TO-REGIONAL PERSPECTIVE OF SOCIOECONOMIC, ENVRIONMENTAL AND HUMANITARIAN IMPACTS OF HIGH-IMPACT WEATHER AND ITS PREDCITION

The body of this lecture will discuss global-to-regional Rossby wave energy dispersion and its role in initiating regional high-impact weather events, such as: i) extreme flooding and wild fires in the North-American Pacific coastal zone; ii) heavy precipitation, and sand and dust storms over North Africa and the impact of these events on food security, epidemical disease and the environment:

- *The socioeconomic and environmental impacts of Saharan dust storms associated with high-wind events in the in the vicinity of the Haggar, Tibesti and Ajr mountains, and the Bodélé depression*: *observations and high-resolution numerical simulations and their role in* locust vector transport, oceanic and continental geo-biochemical processes, and sub-Saharan meningococcal meningitis epidemics.

- *Rossby wave trains and their relationship to the onset of high-impact weather events extending from western North America to Africa and beyond:* anomalous precipitation on the western edge of the Sahara desert and the subsequent initiation of the 2003-2004 African locust plague.

4. CONCLUSION

The capstone of the THORPEX legacy will not be its marginal advancement in predictive skill over what would have taken place through natural evolution of global forecast systems (e.g. Fig. 1), but through its achievements in providing and communicating innovative uses of weather information to natural-hazard managers, environmental policy makers, and global societies at large to enable sound decisions that minimise the vulnerabilities and losses arising from high-impact weather and intra-seasonal climate variability. In this vein, it is imperative that THORPEX carry out research and forecast demonstration projects to assist those emerging nations that are least capable of utilising and participating in the development of advanced weather-forecast systems and their weather-related socioeconomic derivatives. The proposed *Health and Climate Partnership for Africa* (see Rogers 2006, this volume) is one such THORPEX research demonstration project that will focus on improving early warning for environmentally-sensitive diseases in Africa African Health.

Dr. Walter Orr Roberts, (National Center for Atmospheric Research) once said, *"I have a very strong feeling that science exists to serve human welfare. It's wonderful to have the opportunity given us by society to do basic research, but in return, we have a very important moral responsibility to apply that research to benefiting humanity"*.

Acknowledgements: *Section 2 of this abstract incorporates contributions by Rebecca Morse and Lenny Smith appearing in Shapiro and Thorpe (2005).*

REFERENCES

Rogers, David, 2006: Health forecasting in Africa. *Second THORPEX International Science Symposium*, this volume

Shapiro, M.A. and A.J: Thorpe, 2004: THORPEX International Science Plan, Version III. WMO TD-No. 1246, 51pp

Simmons, A.J., and Hollingsworth, A. 2002: Some aspects of the improvement in skill of numerical weather prediction. *Quart. J. Roy. Meteorol. Soc*., **128**, 647-677

PERFORMANCE OF THE LOCAL ETKF IN THE MET OFFICE GLOBAL ENSEMBLE

Neill Bowler, Ken Mylne, Alberto Arribas, Kelvyn Robertson

Met Office, Fitzroy Road, Exeter, EX1 3PB, UK
E-mail: *Neill.Bowler@metoffice.gov.uk*

Abstract: The Met Office has developed a short-range global and regional ensemble prediction system based around the ensemble transform Kalman filter (ETKF). This ensemble has been running in the operational suite since September 2005 as part of a year-long trial. The ETKF is a version of the ensemble Kalman filter which allows computationally efficient update of the ensemble perturbations without performing an analysis.

Upgrades to the initial condition perturbations and stochastic physics schemes have recently been performed. The new initial condition method is called the local ETKF, which provides initial condition perturbations by calculating the ETKF transform matrix for a series of points over the globe, using only observations within a given radius of each point. In order to keep the computation swift, a sparse set of points are used for the calculation of the transform matrices, and these are interpolated to intermediate grid-points.

The local ETKF allows control over the variation of the spread of the ensemble with location, avoiding some of the problems experienced with the ETKF. Tests have shown positive performance overall, with the verifying observation lying outside the range of the ensemble less often than with the ETKF.

Keywords – *ensemble Kalman filter, ETKF, localisation*

1. INTRODUCTION

The Met Office Global and Regional Ensemble Prediction System (MOGREPS) is a short-range ensemble prediction system aimed at providing guidance on the likelihood of severe weather developments in the next three days. This requires high resolution to represent the severity of the winds, so for affordable implementation on current resources we need a limited-area ensemble. For short-period forecasting the singular vector method of ensemble generation is not appropriate, since it does not properly sample initial errors. Instead, after a preliminary idealised study (Bowler, 2006), we chose to implement an ensemble transform Kalman filter (ETKF) (Bishop *et al.*, 2001). To avoid problems with boundary conditions, and because errors over the Atlantic can sometimes be traced back to upstream areas such as the Canadian Arctic, we decided a global ensemble system was needed. The ETKF produces global perturbations at about half the resolution of the main global forecast (90km). These are added to the reconfigured global 4D-Var analysis and the ensemble is run to 3 days. After 6 hours the evolved perturbations are added to the newer North Atlantic and European (NAE) 4D-Var analysis, and the regional ensemble is run to 36 hours at half the resolution of the main NAE run (24km).

The ensemble uses 24 forecasts (1 control and 23 perturbed forecasts) as this offers a compromise between the resolution of each forecast, and the ability of accurately specify the errors in the analysis. The ETKF is equivalent to the EnKF and allows for rapid calculation of the analysis perturbations. The efficiency of the computation relies on the analysis perturbations being in the subspace of the forecast perturbations. Hence, covariance localisation is not normally possible within the ETKF framework.

2. LOCAL-ETKF (L-ETKF)

The initial implementation used a global ETKF for which the scaling of the perturbations was determined globally. This resulted in perturbations which were generally too large in the extra-tropics, where the growth rate due to baroclinic instability is large, and too small in the tropics (figure 1a). The L-ETKF scheme runs a number of regional ETKFs where the ensemble transform is calculated based only on observations and forecasts within a limited area. The transform matrices are then interpolated between the regions in order to create continuous perturbation fields. The set-up of the scheme was constrained by the need to have regions large enough to ensure that each region contained sufficient radiosonde observations to reliably calculate the local scaling, but small enough to allow an effective variation of the scaling across the globe. The compromise reached was to use regions with a radius of 3000km. However a global ETKF is retained and is used to provide perturbations in the tropics and for regions where there are insufficient radiosondes to calculate the scaling. The L-ETKF scheme was introduced into the operational suite on 14th June 2006. Figure 1b shows that the L-ETKF provides a much improved scaling of the ensemble spread with latitude compared to the global ETKF in figure 1a. Prior to the change a common feedback response from forecasters was that perturbations looked unrealistically large in the early time frames of the forecast (3-12 hours), but since the change very few such comments have been received.

a) b)

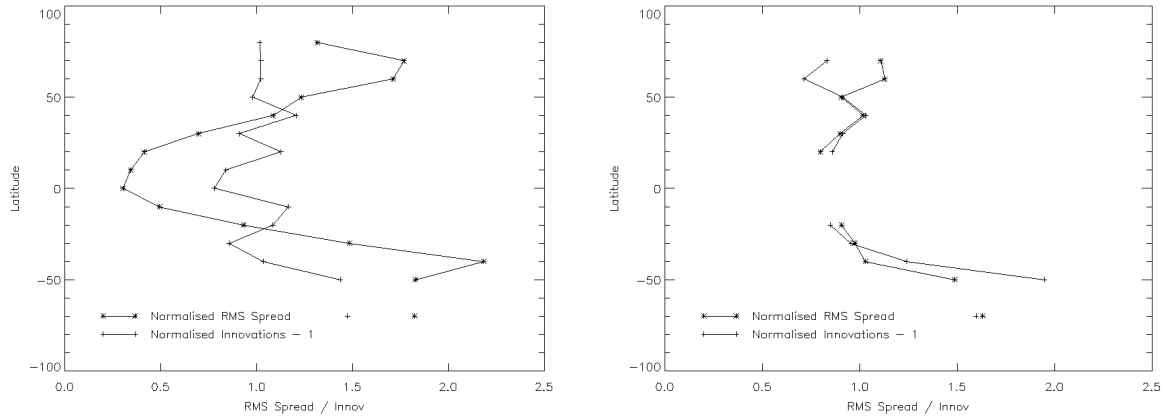

Figure 1: Zonal-mean ensemble spread and 4D-Var innovations (RMS of observations minus background) for radio sonde observations normalised by the background error, as a function of latitude for a) the global ETKF and b) the Local-ETKF. Note that the L-ETKF is not calculated between 20N and 20S.

The local ETKF (along with the stochastic physics scheme SKEB) was introduced in parallel suite 11. The stochastic kinetic energy backscatter (SKEB) scheme aims to backscatter some of the kinetic energy that is excessively dissipated from the model by the semi-Lagrangian advection scheme. Figure 2 shows the results from this trial period of running for forecasts of 500hPa geopotential height verified against analyses over the NAE domain. The local ETKF serves to reduce the spread of the ensemble (figure 2a), though the ensemble still seems over-spread. In spite of the reduction in spread, the frequency with which the verification lies outside the spread of the ensemble is reduced (figure 2b).

a) b)

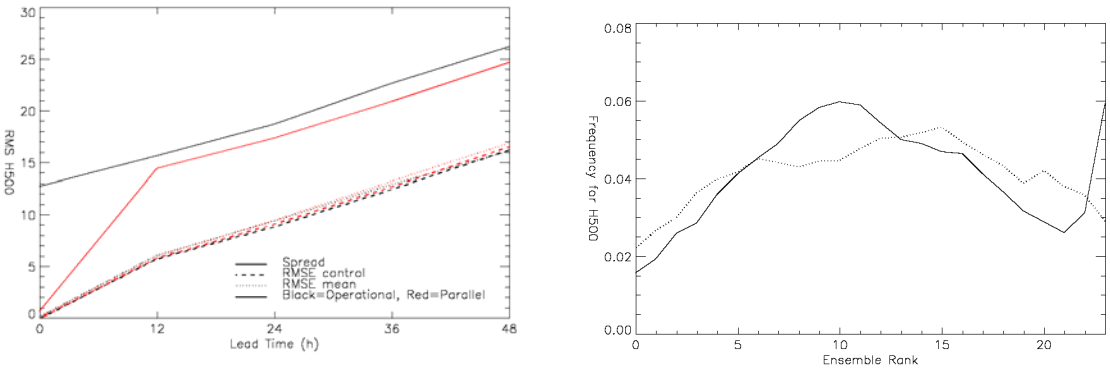

Figure 2: Performance of the MOGREPS global ensemble during parallel suite 11, which included the introduction of the local ETKF and SKEB. a) shows the RMS spread and error of the ensemble mean and control forecasts for the operational (black) and trial (red) ensembles, verified against analyses of 500hPa geopotential height. b) shows the rank-histogram for the operational (solid) and trial (dotted) ensembles.

3. CONCLUSION

A new method for calculating initial condition perturbations has been applied to the MOGREPS ensemble. This allows localisation of the perturbations within the ETKF framework, and therefore control over the regional variation of the spread of the ensemble. This reduces the spread of the ensemble in the extra-tropics while reducing the frequency with which the verification lies outside the spread of the ensemble.

REFERENCES

Bishop, C. H., B. J. Etherton and S. J. Majumdar, 2001: Adaptive sampling with the ensemble transform Kalman filter. Part 1: theoretical aspects, Monthly Weather Review, **129**, 420-436.

Bowler, N., 2006: Comparison of error breeding, singular vectors, random perturbations and ensemble Kalman filter perturbation strategies on a simple model, Tellus A, **58**, 538-548.

ADAPTIVE OBSERVATION IN THE ATLANTIC AND THE MEDITERRANEAN REGION

Alexis Doerenbecher[1]

[1]CNRM-GAME, Météo-France, Toulouse, France

Abstract: The focus of this presentation is adaptive observation on some Mediterranean cases. During the past adaptive observation campaigns Météo–France participated in over the Northern Atlantic (FASTEX 1997, NA-TReC 2003), the targeting guidance that was proposed was based on the model ARPÈGE associated with some first generation techniques. The current plans are to implement some second generation techniques that were investigated for research purpose on FASTEX Atlantic cases, and to adapt them for adaptive observation in the context of severe (not extreme) weather events in the Mediterranean region.

Keywords – CYPRIM, *adaptive observing network, observation sensitivity, 4D-Var, Mediterranean, high impact weather, synoptic scale, mesoscale, optimization, campaign.*

1. INTRODUCTION

Météo–France participated in two field campaigns in which observation targeting was a prime objective. These campaigns took place in the Northern Atlantic (FASTEX 1997, NA-TReC 2003) and focused on the prediction of the synoptic scale features in the storm track. Some experience of the targeting guidance has been gained in that context. Moreover, this experience is complemented by the ongoing research on adaptive observation and on the issues related to the predictability at such scales.

Nowadays, the Mediterranean region and its high impact weather (heavy precipitation, wind storms) draws our attention. The events we are interested are little predictable and are of smaller scale than the synoptic scale. One expects the adjoint-based targeting techniques developed for synoptic features (e.g. 1-2 days range) to be of poor guidance when strictly focusing on such scales. However, the large scale atmospheric environment may be important for the occurrence of such events. Thus, an adaptive observing network optimized for the synoptic scale would still benefit the prediction of mesoscale Mediterranean events. The first stage of this work is to implement the KFS (**K**alman **F**ilter **S**ensitivity, Bergot and Doerenbecher, 2002) with a quasi-operational version of ARPÈGE. This tool will help us to evaluate alternative deployments on few meteorological cases of interest.

In the first part of this long summary, we briefly present a case of heavy precipitation on the Mediterranean. In the second part, we discuss the theory that supports the KFS tool we apply to that Med. case. The last part sketches the planned work and its context.

2. A MEDITERRANEAN CASE

Fall and winter seasons are favourable to high impact weather in the Mediterranean region. Here, we briefly describe a recent case with heavy precipitation over southern France, especially over Corsica. We focus on the 14^{th} of October, 2006. Figure 1 shows the ARPÈGE analysis overlaid with a water vapour SEVIRI image (channel 5) from METEOSAT 8. On this case, the upper trough is located on the western Europe and produces a northward flow above the Mediterranean. The low level flow has some small scale features such as a cyclonic circulation at the east of Corsica and a convergence over Tyrrhenian Sea where the convection occurs. Precipitation also occurs ashore of the Gulf of Lion.

3. WHICH TARGETING TECHNIQUE ?

The targeting guidance produced by the first generation adjoint-based technique used at Météo–France implies the computation of singular vectors (total energy norm, see Palmer *et al.*, 1998 for details). Sensitive areas are derived from a set of leading singular vectors, by vertically integrating the total energy and combining the singular vectors with respect to their growth rate. This technique accounts for the dynamics of the meteorological situation. The sensitive areas show where a modification of the initial conditions (IC) will strongly impact the forecast (see Fig 2). So they do not account for any assimilation process that would modify the IC consistently with the addition of observations. Moreover, this targeting guidance ignores about any aspect of sampling strategy.

The second generation techniques do account for such assimilation aspects, in addition to the dynamical properties of the flow. The KFS may be considered as such a technique. It has been derived from the so-called sensitivity to the observations (Doerenbecher and Bergot, 2001).

As for any other adaptive observation technique, a particular aspect of a forecast $\mathbf{x}^f$ is focused on. Hereafter, it is written as a function: $\mathcal{J}\left(\mathbf{x}^f\right)$ (e.g. the energy of the forecast error at range HH on the domain Ω). The KFS

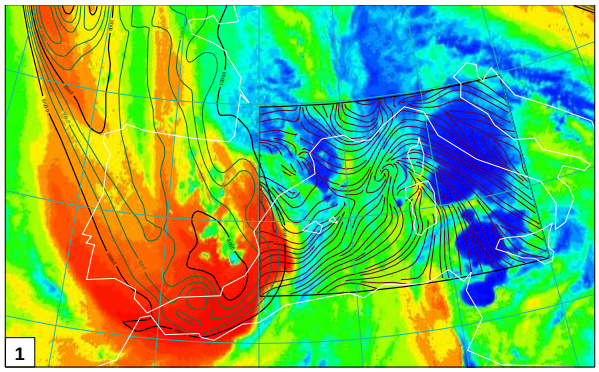

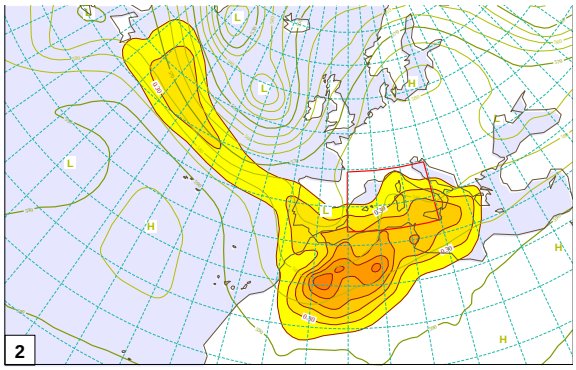

Figure 1 (right): ARPÈGE analysis METEOSAT 8 satellite image valid for the 2006-09-14 at 12 TU. The image is channel 5 (water vapour) of SEVIRI instrument. The deep blue areas show where the upper troposphere contains water and the coverage of convective clouds (sp. east of Corsica). Red areas show dry air from stratosphere associated with the through above western Europe. The fields are the geopotential on 2.0 PV-Unit surface (every 50 dam below 10000 m) and the surface wind at 10 m (streamlines) inside the region of interest that is used for targeting purpose. The low level flow shows a cyclonic circulation of small scale (not yet mesoscale) just at the west of Corsica.

Figure 2 (right): Normalized sensitive area derived from 10 singular vectors computed with ARPÈGE. The targeting time is 2006-09-13 at 00 UT, 36 hours prior to the verification time shown in fig. 1. The overlaid field is the geopotential at 500 hPa (every 50 dam) from a 12 h forecast starting from the 2006-09-12 at 12 UT. These 12 hours stand for the lead time.

relies on a score $\mathcal{S}$ for that function $\mathcal{J}$ applied to $\mathbf{x}^f$ with respect to the (unknown) truth $\mathbf{x}^t$: $\mathcal{S} = \mathcal{J}\left(\mathbf{x}^f\right) - \mathcal{J}\left(\mathbf{x}^t\right)$. Considering that the model is perfect, that $\left(\mathbf{x}^f - \mathbf{x}^t\right)$ is small enough to verify some linear assumption and that the analysis is an unbiased process, one can write the variance of the score $\mathcal{S}$ as follows: $Var\left(\mathcal{S}\right) = \nabla_{\mathbf{x}^a}\mathcal{J}^* \mathbf{A} \nabla_{\mathbf{x}^a}\mathcal{J}$, where $\mathbf{A}$ stands for the matrix of the analysis error covariances. Following the approach of Cardinali (Ecmwf, *personal communication*), $\mathbf{A}\nabla_{\mathbf{x}^a}\mathcal{J}$ can be saved from the computation of the sensitivity to the observations. Indeed, the sensitivity of $\mathcal{J}\left(\mathbf{x}^f\right)$ to the observations $\mathbf{y}^o$ (entering its initial conditions $\mathbf{x}^a$) necessitates to get the adjoint of the assimilation process $\mathbf{K}^*$ which contains the self-adjoint $\mathbf{A}$. As a consequence, the KFS accounts for the location and the error statistics of the observations within the data assimilation system of interest.

The variance of the score may be computed for two observing systems (OS): the routine OS ($\mathbf{y}^o_r$) and the extended OS (comprising routine + adaptive = $\mathbf{y}^o_{rs}$). Thus, one can compute the variation (i.e. reduction) of variance $\Delta Var\left(\mathcal{S}\right)$ due to the addition of a (simulated) set of observations $\mathbf{y}^o_s$. The targeting guidance arises from the evaluation of several alternative supplementary deployment $\mathbf{y}^o_{s_k}, k = 1, 2...N$. We will study and evaluate some possible configurations for such an in-situ observing network. The experiments will be conducted with simulated observations. These observations may comprehend some routine platforms used in an adaptive mode (measurements at extra time, when the location cannot be changed) as well as specific platforms (e.g. research aircraft). The evaluation of the benefit of the added observations on the subsequent forecasts will be possible with the **K**alman **F**ilter **S**ensitivity in ARPÈGE and its 4D-Var.

4. DISCUSSION

This work considering a simulated context is only a first step. This stands as our contribution to the French (national) project CYPRIM. CYPRIM (**Cy**clogenesis and heavy **pr**ecipitation in the **M**editerranean) aims to better understand the Mediterranean high impact weather and to conceive an observing system capable to better control the forecast uncertainties at the scales concerning these weather events. In the longer term, our research plans will match the objectives of the HYMEX project (see paper by Ducrocq and co-author in this book), which considers the implementation of some real-time adaptive observation during EOPs and SOPs.

REFERENCES

Bergot, T., and A. Doerenbecher, 2002: A study on the optimization of the deployment of targeted observations using adjoint-based methods, *Quart. J. Roy. Meteor. Soc.* **128**, 1689–1712.

Doerenbecher, A., and T. Bergot, 2001: Sensitivity to observations applied to FASTEX cases, *Nonlinear Processes in Geophysics* **8** (6), 467–481.

Palmer, T., R. Gelaro, J. Barkmeijer, and R. Buizza, 1998: Singular vectors, metrics and adaptive observations. *J. Atmos. Sci.* **55** (4), 633–653.

OBSERVING SYSTEM EXPERIMENTS USING A SINGULAR VECTOR METHOD FOR 2004 DOTSTAR CASE

Yoshiaki TAKEUCHI [1], Munehiko YAMAGUCHI [1], Takeshi IRIGUCHI [1], Tetsuo NAKAZAWA [2]

[1] Numerical Prediction Division, Japan Meteorological Agency, Tokyo, Japan
[2] Typhoon Research Department, Meteorological Research Institute, Tsukuba, Japan
E-mail: *ytakeuchi@met.kishou.go.jp*

Abstract: Japan Meteorological Agency (JMA) performed Observing System Experiments (OSEs) on a typhoon track forecast to investigate the usefulness of a sensitivity analysis based on a moist singular vector method. The results show the sensitivity analysis using JMA singular vector method may be useful for targeting observations like Dropsonde Observation for Typhoon Surveillance near the Taiwan Region (DOTSTAR).

Keywords – *OSE, typhoon track forecasts, sensitivity analysis, moist singular vector*

1. INTRODUCTION

Dropsonde Observation for Typhoon Surveillance near the Taiwan Region (DOTSTAR) has demonstrated the effectiveness of dropsonde observation on typhoon track forecasts. Japan Meteorological Agency (JMA) has performed several Observation System Experiments (OSEs) for DOTSTAR data of typhoon CONSON, in order to investigate the usefulness of a sensitivity analysis based on a moist singular vector method, which has been developed for typhoon ensemble forecasts planned to be operational in 2007.

2. JMA SINGULAR VECTOR METHOD

A singular vector method is known as a strategy for a sensitivity analysis (Majumdar et al., 2006) as well as for making initial perturbations in an ensemble prediction system (Puri et al., 2001). The linearized model and its adjoint version of JMA singular vector method are derived from the global 4D-VAR analysis system, and consist of full dynamics based on Eulerian integrations and full physical processes containing representations of vertical diffusion, gravity wave drag, large-scale condensation, long-wave radiation and deep cumulus convection. The model resolution is T63 (about 200km grid size at middle latitude) with 40 vertical layers. The norm to evaluate the growth rate of a singular vector is based on a total energy norm (Barkmeijer et al., 2001), but which is adjusted in order to obtain singular vectors explained mainly by wind and specific humidity component below about 300hPa, which are highly likely to relate with the uncertainties on typhoon track forecasts.

3. OSE SET-UP

The sensitivity analysis is performed for typhoon CONSON at 12UTC 8 June 2004 when totally 16 dropsondes were dropped under the DOTSTAR project (Figure 1). In this singular vector calculation, the optimization time interval is 24 hours and a targeting area is set to rectangle, 25N – 30N and 120E – 130E, including CONSON's center position at the optimization time. The result is shown in Figure 2. The sensitive region, which is defined in this study as the distribution of vertically accumulated total energy of the 1st singular vector, is computed around northeast of the typhoon. Four predictions with JMA Global Spectral Model (TL319L40) were performed starting from above time. The four predictions were different only in the use of the DOTSTAR data in the global 4D-VAR analysis; (I) all dropsonde observations were used for making the initial condition, (II) no dropsonde was used, (III) only eight observations within a sensitive region were used, and (IV) only observations outside of the sensitive region were used (Table 1). In these experiments, the typhoon track forecasts are compared with each other.

4. RESULTS

OSEs results are shown in Figure 3. In the comparison of the typhoon track forecasts, CONSON's northeastward movement in the third prediction is similar to that in the first one while in the second and forth ones CONSON stays at the almost same position as an initial position. Furthermore, it is found in an additional experiment that even one dropsonde data within the sensitive region can contribute to the improvement on CONSON's track forecast.

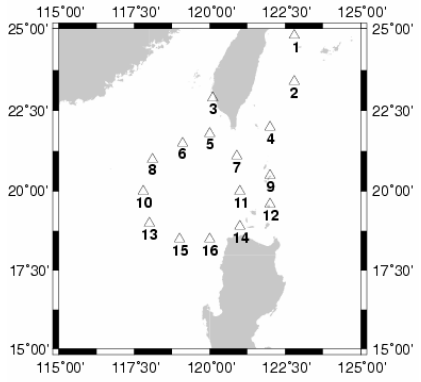

Figure 1. Dropsonde observation points for typhoon CONSON at 12UTC 08 June 2004.

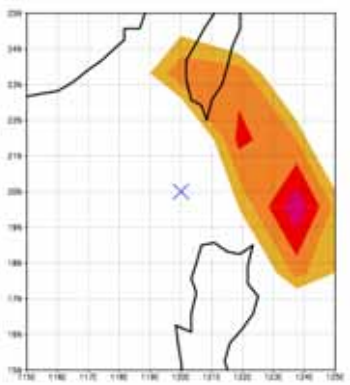

Figure 2. Sensitivity analysis result by JMA singular vector method. The distribution means vertically accumulated total energy by the 1st moist singular vector. Blue point is the CONSON's center position.

Experiment Name	The number of used dropsonde data
(I)	all (1 – 16)
(II)	nothing
(III)	3, 4, 5, 7, 9, 11, 12, 14
(IV)	6, 8, 10, 13, 15, 16

Table 1. Experiment list and dropsonde data which are used in the global 4D-VAR analysis at the corresponding experiment.

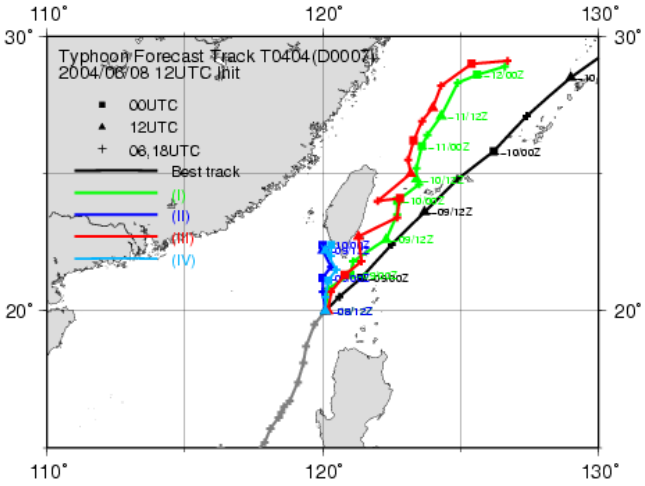

Figure 3. OSEs result on CONSON's track forecast; green line is by exp. (I), blue line is by exp. (II), red line is by exp. (III), and light blue line is by exp. (IV). Black line is the best track of CONSON. Initial time is 12UTC 08 June 2004.

5. CONCLUSION

The OSEs results suggest two conclusion; one is that dropsonde data within the sensitive region is enough to predict typhoon CONSON's track well, and the other is that a sensitivity analysis using JMA singular vector method may be useful for targeting observations like DOTSTAR. In other typhoon cases, for example, typhoon MELOR in 2003 which is also a DOTSTAR case, and typhoon MARIA in 2006, which forecasts may have been sensitive in initial conditions, the singular vector method proves to be useful for targeting observation for tropical cyclones.

Acknowledgements: *DOTSTAR data are used in this study. JMA thanks to the data and DOTSTAR project.*

REFERENCES

Barkmeijer, J., Buizza, R., Palmer, T. N., Puri, K. and Mahfouf, J. F., 2001: Tropical singular vectors computed with linearized diabatic physics. *Quart. J. Roy. Meteor. Soc.*, **127**, 685-708.

Majumdar, S. J., S. D. Aberson, C. H. Bishop, R. Buizza, M. S. Peng and C. A. Reynolds, 2006: A Comparison of Adaptive Observing Guidance for Atlantic Tropical. *Mont. Wea. Rev.*, **134**, 2354-2372.

Puri, K., Barkmeijer, J. and Palmer, T. N., 2001: Ensemble Prediction of tropical cyclones using targeted diabatic singular vectors. *Quart. J. Roy. Meteor. Soc.*, **127**, 709-731.

THE THORPEX INTERACTIVE GRAND GLOBAL ENSEMBLE (TIGGE): CONCEPT AND CURRENT STATUS

Philippe Bougeault
(co-chair, GIFS-TIGGE WG)
ECMWF, Reading, UK

E-mail: *P.Bougeault@ecmwf.int*

Abstract: Nine operational NWP centres producing daily ensemble forecasts to 1-2 weeks ahead have now agreed to deliver in near-real-time a selection of forecast data to the TIGGE data archives. This is offered to the scientific community as a new resource for research and education. The objective of TIGGE is to establish closer cooperation between the academic and operational worlds by encouraging larger use of operational products for research, and to explore actively the concept and benefits of multi-model probabilistic forecasts, with a particular focus on severe weather prediction. The TIGGE data policy is to make each forecast freely accessible via Internet 48h after it was initially issued by the originating centre. Real-time access can also be granted for field experiments or projects of particular interest to THORPEX. The future evolution of TIGGE will comprise archiving additional datasets for limited periods, based on requests from THORPEX working groups, and transitioning to a distributed archive concept (Phase 2). The future operational use of the TIGGE infrastructure as part of a "Global Interactive Forecasting System" will be considered, subject to positive results from research undertaken with the TIGGE data archives.

Keywords – *THORPEX, WMO, TIGGE, Multi-model forecasts*

1. TIGGE OBJECTIVES AND CONCEPT

TIGGE, the THORPEX Interactive Grand Global Ensemble, is a key component of THORPEX: a World Weather Research Programme to accelerate the improvements in the accuracy of 1-day to 2-week high-impact weather forecasts for the benefit of humanity. The first TIGGE workshop was held at ECMWF from 1 to 3 March 2005 and the full workshop report is available on the THORPEX Web site and has been published in the WMO series WMO/TD-No. 1273 WWRP/THORPEX No. 5.

Several objectives for TIGGE were agreed at the Reading workshop, such as: (i) enhancing collaboration on ensemble prediction, internationally and between operational centres and universities; (ii) developing new methods to combine ensembles from different sources and to correct for systematic errors (biases, spread over-/under-estimation); (iii) achieving a deeper understanding of the contribution of observation, initial and model uncertainties to forecast error; (iv) exploring the feasibility and the benefit of interactive ensemble systems responding dynamically to changing uncertainty; (v) future transition towards an operational system.

The data to accumulate in priority in the TIGGE archive were agreed to be: (i) The ensemble forecasts generated routinely (often operationally) at different centres around the world: This is the core data of the TIGGE archive. The total daily data volume is around 200GB. (ii) Observational data and existing datasets including re-analyses and re-forecasts. (iii) Additional special datasets generated by the THORPEX community for specific research and applications.

The technical concept of TIGGE was also discussed. It was judged most effective to develop TIGGE with two different phases: In *Phase-1,* data will be collected in near-real time at a small number of central TIGGE data archives. This can be implemented rapidly at little cost and can handle the estimated 200 GB per day data volumes with current network and storage capabilities. In *Phase-2*, data archives will be distributed over a number of repositories, instead of all being held centrally, but efficient and transparent access to users will be maintained. This is a more flexible solution with the potential to eliminate routine transfers of large data volumes. But this will require substantial software development, in coordination with the WMO Information System, and specific funding.

The workshop was followed by a period of consolidation of the concept. The GIFS-TIGGE working group was appointed to lead the project. Meetings were held to agree the detailed content and format of the initial data base, as well as the exchange procedures. Commitments were sought from potential partners. At the present time, commitments have been received from the following institutions: CMA, ECMWF, and NCAR have agreed to become Archive and Distribution Centres. BMRC, CMA, CPTEC, ECMWF, FNMOC, JMA, KMA, Meteo-France, MS Canada, NCEP, and UKMO have agreed to provide daily forecasts to the above Archive Centres. In addition, the TIGGE Web site will be maintained by ECMWF, the meta-data centre will be maintained by NCAR, and the verification Web site will be maintained by JMA.

Finally it was agreed to maintain the maximum compatibility with the North American Ensemble Forecasting System (NAEFS) and to exchange research results. The scope of the two projects is initially different, but it is believed that TIGGE and the NAEFS will ultimately evolve into a single operational system.

2. TIGGE USERS

TIGGE is developed in view of benefiting to the research community at large and in particular the science working groups of THORPEX. It will also serve a number of research/development projects targeted at specific applications of severe weather forecasts (health, energy, flood warning, fire weather, etc…). The forecast demonstration projects of THORPEX and WWRP (e.g. BeiJing 2008 FDP/RDP), the future field campaigns on adaptive observations and the IPY projects will be active users of TIGGE. Finally the hydrological community (e.g. through HEPEX) is expected to be a strong user of TIGGE data.

3. SOME IMPORTANT TECHNICAL CHOICES

The new WMO standard GRIB2 for gridded data was agreed by all partners to support data exchanges between the data providers and the archiving centres. The archives will also be held in GRIB2. The units, the names of the various fields, the accumulation periods, etc… will be identical for all data providers. A less obvious matter was the choice of grids. As forecast resolutions and grid projections vary widely between the forecast centres, any choice of a common grid would result either in a loss of quality (for the higher resolution systems) or in an artificially high archive volume (for the lower resolution systems). Therefore it was agreed that data providers will provide data on grids of their own choosing, which are as close as possible to the native grid employed to carry out the predictions. The data will be archived on the same grid as received. The data providers will ensure that appropriate software is available to the archiving centres to enable users to interpolate data to latitude/longitude grids and locations of their choosing. They should also ensure that when revisions to their systems are made, the revised interpolation software are communicated to the archiving centres immediately. Finally the archiving centres will endeavour to offer a user-friendly interface based on the interpolation software supplied by the data providers. This should allow easy retrieval of data on grids defined by the users. The user interfaces will allow downloading any set of data (sub-setting and sub-sampling facilities) at single points or on a regular lat-lon grid defined by the user. Special effort will be made to provide quick access to long series of data at a single point, as this is a frequent request from all application-oriented users. Automatic regular requests will also be possible. In Phase 1, each Archive Centre will provide data through a different user interface. However, the data supplied by different Archive Centre should be the same. In Phase 2, the user interface should be unified.

4. ACCESS TO TIGGE DATA

Data providers will supply their products to the Archive Centres under an agreed set of rules, which include re-distribution rights. Access will be provided for Research & Education through a simple electronic registration process, with valid e-mail address and acknowledgment of conditions of supply. Under the simple registration process, access will be given with a delay (48 hours) after initial time of the forecast (reference time of data in GRIB2). Real-time access will be granted in some cases, e.g. for field experiments and projects of special interest to THORPEX. Registration for real-time access will be handled via the THORPEX IPO.

Acknowledgements: *The TIGGE-WG is composed of representatives from the forecasting centres and of the academic community and has hold several meetings to agree the formats and the content of the initial archive. The IT teams at ECMWF, NCAR and CMA have invested considerable work to initiate the routine exchange and accumulation of data in good technical conditions. Beaudouin Raoult is especially acknowledged for his contribution to the project.*

MEDIUM-RANGE ENSEMBLE FORECASTS AT THE MET OFFICE

Richard Swinbank

Met Office, Exeter, U.K.
E-mail: *richard.swinbank@metoffice.gov.uk*

Abstract: The Met Office has recently implemented a 24-member global ensemble forecast extending to 15 days. This is an extended-range version of the Met Office Global and Regional Ensemble Prediction System (MOGREPS), originally developed for short-range forecasts over the UK and Europe. The medium-range forecasts are being stored in the TIGGE archive, and will be used to develop techniques for multi-model ensemble forecasting. This paper describes early results from our global medium-range ensemble forecasts and outlines our plans for future THORPEX research.

Keywords – *Ensemble forecasts, medium-range forecasts, TIGGE, THORPEX*

1. INTRODUCTION

As a major part of our contribution to THORPEX, the Met Office has recently implemented regular medium-range global ensemble forecasts. The medium-range ensemble forecast system is based on the Met Office Global and Regional Ensemble Prediction System (MOGREPS). MOGREPS comprises a regional model (covering the North Atlantic and Europe) with boundary conditions taken from global ensemble forecasts. The 24-member ensemble forecasts are run twice daily. Perturbations to the initial conditions are generated using an Ensemble Transform Kalman Filter (ETKF) method (Bowler, 2006). For the medium-range ensemble forecasts, the global component of MOGREPS has been extended to 15 days. Output from the medium-range forecasts is being stored in the THORPEX Interactive Grand Global Ensemble (TIGGE) archive database.

A key benefit of this research is the prospect of improving the forecasting of high-impact weather and the risks associated with it. In addition, the Met Office is continuing to develop techniques for observation targeting based on output from the ensemble forecasts.

2. ENSEMBLE FORECAST SYSTEM

For THORPEX, the global forecast component of the MOGREPS system has been ported to the ECMWF supercomputer. The global Unified Model is run at a horizontal resolution of 0.83° latitude by 1.25° longitude, with 38 levels. When originally implemented in late March 2006, the physical parameterizations were similar to those used in the global component of the short-range MOGREPS, with a limited implementation of stochastic physics. A new package of physical parameterizations has recently been evaluated (Savage et al, 2006) and will be implemented, in conjunction with compatible stochastic physics schemes, early in 2007.

Initial conditions for the ensemble forecasts are generated by the MOGREPS system at the Met Office, and transferred to ECMWF (see Figure 1). The forecast model produces the TIGGE output fields directly in GRIB format, and these are transferred to the TIGGE archive via the ECMWF MARS archive system. Other output streams are used for verification and to generate products - particularly aimed at forecasting high-impact weather, as described in section 4.

3. MULTI-MODEL ENSEMBLES

As shown in Figure 1, it is planned to combine the Met Office medium-range forecasts with forecasts from other models that will be available via the TIGGE database. Johnson (2006) has used an ensemble test-bed based on simple models to help guide the approach we will use to calibrate and combine the ensemble forecasts. Based on that work, we are currently producing an experimental bias-corrected ensemble mean combining Met Office and ECMWF forecasts. We will continue to develop techniques for multi-model ensemble forecasting, and to evaluate the benefits of a possible future operational multi-model ensemble.

4. FORECASTING HIGH-IMPACT WEATHER

Ensemble forecasts produce a vast amount of data which is hard for forecasters and end-users to interpret. In order to facilitate this process, a suite of intelligent diagnostics needs to be developed, to highlight when high-impact weather is forecast. For example, we have developed a “heat-wave” product to show when successive

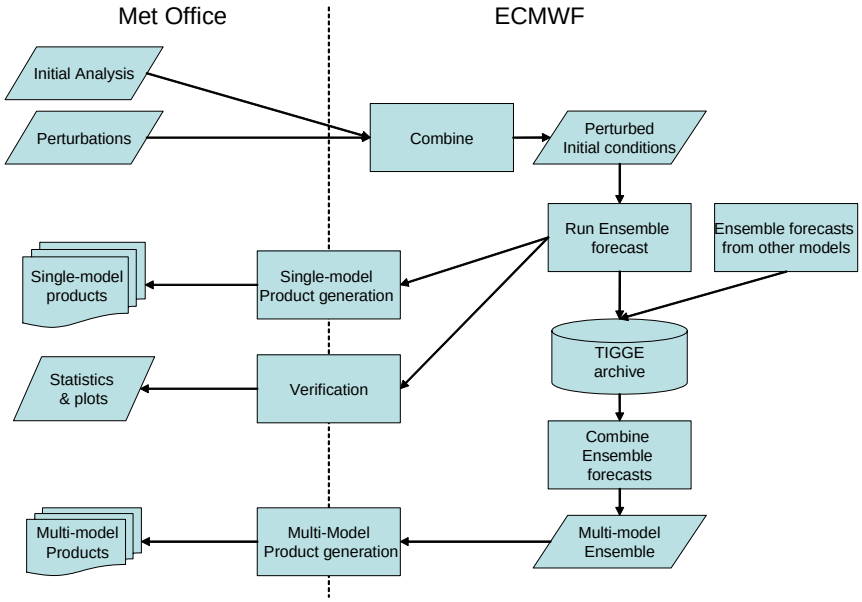

Figure 1. Schematic of the Met Office medium-range ensemble forecast system. At present experimental products and verification statistics are being produced from the single-model forecasts. Work is currently in hand on the combination of forecasts from ECMWF and the Met Office.

day-time and night-time temperatures are likely to exceed specified thresholds. Similar approaches are used to highlight persistent wet or dry periods.

Much of the high-impact weather in Europe is associated with synoptic features. At the Met Office, the ensemble forecast output is automatically analysed to identify extra-tropical cyclones and fronts, with feature-point attributes stored in a cyclone database (Watkin and Hewson, 2006). By processing this information with tailored tracking software, forecasters can be shown how each feature may develop over several days, including the potential for high-impact weather. At longer range, beyond the lifetime of features identified in the initial analysis, the cyclone database can still be used to indicate the likelihood of windstorms.

Alongside work on the forecasting of high-impact weather, we are formulating and prioritising the requirements for forecasts of the socio-economic impacts of the weather. Based on those requirements, we will be developing models to estimate weather impacts based on the ensemble forecast output.

5. OBSERVATION TARGETING

Where diagnostic techniques have highlighted the possibility of severe weather events, observation targeting might be used to reduce uncertainties in the forecast. The Met Office observation targeting system (Bovis, 2006) uses an ETKF-based method to predict "sensitive areas", i.e. those areas where additional observations are expected to reduce the uncertainties in the forecast at a specified place and time. The Met Office observation targeting system was used in the 2003 ATReC experiment (Petersen, 2006), and will also be used to support the planned GFDex and ETReC campaigns in 2007. It will be a component of the Eurorisk-PREVIEW data targeting system, which will be evaluated in an 11-month trial, covering most of 2008.

Acknowledgements: *Kelvyn Robertson and Simon Thompson set up the ensemble forecast suite at ECMWF, and implemented the TIGGE output. I would like to thank the THORPEX project team and many other Met Office scientists for their contributions, and ECMWF for their support.*

REFERENCES

Bovis, K., 2006: Observation targeting using the Met Office Global and Regional Ensemble Prediction System (this volume).
Bowler, N., 2006: Performance of the local ETKF in the Met Office global ensemble (this volume).
Johnson, C., 2006: Combination and calibration of an idealised multi-model ensemble (this volume).
Petersen, G.N., 2006: The impact of A-TReC targeted observations on weather forecasts, applying the UK Met Office forecasting system (this volume)
Savage, N, et al, 2006: Evaluating model errors and predictability in Met Office THORPEX forecasts (this volume)
Watkin. H and T. Hewson, 2006: The development of feature-based diagnostics to assess TIGGE handling of high-impact extra-tropical cyclones (this volume).

Daily Forecast Skill of Multi-Center Grand Ensemble

Mio Matsueda[1], Masayuki Kyouda[2], H. L. Tanaka[3] and Tadashi Tsuyuki[2]

1: Graduate School of Life and Environmental Sciences, University of Tsukuba, Japan
2: Numerical Prediction Division, Japan Meteorological Agency, Japan
3: Center for Computational Sciences, University of Tsukuba, Japan
E-mail: s025304@ipe.tsukuba.ac.jp

Abstract: In this study, we investigated the daily forecast skill of Multi-Center Grand Ensemble (MCGE), consisting of three operational medium-range ensemble forecast data by the Japan Meteorological Agency (JMA), the National Centers for Environmental Prediction (NCEP), and the Canadian Meteorological Center (CMC). The forecast skill was evaluated by RMSE for Z500 over the NH (20°N–90°N) from August 2005 to February 2006. It is found that the effects of multi-model and increasing ensemble size appear in daily score. When RMSE of a single-center ensemble is extremely large, namely a Hight-Impact weather (HIW) occurs, MCGE can avoids being worst score by the effects of multi-model and increasing ensemble size. These effects result from the fact that a certain single-center ensemble is not always most skillful. MCGE contains various possibilities on a HIW. This leads to the avoidance of the worst score of ensemble mean. Also this might lead to the useful probabilistic information on a HIW.

Keywords *– TIGGE, multi-model ensemble, operational ensemble forecast, medium-range forecast*

1. Introduction

Matsueda et al. (2006) constructed the Multi-Center Grand Ensemble (MCGE) forecast, consisting of three operational ensemble forecast data by JMA, NCEP, and CMC, on a quasi-operational level. They have reveal that MCGE forecasts are more skillful than single-center ensemble forecast without weight among ensemble members and bias corrections using monthly deterministic and probabilistic scores, such as Anomaly Correlation (AC), Root Mean Square Error (RMSE), and Brier Skill Score (BSS) for Z500 and T850 over the NH (20°N–90°N) in September 2005. However, their verifications are only for particular month and they didn't discuss on daily forecast skill of MCGE and single-center ensembles.

The purpose of this study is to investigate the daily forecast skill of MCGE in comparison with that of single-center ensembles using RMSE for Z500 over the NH (20°N–90°N) from August 2005 to February 2006. It is imagined easily that the variabilities of forecast skills cased by a HIW, such as blocking, appear more clearly in the daily verification than the monthly verification.

2. Data and Methodology

Medium-Range ensemble forecast data from three operational centers, JMA, NCEP and CMC, are used. The ensemble sizes of JMA, NCEP, and CMC are 25 (25), 44 (11), and 17 (17) per day (run), respectively, as of February 2006. RMSE was calculated for Z500 over the NH (20°N–90°N) from August 2005 to February 2006. Forecast and analysis fields have been interpolated onto a common regular 2.5° × 2.5° grid, and each single-center ensemble has been verified against its own analysis, that is, each control run at initial time is regarded as each analysis. JMA analysis has been adopted as the analysis for verification of MCGE.

Following Matsueda et. al. (2006), we have constructed four ensemble mean forecasts, that is, JMA25, NCEP11, CMC17, and MCGEs (J9N8C8 and J25N44C17) using above three ensembles. JMA25, NCEP11, and CMC17 consist of ensemble members of each EPS initialized at 12 UTC, 12 UTC, and 00 UTC, respectively. J9N8C8, whose ensemble size is same as JMA25, contains JMA ensemble control run, 4 perturbation pairs of JMA, 4 perturbation pairs of NCEP starting from 12 UTC, and 4 perturbation pairs of CMC starting from 00 UTC without weight among ensemble members and bias corrections. J25N44C17 has the maximum ensemble size, namely 86. Initial time of MCGE forecasts is set to 12 UTC.

3. Results

Figure 1 illustrates a scatter diagram of the RMSE of JMA25 versus MCGE improvement rate (MIR) of RMSE for Z500 at 120 hr lead time during period from August 2005 to February 2006. The horizontal axis is the RMSE of JMA25. The vertical axis is MIR defined as $(\mathrm{RMSE}_{\mathrm{JMA25}}\text{-}\mathrm{RMSE}_{\mathrm{J9N8C8}})/\mathrm{RMSE}_{\mathrm{JMA25}}$. The positive (negative) MIR indicates J9N8C8 (JMA25) is more skillful than JMA25 (J9N8C8). MIR becomes zero (0.0) only when RMSE of J9N8C8 is equivalent to that of JMA25, whereas MIR becomes one (1.0) only when RMSE of J9N8C8 is zero (0.0). The white and black circles indicate the verification period from August 2005 to October 2005 (ASON) and that from November 2005 to February 2006 (DJF), respectively.

It is found in Fig. 1 that the frequencies that J9N8C8 is more skillful than JMA25 are 76.5% and 75.0% in ASON and DJF, respectively. This indicates that the effect of multi-model appear in the daily scores. The maximum (minimum) MIRs are 0.28 (-0.08) and 0.18 (-0.15) in ASON and DJF, respectively. In each seasons, the range of positive MIR is comparable without relation to the magnitude of RMSE. This indicates that whether it is an easily-predictable atmospheric field or not, we can obtain a similar MIR. Also, it is noted that when the RMSE of JMA25 is large, MIR tends not to be negative, especially in DJF. When the RMSE of JMA25 is large, RMSEs of another single-center ensemble is not always large (not shown). A certain single-center ensemble is not always most skillful (not shown). Therefore, we can reduce the uncertainty of model, initial value, and so on by replacement of other single-center members by JMA members. It must be noted here that although of course MCGE does not have the worst forecast skill, MCGE does not always have the best forecast skill. This can be expected from Fig. 2.

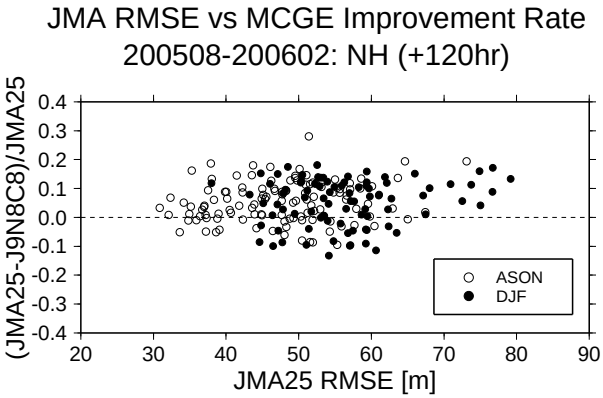

Fig. 1 The scatter diagram of the RMSE of JMA25 versus MCGE improvement rate of RMSE for Z500 at 120 hr lead time from August 2005 to February 2006. The white and black circles indicate the initial time during ASON and DJF, respectively.

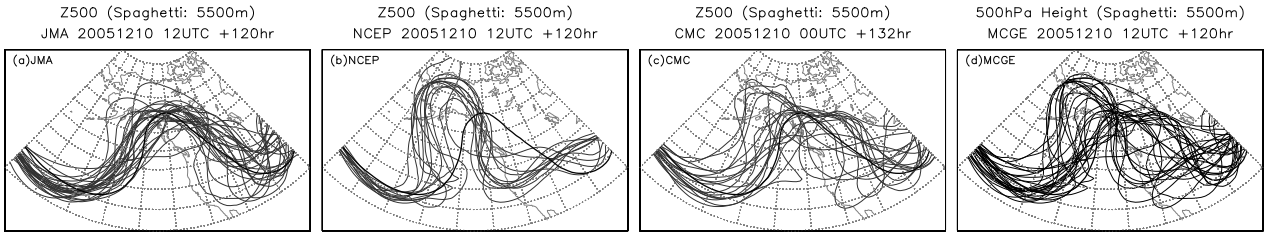

Fig. 2 The Z500 spaghetti diagrams (5500 m) for (a) JMA 120 hr forecast, (b) NCEP 120 hr forecast, and (c) CMC 132 hr forecast initialized on 10th December 2005, and that for (d) MCGE (J9N8C8), valid 12 UTC on 15th December (thin solid line for each ensemble member, thick solid line for JMA analysis at the valid time).

Figure 2 illustrates the spaghetti diagrams (5500m) for (a) JMA, (b) NCEP, and (c) CMC from 00 UTC (CMC) or 12 UTC (JMA and NCEP) on 10th December 2005, and that for (d) MCGE (J9N8C8), valid 12UTC on 15th December. Blocking occurred at the upstream of the Rocky Mountains. All of NCEP ensemble members predicted the wrong locations of the blocking, whereas JMA ensemble members initialized at 12 UTC on 10th December and most of CMC ensemble members predicted the right locations of the blocking. The difference between RMSE of NCEP11 and that of JMA25 is about 30 m. Constructing MCGE by using them, MCGE is less skillful than the best single-center ensemble, namely JMA25, but more skillful than the worst single-center ensemble, namely NCEP11. Precisely because we cannot know that which ensemble member captures a HIW correctly on ahead, it seems to be appropriate to construct MCGE instead of single-center ensemble. It is found from Fig. 2 (d) that MCGE contains various possibilities on a HIW scenario. MCGE might enable us to get a helpful measure of probabilistic information on a HIW in the daily use.

Although it seems to be natural to consider how superior is J25N44C17, which has maximum ensemble size, to JMA25 in operational use of MCGE, the effect of increasing ensemble size, shown in Matsueda et al. (2006), is seen in the daily forecast skill. The frequencies that J25N44C17 is more skillful than JMA25 are 84.9% and 80.7% in ASON and DJF, respectively (not shown).

5. Conclusions

We investigated the daily forecast skill of MCGE, consisting of three operational medium-range ensemble forecast data by JMA, NCEP and CMC, using RMSE for Z500 over the NH (20°N–90°N) from August 2005 to February 2006.

It is found that the effects of multi-model and increasing ensemble size appear in the daily score, same as in the monthly score. The win rates of J8N8C8 (J25N44C17) to JMA25 at 120 hr lead time are 76.5% (84.9%) and 75.0% (80.7%) during ASON and DJF, respectively. When RMSE of a single-center ensemble is extremely large, namely a HIW occurs, MCGE can avoids being worst score by the effects of multi-model and increasing ensemble size. These effects result from the fact that a certain single-center ensemble is not always most skillful. MCGE contains various possibilities on a HIW. This leads to the avoidance of the worst score of ensemble mean. Also this might lead to the useful probabilistic information on a HIW.

Acknowledgments: This work could not have been done without the operational ensemble data of NCEP and CMC. We are especially thankful to NCEP and CMC. A part of the research support comes from Grant-in-Aids (18204043) of the Japan Society for Promotion of Science.

References

Matsueda M., M. Kyouda, H.L. Tanaka and T. Tsuyuki, 2006: Multi-Center Grand Ensemble using three operational ensemble forecasts. *SOLA*, **2**, 33–36.

ORGANIZED TROPICAL CONVECTION AND WEATHER PREDICTION ON SUB-SEASONAL TIME-SCALES

Frederic Vitart [1], Jan Barkmeijer [2]
[1] ECMWF, Reading, UK
[2] KNMI, De Bilt, The Netherlands
E-mail: nec@ecmwf.int, *jan.barkmeijer@knmi.nl*

Abstract:

Keywords – *Madden Julian Oscillation, stratospheric sudden warming, monthly forecasting*

1. INTRODUCTION

A Thorpex interest group (IG2/IG10) has been set up in order to discuss issues relative to sub-seasonal time scales. Two major sources of predictability in the sub-seasonal time scale are the Madden-Julian Oscillation and stratospheric initial conditions. Therefore, most of the discussions within the group have focused on those two topics.

2. The Madden-Julian Oscillation

The Madden-Julian oscillation (MJO) is the dominant mode of variability in the Tropics on time scales exceeding one week and less than a season. It has a significant impact on the Indian and Australian monsoons, on the onset and development of an El-Nino event, and tropical cyclogenesis over the eastern Pacific and the Atlantic basin. Some studies (for example Ferranti et al, 1990) have also provided evidence that the MJO has a significant impact in the extratropics in the sub-seasonal time-scale. Recent studies have shown also an impact on precipitation over Mexico, and China. A. Donald et al (2006) have shown the MJO can influence daily rainfall patterns, even at high latitudes, via teleconnections with broadscale mean sea level pressure (MSLP) patterns. A study by T. Jung (personal communication) also highights a significant impact of the MJO on the 500 hPa geopotential hight in the extratropics.

It is therefore important for the operational monthly forecasting systems to be able to predict the evolution of an MJO event. It is not clear what is the theoretical limit of predictability of the Madden-Julian Oscillation, but statistical predictive models of the MJO display useful predictive skill out to at least 15-20 days lead time (see for example Wheeler 2001). The skill of NWP models is often less than that of statistical prediction techniques. Climate models have also generally a poor representation of the Madden-Julian Oscillation (Slingo, 1996). However, a recent study by Woolnough et al (2006) found that an improved representation of the mixing in the upper ocean, by using a high vertical resolution mixed-layer model, produced an improvement in the MJO forecast, particularly for the phases of the MJO where the convection is active over the Indian Ocean or West Pacific. Vitart et al (2006) have shown that a version of the ECMWF atmospheric model (IFS) coupled to an oceanic-mixed layer model had a predictive skill comparable to current statistical methods.

3. Impact of stratospheric initial conditions

There seems to be consensus about the possibility to improve sub-seasonal forecasting of the tropospheric circulation by using knowledge of the stratospheric circulation (Christiansen, 2005; Charlton et al., 2003). In fact it is found that the best statistical forecasts are obtained when using (lower) stratospheric predictors as opposed to tropospheric predictors. Further, these statistical forecasts perform as well as state-of-the art dynamical seasonal forecast models.

By now there is observational and numerical evidence that stratospheric events often precede tropospheric events, e.g., the Northern Annular Mode configuration. Interestingly, it also seems the case that stratospheric events in their turn may be preceded by a certain preconditioning of the stratospheric or tropospheric circulation (Black and McDaniel, 2006). Improving our understanding of this process will have consequences for sub-seasonal prediction.

There was some concern that NWP models continue to have difficulties in accurately representing the general behaviour of intraseasonal low frequency variability (including blocking events). Models may even show the right statistical behaviour for the wrong physical reasons (Robinson and Black, 2005).

The strong 2006 Stratospheric Sudden Warming (SSW) lead to some discussion. Results of the ECMWF monthly forecasting system showed large differences in ensemble spread from one week to another. Especially, the collapse of the ensemble spread during the maturing phase of the SSW was a striking feature. More or less the same behaviour can be inferred from the JMA ensemble (Mukougawa, personal communication). The apparent change in sensitivity of the stratospheric initial condition during the SSW can not be concluded from singular vector computation for the stratospheric circulation during this period.

REFERENCES

Black, R.X., B.A. McDaniel, and W.A. Robinson, 2006: Stratosphere-Troposphere coupling during Spring onset. J. Climate, 19, 4891-4901.

Charlton, A.J., A. O'Neill, D.B. Stephenson , W.A. Lahoz , and M.P. Baldwin, 2003: Can knowledge of the state of the stratosphere be used to improve statistical forecasts of the troposphere? Quart. J. Roy. Meteor., 129, 3205-3224.

Christiansen, B., 2005: Downward propagation and statistical forecast of the near surface weather. J. Geophys. Res. , 110, D14104.

Donal, A., H. Meinke, B. Power, A. de H.N. Maia, M.C. Wheeler, N. White, R.C. Stone and J. Ribbe, 2006: Near-global impact of the Madden-Julian oscillation on rainfall.

Ferranti, L. , T. N. Palmer, F. Molteni and E. Klinker, 1990: Tropical-extratropical interaction associated with the 30-60 day oscillation and its impact on medium and extended range prediction.

Robinson, D.P., and R.X. Black, 2005: The statistics and structure of subseasonal variability in NASA/GSFC GCM's. J. Climate, 18, 3294-3316.

Slingo, J. and coauthors, 1996: Intraseasonal oscillations in 15 atmospheric general circulation models: Results from an AMIP diagnostic subproject. Clim. Dyn., 12,325-357.

Vitart, F., S. Woolnough, M.A. Balmaseda and A. Tompkins, 2006: Monthly forecast of the Madden-Julian Oscillation using a coupled GCM. Monthly Weather Review, in press.

Woolnough, S. J., F. Vitart and M. A, Balmaseda, 2006: The role of the ocean in the Madden-Julian Oscillation: Sensitivity of an MJO forecast to ocean coupling. Quart. J. Roy. Meteor. Soc., in press.

THE IMPACT OF EXTRATROPICAL TRANSITION ON THE DOWNSTREAM MIDLATITUDE PREDICTABILITY

Patrick Harr[1], Sarah Jones[2]

[1] Naval Postgraduate School, Monterey, CA USA
E-mail: paharr@nps.edu
[2] Institut fur Meteorologie und Klimaforschung, Universitat Karlsruhe / Forschungszentrum Karlsruhe, Karlsruhe, Germany
E-mail: sarah.jones@imk.uka.de

Abstract: The poleward movement of a decaying tropical cyclone often results in a rapidly-moving, explosively-deepening midlatitude cyclone. The re-intensification of the decaying tropical cyclone as an extratropical cyclone depends on the phasing between the remnant tropical circulation and a midlatitude environment that is favorable for midlatitude cyclogenesis. Furthermore, the extratropical transition of a tropical cyclone may result in excitation and dispersion of Rossby waves that have far-reaching impacts on downstream atmospheric conditions. Therefore, the midlatitude flow patterns may be perturbed across individual ocean basins with the potential for nearly hemispheric-scale impacts.

Keywords *– Tropical cyclones, extratropical transition, Rossby waves, ensemble prediction systems*

1. INTRODUCTION

The poleward movement and extratropical transition (ET) of a tropical cyclone (TC) initiates complex interactions with the midlatitude environment that often results in a high-impact midlatitude weather system with strong winds, high seas, and large amounts of precipitation. Although these extreme conditions severely impact the region of the ET, there are significant impacts downstream of the ET event due to the excitation of large-scale propagating Rossby wave-like disturbances (Fig. 1). The occurrence of ET events has been observed to coincide with periods of reduced forecast model skill (Jones et al. 2003). During September 2005 (Fig. 2), the ET of several tropical cyclones over the North Pacific and North Atlantic basins resulted in periods of reduced skill in the Global Forecast System (GFS) of the National Centers for Environmental Prediction (NCEP) and the Navy Operational Global Atmospheric Prediction System (NOGAPS). Based on this type of impact, the THORPEX Working Group on Predictability and Dynamical Processes established Interest Group Four on The Impact of Extratropical Transition on Downstream Midlatitude Predictability.

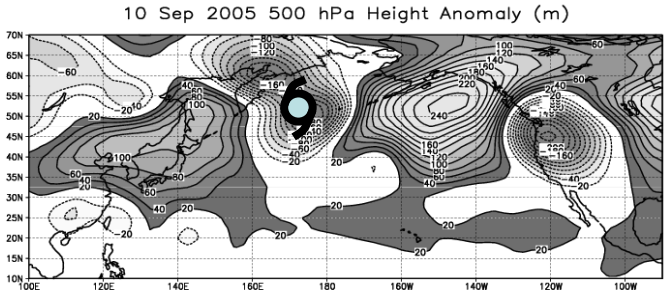

Figure 1. Height anomalies (m, positive contours are shaded) at 500 hPa for 0000 UTC 10 September 2005 computed as a departure from the mean 0000 UTC 10 September values derived from the NCEP/NCAR reanalysis. The location of the cyclone that developed from the extratropical transition of TY Nabi is marked by the tropical cyclone symbol.

2. KEY ISSUES

The primary scientific issues associated with ET and downstream impacts due to ET events may be placed in a framework of mechanisms, predictability, and strategies for increasing predictability. The ET process may be characterized by complex physical mechanisms associated with the decaying TC core, developing regions of low-level frontogenesis, and upper-level outflow into a midlatitude jet streak. To understand the impact of ET on the predictability of high-impact downstream weather events, mechanisms responsible for the generation, intensification, and propagation of the Rossby wave-like disturbances during ET need to be identified. Several aspects of the ET process likely play important roles in the mechanisms responsible for generation of downstream impacts. The impact of the ET event on downstream predictability may be examined in the context

of increased standard deviation in mid-tropospheric heights among ensemble members generated with an operational global ensemble prediction system (Fig. 3). The complex physical and dynamical processes

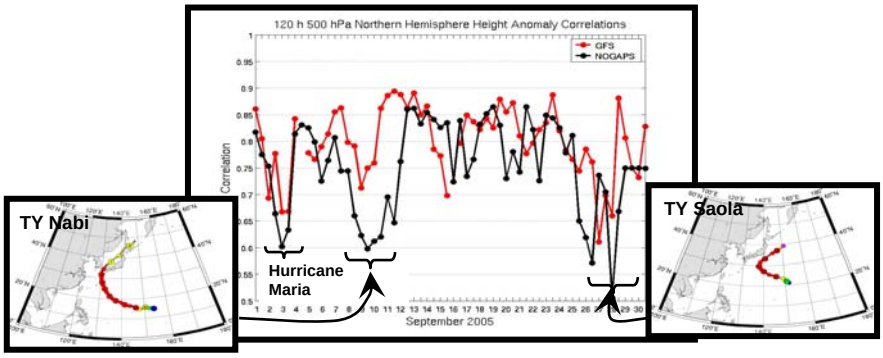

Figure 2. Height anomaly correlations over the Northern Hemisphere for 120-h forecasts from the GFS and NOGAPS models during September 2005. Periods of low correlation values that coincide with the ET of tropical cyclones are labeled. Tropical cyclone track figures courtesy of http://agora.ex.nii.ac.jp/digital-typhoon/.

during ET are extremely sensitive to sources and impacts of initial condition errors and forecast model uncertainty. Therefore, factors that impact forecast model error growth downstream of an ET event must be identified. For example, predictability during an ET event may exhibit large variations due to the phasing between the decaying tropical cyclone and the midlatitude circulation (Klein et al. 2002).

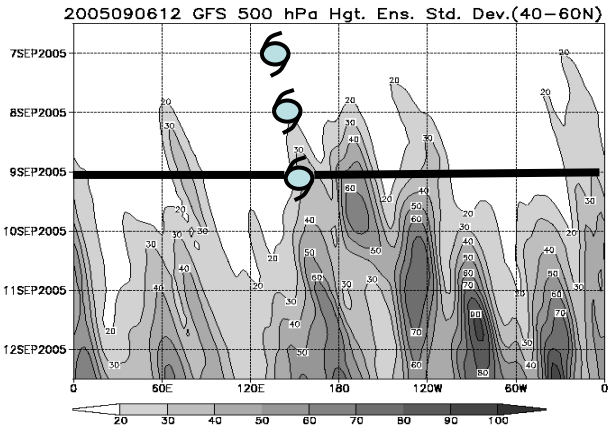

Figure 3. Time-longitude plot of 500 hPa height standard deviation (m) for the GFS ensemble prediction system members initialized at 1200 UTC 6 September 2005. The standard deviation is averaged between 40°N – 60°N. Beginning at 0000 UTC 7 September, which was the recurvature time, the tropical cyclone symbols mark the longitude of TY Nabi. The thick black line at 0000 UTC 9 September marks the time that TY Nabi was extratropical.

3. SUMMARY

In summary, the impacts of an ET event over the western North Pacific may be fast spreading, far reaching, and associated with reduced predictability. A comprehensive program of study is required such that increased understanding of mechanisms responsible for the generation and variation of downstream effects is related to an increase in predictability via improved sampling strategies, data assimilation techniques, and ensemble systems.

Acknowledgements: *Support of the Office of Naval Research, Marine Meteorology Program is acknowledged. The first author also acknowledges support from the World Meteorological Organization.*

REFERENCES

Jones, S. C., and Co-authors,2003: The extratropical transition of tropical cyclones: Forecast challenges, current understanding and future directions. *Wea. Forecasting*, **18**, 1052-1092.

Klein, P. M., P. A. Harr, and R. L. Elsberry, 2002: Extratropical transition of western North Pacific tropical cyclones: Midlatitude and tropical cyclone contributions to reintensification. *Mon. Wea. Rev.*, **130**, 2240-2259.

AMMA AND ASPECTS OF TROPICAL–EXTRATROPICAL INTERACTIONS (PDP WG INTEREST GROUP 9)

Peter Knippertz [1], Sarah Jones

[1] Institute of Atmospheric Physics, University of Mainz, D-55099 Mainz, Germany
E-mail: *knippertz@uni-mainz.de*

Abstract: This paper provides a short overview of the research questions discussed in the interest group 9 (IG9) within the THORPEX working group on Predictability and Dynamical Processes (PDP WG).

Keywords – *THORPEX, PDP WG, IG9, AMMA, West African monsoon, Tropical–extratropical interactions*

1. INTRODUCTION

The WMO/WWRP research programme THORPEX working group on Predictability and Dynamical Processes (PDP WG) has set up interest groups (IGs) to promote THORPEX research for particular subject areas. IG9 is entitled “AMMA and aspects of tropical-extratropical interactions”. AMMA stands for “African Monsoon Multidisciplinary Analysis” and is an international science project funded through various agencies in Africa, Europe and North America. IG9 will consider different aspects of the West African Monsoon and tropical-extratropical interactions on synoptic time scales. Excluded from this are questions directly related to tropical cyclogenesis and to extratropical transition that are covered by IGs 3 and 4.

The first milestone of the IG is a compilation of a summary of the current state of knowledge and key open questions. It will be part of an overview document with the working title "Priority issues for research on predictability and dynamical processes in THORPEX" that serves as a white paper for WWRP/THORPEX PDP research. This document will be finalized shortly after the Second THORPEX International Science Symposium (STISS) in Landshut, 4.–8. December 2006. In order to get an as broad as possible overview over current research we contacted a number of colleagues and asked them to (a) forward information about the IG and its goals to other interested researchers, (b) contribute references to relevant published and unpublished work, (c) write short summary texts to be included in the summary document and (d) send diagrams to be shown in the oral presentation at the STISS. The IG is open to everyone, and discussion and exchange of ideas are facilitated through an automated mailing system operated through the National Center for Atmospheric Research (NCAR) in Boulder (http://mailman.ucar.edu/mailman/listinfo/thorpex-pdp-ig9).

2. LIST OF OPEN QUESTIONS

The following questions serve as guidelines to structure the input from the IG.

(9.1a) How well do we understand the influence of Rossby waves propagating into the Tropics on convection over Africa?

Keywords: Inertial instability, dry intrusions, heat low

(9.1b) How well do we understand the dynamics and predictability of high-impact weather in the subtropics in relation to tropical–extratropical interactions?

Keywords: Heavy precipitation, static stability, dynamic lifting, dust storms

(9.2) How well do we understand the excitation of Rossby-wave trains by African convection?

Keywords: Barotropic modelling, Rossby wave source, waveguides

(9.3) How well do we understand the dynamics and the predictability of the West African Monsoon?

Keywords: Onset, break cycles, heat low dynamics, African Easterly Waves, convection

(9.4) What are the relative roles of initial condition error and model uncertainty over Africa?

Keywords: convection, surface exchange, soil moisture, aerosol (biomass burning/mineral dust), AMMA dry run

(9.5) What are the prospects for ensemble forecasting for Africa?

Keywords: Evaluation, appropriate initial perturbations

(9.6) How well do we understand and can global models represent moisture transport from the Tropics into mid-latitudes?

Keywords: Moisture conveyor belt, atmospheric rivers, tropical waves

3. CONCLUDING REMARKS

Even after the STISS in Landshut everybody is invited to join IG9 by registering at the NCAR-hosted site http://mailman.ucar.edu/mailman/listinfo/thorpex-pdp-ig9. All previous discussion will be available to read on this webpage and input to upcoming draft documents will still be possible and certainly appreciated.

Catarina Cyclone: a hurricane-like cyclone over South Atlantic

Manoel Alonso Gan[1], Everson Dal Piva[2], Vadlamudi Brahamananda Rao[1]
[1] Instituto Nacional de Pesquisas Espaciais – INPE, Centro de Previsão de Tempo e Estudos Climáticos – CPTEC São José dos Campos, SP – Brazil - E-mail: alonso@cptec.inpe.br.
[2] Universidade Federal de Santa Maria – Rio Grande do Sul - Brazil

Abstract: The Catarina cyclone was the first one of its kind in South Atlantic that had characteristics of a hurricane category 1 during its mature phase. It developed in the subtropical latitudes of the South Atlantic in the end of March 2004 close to the core of an occluded extratropical cyclone. The aim of this study is to identity the main atmospheric characteristics and the dynamic processes associated with the evolution of this system. An observational analysis and numerical simulations of the evolution of the Catarina will be presented. The NCEP analysis for 1° latitude x 1° longitude and the BRAMS model are utilized in this study. The preliminary results show that the Catarina cyclone developed in the head of inverted coma cloud and propagated to west during its intensification phase. The interaction of the cyclonic circulation with the warm waters associated with the Brazilian oceanic current was important to the intensification and the atypical displacement to west of this cyclone. In the control experiment the model underestimated the intensity of the cyclone because the Sea Surface Temperature (SST) did not represent well the Brazilian oceanic current. The importance of the surface heat fluxes in the evolution of the Catarina cyclone is also discussed.

Keywords – Catarina Cyclone, tropical cyclone, surface fluxes

1. INTRODUCTION

The Southern Brazil region is normally affected by intense extratropical cyclones, mainly during the period from May to September. When extratropical cyclones move from the cold continent to the ocean water relatively warm they intensify contributing to intense precipitation, strong winds and high ocean waves in the coast of this region (Piva, 2001). However, an atypical situation occurred at the end of March 2004, when a cyclone developed in the subtropical latitudes of South Atlantic, which during its intensification phase had a displacement to west, and in its mature phase acquired characteristic of a tropical cyclone of category 1 or a weak of category 2 according to the Saffir/Simpson scale (Simpson, 1974).

When the Catarina cyclone approached the continent (between 27th and 28th of March 2004), the southern Brazil, mainly to the south of Santa Catarina State and the north of Rio Grande do Sul, was affected by intense rains and gusty winds that scared the population and caused immense damages such as: destroyed the house roofs, interdicted roads, trees overthrown over cars and houses, and oceanic waves of five meters height reached the coast of this region. The damages also occurred in agriculture, with losses in the rice (25%), maize (90%) and banana (90%) culture. According to Santa Catarina civil defense, 23 cities were affected; where 33,165 people lost their houses, and 40,012 constructions were damaged, beyond the register of 4 deaths and 7 sailors remained disappeared.

As the Catarina was the first cyclone with hurricane characteristics observed over South Atlantic Ocean and affected the Southern Brazil coast, the aim of this study is to identity the main atmospheric characteristics and the dynamic processes associated with the evolution of this system.

2. DATA AND METHODOLOGY

In this study we use Infrared GOES satellite picture and the NCEP numerical analyses. for the period from 20th to 28th of March 2004. The BRAMS 3.2 is model used and it is a version 5.04 of RAMS with emphasis in the tropics (Fazenda et al., 2006). We run it with two grids, one with 40 km and the other with 8km. The SST used was the week by mean. The experiments were the control (CONT), TSM field plus 2°C (T2) and without surface heat fluxes (WSHF).

3. OBSERVATIONAL ANALISIS

The origin of this system must be studied since 8 days before the Catarina cyclone hit the Brazilian coast, when along of an intense cold front over South Atlantic, a cyclone developed around 20°S. On 23th of March, the cloudiness associated with this cyclone showed that it was in dissipation phase. But during this day (at 1500 UTC), close to the cyclone center an inverted comma cloud developed. Twelve hours later this cloudiness disorganized, but few hours later a new inverted comma cloud developed embedded in a baroclinic environment. During the next twelve hours, the cloudiness around the head of the inverted comma cloud got the shape of a tropical cyclone type 1, having an eye in the cloudiness center. On day 26th at 1500 UTC the spiral form of the cloudiness was well identified in the satellite picture. At this moment, the cyclone gathered speed to west, what contributed for its approaching to the coast of Santa Catarina and Rio Grande do Sul states on 27th of

March. On the next day, over the continent, the cyclone weakened. Then we can see that the evolution of the Catarina Cyclone has similarities characteristics of some Polar Lows and Mediterranean cyclones.

The pressure NCEP analysis shows well the cyclone position and the displacement, but less visible in the intensity. While the numerical analysis gives 1010 hPa as the pressure in the cyclone center, the observed at São Bento was so low as 974 hPa (Figure 1).

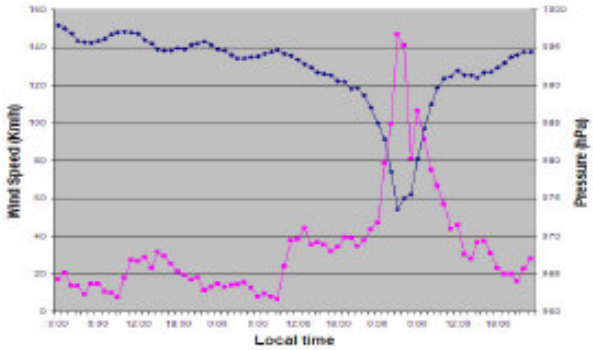

Figure 1. Time evolution of hourly measurements of pressure (in blue, right hand scale) and Wind (in red, left hand scale) from the 26th of March at 00:00 local time to 29th at 00:00 for São Bento (28°36'S, 49°33'W, 135m). From Pezza and Simmonds, 2006).

The upper level analysis shows a bifurcation of the flow over the South America on 22sd of March at 0000 UTC, having an axis trough on southern Brazil, and a ridge on the midlatitudes of South Atlantic around 35°W. The ridge in midlatitudes propagated to east and remained weak on 21st of March at 1200 UTC. The trough over southern Brazil close on 22sd of March, forming a cut-off low that practically remained stationary until the end of the month. This evolution characteristics are similar to many intense cyclones that development close to Southern Brazil coast (Piva, 2001).

4. NUMERIC SIMULATION

The CONT experiment catches the main synoptic characteristics of the Catarina, but the cyclone is not so intense as in observation data. The minimum pressure in the CONT was around 1005 hPa while in São Bento 974-hPa on 28th of March (Figure 1). The surface heat fluxes in the CONT are lower than we expect, being the sensible heat lower than 60 w/m^2 and the latent heat 350 w/m^2. This result shows that week mean SST is not so precise and the model can underestimate the surface heat fluxes and the intensity of the cyclone. Then to turn around this problem we add 2°C in the SST field (T2 experiment). In this experiment the Catarina is more intense with inner pressure around of 996-hPa on 28 March. The problem of this simulation is that the cyclone core is larger than we expect and it is far from the coast. In the WSHF experiment, the minimum pressure observe in the cyclone core was 1015-hPa on 26 March when it dissipates.

5. CONCLUSIONS

In the synoptic analysis discussed in the item previous, we can deduce that the Catarina cyclone had well defined dynamic characteristics, such as: 1) had baroclinic origin in the initial phase, 2) was cut-off of the baroclinic system in its intense phase, the 3) the heat surface flows had contributed to the intensification. Although initially the Catarina cyclone had a development close to an extratropical cyclone core, it had a dynamic support of an upper level trough and in low levels of the surface heat (sensible and latent) fluxes. The cold and dry southerly flow in the west side of the cyclone passed over hotter water associates with the South Atlantic Brazil current. The CONT experiment did not simulate well the intensity of the cyclone, but when we add 2°C in the week SST field the cyclone was simulated to be more intense but weaker than the observed. Other difference in this experiment is that the cyclone had a shorter displacement. In the WSHF the cyclone was weaker and it dissipated early.

Acknowledgments: WMO to provide financial support for the first author to participate in the STSS.

REFERENCES

Piva, E.D.: **Ciclogênese intensa sobre o sul do Brasil.** Dissertação de Mestrado. Instituto Nacional de Pesquisas Espaciais – INPE, São José dos Campos, SP. 2001.

Fazenda, A. L.; Moreira, D. S.; Enari, E. H.; Panetta, J. First time user's guide (BRAMS version 3.2). 24p. 2006.

Pezza , A.b and Simmonds, 2006. Catarina: The first hurricane and its association with vertical wind shear and high latitude blocking. In: ICSHMO, 2006, Foz Iguaçu, Brazil. P353-364. CD-ROM. ISBN 85-17-00023-4.

Simpson, R. H.: The hurricane disaster potential scale. Weatherwise, 27, 169-1186.

ON THE DETERMINATION OF TROPICAL-CYCLONE SIZE AND INTENSITY PARAMETERS

Harry Weber-Philipp

Meteorological Institute, University of Munich, Theresienstr. 37, D-80333 Munich, Germany
E-Mail: harry@meteo.physik.uni-muenchen.de

Abstract: A new model for the automatic determination of size and intensity parameters of tropical cyclones has been developed. For a given operational Dvorak estimate of maximum wind speed at any given date and time during the existence of a tropical cyclone, a consistent set of all relevant storm parameters can be computed.

Keywords – *Pressure-wind relationship, tropical cyclones, synthetic vortices, model initialization*

1. INTRODUCTION

A new model (henceforth referred to as the PW-model) for the determination of the pressure-wind relationship in tropical cyclones (TCs) has been developed on the basis of operational storm parameters such as the outermost closed isobar p_{oci} and its radius r_{oci}, the central pressure p_c or its deviation from a given environmental pressure $dp_c = p_c - (p_{oci} + 1\ hPa)$, respectively, the radius of 34-kt wind speed r_{34}, the radius of maximum wind speed r_m or the maximum wind speed v_m. For any given intensity parameter (e.g. v_m), the storm

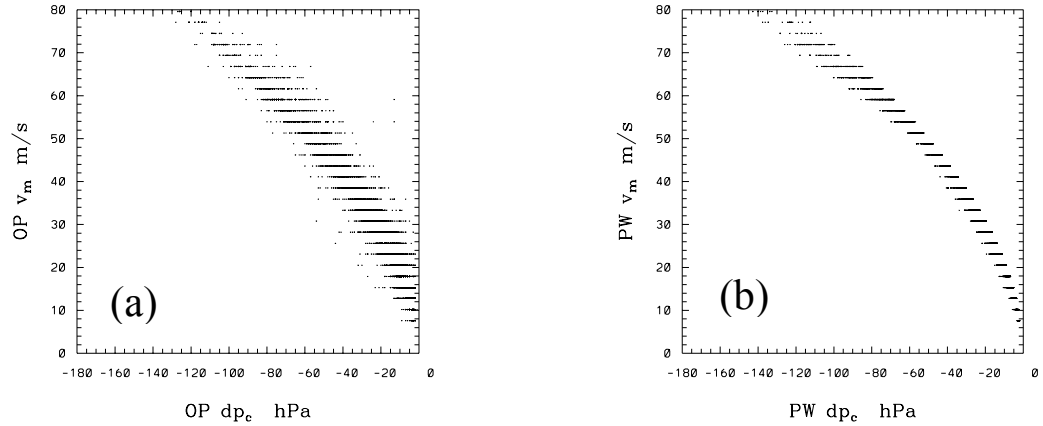

Figure 1. Pressure-wind relationship: v_m as function of dp_c of the (a) A-Decks and the (b) PW-model for all TC cases.

centre latitude and a global mean-sea-level-pressure (MSLP) analysis, the model first produces an estimate of r_{oci} and then computes a consistent set of all other storm parameters by integration of the f-plane gradient wind equation for an inertially-stable, axi-symmetric, tangential wind profile. Beside the retrieval of a complete set of TC parameters from one intensity and one size parameter, the model allows systematic insights in the general relationship between storm parameters and their range of validity. The model was developed and tested using operational advisories (A-Decks) of 11230 global TC cases 2000-2005 given by the Automated TC Forecasting System (ATCF). Results were verified against ATCF best-track data (B-Decks).

2. RESULTS

Figure 1a shows a scatter diagram of the operational estimates (OP) of v_m and dp_c during the years 2000-2005. The relatively large width of the band relating v_m to dp_c is mainly a result of the different pressure-wind relationships used at individual prediction centres to compute p_c from v_m. The same diagram of the PW-model in Fig. 1b, with r_{oci} and v_m as input, has similar characteristics but a smaller band-width that depends only on the centre latitudes of the storms. In contrast to Fig. 1a, the PW-model relation produces larger negative values of dp_c than those estimated routinely in the case of very strong storms. This agrees with the finding that the estimates of v_m in the A-Decks are, on average, 6.2 m/s higher than the corresponding values measured during aircraft missions through 176 Atlantic hurricanes 1996-2001. The operational over-estimation of v_m is suspected to be a result of the incorporation of the speed of translation of tropical cyclones during the determination of v_m.

Figure 2 shows examples of r_m and dp_c of the PW-model, as functions of the input quantities r_{oci} and v_m at a latitude of 20º N. As expected, stronger dependencies exist between r_{oci}, r_{34} (not shown) and r_m, with smaller values of r_m and r_{34} for smaller values of r_{oci}, and between dp_c and v_m. The relationships are non-linear, however, and depend also on latitude: for fixed r_{oci} and v_m, the values of r_m, r_{34} and dp_c become larger at higher latitudes. Note also that the tangential wind speed at r_{oci} (not shown) varies considerably (4-11 m/s, depending mainly on r_{oci} and latitude), emphasizing that r_{oci} cannot be regarded as a true storm size parameter.

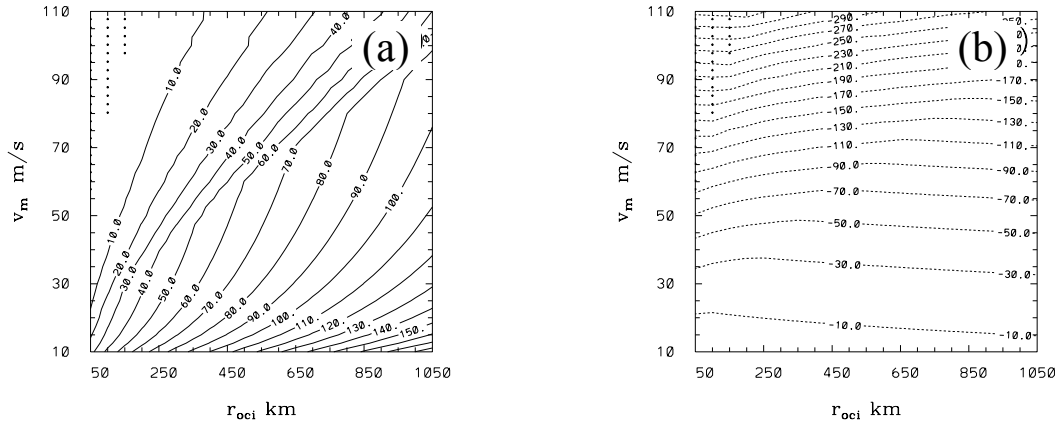

Figure 2. (a) r_m in km and (b) dp_c in hPa of the PW-model as functions of r_{oci} and v_m for a centre latitude of 20º N.

The values of r_m, r_{34} and dp_c of the PW-model agree well with those operationally-observed, as shown in Fig. 3. Mean errors (11230 cases) are –2.4 km for r_m, 22.2 km for r_{34} and 0.3 hPa for dp_c, with standard deviations of 29.3 km, 59.9 km and 5.0 hPa, respectively. In the case of very strong storms, the operational over-estimation of

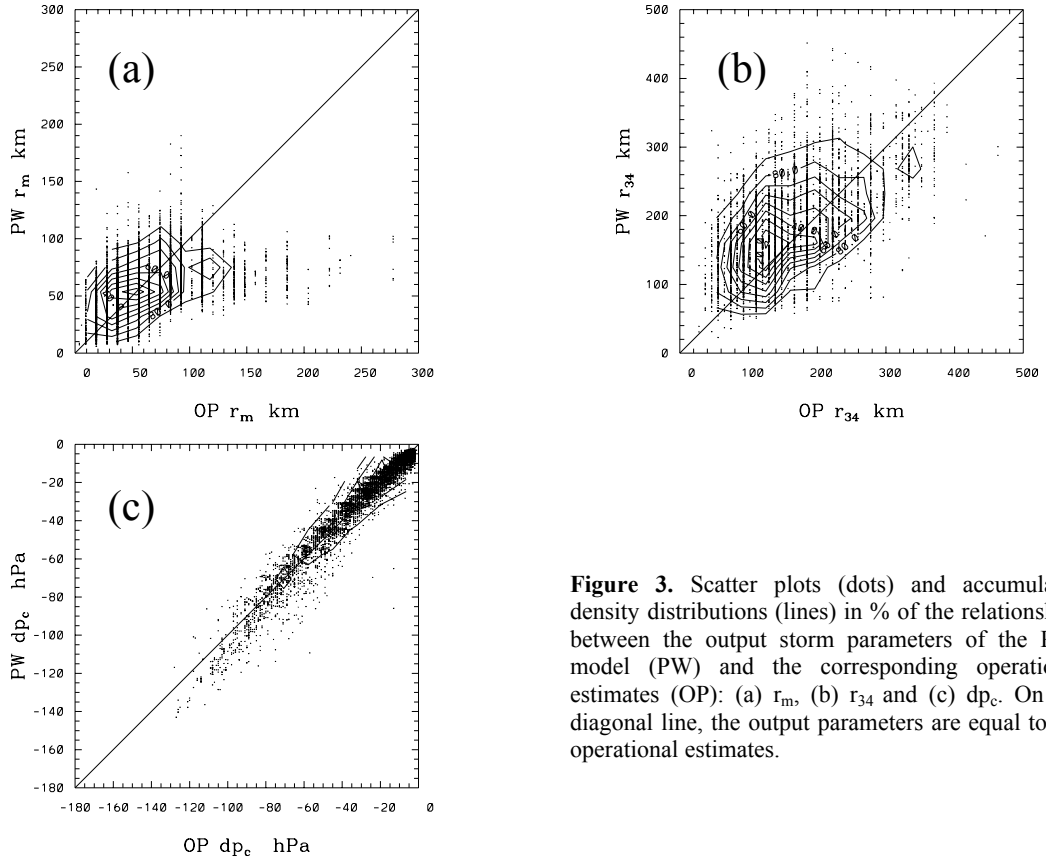

Figure 3. Scatter plots (dots) and accumulated density distributions (lines) in % of the relationships between the output storm parameters of the PW-model (PW) and the corresponding operational estimates (OP): (a) r_m, (b) r_{34} and (c) dp_c. On the diagonal line, the output parameters are equal to the operational estimates.

v_m leads to larger negative dp_c values of the PW-model relative to the operational estimates (Fig. 3c). A comparison of the tangential wind profiles of the PW-model with those measured during 176 aircraft missions through Atlantic hurricanes between 1996 and 2001 shows also good agreement. Using r_m, v_m of the mean tangential wind profile computed from all individual flight passes of one aircraft mission as input, the PW-profiles lie within an envelope defined by the profiles of all individual flight legs in about 81% of all cases analysed. Using r_{oci} and v_m of the A-Decks as input, the above percentage reduces to 55%, but still represents an astonishingly good agreement in view of the possible deviations of the operational estimates of storm structure parameters from their true values.

At present, all prediction centres use different pressure-wind relations to determine the central pressure of a given storm from the Dvorak estimate of v_m. As it is not very likely, however, that the dynamics of a tropical cyclone e. g. in the Atlantic differs from that of a storm in the Pacific, the PW-model could be used for a globally-consistent estimation of storm parameters in contrast to current operational practice. Furthermore, the quality of the results of the PW-model suggests that it could be applied to generate more realistic synthetic vortices during the initialization of numerical prediction models.

HEALTH FORECASTING IN AFRICA

David Rogers

Atmospheric Research and Environment Programme, WMO, Geneva, Switzerland
E-mail: *drogers@wmo.int*

Abstract: This paper describes progress on the development of a THORPEX demonstration project focused on improving early warning of environmentally-sensitive diseases in Africa.

Keywords – *THORPEX, AMMA, MARES, Epidemics, Malaria, Meningitis, Health, Africa, TIGGE*

1. INTRODUCTION

One of the goals of the THORPEX International Research Implementation Plan is to develop a set of demonstration projects to highlight the benefits of THORPEX in specific societal benefit areas (Rogers et al., 2005). In particular, these projects are intended to bridge the gap between developed and developing countries, transferring technical know-how on the one-hand and knowledge of user requirements on the other. Two related programmes, aimed at provided earlier and more useful warnings of impacts on agriculture and health in Africa, are in development. Their utility depends on access to real-time observations and ensemble predictions. The latter are needed on timescales from days to seasons, which requires collaboration and coordination between THORPEX and AMMA (Lebel et al. 2005), and ongoing medical programmes in Africa (e.g., Djingarey 2006). To achieve the cross-disciplinary coordination THORPEX initiated the *Health and Climate Partnership for Africa* as framework for medical practitioners and researchers, and weather and climate scientists to communicate and cooperate.

This paper briefly describes the health problem and the steps that are being taken to apply THORPEX related capabilities to help the medical community improve the timeliness of their interventions to reduce the impact of epidemics.

2. THE HEALTH PROBLEM

The leading causes of morbidity and mortality in sub-Saharan Africa are infectious diseases. Many, such as meningococcal meningitis, malaria, cholera, chikungunya, lymphatic filariasis and rift valley fever, are vector-borne and hence sensitive to weather, climate and other environmental factors. Epidemics of these diseases cause massive disruption to societies and overburden the precarious health system. Malaria, for example, causes more than one million deaths annually with over 90% of the cases occurring in sub-Saharan Africa and most afflicting children under five years of age. Any intervention strategies, including earlier warning of epidemics, must also consider that poor people are most at risk with mortality more than 39% higher in the poorest socioeconomic group than the richest (Mbizvo 2006). Furthermore the cost of malaria care may be as little as 1% of the income of the rich, but can be as much as 34% of the income of the poorest households. Thus, development of an effective health early warning system must consider the following constraints:

- Early warning must consider prevention as well as detection to enable cost effective non-medical interventions;
- Earlier detection of epidemics must enable national health services to scale up interventions in time to cope with the disaster as it unfolds, while not further straining the services beyond their human and financial limits;
- Early warning must focus on high-risk communities – the poor, those at risk because of existing health and nutrition problems, women and children, those living in non-endemic disease areas; and
- Early warning must build on the existing surveillance and monitoring systems, which are the basis for existing warnings

Although the basic associations between the environment and most weather and climate sensitive diseases are understood, these relationships are not sufficiently robust to deliver an immediate improvement in health warnings (Duchemin 2006). Further work is needed to improve biological confirmation of diseases using rapid tests and these must be related to the environmental conditions encountered at the infection sites. Better knowledge of the diseases and the disease vectors is needed to define the environmental role. Accomplishing this requires bridges to be built or reinforced between the health sectors and weather, climate and environmental communities (Duchemin 2006). Existing projects, such as the Malaria: Alerte et Résponse aux Epidémies dans le Sahel (MARES), which already bring together health and atmospheric scientists, provide an opportunity to pilot THORPEX early warning systems cost effectively (Djingarey 2006).

3. WEATHER AND CLIMATE FORECASTS

Advances in probabilistic forecasting of the weather and climate on scales of one day to a season offer new opportunities to provide more useful information about the risk of rain, droughts and dust storms, which coupled with epidemiological studies, may provide early warning of serious health impacts. Weather forecasts have direct application for the early warning of high impact events such as dust, which can trigger a meningitis epidemic or heavy rainfall, which can result in flooding or the onset of the rainy season, which will inhibit the continuance of a meningitis epidemic. Seasonal forecasts are potentially valuable for a range of health issues including disease incidence and the health impacts of food insecurity. Palmer et al. (2004) demonstrated that it is not only possible to forecast probabilities of anomalously high and low malaria incidence with dynamically-based seasonal timescale multi-model ensemble predictions of climate but that, by first establishing the evidence of the relationships of malaria epidemics to climate (Morse et al. 2005) and then tailoring this information to the specific needs of the malaria community it is possible to deliver this information into operational malaria early warning systems (Thomson et al. 2006).

Used together, weather and climate forecasting systems could provide communities with long range outlooks for planning up to 4 months ahead, short range, site specific forecasts of likely events, and near real-time assessments of the life-cycle and severity of an epidemic. Data assimilation tools also provide researchers with the possibility of extending the utility of sparse observations to improve understanding of the relationship between basic environmental parameters and the life cycles of weather and climate related diseases. The TIGGE (THORPEX Integrated Global Grande Ensemble) offers a unique opportunity to use multi-model ensemble forecasts (Richardson et al. 2005) to test the value of a probabilistic health forecasting system.

4. SUMMARY

This project brings together the skills of the THORPEX, AMMA and medical communities in West Africa to develop and test tailored forecasts in support of operational health early warning systems. The project will extend health forecasts to shorter time-scales to allow more timely interventions to reduce the threat of epidemics in high risk regions. It will establish the appropriate temporal and spatial scales at which weather and climate information can provide valuable new information to decision makers for specific health related problems – (week, month, season, decade for village, district, region), and it will improve the capacity of communities to respond to health alerts with non-medical interventions.

Acknowledgements: *The author acknowledges the contribution of many members of the Health and Climate Partnership for Africa who are actively developing and applying health forecasting systems.*

REFERENCES

Duchemin, J.B., 2006: Disease burden in West Africa. Presented at the WMO workshop on Prévoir les effets néfastes sur la santé en Afrique / Forecasting adverse health impacts in Africa, WMO, Geneva, 3-7 April 2006

Djingarey, M. H., 2006: Malaria: Alerte et Résponse aux Epidémies dans le Sahel (MARES). Presented at the WMO workshop on Prévoir les effets néfastes sur la santé en Afrique / Forecasting adverse health impacts in Africa, WMO, Geneva, 3-7 April 2006

Lebel, T., J.-L. Redelsperger, and C. Thorncroft, 2005: The International Science Plan for AMMA. 103pp. Available from http://amma.mediasfrance.org/international/documents/AMMA_ISP_Final_May2005.pdf

Mbizvo, E., 2006: Epidemics in Africa – health and social consequences. Presented at the WMO workshop on Prévoir les effets néfastes sur la santé en Afrique / Forecasting adverse health impacts in Africa, WMO, Geneva, 3-7 April 2006

Morse, A.P., F. Doblas-Reyes, M. B. Hoshen, R. Hagedorn, and T.N. Palmer, 2005: A forecast quality assessment of an end-to-end probabilistic multi-model seasonal forecast system using a malaria model, *Tellus* A, **57** (3), 464-475

Palmer, T.N., A. Alessandri, U. Andersen, P. Cantelaube, M. Davey, P. Délécluse, M. Déqué, E. Díez, F.J. Doblas-Reyes, H. Feddersen, R. Graham, S. Gualdi, J.-F. Guérémy, R. Hagedorn, M. Hoshen, N. Keenlyside, M. Latif, A. Lazar, E. Maisonnave, V. Marletto, A. P. Morse, B. Orfila, P. Rogel, J.-M. Terres, M. C. Thomson, 2004: Development of a European multi-model ensemble system for seasonal to inter-annual prediction (DEMETER). Bulletin of the American Meteorological Society, 85, 853-872

Richardson, D., R. Buizza, and R. Hagedorn, 2005: First Workshop on the THORPEX Interactive Grand Global Ensemble (TIGGE) Final Report. WMO/TD-No. 1273, WWRP/THORPEX No. 5.

Rogers, D. P., M. Béland, P. Bougeault, J. Caughey, Chen Dehui, P. Courtier, E. Manaenkova, M. Miller, K. Mylne, T. Nakazawa, D. Parsons, J. Purdom, K. Puri, D. Richardson, M. Shapiro, A. Thorpe, and Z. Toth, 2005: THORPEX International Research Implementation Plan. WMO / TD-No. 1258, WWRP/THORPEX No. 4, 96pp.

Shapiro, M.A. and A.J: Thorpe, 2004: THORPEX International Science Plan, Version III. WMO TD-No. 1246, 51pp

Thomson, M. C., F. J. Doblas-Reyes, S. J. Mason, R. Hagedorn, S. J. Connor, T. Phindela, A. P. Morse, and T. N. Palmer, 2006: Malaria early warnings based on seasonal climate forecasts from multi-model ensembles. *Nature*, 439, 576-579

MOVING TOWARD USER-RELEVANT VERIFICATION

Barbara G. Brown[1]

[1] Research Applications Laboratory, National Center for Atmospheric Research, Boulder, Colorado, U.S.A.
E-mail: *bgb@ucar.edu*

Abstract: The concept of "user-relevant" verification is explored. A framework is developed to move verification approaches from traditional (primarily administrative-focused) methods to methods that are focused on users' needs for information, and can naturally lead to estimation of forecast value.

Keywords *– Verification, forecast value, forecast users, THORPEX, diagnostic verification methods, features-based verification*

1. INTRODUCTION

Traditionally, the three purposes of forecast verification defined by Brier and Allen in 1951 have been specified in verification and meteorological statistics textbooks (e.g., Wilks 2006); these purposes are "administrative," "scientific," and "economic." In general, most verification measures and approaches have only focused on the administrative goal. The techniques that satisfy the administrative goal are able to provide monitoring information about forecast performance, but they do not provide information that can be used to improve forecasts, or that can aid in decision-making by end users.

In recent years, some efforts have focused on development of verification approaches that provide more diagnostic information regarding forecast performance, indicating which aspects of a forecasting system are in need of improvement (and in what ways), and providing information about the uncertainty in the verification measures. These approaches – including basic diagnostic information about forecast errors, object- and entity-based approaches, and approaches that characterize variations in performance with scale – go part of the way toward user-focused verification. However, close interactions with particular sets of users (including forecast developers) will be required to develop measures that are truly user-focused.

A framework is developed to define the progression of verification methods from traditional approaches to approaches with greater user focus. Within this framework, we consider the research required to achieve greater user relevance in verification in the context of THORPEX.

2. TRADITIONAL AND DIAGNOSTIC VERIFICATION APPROACHES

Traditional forecast verification approaches allow overall monitoring of forecasting performance according to specific criteria (i.e., they may meet certain administrative needs for forecast verification information). However, these measures are limited and not appropriate for many purposes (e.g., they only measure a small set of attributes of forecast quality). They also tend to reward "smooth" forecasts over forecasts containing more detail and they don't provide diagnostic information about which aspects of a forecast need improvement. Thus, the measures-based approaches don't indicate how the forecast can be improved, to aid in forecast development. Finally, such approaches generally are not "informative" to users – they typically are difficult to interpret in terms of relevant characteristics of the forecasts that can be applied in decision making.

What makes a good forecast? Murphy (1993) defined three related aspects of forecast "goodness:" forecast quality (i.e., verification), value (economic and other), and consistency (e.g., provision of information about uncertainty). Traditional verification statistics simply evaluate goodness in terms of the correspondence between forecasts and observations. However, it is easy to demonstrate that forecast goodness depends critically on the use of the forecast. For example, a correct forecast that is displaced in space may be very useful for some users (e.g., for routing aircraft across the continental U.S.) but is worthless for other users (e.g., a watershed water manager). Traditional verification statistics would indicate that such a forecast has no skill, but would not provide any information about the fact that the lack of skill arises from a displacement error.

In contrast, a diagnostic verification approach would dissect the forecast performance into a variety of components or *attributes* of performance, and identify both the good and bad attributes that are relevant for a variety of users.

3. USER-RELEVANT VERIFICATION AND ESTIMATION OF FORECAST VALUE

Diagnostic approaches are one way to make verification information more meaningful to users. Certain forecast quality attributes are clearly more meaningful to certain users than others, and the diagnostic approaches

allow a wide variety of attributes to be computed. New diagnostic features-based approaches (e.g., Davis et al. 2006) also allow users to specify attributes of interest. Stratification of verification results according to meaningful subgroups is a second – and easily implemented – approach toward making verification result more user-focused. Nevertheless, by themselves diagnostic approaches and stratifications only go part of the way toward the provision of information that is truly beneficial and user-focused.

An obvious step toward greater user focus – and the ability to measure forecast value – is the development of connections with specific user groups to determine the forecast performance information that would be most useful, and to provide verification information that is tailored to specific applications. This approach would be especially beneficial for identifying the information required by an objective decision support system. Ultimately, verification information could be tailored to meet the needs of specific user groups.

Finally, user-relevant verification capabilities would aid in the development and application of methods to estimate forecast value. Studies of forecast value require appropriate and meaningful information about forecast quality, to develop and understand the complex link between forecast quality (which the forecasting system controls) and forecast value (which is at least partially under control of the forecast user).

4. FRAMEWORK FOR USER FOCUSED VERIFICATION

A simple framework can be defined for moving from traditional measures-focused approaches to approaches that are user-focused, and eventually to estimates of forecast value that rely on the user-focused verification information. Intermediate steps in this transition include the application of diagnostic and features-based approaches as well as initial identification of users' needs. The framework includes five levels:

- *Level 0*: Conventional measures-based approaches applied; verification approaches meet administrative purposes only;
- *Level 1*: Broad diagnostic approaches applied; user-selectable information is available and user-relevant stratifications are applied;
- *Level 2*: Features-based approaches applied; enhanced diagnostic information provided;
- *Level 3*: User-specific verification approaches and measures are developed through direct interactions with specific user groups;
- *Level 4*: Forecast value estimated, making use of user-focused verification information.

6. CONCLUSION AND FUTURE RESEARCH

Near-term research leading toward user-relevant verification approaches includes development of new diagnostic methods (e.g., ways to view/summarize forecast distributions; Level 1) and features-based approaches (Level 2). In addition, it will be critical to begin to develop connections with specific user groups (e.g., aviation, water resources), and to develop a common language and a process for identifying relevant verification attributes. In the longer term, research will continue to focus on development of diagnostic and features-based approaches (Levels 1-2). In addition, investigations of decision-making strategies for specific users will be required; knowledge of these strategies will lead to identification of meaningful verification attributes (Level 3). Finally, user-specific verification attributes will be applied in forecast value studies (Level 4) and used to investigate relationships between forecast quality (as measured by these attributes) and forecast value.

THORPEX field programs such as the Pacific-Asian Regional Campaign (PARC), and the THORPEX Interactive Grand Global Ensemble (TIGGE) project provide opportunities for the advancement of verification methodologies and development of approaches that are more user-relevant. For example, field programs provide an opportunity to test new methods in practice, and TIGGE will provide a wealth of forecasts that can be used for extensive development and testing of new verification approaches. In both cases, social science and decision-theoretic methods must be integrated in the research process to optimally develop the new methodologies.

Acknowledgements: *NCAR is sponsored by the National Science Foundation. This research is partially in response to requirements and funding by the Federal Aviation Administration (FAA). The views expressed are those of the authors and do not necessarily represent the official policy of the FAA*

.

REFERENCES

Davis, C., B. Brown, and R. Bullock, 2006: Object-based verification of precipitation forecasts, Part I: Methodology and application to mesoscale rain areas. *Monthly Weather Review*, **134**, 1772-1784.

Murphy, A.H., 1993: What is a good forecast? An essay on the nature of goodness in weather forecasting. *Weather and Forecasting*, **8**, 281-293.

Wilks, D., 2006: *Statistical Methods in the Atmospheric Sciences*. Elsevier, San Diego.

NEW APPROACHES TO VERIFYING FORECASTS OF HAZARDOUS WEATHER

Tim Hewson

Met Office, Exeter, U.K.
E-mail: *tim.hewson@metoffice.gov.uk*

Abstract: A new, simple and informative verification measure called the 'deterministic limit' is introduced. It applies to categorical forecasts of a (pre-defined) adverse meteorological event, indicating the lead time beyond which these forecasts are more likely, on average, to be wrong than right. Examples are provided, based on wind speed. These also illustrate the importance of incorporating a suitable frequency-preserving calibration step, to best account for any forecast bias.

Keywords – *verification, hazardous weather, contingency table, deterministic, probabilistic, calibration, THORPEX*

1. MOTIVATION

The practice of weather forecasting, particularly for rare events, has historically been hindered by a lack of clear measures of capability. Forecasters will understand that predicting a day with unusually high maxima - such as 'over 30C at London Heathrow' - is rather easier than predicting a short, intense rainfall event, such as 'more than 10mm in 1 hour at Glasgow airport', but knowledge of exactly how far ahead it is possible to successfully predict such events does not exist. Given the great importance attached, in socio-economic terms, to warning provision, this state of affairs is regrettable. The new 'deterministic limit' verification measure introduced here addresses this problem.

2. DEFINITION AND EXAMPLES

We define the deterministic limit (T_{DL}), for a pre-defined, rare meteorological event, to be '*the lead time (T) at which, over a suitably large and representative forecast sample, number of hits (H) equals the total number of misses and false alarms (X)*' (see Fig. 1a). Null forecasts are ignored, being considered not relevant. The closest counterpart in traditional verification measures is the Critical Success Index (see Jolliffe & Stephenson (2003), Ch 2), which equals $H/(H+X)$. Evidently, at T_{DL}, this is 0.5. What is new here is use of the lead-time dimension.

Choice of CSI=0.5, as opposed to some other value, relates directly to forecast utility. Out of all forecasts, the subset which *is concerned with* the event in question is made up only of the non-null cases (i.e. H+X). So within this subset forecasts are more likely to be right only for $T < T_{DL}$. This gives some justification for using deterministic forecasts at these ranges. Whilst purists will argue that probabilistic forecasts should be used at all leads, it is an inescapable fact that there is and probably always will be customer demand for deterministic guidance. Indeed, introduction of the deterministic limit concept may help attract more customer interest in probabilistic forecasts, notably for $T > T_{DL}$.

One pre-requisite for defining T_{DL} is that H and X should, respectively, decrease and increase monotonically with T. In practice this should be a characteristic of almost every forecast system, though in cases where small sample size obscures this (e.g. Fig. 1a, top) smoothing could be used. In pure model forecasts assimilation-related spin-up problems could also lead to there being short periods, for small T, when $\partial H/\partial T > 0$. However in systems employing 4D-Var this is less likely to be an issue. In terms of benefits, the deterministic limit:

i) is a simple, meaningful quantity that can be widely understood (by researchers, customers etc)
ii) can be applied to a very wide range of forecast parameters
iii) can be used to set appropriate targets for warning provision
iv) can be used to assess changes in performance (of models and/or forecasters)
v) provides guidance on when to switch from deterministic forecasts to probabilistic ones
vi) indicates how much geographical or temporal specificity to build into a forecast, at a given lead

The Lerwick example in Fig. 1a - see caption for full event definition - leads to two conclusions. Firstly, for Force 7 wind predictions, T_{DL} is about 15 hours (marked). For lead times beyond this probabilistic guidance should be used. For Force 8, T_{DL} is less than zero (curves don't cross), implying that probabilistic guidance should be used for all T. In part the reason T_{DL} is smaller for the more extreme winds is the lower base rate - i.e. the climatology (see caption). Base rate should always be quoted alongside the deterministic limit. In another model example (not shown) with site specific exceedance replaced by exceedance within an area, T_{DL} increases. This is due to reduced specificity - (vi) above - which in turn partly relates to a higher base rate. It is generally accepted that forecasts should be less specific at longer leads – this puts this practice onto a much firmer footing.

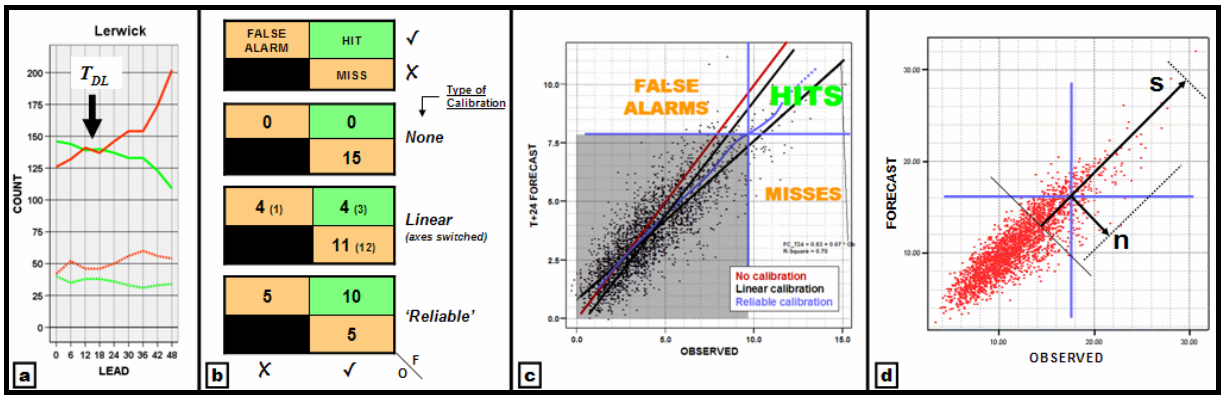

Figure 1: Data for all panels covers a 24 month period from mid 2004, with forecasts provided by the Met Office Mesoscale model (12km resolution). **(a)**: hits (orange) and misses + false alarms (green) for mean wind exceedance, at Lerwick, at a fixed time; top lines for ≥ Beaufort Force 7, base rate = 8% (deterministic limit is marked – assumes curves have been smoothed); bottom lines for Force 8, base rate = 2%. **(b)**: 2x2 contingency tables for T+0 North Rona mean wind ≥29 m/s (~Force 11), with differing calibration methods. **(c)**: Scatter plot for Heathrow mean wind forecasts (m/s) for T+24h; lines show calibration methods; 2x2 contingency table structure for 'Reliable Calibration' method is overlaid. **(d)**: Scatter plot for Heathrow T+6 wind forecasts (m/s), with method for estimating contingency table characteristics illustrated (see text).

3. CALIBRATION

In analysing strong wind data it became apparent that model bias can significantly impact on T_{DL}. Similar problems would likely be encountered for other parameters, such as rainfall. The clearest way round this is to calibrate model output, by site. Figure 1b illustrates the impact that calibration has on model handling at a very exposed site. Clearly a simple approach, using linear regression, is sub-optimal. The alternative, which we call 'reliable calibration', normalises misses to equal false alarms, and in so doing also elevates hits markedly. This method, touched on in Casati et al (2003), is illustrated in Fig. 1c. As the 'contingency table cross' (horizontal and vertical lines) moves along the reliable recalibration curve, the number of points in the right half (=event observed) always matches the number in the top half (=event forecast). Note also how the reliable recalibration curve varies through the data range, sometimes lying between the linear regression lines, sometimes outside.

4. FURTHER DISCUSSION

Evidently the structure of a 'forecast versus observed' scatter plot (for lead time T) is pivotal for determining whether H > X, which in turn indicates whether $T_{DL} > T$: tighter point clustering would naturally be consistent with more hits. A simple first order assumption that there is a linear reduction in point density in the orthogonal directions s and n shown on Fig. 1d, above the threshold in question (with ~ zero density reached at the vectors' ends), leads to the result that $T_{DL} \approx T$ when s ≈ 3n. This implies that if the cross-calibration spread (s) is more than about one third of the along-calibration spread (n), then event forecasts for that T should in general be probabilistic. This reasoning follows in the spirit of Murphy and Winkler (1987), where the importance of considering the joint distribution of forecasts and observations was highlighted.

As Fig 1a illustrates, the error bar on T_{DL} is a function of $(\partial H/\partial T)_{DL}$ and $(\partial X/\partial T)_{DL}$. This can be computed geometrically.

Forecasts of hazardous weather are intrinsically difficult to verify because of low base rates. For the time being this may constrain T_{DL} calculations to focus on thresholds that are less stringent than the ideal. In future we must strive to maximise the verification database by collecting all available data (e.g. 6-hourly maximum wind gusts), by providing model forecasts that are better suited to purpose (e.g. interrogating all model time steps to give 6-hourly maximum gust) and by reserving supercomputer time to perform reruns of new model versions on old cases.

In the context of THORPEX, it is hoped that the deterministic limit concept will assist with long term socio-economic goals, by providing clear guidance on an appropriate structure for warning provision.

REFERENCES

Casati, B., Ross, G. and Stephenson, D.B. 2004. A new intensity-scale approach for the verification of spatial precipitation forecasts. Meteorol. Applications **11**, 141-154.

Jolliffe, I.T. and Stephenson, D.B. (eds), 2003. *Forecast Verification – a Practitioner's Guide in Atmospheric Science*. John Wiley & Sons. Chichester, U.K. 240 pp.

Murphy, A.H. and Winkler, R.L. 1987: A General Framework for Forecast Verification. Mon Wea Rev. **115** , 1330-1338.

BIAS-CORRECTION METHODS APPLIED TO NCEP EPS OUTPUT

Warren Tennant

[1] South African Weather Service (Prediction Research Section), Pretoria, South Africa
E-mail: *warren.tennant@weathersa.co.za*

Abstract: This paper assesses the various bias-correction techniques that have been tested on the NCEP EPS over southern Africa. This includes a time-dependent adaptive correction of 500hPa height data, frequency adjustment of probability forecasts, correction of physical fields before probability calculation and regime-dependent bias correction.

Keywords *– THORPEX, WMO, Bias correction, ensemble probability forecast*

1. INTRODUCTION

The SAWS has been downloading subsets of the National Centers for Environmental Prediction (NCEP) ensemble prediction system (EPS) on a daily basis since 2000. The operational configuration at NCEP used for this study consists of 23 ensemble members per day generated through the use of the breeding cycle (Toth and Kalnay 1993; 1997). Forecasts extend to 16 days ahead at 2.5° resolution. Detail of the various changes that have been made to the NCEP EPS is available online at http://wwwt.emc.ncep.noaa.gov/gmb/ens/index.html). For purposes of a coherent set of forecast data, this paper only assesses the data as described above. However, it must be stressed that the NCEP model performance has been continuously improving through upgraded model physics, resolution and data assimilation and these effects are automatically manifest in these coarser output sets.

2. VERIFICATION METHODS

Verification of pressure-level geopotential heights and sea-level pressure is done by comparing forecasts against the ensemble control run analysis and calculating root-mean-square error and anomaly correlation coefficient scores. Verification of quantitative precipitation forecasts is done using the Equitable Threat Score (ETS) that has the advantage of measuring the fraction of observed and/or forecast events that were correctly predicted but adjusting the score for hits associated with random chance. The skill of probabilistic forecasts is verified using the Brier Skill Score (BSS) decomposed into reliability, resolution and uncertainty, and the Relative Operating Characteristic (ROC).

3. BIAS CORRECTION TECHNIQUES

The bias-correction technique on pressure-level fields was performed as follows. Starting at 1 January 2001, a bias for each forecast lead-time for forecasts valid for the 14-day window period (ending 31 December 2000) was calculated and subtracted from all forecasts valid over the window period. The process was then repeated for each day in turn until 1 January 2005. During this process each particular forecast case was bias-corrected 14 times as the window moved across the time. This iterative process provided more stability to the bias correction process. The latest forecast (simulating an operational environment) was bias-corrected using the mean difference between the standard forecasts and the latest set of iteratively bias-corrected forecasts over the 14-day window. In this way the most up-to-date bias information was used to correct the current forecast. These forecasts (with only one bias-correction step) were saved separately for verification.

Over the southern Africa domain the GFS model exhibits an increasing area-average negative bias with forecast lead-time. The magnitude of the bias is dependent on model resolution, with a larger bias associated with the lower resolution. The bias correction method is successful in reducing the magnitude of the bias considerably throughout the forecast period and also improves forecast skill somewhat, although some of the spatial pattern of the bias remained. Self-Organising Maps (SOMs) were used to generate a catalogue of circulation

regimes based on barotropic kinetic energy. The forecast bias stratified by these regimes showed significant differences and a regime-dependent bias-correction was also tested.

Quantitative precipitation forecast (QPF) fields were calibrated by adjusting the event threshold (i.e. the precipitation forecast amount defining a "yes" or "no" forecast event), so that the forecast frequency matched the observed frequency for the verification period (July 2000 to June 2005). Over the summer rainfall area (characterised by a positive bias), Equitable Threat Scores (ETS) of the calibrated forecasts were improved for light rainfall amounts but deteriorated for heavier rainfall events, as these events are rare and hardly ever reach high probabilities in practice, highlighting the difficulty in calibrating rare events.

A useful EPS product for event forecasting is the probability of the 850-500hPa-thickness field falling below 4200 and 4100gpm. These synoptic situations are good indicators of extreme cold weather and possible snowfall in South Africa, both of which are considered high-impact events in the region. The EPS is able to capture these events adequately for the first seven days of the forecast, as shown by positive Brier Skill Scores (BSS) (Fig. 1). Bias-correction improves the BSS considerably and also improves resolution somewhat.

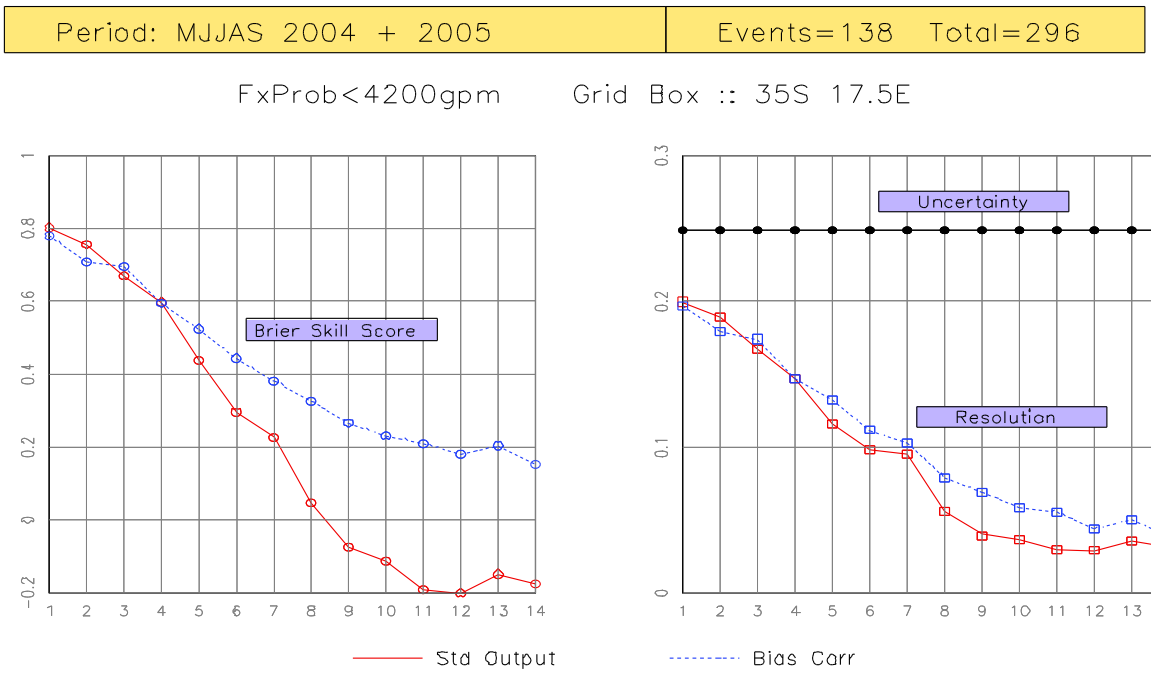

Figure 1. Brier Skill Score decomposition for standard (solid line) and bias-corrected (dashed) forecast probabilities of the 850-500hPa thickness field dropping below 4200gpm at the given grid point.

4. CONCLUSION

Bias-correction of the NCEP EPS is successful in improving probabilistic forecast skill and reducing the bias substantially. Physically-based correction methods work better that probability adjustment techniques, as they address the root of the model error more directly.

Acknowledgements: *The author thanks the WMO and THORPEX-IPO who have sponsored the conference fees and to Zoltan Toth and Kevin Rae who have collaborated on this work.*

REFERENCES

Toth, Z., and E. Kalnay, 1993: Ensemble forecasting at NMC: The generation of perturbations. Bull. Amer. Meteor. Soc., **74**, 2317-2330.

Toth, Z., and E. Kalnay, 1997: Ensemble forecasting at NCEP and the breeding method. Mon. Wea. Rev., **125**, 3297-3319.

TOWARDS SEAMLESS ENSEMBLE FORECASTS AND THE POTENTIAL FOR ALLEVIATION OF HIGH IMPACT WEATHER FOR USERS IN AFRICA

Andrew P. Morse [1], Andre Kamga Foamouhoue [2]
[1] Department of Geography, University of Liverpool, Liverpool, L69 7ZT, U.K.
[2] ACMAD, Niamey, Niger
E-mail: *A.P.Morse@liverpool.ac.uk*

Abstract: Application groups need to be fully integrated in forecast development. Users need to be involved in the development of seamless ensemble prediction systems. There is a great need for the development and support for such integrated forecasting systems in Africa.

Keywords – *Ensemble Forecasting Systems, Seamless Integration, Forecast Users, Applications, Validation*

1. INTRODUCTION

Forecast user communities have grown in recent years often alongside a forecast product community. It is clear that many of the issues encountered by the user and application communities are common to all ensemble prediction system (EPS) regardless of lead time. Producing a seamless integration of climate forecasts, weather forecasts and observations is an important forthcoming community activity e.g. WCRP COPES. However, for these seamless systems to be successful they must include relevant user and application communities from their inception. The integration of user communities has started but it is not universal and the nature of this integration is not clear in many programmes. In this paper, we address how users could make use of a seamless system and how they need to be integrated within project plans. The examples used will be from Africa, which is a continent whose population is highly vulnerable to climate variability particularly at interannual and intraseasonal time scales. The ability in many parts of Africa to mitigate high impact weather events with much shorter forecast lead times and observations is limited due to the lack of resources thus there is a need to construct a seamless end-to-end integrated EPS that gives some forewarning at seasonal timescales that are reinforced at the monthly scale and 'confirmed' at the medium and short range.

2. CURRENT CHALLENGES AND BACKGROUND

There is a strong demand for forecasts from users in Africa. From discussion through AMMA and CLIVAR VACS, it is very clear that users want event specific or intra-seasonal information e.g. rainfall onset, false starts or withdrawals and breakcycle length. This information is best served from seasonal or monthly EPS. Although the intraseasonal detail is provided through dynamic model output, statistical seasonal forecasts should also be included. 'Confirmation' and details can be made at THORPEX scales in a seamless system. The performance of forecast models is poor in West Africa and THORPEX should work to improve the parameterization in forecast models for use in the tropics.

Users are not concerned which forecasting system produces the forecasts and ideally need an integrated system that uses information from all forecast products over a range of forecasting lead times in a seamless interface – issues such as weighting, bias correction and scale all need to be addressed in ways that may be driven by specific user requests. Therefore, users need to be involved from the start in a true end-to-end approach. This has been undertaken with seasonal forecasting in the DEMETER project (Palmer et al., 2004). Users must not become polarised with certain forecasting teams and products i.e. THORPEX users, seasonal users etc.

Only users can help to define relevant and useful skill, utility or cost-benefit of a forecast. In terms of forecast quality both users and forecasters need to be pragmatic, users need to adapt to use the inherent skill contained in the forecast and forecasters need to know the skill of their meteorological forecasts from a user perspective. Downscaling remains an issue; again communities are unaware of each others needs, requirements or constraints. The ENSEMBLES project is linking users with statistical downscalers. For much of Africa, data availability is an issue for statistical downscaling techniques and therefore dynamic downscaling needs to be developed see Cui et al. (this issue).

Users have a need to be forewarned of high impact weather, this is opposed to extremes which are defined from a meteorological and not a user perspective. High impact weather can result from the unusual sequence of non extreme events. Predicting these high impacts events sits more closely within the scope of THORPEX but is shared by other projects such as AMMA and ENSEMBLES.

Users need data in a form they can access this can be a big problem with EPS as the users MUST use all the ensemble members not just the ensemble mean and this is something the forecasting community needs to strongly encourage with pilot demonstrations with selected sample users. Users often require site specific time series of a few key surface variables, which they find difficult to extract from gridded model output.

3. EXAMPLES OF CURRENT PRACTISE

Matthews (2004) described a mechanism by which intraseasonal variability over Africa is modulated by the Madden Julian Oscillation (MJO) It has been shown that the NCEP Global Forecast System (GFS) predicts the large-scale structure of the MJO at medium range (5 days). The ECMWF medium range and monthly forecasting systems predicts the sign of the MJO up to approximately 10 days (ECMWF/ACMAD internal communication). More interestingly, statistical models and subjective guidance of the MJO show useful skill at approximately 20 days lead time e.g. Wheeler and Weickmann 2001.

The late onset of the West African monsoon in summer 2006 is a good example of an intraseasonal monsoon feature that dictated the planting period over parts of the sub-saharan Africa region. A number of farming activities are based on the climatological onset period that occurs in June over most of the Sahel region. In 2006, the rainy season effectively started in mid July after some earlier but insufficient rains for agricultural activity. At ACMAD through monitoring and forecasting of the MJO activity using ECMWF monthly forecasting system and NCEP intraseasonal products, it was possible by late June to issue a simple statement with a big impact like " the 2006 onset is expected to arrive late " and early in July, that is a week or 10 days before the onset, a similar analysis was signalling the onset in mid July. This important information was conveyed to the official media and relevant user groups.

4. THE WAY FORWARD

The scientific gaps in knowledge and know-how can start to be filled through programmes such as THORPEX-AMMA, as funding allows, but the gaps between the scientific forecasting community and the forecast users, decision makers and implementers; remain a substantial challenge. This highlights the need to build cross cutting teams with adequate representation for the user communities, and resourcing, in any forecast development programme. In some displines e.g. agriculture and water resources there is an established interaction between users and forcasters but for health e.g. epidemic early warning, this interaction is in its infancy (see Rogers, this issue). AMMA-THORPEX should be a way of developing a pilot project for picking up on the user requirements that can make use of a 15 day lead time especially for high impact events e.g. long break cycles, false starts of the rains, early or late withdrawal of the rains, prolonged dust events, dry season rainfall (destruction of unharvested crops), dry season cold snaps (cattle deaths and loss of fodder crops), flooding, heat waves - especially in urban centres. Further, user orientated validation and demonstrations could be developed at the AMMA-THORPEX interface. Finally model development - we need to improve the medium range model physics/parameterisation to increase the skill in the monthly and seasonal forecasts, this will require the parameterization to work at the model's lower resolution, when used beyong medium range, or at least degrade gracefully.

5. CONCLUSION

Therefore, AMMA-THORPEX with inputs from other programmes e.g. ENSEMBLES, CLIPS and WCRP-COPES is a framework to demonstrate the potential in existing monitoring and forecasting systems over Africa, build training materials based on case studies, upgrade and run training programs for African forecasters, undertake research to determine and extend the current limit of predictability of the user defined events. We will then be helping to capitalize on substantial efforts made by global weather centres to develop products for Africa. By upgrading forecasting techniques in Africa (with demonstrations and training on EPS, forecasts verification, monitoring of relevant oscillations), we can make a significant improvement on the quality of the forecasts.

Acknowledgements: *APM acknowledges support of the EU FP6 ENSEMBLES and AMMA projects and the NERC AMMA project.*

REFERENCES

Matthews, A.J. (2004). Intraseasonal variability over tropical Africa during northern summer. J. Climate, **17**, 2427-2440.

Palmer,T.N., Alessandri,A, Andersen, U., Cantelaube, P., Davey, M., Déqué, M., Díaz, E., Doblas-Reyes, F.-J., Feddersen, H., Graham, R, Gualdi, S., Guérémy J.-F., Hagedorn, R., Hoshen, M., Keenlyside, N., Latif, M., Lazar,A., Maisonnave, E., Marletto, V., Morse, A.P., Orfila, B., Rogel, P, Terres J.-M, and Thomson, M.C. (2004). Development of a European Multi-Model Ensemble System for Seasonal to Inter-Annual Prediction (DEMETER), BAMS**, 85**, 853-872.

Wheeler, M. and K. Weickmann, (2001). Real time monitoring of modes of coherent synoptic to intraseasonal convective variability. Mon. Wea. Rev., **129**, 2677-2694

WEATHER FOR COCKPIT AND TOWER: THE BENEFIT OF AN IMPROVED WEATHER INFORMATION SYSTEM FOR AVIATION

Thomas Gerz [1] and Michael Theusner [2]

[1] Institut für Physik der Atmosphäre, German Aerospace Center (DLR), Oberpfaffenhofen, Germany
[2] Institut für Meteorologie und Klimatologie, Leibniz Universität Hannover, Hannover, Germany
E-mail: *Thomas.Gerz@dlr.de*

Keywords – *FLYSAFE, severe weather, integrated surveillance system, safety, capacity*

1. INTRODUCTION

Air traffic is expected to triple world-wide within the next 20 years. With the existing on-board and on-ground systems, this would lead to an increase of aircraft accidents, in the same, or a higher proportion. Instead of approximately 30 accidents per year, there could be 90 such accidents in the future annually. This increase is perceived as unacceptable by society and new systems and solutions must be found to maintain the number of accidents at its current low level or to reduce it to even lower levels. Although adverse weather is seldom the exclusive cause of accidents, it is nevertheless one of the most disruptive factors in aviation. It jeopardises safety and economic efficiency of the entire air transportation sector. Moreover, the disturbance caused by any individual weather event depends on a complex network of non-meteorological factors. Therefore, flight dispatchers, pilots and controllers must be equipped with new surveillance systems allowing them to make the right decision at all times. The provision of timely, dedicated and improved weather information for flight crews as well as airline operations centres and air traffic management is an essential part of such a system.

The European Integrated Project FLYSAFE (FLYSAFE 2005) aims at designing, developing and validating a complete Next Generation Integrated Surveillance System (NGISS) for cockpits and Weather Information and Management Systems (WIMS) on the ground. NGISS and WIMS strive to mitigate the potential risk factors “adverse weather“, “traffic” and “terrain” and, thus, contribute to the safety of flights for all aircraft. The WIMS shall provide tailored weather information for aviation on time.

2. WEATHER IMPACT ON AVIATION

It is well noticed by passengers that weather has an impact on the capacity for the air transportation system. An illustration for 2004 is given in Figure 1 for major European airports. According to a maximum growth scenario of future air traffic in Europe (Eurocontrol 2004), big airports will require an increase from 80 movements per hour in 2003 to 160 movements per hour by 2020 to fulfill the demand.

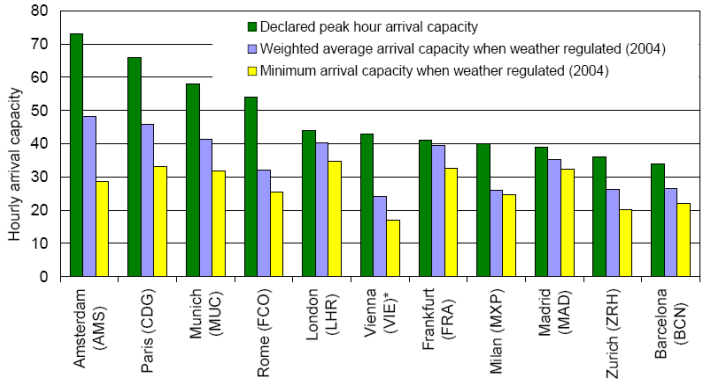

Figure 1. Impact of weather on arrival capacity for major European airports.

More importantly, weather is also a safety issue to aviation. Between 1995 and 2004 177 hull loss accidents were recorded, for 44 of which the cause of the accident is still unknown today or the final report was not available. The remaining 133 accidents were attributed to have resulted from the following causes: flight crew (56%), airplane (17%), weather (13%), misc./other (6%), maintenance (4%), airport/air traffic control (4%).

Thereby, weather has to be considered to play an even larger role than can be deduced from the numbers given above as it often is a contributing factor. Wrong decisions by the flight crew lead to accidents more frequently under adverse weather conditions than in fine weather. Despite that fact, the primary cause of such an accident would be attributed to the flight crew and not to weather.

The most prominent atmospheric hazards to aviation are strong wind and wind shear (downbursts, microbursts), turbulence (convective and clear air), icing, visibility (fog, strong precipitation), lightning, and hail. Furthermore, aircraft wake vortices and volcanic ash have to be mentioned here since they are, though no weather phenomena by themselves, transported and diluted by atmospheric processes. Within the FLYSAFE project the weather hazards thunderstorm, in-flight icing, wake vortices, and clear-air turbulence have been selected for closer inspection (Figure 2).

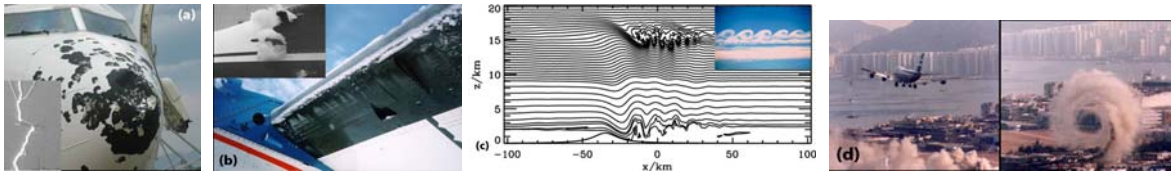

Figure 2. Weather hazards for aviation: (a) B737 after flight through a thunderstorm with large hail, (b) icing on wing and sensors of a Do 28, (c) simulation and photography of breaking gravity waves as a source of clear-air turbulence, (d) aircraft vortex made visible by industrial smoke.

3. THE FLYSAFE CONCEPT

One object in FLYSAFE is the development of a set of expert systems for these four hazards, the 'Weather Information Management Systems' (WIMS), which shall enable all aircraft to get timely, dedicated, and improved weather information. The WIMS provide all atmospheric data which are necessary to describe the hazards and to suggest alternative trajectories.

The flow of information starts from the observed or forecast hazards, through the WIMS to a ground-based weather processor which transfers the information to the aircraft, air traffic control and management and the airline operation centres. Atmospheric phenomena and weather hazards that impact the aircraft are monitored by observation systems (satellite, aircraft, radar networks, wind-temperature profilers, LIDAR, etc.), but also by the pilot and by various on-board weather sensors. The observation data will be processed by each WIMS, using dedicated and up-to-date forecasting and nowcasting tools. The optimum information about type, location and strength of the respective weather hazard will be evaluated and formatted as object-oriented or gridded 3-D data, respectively 4-D data if several output times are considered.

The WIMS products will be submitted to the 'Ground (based) Weather Processors' which store the information and tailor the data in a consistent and timely way to meet the specific requirements of the aircraft. The resulting 'corridor weather' is communicated to the aircraft systems where it will be fused with data from on-board sensors and displayed to the pilot. At the same time the weather hazard information is also available for AOC, ATM and ATC.

Weather information is required 24 hours in advance by AOC and ATM for planning on a strategic scale (e.g. long-haul flights) and down to the order of a few minutes (e.g. wake vortex warnings at the final approach) or an hour (e.g. thunderstorm warnings) for alerting air crews and ATC on a tactical scale. Such a large diversity of scales and terms cannot be addressed with a single technique. Weather forecasting techniques, which rely on numerically solving the equations of state of the atmosphere and provide 'long-term' predictions of more than an hour, and the nowcasting techniques, which combine recent weather monitoring data with simpler 'short-term' predictions of minutes to an hour, must be used in smart combination to obtain optimum results for aircraft en-route as well as flying in the terminal area.

4. CONCLUSION

The products of the Integrated Project FLYSAFE will in particular enhance the on-board awareness of adverse weather elements and the capability of the flight crew to make the right and flight-optimum decisions. For example, the different hazard volumes of lightning, hail and turbulence in the upper part of a thunderstorm will be displayed in the cockpit. Compared to today's rule of thumb methods by day and nothing during night operations, the FLYSAFE outcome will allow rational distance keeping from thunderstorms during cruise flight and it may possibly lead to less disturbed routings around weather systems allowing more traffic to be handled.

Acknowledgements: *The Integrated Project FLYSAFE is funded by the European Commission under contract number FP6 – 516167.*

REFERENCES

Eurocontrol 2004: Challenges to Growth, 2004 Reports (CTG04).
FLYSAFE 2005: see http://www.eu-flysafe.org/Project_Overview.html

GROUND-BASED AND AIRBORNE OBSERVATIONAL NEEDS FOR THORPEX

Roger M. Wakimoto
Earth Observing Laboratory, NCAR, USA
E-mail: *wakimoto@ucar.edu*

Abstract: The presentation at the symposium will describe ground-based and airborne observational needs for THORPEX. The current capabilities as well as planned instrument development will be highlighted.

Keywords *– THORPEX, Observations*

1. INTRODUCTION

One of the major objectives of THORPEX is to improve the accuracy of one-day to two-week forecasts of high impact weather for the benefit of society, the economy and the environment and to increase the effectiveness of advanced warnings of high impact weather globally. One of the ways to meet this objective is by evaluating the impact of static and targeted observations from ground-based and airborne platforms. The plethora of satellite observations is also critical but this will be the focus of another presentation. This talk will provide a broad overview of some of the observational platforms that are currently in operation and some that are planned.

2. AIRBORNE AND GROUND-BASED SYSTEMS

The success of the driftsonde activity during AMMA is a coup for THORPEX. It was clearly shown that it is possible to launch a gondola and have it "drift" with a tropical depression while deploying dropsondes in targeted regions. Future field experiments with the driftsonde are planned for Asia and will be a focus for the THORPEX community in the coming months. The growth of AMDAR and ACARS observations is filling in data gaps along the commercial airline flight paths over the oceans. Incorporating these data in forecasts has been shown to have a positive impact.

Small UAVs have already been deployed in hurricanes. The use of UAVs may see tremendous growth in the future which will lead to a greater push toward miniaturization of sensors. This trend will ultimately benefit the development of smaller instrument packages that will fly on manned aircraft. These larger aircraft such as NCAR's HIAPER and DLR's HALO, with their current and planned remote sensing and in situ instruments, will allow us to more efficiently probe the atmosphere in regions that were previously difficult to reach.

Surface-based instruments will also play a key role in helping THORPEX meet its objectives. It is believed that the overarching theme with these platforms is "integration." One way to integrate is by networking a number of surface stations together such as been done in the mountainous regions of the western United States. Integrating the WSR-88d Doppler radar network was shown to be feasible using CRAFT (Collaborative Radar Acquisition Field Test). The radar data collected and archived led to improved understanding of the propagation of mesoscale convective systems across the United States.

Another important way to integrate surface observations is by combining sensors into a single platform. The NCAR ISS (Integrated Sounding System) consists of a RASS, GPS radiosonde sounding system, wind profiler, 10-m meteorological tower, and surface mesonet station. A mobile system has been developed that will allowed for targeted observations such as near a coastline. The advantage of this type of platform is that the individual components might be "off the shelf" items and, therefore, not expensive to assemble. However, successful integration of the sensors would result is a state-of-the art observational platform.

These and other examples will be discussed at the THORPEX Symposium.

RECENT CHANGES IN ATMOSPHERIC CIRCULATION REGIMES OVER NORTHERN EURASIA AND SUGGESTION TO REDESIGN RAOB NETWORK

Oleg M. Pokrovsky

Main Geophysical Observatory, St. Petersburg, 194021, Russia
E-mail: *pokrov@main.mgo.rssi.ru*

Abstract: Enhanced meridionality of the airflow in Northern Asia appeared to be a result of rapid warming in Arctic Ocean. The Siberian RAOB networks optimal configuration scenarios is considered after substantial changes in atmospheric circulation regimes.

Keywords – *atmospheric circulation regimes, arctic dipole, Northern Siberian Oscillation, RAOB optimal design*

1. INTRODUCTION

Global warming leads to a rapid ice melting in Eastern Artic Ocean and, primarily, in Kara and Laptev Seas. Some experts considered this phenomenon as a cause of recent changes in atmospheric circulation regimes in Northern Eurasia: appearance of long-lived low atmospheric pressure patterns during warm part of year and a high ones – during cold period over Eastern Arctic Shelf Seas. The EOF analysis of the SLP fields in high latitude belt of Northern Hemisphere revealed a phenomenon of *Arctic dipole* enhanced during last decade (Wu et, al, 2004). A winter of 2005/2006 demonstrated the extreme high atmospheric pressure and height field anomalies in troposphere, which blocked a normal zonal flow in Northern Eurasia and generated an intensive cold air outbreaks to Eastern/Southern Europe and to Central Asia. Low atmospheric pressure anomaly in August/September led to appearance of a strong meridional flow and to delay in autumn development in Northern Eurasia. These changes determine a growing role of Russian RAOB network located at Arctic coast to gain better understanding of new circulation regimes and to provide more accurate and spatially detailed data for NWP models. A low accuracy of remote sensing data on wind velocity components in this area is another motivation to improve state of Siberian RAOB network. Siberian RAOB network has been degrading during nineties of last century. Most of remained sites are located in habitant regions of Western and Southern Siberia. This paper is focused to develop several optimal scenarios to redesign an existed network by redistribution of stations and network extension in Northern and North-Eastern Siberia regions. This task was formulated among others in a list of science questions where THORPEX can help (Global Atmospheric Research Program. - CBS/OPAG-IOS/ODRRGOS-Doc 7.1, WMO Geneva, 8.07.2004).

2. CHANGES IN THE ATMOSPHERIC CIRCULATION REGIMES

Objective classification of two component vector wind and scalar height daily grid fields for North Asia by fuzzy logic tools permits us to reveal major regimes of atmospheric circulation and acquire statistical properties of corresponding classes (Pokrovsky, et al, 2002). Enhancement of Arctic dipole (presence of two atmospheric pressure anomaly extremes of opposite signs in Eastern and Western Hemisphere (fig.1)) leads to activation of wind meridional component. Warming water pool in Autumn Kara Sea causes an atmospheric convection with low atmospheric pressure anomaly. It enforces northeastward winds from low latitudes. Rapid reduction in Kara Sea ice extent and positive trend of local sea surface temperature in September is major reason of Arctic dipole phenomenon and appearance of *North Siberian Oscillation*. As a result a warm fall season prolongs in Northern Asia. Opposite pressure anomaly dominates in winter: high atmospheric pressure over Russian Arctic strongly impacts on zonal flow over Eurasia. Cold air outbreaks from high latitudes governed by southwestward and southward winds cause rapid cooling in most areas of Eastern Europe and Central Asia in winter time. Unfortunately, now there is only one RAOB station at Russian Arctic coast (Island Dixon) provided a sustainable data flow on the temperature, height and wind profiles twice per day.

3. RAOB NETWORK DISTRIBUTION SCENARIOS

Our approach is based on maximizing of the information content of observing data with account to composite of the height and wind fields (H500, U700 and V700). Information model of Siberian observing system based on Kalman filter methodology was developed and applied to determine corresponding target function (Pokrovsky, 2000, 2004). Implementation of numerical optimal search algorithm leads us to acquisition

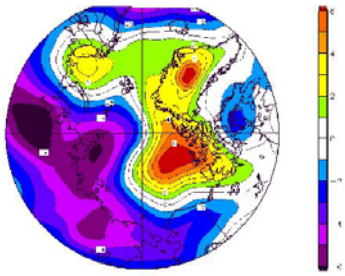

Figure 1. Demonstration of Arctic dipole: sea level pressure composite (mb) for September 2006 minus September 2003

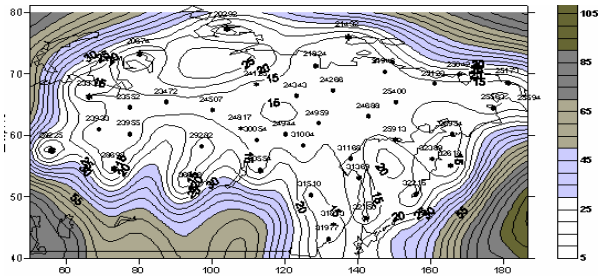

Figure 2. Siberian RAOB optimal configuration (42 sites) and H500 objective analysis error fields (m)

of consecutive sequence of optimal designs for RAOB network with various numbers of stations. Our study showed that total site numbers should lies between 14 and 42. Former is designed as minimal network, latter – as sufficient one. *Minimal network* provides a minimal representation of the *statistically homogeneous zones* (each of them is an approximately isotropic and homogeneous random field). *Sufficient network* provides a *proportional representation* of these zones with account to corresponding information contents. Each of scenarios assumes a recovering of currently closed RAOB stations located in North and North-Eastern Siberia. RMS (root mean square) error fields for major meteorological variables describe an efficiency of network design. Fig.2 shows that H500 RMS does not exceed 20 m over Siberia in the case of sufficient network scenario assumed presence of 42 sites. Optimal design provides the objective analysis RMS values improvement at 30-40% for wind components with account to current network state. Optimal network gains also an advantage in objective analysis accuracy for temperature and height fields with account to the existed network and remote sensing systems. Former is due to absence of data in some atmospheric circulation key areas, latter - to considerable contamination of outgoing radiation by cloudiness. Heavy clouds occur most part of the year in Arctic coast areas. H500 objective analysis accuracy providing by optimal RAOB is equal to 30-45 m, while existed network delivers only 60-70 m and NOAA remote sensing system - about 70-80 m. Existing network mainly covers the interior Siberian areas. In contrast, the optimal sets have a priority along Arctic and Pacific Ocean coasts. It was found that atmospheric pressures/heights and wind direction have maximal variance just in these regions.

4. CONCLUSION

Activation of Arctic dipole and Northern Siberian Oscillation leads to enhancement of northward (late summer and autumn) and southward (winter) meridional circulation. Large masses of arctic cold air crosses the Northern Eurasia and can cause substantial and rapid changes in weather patterns by means of hot and wet air condensation in some remote regions of Central, South and South-East Asia and consequent extreme rains and floods. It is necessary, keep in mind, that satellite remote sensing systems are not sufficiently efficient because of heavy cloudiness occurring here during most part of year. Such cloudiness contaminate radiance signal detected by satellite radiometers. Therefore, RAOB network of Northern Asia, primarily, in Northern Siberia, should be properly extended by means of recovering of many among now closed stations. We offered to perform some experiments with Siberian RAOB network data in frame of the Asian regional THORPEX program to verify our scenarios of network configuration.

REFERENCES

Pokrovsky O.M., 2000: Direct and Adjoint Sensitivity Approach to Impact Assessment of Ground-Based and Satellite Data on Weather Forecasting. *Proceedings of Second CGC/WMO Workshop on the Impact of Various Observing Systems on Numerical Weather Prediction.* World Weather Watch Technical Rep. N 19 (WMO/TD N1034), WMO, Geneva, p.99-118.

Pokrovsky O.M., Roger H.F. Kwok and C.N. Ng , 2002: Fuzzy logic approach for description of meteorological impacts on urban air pollution species: a Hong Kong case study.- *Computers and Geosciences*, **28**, N 1, p. 119-127.

Pokrovsky O.M., 2004: Optimization of Siberian RAOB network by Maximization of Information Content. *Proceedings of Third CGC/WMO Workshop on the Impact of Various Observing Systems on Numerical Weather Prediction*. World Weather Watch Technical Rep. WMO/TD N1228, WMO, Geneva, p.270-282.

Wu, B., J. Wang, J.E. Walsh, 2005: Dipole forcing and Arctic sea ice motion, *J. Climate*, **19**, p.210-225.

FINITE AMPLITUDE THRESHOLD BEHAVIOR OF DIABATIC ROSSBY VORTEX FORMATION

Richard W. Moore[1], Michael T. Montgomery

[1] Institute for Atmospheric and Climate Science, ETH-Zurich, Switzerland
E-mail: *richard.moore@env.ethz.ch*

Abstract: A suite of idealized, full-physics mesoscale model simulations are used to: i) diagnose the physical processes that allow a pre-existing, low-level vortex to begin to grow in a moist baroclinic atmosphere and ii) identify a necessary initial amplitude threshold for disturbance growth. The formation of a growing disturbance, termed a diabatic Rossby vortex, requires the presence of near-continuous convection for a finite period of time before the mutual interaction of two diabatically-generated potential vorticity anomalies can overcome frictional dissipation. The amplitude threshold is found to be a function of both environmental parameters (baroclinicity and moisture content) and the strength of an initial disturbance.

Keywords – *THORPEX, Moist Cyclogenesis*

1. INTRODUCTION

A number of studies investigating a variety of atmospheric phenomena have illustrated that diabatic processes often play an integral role in the formation and amplification of short-scale disturbances in a moist baroclinic atmosphere. A low-level cyclonic disturbance can grow, even in the absence of upper-level forcing, via the near constant production of potential vorticity (PV) associated with cloud diabatic processes (Snyder and Lindzen 1991; Montgomery and Farrell 1992; Parker and Thorpe 1995; Moore and Montgomery 2004). This type of disturbance, where the PV tendency due to diabatic heating acts in a similar manner to that of the meridional advection of PV in a classical Rossby wave, has been termed a diabatic Rossby vortex (DRV).

While the bulk of previous work has focused on the characteristics of growing disturbances, an equally important issue concerns the formation of an amplifying disturbance. Via what avenue does a small-scale, yet finite amplitude, perturbation transform into a DRV? Are there instances where such a transformation does not occur? This work will attempt to address these questions.

2. MODEL FORMULATION

The PSU-NCAR Mesoscale Model (MM5) with an idealized initial condition is used for all simulations. The initial condition is composed of a surface concentrated, warm core vortex (with zero quasigeostrophic PV in the interior of the domain) superposed on the southern side of a moist baroclinic zone over an ocean surface.

To ascertain the general features of the DRV formation process, a 'control' simulation is made. The maximum vertical wind shear of 1.5 ms^{-1} km^{-1} is found at the center of the baroclinic zone at approximately 45N and the lower atmosphere is sub saturated (80% relative humidity from the surface to 800 mb). The initial vortex is characterized by a positive 3K perturbation in the potential temperature field on the lower boundary and is centered at 35N (Fig. 1a). There is a 3.5 mb pressure depression and a 4.5 ms^{-1} maximum wind flow at a radius of about 300 km associated with the perturbation vortex.

An advantage of this particular model formulation is the ease with which one can vary the parameters most applicable to DRV formation; namely, the strength of the baroclinic zone, the moisture content and the initial strength of the perturbation vortex. To determine the sensitivity to each of these parameters, a number of model simulations are made during which a single parameter is varied from the control simulation.

3. RESULTS

In an initially sub saturated environment, two distinct stages of development are necessary before an incipient disturbance begins to grow. Environmental pre-conditioning involves the moistening of the lower atmosphere downshear of the pre-existing vortex via the warm, moist advection that results from the interaction of the incipient vortex with the baroclinic zone. Subsequent to air parcel saturation, near-continuous cloud diabatic processes serve to create the characteristic DRV PV structure: a positive anomaly and a negative anomaly in the lower and mid-troposphere, respectively, tilted downshear with height.

The associated temperature anomaly and diabatic heating rate at day 4.5 of simulation time (approximately half a day after the incipient disturbance begins to grow) are presented in Fig. 1b. Diabatic processes have

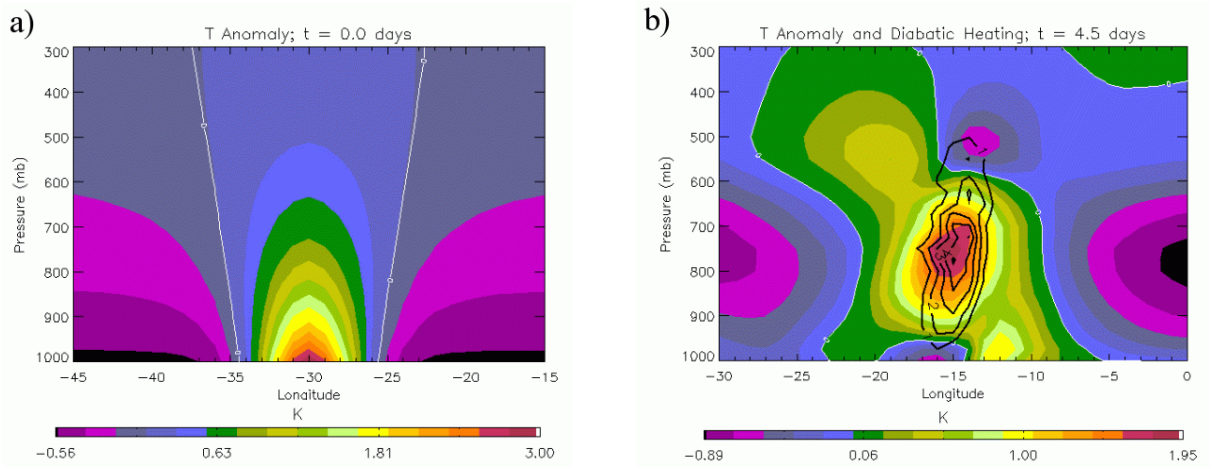

Figure 1. Vertical cross section of the temperature anomaly (K; shading) and positive diabatic heating rate (K day-1; black contour) through the center of circulation at: a) day 0, 35N and b) day 4.5, 40N.

significantly altered the structure of the initial vortex by this time. From an energetics perspective, the DRV begins to grow once the diabatic production of eddy available potential energy (a quantity directly related to the covariance of the temperature anomaly and the diabatic heating rate) becomes large enough to overcome frictional dissipation. This occurs once the dipole PV structure has achieved sufficient coherence and amplitude.

The results of a suite of sensitivity simulations identify an amplitude threshold for DRV formation. The DRV growth mechanism requires the presence of baroclinicity and moisture. Given the parameter space explored here, an initial perturbation vortex of sufficient amplitude is also found to be necessary for a growing disturbance to emerge within a subjectively defined 'reasonable' amount of time (10-days of model simulation). For all three of these requisite ingredients, there exists a non-zero threshold value below which DRV formation does not occur. The key factor that determines whether or not a DRV forms is directly related to the local-scale forcing of convection. The forcing must be sufficiently strong and invariant to ensure the presence of near-continuous cloud diabatic processes for a finite period of time.

4. DISCUSSION

The results of this study, in conjunction with previous work, illustrate that DRV formation and growth pose a difficult challenge for the forecasting community. The predicted sensitivity to the local environment and the perturbation field imply a clear picture of both is necessary for an accurate forecast. This result highlights the need for further research into alternate techniques such as adaptive observations and singular vector approaches that may provide further insight into the information content necessary for an accurate forecast. It also provides a strong argument for the use of advanced modelling techniques that emphasize the importance of observational data (such as four dimensional data assimilation), as well ensemble forecasting approaches that attempt to account for a large sensitivity to the initial conditions.

REFERENCES

Montgomery, M. T. and B. T. Farrell, 1992: Polar Low Dynamics. *J. Atmos. Sci*. **49**, 2484-2505.

Moore, R. W. and M. T. Montgomery, 2004: Reexamining the Dynamics of Short-Scale, Diabatic Rossby Waves and Their Role in Midlatitude Moist Cyclogenesis. *J. Atmos. Sci*. **61**, 754-768.

Parker, D. J. and A. J. Thorpe, 1995: Conditional Convective Heating in a Baroclinic Atmosphere: A Model of Convective Frontogenesis. *J. Atmos. Sci*. **52**, 1699-1711.

Snyder C. and R. S. Lindzen, 1991: Quasigeostrophic Wave-CISK in an Unbounded Baroclinic Shear. *J. Atmos. Sci*. **48**, 78-86.

INFLUENCE OF LARGE-SCALE PRECIPITATION ON THE PREDICTABILITY OF BAROCLINIC SYSTEMS

Olivier Rivière[1], Guillaume Lapeyre[1], Olivier Talagrand[1]

[1] Laboratoire de Météorologie Dynamique (IPSL), ENS, Paris, France
E-mail: *oriviere@lmd.ens.fr*

Abstract: The development of atmospheric perturbations is primary driven by baroclinic instability processes. However water vapour may play an important role in the formation of intense storms through the release of latent heat by large-scale precipitation. The processes involved in this dynamics are not completely understood yet. We investigate the mechanisms leading to the development of moist synoptic perturbations, and in particular the interaction between baroclinic and moist processes. For this purpose we use primitive-equation simulations and examine the sensitivity of moist singular vectors to the strength and spatial distribution of latent heating. Our aim is to understand how the spatial distribution of water vapour relatively to the characteristics of the large-scale jet affects the growth rate of synoptic perturbations. For this purpose, we use a novel technique called Conditional Nonlinear Optimal Perturbations (CNOPs) to assess the effect of the nonlinearities in the intensification of moist synoptic systems. CNOPs are a generalization of singular vectors as they are perturbations with a given initial energy, evolving nonlinearly and reaching maximum amplification (for all perturbations with same initial energy) over a finite time.

Keywords – *Predictability, water vapour, latent heat release, singular vector, moist baroclinic instability.*

1. INTRODUCTION

The cases of the European Christmas 1999 storms showed that water vapour can play an important role in the storm intensification since a structure with high water vapour was observed in the region of strong development (Wernli et al, 2002; Hoskins and Coutinho, 2005). Water vapour directly affects the dynamics of synoptic perturbations through latent heat release associated with large-scale precipitation. Many studies in the 80s have shown that this effect tends to increase the linear baroclinic instability of synoptic waves leading to stronger cyclogenesis. Recently, two important mechanisms that may have a profound impact on synoptic systems have been identified. First, it was recognized both by theoretical studies (Lapeyre and Held 2004) and by analysis of individual cases (Hoskins and Coutinho 2005) that the spatial distribution of water vapour compared to the distribution of potential vorticity is essential to promote the intensification of storms: if water vapour is present at the beginning of the storm development, it can efficiently intensify that development. Second, latent heat release may critically modify the dynamics of synoptic systems. The paradigm of the "diabatic Rossby wave" (Parker and Thorpe 1995), that is a Rossby wave that maintains and develops through latent heat release (whereas standard Rossby waves maintain and develop through the interaction of upper and lower tropospheric disturbances) has been invoked to explain the dynamics of moist synoptic eddies and seems to be at play for systems with high water vapour (Lapeyre and Held 2004, Moore and Montgomery 2005).

2. A NONLINEAR APPROACH TO PERTURBATION GROWTH

In order to investigate the role of water vapour in the storm development, we make use of a new technique that extends singular vector analysis to the nonlinear regimes. Singular vectors (SV) are constructed as linear perturbations of a given trajectory that have the largest growth over a given time period and for a given norm. However, processes such as latent heat release are strongly nonlinear (since precipitation is triggered at a particular threshold). Mu et al. (2004) have developed a new technique called CNOPs (Conditional Nonlinear Optimal Perturbations) which are perturbations with a given initial energy and having the largest nonlinear growth over a finite time. CNOPs have the advantage of having a definite sign (whereas both positive and negative SVs have the same growth rate). They can be computed using numerical techniques available for nonlinear optimization problems such as quasi-Newton method and interior point algorithm. We used this technique within a GCM at resolution T42 with 15 vertical levels, resolving large-scale precipitation and including surface drag and a simple vertical diffusion scheme. We computed the first SV and CNOP in our model for a time period of 24h and using a dry norm (kinetic + potential energy) and compared their growth rate as a function of their sign. The initial CNOP amplitude corresponds roughly to a maximum value of 3K. As shown in Table 1, the SV in the nonlinear model has a limited growth compared with its potential in the linear regime. The nonlinearities give rise to different amplifications for +SV and –SV. The CNOP is able to have a sustained growth in the nonlinear regime quite similar to the SV in the linear regime. Preliminary results show that CNOP tend to stay quite linear during their time evolution and have spatial properties in common with SV structures. It is hypothesized that they adapt to maintain their growth rate using wave-mean flow interactions. We are currently investigating this behaviour in a Quasi-Geostrophic model of baroclinic instability.

Initial perturbation	+SV	-SV	CNOP	-CNOP	SV in linear model
Amplification over 24h	20.5	19.7	28.6	22.2	30.6

Table 1. Final energy for different structures in the nonlinear models and for the SV in the linear model. For each structure, we examine both its amplification (+SV, CNOP) and the amplification of its opposite (-SV, -CNOP).

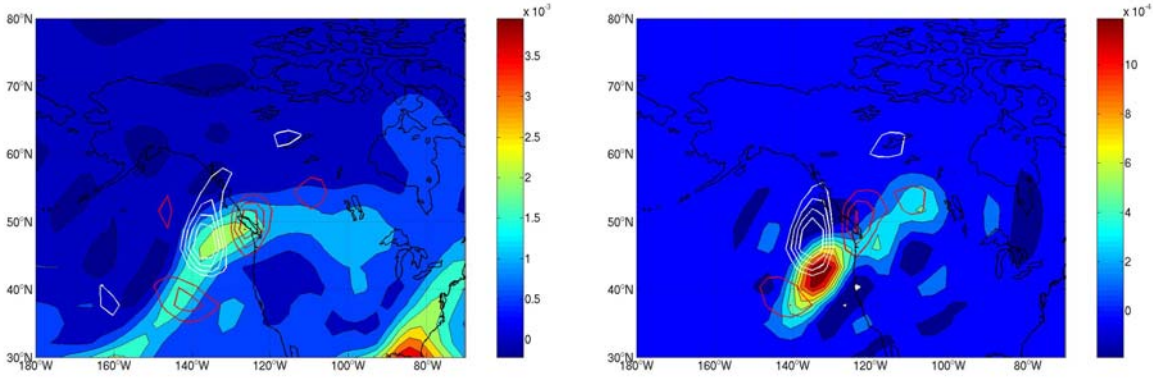

Figure 1. Experiments with perturbed/unperturbed water vapour on trajectory at initial time: Left: Water vapour of the unperturbed trajectory (in colour) and corresponding SV (white and red contours). Right: perturbed water vapour (in colour) and SV of the new trajectory (white and red contours).

3. IMPORTANCE OF WATER VAPOR SPATIAL DISTRIBUTION

Computing SV using water vapour in the norm is problematic since the initial water vapour of the perturbation is transformed into sensible heat whenever and wherever it rains on the trajectory. This is because the saturation threshold of the trajectory still applies to the linearized precipitation. Using the same approach as CNOP, we can treat water vapour in a different way by *modifying the water vapour of the trajectory itself*. If we denote trajectory variables as X0 and δX0, perturbation as δX', the final perturbation along a modified trajectory X0+δX0 reads δX'(T)= M(X0+δX0+δX')-M(X0+δX0) where M is the model from t=0 to the optimization time T. One can then try to find the optimal δX0(t=0) resulting in the largest amplification of $\|\delta X'(T)\|/\|\delta X'(0)\|$. This can be done using a numerical algorithm analogue to the CNOP computation. For this, we consider only a dry norm to compute the amplification rate of δX' while δX0 is a perturbation of water vapour, under the constraint that the total water vapour of the modified trajectory is under saturated. Figure 1 shows the result of such a procedure and in this case the amplification rate over 24h increases from 28.6 to 39. Interestingly the water vapour modification is strongly localized in space in the region of the singular vectors. Such a method may help in understanding the relationship between water vapour and the dynamical structures.

4. CONCLUSION

To better understand the role of water vapour in the predictability of synoptic systems we are currently using new tools that quantify the development of nonlinear moist perturbations. First, we compute CNOPs which are a generalization of singular vectors to the nonlinear regime. These structures strongly amplify in the nonlinear regime, contrary to SV, and share some common properties with SV. Second, we assess the sensitivity of the background distribution of water vapour by finding which modifications of the trajectory water vapour can lead to the largest growth of SV on the modified trajectory. Such an analysis allows identifying regions of space where water vapour plays a significant role in the dynamics.

REFERENCES

B. Hoskins and M. M. Coutinho, 2005: Moist singular vectors and the predictability of some high impact European cyclones, Q. R. Meteorol. Soc. **131**, 581-601.

G. Lapeyre and I. M. Held, 2004: The role of moisture in the dynamics and energetics of turbulent baroclinic eddies, Atmos Sci. **61**, 1693-1710.

R. W. Moore and M. T. Montgomery, 2005: Analysis of an Idealized, Three-Dimensional Diabatic Rossby Vortex: A coherent Structure of the Moist Baroclinic Atmosphere, J. Atmos Sci. **62**, 2703-2725.

M. Mu, L. Sun and H. A. Dijikstra, 2004: The sensitivity and stability of the ocean's thermohaline circulation to finite amplitude perturbations, J. Physical Oceanog. **34**, 2305-2315.

D. J. Parker and A. J. Thorpe, 1995: Conditional convection heating in a baroclinic atmosphere: a model of convective frontogenesis, J. Atmos. Sci. **52**, 1699-1711.

H. Wernli, S. Dirren, M. A. Liniger and M. Zillig, 2002: Dynamical aspects of the life cycle of the winter storm 'Lothar', Q. J. R. Meteorol. Soc. **128**, 405-429.

CALIBRATION AND POST-PROCESSING METHODS TO COMBINE ENSEMBLES FROM MULTIPLE SOURCES - THE NAEFS EXPERIENCE.

Laurence J. Wilson[1], Stéphane Beauregard, Bo Cui, Yuejian Zhu, Zoltan Toth and Richard Verret

[1] Meteorological Research Division, Environment Canada, Montreal, Canada
E-mail: *lawrence.wilson@ec.gc.ca*

1. INTRODUCTION

The North American Ensemble Forecast System (NAEFS) project has as its major goal the preparation and dissemination of forecast products in real time created from the combined Canadian and NCEP ensembles. It was understood very early in the project that both ensembles would need to be corrected for biases in their first (mean) and second (variance) moments before they could be effectively combined into one ensemble. If bias correction is not carried out, then the combined ensemble is likely to exhibit "false" spread due only to systematic error differences between the two component ensembles.

There are many methods available for bias-correction, including simple removal of the mean error, various forms of regression, recursive correction methods of the Kalman filter type, and Bayesian methods. These methods will be more fully enumerated and compared in the presentation. It was necessary for the first implementation of NAEFS to choose a method which worked and which could be easily implemented into an operational schedule. Since there was not a lot of time for comparative evaluation of different methods, one method was chosen, a recursive decaying weight method (Cui et al, 2004), for the first version of NAEFS. This method corrects only the first moment; other methods are in development for both first and second moment correction.

Examples of recent results are shown in the next two sections, first for the decaying weight scheme now being implemented into NAEFS, and second for Bayesian model averaging (BMA), which is under development for correction of the ensemble spread.

2. THE DECAYING WEIGHT BIAS CORRECTION

For 35 of the 50 forecast variables that are exchanged as part of NAEFS, the decaying weight bias correction is applied to each ensemble separately, referenced to each center's own analysis. The correction is of the form,

$$(1\text{-}w) * \text{prior time mean estimate} + w * (f - a)$$

where the "prior time mean estimate" is the average error over the previous 50 days, "f" is the forecast, "a" the analysis, and w a weight set to 0.02 after testing of different values. The prior time mean estimate is updated daily and the full correction is applied to the next forecast.

The top two panels of figure 1 show an example of the effect of the correction on nearly two months of 500 mb heights. The rank probability skill score is shown, against long term climatology for the two individual ensembles and for the combined ensemble, before and after bias correction. In this case, the Canadian ensemble has been corrected to, and verified against the NCEP analysis. It can be seen that the bias-corrected combined ensemble is slightly more skillful than either of the two ensembles at all forecast ranges. The bottom panel of figure 1 shows more directly the effect of the bias correction on the NCEP ensemble.

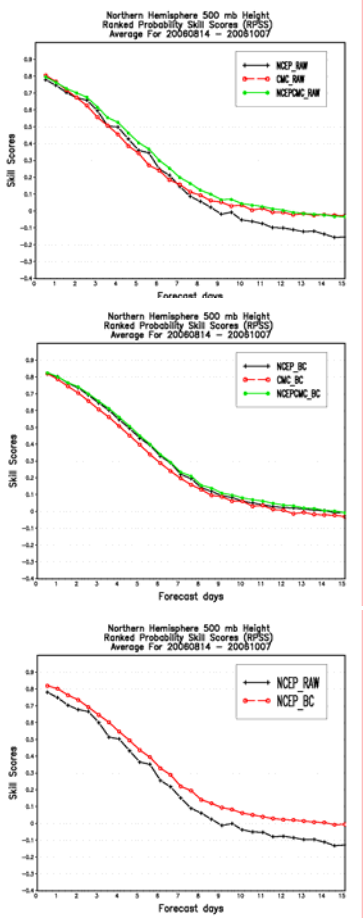

Figure 1. RPSS of uncorrected (top) and corrected (middle) 500 mb forecasts from the NCEP and Canadian ensembles over North America, for 2 months. The bottom panel shows the effect of the bias removal on the NCEP forecasts

3. BAYESIAN MODEL AVERAGING (BMA)

BMA is a method of correcting the spread of a bias-corrected ensemble based on a training sample of forecast realizations. As with other ensemble correction techniques that might be considered for operational use, the BMA must be applicable to relatively small samples. This is especially true of multi-model ensembles from different sources,

since changes to any of the component ensemble systems destroy the statistical stationarity of the training sample. With ensembles from multiple sources, changes to the combined system are therefore to be expected to be more frequent than for any of the component systems. Accordingly, we tested BMA on short samples for single station forecasts of surface temperature, settling on a training period of 40 days following tests on periods of different lengths.

In our experiment (Wilson et al, 2007), the BMA was performed for 23 Canadian stations, through one year of data. The BMA was trained on the previous 40 days, then used to correct the next day's forecast, as independent data. Figure 2 summarizes the results in terms of the continuous ranked probability skill score, as a function of projection time, based on a sample of about 8000 cases. The curves shown are: 1. The original uncorrected 16- member ensemble ("standard"); 2. The ensemble with bias removal based on bivariate regression only ("regression"); 3. BMA, applied to bias corrected forecasts using regression ("BMA"); 4. The original 16 member ensemble with the control and full resolution forecast added as members ("standard18"); 5. The original 16 member ensemble with bias correction by subtraction of mean error only ("regressionb1"); 6. BMA using the bias correction as in 5 ("BMAb1"); and 7. BMA for the 18 member ensemble with bias removal as in 5 ("BMA18").

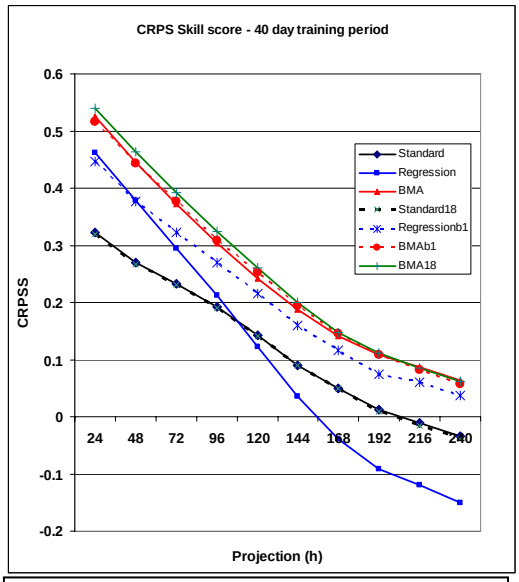

Figure 2. CRPS Skill Score vs. climatology for various tests of BMA on 23 Canadian stations, for 2m temperature. One year of independent data. See text for explanation of the plotted curves.

It can be seen from this figure that there is positive skill in the forecasts with respect to climatology out to day 8 for both original ensembles, that correction of the mean error improves the skill by 5 to 10 percent at all projections, and that the BMA adds a further improvement of 2 to 3% at all projections. While the original ensembles don't show any noticeable difference in skill between 16 and 18 members, the BMA has succeeded in extracting additional predictive information from the extra two members, leading to a further improvement to the CRPSS in the first 6 days of the forecast. This is a significant result, for it points out the advantage of BMA for extraction of unique predictive information from members from different sources. The only exception to the generally positive result is the performance of the regression-based bias correction. This is due to the tendency for the regression, which was applied separately to each member, to result in greater colinearity in the forecasts, and reduced ensemble spread at longer projections. As shown in the figure, skill decreases much more rapidly for these forecasts.

4. CONCLUSION

Both the decaying weight bias correction and BMA show considerable promise for use to correct errors in the first two moments of ensemble distributions. BMA has been shown to conveniently extract predictive information from ensemble members from different sources, and thus is flexible for application to the multimodel context. The methodology for these applications is still under development. In future, it will be advisable not only to continue to refine the methodology for these techniques but also to compare with other methods for generating calibrated ensemble distributions, such as dressing methods, other forms of Bayesian methods, and other forms of bias correction. Such efforts will not only benefit NAEFS in an operational context, but will be an advantage to the effective use of TIGGE data.

REFERENCES

Cui, B., Z. Toth, Y. Zhu, D. Hou, D. Unger, and S. Beauregard, 2004: The Trade-off in Bias Correction between Using the Latest Analysis/Modeling System with a Short, vs. an Older System with a Long Archive. Proceedings, First THORPEX International Science Symposium, Montreal, Dec. 2004.

Wilson, L. J., S. Beauregard, A. E. Raftery, and R. Verret, 2007: Calibrated Surface Temperature Forecasts from the Canadian Ensemble Prediction System Using Bayesian model Averaging. Mon. Wea. Rev. In Press.

DEMONSTRATION OF PROBABILISTIC HYDROLOGICAL AND ATMOSPHERIC SIMULATION OF FLOOD EVENTS IN THE ALPINE REGION (D-PHASE)

Mathias W. Rotach[1] and Marco Arpagaus[1]

[1] MeteoSwiss, Zurich, Switzerland
E-mail: *mathias.rotach@metoeswiss.ch*

Abstract: The fourth phase of the Mesoscale Alpine Programme (MAP), called MAP D-PHASE and approved as the second Forecast Demonstration Project (FDP) of World Weather Research Programme (WWRP), aims at demonstrating some of the many achievements of MAP, in particular *the ability of forecasting heavy precipitation and related flooding events in the Alpine region*. It mainly builds on the MAP achievements with respect to understanding orographic precipitation, high-resolution numerical modelling, hydrological modelling, hydrological modelling, radar technique and ensemble forecasting. The demonstration period of MAP D-PHASE, will be June to November 2007, encompassing the 'classical' MAP period (September – November) as well as the *Convective and Orographically-induced Precipitation Study* (COPS) observation programme (June – August). MAP D-PHASE will address the entire forecasting chain ranging from limited-area ensemble forecasting, high-resolution atmospheric modelling (km-scale), hydrological modelling, and nowcasting to decision making by the end users, i.e., it is foreseen to set up *an end-to-end flood forecasting system.* A focus is given to ensemble forecasting techniques, both in the atmospheric and hydrological components of the system. Examples of probabilistic meteo-hydrological forecasts, as they will be evaluated and assessed during the Forecast Demonstration Project will be given. Also the potential for a high-resolution poor man's ensemble system from the many participating km-scale advanced atmospheric models will be discussed. Finally, the relation to TIGGE, and in particular common data definitions and needs will briefly be addressed.

Keywords: *MAP, flood forecast, heavy precipitation, probabilistic forecast, end-to-end forecasting system*

1. INTRODUCTION

The Mesoscale Alpine Programme (MAP) was the first Research and Development Project (RDP) of the World Weather Research Programme (WWRP) of WMO. It has seen three phases so far: a development phase when the plans were made and the project was designed, the field phase with the Special Observing Period in fall 1999, and the analysis phase that is still ongoing and has brought a wealth of exciting new results and insight in mountain meteorology (Bougeault et al. 2001; Volkert 2005). In October 2005 WWRP endorsed D-PHASE as MAP's *Forecast Demonstration Project* (FDP), the second after the one associated with the Sydney 2000 Olympics (Keenan et al. 2004**)**. The acronym D-PHASE (**D**emonstration of **P**robabilistic **H**ydrological and **A**tmospheric **S**imulation of flood **E**vents in the Alpine region) reflects the MAP community's choice of *heavy (orographic) precipitation* as the theme for the forecast demonstration project.

As an FDP, D-PHASE aims at demonstrating progress in operationally forecasting high-impact weather of international relevance (heavy precipitation and related flooding events). Also it will rely on clear and pre-defined evaluation protocols. It is finally committed to the societal aspect of weather related research by envisaging an end-to-end forecasting system encompassing the entire forecasting chain from the atmospheric modeling over the hydrological modeling to observations / nowcasting to the end users.

2. GOALS OF D-PHASE

The main objective of the MAP D-PHASE is to demonstrate the benefits in forecasting heavy precipitation and related (flash) flood events, as gained from the improved understanding, refined atmospheric and hydrologic modelling, and advanced technological abilities acquired through research work during MAP. Specifically, an end-to-end forecasting system for Alpine flood events is being set up to demonstrate state-of-the-art forecasting of precipitation-related high-impact weather. This system will include probabilistic forecasting based on ensemble prediction systems with a lead time of a few days, followed by short-range forecasts based on high-resolution atmospheric and hydrologic models for selected regions or catchments, and completed with real-time nowcasting and high-resolution observational information. Throughout the forecasting chain, warnings will be issued and re-evaluated as the potential flooding event approaches, allowing forecasters and end users to alert and make decisions in due time. A schematic of the end-to end forecasting system is displayed in Fig. 1 showing the time line (from top to bottom) with early probabilistic (pre-) alerts, followed by high-resolution deterministic models closer to a possible event, hydrological modelling in catchments of interest and, finally, the use of latest observations and nowcasting tools for the final decision making at intervention level. All products will be evaluated both objectively using high-resolution surface and atmospheric observations, and subjectively by feedback to be submitted by users of the information at all stages (atmospheric and hydrological forecasters, end users).

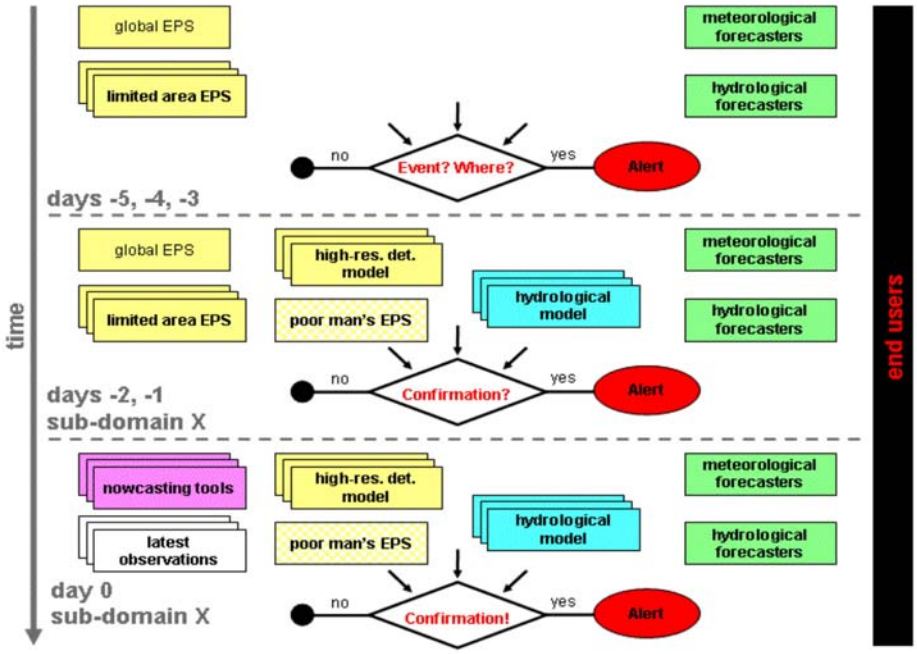

Figure 1. Sketch of the sequence of different components (model systems and types, forecasters) in the end-to-end forecasting system for D-PHASE. Note that time is running from top to bottom.

3. CONTRIBUTIONS AND ORGANISATION

Contributions to D-PHASE will be made by some 3 regional (atmospheric) ensemble systems, about 10 different atmospheric high-resolution models, about the same number of hydrological models and several nowcasting tools. Model products are exchanged bilaterally between collaborating teams in the modelling chain in such a way that for example an atmospheric modeller submits predefined model fields to a hydrological modeller who uses the information as input to the hydrological model. At the same time possible alerts are transferred that are based on the requirements of the respective hydrological modeller or his/her 'customer' (i.e. an end user in the respective catchment). All this information is transferred in parallel to a Visualisation Platform so that in case of an alert (for example: precipitation in catchment X exceeding 100 mm/24h) each person active in the forecast chain can assess all available information for the region of interest. As an example, end user X (a lake manager, say, in the Lago Maggiore catchment) receives a pre-alert based on the forecast from atmospheric model m5 that fed into hydrological model h2 to produce a foreseen runoff that in his experience leads to a lake level exceeding thresholds. As in this hypothetical case the exceedance may crucially depend on heavy precipitation, end user X may want to assess the predictions of other atmospheric models for the same region. Possibly even other hydrological mode results may be available on the Visualisation Platform. The latter will also be used by both atmospheric and hydrological forecasters in their decision finding process when alerts need to be issued. Finally, all data, including alerts and feedback will be stored in a data archive that is being set up in collaboration with COPS (Convective Orographic Precipitation Study; Behrendt, Wulfmeyer et al. 2006) for an a posteriori verification and evaluation.

D-PHASE is organised in four working groups ('Data Interface', 'Data Policy', 'Hydrology and End Users', 'Verification') that are mainly responsible for defining the needs of the different communities, common lists of variables, common formats and transfer procedures. A scientific Steering Committee oversees the development and defines the overall strategy. Finally a Program Office has been established at MeteoSwiss with the second author of this abstract serving as the D-PHASE coordinator. More detail on the project goals and procedures as well as information on names and contributions by various individuals and institutions can be found at www.map.meteoswiss.ch/d-phase.

REFERENCES

Behrendt A., Wulfmeyer V. et al., 2006: Convective Orographic Precipitation Study, COPS, *Proceedings 1st D-PHASE Scientific Meeting*, November 6-8 2006, Vienna, A, p29.

Bougeault, P., P. Binder, A. Buzzi, R. Dirks, R. Houze, J. Kuettner, R. B. Smith, R. Steinacker, and H. Volkert, 2001: The MAP Special Observing Period. Bull. Amer. Meteorol. Soc. **82** , 433-462.

Keenan T.D. et al., 2004: Foreword to the special issue of *Weather and Forecasting*, **19**, 5-6.

Volkert H, 2005: The Mesoscale Alpine Programme (MAP): A multi-facetted success story, *Proceedings ICAM/MAP*, Zadar, 23-27 May 2005; online: http://www.map.meteoswiss.ch/map-doc/icam2005/pdf/sesion-15/S15-01.pdf

CALIBRATION OF THE EUROPEAN REGIONAL MULTI-MODEL ENSEMBLE SRNWP-PEPS

Michael Denhard & Sebastian Trepte

Deutscher Wetterdienst, Offenbach, Germany
E-mail: *michael.denhard@dwd.de*

Abstract: Bayesian Model Averaging (BMA) is used to calibrate SRNWP-PEPS ensemble forecasts.

Keywords – *Ensemble, Calibration*

1. INTRODUCTION

The experimental Poor Man's Ensemble Prediction System of the EUMETNET SRNWP Program (SRNWP-PEPS, see http://www.dwd.de/PEPS) was established in the beginning of 2005. It incorporates 23 limited area forecast models of 20 European weather services. The PEPS probability products are redistributed to the contributing weather services on an operational basis four times a day. Ensemble means and probability products are available for precipitation, 10m wind speed, wind gust speed and maximum/minimum temperatures and provide forecasts up to 48h using 12h and 24h accumulation periods.

The basic PEPS assigns equal weights to the ensemble members and uses a nearest neighbour grid mapping for the interpolation of the different model grids to the reference PEPS grid. The forecasters at DWD found that this system already generates very stable forecasts and provides a useful guidance in situations when single models show great differences. However, these simple probabilistic PEPS forecasts are biased and uncalibrated. The Talagrand-diagram of the "raw" PEPS forecasts in figure 1 of the maximum temperature in March shows that in many cases the ensemble forecasts are colder than the observation. A forecast system is calibrated, if Intervals or events that we declare to have probability P happen a proportion P of the time. Of course, calibration is necessary but not sufficient: ensemble forecast distributions are supposed to be sharp. Prediction intervals must be narrower on average than those obtained from climatology.

2. METHOD AND DATA

To be able to generate calibrated and sharp PEPS forecasts the Bayesian Model Averaging technique (BMA, Raftery et. al., 2005), developed at the University of Washington, was established at DWD. Raftery et al. (2005) additionally provides an overview of alternative techniques for ensemble calibration. The BMA fits a parametric distribution function to the forecast error distributions of each ensemble member so that the weighted sum of the single member distributions is calibrated and sharp. In addition to BMA a simple linear bias correction scheme is applied. We will show results of BMA calibrated PEPS forecasts for 2m temperature and surface wind data of 2005 and 2006 using station data from Germany. A sub-ensemble from the SRNWP-PEPS of 14 members with a constant ensemble size over Germany is used. The training period covers 25 days. Work on the calibration of PEPS precipitation forecasts is in progress and will be based on the BMA proposed by McLean Sloughter et al., 2006.

3. RESULTS

Figure 1 shows that BMA is able to produce calibrated PEPS forecasts with a flat PIT-histogram. When comparing the three error distributions of the raw ensemble, the ensemble with bias correction only and the fully calibrated ensemble, it can be seen that the bias correction underestimates negative and overestimates positive errors. This is corrected by BMA. There is an overall gain in the mean absolute error (MAE) of about 0.2°K using the fully calibrated BMA ensemble which means that the calibrated forecast distributions of 2m maximum temperature are sharper than those from the raw ensemble. This is obtained by giving significant weights only to a small number of models that outperform the other ensemble members during the training period. From January to March 2006 this number is in the order of 4.

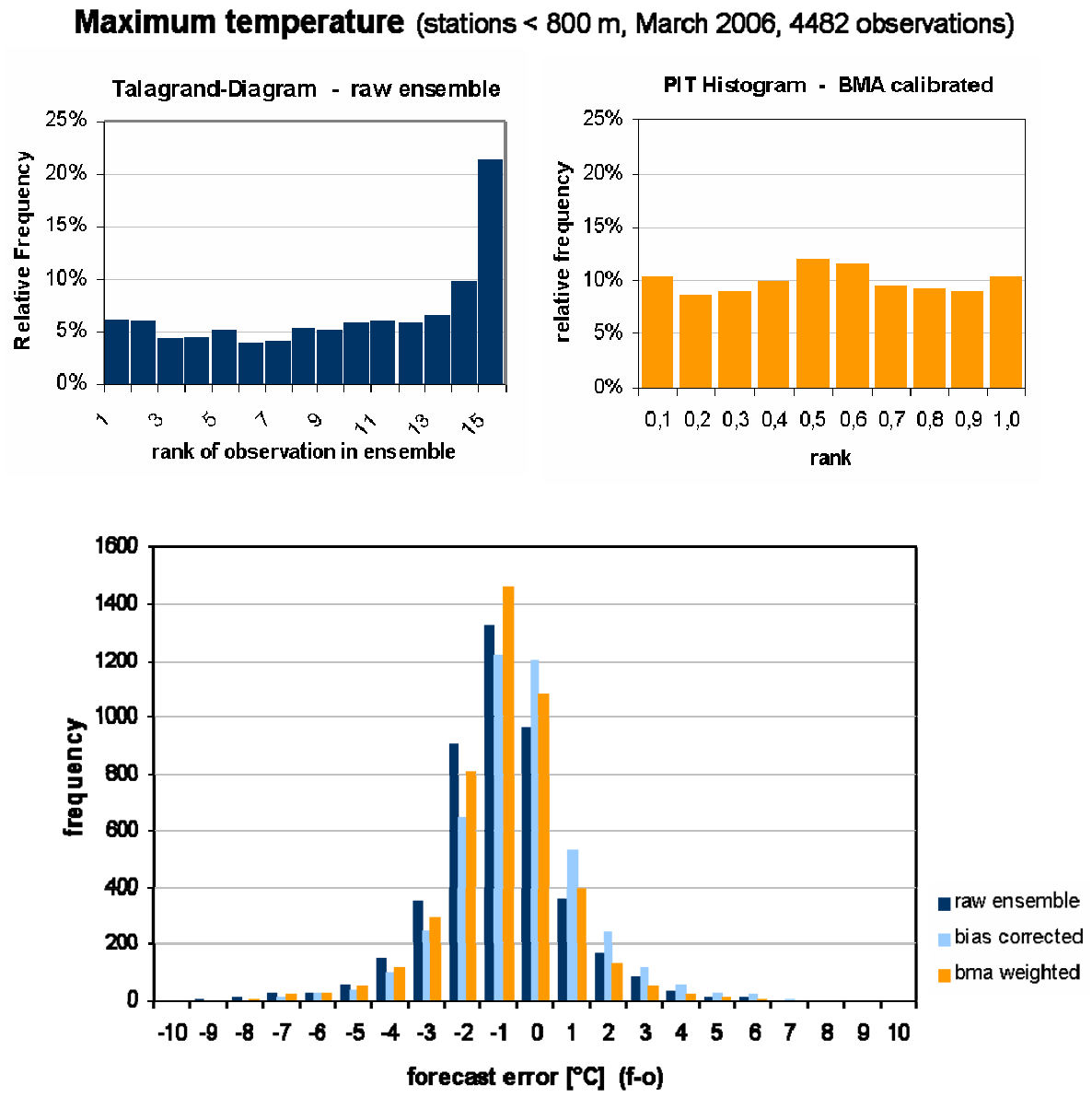

Figure 1. Talagrand-diagramm of the raw and PIT-histogram of the BMA calibrated SRNWP-PEPS forecasts of maximum temperature in March 2006 (upper panels). The lower panel shows the error distributions of the raw, the bias corrected and the fully calibrated (bias correction + BMA) ensemble forecasts.

4. CONCLUSION

The BMA is able to produce calibrated and to some extend sharper forecast distributions from the raw SRNWP-PEPS. We are planning to start the operational distribution of calibrated PEPS products in Spring 2007.

Acknowledgements: *Many thanks go to the director of the EUMETNET SRWNP program Jean Quiby.*

REFERENCES

Raftery, A., T. Gneiting, F. Balabdaoui and M. Polakowski, 2005: Using Bayesian Model Averaging to Calibrate Forecast Ensembles. Monthly Weather Review **133** , 1155-1174.

McLean Sloughter, J., A. Raftery and T. Gneiting, 2006: Probabilistic Quantitative Precipitation Forecasting using Bayesian Model Averaging,Technical Report no. 496, Department of Statistics, University of Washington

AN INTERMEDIATE–COMPLEXITY MODEL FOR DATA ASSIMILATION

Martin Ehrendorfer[1] and Ronald M. Errico[2,3]
[1]Institute of Meteorology and Geophysics, University of Innsbruck, Innsbruck, Austria
[2]Goddard Earth Science Technology Center, University of Maryland Baltimore County, MD, USA
[3]Global Modeling and Assimilation Office, NASA Goddard Space Flight Center, MD, USA

Abstract: In the process of assessing properties of data assimilation methods, it is critical to study these methods within the framework of models that faithfully resemble atmospheric properties, such as time scales, dynamics, and error growth behavior. At the same time, models used for exploring properties of data assimilation methods need to be restricted in terms of their resolution and complexity to allow for extended experimentation in spite of the high computational expense of most data assimilation methods. A model with realistic behavior and intermediate complexity that is based on the nonlinear quasigeostrophic potential vorticity equation is presented here. It contains a number of physical processes, such as climatological forcing, diffusion, and damping to match observed atmospheric properties; its dynamical core is spectral. The model properties are compared against atmospheric properties in terms of energy spectra, time-mean and transient behavior, as well as in terms of singular-vector perturbation growth. The model behaves realistically at a variety of resolutions (horizontal and vertical). It is well suited for data assimilation studies due to its comparatively small numerical cost and the fact that it contains a complete tangent-linear and adjoint package.

Keywords: quasigeostrophic dynamics, data assimilation, predictability, mean and transient flow components

1. Introduction and Motivation

The primary objective of data assimilation is the construction of an optimal estimate of the atmospheric state by blending a priori and observational information. A variety of techniques have been proposed to address this objective, among them variational, sequential, and ensemble–based methods. In the process of assessing the properties of these data assimilation methods, it is critical to study them in the framework of models that faithfully resemble atmospheric properties, such as time scales, dynamics and error growth behavior. At the same time, due to the high computational expense of most data assimilation methods, models used for exploring properties of data assimilation methods need to be restricted in terms of their resolution and internal complexity.

2. Model Description: Dynamics, Discretization, and Physics

A model possessing both of the above properties (realistic behavior and reduced complexity), named **AMIC** (**A**tmospheric **M**odel of **I**ntermediate **C**omplexity) is presented here. AMIC is based on the QG potential vorticity (PV) equation. It uses a spectral representation in the horizontal. It may be run for variable choices of horizontal and vertical resolution.

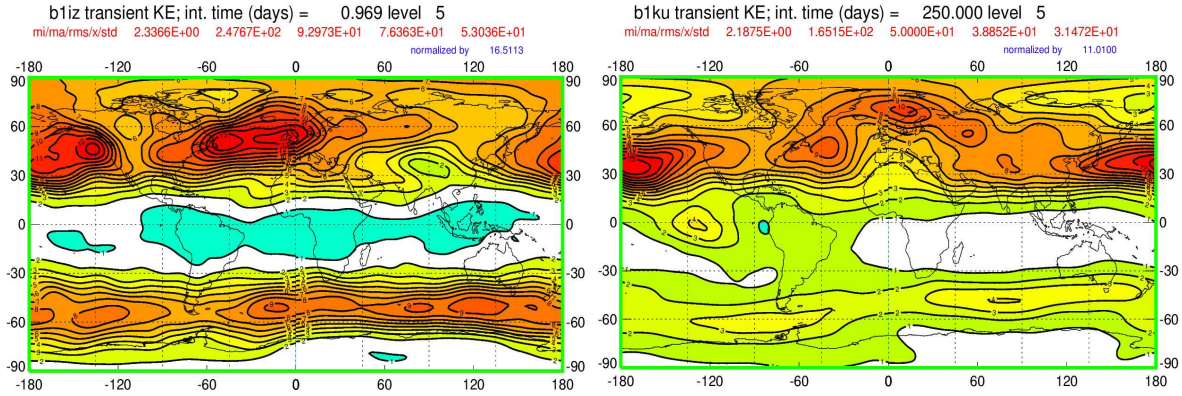

Figure 1: Kinetic energy in J/kg of the transient flow component at around 500 hPa. Left panel: observed, normalized by 16.51 (derived from ECMWF analyses over 2000–2005); right panel: AMIC model results, normalized by 11.01, obtained at resolution T106L9, with a relaxation time scale of $\tau = 20$ days.

In its spirit, AMIC is similar to the model described by Marshall and Molteni (1993) (see also, Molteni 2003; Lapeyre and Held 2004) and it also uses that same vertical discretization (Ehrendorfer 2000). However, AMIC possesses different physical processes that may be summarized as ($\hat{q}_{n,m}$ and $q_{n,m}$ are spectral components of relative and absolute QG PV):

$$\frac{\partial}{\partial t}\hat{q}_{n,m} = F_{n,m} - \tau^{-1}(q_{n,m} - \bar{q}_{n,m}) + \nu_\alpha d_n(q_{n,m} - \bar{q}_{n,m}) + S_{n,m} - k_v(\sigma)\zeta_{n,m} \ . \qquad (1)$$

In eq. (1), the second term on the right–hand–side represents a relaxation term (that is proportional to the difference of PV and a climatological reference PV) with relaxation time τ. The third term is a diffusion term (treated fully implicitly) consisting of contributions proportional to ∇^2 and ∇^6 of the deviation of PV from the climatological PV, with an e–folding time scale for the smallest spatial scales given by τ_ν. The fourth term describes the inclusion of a constant PV source that is added to the actual PV tendencies. This constant PV source is computed from model tendencies that take into account the specific relaxation and diffusion settings – as set for a given model run. As a result, the long–term time mean of the model's time tendency should be close to zero (e.g., Barkmeijer et al. 2003). The last term in (1) denotes linear low–level

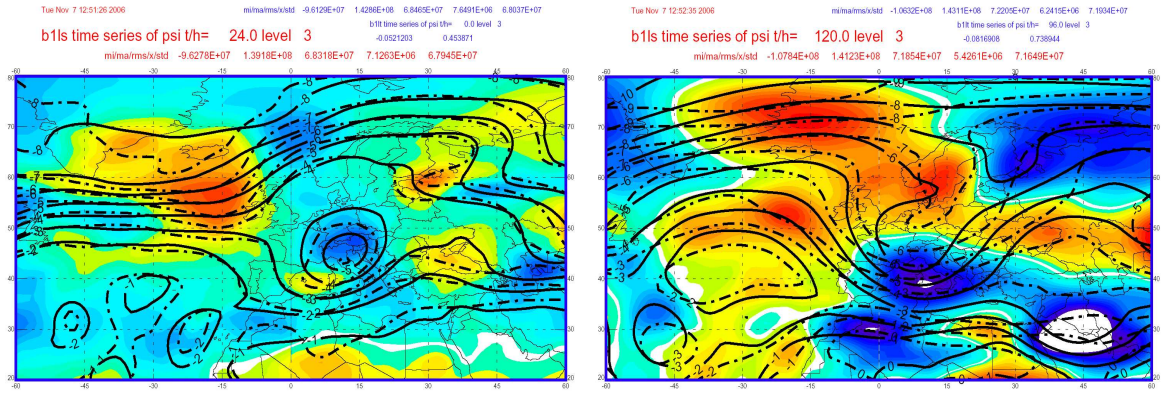

Figure 2: AMIC forecasts at 300 hPa verifying at the same time, but started from initial conditions 24 hours apart. Isolines show geostrophic streamfunction in units of 10^7 m^2 s^{-2}. In the left panel the 24–hour forecast (solid black contours) for 22/08/2005/00UTC and the analysis (black dashed contours) are shown; the right panel shows the 5–day forecast (solid) versus the 4–day forecast (dashed) for 26/08/2005/00UTC. Shading indicates the difference between the longer and the shorter lead–time forecasts (solid minus dashed contours). The color scale ranges from -1.5 (blue) units to $+1.5$ (red) units. The global rms difference between forecasts is 0.45 units in the left panel, and 0.74 units in the right panel.

damping following the specifications of Held and Suarez (1994); its inclusion was found necessary to prevent very small–scale SV structures at the lowest model levels from appearing when the model is used at resolution T106L9, representing the important boundary–layer damping effect. The model presently uses no orography. The adjoint of this model has been developed as well. The observed fields needed to compute the input to these physics consist of January ECMWF analyses of relative vorticity for the years 2000–2005.

3. Properties of the Model: Transients and Predictability

It can be seen from Fig. 1 that the QG model exhibits reasonably realistic behavior in terms of the kinetic energy of the transient flow. Structures in the northern hemisphere are well reproduced, being, however, too small by approximately a factor of two. It appears to be difficult to correctly describe the transient behavior in the southern hemisphere. However, the use of $\tau = 20$ days shows a marked improvement in southern hemisphere transient activity as compared to using $\tau = 10$ days (not shown). Further details concerning the behavior of this model may be found in Ehrendorfer (2005) and Ehrendorfer (2006b). In terms of predictability and the divergence of initially close model states, Fig. 2 clearly demonstrates the error growth behavior of AMIC, as found in other much more realistic atmospheric prediction models, too (Ehrendorfer 2006a).

4. Discussion and Concluding Remarks

The spectral QG model AMIC has been discussed. This model possesses simplified physics used to tune its behavior towards observed January conditions. While it is easy to reproduce the observed *mean* state through a strong relaxation term, using a small τ in eq. (1), such tuning counteracts the strength of the *transient* component of the flow. However, a correct time–mean is needed to provide energy to the transient flow components. It is thus necessary, in general, when tuning models of the type presented here, to balance between the realism of the time–mean flow and the strength of the transient flow. Such balancing is successfully achieved here. AMIC kinetic energy spectra clearly reveal a spectral slope of minus three (not shown). It is difficult to get the transient flow in the summer hemisphere right (Fig. 1), since it is convectively, as well as dynamically driven, with the former not modeled. AMIC appears to model correctly the time scales for instabilities which is critical for data assimilation studies since these time scales determine asymptotic data assimilation results that depend on the balance between short–term error growth and the correction of the background by observations in the analysis step.

In terms of the assessments discussed or shown – such as mean flow, kinetic energy of mean and transient flow components, energy spectra, long–term behavior, and error growth – AMIC shows realistic behavior compared to observed atmospheric conditions. The model is of intermediate complexity and thus fully suited for performing extensive suites of data assimilation experiments. AMIC is therefore arguably a useful tool for further data assimilation and predictability studies, also since it includes tangent–linear and adjoint code.

References

Barkmeijer, J., T. Iversen, and T.N. Palmer, 2003: Forcing singular vectors and other sensitive model structures. *Quart. J. Roy. Meteor. Soc.*, **129**, 2401–2423.

Ehrendorfer, M., 2000: The total energy norm in a quasigeostrophic model. *J. Atmos. Sci.*, **57**, 3443–3451.

Ehrendorfer, M., 2005: Second Interim Report 2005 ECMWF Special Project – SPATME02 "Mesoscale Predictability and Ensemble Prediction". [Available from ECMWF, Shinfield Park, Reading RG2 9AX, England].

Ehrendorfer, M., 2006a: The Liouville equation and atmospheric predictability. In: *Predictability of Weather and Climate*, T. Palmer and R. Hagedorn (Eds.), pp. 59–98. Cambridge University Press, Cambridge, UK, 702 pp.

Ehrendorfer, M., 2006b: Third Interim Report 2006 ECMWF Special Project – SPATME02 "Mesoscale Predictability and Ensemble Prediction". [Available from ECMWF, Shinfield Park, Reading RG2 9AX, England].

Held, I.M., and M.J. Suarez, 1994: A proposal for the intercomparison of the dynamical cores of atmospheric general circulation models. *Bull. Amer. Meteorol. Soc.*, **75**, 1825–1830.

Lapeyre, G., and I.M. Held, 2004: The role of moisture in the dynamics and energetics of turbulent baroclinic eddies. *J. Atmos. Sci.*, **61**, 1693–1710.

Marshall, J., and F. Molteni, 1993: Toward a dynamical understanding of planetary-scale flow regimes. *J. Atmos. Sci.*, **50**, 1792–1818.

Molteni, F., 2003: Atmospheric simulations using a GCM with simplified physical parameterizations. I: model climatology and variability in multi–decadal experiments. *Climate Dynamics*, **20**, 175–191.

DOES THE GLOBAL OBSERVING SYSTEM CONTAIN A 'SATELLITE ACHILLES HEEL'?

Andy Lawrence, Martin Leutbecher and Tim Palmer

European Centre for Medium-Range Weather Forecasts, Reading, UK
E-mail: *a.lawrence@ecmwf.int*

Abstract: Singular vectors can identify dynamically sensitive structures of the atmosphere. Initial errors in the directions of the leading singular vectors are assumed to explain a significant fraction of the forecast error for a specific verification region and forecast range. The structure of these optimal perturbations depends on the choice of initial-time metric. Singular vectors based on the total energy metric are compared with singular vectors based on an estimate of the analysis error covariance metric coming from a 4D-Var assimilation scheme (the so-called `Hessian' metric). The characteristics of the different sets of singular vectors at initial time present important implications for observation targeting. In order to constrain initial errors with structures that are shallow or are located below cloud in the mid/lower troposphere, in-situ observations are expected to be more suitable than satellite radiances if one considers upgrades of the observing network during a single assimilation cycle. Upgrades of the observing network that persist for several assimilation cycles will also increase the accuracy of the background field. However, this effect has not been quantified in this study.

Keywords – *Observation Targeting, Singular Vectors*

1. INTRODUCTION

Certain regions of the globe are well represented by ground-based and airborne observations (i.e. USA, Europe), but there are many regions (i.e. Poles, Southern Oceans) that have few in-situ measurements due to geographical or logistical constraints. These regions of low observation density can generate errors that contribute to a reduction of forecast skill and lead to inaccurate predictions of important meteorological events. Satellite data provides the most comprehensive observational coverage of remote regions, but can fail to detect structures that are shallow or beneath cloud. If these structures contain important dynamical and statistical information, then supplemental sampling using ground, aircraft and ship-based observations may be beneficial. This study aims to address if there is a credible limitation to the sampling of these structures via satellite (a so-called 'Satellite Achilles Heel'). If so, this represents a viable case for the use of in-situ measurements for improving weather forecasting of short-range events, which forms one of the central scientific questions of THORPEX.

2. SINGULAR VECTOR COMPARISONS

Singular vectors define the most unstable perturbations from an initial (analysis) time to a final (forecast) time. If computed using an appropriate metric or 'norm', they are particularly useful for diagnosing the most dynamically-sensitive structures that contribute to a majority of the forecast error. Sensitive regions derived from these structures identify where observations should be taken for optimum benefit to the forecast. The total energy norm provides a first-order approximation to the analysis error covariance matrix (Palmer, 1998), whereas the Hessian norm can be shown to be equal to the inverse of the analysis error covariance matrix (Barkmeijer, 1998).

The structure of Total Energy and Hessian singular vectors targeted on Europe have been examined for numerous cases using a T42 dry tangent linear/adjoint model and a 48-hour optimisation time. Hessian Singular vectors were computed with two configurations: (a) using the background error covariance matrix only ('partial' Hessian) and (b) using both the background and observational error covariance matrices ('full' Hessian) to estimate the value of the observational component. The structures of the leading singular vectors using these formulations are shown for a representative case in December 2003 in figure 1. For the case of the total energy norm, shallow, tilted structures are present in the lower and middle regions of the atmosphere, consistent with the tilt against vertical shear often seen in examples of baroclinic structures. The full Hessian exhibits similar structures in the lower atmosphere. However, the structures of the singular vectors based on the partial Hessian are spatially larger with smaller maximum amplitudes. This indicates that the inclusion of the observational information (in the full Hessian) penalises the large-scale equivalent barotropic modes (that manifests in the partial Hessian), leaving smaller-scale baroclinic-type structures in the lower troposphere (similar to the types of modes obtained using a total energy initial norm).

By using numerous methods to compare the structural differences of the singular vector formulations (i.e. wavenumber spectra, vertical energy profiles), it can be determined if these results are generic, which would suggest particular implications for observation targeting. Assuming the structures of the leading singular vectors are representative of the forecast error, it is important to accurately measure these structures at initial time to monitor their development. The relatively low altitude and shallow, baroclinic nature of the TESV and HSV

structures may present a problem for satellite sampling over a single assimilation cycle. Tropospheric temperature profiles can be conveniently sampled by high-spectral-resolution infrared radiometers in clear-sky conditions, but the presence of cloud significantly reduces the radiance signal. Also, the weighting functions employed in remote sensing used to interpolate between the observed vertical levels often smooth out the detail in shallow structures. Thus, features that develop into the forecast error structures may not represented correctly without the use of high-resolution observations in the vertical that traditional in-situ techniques employ.

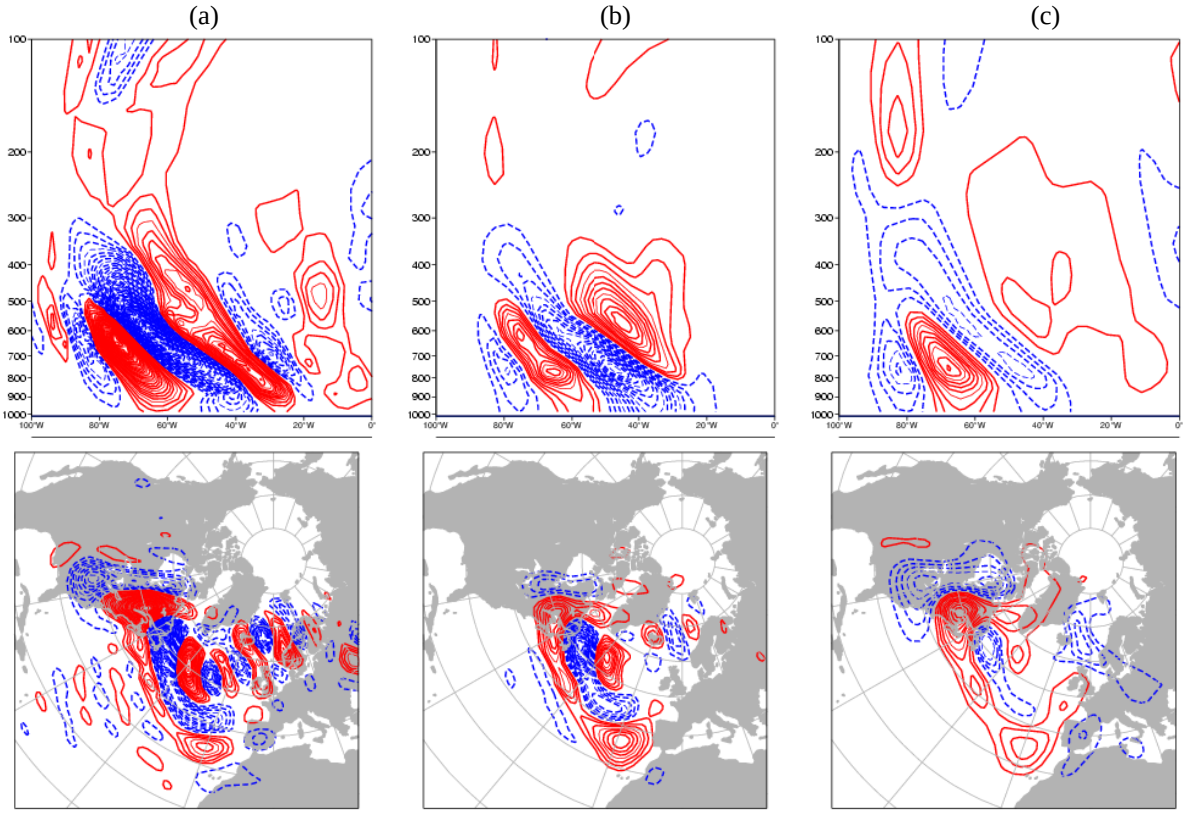

Figure 1. Vertical cross-sections along 50^{o}N (top) and plan views at ~750 hPa (bottom) of initial temperature fields for the leading singular vectors for (a) TESVs, (b) full HSVs and (c) partial HSVs for 23 December 2003 (12UT). Contours are at intervals of 0.0025K.

3. CONCLUSIONS

The singular vector structures derived from the Hessian norm are heavily dependent on observational information. In this study, where a single assimilation cycle is considered, the sensitive structures (using total energy and full Hessian norms) tend to be located within cloud-layers and may cause satellite radiance information to be partially or wholly obscured. Under these circumstances, in-situ measurements may be beneficial. If considering several assimilation cycles and using 4D-Var assimilation techniques, one can assume that this will increase the accuracy of the background field. Therefore it is important to recognise that further development of this background component within the Hessian norm may help to improve analysis error covariance definition. This, along with improvements of tangent-linear, adjoint and forecast models enhance the ability to interpolate data spatially and temporally from well-observed regions to remote areas. Despite satellite technology continuing to advance into increasingly cost-effective methods for gaining global observation coverage, any further experimentation to explore these extended issues should cater for both advances of instrumentation techniques and observation targeting methodology.

Acknowledgements: *This work received financial support via a THORPEX-Vaisala Fellowship.*

REFERENCES

Barkmeijer, J., M. V. Gijzen and F. Bouttier, 1998 : Singular vectors and estimates of the analysis-error covariance matrix, *Quarterly Journal of the Royal Meteorological Society*, **124**, 1695-1713.
Palmer, T. N., R. Gelaro, J. Barkmeijer and R. Buizza, 1998, Singular vectors, metrics and adaptive observations, *Journal of the Atmospheric Sciences*, **55**, 633-653.

THE GREENLAND FLOW DISTORTION EXPERIMENT

Guðrún Nína Petersen [1], Ian A. Renfrew, G. W. Kent Moore, Haraldur Ólafssons and Jón Egill Kristjánsson

[1] School of Environmental Science, University of East Anglia, Norwich, UK
E-mail: *g.n.petersen@uea.ac.uk*

Abstract: The Greenland Flow Distortion Experiment (GFDex) is a international fieldwork and modelling based project, with the fieldwork part taking place in 2007. It will investigating the role Greenland plays in distorting atmospheric flow over and around it, affecting local and remote weather systems and, via air-sea interaction processes, the coupled climate system.

Keywords *– THORPEX, IPY, Greenland, tip jet, barrier wind, mesoscale cyclones, targeted observations*

1. INTRODUCTION

The Greenland Flow Distortion Experiment (GFDex) is an international fieldwork and modelling-based programme taking place year 2006-2008. It investigates the role that Greenland plays in distorting atmospheric flow over and around it, affecting local and remote weather systems and, via air-sea interaction processes, the coupled climate system.

The field campaign will take place in February and March 2007. The FAAM (the Facility for Airborne Atmospheric Measurements), operating from Keflavík, Iceland, will be used to make detailed *in situ* measurements of intense atmospheric forcing events that are thought to be important for modifying the ocean in this area; tip jets, barrier winds and mesoscale cyclones. Greenland's role in atmospheric flow predictability will also be investigated using targeted observations.

2. BACKGROUND

Greenland has a major influence on the weather and climate of the North Atlantic and Western Europe. It deflects flow both over and around itself, i.e. distorting the atmospheric flow, with both local and remote consequences. High wind weather phenomena in Greenland's vicinity that have serious impact on maritime and other human activities are e.g. tip jets and reverse tip jets: westerly and easterly low-level wind jets initiated at Cape Farewell; barrier winds: low level wind jets along the south-eastern coast of Greenland and mesoscale cyclones or polar lows: 100-500 km scale cyclones that are common in this area. These weather systems present a much immediate modelling and prediction challenge which has not been addressed, largely due to the relatively few *in situ* observations in this geographically remote region. These same mesoscale weather systems may also induce large air-sea exchanges of heat, moisture and momentum (Pickard *et al.*, 2003; Moore and Renfrew, 2005) and thus play a key role in controlling the coupled atmospheric-ocean climate system. Furthermore, the region over and around Greenland has been shown to be often highly sensitive to the growth of small initialization errors in numerical weather forecasts.

3. OBJECTIVES

The key objectives of the project are to:

- Improve our understanding and ability to predict interactions between the atmospheric circulation and the topography of Greenland, both locally and downstream over Western Europe.
- Obtain hitherto rare *in situ* observations of high-impact weather systems and their associated air-sea fluxes in the coastal seas of Greenland.
- Improve the numerical modelling of these weather systems, testing e.g. the boundary-layer and turbulence parametrisations, and thus improving the quality of the atmospheric forcing fields that are essential for accurate atmosphere-ocean coupling and the thermohaline circulation.
- Increase knowledge of the sensitivity of the large-scale downstream flow to the flow distortion caused by Greenland; thereby investigate the prediction of high-impact weather systems over Europe through the use of targeted observations upstream in sensitive areas of the flow.

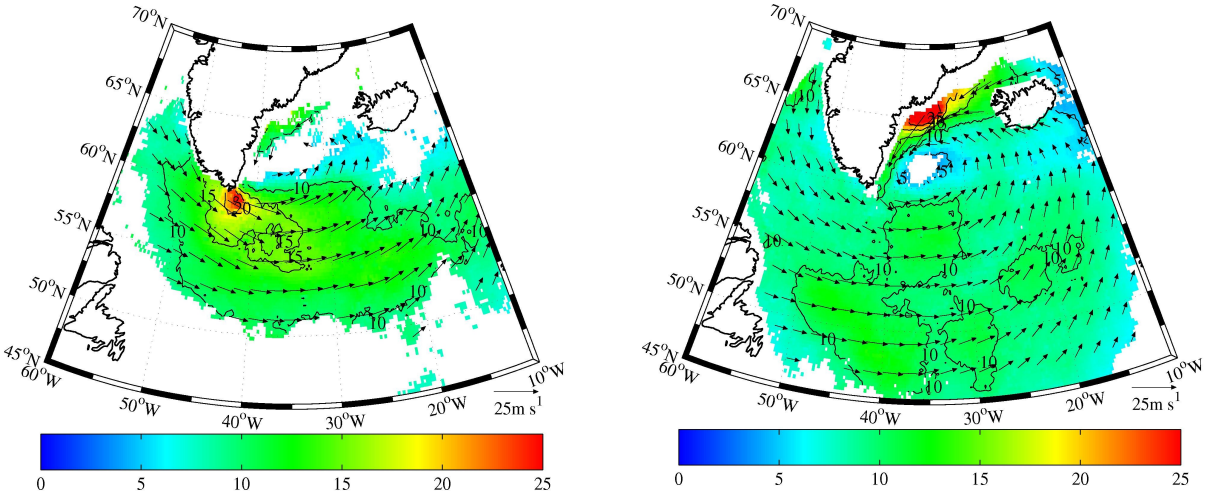

Figure 1. Surface wind speed and wind vectors associated with, left, tip jet events and, right, barrier wind events (Denmark Strait South) from QuikSCAT climatology. Only statistically significant data are shown. From Moore and Renfrew (2005).

4. METHODOLOGY

During the GFDex field campaign, that takes place 16 February - 12 March 2007 the FAAM will be used to obtain *in situ* observations of tip jets, barrier winds and mesoscale cyclones. For each case, a high level dropsonde flight component will map out the general structure of the system and a low-level boundary layer component will measure the boundary layer structure and associated air-sea turbulent fluxes. In order to identify sensitive region, the European Centre for Medium Range Forecasts (ECMWF) will provide singular vector sensitive area predictions (SAP) and the UK Met Office SAPs based on the ensemble transform Kalman filter (ETKF), both with verification areas over Europe. Targeted observations will be carried out when sensitive areas are within the range of the aircraft. Dropsondes will also be released outside of SAPs. These will act as additional "random distribution" observations and thus can be used as controls in the impact assessment studies.

Numerical modelling experiments of the high impact local weather systems will evaluated and refined using the aircraft based observations. This will increase our understanding of these systems and, through comparison with other observations and data sets, provide accurate fields of air-sea heat and moisture fluxes for driving ocean and climate models. Furthermore, modelling will be used to assess any improvement from the additional targeted observations.

The GDFex is an international project with participants from the UK, Canada, Norway and Iceland with the UK Met Office and the ECMWF as project partners providing SAPs. It is a part of IPY-THORPEX and is funded by Natural Environment Research Council, Canadian Fund for Climate and Atmospheric Sciences, European Fleet for Airborne Research and EUCOS. Further information on GFDex and its development can be found on the web site: http://lgmacweb.env.uea.ac.uk/e046/research/gfdex/index.htm

5. SUMMARY

GFDex is an project investigating Greenland role in distorting the atmospheric flow over and around it, affecting local and remote weather systems and, via air-sea interaction processes, the coupled climate system. The objectives of the project will be met through a 3-week instrumental aircraft field campaign and numerical modelling. The campaign will provide some of the first detailed *in situ* observations of the intense forcing events that may play an important role in controlling the coupled atmospheric-ocean climate system. The GFDex aims to improve the understanding and thereby enabling improve prediction of Greenland's interaction with the atmosphere on both short and long time scales.

REFERENCES

Moore, G. W. K. and I. A. Renfrew, 2005: Tip jets and barrier winds: A QuikSCAT climatology of high wind speed events around Greenland. *J. Climate* **18**, 3713-3725.

Pickart, R. S., M. A. Spall, M. H. Ribergaard, G. W. K. Moore, and R. F. Milliff, 2003: Deep convection in the Irminger Sea forced by the Greenland tip jet. *Nature* **424**, 152-156.

THORPEX PACIFIC ASIAN REGIONAL CAMPAIGN: ASIAN PERSPECTIVE

Tetsuo Nakazawa

Meteorological Research Institute, Japan Meteorological Agency, Tsukuba, Japan

E-mail: *nakazawa@mri-jma.go.jp*

Keywords – *Regional Observational Experiment, Typhoon Forecast, Targeting Observation*

1. INTRODUCTION

Typhoon is one of the most severe weather phenomena in Asia. Every year, we experience many casualties and huge economic loss due to typhoon. It is urgently required to provide better typhoon forecast in longer lead-time to the society. Thus the Asian THORPEX Regional Committee (ARC) originated the special observation experiment in 2008 for typhoon (typhoon targeting observation) over the western Pacific. The plan of the experiment expanded to cover whole Pacific basin to collaborate with the North America THORPEX Regional committee, and the experiment is now called THORPEX Pacific Asia Regional Campaign (T-PARC). In this talk we present the overview and science issues of the Asian component of the T-PARC.

2. T-PARC

The objectives of Asian component of the T-PARC are summarized below.

I To describe and document the space-time evolution of the atmospheric circulation for better understanding of the predictability.

II To identify the influence of the atmospheric circulation to the downstream Rossby wave propagation to generate high-impact weather in Asia and North America.

III To demonstrate the capability of the THORPEX Interactive Grand Global Ensemble (TIGGE) for the societal and economical applications.

ARC identified four high-impact weathers : typhoon, heavy rainfall during the rainy season, dust storm and the Madden Julian Oscillation. T-PARC is the first observational experiment in the ARC.

3. TYPHOON TARGETING OBSERVATION

One of the challenging attempts during the T-PARC in Asia is typhoon targeting observation by several observational platforms; in-situ observation of manned/unmanned aircrafts, driftsondes or satellite remote-sensing data. Over the Atlantic hurricane reconnaissance flights are operational for many years, however, after 1987 there has been no operational typhoon reconnaissance flights over the western North Pacific. Recently the project of DOTSTAR (Dropsonde Observation for Typhoon Surveillance near the TAiwan Region) has begun GPS dropsonde airborne observation of typhoons over the region since 2002. The Japan Meteorological Agency (JMA) and several operational centers verified the impact of the sounding data obtained from DOTSTAR and concluded that the typhoon track forecast improved significantly (Wu et al., 2005, 2006) using DOTSTAR data. Some examples will be reported in this conference by JMA (Takeuchi et al., 2006).

The high-temporal and limited-area wind information near typhoon from satellites will be also utilized during the experiment. MTSAT-1 and MTSAT-2 have rapid scanning functions to observe not only full earth and hemisphere but also limited particular area. The rapid scanning will provide us detailed 3-D structure of typhoon; eye-wall, cumulus convections, rain bands and the wind in lower and upper troposphere.

REFERENCES

Takeuchi, Y., M. Yamaguchi, T. Iriguchi and T. Nakazawa, 2006: Observing System Experiments using a singular vector method for 2004 DOTSTAR case. 2nd THORPEX International Science Symposium (This Symposium).

Wu, C.-C., P.-H. Lin, S. D. Aberson, T.-C. Yeh, W.-P. Huang, J.-S. Hong, G.-C. Lu, K.-C. Hsu, I.-I. Lin, K.-H. Chou, P.-L. Lin, and C.-H. Liu, 2005: Dropwindsonde Observations for Typhoon Surveillance near the Taiwan Region (DOTSTAR): An overview. *Bull. Amer. Meteor. Soc.*, **86**, 787-790.

Wu, C.-C., K.-H. Chou, P.-H. Lin, S. D. Aberson, M. S. Peng, and T. Nakazawa, 2006: The impact of dropsonde data on typhoon track forecasts in DOTSTAR. Submitted to *Weather and Forecasting*.

SOUTHERN HEMISPHERE PERSPECTIVE OF THORPEX

Neil Gordon [1] and Kamal Puri [2]

[1] Meteorological Service of New Zealand, Wellington, New Zealand. Email: *Neil.Gordon@metservice.com*
[2] Commonwealth Bureau of Meteorology, Melbourne, Australia. Email: *K.Puri@bom.gov.au*

Abstract: A Southern Hemisphere Science Plan has been developed, and a Regional THORPEX Committee established. The Science Plan, and the activities which are being formulated in an associated Implementation Plan, recognise the unique geographical and meteorological features of the Southern Hemisphere, as well as focussing on the needs and capabilities of the countries in the region.

Keywords – *THORPEX, WMO, Southern Hemisphere, MJO, Antarctica.*

1. INTRODUCTION

A Southern Hemisphere THORPEX Science Plan has been developed by scientists interested in Southern Hemisphere meteorology. The draft was prepared by correspondence, and refined following a workshop in Melbourne, Australia in November 2005, and the WWRP/THORPEX Conference in Cape Town, South Africa in February 2006. At the conclusion of the Conference it was agreed to form a Southern Hemisphere Regional THORPEX Committee to take the Science Plan forward, and develop an associated Implementation Plan. The Committee includes scientists from Australia, New Zealand, Indonesia, the Cook Islands, Argentina, Brazil, Chile, Kenya and South Africa.

This presentation will describe the key features of the Science Plan, (available at http://www.wmo.int/thorpex/doc/Shem_THORPEX_fin4.doc) and report progress towards the development of the Implementation Plan and expected activities.

2. RATIONALE FOR A SOUTHERN HEMISPHERE REGIONAL FOCUS

The Southern Hemisphere Science Plan emphasises a number of geographical and meteorological features that are unique to the hemisphere. These include (i) a large percentage of the Southern Hemisphere is covered by oceans, leading to logistical challenges for data collection and the important role of satellite data; (ii) the various countries of the hemisphere have strongly overlapping problems associated with the monitoring and forecasting of weather and climate; (iii) large differences from the Northern Hemisphere in terms of the meteorology on the 1-day to 2-week timescale which is partly due to the weaker orographic and continental forcing of the Southern Hemisphere flow; (iv) the peculiar feature of the Southern Hemisphere summer circulation characterized by three major subtropical fronts (South Pacific Convergence Zone - SPCZ, South Atlantic Convergence Zone - SACZ and South Indian Convergence Zone –SICZ); (v) the role of Antarctica.

Discussions amongst scientists during the preparation of the plan revealed a commonality in forecast problems across the hemisphere. Examples include fire weather; the role of the Madden Julian Oscillation; flooding from cut-off lows off the east coast of Africa, South America and Australia; widespread flooding and loss of life associated with tropical cyclone landfall; and blocking anticyclones leading to extended heat-waves. There is also a common focus on improving forecast system performance through the assimilation of satellite observations in high-resolution limited area models.

3. DATA ASSIMILATION & OBSERVING STRATEGIES, INCLUDING OBSERVING SYSTEMS

Many Southern Hemisphere countries have relatively small economies, with a high dependence on agriculture and tourism. It is expensive to maintain remote observing sites in the large oceanic expanses, and many of the larger landmasses have data sparse interiors. Any THORPEX observing system experiments are likely to be relatively small scale, or building on the results of regional field experiments such as TWP-ICE, or in association with other programmes such as IPY. The overall focus is likely to be on exploitation of satellite data and optimising benefits from in situ observing. While very few Southern Hemisphere centres are in a position to contribute to advancing medium range model forecast skill, many are involved in various limited area modelling systems.

Given these factors, the activities in the area of observing and data assimilation are expected to include:

- Promoting the use of new observing systems suited for Southern Hemisphere use, including ASAP and AMDAR

- Assessing information from studies that assimilate routinely available observation network reports and making appropriate recommendations for adjusting networks and for further investigation
- Determining the impact of different/new systems (such as AMDAR humidity) on a research basis
- Collaboration between centres interested in Southern Hemisphere NWP in general and data assimilation in particular
- Data assimilation in the tropics
- Characterization of background errors in the tropics and Southern Hemisphere, including their estimation, specification and evolution for high resolution NWP
- Methods for processing and assimilating high volume satellite data, including observation error characterization, forward modelling, data thinning and compression

4. PREDICTABILITY AND DYNAMICAL PROCESSES

Various significant phenomena which affect one or more regions of the Southern Hemisphere, and are documented in the Science Plan, include tropical cyclones, cut-off lows, intense extratropical cyclones, cold fronts, the South American Low Level Jet (SALLJ) east of the Andes, mesoscale convective systems, longer timescale influences such as the Madden-Julian Oscillation (MJO), and intense weather events in Antarctica and high latitudes which subsequently impact middle latitudes. Although some phenomena such as tropical cyclones are already covered under both the World Weather Research Programme (WWRP) and the Working Group on Tropical Meteorology Research Programme (WTMRP), the emphasis under THORPEX should be on predictability studies and on extending the range of prediction out to a week and longer.

One particular activity being considered for the Implementation Plan is setting up a publicly accessible web page to monitor predictability and dynamical processes in real time; this should encourage communication and interactions amongst the Southern Hemisphere countries. Other particular focuses are expected to be tropical systems including tropical cyclones, the MJO, and Antarctic and Southern Hemisphere polar latitudes phenomena.

5. SOCIETAL AND ECONOMIC APPLICATIONS

The Southern Hemisphere Science Plan recognises the crucial role of applications as part of the THORPEX programme, with its end-to-end focus. There is a need to exploit *existing* as well as improved prediction systems to bring benefits to society, economies and the environment. In both the global context and for the Southern Hemisphere specifically, it is important to note that the term “high-impact weather forecast” does not equate solely to forecasts of severe weather. Forecasts will have high impact if they enable users to make weather-related decisions that make a significant difference.

The challenge for many developing countries in *both* hemispheres, but particularly in regions such as southern Africa, lies in the application of sophisticated new technologies, developed in first world environments, to the benefit of communities at risk in developing environments, allowing them to take efficient advantage of weather forecasts, reducing their vulnerabilities, and increasing their coping capacities.

Planned Southern Hemisphere activities in this area include compiling systematic inventories of high impact weather forecast opportunities, developing new user-specific weather products and applications through engagement of end users, communication of forecast uncertainty, promote the availability and use of existing model guidance products, estimating the net benefits of improved forecasting systems, and collaboration with other THORPEX regional programmes and WMO initiatives.

6. CONCLUSION

THORPEX has been a valuable catalyst for collaborative effort amongst scientists from Southern Hemisphere countries who have worked together to prepare a Science Plan focussing on unique Southern Hemispheric characteristics, and who are now formulating an associated Implementation Plan. This will result in a coordinated Southern Hemisphere THORPEX activity, involving scientists in a number of interested Southern Hemisphere countries; arguably the first time such a coordinated activity has occurred in our hemisphere.

THE CHALLENGE OF ORGANIZED TROPICAL CONVECTION IN THE THORPEX ERA

Mitchell W. Moncrieff [1] and Duane Waliser

[1] Cloud Systems Group, Mesoscale and Microscale Meteorology Division, NCAR, Boulder, Colorado, USA
E-mail: *moncrief@ucar.edu*

Abstract: The modern approach to multi-scale convective organization, notably in the context of the Madden-Julian Oscillation (MJO), involves cloud-system resolving simulation, dynamical theory, and observations. Advances in these areas are summarized. An integrative initiative is proposed: *TRopical Observations and Predictions for Improving Convective System Simulation (TROPICSS*) focused on the meso-to-global and diurnal-to-subseasonal range of scales. Integration of cloud-system models with space-based measurements is an important part of this initiative.

1. INTRODUCTION

Precipitating convection is the building block of tropical weather systems and scale-interaction with the Earth's global climate. The ubiquity of convective organization was first identified during the GATE field campaign in the 1970's and confirmed during TOGA COARE in the 1990s. Satellite measurements show tropical convection is organized on a hierarchy of scales (cumulonimbus, mesoscale convective systems, superclusters) embedded in the Kelvin-Rossby wave environment of the deep tropics. While the Madden-Julian Oscillation (MJO) is the outstanding example, convective organization is widespread occurring within the ITCZ, the monsoons, and over continents (tropics and higher latitudes). The genesis of the MJO is a key issue in regard to the generation of planetary waves which influence global weather through the teleconnection mechanism. The reader is referred to ECMWF (2003), Waliser et al. (2006), and Zhang (2005) for background.

The multi-scale organization of precipitating convection and its approximation in global models is ripe for advancement as a result of advances in theory, simulation and observations. Global models that operate convective parameterizations struggle with the MJO. Figure 1 summarizes pertinent issues. On the other hand, cloud-system resolving models (CRM) are relatively successful because the dynamics of convective organization (e.g., propagation, structure, life-cycle, and upscale transport) are represented explicitly. It will be decades before climate-change models resolve convection so the parameterization of convective organization is salient.

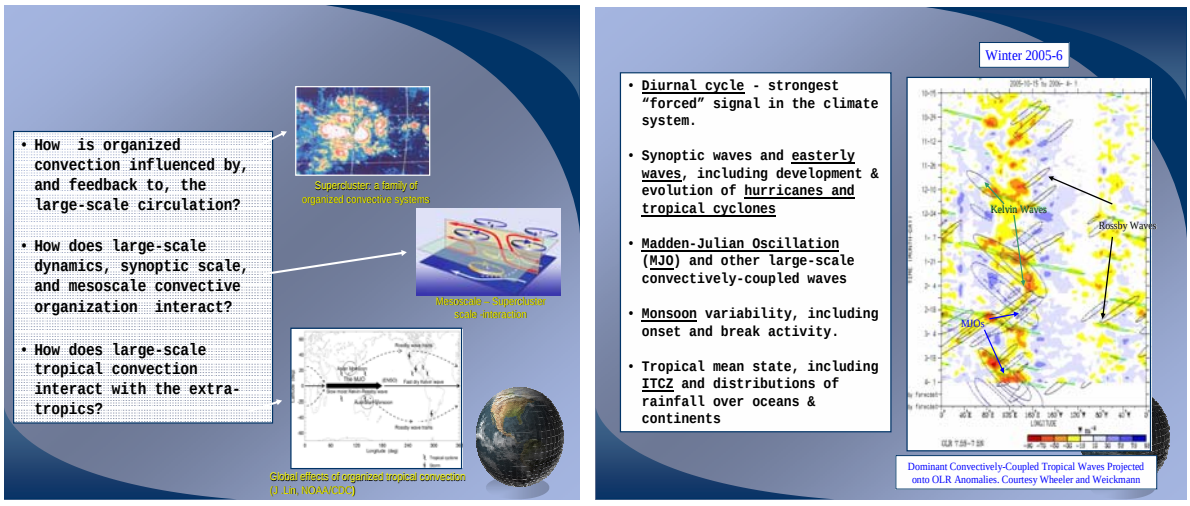

Figure 1. Multi-scale organization of tropical convection is a grand challenge in the prediction of weather and climate.

2. INTEGRATIVE APPROACH

Significant progress is anticipated based on advances in numerical simulation and theory. The fidelity of the early CRMs in simulating squall lines and mesoscale convective systems has long been recognized. Modern CRMs take a vital further step - quantifying interaction and coupling between convection and the large-scales of motion. Figure 2 (left) summarizes four categories of explicit model: global CRMs, super-parameterized models, scaled-equation models (DARE), tropical channel/nested models.

The CRM simulation results are underpinned by the theory of convective organization (Fig. 2, right). The concept of convective organization is rooted in control by vertical shear, self-organization by downdrafts, and

the upscale effects of organized transport (especially momentum transport). These principles have been generalized to explain interlocked scales of convective organization associated with the MJO and convectively-coupled waves (Moncrieff 2004; Biello and Majda 2005).

The dynamic range of modern CRMs (up to global scale) is too large to be validated by field-campaign data alone. A combination of field-campaign data and remotely-sensed data is essential. The suite of modern satellite measurements is unprecedented. Of particular interest is the vertical profiling of moist physics: TRMM (precipitation), CloudSat (light precipitation and condensate) and Calipso (thin cirrus and aerosol); MODIS (cloud characteristics); AIRS, AMSRE, and COSMIC (environment); CERES (top-of-atmosphere energy budget); and ocean surface winds (QuickScat).

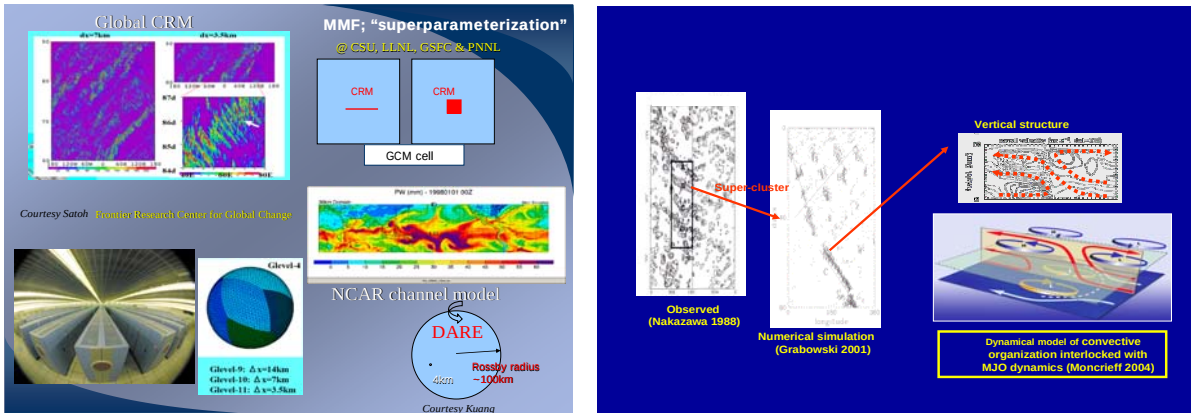

Figure 2. Left, categories of explicit model: global cloud-system resolving, super-parameterization, tropical channel, and scaled-equation approach (DARE). Right, super-parameterization generates MJO-like system and this system approximated by a dynamical model of organized convection interlocked with a Rossby-gyre circulation.

3. TROPICSS

We propose an new initiative called *TRopical Observations and Predictions for Improving Convective System Simulation (TROPICSS)* involving a combination of theory, simulation and observational analysis. This is a comprehensive and integrative approach to tropical convection and its cross-scale interaction. A bottleneck to progress is the lack of integrated satellite datasets for model validation. A practicable phased is:

- PHASE I: Pilot simulations employing large-domain/nested CRM simulations of MJO events driven by global analysis and specified SST; TRMM and A-train measurements for model validation.
- PHASE II: Simulation of the full tropics in global CRMs/nested global models in a *Year of Tropical Convection, YOTC*; produce integrated observational datasets for model verification.
- Phase III: 'Virtual global experiments' extending TROPICSS to global CRMs; quantify tropics-extratropics interaction; improve global models; integrated observational datasets for model verification.

4. CONCLUSION

Quantification of the effects of convective organization on global scales is now tractable on meso-to-global and diurnal-to-subseasonal scales using the super-parameterization and CRM approaches. This gives prospect for improving contemporary global models and also parameterizations of convective organization for future Earth-system models. It is anticipated that TROPICSS will unify tropical research and directly involve the developing nations (Africa, China, and India) that reside wholly or partly within the tropics.

REFERENCES

ECMWF, 2003: Proceedings ECMWF/CLIVAR Workshop on *Simulation and Prediction of Intra-seasonal Variability with Emphasis on the MJO*, 3-6 November, 2003, 269pp.

Biello, J.A., and A.J. Majda, 2005: A new multiscale model for the Madden-Julian Oscillation. *J. Atmos. Sci.*, **62**, 1694-1721.

Moncrieff, M.W., 2004: Analytic representation of the large-scale organization of tropical convection. *J. Atmos. Sci.*, **61**, 1521-1538.

Waliser, D., K. Weickmann, R. Dole. S. Schubert, O. Alves, C. Jones, M. Newman, L.-L. Pan, A. Roubicek, A. Saha, C. Smith, H. van den Dool, F. Vitart, M. Wheeler, and J. Whitaker, 2006: The Experimental MJO Prediction Project. *Bull. Amer. Meteorol. Soc.*, **87**, 425-431.

Zhang, C., 2005: Madden-Julian Oscillation. *Rev. Geophys.*, **43**, doi:10.10289/2004RG000158.

Introduction to the joint AMMA–THORPEX Working Group

Ernest Afiesimama[1], Sarah Jones[2], David Parsons[3], Florence Rabier[4], Chris Thorncroft[5], Zoltan Toth[6]

[1] Regional Meteorological Research Institute, Oshodi, Lagos, NIGERIA. E-mail: ernafies@yahoo.com
[2]Institut fuer Meteorologie und Klimaforschung, Universitaet Karlsruhe, GERMANY
[3] National Center for Atmospheric Research, US
[4] Meteo-France, FRANCE
[5] University at Albany, SUNY, Albany, New York, US
[6] Environmental Modeling Center, NOAA/NWS/NCEP, US

1.0 INTRODUCTION

The joint AMMA-THORPEX working group was set up as one of five science working groups in the framework of African Monsoon Multidisciplinary Analyses (AMMA) International, specifically to link AMMA and THORPEX activities related to the West African Monsoon. The group is concerned with high impact weather over West Africa (onset and duration of wet/dry spells including monsoon onset; risk of heavy rainfall/floods), the downstream Atlantic (tropical cyclogenesis and intensity change, role of the Saharan Air Layer), and the extratropics (extratropical transition, excitation of Rossby wave trains).

One of the main priorities of the group is to assess the impact of the additional data gained during the AMMA Enhanced Observing Period (EOP) of 2005-2007 and the Special Observing Period (SOP) in 2006 on numerical weather prediction for West Africa. Of particular interest are data, which have been collected from the enhanced radiosounding network and the driftsonde campaign. AMMA scientists working with National Meteorological and Hydrological Services (NMHSs) and other research institutions in West Africa have upgraded the regional soundings network, reestablished stations that were down in recent years (e.g. Abidjan), and established several new stations (e.g Tamale, Abuja, etc). This effort has also included improvements to the transmission of data to the global telecommunication system (GTS). All these have been major effort involving several hundred people and substantial coordination by AMMA.

2.0 AMMA-THORPEX ACTIVITIES

During the period 2005 – 2006, a number of activities have taken place especially in short and medium range forecasting using models from global and regional modelling centres. New forecasting tools and products were developed with observing strategies that will improve weather predictions over West Africa. Some details are highlighted below.

2.1 Data Impact Studies

AMMA is working with THORPEX to coordinate a number of data impact studies. The ultimate aim is to make recommendations for what the future observing system should be in the West African region that will support prediction of high impact weather. AMMA will ensure that the benefits for improved weather prediction are associated with and judged by their impact on African societies. The societal impacts work related to THORPEX is being coordinated by AMMA-THORPEX and the group responsible for the prediction of Climate Impacts. The main partners here are ECMWF, Meteo-France, NCEP, NRL, UKMO and University of Miami.

2.2 Development and assessment of new forecast tools and products

AMMA scientists have developed and established an impressive forecasting effort for the AMMA SOP. Tailored products and software have been developed and others still being developed by AMMA for the region and African forecasters have been trained to use them. The AMMA forecasting team consists of AMMA scientists and forecasters from NMHSs. Discussions have started to explore ways that we can sustain these efforts and in the long-term see if they can be transferred to other regions on the continent.

2.3 Adaptive Observations and Ensemble Forecasting

The question of whether an adaptive observing strategy should be considered during the SOP was raised and it was concluded that we do not know whether techniques applied elsewhere to calculate sensitive areas are appropriate for West Africa. This is an area where AMMA-THORPEX working group with THORPEX scientists will coordinate research to address this question using the data gained during the EOP/SOP. The work has implications for the design of ensemble perturbations also. Key partners are ECMWF, NCEP, NRL, University of Miami, and University of Reading.

3.0 CONCLUSION

AMMA-THORPEX working group as one of the five science working groups of African Monsoon Multidisciplinary Analyses (AMMA) has been established with the view to examining high impact weather over West Africa, the tropical Atlantic and the extratropics. The group is also involved in the development and assessment of new forecast tools and products for users community in West Africa and impacts, which the additional observational data during the special observing period in 2006 will have in predictability studies.

References

http://www.amma-international.org
http://www.amma-international.org/science/scientificGroups/WG5/index
http://www.wmo.int/thorpex

THE CONVECTIVE AND OROGRAPHICALLY-INDUCED PRECIPITATION STUDY (COPS) 2007 AND ITS LINKS TO THORPEX

Andreas Behrendt[1], Volker Wulfmeyer[1], Christoph Kottmeier[2], Ulrich Corsmeier[2],
Martin Hagen[3], George Craig[3], Hans-Stefan Bauer[1],
and the COPS International Science Steering Committee

[1] Institute of Physics and Meteorology, University of Hohenheim, Stuttgart, Germany
[2] Institute of Meteorology and Climate Research, University/Forschungszentrum Karlsruhe, Germany
[3] Institute of Atmospheric Physics (IPA), DLR Oberpfaffenhofen, Weßling, Germany

E-mail: *behrendt@uni-hohenheim.de*

Abstract: A refined model representation of atmospheric processes (e.g., by improved parameterizations, new model physics, assimilation of additional data) needs to be developed and tested for the next generation of upcoming high-resolution models to advance the forecast skills of convective precipitation events, especially in orographically-complex terrain. This need forms the motivation for the Convective and Orographically-induced Precipitation Study (COPS). COPS will be conducted in Southern Germany and North-Eastern France in summer 2007. COPS was endorsed as a Research and Development Project of the World Weather Research Programme (WWRP) and strong collaboration exists with the WWRP Forecast Demonstration Project of the Mesoscale Alpine Project (MAP D-PHASE). During COPS a synergy of state-of-the-art remote sensing systems, ground-based and airborne, partly scanning and employed for the first time, will be combined with in-situ instruments. COPS was initiated as part of the Germany priority program on quantitative precipitation forecast and is embedded in a 1-year general observations period (GOP). Scientists not only from Germany and France but also from the UK, USA, Austria, Italy, Switzerland, and the Netherlands contribute to the COPS instrumentation. Strong links to THORPEX are manifest by the European THORPEX Regional Campaign 2007 which is closely coordinated with COPS.

Keywords – quantitative precipitation forecast, data assimilation, COPS, ETReC07, MAP D-PHASE, convection

1. INTRODUCTION

In low-mountain regions, which cover a large fraction of the Earth's land surface, the relevant processes leading to convective precipitation are still hardly understood. This is especially unsatisfactory as many severe weather events are related to convective precipitation. Correspondingly, the overarching goal of the Convective and Orographically-induced Precipitation Study (COPS, http://www.uni-hohenheim.de/cops/) is to

"Advance the quality of forecasts of orographically-induced convective precipitation by 4D observations and modeling of its life cycle".

2. COPS PERIOD, DOMAIN, AND MEASUREMENT STRATEGY

COPS will take place in Southern-Western Germany and North-Eastern France between 1 June and 31 August, 2007, and covers the Black Forest, the Swabian Jura, and the Voges Mountains (Fig. 1). This area is characterized by high summer thunderstorm activity and particularly low skill of numerical weather prediction models. Within COPS the physical and chemical processes responsible for the deficiencies in quantitative precipitation forecast over low-mountain regions shall be identified and their model representation shall be improved. An important tool to achieve this is the assimilation of new data to mesoscale models, e.g., from state-of-the-art lidar systems, to separate errors in the initial fields from errors due to inadequate parameterizations. Furthermore, re-analyses testing the assimilation of different data, allow to investigate the sensitivity of the models and to study eventually the predictability of quantitative precipitation forecasts. Four working groups form the basis of COPS: Convective initiation (CI), Aerosols and cloud microphysics (ACM), Precipitation processes and life cycle (PPL), and Data assimilation and predictability (DAP). Different types of remote sensing systems (Fig. 2) shall be collocated at 5 supersites which form an east-west transect in the COPS region. At one of these sites in the Northern Black Forest, the Mobile Facility of the US Atmospheric Radiation Measurement (ARM) Program (Fig. 1 and 3) will be operated from 1 April to 31 December 2007 and collect detailed meteorological data within this extended period (www.arm.gov/sites/amf.stm).

3. LINKS TO THORPEX

The European THORPEX Regional Campaign 2007 (ETReC07) will be closely coordinated with COPS (Fig. 3) and targeted observations for the COPS domain shall be performed. For this, additional radiosondes, AMDAR and ASAP data shall be complemented with airborne water vapour DIAL and Doppler lidar measurements of the DLR Falcon aircraft. The COPS data set will allow then a detailed verification of the impact of the targeted observations.

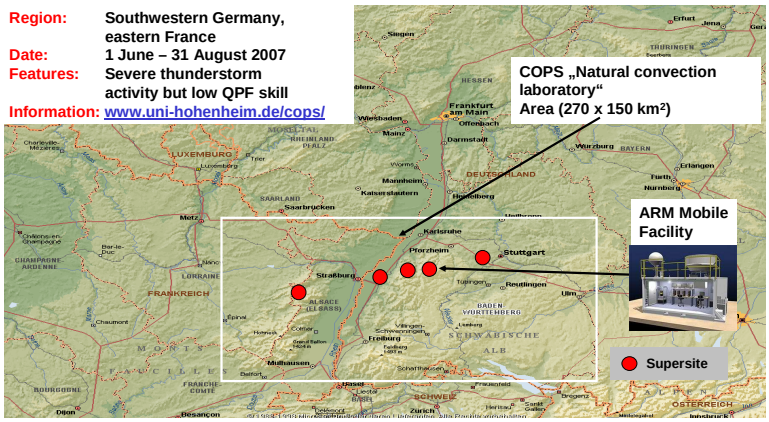

Figure 1. COPS domain in North-Eastern France and South-Western Germany covering the Voges Mountains, the Black Forest, and the Swabian Jura. 5 supersites form a east-west transect in the region. In addition to the instruments at the supersites, 8 aircrafts will perform measurements during COPS and, e.g., dense networks of rain gauges, meteorological stations, GPS sensors, energy balance/flux stations, soil moisture sensors, will be set up.

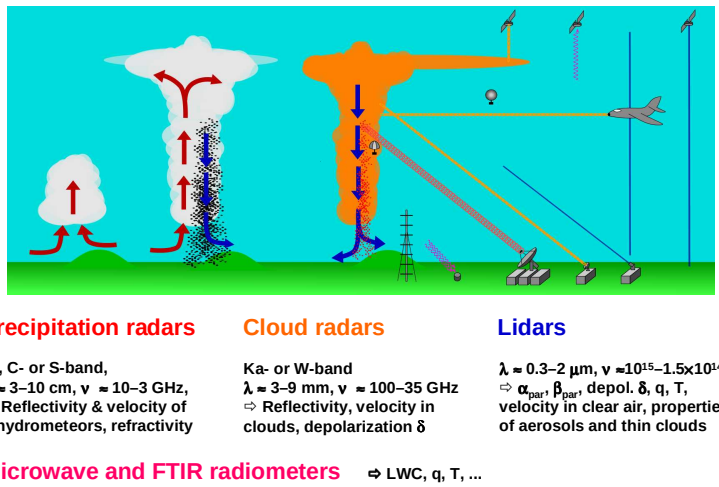

Figure 2. During COPS, high-resolution data sets covering the entire evolution of convective precipitation events will be collected with a large suite of different types of remote sensing systems. Most of these instruments will be collocated at the supersites so that also synergetic data products can be derived.

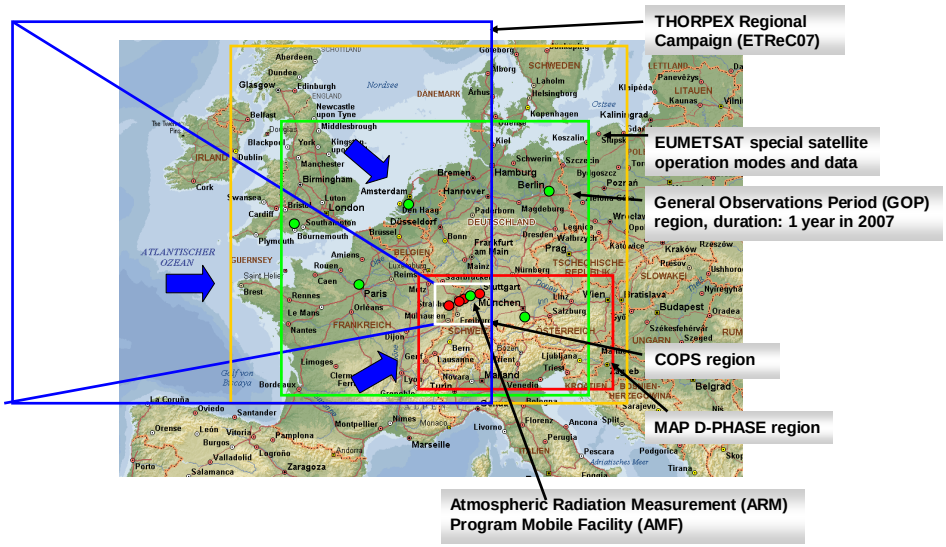

Figure 3. Domains of the European activities during COPS in 2007. The European THORPEX Regional Campaign (ETReC07) will be coordinated with COPS and targeted observations shall be performed for the COPS region. The COPS data set will allow a detailed verification.

HYDROLOGICAL CYCLE IN THE MEDITERRANEAN EXPERIMENT (HyMeX): TOWARDS A MAJOR FIELD EXPERIMENT BETWEEN 2009 AND 2012

Véronique Ducrocq[1], P. Drobinski, K. Béranger, F. Carlotti, C. Claud, G. Delrieu, A. Doerenbecher, F. Dulac, X. Durrieu de Madron, F. Elbaz, R. Escadafal, C. Estournel, H. Giordani, C. Guieu, J. Guiot, S. Hallegate, M. Kageyama, P. Lachassagne, L. Li, E. Martin, F. Médail, R. Moussa, M. Plu, L. Prieur, S. Rambal, D. Ricard , J.-C. Rinaudo, F. Roux, S. Somot, I. Taupier-Letage

[1] CNRM, Météo-France, Toulouse, France
E-mail: veronique.ducrocq@meteo.fr
http://www.cnrm.meteo.fr/hymex/

Keywords – *Hydrological cycle, Mediterranean region, Field experiment.*

1. INTRODUCTION

The Mediterranean basin has quite a unique character that results both from physiographic conditions and historical and societal development. The region features a near closed sea surrounded by very urbanized littorals and mountains from which numerous rivers originate. This results in a lot of interactions and feedbacks between oceanic-atmospheric-hydrological processes that play a predominant role on climate and its ecosystems. These processes frequently cause extreme events that produce heavy damages and human losses; heavy precipitation and flash-flooding during the fall season, severe cyclogeneses associated with strong winds and large swell or droughts accompanied by forest fires during summer are examples of Mediterranean high-impact weather events. The capability to predict such dramatic events remains weak because of the contribution of very fine-scale processes and their non-linear interactions with the larger scale processes. Progress in the understanding of the Mediterranean climate has thus important environmental, societal and economical implications. There is a clear lack of an experimental project relying on up-to-date innovative instrumentation in order to go one step further in the understanding and predictability of the Mediterranean weather events; such a major experimental project is now envisaged in the Medex Phase 2 framework in 2010 (or 2011).

2. THE HYMEX CONTEXT

In France, the research community has also recognised the necessity to develop a major multi-disciplinary and multi-scale experimental project to address the main issues related to the Mediterranean coupled system within the 2009-2012 period. The hydrological cycle in the Mediterranean region has been identified as a key scientific, environmental and socio-economic issue that has to be addressed within such experimental project. The HyMeX (HYdrological cycle in the Mediterranean EXperiment, http://www.cnrm.meteo.fr/hymex/) project aims at a better quantification and understanding of the hydrological cycle and related processes in the Mediterranean, with emphases put on high-impact weather events and regional impacts of the global change including that on ecosystems and the human activities. A phasing of the special observing period with a THORPEX European Regional Campaign in 2010 (or 2011) in connection with the Medex Phase 2 is looked for.
A white book for HyMeX is currently written by a panel of French scientists (listed here as co-authors) in atmosphere, hydrology and ocean sciences. It aims at highlighting some key open scientific questions related to the study of the water cycle at different time and temporal scales in the Mediterranean. It is planned to be largely debated with the research community during the first HyMeX workshop in January 2007. STISS also constitutes one of the opportunities to discuss and integrate propositions of the international community.

3. HYMEX SCIENTIFIC TOPICS

HyMeX scientific objectives are currently organized around the six following topics:
- *Water budget of the Mediterranean sea:* The Mediterranean sea is characterized by a negative water budget (excess evaporation over freshwater input) balanced by a two-layer exchange at the Strait of Gibraltar composed of a warm and fresh upper water inflow from the Atlantic superimposed to a cooler and saltier Mediterranean outflow. Light and fresh Atlantic waters are transformed into denser waters through interactions with the atmosphere that renewals the Mediterranean waters at intermediate and deep levels and generates the thermohaline circulation. Although the scheme of this thermohaline circulation is more and more understood, little is known about its variability at seasonal and inter-annual scales. For example, a better understanding of the formation of Levantine Intermediate Water (LIW) in the eastern Mediterranean is needed because LIW plays a major role in the formation of other kind of dense waters in the whole Mediterranean and its signature is still visible in the Mediterranean outflow water at the Strait of Gibraltar. The budget of the Mediterranean sea has also to be examined in the context of the global warming, and in particular by highlighting the impact of an increase of SST on high-impact weather frequency and intensity.

- *Water resources-hydrological continental cycle:* The rainfall climatology of the Mediterranean region is characterized by dry summers frequently associated with very long drought periods, followed by fall and winter precipitation that are mostly very intense. This results in a high daily/seasonal variability in river discharge, soil water content, vegetation characteristics, for which the interaction with the atmosphere is not well known. This includes for example the impact of the large extension forest fires associated with drought during summer on the evapotranspiration component of the hydrological cycle. The role of the surface states (landuse/landcover) and of the soils on the modulation of the rainfall needs also to be better understood. Hydrological and hydrogeological transfer functions are also characteristic of the Mediterranean basin, notably because of the specificities of the peri-mediterranean karstic and sedimentary aquifers. Progress in their understanding is of primary importance for the development of integrated management of the hydrosystems (exploitation of the groundwater resource, mitigation of the flood risk, preservation of the water quality), and its adaptation to the climate change.
- *Heavy precipitation and flash-flooding:* During the fall season, western Mediterranean is prone to heavy precipitation and devastating flash-flooding and floods. Daily precipitation above 200 mm are not rare during this season, reaching in some cases exceptional values of 700 mm recorded in September 2002 during the Gard (France) catastrophe. Large amounts of precipitation can accumulate over several day-long periods when frontal disturbances are slowed down and strengthened by the topography (e.g. Massif Central and the Alps), but also, huge rainfall totals can be recorded in less than a day when a mesoscale convective system (MCS) stays over the same area for several hours. Whereas large scale environment propitious to heavy precipitation is relatively well known, progress has to be made on the understanding of the mechanisms that govern the precise location of the anchoring region of the system as well as of those that produce in some cases uncommon amount of precipitation. The consequences of the intense precipitation events are amplified by the specific topography of the region with numerous small and steep river basins, and also by the predominance of karstic aquifers, resulting in flash-flooding.
- *Dense water formation:* The transformation of incoming Atlantic Water into denser waters occurs mainly during the winter when high evaporation and cooling cause oceanic convection. Deep offshore winter convection happens mainly in four major sites (the Gulf of Lion in the western Mediterranean, and, in the eastern Mediterranean, the Adriatic sea, the Aegean sea and the Levantine basin). Intense Mediterranean cyclogeneses and regional high winds (e.g. Genoa cyclone and Mistral for western Mediterranean) contribute to intense air-sea heat exchanges and sea surface cooling resulting in strong vertical mixing within convective chimneys of diameters of several kilometres. Hydrological and dynamical characteristics and inter-annual variability of the convection, in particular in terms of spatial extent, occurrence and time duration associated to the chimneys, need to be better documented in order to stress the respective role of the atmospheric forcing and oceanic processes (such as mesoscale eddies and submesoscale vorticies) and to progress in the modelling of these processes. Ecosystems functioning are strongly related to this complex dynamic and its impact needs to be addressed.
- *Coastal dynamics*: A good knowledge of the water circulation and mixing in the coastal zone are keys to understand the transport and transformation of continental rivers and aquifers inputs (biogeochemical and sediment transport), the cycle of major constituents in the coastal zone as well as the formation and cascading of dense waters toward the open sea. Momentum transfer from atmospheric winds largely govern the residence time of the water and nutriments within the continental shelves. The functioning of the coastal zone is therefore very sensitive to the fine scale spatial and temporal variability of the low-level wind field in this region, which result from not well known interactions with the complex topography of the Mediterranean region.

4. HYMEX EXPERIMENTAL STRATEGY

The experimental strategy will be refined in the future based on the outcome of the white book and its discussion with the national and international communities and projects. For the time being a two-level nested experimental strategy for the field campaign is envisaged:

- *an enhanced observation period (EOP) lasting four years [targeted date: 2009-2012],* which consists in enhancing the current operational observing systems and existing observatories in hydrology, oceanography and meteorology. The main objective of the EOP is to gather and provide additional observations of the whole coupled system that support analysis of the seasonal-to-interannual variability of the water cycle. As high-impact weather events are concerned, a long observation period (4 years) is needed in order to get a chance of documenting some of them.
- *a special observation period (SOP) envisaged in 2010 or 2011,* which will aim at providing detailed and specific observations to study key processes of the water cycle in the Mediterranean region. This SOP should be in phase with a THORPEX European Regional Campaign in 2010 (or 2011) in connection with the Medex Phase 2.

Acknowledgements: *The preparation actions of the HyMeX project (white book writing, HyMeX workshop, etc) are supported by the "Institut National des Sciences de l'Univers (INSU)" of CNRS and Météo-France.*

VULNERABILITY TO FLASH FLOOD
THE PROBLEM OF DECISION-MAKING IN CRISIS SITUATIONS

Céline Lutoff [1], Isabelle Ruin

[1] PACTE, Alpine Geography Institute, Joseph Fourier University, Grenoble, France
E-mail: *celine.lutoff@ujf-grenoble.fr*

Abstract: This communication focuses on the first results of a survey, concerning people's knowledge of flash floods, their perception of danger and their responses to the flash flood hazard. This study helps to understand flash flood vulnerability factors better, as understanding may be one of the key points necessary to improve operational warning systems as well as to orient future research into hydro-meteorological hazards.

Keywords – *Flash Floods, Vulnerability, Perception of risks, Gard (France)*

1. INTRODUCTION

Flood risks concern 4% of metropolitan France's territory or some two million people (Hubert, G. and Ledoux, B., 1999). Flash floods in southern regions are the most dangerous as they affect targets that are difficult to protect, such as isolated dwellings, road users and eco-tourists. Flash flood risks are the result of the interaction between hazard and vulnerability, i.e. the rapid concentration of storm water in small drainage basins and the fragility of exposed elements (people, buildings, infrastructure, communication networks, and social and economic activities, etc).

Due to the spatio-temporal characteristics of this type of flood, i.e. the variability in rainfall and drainage basin response times, flash flood deaths are often correlated with inappropriate behaviour during crisis periods. In both France and US, studies have shown that about half of the flash flood related deaths concern people driving their vehicles during the flood (Antoine et al., 2001; Gruntfest, E.C. and Handmer, 2001). In flood plains, people usually considered "at risk" are generally those who are physically unable to respond to warnings, such as older people, the disabled and children. Nevertheless, less attention is paid to people who cannot be easily reached by warning messages, e.g. all those moving in an affected area at a critical time. With flash floods, the suddenness of onset and the difficulty of determining where the danger lies in small drainage areas and along roads make such people particularly exposed to risk.

On the basis of these observations, our research focussed on mobile populations in order to better understand why people expose themselves to danger, and what vulnerability factors underlie such behaviour.

2. TOURISTS AND RESIDENTS SURVEY

Vulnerability may be evaluated by analysing processes leading to inappropriate decisions in a crisis situation (Thouret & D'Ercole, 1996). In order to quantify these processes we carried out a major questionnaire based on surveys among tourists and residents in a region especially prone to flash floods in the south of France.

268 tourists and 734 residents were interviewed during autumn 2004 in the Gard region. A large part of the questionnaire deals with 3 main points :

- Knowledge of hazards
- Prevention and information tools
- Supposed behaviour during crises.

We based this work on several hypotheses.

1. Knowledge of local environment : the better the environment is known, the greater the perception of the risks and the more adapted the behaviour.
2. Experience of floods : people who have already experienced floods are more prepared for that sort of crisis.
3. Correlation between perception and behaviour : following Kates studies (1970), we can assume that perception of risks and behaviour during crisis are related.
4. Vulnerability factors : social factors (age, gender, social level, etc.) may have impacts on hazards and knowledge prevention tools, and on behaviour during crisis.

3. SOCIAL VULNERABILITY FACTORS

Data analysis is still in progress. Here, we present some results after a first analysis of the surveys. These results will be completed in the future. What we are mainly concerned with, for the moment, is to identify social vulnerability factors (related to hypothesis 4). Here are some examples of results we will present in this communication.

As a first observation, age seems to be one of the most significant factors, both for residents and tourists. It influences knowledge of hazards : older people are more aware than others of the dangers of flooding. There is a correlation with age : the older the people, the more they know about the risk.

This greater knowledge seems to have an positive impact on some behaviour. For instance, behaviour in response to a weather alert is more adapted for older people. However, age can also have a negative impact as in the case of evacuation. Most people who don't want to leave during an evacuation belong to the youngest and the oldest groups.

For tourists, one other vulnerability factor is the origin. Foreigners and especially non francophe tourists seem to be the most vulnerable. They have a poor knowledge of risks and of French protection measures.

The presentation will identify other social factors of vulnerability and some other answers in relation to our hypotheses.

4. CONCLUSION

In conclusion, we can say that this study has already provided some answers to vulnerability questions concerning flash floods. Age, local environment knowledge and in some cases flash-flood experience have an impact on behaviour and mobility during crises. Other results will complete these first findings to improve our knowledge about social vulnerability and to understand the individual decision-making process in crisis situations.

Acknowledgements: *Fondation MAIF (France) provide financial assistance for this study.*

REFERENCES

Hubert, G. and Ledoux, B., 1999: *Le coût du risque. Evaluation des impacts sociaux économiques.* Presses de l'Ecole Nationale des Ponts et Chaussées, Paris, France, 232 p.

Antoine et al., 2001: *Les crues meutrières, du Roussillon aux Cévennes.* Annales de géographie, n° 622, pp. 597-623

Gruntfest, E.C. and Handmer, 2001: *Coping with flash floods.* Dortrech, Kluwer, 322 p.

Thouret, J.C. & D'Ercole, R., 1996: *Vulnérabilité aux risques naturels en milieu urbain : effets, facteurs et réponses sociales*. Cahier des Sciences Humaines 32, n°2, pp. 407-422

Kate, R.W., 1970: *Natural Hazard in Human Ecological Perspective : hypothesis and models*. Natural Hazard Research Papers. Department of Geography of Toronto, vol 14, 27p.

ASSISTANCE OF THE MARINE WEATHER FOR ARTISANAL AND INDUSTRIAL FISHING

Mamina Kamara

Météo. Nat. Senegal, Dakar, Senegal
E-mail: *maminakamara@yahoo.fr*

PROBLEMATIQUE

La position géographique du Sénégal laisse sur sa façade occidentale les eaux de l'océan atlantique.Avec 700 km de cotes, l'ampleur du domaine maritime est considérable et représente la principale ressource économique du pays.

La pêche constitue le premier pilier de l'économie sénégalaise avec un chiffre d'affaire d'environ 200 milliards de francs CFA.Trois entités mènent des activités intenses en mer ;il s'agit de la pêche artisanale avec 80% du total des débarquements globaux,joue un rôle de premier plan.Il mobilise 12000 pirogues recensés et 60000 pécheurs .Ensuite la pêche industrielle avec prés 5000 escales de navires par an,sans compter ceux qui passent au large du Sénégal.Enfin le transport des passagers et fret maritimes suivant axe Dakar,Banjul,Ziguinchor,Cap Skiring, Gorée et Mbour.

Cependant le secteur de la pêche est soumis aux aléas climatiques qui rendent périlleuses ses activités.La Direction de la Météorologie Nationale dans sa mission première de sécurité et de prévention des catastrophes naturelles peut jouer un rôle important.

L'information météorologique utilisée à temps réel permet de :

- Planifier les opérations d'urgence en mer (opération de recherche et de sauvetage en mer) pour la sauvegarde des vies et protection des biens.
- D'orienter les flottes de pêches vers des zones où la configuration des températures et la circulation des océans sont particulièrement favorables à certaines espèces de poissons.
- Faciliter la navigation maritime internationale, nationale, la pêche et les autres activités maritimes déployées sur la Cotes, le Large et au Grand Large.
- D'élaborer le routage des navires qui se fondent sur les prévisions du vent, et des vagues fournies par des models modernes de prévision du temps et de l'état de la mer pour choisir un itinéraire recommandé qui réduise au minimum la durée de la traversée et les coûts d'exploitation.
- De réaliser d'appréciables économies en carburant, en finance et surtout gagner en confort et sécurité.
- Contribuer au plan de lutte contre la pollution marine, consécutive à un déversement accidentel d'hydrocarbures, d'une rupture d'oléoduc ou la perte d'un pétrolier ; si l'on sait que le port autonome de Dakar reçoit en moyenne par an un million de tonnes d'hydrocarbures ainsi que la dispersion dans l'atmosphère des gaz toxiques et inflammables dus à l'éruption d'un puit de gaz ou à un rejet accidentel.

Le début de l'exploitation du pétrole par la Mauritanie constitue une menace sérieuse de pollution en cas d'accidents vue la direction dominante du flux et des courants marins vers les cotes sénégalaises.

Compte tenue de toutes ces préoccupations,il est donc tout naturel que le Sénégal ou l'activité maritime est l'une des principales activités économiques ,puisse disposer d'un service météorologique opérationnel,capable de répondre aux nombreuses sollicitations des usagers de la mer,notamment les pécheurs.

BULLETINS DE SECURITE DE LA METEO MARINE

La direction de la météorologie Nationale du Sénégal se conforme à la réglementation internationale définie dans le cadre du Système mondial de détresse et de sécurité en mer **(SMDSM)** établi au titre de la convention internationale pour la sauvegarde de la vie humaine en mer (convention **SOLAS**).Les bulletins de sécurité du service de la météo marine concernent le bulletin **« Cotes »**(jusqu'à 20 milles des cotes), bulletin **« large »** (jusqu'à 200 milles), bulletin **Spécial Port** (prévisions de houle et marées), bulletin **Pic et Direction des Vagues** (pour chaque station côtière).A ces bulletins réguliers diffusés à une heure fixe est émis un **Bulletin Météo Spéciale (BMS)** dés que les conditions météorologiques actuelles ou prévues présentent un danger pour la navigation**.** Ils sont repartis en deux groupes.

1) Bulletins gratuits conformément à la mission de service public : production régulière des bulletins « Cotes » pour 24 heures (ex : grande cote, petite cote, cote sud), bulletin « Large », « bulletin météo spéciale » (BSM).
2) Bulletins à caractère commercial par la signature de protocoles d'accord, de conventions entre la direction de la météo nationale et les clients ou usagers, surtout portant sur des échéances moyennes à longues (ex : bulletin « Cote » par zones, « BMS » par zones, bulletin « Spécial Port », routage des navires, suivi de pollution, prévision de surcote, annuaires des marées, consultations et expertises).

L'objectif spécifique recherché est le renforcement institutionnel mais surtout une meilleure visibilité des activités de la Direction de la météorologie nationale afin d'assurer au mieux sa mission de service public dans le cadre de la sécurité en mer et pour l'optimisation et une rentabilité des activités de pêche.

MOYENS DE DIFFUSION DES BULLETINS DE METEO MARINE.

Actuellement la diffusion des avis et prévisions météorologiques à travers des bulletins de sécurité se fait essentiellement par fax et occasionnellement par téléphone, radio bande FM, radio côtière et par Internet.
La direction de la météorologie nationale est à la recherche des moyens additionnels plus efficients pour permettre aux usagers et clients une meilleure réception et à temps réel de l'information météorologique.Vu la modestie de son budget pour faire face à ces investissements, le soutien de l'état et des bailleurs de fond à travers les organismes internationaux est nécessaire pour l'acquisition de ces outils de communication.
Pour la **bande Côtière** (jusqu'à 20 milles au large) : besoins en équipement : VHF, Téléphone, SMS, Serveur vocale, Internet, fax, radio etc.
Bulletin **Large** (jusqu'à 200 ou 300 milles au large) : besoins en équipement : Emetteurs en BLU, NAVTEX, Worldspace, Inmarsat C

DESTINATAIRES

Télévision nationale (bulletin météo à la TV)
Direction de la protection et de la surveillance de la pêche (DPSP).
Port Autonome de Dakar (PAD).
Marine Marchande.
Direction de la pêche.
SOMAT (bateau « **WILIS »**)
Chaloupe de Gorée
Dakar NAVE
Fédération des syndicats de pécheurs et Mareyeurs (FENAGIE-PECHE) et autres usagers.

SENSITIVITY OF ENSEMBLE FORECASTS OF EXTRATROPICAL TRANSITION TO INITIAL PERTURBATIONS TARGETED ON THE TROPICAL CYCLONE

Doris Anwender[1], Martin Leutbecher, Sarah Jones, and Patrick Harr

[1] Institut für Meteorologie und Klimaforschung, Universität Karlsruhe, Karlsruhe, Germany
E-mail: doris.anwender@imk.uka.de

Abstract: In this paper experiments designed to investigate the impact of the new initial perturbations on the predictability of extratropical transition and the downstream flow are described. Ensemble forecasts using the current operational configuration but with no stochastic physics are compared with experiments that are identical except that the targeting for a specific tropical cyclone is switched off.

Keywords – *Extratropical transition, Ensemble prediction, singular vectors, ECMWF*

1. INTRODUCTION

The reduced predictability associated with the extratropical transition of tropical cyclones presents a severe challenge for numerical weather prediction. Guidance with respect to the uncertainty associated with extratropical transition can be obtained from ensemble prediction systems that calculate a certain number of forecasts from perturbed initial conditions in addition to the deterministic forecast. This allows probability forecasts to be made. In the ECMWF Ensemble Prediction System (EPS) 50 initial perturbations for the ensemble members are obtained by calculating extratropical singular vectors that identify all regions in the atmosphere polewards of 30° where maximal error growth is possible in a certain time interval. In addition singular vectors are calculated with linearised diabatic physics only for areas targeted around tropical cyclones. In order to avoid double counting singular vectors the target areas used to be restricted to the tropical belt (25°S – 25°N). However, a tropical cyclone often exists polewards of 30° especially when it undergoes extratropical transition. In the recent upgrade to the ECMWF EPS the calculation of the initial perturbations targeted on tropical cyclones has been modified so that they can be applied to tropical cyclones as they move into the midlatitudes.

Tests of the new configuration as implemented on 28 September 2004 have been conducted at ECMWF for certain tropical cyclones (Leutbecher and Paulsen, 2004). In the case of FABIAN (2003), for example, calculations of the tracks with the new configuration show a splitting of the ensemble members in two distinct branches which cannot be seen in the calculation with the old configuration (Fig. 1). The monomodal distribution of tracks changes to a bi-modal one. Furthermore, a larger number of ensemble members can be found close to the observed track.

In this paper we present experiments designed to investigate the impact of the new initial perturbations on the extratropical transition of tropical cyclones and the downstream flow in ensemble forecasts. In experiments with the ECMWF EPS we want to separate the effect of the initial perturbations on the EPS forecast from the other changes made in the new configuration.

2. EXPERIMENTS

In experiments with the ECMWF model system we reran EPS forecasts for the tropical cyclone TOKAGE (2004) using the new configuration with the resolution TL255 and 40 level. In order to identify the impact that is caused by the initial perturbations alone we switch off the stochastic physics for all experiments. This is important because the influence of the stochastic physics cannot be assigned clearly either to the tropical cyclone or to the midlatitude flow. We ran experiments without initial perturbations targeted for TOKAGE and compared them to the runs with perturbations.

3. RESULTS

The ensemble track forecast without perturbations from 16 October 2004 12 UTC (Fig. 1 a) shows an insufficient spread at the point of recurvature, i. e. after 48 h, as the analysis lies outside of the spread. The deterministic forecast can be seen at the western edge of the ensemble members. Furthermore, at ET time and thereafter (dashed black line) all but four ensemble members show TOKAGE well to the north of the analysis. In the ensemble track forecast from the same time with perturbations targeted on TOKAGE (Fig. 1 b) the spread around the time of recurvature is much larger so that both the analysis and the deterministic forecast fall within the spread. The region around the analysis at and after ET time is covered well with ensemble tracks and several members agree with the analysis.

To quantify the influence of the initial perturbations targeted on TOKAGE the difference between the root mean square difference (RMSD) of the ensemble members relative to the control forecast with and without

perturbations has been calculated for forecasts from 16 and 18 October 2004 12 UTC. The results for 16 October are shown in Hovmoeller plots of 200 hPa (Fig. 2 a) and 500 hPa (Fig. 2 b) heights averaged over 40° - 50° N in Fig. 2.

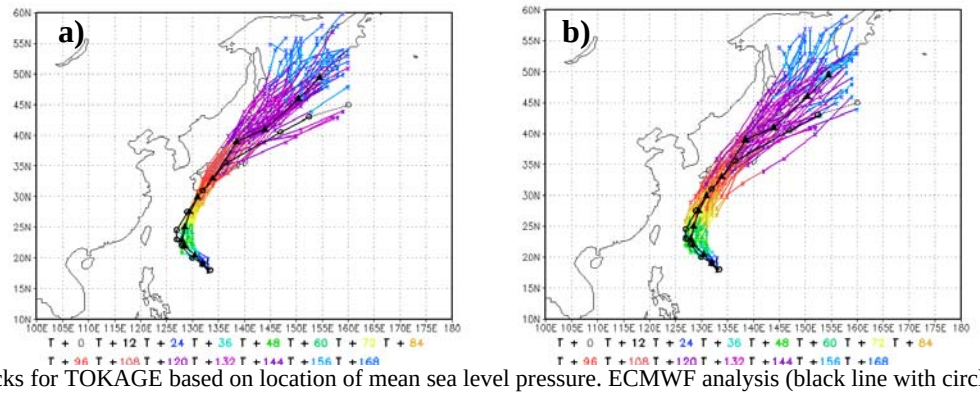

Fig. 1: Tracks for TOKAGE based on location of mean sea level pressure. ECMWF analysis (black line with circles, dashed after ET), deterministic forecast (black line with triangles) and ensemble forecast (colours) from 16 October 2004 12 UTC for 7 days. Forecast a) without and b) with perturbations targeted on TOKAGE.

A signal which originates at the ET time and position of TOKAGE and a second stronger one that originates 48 (200 hPa) to 24 h (500 hPa) before ET time downstream of the ET event propagates downstream and broadens with increasing forecast time (Fig. 2). In the 200 hPa plot (Fig. 2 a) the maxima are shifted slightly to the west. They cover a larger area and have higher values than in the 500 hPa plot (Fig. 2 b) but compared to their total value of RMSD (not shown) they make up about the same percentage, i. e. up to 25 %, at both levels. The percentage downstream is higher at both levels than that in the plume directly originating from TOKAGE.

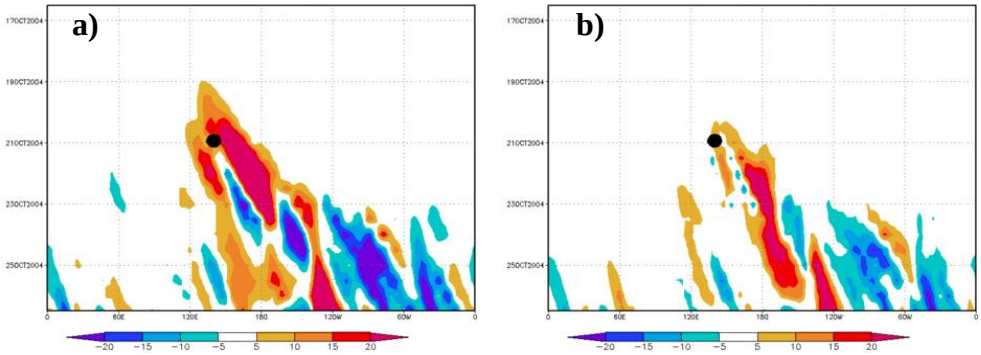

Fig. 2: Forecast from 16 October 2004 12 UTC. RMSD of ensemble forecast with perturbations minus RMSD of ensemble forecast without perturbations around TOKAGE at a) 200 hPa and b) 500 hPa.

To be able to investigate the synoptic patterns, groups of ensemble members that contribute in a similar way to the main patterns of variability have been formed. For this purpose an analysis method consisting of a combination of EOF analysis and clustering of the principal components has been applied to the potential temperature on the dynamic tropopause.
For the forecast with perturbations targeted on TOKAGE for 21 October 2004 00 UTC initialized on 16 October 2004 12 UTC the method yields five clusters. The form of a characteristic trough-ridge-trough pattern consisting of the trough that interacts with TOKAGE, the ridge directly downstream and the trough downstream of the ridge is quite different. Three of them show a very strong, one a moderate to strong and one a weak re-intensification of TOKAGE after its ET in terms of surface pressure. The depth of the surface pressure in the analysis lies in between the clusters that show moderate to strong and weak re-intensification. A comparison with the same clusters of the ensemble members calculated without perturbations targeted on TOKAGE illustrates nicely that the analysis in that case would lie outside of the ensemble because all the five clusters show a stronger re-intensification than seen in the analysis. Furthermore, these patterns show less variability in the representation of the trough-ridge-trough pattern and in the position of TOKAGE that is forecast incorrect in all of them.

Acknowledgements: ***This work received support from the Office of Naval Research, Marine Meteorology. We are grateful to the ECMWF for providing ensemble data as part of a special project.***

REFERENCES

Leutbecher, M., and J. E. Paulsen2004: Revised initial condition perturbations for the EPS and the 28r3 EPS e-suite. ECMWF memorandum research department.

WRF SIMULATION AND DIAGNOSIS OF THE EXTRATROPICAL TRANSITION OF IRENE (2005)

Christopher Davis[1], Sarah Jones and Michael Riemer
[1] National Center for Atmospheric Research, Boulder, Colorado, USA
E-mail: *cdavis@ucar.edu*

Abstract: A realistic simulation of the extratropical transition of hurricane Irene (2005) is examined to deduce the mechanism by which the vortex transitions from a hurricane structure to a frontal cyclone. The simulation (actually a real-time forecast) uses a storm following nest with a grid increment of 4 km. Diagnosis indicates that the lower-tropospheric warm-core vortex is initially highly resistant to increasing vertical shear. Convection continually develops on the downshear side of the vortex and organizes to the point where a new storm center forms. Large deformation is then induced around the new center, destroying the original warm-core vortex within a few hours. The new vortex rapidly acquires frontal characteristics and features hurricane-force winds on its flank during the structural adjustment.

Keywords – *THORPEX, WMO, Extratropical Transition*

1. INTRODUCTION

As discussed in Jones et al. (2003) a key aspect of extratropical transition (ET) is the downstream development it can induce. The uncertainty in the interaction of the tropical cyclone with the mid-latitude jet is a key component of the noted hemispheric decline in predictive skill in global models. One of the key contributors to the uncertainty is the development of the downstream ridge connected with the outflow of the tropical cyclone. The dynamics of this ridge development, fundamentally involving diabatic heating, is, in turn, related to properties of the jet and properties of the impinging tropical cyclone as transition occurs. Thus far, little is known about how the significant structural changes to the vortex occur during ET. In particular, the warm-core structure is maintained in some cases long after the vortex experiences significant westerly shear. In this paper, we utiltize fully explicit simulations of hurricane Irene (2005) with the Weather Research and Forecasting (WRF) model (Skamarock et al. 2005), focussing on the processes by which Irene became a frontal cyclone.

2. MODEL CONFIGURATION

The WRF simulation used a 2-way nested configuration featuring a 12-km outer fixed domain with a movable nest of 4-km grid spacing centered on the minimum 500 hPa geopotential height. Nest repositioning was calculated every 15 simulation minutes. On the outer 12-km domain we used the Kain-Fritsch cumulus parameterization, but the inner domain had no parameterization. Both domains used the WSM3 microphysics scheme (Hong et al. 2004) that predicted only one cloud variable (water for $T > 0^oC$ and ice for $T < 0^oC$) and one hydrometeor variable, either rain water or snow (again thresholded on 0^oC). Both domains also used the Yonsei University (YSU) scheme for the planetary boundary layer (Noh et al. 2001). The forecasts were integrated from 00 UTC, initialized using the Geophysical Fluid Dynamics Laboratory (GFDL) model, with data on a $1/6^o$ latitude-longitude grid. Lateral boundary conditions were also taken from the GFDL model.

3. RESPONSE OF VORTEX TO SHEAR

As Irene progressed poleward, the vertical wind shear (in the 1-6 km MSL layer) increased in magnitude, being generally westerly (Fig. 1a). The shear remained roughly 10 m/s in the layer, with small oscillations, for more than 12 h. In response, the tilt of the vortex increases gradually, with cyclonic precession apparent during a 12 h period prior to 22 h. The tilt then stabilizes at about 60-80 km, oriented slightly to the left of the shear vector, for more than 12 h. Despite a relatively steady tilt, the vortex during this period is far from steady. Near the beginning of the period (22 h), the structure still resembles a hurricane (Fig. 1c), albeit highly asymmetric with convection confined to the left of the downtilt direction. The persistent forcing of the shear apparently allows the convection to grow in strength and organize its own vortex, to the point where this vortex becomes the dominant circulation by 31 h (Fig. 1d). As the parent vortex collapses in the presence of strong horizontal deformation exerted by the new vortex, the PV gradient on the east side strengthens markedly and a hurricane-force (50 m/s) low-level jet develops, representing a temporary reintensification of the storm (not shown). As the new center develops, it taps the enhanced baroclinity (in approximate balance with the increased shear at a higher latitude), and begins generating frontal structures recognizable as an extratropical cyclone, but still on a scale of only a few hundred kilometres. Beyond this time, the scale continues to grow, a deep-tropospheric upshear tilt tendency occurs (red line in Fig. 1b) and the cyclone completes its transition.

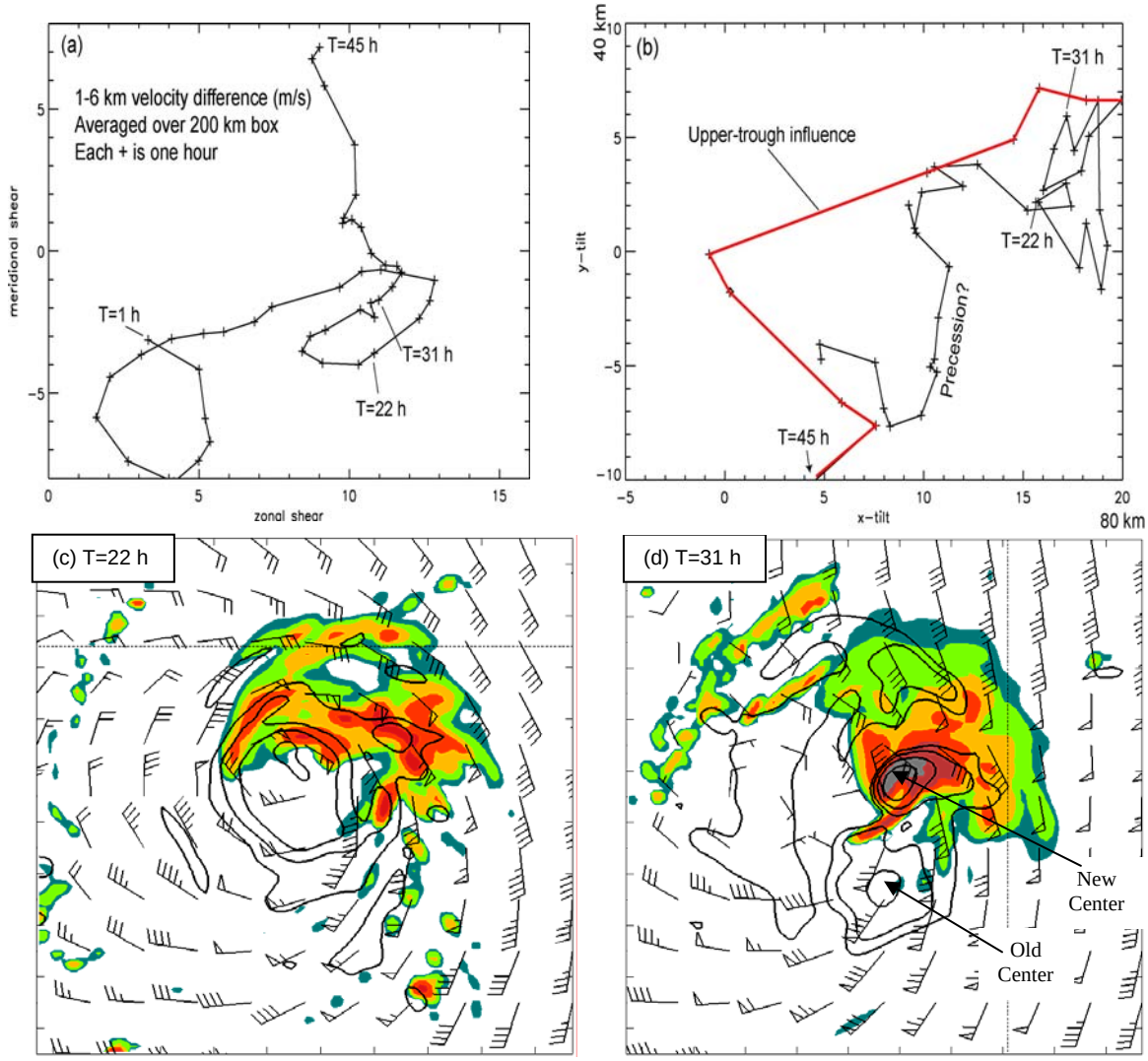

Figure 1. (a) 1-6km vertical wind difference over 200 km box centered on storm (and domain) center; (b) tilt, defined as position of PV maximum averaged over 80-km box at 6 km minus PV maximum over 80-km box at 1 km MSL; (c) Rain water mixing ratio at 10 m MSL (dark green = 0.1 g/kg, light green = 0.2 g/kg, light orange = 0.4 g/kg, bright orange = 0.8 g/kg, dark red = 1.6 g/kg, gray = 3.2 g/kg), wind at 500 m MSL and PV on 310 K isentropic surface (contoured at 2, 4, 8 and 16 PV Units). Each tick in (c) and (d) is 40 km.

4. CONCLUSION

The primary vortex in Irene appears highly resistant to rather strong shear imposed, but the increasingly strong asymmetric convection brought about by the shear allows for a rapid transition to a new dominant circulation. Once this happens, the demise of the original hurricane vortex occurs in a few hours. The warm core becomes highly elongated and disappears rapidly, perhaps as a result of adiabatic ascent within a developing frontal zone south of the new cyclone center.

REFERENCES

Hong, S.-Y., J. Dudhia, and S.-H. Chen, 2004: A revised approach to ice microphysics process for the bulk parameterization of clouds and precipitation. *Mon. Wea. Rev.*,**132**, 103-120.

Jones, S. C, P. A. Harr, J. Abraham, L. F. Bosart, P. J. Bowyer, J. L. Evans, D. E. Hanley, B. N. Hanstrum, R. E. Hart, F. Lalaurette, M. R. Sinclair, R. K. Smith, and C. Thorncroft, 2003: The Extratropical Transition of Tropical Cyclones: Forecast Challenges, Current Understanding, and Future Directions. *Wea. And Forecasting*, **18**, 1052–1092.

Noh, Y., W. G. Cheon, and S. Raasch, 2001: The improvement of the K-profile model for the PBL using LES. Preprints of the International Workshop of Next Feneration NWP Model, Seoul, South Korea, 65-66.

Skamarock, W. C., J. B. Klemp, J. Dudhia, D. O. Gill, D. M. Barker, W. Wang and J. G. Powers, 2005: A Description of the Advanced Research WRF Version 2. NCAR Technical Note TN-468+STR. 88 pp.

SIMULATIONS OF THE INTRA-SEASONAL OSCILLATION IN THE TROPICS WITH ENSEMBLE TECHNIQUES

Takeshi Enomoto[1], Shozo Yamane[2], Takemasa Miyoshi[3]

[1] Earth Simulator Center, Japan Agency for Marine-Earth Science and Technology (JAMSTEC),
3173-25, Showamatchi Kanazawa-ku, Yokohama, Kanagawa 236-0001 Japan
Email: eno@jamstec.go.jp
[2] Chiba Institute of Science/Frontier Research Center for Global Change, JAMSTEC
[3] Numerical Prediction Division, Japan Meteorological Agency

Abstract: This study examines initial perturbations generated by ensemble techniques in an attempt to better simulate the intra-seasonal oscillation in the tropics using an atmospheric general circulation model. Perturbations generated by the local ensemble transform Kalman filter (LETKF) are compared with those generated by the breeding method. Perturbations by the breeding method mainly represent baroclinic instabilities in the extratropics. Perturbations by LETKF have large moist energy in the tropical lower troposphere as well. This is a favourable feature for simulations of the tropical intra-seasonal oscillation. Another interesting property of perturbations by LETKF is that the ensemble spreads seem to lead convective activities. This implies that locations and/or intensity of tropical convection differ among ensemble members. Comparisons between the two methods provide insights into the nature of the intra-seasonal oscillation and useful information on the methodology to generate ensemble perturbations.

Keywords—*Breeding method, Local Ensemble Transform Kalman Filter, the Madden-Julian Oscillation (MJO)*

1. INTRODUCTION

A Rossby wave-packet induced from a convectively active region often causes high-impact weather events along the mid-latitude jet. A convective flare-up is often caused by the intra-seasonal oscillation known as the Madden-Julian Oscillation (MJO). Thus, in order to improve the forecast of the high-impact weather in mid-latitudes beyond several days to a few weeks, it is essential to better predict convective activities in the tropics.

Initial perturbations used in the current mid-range forecast systems are not satisfactory for the tropical disturbances. Singular (Palmer et al. 1992) and bred (Toth and Kalnay 1993) vectors essentially aim at capturing the extratropical synoptic disturbances. Japan Meteorological Agency uses the breeding method with larger rescaling factor for humidity in the tropics in order to account for larger uncertainty with moisture (Kyouda 2006). In order to further improve the representation of MJO in JMA's ensemble prediction system, Kubota et al. (2006) proposed a method to generate perturbations for MJO. They use kinetic energy or velocity potential at 200 hPa as a norm and reduce amplitudes in the extratropics in a Gaussian form centred at the equator.

Hamill et al. (2000) and Wang and Bishop (2003) argue that the masked rescaling factor introduces noise probably due to spurious equatorial wave source in data-sparse tropical regions. Their results indicate that the use of perturbations generated with an ensemble Kalman filter (EnKF) technique is promising since it provides a *masking of the day*.

In this study, the perturbations generated by the local ensemble transform Kalman filter (LETKF) are examined and compared against those by the breeding method, focusing upon the tropics in particular. This abstract briefly introduces our LETKF system in Section 2 and some features of the generated perturbations in Section 3.

2. ALERA: AFES-LETKF EXPERIMENTAL REANALYSIS

An experimental reanalysis dataset has been created on the Earth Simulator using a system composed of AFES (AGCM for the Earth Simulator, Enomoto et al. 2006) and LETKF (Miyoshi and Yamane 2006). Using a T159/L48 (triangular truncation at total wavenumber 159, corresponding to about 80-km mesh and 48 layers) resolution, the AFES-LETKF system has been running stably over 17 months from 12 UTC, 1 May 2005 (Miyoshi 2006, poster D25). Most of the observational data used in the operational analysis at JMA except for satellite radiances are assimilated. We named this dataset ALERA (AFES-LETKF Experimental ReAnalysis).

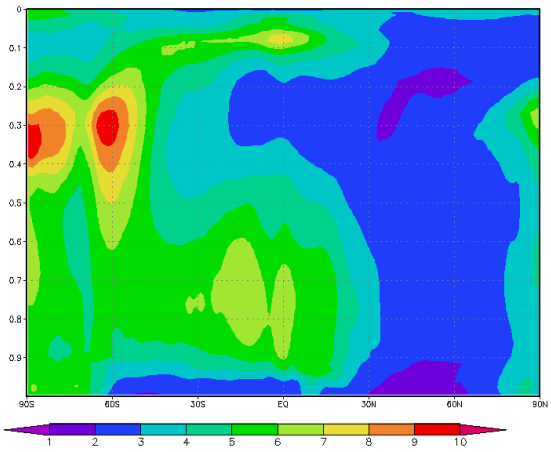

Figure 1. Distribution of the zonal mean total energy norm (J kg^{-1}) averaged between 0 UTC, 22 to 31 Mar 2006 in ALERA. The vertical axis is in σ coordinates.

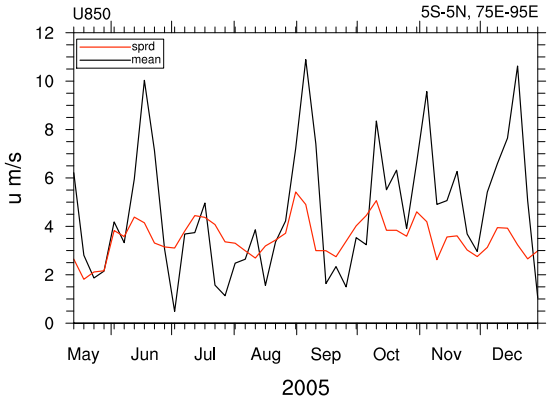

Figure 2. Time evolutions of the mean and spread of the zonal wind speed (m s^{-1}) at the 850-hPa level averaged in the equatorial eastern Indian Ocean (5°S– 5°N, 75°E–95°E). The pentad mean data is smoothed with 3-pentand running mean.

3. PERTURBATIONS IN ALERA

The perturbations in ALERA appear to be favourable for simulating the MJO since the perturbation amplitude is large and the ensemble spreads appear to lead the convective activity in the tropics.

There is a maximum of the zonal mean total energy in the tropical middle- to lower-troposphere in ALERA (Fig. 1), where humidity contributes the most. Such a peak is not usually found in the breeding or singular vector methods. It is speculated that EnKF ensemble updates acts as a flow-dependent masking without excessive influences from the midlatitudes and enables to capture instabilities peculiar to the tropics.

Both the ensemble mean and spead of the zonal wind speed at the 850-hPa level in the equatorial eastern Indian Ocean fluctuate at intra-seasonal time scales (Fig. 2). It is interesting to note that the correlation is the largest at 1-pentad lead of the spread. It implies that the intensity and location of convection differ among ensemble members at the leading-edge of the MJO.

4. DISCUSSION

The perturbations in ALERA seem to reasonably capture the uncertainty associated with the intra-seasonal signal. It is planned to verify the performance of ensemble forecasts from these perturbations.

REFERENCES

Enomoto, T., A. Yoshida, N. Komori, and W. Ohfuchi, 2006: Description of AFES 2: improvements for high-resolution and coupled simulations. *In High Resolution Numerical Modelling of the Atmosphere and Ocean. W. Ohfuchi and K. Hamilton (eds)* , Springer, New York, in press.

Hamill, T.M., C. Snyder, and R.E. Morss, 2000: A comparison of probablistic forecasts from bred, singular vector, and perturbed observation ensembles. *Mon. Wea. Rev.*, **128**, 1835–1851.

Kubota, T., H. Mukougawa, S. Maeda, H. Sato, T. Iwashima, 2006: Predictability of intraseasonal oscillation in the tropical atmosphere. *Annals of Disas. Prev. Res. Inst.*, Kyoto Univ., **49B**, 411–421.

Kyouda, M., 2006: Chapter 3.1 The one-week ensemble prediction system. *In Introduction of Ensemble Technique to short- and medium-range forecasting —With the aim of the improvement in the forecast skill of extreme weather event—, Annual NPD/JMA report*, Separated Vol. **52**, 23–33.

Palmer, T.N., F. Molteni, R. Mureau, R. Buizza, P. Chapelet, and J. Tribbia, 1992: Ensemble prediction, *ECMWF Research Department Tech. Memo.*, **188**, 46pp.

Miyoshi, T., S. Yamane, and T. Enomoto, 2006: Experimental reanalysis using AFES-LETKF at a T159/L48 resolution, *Proceedings of the Second THORPEX International Symposium Symposium*, 4–8 Dec. 2006, Landshut, Germany.

Miyoshi, T. and S. Yamane, 2006: Local ensemble transform Kalman filtering with an AGCM at a T159/L48 resolution. *Mon. Wea. Rev.*, submitted.

Toth, Z. and E. Kalnay, 1993: Ensemble forecasting at NMC: the generation of perturbations. *Bull. Amer. Meteor. Soc.*, **74**, 2317–2330.

Wang, X. and C.H. Bishop, 2003: A comparison of breeding and ensemble transform Kalman filter ensemble forecast schemes. *J. Atmos. Sci.*, **60**, 1140–1158.

INTRASEASONAL VARIABILITY IN A DRY ATMOSPHERIC MODEL

Hai Lin [1], Gilbert Brunet and Jacques Derome

[1] Recherche en prévision numérique, Meteorological Service of Canada, Dorval, Québec, Canada
E-mail: *hai.lin@ec.gc.ca*

Abstract: A long integration of a primitive equation dry atmospheric model with time-independent forcing under boreal winter conditions was analyzed. Significant tropical intraseasonal variability (TIV) that has a Kelvin wave structure was found in the model atmosphere. Coherent eastward propagations in the 250 hPa velocity potential and zonal wind were observed, with a speed of about 15 m s^{-1}. The oscillation is stronger in the eastern Hemisphere than in the western Hemisphere. It is evident that tropics-extratropics interactions are responsible for the simulated intraseasonal variability.

Keywords *– THORPEX, WMO, MJO, intraseasonal variability, simple model.*

1. INTRODUCTION

In most existing theories, moisture and deep convections are considered crucial to the Madden-Julian oscillation (MJO) since the tropical latent heat serves as an energy source to support the large-scale oscillation against damping. Other mechanisms such as extratropical influence have also been suggested. The relative importance of tropical and extratropical contributions, however, is unclear. In the present study, we use a dry atmospheric model to study the tropical intraseasonal variability (TIV) that is generated in the absence of moisture and tropical convections. The structure and behaviour of this TIV are analyzed in detail, and compared with the MJO.

2. THE MODEL AND DATA

The simple general circulation model (SGCM) as described in Hall (2000) is used in this study. It is a global spectral model with no moisture representation. The resolution used in this study is T31 with 10 vertical levels. An important feature of this model is that a time-independent forcing is used that is calculated empirically from observed daily data. This forcing is obtained as a residual for each time tendency equation by computing the dynamical terms of the model, together with the dissipation, with daily global analyses and averaging in time.
All the processes that are not resolved by the model's dynamics are thus included in the forcing. The daily data used to calculate the forcing is the National Centers for Environmental Predictions (NCEP) and the National Center for Atmospheric Research (NCAR) reanalyses. Data of 30 winters from 1969/70 to 1998/99 are utilized, where the winter is defined as the 90 day period starting on December 1.

With the time-independent climatological forcing, a perpetual Northern Hemisphere winter integration of 3660 days is conducted starting from an observed initial condition. Daily output is saved for analysis. The period of the first 40 days is taken as a spin up of the model, and is not used.

3. SIMULATED TROPICAL INTRASEASONAL VARIABILITY

Space-time power spectrum analyses are performed on the 250 hPa zonal wind and velocity potential averaged between 5ºS and 5ºN. The results indicate a planetary scale disturbance with intraseasonal time scales that propagates eastward at a speed of 15~20 m/s. Time-longitude distribution of the velocity potential field at the equator reveals a coherent eastward propagations with a wavenumber one structure. The low-frequency wave is stronger in the eastern Hemisphere than in the western Hemisphere.

An Empirical Orthogonal Function (EOF) decomposition is applied to the daily data of the 20-100 day filtered 250 hPa velocity potential. Both EOF1 and EOF2 have a mainly zonal wavenumber one structure. They account for 34% and 30% of the 20-100 day variance, respectively. Time lag correlation between the principal components (PC) of these two EOFs reveals that they represent an eastward propagating planetary scale wave.

A linear combination of these two PCs is used to represent the TIV index. Lag regressions are calculated between the TIV index and some 20-100 day filtered 250 hPa variables averaged for the band 10ºS-10ºN. The result reveals that the TIV represents an equatorial Kelvin wave, where positive (negative) geopotential height anomalies are paired with westerly (easterly) wind anomalies in the eastern Hemisphere. The TIV has a maximum amplitude in the upper troposphere.

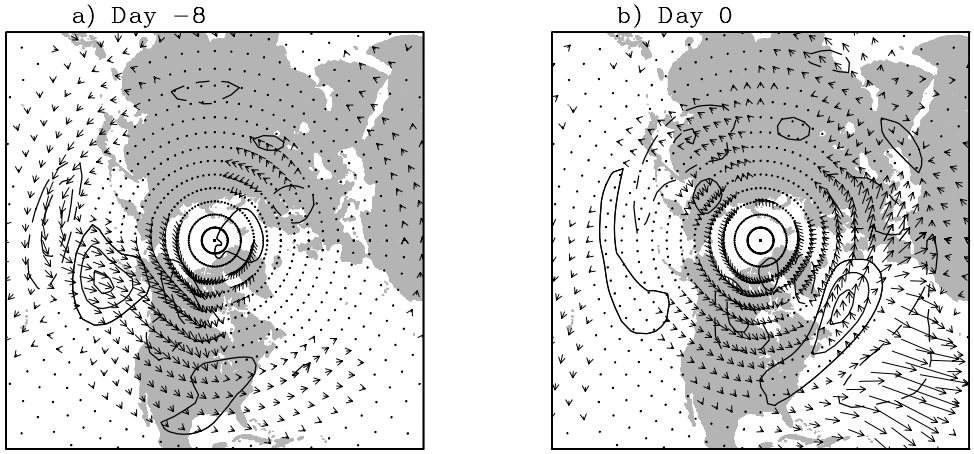

Fig.1 Wave activity flux (vectors) and the potential vorticity anomaly (contours) associated with the TIV. Amplitude corresponds to one standard deviation of the TIV index. Contour interval for the PV anomalies is 0.3 pvu. Zero line is omitted. Contours in dash and solid are of negative and positive values, respectively.

Significant difference exists between the model simulated TIV and the observed MJO. Firstly, the TIV has a faster phase speed than the MJO. Secondly, the TIV has mainly a Kelvin wave structure, and the Rossby wave gyre that is observed to be dragged along with the divergence in the eastern hemisphere in the MJO is not simulated.

4. EXTRATROPICAL COUPLING WITH THE TIV

Lag regressions of the 250 hPa streamfunction with the TIV index indicate that a global low-frequency signal in the rotational circulation is associated with the simulated TIV. In the eastern Hemisphere, couplets of cyclonic and anticyclonic circulation anomalies straddling the equator propagate eastward up to west of the date line. In the extratropical region, the pattern seems to develop in situ with little evidence of a phase propagation. In the extratropical Pacific and North American region, the signal communicates with the downstream anomalies in the form of a wave train. In the North Atlantic area, intensification of anomalies with a dipole structure is followed by the development of another tropical couplet of circulation anomalies near the Greenwich longitude.

Wave activity flux vectors are calculated based on lag-regression maps of the 250 hPa streamfunction with respect to the TIV index. Fig. 1a and b depict the wave activity flux at Day –8, when there is upper convergence over the western equatorial Pacific, and Day 0, when upper divergence happens over equatorial Africa and the Indian Ocean, respectively. Also shown on the maps as contours is the potential vorticity (PV) anomaly. The square of the PV anomaly is proportional to the wave activity. The wave activity propagates from the Tropics to the middle and high latitudes in the Pacific region, implying a tropical influence in this sector. On the other hand, in the Atlantic sector, there is a strong wave activity flux from the middle latitudes southward into the Tropics, implying an extratropical influence. These fluxes of wave activity are coupled with the divergent flow in the Tropics. The northward wave activity flux occurs when the tropical convergent (divergent) center moves into the western Pacific, while the development of the tropical Atlantic divergent flow occurs when strong southward wave activity flux makes its way into the Tropics.

The ultimate energy source of the simulated TIV is likely located in the extratropical atmosphere. A part of the energy comes from the mean flow though barotropic conversion in the westerly jet exits. Transient eddy activity also contributes to the TIV, especially in the North Atlantic area, where the vorticity flux convergence by transients reinforces the low-frequency flow.

5. DISCUSSION

The generation of the TIV in the dry model suggests a possible mechanism for the MJO. On the other hand, the fact that some of the key features of the MJO are missing in the dry model simulation indicates that tropical deep convective processes are indeed important for the observed MJO.

REFERENCES

Hall, N. M. J., 2000: A simple GCM based on dry dynamics and constant forcing, J. Atmos. Sci., **57**, 1557-1572.
Lin, H., G. Brunet, and J. Derome, 2006: Intraseasonal variability in a dry atmospheric model, J. Atmos. Sci., in press.

SUB-TROPICAL SYNOPTIC-SCALE FORCING OF EXTRA-TROPICAL FLOW: DIAGNOSTIC ANALYSIS AND MODEL SIMULATIONS

Thomas Spengler [1], Cornelia Schwierz [2], Huw C. Davies [1]

[1] Institute for Atmospheric and Climate Science, ETH Zurich, Zurich, Switzerland
[2] Institute for Atmospheric Science, University of Leeds, Leeds, United Kingdom
E-mail: *thomas.spengler@env.ethz.ch*

Abstract: A model-based study is undertaken of the transient influence of sub-tropical synoptic-scale forcing upon the extra-tropical flow. To this end the adiabatic version of the ECMWF Integrated Forecast System (IFS) is run in the Held-Suarez setting, and a comparison is made between a control run and one where the model's sub-tropics is subjected to an additional specified thermal forcing.
Diagnostic analysis indicates that the transient response to the forcing in the extra-tropics takes the of a coherent downstream development on the extra-tropical wave guide rather than following a great-circle ray path. The nature of the response is found to be sensitive to the location, size and magnitude of the forcing and to the structure and strength of the jet. An interpretation of the results is proffered in terms of simple wave transmission, propagability and excitation.

Keywords **–** Downstream development, MJO, Rossby Wave propagation, Wave guide

1. INTRODUCTION

An event of intense localized and organized convective activity in the tropics (e.g. the ENSO convective region and the MJO) constitutes a large-amplitude coherent flow feature in an otherwise comparatively quiescent ambient environment. Such events are thought to play a major role in initiating Rossby Wave trains that propagate out of the tropics (c.f. the Pacific North American teleconnection pattern of the Pacific (Wallace and Gutzler, 1981; Simmons et al, 1983). Likewise organized activity in the sub-tropics (e.g. hurricanes / typhoons), although smaller in scale, can also exert a direct impact upon the extra-tropics before and during an extra-tropical transition..

The representation of the foregoing convective-related tropical flow phenomena are not always adequately simulated in operational NWP models, and hence this can lead to the non-capture of their effect upon the extra-tropics with an accompanying loss of predictability in the latter region.

The present model-based study examines the meridional transmission and downstream effect of sub-tropical forcing upon the flow on the mid-latitude wave guide. Idealized simulations are conducted with a local specified tropical heating distributions of different amplitude, scale and location to examine the nature and sensitivity of the response .

2. MODELS AND METHODS

The adiabatic version of the ECMWF IFS, a global spherical model with hybrid coordinates, is used with a resolution of T159 in the horizontal and 60 levels in the vertical. The model is set to run in the Held-Suarez setting, which resembles a temperature relaxation to an atmospheric state yielding one tropospheric mid latitude jet in each hemisphere and experiments are carried out with and without orography. In addition a specified thermal forcing is applied to simulate in a rudimentary fashion aspects of the diabatic heating of the MJO or tropical cyclones.

To illustrate the impact of the forcing we diagnose the difference between the forced minus the unforced forecast of geopotential on 200 hPa in relation to the main PV gradient of the extra-tropical wave guide. This is complemented by heuristic theoretical considerations of barotropic Rossby Wave propagation through a latitudinally varying zonal flow at low-latitudes.

3. RESULTS

The experiments conducted without orography show that the difference between the diabatically forced and control simulations capture a significant downstream signal on the extra-tropical PV wave guide. After day 5 a coherent wave pattern is evident on the jet stream and it extends some 4000-6000 km downstream from the forcing. A series of simulations indicate that the response is sensitive to the lateral separation of the forcing and

the wave guide. In effect the signal first increases in amplitude as the separation reduces, but there an optimum separation and thereafter the downstream response diminishes and the structures become less coherent.

The inclusion of orography induces a zonal asymmetry of the time mean jet with a maximum in the western Pacific that is distinctly stronger than its non-orographic counterpart, and a secondary and weaker maximum in the western Atlantic. These changes to the time-mean features are akin to the real atmospheric counterpart features.

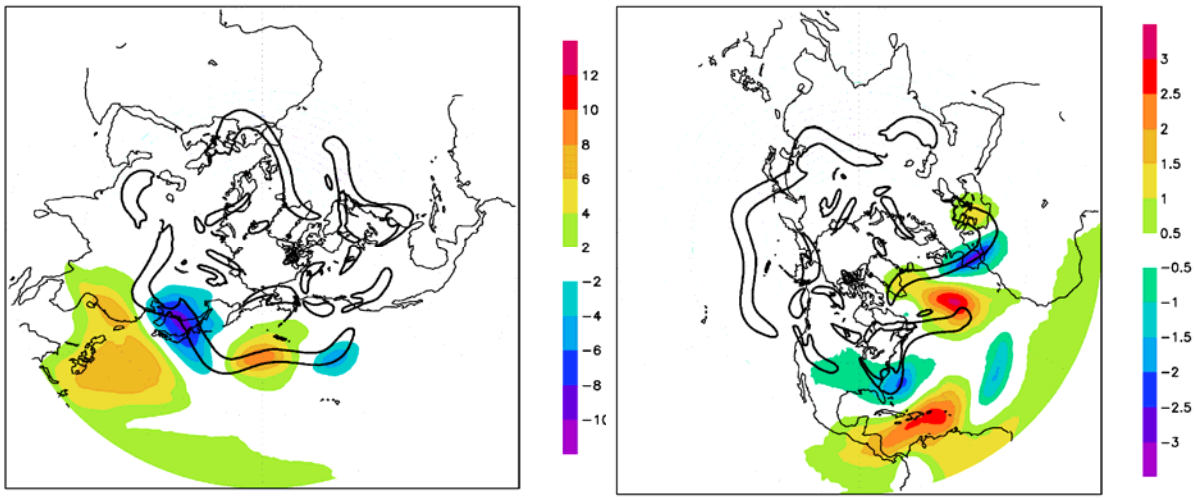

Figure 1. Difference in geopotential (forced minus unforced forecasts) on 200 hPa. Contours indicating PV gradient exceeding 1 PVU/1000 km on 315 K. Left panel: forcing centred at 10 N 120 E for; right panel: forcing centred at 10 N 70 W; both for set up including orography.

For this refined setting the extra-tropical response is different and distinctive. On the one hand a forcing located directly equatorward of the stronger Pacific jet stream results in a much reduced signal, and indeed a significant downstream response is only attained when the forcing is positioned closer to the PV gradient. On the other hand a forcing located more westward at the longitude of the jet stream's entrance resembles that obtained in the non-orography simulation (see Fig. 1a). In effect there are indications that it is not only the strength and position of the forcing that influences the downstream response but also the 'sharpness' of the PV gradient. For smaller scale forcing in the tropical western Atlantic the subsequent response extends to the neighbourhood of the Mediterranean within 5 days (see Fig 1b).

A common feature of the simulations was the absence of Rossby wave propagation on great circles equatorward or polewards of PV wave-guide, but rather a downstream propagation along the wave guide (c.f. Schwierz et al 2002). Insight can be sought by considering the meridional propagation of two-dimensional perturbations embedded within a barotropic atmosphere on an equatorial β-plane. In line with the foregoing meridional propagation is only possible through regions of weak shear, and for typical atmospheric values the response is expected to be strongly evanescent.

4. CONCLUSIONS

Significant downstream development on the mid latitude PV wave guide can be triggered by distant forcing in the tropical/subtropical region. The response is dependent on the forcing (position, size and strength) and on the wave guide itself (structure and strength). The results have implications for extra-tropical medium range predictability in the presence of an MJO or tropical cyclones.

Acknowledgments: *We thank MeteoSwiss for providing access to ECMWF data and CPU usage. Special thanks are also due to ECMWF (Nils Wedi) for their great assistance in getting started with PrepIFS, model-setup and MetView.*

REFERENCES

Schwierz, C., S. Dirren and H. C. Davies: Forced waves on a zonally aligned jet. J. Atmos. Sci.. **61**, 73-87.

Simmons, A. J., J. M. Wallace and G. W. Bratstator: Barotropic wave propagation and instability, and atmospheric teleconnection patterns. J. Atmos. Sci. **40/6**, 1363-1392.

Wallace, J. M. and D. S Gutzler, 1981: Teleconnection in the geopotential height field during the northern hemisphere winter. Mon. Weather Rev. **109**, 784-812.

WEST AFRICA WEATHER FORECASTING IN AMMA-UK: A FRIST CASE STUDY

Xuefeng Cui[1], Christophe Messager[2], and Andrew Morse[1]

[1] Department of Geography, University of Liverpool, Liverpool, UK
[2] Institute for Atmospheric Science, University of Leeds, Leeds, UK
E-mail: *x.cui@liv.ac.uk*

Abstract: One of the main objectives of African Monsoon Multidisciplinary Analyses – UK (AMMA-UK) is to improve the understanding of West African Monsoon (WAM) and its prediction from days to weeks. A nested Met Office Unified Model (UM) system with horizontal resolution up to several kilometres will be set up for West African area. Using better validation data obtained through the international AMMA measurement campaign, we aim to improve the model's representation of the land surface processes, convection and the monsoon dynamics.

A first 10-day forecast of August 2005 with the global UM demonstrates that our model could simulate relatively realistic daily rainfall during the first 3 days with slower westward movement, which is associated with the representation of African Easterly Jet. The model fails to reproduce the new strong convective systems starting since the third forecast day due to no assimilation implemented. The UM mesoscale simulation provides more small scale events compared to the driving global model but mostly restricted by the driving field as well. Both the two simulations show very good agreement with limited available observations of surface temperature. This study is still in its starting phase but the outcome would greatly increase confidence in our ability to model and predict the underlying dynamics of climate in this region.

Keywords – *West African Monsoon, AMMA, Dynamical Downscaling, Unified Model UM*

1. INTRODUCTION

Climate variability in West Africa, spanning a large range of scales from intraseasonal to decadal, is under the control of a dominant atmospheric feature that occurs in summer: the West African Monsoon (WAM). The variability of the WAM has always been difficult to analyse, firstly because of the complex interaction between the atmosphere, the biosphere and the hydrosphere that control its dynamics and the life cycle of the associated convective systems, but also because of the scarcity in situ data (Montmerle et al. 2006). This has motivated the African Monsoon Multidisciplinary Analyses (AMMA) international research project, whose main objective is to perform detailed studies of the multi-scale physical and chemical processes that influence the land-ocean-atmosphere system over this area (For details see http://www.amma-international.org/). One of the core objectives of AMMA is to develop numerical modelling systems which could resolve microclimate, land surface processes, mesoscale convective systems (MCSs), WAM evolution with the help of the high quality interdisciplinary observations made available in the project. With the improvement of weather and climate prediction, an early warning system could be developed in this region for malaria, catastrophic flooding or prolonged dry spells, e.g. droughts or long break cycles in the monsoon.

Model simulations at mesoscale and at cloud scale are essential to analyse the processes leading to the organization of convection and to study the impact of MCSs on the monsoon flux at a synoptic scale through the water and energy cycles. Usually, mesoscale models are initialized and driven at the lateral boundaries using large-scale analyses provided by global models. Errors in global models will be possibly transported into the mesoscale domain through boundaries. Therefore, it is essential to develop and validate the dynamical modelling systems covering from global model to mesoscale in West Africa. In this context, a first case study was setup in this paper to demonstrate 1) the forecast performances of UM at global scale in term of large-scale dynamical circulations and its associated convection processes; 2) the improvement of UM mesoscale compared to driven global model in representation of MCSs, the major rain-producing systems.

2. MODEL AND EXPERIMENTAL SETUP

The New Dynamics Unified Model version 6.1 (UM6.1) developed developed at the UK Met Office was implemented in this study. The global experiment is run with a horizontal resolution of 60 km and 38 vertical levels up to 39.5 km. It was initialized from European Centre for Medium-Range Weather Forecast (ECMWF) analysis data at 00 UTC of 27th August 2005 and kept running for 10 days without any data assimilation. The time step is chosen at 20 minutes and 6-hourly output is analyzed. In addition to running at global scale, the non-hydrostatic UM has the capacity to run at a very small grid scale up to 1 km. In this study we run the mesoscale model at resolutions of 20 km and 12 km. The mesoscale model is initialized from the same ECMWF dump file

and then nudged with the global model output at lateral boundaries every hour. The experiments are only performed for 3 days with time step of 5 minutes.

3. VILIDATION DATA

National Centers for Environmental Prediction-National Center for Atmospheric Research (NCEP/NCAR) four times daily reanalysis (Kalnay et al. 1996; http://www.cdc.noaa.gov/cdc/data.ncep.reanalysis.html) is used to compare with our model simulated atmospheric circulation. Global Precipitation Climatology Project (GPCP) 1-degree daily (1DD) observation-only combined dataset is used to validate model simulated rainfall together two satellite rainfall datasets: 3-hourly NOAA Climate Prediction Center (CPC) Morphing Technique (CMORPH; http://www.cpc.ncep.noaa.gov/products/janowiak/cmorph_description.html) and daily CPC Africa Rainfall Estimation (RFE2.0; http://www.cpc.ncep.noaa.gov/products/fews/data.shtml) rainfall estimates. For surface temperature, we are using the 3-hourly Meteorological Interactive Data Access System (MIDAS) Land Surface Observation Station Data from British Atmospheric Data Centre (BADC; http://www.badc.ac.uk).

4. RESULTS AND ANALYSIS

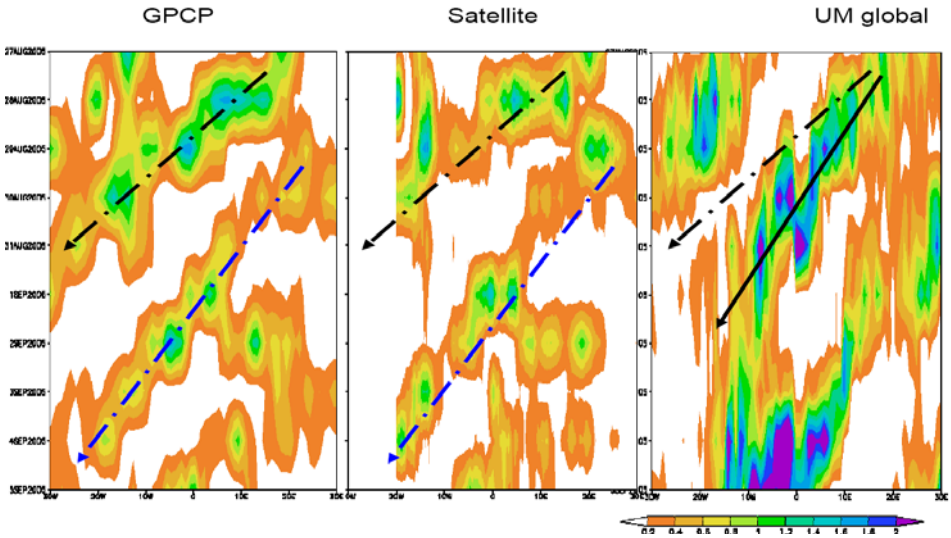

To be brief in this abstract, only a longitude-time section of daily rainfall comparison between observation and global model simulation are presented below. The other analyses will be presented during the conference. The results demonstrate that our UM forecasts reasonably well the first 3 days daily rainfall with slightly slower westward movement (shown as the dark arrow in the figure). The model fails to reproduce the second strong convection system starting the third day (blue arrow in the left panels). The rainfall performances are closely associated with the AEJ representation in the model. The mesoscale simulation shows more small scale events but largely restricted by the driving global model. Surface temperature simulated by both models agrees weel limited station observations.

5. CONCLUSION

A first case study is performed in this study to investigate the forecast capacity of the nesting model system from global to mesoscale in representation of African Easterly Jet, Mesoscale Convection Systems, and more importantly, the most useful parameters for application users: precipitation and surface temperature. The results demonstrate that our model forecast reasonably well the first three days daily rainfall with slightly slower westward movement associated with AEJ performances but fails to reproduce the new strong convection system. The mesoscale model shows more small scale events but largely restricted by the driving global model. With the high quality observations made available by AMMA, the outcome of this study would greatly increase confidence in our ability to model and predict the underlying dynamics of climate in this region.

REFERENCES

Montmerle, T., J. Lafore, L. Berre, and C. Fischer, 2006: Limited-area model error statistics over Western Africa: Comparisons with midlatitude results. Q. J. R. Meteorol. Soc., **132**, 213-230.

OBSERVATION IMPACT MONITORING WITH A DATA ASSIMILATION ADJOINT

Rolf Langland[1], Nancy Baker[1], Randal Pauley[2], Tim Hogan[1], Patricia Pauley[1], Liang Xu[1], Ben Ruston[1]

[1]Naval Research Laboratory, Monterey, CA, USA 93943
[2]Fleet Numerical Meteorology and Oceanography Center, Monterey, CA, USA 93943
E-mail: rolf.langland@nrlmry.navy.mil

Abstract: An adjoint-based technique to estimate the impact of observations on short-range forecast errors in operational NWP is described. The procedure is computationally affordable and provides valuable information about observations and the performance of the data assimilation procedure.

Keywords – Satellite and in-situ observations, data assimilation, adjoint methods, forecast impact

1. INTRODUCTION

In numerical weather prediction (NWP), there is an increasing need to develop and apply methods for monitoring the impact and value provided by atmospheric observations used in data assimilation. Significant investments have been made to develop new satellite observing systems (AMSU, AIRS, HIRS, SSM/I, etc.) and the efforts to use these data to improve NWP also involves considerable research and computational expense (Rabier 2005). It is recognized that larger amounts of satellite observations benefits NWP yet, from a diagnostic perspective, it can be difficult to quantity the relative value of the many types of data that are assimilated. For example, when 300 channels of an infrared imager are assimilated, what is the relative benefit, in terms of forecast skill, provided by each of these channels? The adjoint-based method described in this paper can be used to answer these types of questions, by providing quantitative information about the impact of all observations assimilated by an operational NWP system.

2. METHODODOLGY

The essential steps involved in adjoint-based observation impact estimates are described by Langland and Baker (2004), LB04 hereafter. The measure of observation impact is defined as the *difference* between forecast errors on an analysis and a background trajectory, whose initial conditions are separated by six hours. For example, we use δe_{24}^{30} to represent an adjoint-based estimate of $e_{24} - e_{30}$, the difference between the 24h error of a forecast started from 00UTC (the start of the analysis trajectory) and the 30h error of a forecast started from 18UTC (the start of the background trajectory). The effect of the observations that are assimilated at 00UTC is to move the forecast from the background trajectory to the new analysis trajectory, which produces a different forecast error. The difference of forecast errors on these two trajectories is due solely to the assimilation of the observations, and the separate forecast impact of *every assimilated observation* can be quantified using this approach. For each observation, the "observation impact" is obtained as the product of the observation innovation value and the observation sensitivity (see LB04 for details). The calculation requires adjoint versions of the forecast model and the data assimilation procedure and, as described by LB04, we use the forecast model adjoint to compute sensitivity gradients on both the analysis and background trajectories to obtain higher accuracy. The computational cost of producing the observation impact information using the adjoint system is about the same as a re-run of the regular analysis and forecast model. It should be noted that this method evaluates the impact of *all observation data simultaneously*, in contrast to conventional data-denial sensitivity studies that estimate the forecast impact for *subsets of observations* that are withheld from (or added to) the analysis.

3. OPERATIONAL APPLICATIONS

Currently, at NRL-FNMOC, adjoint-based observation impact is run once per day for the 00UTC operational and beta-runs of NAVDAS[1]-NOGAPS[2], using vertically-integrated, moist energy-

[1] NAVDAS – NRL Atmospheric Variational Data Assimilation System
[2] NOGAPS- Navy Operational Global Atmospheric Prediction System

weighted global 24h forecast error as a costfunction. The observation impact information is examined on a regular basis and is used to make decisions for quality control and to help decide which features of the data assimilation procedures may need improvement – for example, the observation error statistics or bias correction. Typically, the most useful information is provided in summaries of observation impact results compiled for at least one month, to provide a representative statistical sample. Our results over the past two years confirm that the adjoint-based observation impact information can identify specific observations with data quality problems - for example, individual radiosonde, land, or ship data that provide non-beneficial impact due to instrument problems, inaccurate metadata, or other issues. The information can also be partitioned for each observation variable so that a station can be blacklisted for just temperature, humidity, or wind observations. In a recent case, observation impact information was used to detect a data processing problem that affected the quality of geostationary satellite wind observations over a particular region of the southern hemisphere – the data-provider was notified and the problem was corrected. In a beta (pre-ops parallel test) forecast context, the observation impact can be used as an additional check on the forecast impact of new observations before transition to actual operations.

4. RESEARCH APPLICATIONS

In Langland (2005) the observation impact procedure was used to evaluate the impact of targeted observations obtained during the North Atlantic THORPEX TReC field program that took place in late 2003. It was found that targeted dropsondes have a relatively large impact *per-observation* on forecast skill, but a modest total impact compared to other observing systems that provide much larger amounts of data. As the amount of satellite data assimilated for NWP continues to increase substantially, the impact produced by small sets of dropsondes may become less significant, which is an important consideration for future targeting programs.

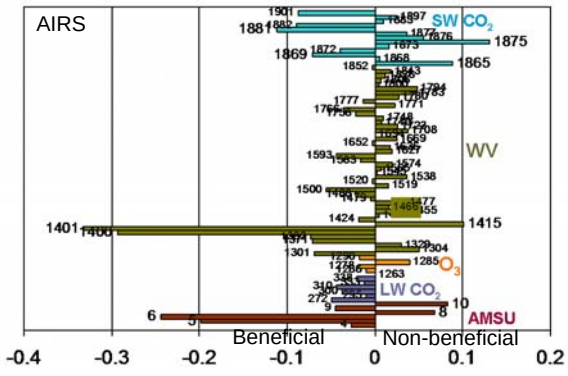

Fig. 1: Impact (J kg^{-1}) of AIRS observations on 24h global forecast error in NOGAPS/NAVDAS, as a function of channel number. Data assimilated at 00UTC, 14-19 Aug 2006. Negative values equal forecast error reduction (beneficial impact).

Observation impact information is also being used at NRL in a research mode to address other data assimilation issues, including channel selection for new satellite instruments such as the AIRS. Fig. 1 illustrates the distribution of beneficial and non-beneficial forecast impact as a function of AIRS channel for a 6-day period in Aug. 2006. Note that non-beneficial impact does not necessarily imply poor data quality – limitations of the data assimilation procedure and background quality also play a role in how well data are used. The adjoint-based approach to observation impact allows us to examine the separate impacts of hundreds or thousands of individual observation channels – information that would be difficult or impractical to obtain by conventional data denial experiments. At present, we compute observation impact for NAVDAS, which is a 3d-VAR analysis in observation-space. We have also developed and tested observation impact in a 4d-VAR context with the adjoint of NAVDAS-AR (accelerated representer, Xu et al. 2005, Rosmond and Xu 2006).

Acknowledgements: *This work is supported by the Naval Research Laboratory and the Office of Naval Research, under Program Element 0602435N, Project Number BE-435-037.*

REFERENCES

Langland, R.H., 2005: Observation impact during the North Atlantic TReC-2003. Mon. Wea. Rev., 133, 2297-2309.

Langland, R. H., and N. L. Baker, 2004: Estimation of observation impact using the NRL atmospheric variational data assimilation adjoint system. Tellus, 56A, 189-201.

Rabier, F., 2005: Overview of global data assimilation developments in numerical weather prediction centres. Q.J. R. Meteorol. Soc., 131, 3215-3233.

Rosmond, T., and L. Xu, 2006: Development of NAVDAS-AR: nonlinear formulation and outer-loop tests. Tellus, 58A, 45-58.

Xu, L., T. Rosmond, and R. Daley, 2005: Development of NAVDAS-AR: Formulation and initial tests of the linear problem. Tellus, 57A, 546-559.

ASSESSING THE LOCAL ENSEMBLE TRANSFORM KALMAN FILTER AND ITS ASSIMILATION OF AIRS OBSERVATIONS

Elana Fertig[1], H. Li, J. Liu, J. Aravéquia, B.R. Hunt, E. Kalnay, E.J. Kostelich, I. Szunyogh, R. Todling

[1] Department of Mathematics and Institute of Physical Science and Technology, University of Maryland, College Park, MD, USA
E-mail: *ejfertig@math.umd.edu*

Abstract: The Local Ensemble Transform Kalman filter (LETKF) is applied to the NASA fvGCM to assimilate simulated rawinsonde observations. The LETKF analysis is found to have significantly less error than that obtained from the operational 3D-VAR scheme, NASA PSAS, and is found to have significantly less error. This scheme is also used to assimilate AIRS observations on the NCEP GFS. The addition of AIRS retrievals significantly improves the resulting analysis and forecasts. Ultimately, LETKF will be applied to assimilate AIRS radiances.

Keywords *– Data assimilation, ensembles, satellite observations*

1. INTRODUCTION

The Local Ensemble Transform Kalman Filter (LETKF, Hunt et al., 2006) efficiently assimilates observations while accounting for the "errors of the day" (Kalnay, 2002). Motivated by its accuracy and efficiency, LETKF is applied to the NASA fvGCM to assimilate simulated rawinsonde observations. The accuracy of this analysis is compared to that obtained from the operational 3D-VAR scheme, NASA PSAS, and is found to have significantly less error. Szunyogh et al. (2006) found similar results on the NCEP GFS model for real rawinsonde observations. We use the implementation of LETKF on the NCEP GFS to assimilate AIRS retrievals. These retrievals are observed to have a significant positive impact on the LETKF analysis.

2. LOCAL ENSEMBLE TRANSFORM KALMAN FILTER

LETKF updates an ensemble of background model states. The background is estimated by the ensemble mean of these model states and the background error covariance by their sample covariance. Like Bishop et al.'s (2001) Ensemble Transform Kalman filter, LETKF performs this update in the space spanned by the ensemble. Specifically, the mean analysis state can be thought of as the linear combination of the background ensemble members that best fits the available observations (Hunt et al., 2006). In this way, LETKF can be applied to assimilate observations at their observation time by seeking the linear combination of the ensemble trajectories which best fits the observations available between analysis times (Hunt et al., 2004).

Like Ott et al. (2004), LETKF obtains a local analysis for each model grid point independently. Specifically, it updates the state at each grid point using only those observations within a specified local region centered at this grid point. Because the update is independent for each grid point, LETKF can be implemented in a very parallel fashion. Furthermore, within this local region the dynamics can be presumed to be low-dimensional, enabling LETKF to use a small, 40 member ensemble (Szunyogh et al., 2005; Liu et al., 2006).

3. PERFECT MODEL EXPERIMENTS ON THE NASA fvGCM

We compare LETKF to the operational 3D-VAR data assimilation scheme, NASA PSAS, on the NASA fvGCM (GEOS4). This comparison is made in the perfect model scenario. That is, integrating the model for two months from the operational analysis at 18Z December 16, 2002 provides a known true state of the atmosphere. We simulate observations by interpolating the true state to real rawinsonde locations and adding zero mean, Gaussian noise with standard deviation of real instrument error. The resulting analyses using these observations obtained by LETKF and PSAS are compared to the truth.

The results of this study are described in depth in Liu et al. (2006). We find that LETKF improves the analysis because it can capture the errors of the day, while PSAS cannot. The percentage improvement of the LETKF analysis over the PSAS analysis is significant over the entire globe, typically at 30% and reaching 50% in the Southern Hemisphere. However, the LETKF analysis has a problem updating the background at the poles, which is particularly apparent when assimilating real observations. We believe that these problems are associated with the grid point localization we have used in this version of the LETKF, whereas a localization based on observation distance implemented on the NCEP GFS is not affected by the pole problem.

4. ASSIMILATING AIRS RETRIEVALS

Because of the analysis errors apparent at the poles in the fvGCM, we have switched to a version of the LETKF implemented on the NCEP GFS with observation based localization. For this model, Szunyogh et al. (2006) have demonstrated that the LETKF analysis and resulting forecasts are better than those obtained from the operational 3D-VAR scheme (SSI) when assimilating all conventional, non-radiance observations. Therefore, we use this implementation of LETKF on the NCEP GFS to assimilate AIRS retrievals provided by Chris Barnet, which use the retrieval algorithm described in Susskind et al. (2003, 2006). Furthermore, as described in Section 2, the implementation of LETKF employed here assimilates the AIRS retrievals at the correct time. We find that the AIRS retrievals have a significant positive impact on the analysis and corresponding forecasts obtained from LETKF. Their improvement is largest in the Southern Hemisphere, but is still significant in the Northern Hemisphere. It is remarkable that the impact of AIRS retrievals is consistently positive even in the Northern Hemisphere, and becomes neutral only when AIRS data is missing.

5. CURRENT WORK

We are currently planning to use LETKF to assimilate AIRS retrievals generated by other schemes in order to compare the quality of these retrievals. We are further extending LETKF to assimilate AIRS radiances on the NCEP GFS. The ensemble scheme should have a particular advantage for assimilating these observations because LETKF does not require either the adjoint or Jacobian of the forward operator. Furthermore, we have shown the potential impact of these radiance observations (Aravéquia et al., 2006). We will compare the results obtained from assimilating clear radiances and those obtained from assimilating cloud cleared radiances which are much more abundant.

Acknowledgements: *Chris Barnet provided the AIRS retrievals, and discussions with the AIRS Science Team were useful. This work has been funded by NASA grants NNG04GK29G and NNG04GK78A.*

REFERENCES

Aravéquia, J.A., E. Kalnay, E.J. Fertig, H. Li, and J. Liu, 2006: Observation operator and estimation of uncertainty in the assimilating of AIRS radiances using ensemble Kalman filter. 15th International TOVS Study Conference, 4-10 October, 2006, Martea, Italy.

Bishop, C., B. Etherton, and S. Majumdar, 2001. Adaptive sampling with the ensemble transform Kalman filter. Part I: Theoretical aspects. *Monthly Weather Review* **129**, 420–436.

Hunt, B.R., E. Kalnay, E.J. Kostelich, E. Ott, D.J. Patil, T. Sauer, I. Szunyogh, J.A. Yorke, and A.V. Zimin, 2004: Four-dimensional ensemble Kalman filtering. *Tellus* **56A**, 273–277

Hunt, B.R., E.J. Kostelich, and I. Szunyogh, 2006: Efficient data assimilation for spatiotemporal chaos: a local ensemble transform Kalman filter. *Physica D* (submitted).

Kalnay, E. 2002. *Atmospheric Modelling, Data Assimilation, and Predictability*. Cambridge University Press, New York.

Liu, J., E.J. Fertig, H. Li, I. Szunyogh, B.R. Hunt, E. Kalnay, E.J. Kostelich, and R. Todling, 2006: Application of Local Ensemble Transform Kalman Filter: perfect model experiments with NASA fvGCM model. 86th AMS Annual Meeting. Jan26-Feb2, 2006, Atlanta, GA, US. (Peer reviewed manuscript in preparation).

Ott, E., B.R. Hunt, I. Szunyogh, A.V. Zimin, E.J. Kostelich, M. Corrazza, E. Kalnay, and J.A. Yorke, 2004: A local ensemble Kalman filter for atmospheric data assimilation. *Tellus* **56A**, 415–428.

Susskind, J., C.D. Barnet, and J.M. Blaisdell, 2003: Retrieval of atmospheric and surface parameters from AIRS/AMSU/HSB data in the presence of clouds. *IEEE Trans. Geosci. Remote Sens.* **41**, 390-409.

Susskind, J., C.D. Barnet, J.M. Blaisdell, L. Iredell, F. Keita, L. Kouvaris, G. Molnar, and M.T. Chahine, 2006: Accuracy of geophysical parameters derived from Atmospheric Infrared Sounder/Advanced Microwave Sounding Unit as a function of fractional cloud cover. *J. Geophys. Res.* **111,** doi:10.1029/2005JD006272, 19 pgs.

Szunyogh, I., E.J. Kostelich, G. Gyarmati, D.J. Patil, B.R. Hunt, E. Kalnay, E. Ott, and J.A. Yorke, 2005: Assessing a local ensemble Kalman filter: Perfect model experiments with the National Centers for Environmental Prediction global model. *Tellus* **57A**, 528–545.

Szunyogh, I., E.J. Kostelich, G. Gyarmati, E. Kalnay, B.R. Hunt, E. Ott, and J.A. Yorke, 2006: Assessing a local ensemble Kalman filter: Assimilating real observations with the NCEP global model. In preparation for submission to *Tellus A.*

IMPACT OF ESTIMATED LAND EMISSIVITIES FROM SATELLITE MICROWAVE OBSERVATIONS IN THE 4D-VAR SYSTEM AT METEO-FRANCE

Fatima Karbou, Élisabeth Gérard and Florence Rabier
CNRM / GAME, Météo-France, 42 avenue Coriolis, 31057, Toulouse, France
E-mail: *florence.rabier@meteo.fr*

Abstract: Satellite microwave observations are still more intensively used over oceans than over land in many weather prediction centres. However their assimilation might be needed in some land areas which are not adequately covered by conventional observations and where hight impact weather can occur, such as Africa for instance. This paper describes the studies conducted at Météo-France in order to assimilate more microwave channels from different sensors over land. In order to reduce the uncertainties about the land emissivity estimation, three land surface parameterisations have been tested in the framework of 4D-VAR assimilation. Some assimilation results are presented in this paper.

Keywords – *Microwave observations, Land, Data assimilation.*

1. INTRODUCTION

Satellite microwave measurements obtained from AMSU-A, AMSU-B and SSM/I like instruments are known to be very useful for atmospheric applications. These observations could be used for atmospheric temperature and humidity monitoring as well as for retrieving surface information. The lesser sensitivity of microwave observations to clouds allows their use in most atmospheric situations. Till now, microwave measurements are more intensively used over oceans than over land. Indeed, uncertainties about the surface temperature and emissivity are larger over land than over oceans. In the present work, three new land emissivity parameterisations have been used in order to better estimate the land emissivity and/or skin temperature (Karbou et al. 2006a). the first parameterisation uses an averaged emissivity climatology obtained using data from two weeks prior to the assimilation period. Within the second land parameterisation the emissivity is dynamically estimated for each instrument at selected frequencies and then allocated to the remaining channels. The second parameterisation is based on the first one with the addition of skin temperature estimates from selected frequencies. During the assimilation, channels that were used for dynamical estimation of emissivity or skin temperature are discarded from any other computations or diagnostics. In the framework of 4D-Var assimilation, several experiments have been conducted using the new parameterisations in order to examine the feasibility of assimilating more microwave observations over land.

2. SATELLITE MICROWAVE OBSERVATIONS AND EMISSIVITIES

The Advanced Microwave Sounding Units (AMSU) A and B are on board the polar orbiting satellites of the National Oceanic and Atmospheric Administration (NOAA), of the National Aeronautics and Space Administration (NASA) and also on boad the Metop mission. The Special Sensor Microwave / Imager (SSM/I) sensors are on board the operational Defense Meteorological Satellite Program (DMSP) since 1987. AMSU-A instrument have channels near the 50-60 GHz oxygen band and is therefore designed for atmospheric temperature sensing whereas AMSU-B is dedicated to humidity probing (with channels near the 183.31 GHz water vapour absorption line). Both instruments have channels that receive a strong contribution from the surface (23.8, 31.4, 50.3, 89, and 150 GHz, called hereafter surface channels) and provide measurements with a mixed polarisation together with a varying observation zenith angles (from -58° to 58°). SSM/I imager provides observations at 19, 22, 37, and 85 GHz, with horizontal and vertical polarisations (only vertical for the 22 GHz channel) and at a fixed zenith angle (53°).

Currently, the Météo-France 4D-VAR system uses Grody (1988) or Weng et al. (2001) models to get emissivity estimates at AMSU frequencies and constant emissivities for SSM/I channels. If the emissivity models help assimilating channels that receive a weak contribution from the surface, their use for surface channels is less successful. In fact, to give emissivity estimates with an accuracy that meets the Numerical Weather Prediction (NWP) requirements, the emissivity models require reliable but badly needed input parameters (soil moisture, vegetation description, soil roughness, among others).

As an alternative to emissivity models, direct emissivity computations using satellite observations have been conducted. For a selected surface channel, the microwave emissivity is derived by removing the rain free atmospheric contribution to the observation using the RTTOV model (Eyre 1991; Saunders et al. 1999, Matricardi et al. 2004). Short range forecast temperature and humidity fields are used to feed the radiative transfer model as well as the short range forecast of the surface temperature. Figure 1 compares mean emissivity maps for SSM/I channel 1 (19V GHz) obtained using the operational model and using SSM/I observations.

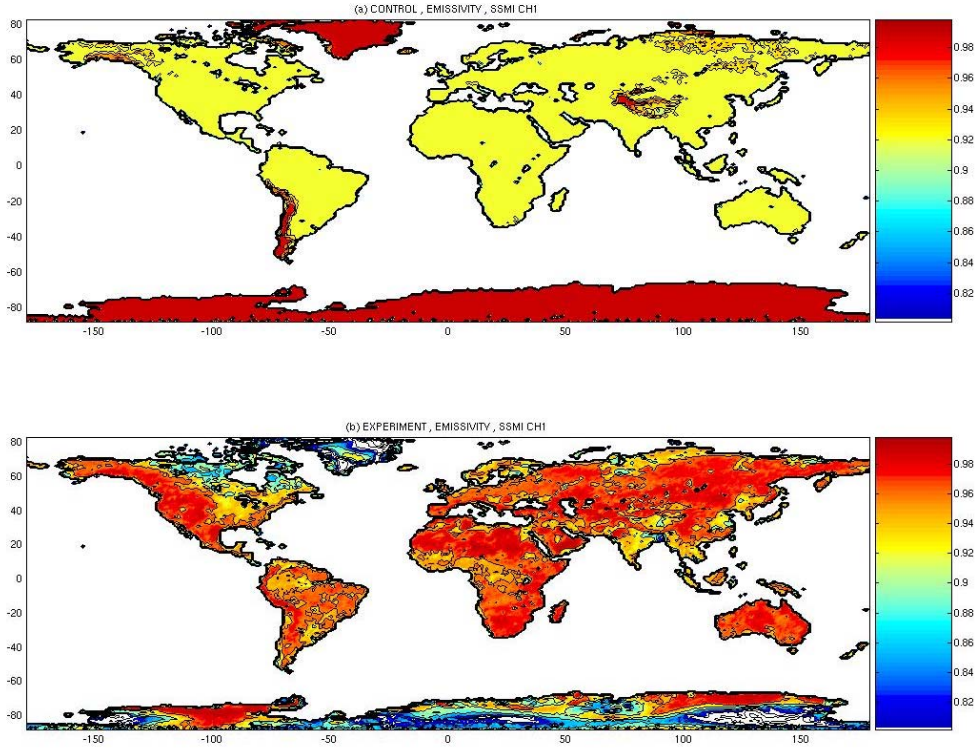

Figure 1. Mean emissivity maps averaged over a two-week period (from 01/08/2005 to 14/08/2005) (a) obtained from the operational model and (b) directly calculated from SSM/I observations.

3. ASSIMILATION EXPERIMENTS

In this paper, we used the Météo-France assimilation and forecast model system (ARPEGE) that uses a 6-hour time window and a multi-incremental 4D-VAR (Courtier et al. 1994; Veersé and Thépaut 1998; Rabier et al. 2000). For satellite radiance assimilation, our observation operator is the RTTOV radiative transfer model. Several assimilation experiments have been performed over different periods during 2005 and using the new land surface parameterisations together with a control experiment that uses the operational model. The parameterisations were applied to AMSU-A, AMSU-B and SSM/I observations. Table 1 describes the different assimilation experiments.

Experiment	sensors	Channels used	Land scheme
Control		As in the operational	operational
AMSU_DYN	AMSU-A & -B	Addition of channels: 1, 2, 4 and 15 (AMSU-A) and 2, 3, 4, 5 AMSU-B over land	Dynamical emissivity estimation at channel 3 AMSU-A (50 GHz) and at channel 1 AMSU-B (89 GHz)
AMSU_ATLAS	AMSU-A & -B	Addition of channels: 1, 2, 4 and 15 (AMSU-A) and 2, 3, 4, 5 AMSU-B over land	Use of an averaged atlas
AMSU_SKIN	AMSU-A & -B	Addition of channels: 1, 2, 4 and 15 (AMSU-A) and 2, 3, 4, 5 AMSU-B over land	Averaged emissivity atlas + dynamical skin temperature estimation at channel 3 AMSU-A (50 GHz) and at channel 1 AMSU-B (89 GHz)
SSMI_DYN	SSM/I	Addition of SSM/I channels 3, 4, 5, 6, and 7 over land	Dynamical emissivity estimation at channel 1 (19V GHz) and at channel 2 (19H GHz)

Table 1. An overview of the assimilation experiments.

4. IMPACT ON THE OBSERVATION OPERATOR PERFORMANCES

The land schemes have been evaluated by looking at the performances of the RTTOV brightness temperature (Tb) simulations over land. For all schemes, and by comparison to the control experiment, the Tb simulations are in better agreement with the observations. The First guess departures (observations-simulations) statistics are improved and we noticed an increase of the number of assimilable observations (up to 150% for AMSU-B channel 2 (150GHz)). Figure 2 shows the mean First guess departures obtained over a two week period for SSM/I channel 3 (22V GHz) from (a) the control experiment and (b) from the SSMI_DYN experiment. It should be mentioned that within the SSMI_DYN experiment, the emissivity derived at channel 1 (19V GHz) has been used for all SSMI channels that have a vertical polarisation. In the same manner, emissivity derived at SSM/I channel 2 (19H) has been used for SSMI channels having a horizontal polarisation.

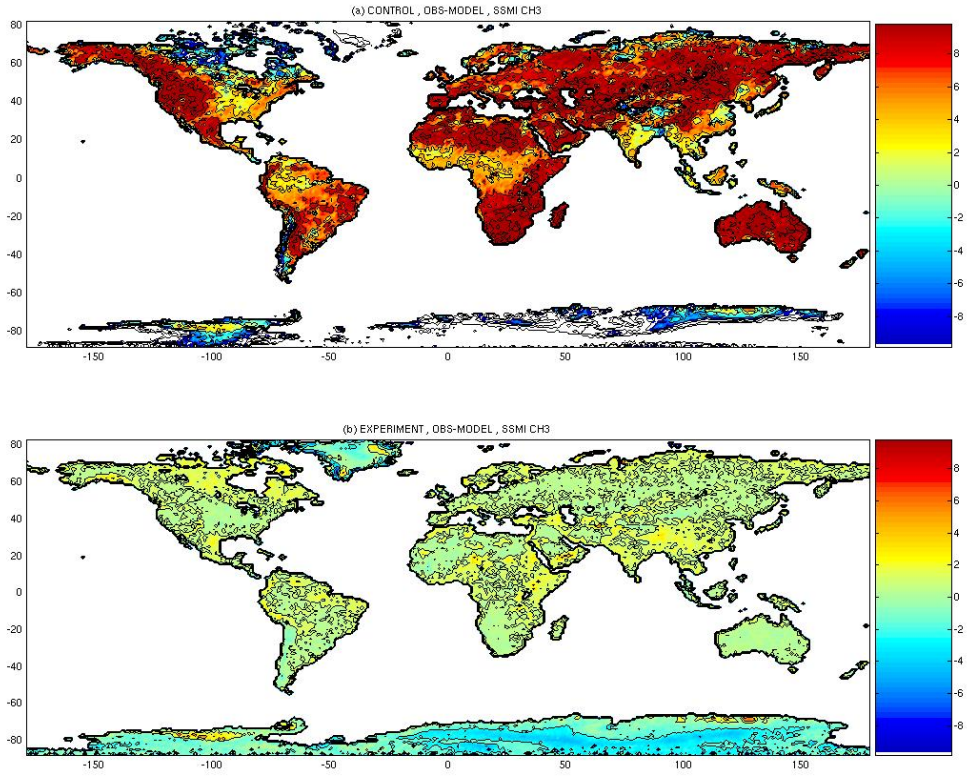

Figure 2. Mean first guess -departure maps for SSM/I channel 3 (22V GHz) averaged over a two week period (from 01/08/2005 to 14/08/2005) obtained (a) from the control, (b) from the experiment SSMI_DYN.

5. IMPACT ON THE ANALYSED AND FORECASTED FIELDS

The different assimilation experiments have also been evaluated by looking at the analysis and forecast fields (Gerard et al. 2006, Karbou et al. 2006b). For all experiments that use an updated surface emissivity scheme, a global drying of the atmosphere over land and a global moistening of the atmosphere over sea are observed. This effect was particularly beneficial to areas famous for their lack of strato-cumulus clouds like in the Guinea Gulf and also to too rainy areas (in particular Central Africa and Arabia). The African monsoon was seen to be displaced in the analysis and forecasts using these new data over land, consistently with other observations. The forecast scores are globally positive for humidity and temperature. Further experiments, focussing over Africa during the AMMA experiment in 2006 will be conducted. The wealth of extra data collected during the experiment will help to validate the approach.

REFERENCES

Courtier, P., J. N. Thépaut, and A. Hollingsworth, 1994, A strategy for operational implementation of 4D-Var using an incremental approach. Q. J. R. Meteorol. Soc. 114, 1321-1387.

Eyre, J. R. 1991, A fast radiative transfer model for satellite sounding systems. ECMWF Tech. Memo. 176, 28 pp.

Gérard, E., F. Karbou, F. Rabier, and Z. Sahlaoui, 2006, Assimilation of SSM/I radiances over sea and over land at Météo-France, *Quart. J. Roy. Meteor. Soc*.,To be submitted.

Grody, N. C. 1988, Surface identification using satellite microwave radiometers, *IEEE Trans. On Geoscience and Remote Sensing*, 26,850-859.

Karbou, F., E. Gérard, and F. Rabier, 2006a: Microwave Land Emissivity and Skin Temperature for AMSU-A & -B Assimilation Over Land, *Quart. J. Roy. Meteor. Soc*., Vol. 132, No. 620, Part A.

Karbou, F., E. Gérard, F. Rabier, E. Bazile, 2006b: Impact of Microwave Land Emissivity from AMSU Measurements in the 4D-Var system at Météo-France, *Quart. J. Roy. Meteor. Soc*., To be submitted.

Matricardi, M., F. Chevallier, G. Kelly, and J. N. Thépaut, 2004, An improved general fast radiative transfer model for the assimilation of radiance observations, *Quart. J. Roy. Meteor. Soc*., 130, 153-173.

Saunders, R. W., M. Matricardi, and P. Brunel, 1999, An improved fast radiative transfer model for assimilation of satellite radiance observations, *Quart. J. Roy. Meteor. Soc*., 125, 1407-1425.

Rabier F., H. Jarvinen, E. Klinker, J. F. Mahfouf and A. Simmons, 2000, The ECMWF operational implementation of four dimentional variational assimilation. I: Experimental results with simplified physics. Q. J. R. Meteorol. Soc. 126, 1143-1170.

Veersé, F. and J. N. Thépaut 1998 Multiple truncation incremental approach for four dimensional variational data assimilation. Q. J. R. Meteorol. Soc. 124, 1889-1908.

Weng, F., B., Yan, and N. Grody, 2001 A microwave land emissivity model. J. Geophys. Res. 106, D17, 20,115-20,123.

NOTE from the editor:

The size of this abstract exceeds the 2-page specification by far. It was only included as an exception as the other contributors followed the guidelines

EXPLOITATION OF SATELLITE DATA FOR NWP

Roger Saunders[1] and Stephen English[1]

[1] Met Office, Fitzroy Rd, Exeter, EX1 3PB, United Kingdom
E-mail: *roger.saunders@metoffice.gov.uk*

Abstract: The satellite data assimilated in numerical weather prediction models is described using the Met Office model as an example. The impact of the satellite data on the forecasts using the Met Office 3D-Var assimilation is also documented.

Keywords *– Satellite Data, NWP, Data Assimilation*

1. INTRODUCTION

Over the last decade the use of satellite data in numerical weather prediction (NWP) models has expanded significantly both in terms of data volumes and diversity in the type of satellite observation. The main impetus for this has been the significant improvement in forecast performance which can be directly attributed to the use of the satellite data improving the model initial state. This has been a major success story for mankind enabling significantly better forecasts of severe weather phenomenon and hence providing more informed and earlier guidance to the general public.

The pre-processing and delivery of satellite data to NWP centres has also improved in recent years with the majority of the data arriving within 3 hours of the measurement time which is essential for the data to be used before the model cut-off times which are under constant pressure to be reduced. In parallel to the availability of the new satellite data the data assimilation systems have also been modified to make use of the concept of variational data assimilation (Lorenc, 1986) which takes into account the spatial and temporal changes in the model to make optimal use of the observations at the actual measurement time. In addition the variational assimilation allows the use of the actual measured quantity (e.g. top of atmosphere radiances) instead of relying on retrieved profiles of model variables (e.g. retrieved temperature profiles) and this has been shown to be beneficial as it removes any 'first guess dependence' in the retrieval which may be inconsistent with the model. Most NWP centres are now using a 4D-Var assimilation (Rabier *et. al.*, 2000) which allows for changes in space and time.

2. SATELLITE DATA USED AT MET OFFICE

The satellite data currently being received and operationally assimilated in the Met Office models is outlined in Table 1. It is worth noting that only a small fraction of the satellite data is actually assimilated due to various factors. The first reason is simply a resources problem of the computing power available being unable to assimilate all the available observations. Each radiance observation requires a radiative transfer model calculation which can be expensive if many thousands of channels/observations have to be simulated. The second reason is that the model spatial resolution is currently of order 50km and so observations cannot be used

Observation group	Observation Sub-group	Items used	# daily extracted	% used in assimilation
Satellite-based vertical profiles of Temperature and humidity	AMSU-A/B + MHS NOAA-15/16/18 AIRS AQUA SSMIS GPS-RO CHAMP/GRACE	'Clear' top of atmosphere radiances directly assimilated Refractivity profile	430000 36000 2700000 300	3 4 0.6 35
Satellite atmospheric motion vectors	GOES 10,12 BUFR Meteosat 5, 8 BUFR MTSAT SATOB MODIS Polar BUFR	High resolution IR winds IR, VIS and WV winds IR, VIS and WV winds IR and WV winds	110000 190000 4000 42000	10 5 55 6
Satellite-based surface winds	SSM/I-13 Seawinds ERS-2 scatt	1DVAR wind speed retrieval NESDIS/ESA retrieval of ambiguous winds. Ambiguity removal in 4DVAR.	3000000 1800000 140000	1 1.5 1.5

Table 1. *Satellite data currently used at the Met Office as of October 2006.*

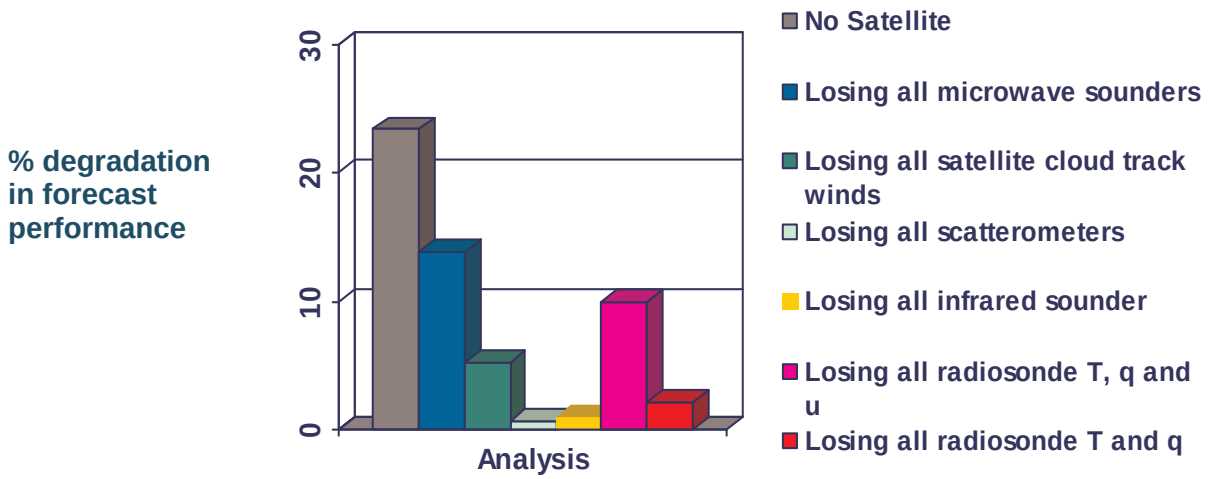

Figure 1. *Impact of satellite and radiosonde observations in the Met Office global model*

on a denser grid. Thirdly the satellite observations often have horizontally correlated biases over length scales of a few hundred kilometres and so using a high density of observations can bias the assimilation in an inappropriate manner. The recent launch of the European METOP polar orbiting satellite will soon provide additional sensors to those listed in Table 1 (i.e. AMSU-A, MHS, HIRS, IASI, ASCAT, GRAS, GOME-2) all of which will be used in NWP models in the near future enhancing the global coverage. The continued increase in the number of satellite sensors and for some sensors large increases in data volume will present a challenge to the NWP centres to use these new data in the coming decade. Also with NWP models becoming more sophisticated, representing minor gases in addition to water vapour, more sensors and/or channels from existing sounders will also be required to provide data on the minor gas concentrations.

3. SATELLITE DATA IMPACTS

The impact of the different satellite observation types on the forecast is shown in Figure 1 in the Met Office 3D-Var system. The plot shows the degradation in forecast skill for a 'basket' of key forecast fields over several forecast ranges from 1 to 5 days verified by the NWP analysis for the valid forecast time. The main conclusion from this plot is that the loss of all the satellite data (grey bar) degrades the forecasts by more than ***twice*** as much as the degradation when radiosondes (purple bar) are removed from the system. The second point is that the microwave sounder radiances provides the main contribution to the impact with smaller contributions from the infrared sounder radiances, surface and cloud motion winds. Note that greater impact from the infrared sounder data will be expected when more of the high spectral resolution data (e.g. AIRS and IASI) are assimilated. The microwave sounder provides 6 times more impact for temperature and humidity fields than the radiosondes but note the radiosonde winds are still important. Satellite cloud track winds have a good impact and scatterometer surface winds also have a smaller but significant impact and are important for improving the forecasting of tropical cyclones. More details on these observation system experiments can be found in English *et. al.* (2004).

For the future the hope is that using more of the satellite data over land, sea-ice and over cloud will increase the impact of these data. In addition new sensors such as IASI, a high spectral resolution infrared interferometer for better temperature, humidity and trace gas profiles and ADM-Aeolus a doppler wind lidar for 3D winds in the troposphere will provide significantly more benefits to the NWP models of the future.

REFERENCES

English, S., Saunders, R., Candy, B. Forsythe and Collard, A. 2004: Met Office Satellite Data OSEs. *Proc. of 3rd WMO workshop on the impact of various observing systems on NWP, Alpbach Austria 9-12 Mar 2004 pp 146-156.*

Lorenc, A. 1986: Analysis methods for numerical weather prediction. *Quart. J. Roy. Meteorol. Soc.* **112** *pp 1177-1194.*

Rabier, F., Järvinen, H. Klinker, E., Mahfouf, J-F. and Simmons A. 2000: The ECMWF operational implementation of four dimensional variational assimilation Part I: Experimental results with simplified physics. *Quart. J. Roy. Meteorol. Soc.* **126** *pp 1143-1170.*

TOWARDS MORE ACCURATE WATER VAPOUR OBSERVATIONS: AIRBORNE LIDAR MEASUREMENT EXAMPLES AND CHARACTERISTICS

Christoph Kiemle[1], Harald Flentje[2], Andreas Dörnbrack[1], Andreas Fix[1] and Gerhard Ehret[1]

[1]DLR, Institut für Physik der Atmosphäre, Oberpfaffenhofen, Germany
[2]Deutscher Wetterdienst, Observatorium Hohenpeissenberg, Germany
E-mail: *Christoph.Kiemle@dlr.de*

Abstract: Airborne differential absorption lidar measurements of mid-latitude, subtropical and tropical water vapour were performed during several recent campaigns over North and South America, and Australia, as well as on the corresponding long-range transfer flights from and to Germany with the DLR "Falcon" research aircraft. These include tropospheric as well as lower stratospheric observations. Complex advection and rapid vertical transport associated with meso- and synoptic scale dynamical processes reflect in inhomogeneous water vapour distributions along the flight paths, as observed by the lidar. The tropical (Hadley) circulation, stratospheric intrusions and humidity transitions between different air masses are clearly detected. The measurements are compared to operational ECMWF analyses interpolated in space and time to the flight path. The relevant transport processes are adequately represented in the analyses as long as vertical and horizontal scales exceed roughly 0.5-1 km in the vertical and 50 km horizontally, while smaller structures and larger gradients are smoothed out. On the longer term, space-borne lidar instruments may provide unprecedented high-resolution (especially in the vertical) and high-precision, low-bias observations of water vapour throughout the troposphere with high added value to next generation observing systems for assimilation into NWP models.

Keywords – *Airborne Lidar, Water Vapour Observations, Stratospheric Intrusions.*

1. INTRODUCTION

Water vapour, the most important greenhouse gas, controls cloud formation and the evolution of weather systems. As its tropospheric concentration may rapidly vary over four orders of magnitude, accurate monitoring especially in the upper troposphere and lower stratosphere (UT/LS) and in remote areas remain important scientific and logistical issues. Water vapour assimilation is still limiting the accuracy of numerical weather prediction (NWP) models, most of which are based on lower and middle tropospheric humidity from regular radiosonde soundings that do not provide reliable humidity profiles at altitudes > 300 hPa or in dry regions < 0.1 g/kg. Moreover, major "birth" regions of severe continental weather to which short-term forecast errors are most sensitive are often only covered by few radiosonde stations. It is therefore obvious to question the accuracy of water vapour distributions in weather services' analyses, particularly with respect to the scales, lifetime and geographical location of investigated structures.

2. OBSERVATIONS

Between 2002 and 2005 the DLR Falcon research aircraft performed long-range transfer flights to various remote campaign destinations in Oklahoma, Brazil and Australia, carrying the water vapour Differential Absorption Lidar (DIAL) in nadir looking arrangement. The DIAL transmitter is based on a Nd:YAG pumped, injection seeded KTP-OPO (Optical Parametric Oscillator) which produces 18 mJ per pulse at 925 nm at 100 Hz. Atmospheric backscatter is measured simultaneously. Using the 925 nm spectral region allows to cover typical water vapour concentrations from the PBL to the upper troposphere with vertical and horizontal resolutions of some 100 m to 1 km and few km to about 10 km, respectively. Main sources of systematic errors are the uncertainty in the determination of the water vapour absorption line cross section (5% estimated uncertainty), laser spectral impurity (1-2%), atmospheric temperature uncertainty (<1%), and the Rayleigh-Doppler absorption line broadening (<1.5%), about 5% in geometric total (Poberaj et al., 2002). The statistical error, controlled by horizontal and vertical averaging, mostly remains below 10%.

Water vapour and aerosol/cloud distributions have been measured with the DLR airborne DIAL in May 2002 during the transfer flights to the International H2O Project (IHOP_2002) across the Northern Atlantic Ocean (Figure 1). The flights went from Germany via Iceland, Greenland and Canada to Oklahoma. Owing to intense dynamical activity over the Atlantic a variety of complex atmospheric structures was observed during the transects such as stratospheric intrusions, PV streamers, frontal zones, gravity waves, convection and patches of vertical turbulence. Stratospheric intrusions and extended extremely dry layers even in the lower troposphere turn out to be the normal case rather than the exception in this part of the globe. The large dynamical range of tropospheric water vapour is impressively demonstrated. Large gradients in the H_2O and backscatter fields dominate the scene and in general can *qualitatively* be reproduced by mesoscale simulations and even to a large extent by ECMWF analyses. However, the gradients and the minimum mixing ratios can not yet be satisfactorily reproduced in a quantitative sense (Flentje et al., 2005).

Figure 2 shows water vapour lidar results of another long-range flight of the DLR Falcon between Dubai and Hyderabad (India) on its way back from a campaign in Australia in late 2005. T799/L91 operational analyses of the European Centre for Medium Range Weather Forecast (ECMWF), interpolated linearly in space and time to the transfer flight path are used for the comparison to the lidar observations. The large-scale circulation is reproduced by the ECMWF analyses but differences are found at smaller scales where strong gradients occur and rapid temporal development takes place due to advection perpendicular to the measurement plane.

The long-range water vapour lidar data will be used for assimilation experiments with the ECMWF global model. First test experiments indicate a reduction of the model's first-guess errors of the water vapour column in the vicinity of the observations. However, this has to be consolidated with further experiments.

3. CONCLUSIONS AND OUTLOOK

Airborne lidar provides unprecedented high-resolution (especially in the vertical) and high-precision, low-bias observations of water vapour throughout the troposphere. Future space-borne lidar instruments could be of high added value to next generation observing systems for NWP because, unlike passive remote sensors, lidar measurements are basically calibration-free, do not depend on a-priori information and are not biased by surface albedo variations, aerosols or clouds. The potential benefit of such new-quality water vapour observations to NWP models could be threefold: First, the exact 4-D location of intrusions of stratospheric dry air into the upper and middle troposphere will help constrain the model dynamics when using variational assimilation techniques. Similar to the construction of motion vectors from cloud tracking, the tracking of stratospheric intrusions in lidar water vapour observations will provide motion vectors in cloud-free regions and in typically highly-sensitive regions like the North Atlantic storm track area where intrusions often occur. Second, latent heat release from the evolution of convective systems influences the local and mesoscale dynamics; here, more accurate water vapour observations prior to the initiation of strong convection would directly improve the model performance when appropriately assimilated. Last not least, the model physics would be improved through better subgrid scale parameterisations from process studies based on the high resolution observations.

REFERENCES

Flentje, H., A. Dörnbrack, G. Ehret, A. Fix, C. Kiemle, G. Poberaj and M. Wirth, 2005: Water vapour heterogeneity related to tropopause folds over the North Atlantic revealed by airborne water vapour differential absorption lidar, *JGR* Vol. 110, D03115, doi: 10.1029/2004JD004957.

Poberaj, G., A. Fix, A. Assion, M. Wirth, C. Kiemle, and G. Ehret, 2002: All-Solid-State Airborne DIAL for Water Vapor Meas. in the Tropopause Region: System Description and Assessment of Accuracy, *Appl. Phys. B* 75, 165-172.

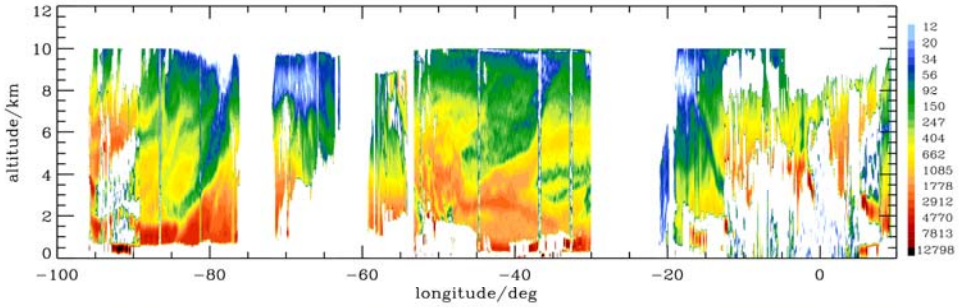

Figure 1. Vertical tropospheric cross section of water vapour mixing ratio (mg/kg) over the North Atlantic. The vertical lidar resolution is 0.5 km. The observed intrusions of dry stratospheric air into the troposphere are associated to the complex dynamics of subsequent synoptic systems. See Flentje et al., 2005.

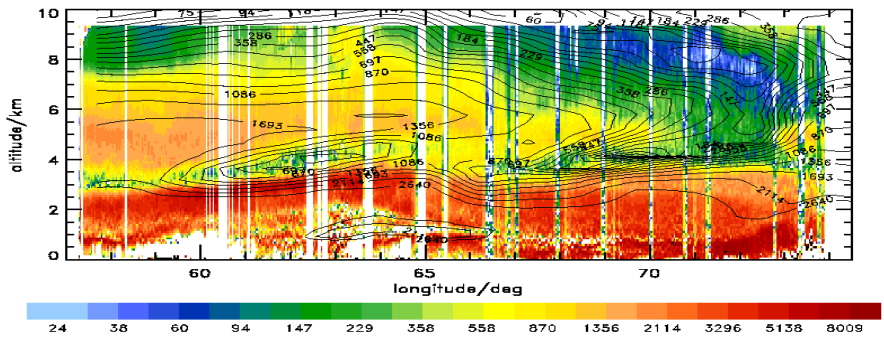

Figure 2. Lidar cross section of water vapour volume mixing ratio (µmol/mol; colours) with ECMWF analysis (T799/L91; lines) interpolated to the flight path. The stratospheric intrusion is well captured by the model; smaller scale and boundary layer humidity variations are smeared or not represented.

ADM-AEOLUS: ESA'S DOPPLER WIND LIDAR MISSION

Paul Ingmann[1], Anne Grete Straume[1], Dulce Lajas[1] and the ADM-Aeolus Mission Advisory Group[2]

[1] ESA/ESTEC, Mail-code EOP-SMA, Mission Science Division, Postbus 299, NL-2200 AG Noordwijk, The Netherlands, e-mail: *paul.ingmann@esa.int*

[2] E. Andersson, ECMWF; A. Dabas, Météo France; P. Flamant, LMD; E. Källén, MISU; P. Menzel, NOAA; D. Offiler, UKMO; O. Reitebuch, DLR; L.-P. Riishøjgaard, NASA-GSFC/GMAO, H. Schyberg, met.no; A. Stoffelen, KNMI; M. Vaughan, MMA; W. Wergen, DWD

Abstract: ADM-Aeolus will be the first active remote sensing satellite mission to provide global wind profiles for real-time use in numerical weather prediction. The mission is expected to pave the way for future operational meteorological satellites dedicated to measure the Earth's wind fields. The instrument is the second ESA Earth Explorer Core Mission scheduled for launch in 2008.

Keywords: *Doppler wind lidar, global wind profiles, numerical weather prediction*

1. INTRODUCTION

The first European satellite-based wind lidar concept was developed in the 1980's. These preparatory activities, including theoretical studies, technical developments and field campaigns, are described in "Report for Mission Selection" (ESA, 1999). This report was presented to the European Earth Observation community at the Earth Explorer selection meeting, and in 1999 ADM-Aeolus was selected for implementation as the second Earth Explorer Core mission. The launch is scheduled for autumn 2008. More details can be found on the ADM-Aeolus homepage (http://www.esa.int/esaLP/LPadmaeolus.html).

2. MOTIVATION

		PBL	Tropo	Strato
Vertical Domain	[km]	0-2	2-16	16-20 (30)
Vertical Resolution	[km]	0.5	1.0	2.0
Horizontal Domain		global		
Number of Profiles	[hour^{-1}]	> 100		
Profile Separation	[km]	> 200		
Horiz. Integration Length	[km]	50		
Accuracy (HLOS)	[ms^{-1}]	1	2	3 (5)
Data Availability	[hour]	3 (goal: 0.5)		
Length of Data Set	[yr]	3		

The primary aim of ADM-Aeolus is to provide global observations of vertical wind profiles from the troposphere and lower stratosphere. Presently, the sampling of the 3-dimensional wind field in large parts of the tropics and over the major oceans is far from sufficient in the global observation system (GOS). This leads to major difficulties both in the studying of key processes in the coupled climate system and in the further improvement of numerical weather prediction (NWP).

Table 1. The ADM-Aeolus observational requirements. Additional mission capability is shown in brackets. HLOS: Horizontal Line-of-Sight wind.

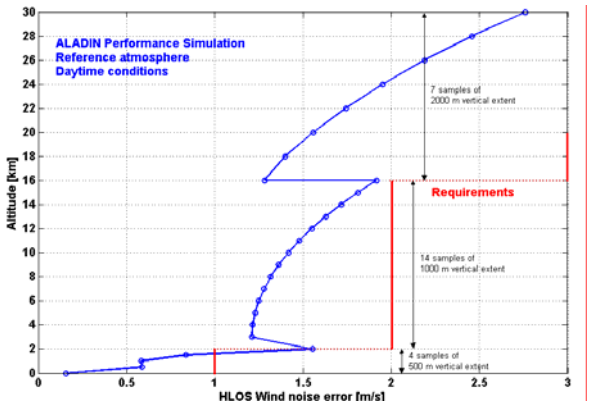

Figure 1: ADM-Aeolus measurement performance estimates from the surface up to 30 km altitude. The red line indicates the observational requirements as given by Table 1.

For a mission intended to demonstrate the feasibility of a full-scale space-borne wind observing system, the requirements on data quality and vertical resolution are the most stringent and most important to achieve. The derivation of the horizontal coverage specification is supported by weather forecast impact experiments, which include the inputs of the conventional wind-profile network. The coverage specification is also compatible with the World Meteorological Organisation (WMO) threshold requirements (e.g. WMO, 2001). Table 1 provides an overview on the ADM-Aeolus requirements. Figure 1 illustrates the expected measurement performances versus height.

ADM-Aeolus is also expected to give information on wind variability as caused by e.g. clear-air turbulence. After its products have been thoroughly validated, it can also be used for comparison and validation of other satellite-based wind and aerosol products.

As a backscatter lidar ADM-Aeolus will deliver height profiles of backscatter and extinction coefficients, and of the lidar ratio. From these parameters it is possible to retrieve cloud and aerosol information such as cloud-top height, the detection of multi-layer clouds and aerosol stratification, cloud and aerosol optical depths (integrated extinction profiles), and cloud and aerosol type (lidar ratio).

A more extended overview on the scientific motivation behind the Atmospheric Dynamics Mission (ADM-Aeolus) can be found in Stoffelen et al. (2005).

3. TECHNICAL AND MEASUREMENT CONCEPTS

The core element of the ADM-Aeolus mission is ALADIN (Atmospheric LAser Doppler INstrument). The laser source is based on a single mode, 120 mJ, 100 Hz pulse repetition frequency, diode pumped and frequency tripled (355 nm) Nd-YAG laser. A 1.5 m diameter Cassegrain afocal telescope is used as transceiver for both transmitting and receiving.

The emitted laser pulse is backscattered in the atmosphere by air molecules (Rayleigh scattering) and particles (Mie scattering), and by the Earth's surface. ADM-Aeolus measures the Rayleigh and Mie signals separately with two receivers. Wind, aerosol and cloud observations are derived from the measured Doppler shift of the backscattered light along the lidar line-of-sight (LOS) (figure 2). The laser will be operated over typically 7 seconds, followed by a 21 seconds period where the laser is switched off. In this 7-second measurement period the satellite will have travelled approximately 50 km and thus the wind and particle properties fields will have been effectively averaged over this distance in the propagation direction. The vertical height resolution is determined by the length of the time-window chosen for the signal accumulation of the return signal.

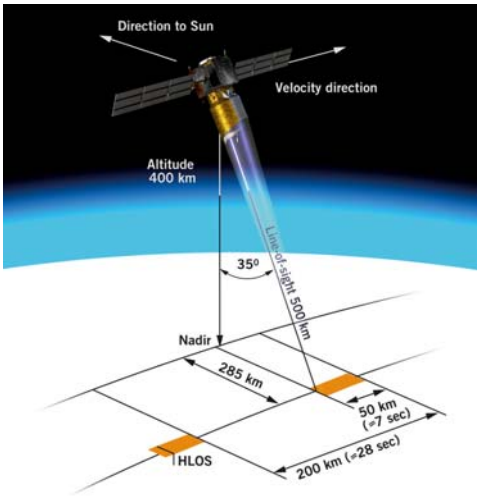

ADM-Aeolus will provide about 3,000 globally distributed wind and particle properties profiles per day at typically 200 km separation along the satellite track down to the surface for clear air and above thick clouds. Wind information within and below thin clouds or at the top of thick clouds is also attainable. A near real-time delivery of data to the main NWP centres is anticipated.

Figure 2. The ADM-Aeolus measurement and sampling concept: The lidar emits a laser pulse towards the atmosphere, then collects and samples the magnitude versus frequency of the backscattered signal. The received signal frequency is Doppler-shifted with respect to the emitted laser light due to the spacecraft motion, the Earth rotation and the wind velocity. The lidar measures the wind projection along the laser line-of-sight (LOS), using a 35° slant angle versus nadir.

4. CONCLUSIONS

Accurate wind profile observations are needed to improve NWP and climate analysis. A feasible concept for a Doppler wind lidar demonstrator (ADM-Aeolus) has been developed and will be implemented as ESA's second Earth Explorer Core Mission. Various scientific and campaign activities are being and will be performed in parallel to the technical activities. These have demonstrated the improvement of NWP forecasting through the inclusion of ADM-Aeolus measurements in the global observation system. Furthermore, the capability of ADM-Aeolus to measure aerosol and clouds optical properties to contribute to a long-term dataset from CALIPSO to EarthCARE has been demonstrated. The ADM-Aeolus launch is scheduled for late 2008. The further adaptation of ADM-Aeolus for full operational use is being studied.

REFERENCES

European Space Agency (ESA), (1999) Atmospheric Dynamics Mission. Report for Mission Selection, ESA SP-1233(4), 157p.

Stoffelen, A., Pailleux, J., Källén, E., Vaughan, J. M., Isaksen, L., Flamant, P., Wergen, W., Andersson, E., Schyberg, H., Culoma, A., Meynart, R., Endemann, M. and Ingmann, P., (2005) The Atmospheric Dynamics Mission for Global Wind Measurement. Bull. Amer. Meteorol. Soc., **86,** pp 73-87.

World Meteorological Organisation (WMO), (2001) Statement of Guidance Regarding How Well Satellite Capabilities Meet WMO User Requirements in Several Applications Areas. Sat-26, WMO/TD No.1052, 52p.

THE STRONG JET STREAM OVER THE NORTH PACIFIC IN NOV-DEC 2005: SEASONAL SENSITIVITY AND FORCING, RESPONSE, FEEDBACKS

Klaus Weickmann[1], Edward Berry[2] and Prashant Sardeshmukh[1]
[1]NOAA/ESRL/Physical Sciences Division, Boulder, CO, USA
E-mail: klaus.weickmann@noaa.gov

Abstract: A case study of the multi-time scale behavior of the global circulation is presented using zonal mean momentum budgets, a synoptic-dynamic model and synoptic analysis of tropical-extratropical interactions. The forcing and poleward movement of zonal flow anomalies is examined including the role of eddies and physical processes.

Keywords: *THORPEX, WMO, weather-climate*

1. INTRODUCTION

The sensitivity of the November-December base state to positive convective forcing over the tropical northwest Pacific has been proposed in recent studies by Newman and Sardeshmukh (1998) and Blade et al. (2007). During November-December 2005, the maturing La Nina and the overall global warming trend in warm pool SSTs led to an SST pattern that left the west Pacific warmer than if there were no trend. Given the above studies and recent statistical results, this season would be favorable for positive PNA patterns as convection becomes active and oscillates over the tropical northwest Pacific.

During November-December 2005, two periods of strong mid-latitude westerly flow were observed in the zonal mean zonal wind and the zonal wind over the Asia-North Pacific region. Each lasted ~20 days and went through a well-defined cycle of growth and decay of zonal mean anomalies. Positive momentum tendencies started south of 30N, and spread slowly poleward and equatorward with time. In late November and early December, the southward shifted jet weakened and ridging was observed over the east North Pacific with cold conditions over the USA during late November to mid-December 2005. The dominance of the strong mid-latitude westerly flow during the two months might be initially attributed to the seasonal sensitivity although feedbacks are clearly also important as is the constant forcing by the MJO and other tropical wave modes. In this study, a synoptic description of both tropical convective flareups and extratropical waves is combined with an analysis of the zonal mean momentum budget to help understand the unusual strength of the jet stream during Nov-Dec '05 despite the La Nina tropical convective forcing.

2. MJO-LIKE VARIABILITY

After global warming and the maturing La Nina, the remaining "big picture" consists of five MJO-like events shown in Fig. 1. Each case has tropical convection anomalies that extend east over the tropical northwest Pacific to at least 140E. All produce westerly flow anomalies that start in the tropics and move both north and south from the starting point. The pattern is clear enough even in the relative AAM tendency contours shown in Fig. 2. When starting on the equator the tendency pattern is symmetric between the two hemispheres, e.g., event 3 in late Jan '06. For the vertically integral budget, individual maxima are caused or dominated by four processes: momentum flux convergence by zonal eddies, the mountain torque, the frictional torque and the coriolis torque. In fact, the mix and timing of the different processes that contribute to the coherent poleward moving features is different during these five events. However, in a broad sense tropical convective forcing combines with mountain effects and cold surges and together produce the eddies that change the zonal mean flow, which then feed back on the initial forcing. One simplification one can make in the budget is that the frictional torque acts primarily to damp the momentum anomalies, with a 6-10 day decay time scale.

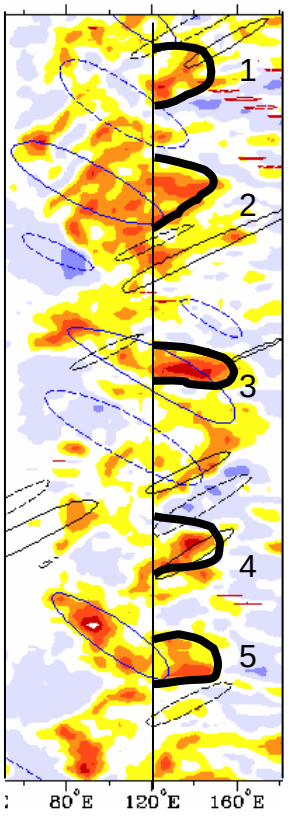

Figure 1. OLR fluctuations 15N-5N over the Indo-Pacific Nov-Mar.

3. SYNOPTICS DURING NOVEMBER 2005

Weickmann and Berry (2006) provide a multiple time scale, synoptic framework to aid with interpretation and attribution of the evolving weather and climate. Sometimes the synoptic evolution is clear and the initial forcing process can be identified. For example, the start of the first event during 7-11 November is a good example of a direct link between tropical convection and a

wave energy pulse that affected the Rossby wave structure near Kamchatka, leading to a recurring blocking pattern. Negatively tilted eddies fluxed momentum southward leading to the positive tendency near 25N durig event 1. Once an event starts other processes can initiate a feedback that can be either positive or negative. For example, the Kamchatka block might be viewed as aiding the buildup of cold air over Siberia, which in turn can lead to a positive feedback as momentum sources from Asian topography will then tend to be positive also. In fact, the strong tendency in the event 1 at around 20 November 2005 is produced both by a positive mountain torque over Asia and advection of momentum by the Hadley circulation, which is concentrated over a La Nina-shrunken warm pool.

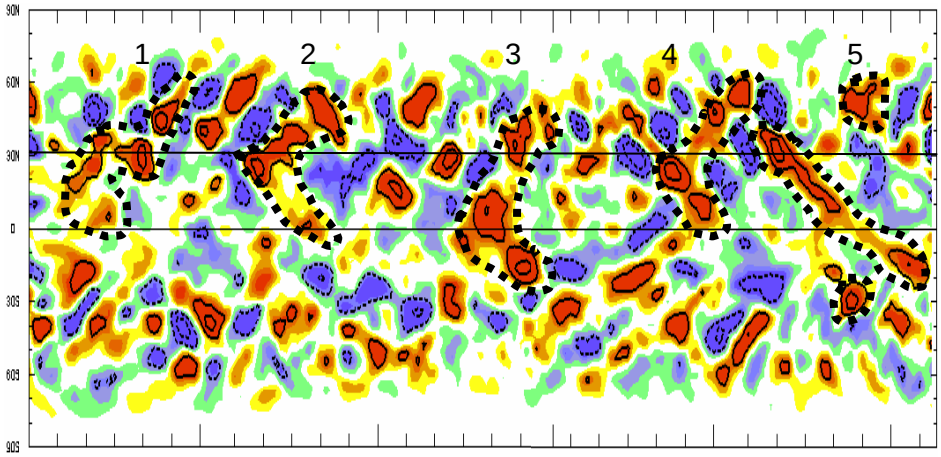

Figure 2. The relative AAM tendency during Nov-Mar 2006. Maxima represent ~0.2 m/sday vertical and zonal mean tendency. Five positive tendency events are shown.

4. MOMENTUM BUDGET DURING DECEMBER 2005

A detailed analysis of the latitude-pressure momentum budget during the start of the second event (7-12 December 2005) is seen in Fig. 3 using NCEP reanalysis pressure level data. The observed momentum tendency has a well-defined tripole structure, which is deep and uniform at 60N but becomes progressively shallower and more focused at ~40N and 25N. The conventional budget has a large dipole-like budget residual in the latitude-pressure plane (not shown). Applying the baroclinic χ-problem to the daily data (Sardeshmukh and Hoskins, 1987) "cleans up" the residual reasonably well, except over the equator where it increases them.

An initial interpretation of the zonal mean dynamics is obtained by examining how the left and right panels of Fig. 3 give rise to the relatively simple structure seen in the middle panel. The important physical processes at the different latitudinal centers of action are: 60N) a flux convergence of momentum by zonal eddies with some help from the mass circulations at low levels, 40N) an eddy flux divergence in mid-levels and an enhanced Ferrel cell at around 300mb, and 25N) a poleward shift in the momentum source produced by the Hadley cell combined with the mountain torque in lower levels.

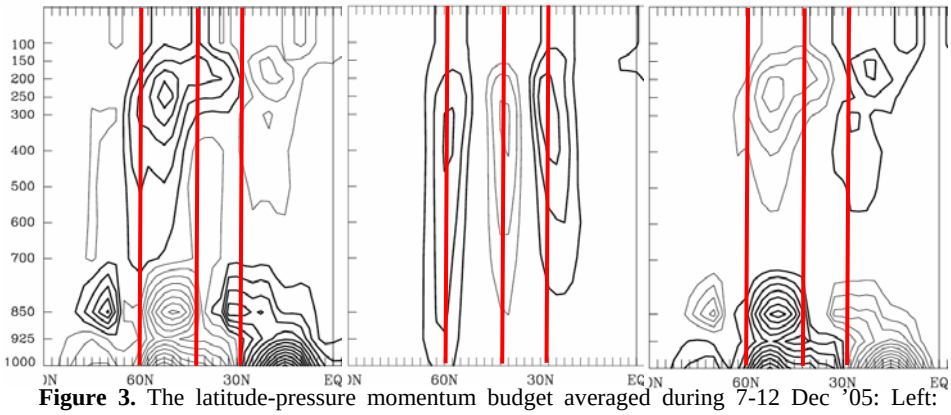

Figure 3. The latitude-pressure momentum budget averaged during 7-12 Dec '05: Left: convergence of eddy momentum fluxes, mountain torques and surface friction, right: momentum advection by Hadley / Ferrel cells (0.2 CI), center: momentum tendency (.05 CI).

The results of a more consistent treatment of mountain forcing and a further "clean up" of the residual will be presented at the meeting, as well as a discussion of the three lines on Fig. 3.

.

REFERENCES

Newman, N. and P.D. Sardeshmukh, 1998: The impact of the annual cycle on the North Pacific/North American response to remote low-frequency forcing. J. Atmos. Sci., 55, 1336-1353.

Sardeshmukh, P.D. and B.J. Hoskins. 1987: On the derivation of the divergent flow from the rotational flow: the χ problem. Q.J.R. Meteor. Soc., 113, 339-360.

Weickmann, K.M. and E. Berry, 2006: A synoptic-dynamic model of subseasonal atmospheric variability. Mon. Wea. Rev., in press.

THE INTENSE JET STREAM OF DECEMBER 1999: AN OUTCOME OF TROPICAL-EXTRATROPICAL TRANSITION?

Didier Ricard [1], Philippe Arbogast, Fabien Crépin, Alain Joly

[1] Centre National de Recherche Météorologique, Météo-France, Toulouse, France
E-mail: *didier.ricard@meteo.fr*

Abstract: At the end of December 1999, two very powerful and devastating extratropical cyclones stroke western Europe. These two storms were associated with an upper-level zonal jet remarkable by its intensity and by its large extension over the Atlantic Ocean. In this study, we focus on the likely relationships between the exceptional features of this jet stream and some heavy precipitation that occurred over Central America during mid-December. Indeed, a Rossby wave train excited by the strong convective activity over this area is likely to play a key role in this teleconnection. To assess this tropical-extratropical interaction, numerical experiments have been performed with the French global model ARPEGE. First, the effects of convection have been neutralized inside a domain localized over Central America. Then, a new strategy for combining model and observations has been devised. Within a selected window, parametrized latent heating is deduced from TRMM precipitation data, translated in terms of PV source and incorporated into the model using PV inversions. These simulations show in particular that the convective activity over Central America triggers a wave train that propagates along the North Atlantic jet stream and interacts with it in the sense of strengthening it somewhat.

Keywords – *TRMM precipitation data, Rossby wave trains, teleconnection, PV inversion, jet stream.*

1. INTRODUCTION

Two powerful and devastating extratropical cyclones stoke Western Europe between the 26 and 28 December 1999 causing huge damages (more than 15 billions euros) and many casualties (more than 90 people). These two bomb storms were associated with an upper-level zonal jet remarkable by its strength (more than 100 m/s) and its extension over the Atlantic Ocean (from Florida to the western French coast).

Very early after the storms a hypothesis was emitted by Anders Persson that the exceptional characteristics of this North Atlantic jet could be linked to some heavy precipitation that occurred over Central America during mid-December. This assumption is based on the teleconnection behaviour of the atmosphere. Indeed, on annual and interannual scales, Yang and Webster (1990) showed that the location and intensity of the extratropical westerly jet streams are closely related to tropical diabatic heating. Moreover, examining the linear response to tropical forcing of a baroclinic model linearized about the 300 hPa climatological mean January flow, Simmons et *al.* (1983) showed a link between these two remote areas. Using a similar model, Hoskins and Ambrizzi (1993) found that a perturbation vorticity source centred at (0, 90W) produces a north and northeasterly propagating wave train that enters the North Atlantic jet region.

Here, in this study, numerical experiments are performed with a primitive-equation model to investigate the likely submonthly tropical-extratropical relationship.

2. MODEL AND DATA

The model used for the numerical experiments is the French operational global hydrostatic model ARPEGE (41 level, T358 resolution). All the experiments start at 00 UTC 11 December 1999 and end at 00 UTC 27 December 1999. The choice of this duration results from a compromise between the inevitable growing forecast error and the triggering of interaction between the tropics and mid-latitudes. Indeed, this period encompasses the heavy precipitation events over Central America and the establishment of the North Atlantic jet stream.

First, the effects of convection have been neutralized inside a domain [20-0N,270-300W] localized over Central America. For that, inside this domain the latent heat release from precipitation is not taken into account and there is no wind tendency from convection during the model integration (hereafter referred as NOCONV, see Table 1). Thus, the effects of convection are assessed by comparison with a reference experiment (noted as REF) performed without any modification.

Experiment	Beginning Day 1	End Day 17	Convection suppressed over Central America	PV injections over Central America
REF	11/12/1999	27/12/1999	NO	NO
NOCONV	11/12/1999	27/12/1999	YES	NO
INV	11/12/1999	27/12/1999	YES	YES

Table 1. Characteristics of experiments.

In a new approach devised for this study, latent heating is deduced from daily TRMM precipitation data (from the Climate Prediction Center). It is translated in terms of PV source and then incorporated every 6 hours into the model using PV inversions. In this simulation (noted as INV), we want to provide to the model a representation of convective events derived from observations, since, as in the NOCONV experiment the convection effects from parametrisation are neutralized.

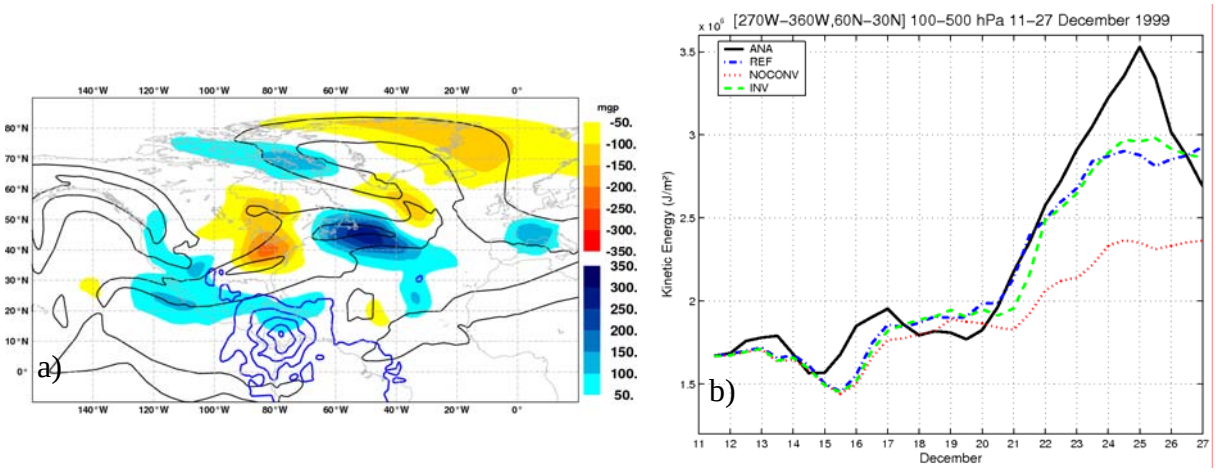

Figure 1. (a) 250-hPa geopotential height anomalies for REF minus NOCONV at day 3 (00 UTC 13 December 1999) (blue lines, contour interval 5 mgp) and at day 9 (12 UTC 19 December 1999) (positive values in blue scale, negative values in red scale, contour interval 50 mgp), wind speed at day 9 (black lines, contour interval 30 m/s). (b) Time evolution of the kinetic energy (J/m²) integrated over the Atlantic Ocean (between 260-360W, 30-60N, 500-100 hPa) for ARPEGE analyses and the three experiments.

3. RESULTS

Figure 1a shows the 250 hPa geopotential height anomalies induced by the convective activity for the difference between the REF and NOCONV experiments. Indeed, by day 3, there is an upper-level anticyclonic anomaly over Central America. The following days, this anticyclonic circulation intensifies and the anomaly propagates toward the north west. It reaches the jet stream localized over Texas. Then, there are propagations over the Atlantic Ocean towards the northeast and over North America. The jet streams (or the band of enhanced PV gradients) act as waveguides. By day 9, there is a succession of positive and negative anomalies. This structure is much alike a Rossby wave train.

The difference between the INV and the NOCONV experiments shows a similar behaviour. The PV injections based on precipitation data induce the excitation of wave trains that propagate along the jet streams.

Moreover, these anomalies have an effect on the jet structure. Indeed, figure 1b represents the evolution of kinetic energy integrated over the Atlantic Ocean for the three experiments and for the analyses. As the analyses, the REF experiment succeeds in reproducing the growth from the 20 December but the maximum reached is lower. For the NOCONV experiment, the growth of kinetic energy is largely attenuated. For the INV experiment, the increase is relatively the same as for the REF one, the maximum is a little higher. Globally, the jet is more intense for the INV experiment.

4. CONCLUSION

This study shows that the heavy precipitation events over the Central America area seems to play a significant role in the intensification of the jet over the Atlantic Ocean since this jet weakens when removing the effects of convection (NOCONV experiment) and strengthens when reintroducing the effects of convection by PV injections derived from precipitation observations (INV experiment). The mechanism of the interaction between these two remote areas can be described using Rossby wave propagation.

REFERENCES

Hoskins, B., and C. Ambrizzi, 1993: Rossby wave propagation on a realistic longitudinally varying flow. *J. Atmos. Sci*, **12,** 1661-1671.

Simmons, A. J., J. M. Wallace and G. W. Branstator, 1983: Barotropic Wave Propagation and Instability, and Atmospheric Teleconnection Patterns. *J. Atmos. Sci*, **40,** 1363-1392.

Yang, S., and P. J. Webster, 1990: The effect of summer tropical heating on the location and intensity of the extratropical westerly jet streams. *J. Geophys. Res.*, **95**, 18 705-18 721.

WHAT DO WE LEARN FROM PIECEWISE POTENTIAL VORTICITY INVERSION?

Joseph Egger[1] and Klaus-Peter Hoinka

[1]Meteorologisches Institut, Universität München, Germany

1. INTRODUCTION

Potential vorticity (PV) is the key variable of quasigeostrophic theory. It is conserved in adiabatic inviscid flow. Quasigeostrophic potential vorticity (PVg) can be inverted solving an elliptic partial differential equation to obtain the geostrophic streamfunction. These basic features of quasigeostrophic potential vorticity can be carried over to more general versions of potential vorticity. Given, in particular, a distribution of Ertel's potential vorticity

$$PV = \rho^{-1} \, (2\vec{\Omega} + \vec{\zeta}) \times \nabla \, \theta$$

it has been demonstrated by Hoskins et al. (1985), Thorpe (1985) and others that all dynamical flow variables can be obtained from the PV-distribution through an iterative inversion procedure which assumes a dynamic balance and hydrostatic conditions. Moreover, some variables have to be known at the boundaries. Hoskins et al. (1985) had a large impact on the diagnostics of synotic-scale flows because of the 'PV-thinking' suggested by the inversion. Given, for example, a localized center of potential vorticity in the upper troposphere, piecewise inversion of this anomaly appears to allow to calculate the winds 'induced' by this anomaly throughout the atmosphere. If there is another anomaly, say, close to the ground, it appears to be straightforward to quantify the impact of the upper PV-anomaly on the lower one and viceversa. The same argumentation applies to horizontally separated anomalies.

While Hoskins et al. (1985)described these partial inversions and the related dynamic interpretations in a suggestive but qualitative manner, it was not for long that actual piecewise inversions have been carried out for idealized and observed flows. To give just two examples, Robinson (1987) calculated via inversion of PVg the flows induced at the levels above a certain height by those prescribed or observed below. Davis and Emanuel (1991) analyzed cyclone development using piecewise inversion.

The technique of piecewise inversion suggests the obvious question how such instantaneous interactions over long distance are possible? After all, the prognostic equation for PVg is completely local and appears not to allow for such long-distance interactions.

2. SIMPLE IDEALIZED CASES

We consider first simple barotropic Rossby waves in a channel where piecewise inversion is easily possible. The ridge of the wave is an area of negative PVg while the trough represents one of positive PVg. It is straightforward to show that there exists a wide class of streamfunction configurations in the trough region which give all the same result with respect to the 'induced' winds in the ridge region. This means that the piecewise inversion of the PVg in the trough region does not lead to a meaningful result with respect to the ridge region. The mathematical reasons for this result are given.

The simple example helps also to elucidate the role of boundary conditions. The interpretation of temperature anomalies at the boundary as PV-anomalies is found to be ambiguous.

3. POTENTIAL TEMPERATURE INVERSION

It is proposed in view of these difficulties to perform a potential temperature 'inversion'. Given the atmospheric pressure at one level and observations of the potential temperature, it is a simple matter to derive from that density, pressure and temperature. Geostrophic balance gives the winds. This inversion is much simpler to implement than the PV-inversion and gives results of at least equal quality. Moreover, potential temperature is conserved the same way as is PV. Interaction of PV-anomalies over horizontal distances do not exist in this case. Those in the vertical reduce to hydrostatic effects.

4. OBSERVED CASES

ERA40 data are used to derive covariances of flow variables with the Alpine mountain torque in the Mediterranean. It is shown that these covariances can be treated the same way as anomalies in the more conventional analyses. In particular, PV anomalies can be inverted as can potential temperature anomalies. The analysed cases are similar to events of Alpine lee cyclogenesis where positive PV anomalies cross the Alps and a low forms at the surface. Given an instant of this flow development we are able to alter substantially the PV-distribution at upper levels. It is shown that this drastic change, if carried out hydrostatically, has no effect on the surface low. This demonstrates that there is no impact of the upper-level PV-anomaly on the low-level flow except what is implied by the hydrostatic relation.

REFERENCES

Davies, C.A. and K.E. Emanuel, 1991: Potential vorticity diagnosis of cyclogenesis. Mon. Wea. Rev., **119**, 1929 - 1953.

Hoskins, B.J., M.E. McIntyre, and A.W. Robertson, 1985: On the use and significance of isentropic potential vorticity maps. Q. J. R. Meteorol. Soc., **111**, 877 - 946.

Robinson, W.A., 1987: Two applications of potential vorticity thinking. J. Atmos. Sci, **44**, 1554 - 1557.

Thorpe, A.J., 1985: Diagnosis of a balanced vortex structure using potential vorticity. J. Atmos Sci, **42**, 397 - 406.

A REVISION OF THE LORENZ'S CHAOTICITY PARADIGM AND ITS CONSEQUENCE FOR THE EXTENDED-RANGE WEATHER FORECASTING PROBLEM

Dmitry M. Sonechkin

P.P. Shirshov Oceanology Institute, Russian Academy of Sciences
and Hydrometeorological Research Centre of Russia, Moscow, Russia
E-mail: *dsonech@mecom.ru*

Abstract: A critical consideration and re-formulation of the famous chaoticity paradigm of Ed Lorenz are given in order to indicate a possible way to overcome the present-day weekly predictability limit.
Keywords *– unpredictability of weather, co-existence of chaos and order in the weather dynamics, synchroneity in the propagation of planetary waves within the extratropical westerlies, a quasi-synchronous forecasting model, THORPEX.*

1. INTRODUCTION

At the beginning of the 1980s, Ed Lorenz analyzed the reliability of weather forecasts of ECMWF and assumed that the predictability limit for forecasts of day-to-day weather variations can reach one month. This optimistic assumption was, on the whole, subsequently confirmed by other researchers. However, the present-day forecasting models based on the system of the primitive equations have virtually exhausted their capacity to predict for one week ahead only. The aim of this report is to indicate a possible method to realize the Lorenz's optimistic assumption.

2. THEORETICAL BASIS OF THE METHOD

Nonlinearity is a basic property of the real-world climate dynamics. The advection is an essentially nonlinear process. It re-distributes air masses with their specific properties like temperature, humidity etc. In turn, this re-distribution transforms the advection itself. Even small changes of the advection affect the followed re-distribution of air mass properties. It is the reason of the general instability of atmospheric motions, their chaoticity and unpredictability for the more or less distant future. The power spectra of higher-frequency atmospheric motions within the direct enstrophy cascade (the periods from one day up to one week) and the inverse energy cascade (the periods from one week up to one-two months) of the atmospheric macroturbulence are obviously continuous and without any power energy peaks. Such shape of these power spectra is inherent to the truly chaotic dynamics. The atmospheric chaos admits the uninterrupted up-scale propagation of forecasting model errors from smallest scales where these errors were initially excited by imperfectness of initial data. This up-scale error propagation constitutes the essence of the Lorenz's chaoticity paradigm, and implies to use a probabilistic formulation of the extended-range forecasting problem (the so-called ensemble forecasting approach).

But the general chaoticity of the weather dynamics does not exclude some mutual adjustments of the heterogeneous and multiscale atmospheric motions, i.e. the atmospheric chaos can co-exists with an atmospheric order. Some kinds of such order reveal themselves already within the direct enstrophy cascade. Examples are the well-known quasihydrostaticity and quasigeostrophicity phenomena. It has been shown (Vlasova et al., 1989) that the motions within the inverse energy cascade are mutually self-adjusted even more. This new kind of the atmospheric order reveals itself as a synchroneity in the propagation of planetary waves within the extratropical westerlies.

3. A FORECASTING MODEL WITHOUT WEEKLY PREDICTABILITY LIMIT

It has been then hypothesized that errors of initial data destroy the planetary wave synchronization, and this circumstance implies the premature predictability loss in extended-range weather forecasts. This hypothesis was used to develop a new system of the hydrodynamical equations called the quasisynchronous forecasting model (Sonechkin et al., 1995). The version of the QS-model created at the middle of 1990s is hemispheric. It is based on a spectral form of the barotropic vorticity equation. The spectral resolution of the QS-model was chosen to be very low (the maximal zonal wave number is equal to 10 only!). Despite of this the model really reveals an ability to overcome the weekly predictability limit. The output product of this model consists of eight consequent 5-day mean H500 fields, and so a forecast can be given for an entire month with 10-day lead time. Fig. 1 shows such a monthly forecast for May 2006. This forecast is prominent by the domination of a zonal flow in the initial H500 field (on April 16-21), the transition to a blocking structure during the first decade of May and then reverting to westerlies. Even if with some errors the model forecast reproduced this transition.

4. CONCLUSION

Thus, a certain success in the monthly weather forecasting was obtained by running a very simple forecasting model (a toy-model in fact!). One can believe that much more successful forecasts can be obtained by running the primitive equations under the condition of an artificially forced synchronization of the planetary wave dynamics (by means of a special initialization of the primitive equations).

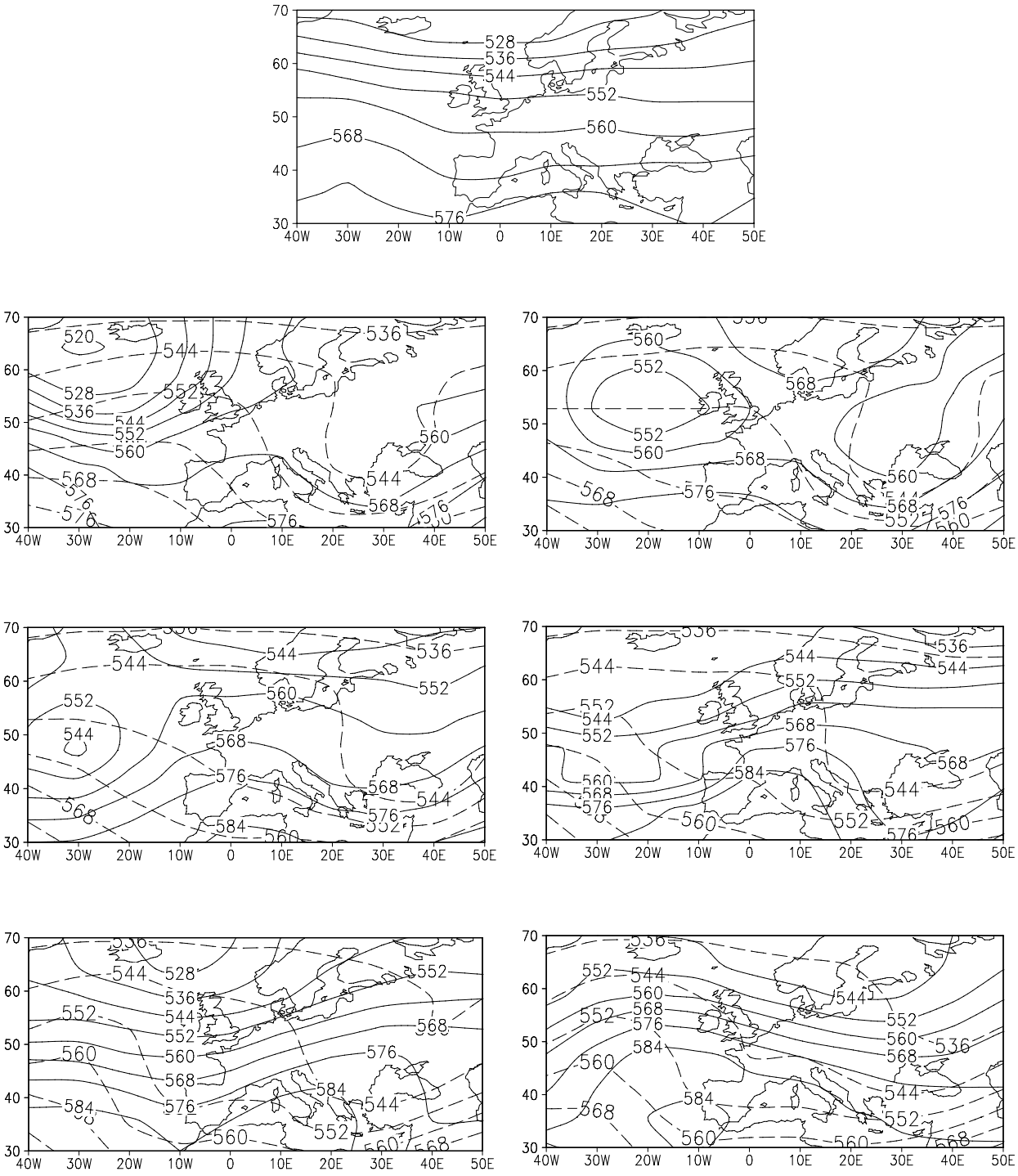

Figure 1. An example of the forecast of 5-day mean H500 fields (an Europe – North Atlantic area) in May 2006 prepared with a 10-day lead time. The initial H500 field on April 16-20, 2006 is shown with solid contour lines at the top of the figure. Below the actual and forecasted H500 fields for pentads in May 2006 are shown with solid and dashed contour lines respectively (the pentads on April 21-25 and 26-30, 2006 are not shown).

REFERENCES

Sonechkin D.M., Samrov V.P., Zimin N.E., 1995: The model averaged with respect of planetary wave phases reveals the ability to overcome the weekly predictability limit. Mon. Wea. Rev. **123**. 2461-2473.

Vlasova, I.L., N.E., Zimin, D.M., Sonechkin, 1989: Relaxation oscillations and phase synchronization of planetary waves. Soviet Meteorol. Hydrol., **11**, 24-31.

EVOLUTION IN GLOBAL WEATHER RESEARCH: FROM GARP TO THORPEX

Hans Volkert

Institut für Physik der Atmosphäre, Deutsches Zentrum für Luft- und Raumfahrt, Oberpfaffenhofen, Germany
E-mail: *hans.volkert@dlr.de*

Abstract: THORPEX is the largest current international initiative to enhance progress in the science application of weather forecasting. The endorsement under the World Weather Research Programme of WMO underscores the global scale of the initiative. During the 1960ies the Global Atmospheric Research Programme (GARP) played a similar role. This contribution collects factors that were conducive to the definition, execution and end of GARP in order to shed some light onto non-science forcing factors for the definition and execution of large scale international cooperation in the atmospheric sciences.

Keywords – *THORPEX, GARP, International Research Programmes, History of Meteorology*

1. INTRODUCTION

Funding agencies and international bodies require current weather oriented research programmes to explicitly consider the societal impact of, say, improved forecasts. In other words the usefulness of curiousity driven and applied research is to be quantified. A line of reasoning in the opposite direction can be taken in order to elucidate how definition and development of broader research initiatives are influenced by societal, political and technological tendencies during the periods when they were conceived. Shifts of emphasis between atmospheric science topics 'Weather' and 'Climate' can be observed as well.

A brief inspection of the sequence from the 'Global Atmospheric Research Programme' (GARP; 1960-1980) via the 'Mesoscale Alpine Programme' (MAP, 1995-2005) sheds light onto the various mechanisms how partly informal inter-national and inter-institutional cooperations can be set in motion and eventually work. Such findings at the border between sciences (atmospheric physics) and humanities (history of science, sociology) are considered of significant value for the further development of 'THORPEX, A World Weather Research Programme' scheduled for the decade 2005-2015.

2. GLOBAL ATMOSPHERIC RESEARCH PROGRAMME (GARP)

Many of the currently active atmospheric scientists remember GARP as *the* example of large scale international collaboration when they received their academic training. This unprecented enterprise was coordinated and overseen by a joint organisation committee between WMO (http://www.wmo.int) and the International Council for Science (ICSU; http://www.icsu.org). The participants of the 6th session held in October 1971 in Downsview, Canada, exemplify calibre and internationality of the enterprise (Figure 1). Large scale field campaigns like the GARP Atlantic Tropical Experiment (GATE, 1974), the Monsoon Experiment (MONEX; winter M. 1978/79, summer M. 1979) and the Alpine Experiment (ALPEX,1982) delivered a wealth of non-routine datasets for the growing capability to simulate regional to global weather patterns in research and operational modes. The First GARP Global Experiment (FGGE, Dec. 1978 – Nov. 1979) set out to establish an enhanced resolution dataset covering the entire globe and a full annual cycle (special issue *WMO Bulletin*, No. 3, Vol. **53**, 2004). FGGE was later termed 'Global Weather Experiment' and can be seen as a root to THORPEX.

The genesis of GARP, however, is much less present in the memory of the scientific community. As Erik Conway (2006), a science historian affiliated with NASA, describes in detail, the definition of GARP resulted from an US-initiative to bring science-based issues into the USA-USSR 'space-race'. The development of meteorological satellites (the TIROS series), the US federal legislation which led to the foundation of NASA as a civilian endeavour and the large public interest in the early satellite images are described as important factors for the early planning phase of what later became a fully international enterprise termed GARP. It took years to interest personalities of high standing in atmospheric physics like Harry Wexler, Victor Bugaev and Jule Charney to develop an appropriate research proposal. The report 'Feasibilty of a global observation and analysis experiment' (Charney et at. 1966) proved to be a milestone. Note that 'forecasting' is not mentioned explicitly.

Conway also describes how the GARP activities developed during the 1970ies, that some activities only took place after several years of delay and that the change in the US administration after 1980 inhibited a direct prolongation of the weather oriented initiative. In the international research arena new initiatives like the World Climate Research Programme (WCRP; from 1980) profited from the experiences made during GARP.

3. REGIONAL EXPERIMENTS SERVING AS A BRIDGE

ALPEX had its field phase in spring 1982, when GARP in general was no longer supported by the US administration. The exploration of lee-cyclogenesis over the northern Mediterranean proved to be a major area of

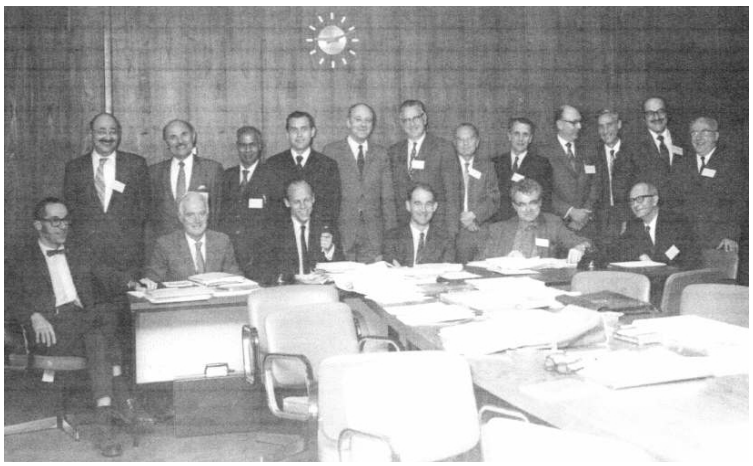

Figure 1. Participants at the 6th session of Joint WMO/ICSU GARP Organisation Committee in Downsview, October 1971: Standing (left to right): Fred Shuman (USA), Morris Tepper (USA), Pisharoth Pisharoty (India), Valentin Meleshko (USSR), Pierre Morel (France), Verner Suomi (USA), Fritz Möller (Germany), John Sawyer (UK), Arnold Glaser (WMO/USA), E.M. Dobryshman (WMO/USSR), Joseph Smagorinsky (USA), Viktor Bugaev (USSR); sitting: Stanley Ruttenberg (USA), Oliver Ashford (WMO/UK), Bo R. Döös (Sweden), Bert Bolin (Sweden), Robert Stewart (Canada), Warren Godson (Canada).
source: http://www.cmos.ca/Metphotos/

scientific advance. As the desired cross-Alpine flows did not occur, step-in mountain wave missions were flown across the neighbouring ranges of Pyrenées and Dinaric Alps (bora flows). The former examples later helped to initiate a separate research programme PYREX, jointly organized by the meteorological services of France and Spain, with a field phase in autumn 1990 (cf. Bougeault et al., 1997). From 1994 onwards research teams with experiences in ALPEX and PYREX formed the kernel to define a research initiative termed Mesoscale Alpine Programme (MAP) to tackle similar issues with the latest observational and modelling techniques, but enlarged by the demand to better forecast heavy precipitation over the Alps. Furthermore a close cooperation was included with hydrological applications also aiming at improved early warnings (Bougeault et al., 2001).

4. GLOBAL AGAIN: THE WORLD WEATHER RESEARCH PROGRAMME AND THORPEX

The WMO Executive Council endorsed in 1998 the proposal by the Commission for Atmospheric Sciences (CAS) to establish a World Weather Research Programme (WWRP) with a mission to develop improved and cost effective forecasting techniques, with an emphasis on high impact weather and to promote their application among Member States. MAP was then accepted as the first research and development project (RDP) of WWRP. Meanwhile THORPEX constitutes the by far largest RDP initiative, while MAP D-PHASE became endorsed as a forecast demonstration project (cf. Rotach and Arpagaus, this volume, p.54). The integration of societal impacts, *i.e.* the benefits of WWRP research for the society at large, became a mandatory ingredient of all WWRP initiatives. As shown above for GARP, it appears to be of similar importance to reflect how different societies and their political systems influence the development of research programmes also in fields as atmospheric science, which may appear quite apolitical at first sight.

5. CONCLUDING REMARKS

Weather and climate research has matured to a degree that historians of science started to bring the geographical, technological, and societal aspects into a perspective that unites sciences and humanities (e.g. Fleming et al., 2006). It appears that a decadal project of global extent, but with implications to the regional scale, like THORPEX can especially profit when the extra-science forcings are explicitly considered and the additional expertise of the history of our science is used – all the more when links to current climate research are sought and highly topical issues like geo-engineering are discussed.

Acknowledgements: *The open attitude of Erik M. Conway is acknowledged with gratitude for making me familiar with and letting me quote from his not yet published article.*

REFERENCES

Bougeault, P., B. Benech, P. Bessemoulin, B. Carissimo, A. Jansa Clar, J. Pelon, M. Petitdidier, and E. Richard, 1997: PYREX: A summary of findings. Bull. Am. Meteorol. Soc., **78**, 637-650.

Bougeault, P., P. Binder, A. Buzzi, R. Dirks, R. Houze, J. Kuettner, R.B. Smith, R. Steinacker, and H. Volkert, 2001: The MAP Special Observing Period. Bull. Am. Meteorol. Soc., **82**, 433-462.

Charney, J., R. Fleagle, V. Lally, H. Riehl, and D. Wark., 1966: The feasibility of a global observation and analysis experiment. National Academy of Sciences/National Research Council, publ. no. 1290, Washington, DC.

Conway, E., 2006: The world according to GARP: Scientific internationalism and the construction of global meteorology, 1961–1980. Unpublished manuscript, NASA history dept., JPL site, 30 pp.; available from Erik.M.Conway@jpl.nasa.gov .

Fleming, J.R., V. Jankovic, and D.R. Coen (eds.), 2006: *Intimate universality: Local and global themes in the history of weather and climate.* Science History Publications, Sagamore Beach, MA, USA, ISBN 0-881353671, xx + 284 pp.

THE EFFECTS OF INTENSE WEATHER SYSTEMS OVER THE CHIAPAS STATE OF MEXICO

Ricardo Prieto-Gonzalez [1], Martín Mundo-Molina [2], Juan M. Caballero [3]

[1] Mexican Institute for Water Technology, Jiutepec, Morelos, Mexico
E-mail: *rprieto@tlaloc.imta.mx*
[2] Autonomous University of Chiapas, Tuxtla Gutierrez, Chiapas, Mexico
E-mail: *ic_ingenieros@yahoo.com.mx*
[3] Mexican Navy, Mexico City, Mexico
E-mail: *jmcaballero@semar.gob.mx*

Abstract: This talk will give a review of the meteorological and social conditions of Chiapas, as well as a proposed regional weather forecast system, which takes into account the socio-economic conditions and the history of disasters, in order to be able to prevent regions and communities most vulnerable to specific type of weather events, with an advanced notice of, at least, 72 hours.

Keywords *– THORPEX, SERA, Chiapas, Mexico*

1. INTRODUCTION

Chiapas is the southernmost state of Mexico. With a population around 4 million, Chiapas' society is composed by a wide variety of people, going from indigenous almost isolated communities, to modern cities. Most of the population in the state lives on poverty conditions. Sharing the border with Guatemala, Chiapas has a high flux of migrants and trade, coming from Central and South America.

The state of Chiapas is under the influence of important synoptic and mesoscale weather systems, such as the intertropical convergence zone, tropical easterly waves, and tropical cyclones. The rainfall season in the state is during the summer and fall, having a midsummer period of relative drought. Historically, the weather systems that affect the state had produced a large number of disasters, such as those produced by hurricane Mitch on 1998 and tropical Storm Larry on 2003. The most recent disaster event is the floods caused by hurricane Stan of 2005, which killed over 100 people, with multimillion dollar costs in damages.

2. THE MAP OF RAIN ASSOCIATED RISKS OVER CHIAPAS

Chiapas topography is quite complex, with mountainous terrain over most of the state, and very steep slopes in several regions. These characteristics, combined with important moisture fluxes arriving from the Pacific Ocean which are torrential rain producers, and the location of small cities, towns and villages over the flat regions next to the coast, creates an important band of high risk areas over the southern part of the state.

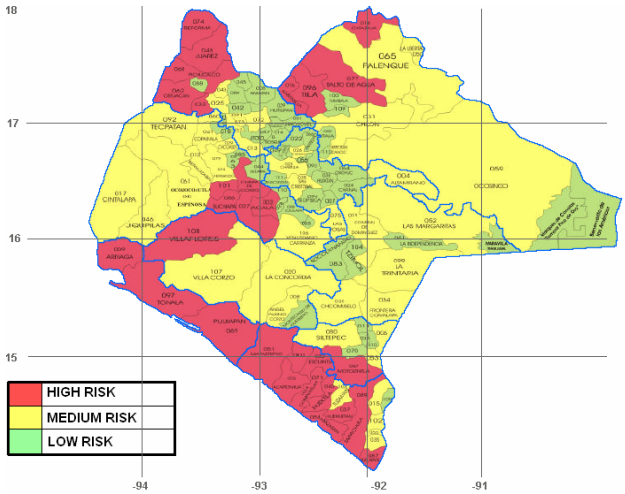

Figure 1. Map of rainfall associated risks over Chiapas, which is divided into socio-economic regions and municipalities. High risk areas are concentrated mainly over the southern region.

Figure 2 shows the flooding effects produced during October, 2005, over: a) Isolated communities of the sierra, and, b) A city located next to the steep slopes of the mountains of southern Chiapas. These types of effects have been recurrent over the years and the society response to prevent rainfall associated disasters, at the present time, is not efficient.

a)  b) 

Figure 2. During the presence of hurricane Stan in October, 2005, several days of continuous rains produced flooding events that destroyed populated areas over extended areas of southern Chiapas.

3. A WEATHER FORECASTING SYSTEM THAT USES SOCIO-ECONOMIC INFORMATION IN ORDER TO REDUCE WEATHER ASSOCIATED DISASTERS OVER CHIAPAS

To the physical complexity associated to an extreme weather event, it is added the social and economical complexity of the population which can be affected. Therefore the response of the protection system requires a full knowledge of the meteorological and socio-economic conditions.

The technological tools of our time can be used during emergency situations in order to take appropriate and timely decisions. Meteorological real-time information can be downloaded automatically in order to save time to the forecasters on duty. Satellite imagery, weather forecasts, real-time weather observations at different levels, can be used into a system which can be downscaled to municipal (county) scale. The social and economic information should complement the physical information in order to automatically produce the actual and future (3 or more days in advance) risks scenarios.

A prototype of a forecasting system which uses the meteorological, social and economical conditions for the state of Chiapas has been constructed, which can be used to take appropriate decisions and prevent future weather associated disasters. This system also includes the history of recent disasters over the state, divided down to municipal (county) scale. The system is available through a web page which is actualized automatically, taking into account the rapid evolution of the atmospheric systems and the need to foresee possible local weather effects.

4. CONCLUSION

The search and analysis of weather and socio-economic information to prevent weather associated disasters can be a time consuming task. Local civil protection systems require a full knowledge of the situation for its use in timely and appropriate decision taking under the presence of extreme atmospheric phenomena. This work proposes the construction of an automatic system, which is able to downscale the most important information to be used by local authorities without the difficulties of searching it under high stress situations. The involvement of regional and local protection authorities, scientists and population is an important task during the design of effective weather warning tools.

Acknowledgements: *FOMIX CONACYT-CHIAPAS provided financial assistance for this work.*

A SOCIETAL AND ECONOMIC RESEARCH AND APPLICATIONS AGENDA FOR THE NORTH AMERICAN THORPEX PROGRAMME

Brian N. Mills[1], Rebecca E. Morss, Jeffrey K. Lazo, Harold E. Brooks, Barbara G. Brown, and Philip T. Ganderton
[1]Adaptation & Impacts Research Division, Environment Canada, Waterloo, Canada
E-mail: Brian.Mills@ec.gc.ca

1. INTRODUCTION

As outlined in the THORPEX International Science Plan (Shapiro and Thorpe, 2004) and informed by the International Societal and Economic Research and Applications Working Group (SERA-WG, 2006), proposed THORPEX SERA activities range from primary research to application development to capacity building. These activities will come to fruition through efforts within national, regional and international programmes. At the regional scale, priorities have been defined for the Southern Hemisphere (Gordon et al., 2006) and efforts are underway or planned in the Asian and European committees.

Research priorities for the SERA component of North American (NA) THORPEX were the subject of a recent workshop held August 2006 in Boulder, Colorado. The workshop included more than 40 U.S., Mexican and Canadian researchers and practitioners representing a cross-section of disciplines. Discussion papers addressing four SERA themes were solicited in advance of the workshop and, together with a series of plenary presentations, served as the primary catalyst for discussion. This paper provides a partial synthesis of the following five priority topics that emerged from the deliberations and received general support from participants: 1) Understanding the use of forecast information in decision making, 2) Communicating weather forecast uncertainty, 3) User-relevant verification, 4) Estimating the economic value of weather forecasts, and 5) Developing decision support tools and systems. Although these priorities are based on the workshop proceedings, they are the authors' views rather than an explicit account of the meeting.

2. PRIORITY RESEARCH TOPICS

Understanding the use of forecast information in decision making. Weather forecasts provide information that people can use in decisions, affecting outcomes. Three key research questions are: 1) how do decision makers in these diverse contexts interpret weather forecast information, 2) how do they combine forecasts with other information in their decision processes, and 3) what constrains their use of current or improved forecast information. Research is needed both in specific decision environments, for example emergency management, and across a variety of contexts in order to compare and draw broader conclusions. A variety of methods are available to tackle these questions, including those that assume an optimizing decision maker (e.g., cost–loss and more complex prescriptive model experiments), and those that examine decisions in real contexts. For the latter type of study, fields such as decision sciences, behavioural psychology, sociology, and geography offer a great variety of tools (e.g., ethnographic studies; surveys, interviews, and focus groups).

Communicating weather forecast uncertainty. The rapid evolution of techniques for estimating weather forecast uncertainty has not been paralleled with concomitant advances in understanding of how to effectively communicate such information to users. Forecast-related decisions under uncertainty are often complex, incorporating information and compiling uncertainty from multiple sources. Simply providing more information, without considering this complexity, may not benefit many users. Important research questions include: 1) how do users interpret forecast uncertainty, 2) how do they respond to different forms of uncertainty communication (in terms of both the medium and the message), and 3) how do they incorporate forecast uncertainty into decisions. Related areas of inquiry include the role of uncertainty thresholds, risk perceptions, and preferences interact in individual decision-making. Studies are needed for a variety of users in different decision contexts, for both hazardous and routine weather forecasts. Ideas, methods, and results developed in other decision-making contexts can be applied to weather forecasts and tested in laboratory and field settings.

User-relevant verification. Forecast verification is the process of evaluating the quality of forecasts and typically involves calculating relatively simple metrics that compare point forecasts to corresponding observations. Traditional verification methods generally provide little information that can help improve forecasts (the scientific purpose), benefit users' decisions (the economic purpose), or estimate forecast value. Addressing this concern requires an understanding of the types of verification information that could benefit users, research on user-relevant features-based and scale-sensitive approaches, and the development and testing of new diagnostic methods (i.e., ways to view and summarize forecast error distributions) for evaluating user-relevant variables. Other areas of research include understanding how to effectively communicate verification information to users and investigating the relationship between forecast quality and value. Conducting this research requires interdisciplinary collaborations among meteorologists, verification experts, social scientists, and users. One approach is to undertake case studies to conceptualize, develop, and employ user-relevant verification approaches for several different users and forecast attributes. Each case study would involve understanding users' forecast and verification-related needs through methods such as interviews, surveys, and

focus groups, combined with expertise in developing verification techniques. From these case studies, more general approaches to user-relevant verification might then be developed.

Estimating the economic value of weather forecasts. In economic terms, the value of improved forecasts is measured by individual or aggregate changes in well-being (utility). Key research areas include estimating the value of different forecast modifications (i.e., changes in forecast attributes) and evaluating various users' preferences among forecast modifications. Both can be studied using well-established tools (e.g., revealed- and stated-preference approaches) that economists have developed to value other non-market goods. Techniques from behavioural economics may also be employed; for example, preferences for different types of forecast information can be studied using laboratory experiments that give real or simulated users controlled information and decision sets. Forecast value may also be estimated using methods, such as hedonic pricing or sector- or firm-specific case studies, that draw on market data. Using cost-benefit analysis techniques, forecast valuation results can be integrated with cost information and meteorological knowledge to evaluate the overall societal costs and benefits of different forecast modifications.

Developing decision support tools and systems. Decision support systems (DSSs) and tools serve as a bridge to connect particular users with weather information providers. User engagement is likely the most important prerequisite for successful DSSs, facilitating greater understanding of users' problems, needs, and decision-making contexts, and promoting adoption of the tool and use of the information it provides. A major decision support priority is developing systems and tools that will enable users to incorporate THORPEX-related forecasts into decisions, particularly those enhanced with uncertainty information (e.g., generated through the TIGGE). Studies should be performed both to facilitate new uses of forecasts in well-served sectors and to benefit new user groups. One mechanism for conducting these studies is decision support testbeds, in which new approaches and technologies are developed and evaluated in conjunction with other user-oriented research.

3. IMPLEMENTATION OF A NORTH AMERICAN SERA AGENDA

Although many disciplines were represented at the workshop, a broader, more substantive and sustainable community is required to further specify and implement an integrated NA SERA research agenda. This will involve developing collaborations with forecast users and entraining additional social and atmospheric scientists, particularly early-career researchers and practitioners, to work in productive interdisciplinary SERA projects. Human resources must be complemented with sufficient financial support and other research infrastructure to fulfill the NA-SERA agenda. Assembling a series of small but dedicated long-term grants for SERA research and ensuring that THORPEX project proposals from other working groups explicitly include a funding element for socio-economic analysis, will help address financial issues. Developing publicly accessible information resources (e.g., annotated bibliographies of existing SERA studies, meta-databases of socio-economic data/information) would provide the information foundation on which to construct a solid SERA programme. With these elements in place, NA THORPEX SERA has a chance to flourish and realize some of the long-recognized potential so often promised in past applied meteorology colloquia, symposiums and workshops.

Acknowledgements: *This abstract is based on a longer manuscript being prepared by the authors (Morss et al., n.d.). The authors acknowledge David Parsons and Gregory Holland for serving on the workshop organizing committee and all of the workshop participants for their contributions and ideas. The workshop was funded through an NCAR Opportunity Fund grant and the THORPEX International Program Office.*

REFERENCES

Gordon, N., A. Angari, M.A. Gan,J.L. McBride, E. Poolman, K. Puri, C.P. Rousseau, I. Simmonds, P. Steinle, M.J. Uddstrom and W.J. Tennant, 2006: *Southern Hemisphere THORPEX Science Plan.* Southern Hemisphere THORPEX Regional Committee. 56pp. http://www.wmo.int/thorpex/publications.html

Morss, R., J. Lazo, H. Brooks, B. Brown, P. Ganderton and B. Mills, n.d.: Societal and Economic Research and Application Priorities for the North American THORPEX Program, submitted to *Bulletin of the American Meteorological Society*.

SERA-WG, 2006: Meeting report of the THORPEX SERA Working Group, March 2006, Reading, UK. http://www.wmo.int/thorpex/reading_meeting.html

Shapiro, M.A. and A.J. Thorpe, 2004: *THORPEX International Science Plan, Version III*. WMO/TD-no. 1248, 57 pp.

TRANSFER OF REGIONAL NWP CAPABILITIES TO DEVELOPING COUNTRIES: THE HRM OF THE DEUTSCHER WETTERDIENST

Detlev Majewski

Deutscher Wetterdienst, Offenbach, Germany
E-mail: detlev.majewski@dwd.de

Abstract: Deutscher Wetterdienst provides the HRM (High resolution Regional Model) and lateral boundary data (from forecasts of the global model GME) to any National Meteorological Service (NMS) worldwide free of charge. For many services HRM is the first numerical weather prediction (NWP) system running operationally. HRM could serve THORPEX SERA as an example of a successful and sustainable transfer of regional NWP capabilities to developing countries.

1. INTRODUCTION

The population in developing countries critically depends on reliable regional weather forecasts because high impact weather events like torrential rain or gale force winds pose a severe thread to life and safety. Global model forecasts, available on the Global Telecommunication System (GTS) of the World Meteorological Organization (WMO), are not well suited as the basis of regional forecasts for such countries as they lack the necessary spatial and temporal resolution. Moreover, the limited set of forecast parameters provided by the global forecasting centres does not allow to run local applications like hydrological forecast models or emergency response systems.

Therefore an increasing number of NMSs in developing countries introduces regional NWP models as the basis of their forecast production suite. Deutscher Wetterdienst (DWD) supports these services by offering the HRM, lateral boundary data from the global model GME (Majewski et al., 2002), and annual training workshops in NWP. This paper describes the HRM system, the transfer of regional NWP capabilities from DWD to developing countries and discusses the process and its constraints taking Kenya and Vietnam as typical examples.

2. OVERVIEW OF A REGIONAL WEATHER FORECASTING SYSTEM AND THE HRM

Figure 1 shows the main components of a regional weather forecasting system, connected by the data flow including observations, NWP results, follow-up applications and final forecast products for various customers.

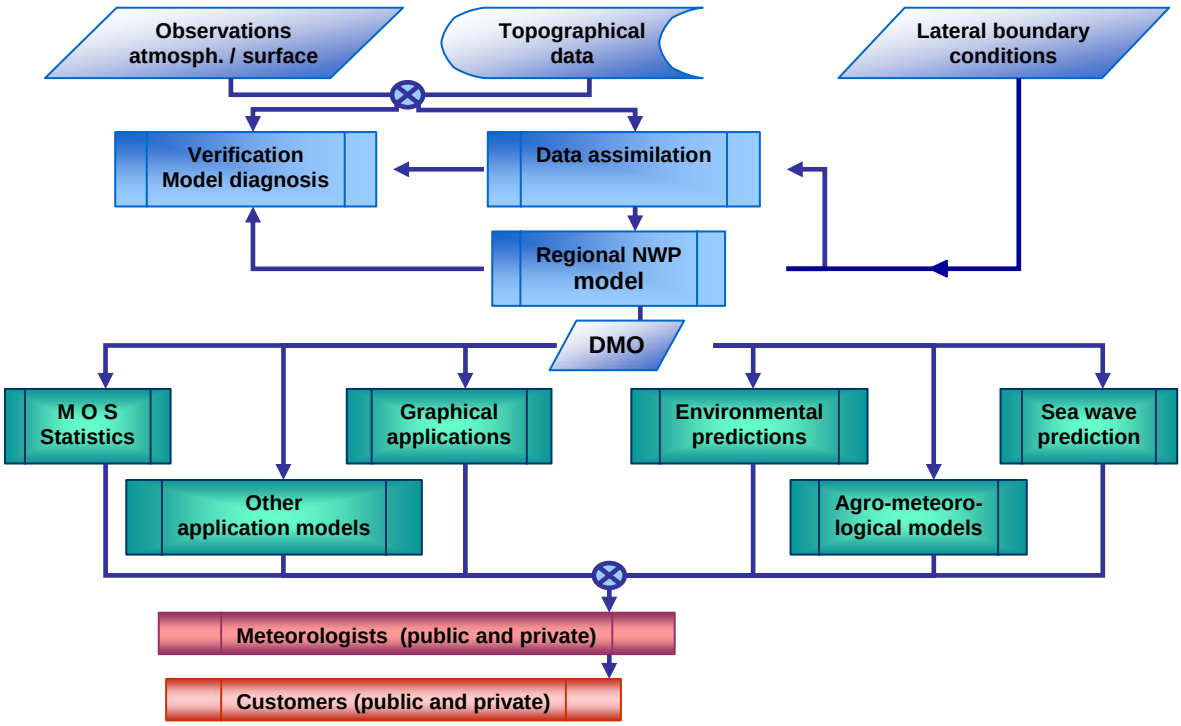

Figure 1. Main components of a regional forecasting system and corresponding data flow.

DWD provides the following NWP components: regional forecast model HRM including 3D-Var assimilation scheme, topographical data sets for any region worldwide, lateral boundary conditions based on the global model GME and a sophisticated verification package developed by DGCAM (Oman).

The HRM system is usually introduced at the NMS of a developing country in a stepwise approach taking the scientific and technical skills of the local staff into account. Initially, the HRM forecasts are based on global analyses, interpolated to the regional domain of interest. Main effort during the first phase is concentrated on operational implementation, forecast product generation and training of staff. As the second step which involves a first usage of local observations, a verification scheme is introduced which provides the NWP group with the benchmark necessary for any work on model improvement and the forecasters with objective information about the strengths and weaknesses of the HRM for their region. Finally, regional high resolution data assimilation using all local observations can be introduced after a few years if the NWP group gained sufficient scientific and technical skills.

3. HRM IN KENYA AND VIETNAM

To run a regional NWP system with a grid spacing of 10 to 20 km for a domain of some 2000x2000 km^2 required a Million US$ supercomputer a decade ago. Today a PC cluster for less than 50.000 US$ allows to produce operational regional meso-ß scale forecasts. Free (open source) operating systems, compilers, data base management and graphics software packages reduce the licence fees for the NWP system to a minimum. The rapid development of the internet as a fast, reliable and cheap worldwide communication link enables the transfer of lateral boundary conditions from the DWD to any NMS running HRM operationally. Thus the NMS of a developing country can implement an operational regional NWP system based on the HRM at rather modest investments in hard- and software. Currently more than 20 NMSs, for example Brazil, Bulgaria, China (RMS Guangdong), Kenya, Mozambique, Oman, Philippines, Senegal and Vietnam, base their operational NWP system on the HRM (see also http://www.met.gov.om/hrm/).

The co-operation between DWD and Kenya Meteorological Department (KMD) started in 2001. One scientist of KMD implemented the HRM for a domain of 97x97 grid points with a grid spacing of 28 km on a single processor PC. Main tasks included the control of the operational suite, provision of products (http://www.meteo.go.ke/nwp/) and the training of forecasters in the interpretation of HRM forecasts. In 2006, KMD acquired a 4-processor PC cluster which allowed to reduce the grid spacing of the HRM from 28 to 14 km. Since the NWP group at KMD consisted of just one scientist until 2005 no real model development was possible but HRM was basically used as a “black box”.

The co-operation between DWD and the Hydrometeorological Service (HMS) of Vietnam started in 2001, too, and it included from the start the Meteorological Departments of Vietnam National University (VNU, Hanoi) and of University of Munich (MIM). This early involvement of universities and the strong commitment of HMS Vietnam towards NWP formed the basis of a rapid build-up of local NWP capabilities. A task sharing between VNU and HMS is implemented where VNU takes care of developing, testing and evaluating new components like verification or data assimilation, and HMS incorporates them in the operational suite. Since 2004 a joint project of the four partners, named “Improved quantitative precipitation forecasting in Vietnam” and funded by the German DFG and the Vietnamese Ministry of Science, Technology and Environment, provides financial resources for research visits. In this framework, six scientists from Vietnam and five from Germany co-operated on various NWP tasks. The successful transfer of NWP capabilities is visible by Vietnamese studies (Lê Đuc et al., 2005) in the field of convective parameterizations (e.g. Tiedtke vs. Betts-Miller schemes), data assimilation (3-D Var and soil moisture assimilation) and parallelization (2-D domain decomposition of the HRM based on MPI).

4. CONCLUSION

The transfer of regional NWP capabilities to developing countries can be successful and sustainable if performed in a step-by-step approach taking the available local knowledge into account, involving local universities at an early stage of the process, assigning the project adequate local human resources and restructuring the NMS to make best use of the new NWP products. In this respect, THORPEX SEA could benefit from DWD’s experience.

REFERENCES

Majewski, D., Liermann, D., Prohl, P., Ritter, B., Buchhold, M., Hanisch, T., Paul, G., Wergen W. and Baumgardner, J., 2002: The Operational Global Icosahedral-Hexagonal Grid Point Model GME: Description and High Resolution Tests. Mon. Wea. Rev. **130**, 319-338.

Lê Đuc, Lê Công Thành, Kieu Thi Xin, 2005: On the high resolution regional weather forecast model (HRM) and forecasting tropical cyclone motion over the South China Sea, Vietnam Journal of Mechanics, **27**, 193-203.

Part B

Extended abstracts of

Poster presentations

The order is alphabetical following the THORPEX working goups and within numbered consecutively (nn = 01,…, max)

Dnn	for	DAOS:	Data Assimilation and Observing Strategies
Onn	for	OS:	Observing Systems
Pnn	for	PDP:	Predictability and Dynamic Processes
Snn	for	SERA:	Societal and Economic Research and Applications
Tnn	for	TIGGE:	THORPEX Interactive Grand Global Ensemble

IMPACT OF GOES RAPID-SCAN WIND OBSERVATIONS ON NOGAPS NORTH ATLANTIC HURRICANE FORECASTS

Rolf Langland[1], Chris Velden[2], Patricia Pauley[1]

[1]Naval Research Laboratory, Monterey, CA, USA
[2]University of Wisconsin, CIMSS, Madison, WI, USA
E-mail: rolf.langland@nrlmry.navy.mil

Abstract: Data assimilation experiments are being conducted to determine the impact of rapid-scan wind observations on North Atlantic hurricane forecasts in the NOGAPS forecast model. In the case studied so far, results indicate a 25% improvement in the 72hr track forecast of Hurricane Katrina landfall on the Gulf Coast, from wind data added over North America and Gulf of Mexico. Studies of additional storms are in-progress.

Keywords – Data assimilation, satellite wind observations, targeted observing, hurricane forecasting

1. INTRODUCTION

Despite improvements in numerical forecasts of hurricane track, there remains significant potential for additional reduction in forecast track error, even at the 48-72hr range. The use of targeted observations is one strategy currently being used to improve hurricane track forecasts (Aberson 2003, Wu et al. 2005). Typically, hurricane targeted observing has involved sets of 10-30 dropsonde profiles, deployed by reconnaissance aircraft in an area around the storm. In some cases, the locations of these dropsondes are determined by guidance from objective targeting methods, including the Ensemble Transform Kalman Filter or singular vectors (Majumdar et al. 2006). While targeted dropsondes improve some hurricane track forecasts by as much as 10-20%, the forecast impact that can be provided by intermittent small sets of dropsondes is inherently limited. In general, it is believed (Langland 2005) that increased impacts from targeted observations will require: 1) larger amounts of observation data in target areas, 2) more-frequent, if not continuous, observations of target areas, and 3) more-complete spatial coverage of target area dynamical structures, beyond the placement of a few observations in localized areas of maximum sensitivity. These requirements for improved observational coverage of target areas are perhaps most feasibly addressed by considering enhanced satellite-observations as a primary source of targeted data. One such source of observation data are rapid-scan wind observations (RS-winds) produced from geostationary satellite imagery. Special sets of these wind data using GOES-12 were produced for major North Atlantic hurricanes during the 2005 season, and are used for the data impact experiments in this project. The RS-winds are more accurate than routinely-produced GOES winds (Velden et al. 2005), and are also provided and are also provided with an experimental quality indicator for improved data thinning and assimilation.

2. METHODOLGY

We use the forecast model NOGAPS[1] (T239L30), and the data assimilation procedure NAVDAS[2] , which performs a 3d-Var analysis. NOGAPS currently provides hurricane track predictions which are among the most skillful of any operational forecast model. In these experiments we use a 6-hr data assimilation cycle, which is the operational configuration for NAVDAS. The observations assimilated include rawinsondes, dropsondes, land and ship-surface data, commercial aircraft observations, scatterometer surface winds, SSM/I surface winds, SSM/I precipitable water, AMSU-A radiances, MODIS winds, and geostationary satellite wind data. A thinning algorithm is applied to the AMSU-A data. In NOGAPS a synthetic observation bogus is used to improve the initial state representation of the hurricane vortex, extending outward about 600km from the storm core. Both the regular and rapid-scan satellite wind data are assimilated as super-obs, which combine information from more than one original wind observation data. RS-winds are provided at hourly intervals in the region 15N-60N, 60W-110W (Fig. 1). This can be considered a "targeted" application of the RS-winds, in the sense that a particular region for supplemental data has been identified, and the additional wind observations in this region cover the area most likely to influence the forecast of hurricanes reaching the U.S. coastline.

[1] NOGAPS- Navy Operational Global Atmospheric Prediction System
[2] NAVDAS – NRL Atmospheric Variational Data Assimilation System

3. HURRICANE KATRINA RESULTS

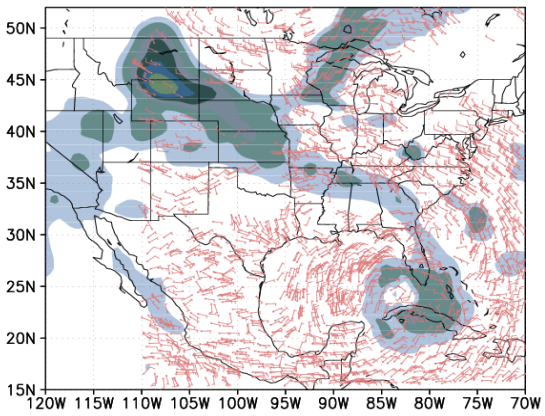

Fig. 1: RS-wind distribution at 0000UTC 27 Aug 2006 (2426 super-obs) and sensitivity of 72h forecast error to initial conditions at this time.

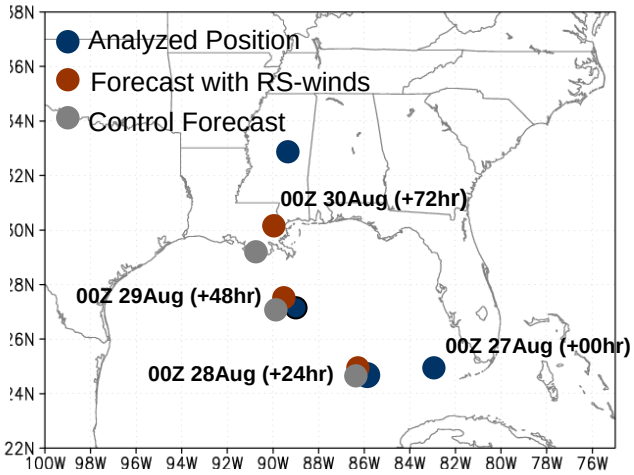

Fig.2: Forecast and analyzed positions of Hurricane Katrina from 00UTC 27Aug – 00UTC 30 Aug 2006.

In this experiment, we have a set of control forecasts which use the full set of operational observation data (no RS-winds) and an alternate forecast sequence in which RS-winds are assimilated every 6-hr starting at 0000UTC 20Aug 2006, leading up to a 72-hr forecast of Hurricane Katrina started at 0000UTC 27Aug 2006. Figure 1 illustrates the distribution of the RS-wind observations (superobs) assimilated in NAVDAS at 00UTC 27Aug 2006. The RS-winds are assimilated only if the data are provided exactly at the analysis times of 0000UTC, 0600UTC, 1200UTC and 1800UTC, so that we use here only about 1/6 of the total available RS-wind observations – later experiments will include the RS-wind data at other observation times.

The shading in Fig. 1 is the vertically-integrated sensitivity of the 72hr NOGAPS forecast error to the initial condition wind and temperature (combined with an energy weighting), from the control run which does not use RS-wind observations. This sensitivity pattern suggests that the Katrina forecast from 00UTC 27 Aug is most sensitive to initial conditions in a region around the storm itself (~25N, 83W) and also over upstream areas of the central United States. We do not attempt to target RS-winds specifically to the evolving positions of these localized sensitivity features, because they are all within the larger RS-wind observing domain of 15N-60N, 60W-110W.

The 72h control forecast of Katrina (Fig. 2) has a track error of about 375 km, which is slightly larger than the average NOGAPS 72h hurricane forecast track error of 326 km during the 2005 season. The 72h RS-wind forecast track error is about 275 km, 25% less than the control forecast track error. However, both forecasts place the storm south of the analyzed position at 72hr, suggesting that interaction of the northward-moving Katrina with the steering flow is still not correctly represented. A possible explanation is the sparsity of RS-wind observations over some parts of the United States.

In the next phase of this project, we will study the impact of RS-winds on forecasts of other hurricanes during the 2005 season, including Ophelia, Rita, and Wilma. In addition we will perform data impact studies using the 4d-Var data assimilation capability provided by NAVDAS-AR (Xu et al. 2005) and tests of the new wind quality indicators.

Acknowledgements: *This work is supported by the Naval Research Laboratory and the Office of Naval Research, under Program Element 0602435N, Project Number BE-435-037, and ONR Contract No. N00014-05-1-0494*

REFERENCES

Aberson, S. D., 2003: Targeted observations to improve tropical cyclone track forecasts. Mon. Wea. Rev., 131, 1613-1628.

Langland, R. H., 2005: Issues in targeted observing. Q.J.R. Meteorol. Soc., 131, 3409-3425.

Majumdar, S. J., and co-authors, 2006: A comparison of adaptive observing guidance for Atlantic tropical cyclones. Mon. Wea. Rev., 134, 2354-2372.

Velden, C., and co-authors, 2005: Recent innovations in deriving tropospheric winds from meteorological satellites. Bull Amer Meteorol. Soc., 86, 205-223.

Xu, L., T. Rosmond, and R. Daley, 2005: Development of NAVDAS-AR: Formulation and initial tests of the linear problem. Tellus, 57A, 546-559.

Wu, C.-C., 2005: Dropwindsonde observations for typhoon surveillance near the Taiwan region (DOTSTAR). Bull. Amer. Meteorol. Soc., 86, 787-790,

INTERPRETATION OF TROPICAL CYCLONE ADAPTIVE OBSERVING GUIDANCE

C. A. Reynolds [1], M. S. Peng, S. J. Majumdar, S. D. Aberson, C. H. Bishop, R. Buizza

[1] Naval Research Laboratory, Monterey, CA, USA
E-mail: *carolyn.reynolds@nrlmry.navy.mil*

Abstract: Singular Vector and Ensemble Transform Kalman Filter adaptive observing guidance products for Atlantic tropical cyclones are compared using composite techniques that allow us to quantitatively examine differences in the spatial structures of the guidance maps, and relate these differences to the approximations of the respective techniques.

Keywords – *Tropical Cyclones, Adaptive Observing, Singular Vectors, Ensemble Transform Kalman Filter*

1. INTRODUCTION

Objective adaptive observing techniques have been applied for a decade to identify tropospheric regions in which additional observations are expected to improve forecasts of mid-latitude winter storms To study the feasibility of applying the objective techniques to the TC problem, Majumdar et al (2006) compared the current ensemble wind variance method with these objective techniques. Their findings indicated lower similarity between the guidance maps produced using different methods than between those produced using the same method but different forecast systems. In this follow-on study, we compare these methods in another manner, using composite techniques that allow us to quantitatively examine differences in the spatial structures of the guidance maps, and relate these differences to the approximations and constraints of the different methods. The degree to which these differences result from differing analysis error variance assumptions is also examined.

2. METHOD

We compare Ensemble Transform Kalman Filter (ETKF) and Singular Vector (SV) adaptive observing products for 78 cases of 2-day tropical cyclone (TC) forecasts in the Atlantic Basin during the 2004 hurricane season. The ETKF and SV methods consider error propagation from the observing (analysis) time t_a into a given forecast verification region at a verification time t_v, 2 days after t_a. All sets of guidance use ensembles (ETKF/Variance) or non-linear trajectories (SVs) initialized at time t_i, at least 48h prior to t_a.

The ETKF products are based on a 50-member ensemble from the European Centre for Medium-range Weather Forecasts (ECMWF) and a 20-member ensemble from the National Centers for Environmental Prediction (NCEP). Total Energy (TE) SVs are computed using both the ECMWF and Naval Research Laboratory (NRL) forecast systems. In addition, variance (VAR) SVs are computed using estimates of analysis error variance from the NRL Atmospheric Variational Data Assimilation System (NAVDAS) and from the NCEP and ECMWF ETKF products. See Majumdar et al (2006) and Reynolds et al (2006) for more details.

3. RESULTS

The TESV and ETKF summary maps averaged over the 78 cases are shown in Figure 1. All four summary maps have large average values in the vicinity of the tropical cyclone storm track. Both TESV products also have large values over central and western North America. Composite results centered on the storms (not shown), indicate that when TESV maximum targets are remote from the storm, they occur almost exclusively to the north west of the storm. In contrast, the ETKF summary maps have significant amplitude over the northern North Atlantic. The differences between the ECMWF and NCEP ETKF summary maps reflect differences in the ensemble variances, in turn reflecting differences in ensemble construction, resulting in, e.g., significantly larger ensemble variances and summary map values over the central and eastern subtropical Atlantic for the NCEP ETKF than for the ECMWF ETKF.

One reason the TESV products have significant signal over North America is that the calculation considers "dynamics only", and does not use information about expected spatial variations in estimated analysis error variance. One way to introduce information about expected error statistics is to constrain the SVs at initial time using estimates of analysis error variance. This will result in a modulation of the SV signal away from regions where the analysis error variances is expected to be small. The resulting product is actually very sensitive to the estimate of analysis error variance used (Fig. 2). Using the NAVDAS estimate, which is based on static background error statistics, results in a slight modulation of the guidance products away from the well-observed eastern US. Use of the ETKF-based analysis error estimate, which has strong flow dependence, results in a

significant modulation of the SV product, with fewer maxima over central and western North America than the TESVs, but also fewer maxima over the central and eastern North Atlantic than the ECMWF ETKF.

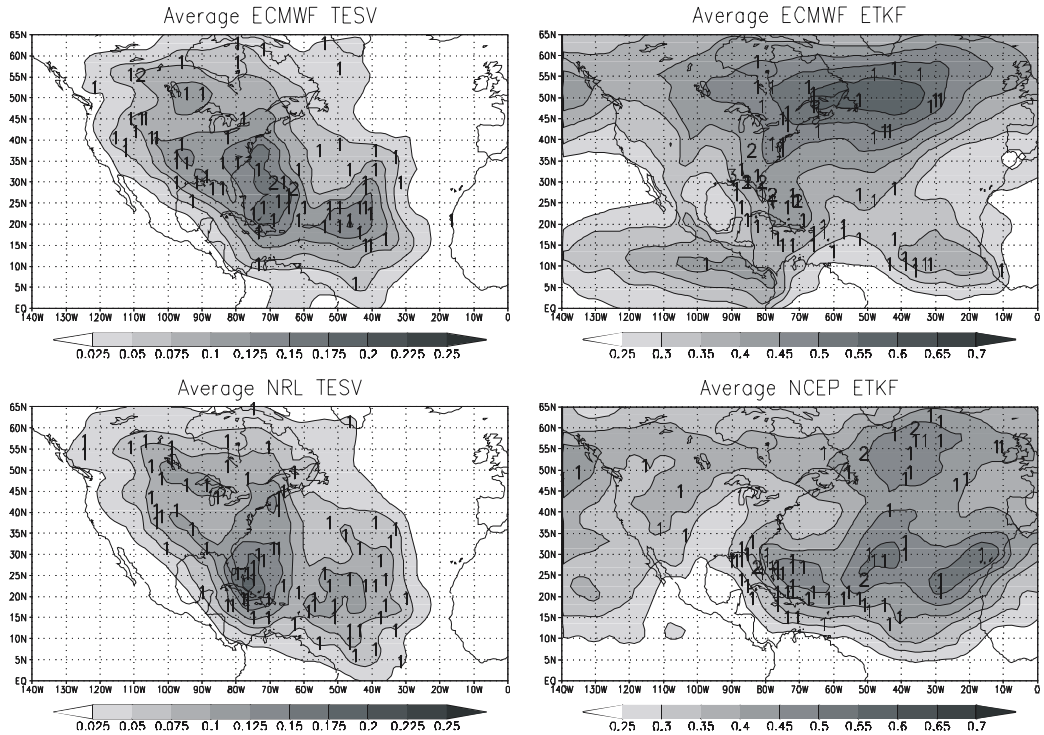

Figure 1. Average summary maps for the ECMWF and NRL TESVs (left) and the ECMWF and NCEP ETKF (right), given by shading. Numbers indicate the locations of the maxima of the 78 individual summary maps.

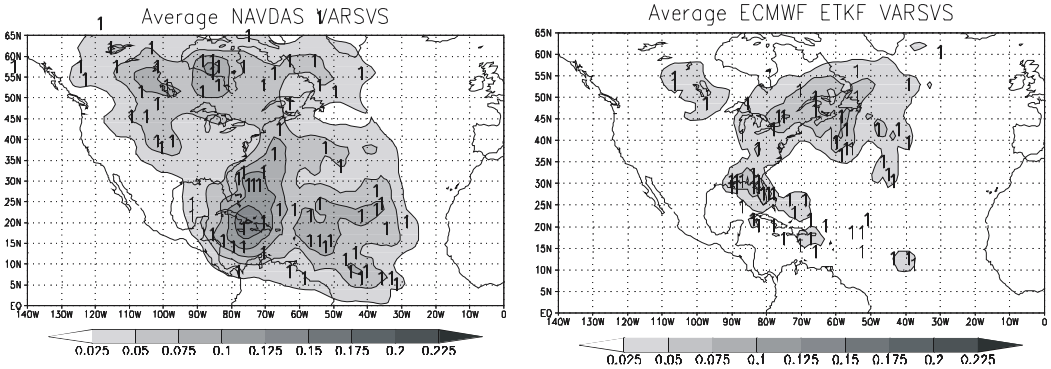

Figure 2. As in Figure 1 but for the NAVDAS VAR SVs (left) and the ECMWF ETKF VAR SVs (right).

6. CONCLUSION

The structural differences between the ETKF and SV target products reflect the differences in the techniques themselves. The TESV targets over the eastern US reflect the fact that this calculation is based on "dynamics only". On the other hand, ETKF products reflect the characteristics of the ensemble on which they are based. VAR SV products are very sensitive to the type of analysis error variance estimate used to constrain them.

Acknowledgements: *S. Majumdar and S. Aberson acknowledge financial support from the NOAA Joint Hurricane Testbed and Z. Toth and the Environmental Modeling Center at NCEP for the provision of an account on the IBM SP supercomputer. C. Bishop, M. Peng, and C. Reynolds acknowledge the support of Office of Naval Research under program element 0601153N, project number BE-033-03-4M.*

REFERENCES

Majumdar, S. J., Aberson, S.D., Bishop, C. H., Buizza, R., Peng, M. S., and Reynolds, C. A. 2006: A Comparison of Adaptive Observing Guidance for Atlantic Tropical Cyclones, Mon Wea. Rev., 134, 2354-2372.

Reynolds, C. A., M. S. Peng, S. J. Majumdar, S. D. Aberson, C. H. Bishop, and R. Buizza, 2006: Interpretation of Adaptive Observing Guidance for Atlantic Tropical Cyclones. Submitted to Mon. Wea. Rev.

THE IMPACT OF A-TREC TARGETED OBSERVATIONS ON WEATHER FORECASTS, USING THE UK MET OFFICE FORECASTING SYSTEM

Guðrún Nína Petersen [1] and Alan J. Thorpe

[1] School of Environmental Science, University of East Anglia, Norwich, UK
E-mail: g.n.petersen@*uea.ac.uk*

Abstract: The influence of A-TReC targeted observations on forecasts made with the UK Met Office global operational system is presented. The impact of the observations reaches the verification area at verification time. However, this does not always result in a forecast improvement.

Keywords *– THORPEX, A-TReC, targeted observations*

1. INTRODUCTION

The North Atlantic THORPEX Regional Campaign (A-TReC) took place October-December 2003. Its main objectives were to test real time quasi-operational targeting of observations using a variety of observational platforms. The focus was on improving short range, 24-72 hours, regional scale numerical weather forecasts over Europe and the eastern coast of North America. In total 21 cases were targeted during the campaign, some on multiple days, resulting in 40 targeted events. During the campaign as targeting time was approached the uncertainties in the forecasts decreased and there was often small uncertainty remaining at targeting time (Mansfield *et al.*, 2005). Given the generally small forecast uncertainties during the campaign, large forecast improvements were not likely, but rather small improvements or deteriorations in the forecast skill were expected.

This study evaluates the impact of the A-TReC additional observations on the forecasts made with the UK Met Office global operational system. The observational impact on the forecasts as well as the effect on the forecast error is evaluated.

2. EXPERIMENTAL SETUP

Of the 40 targeted events, 38 were used in this study. For each event three forecasts were made, 'Control', 'Atarg' and 'ATReC'. The difference between the forecasts is listed in Table 1. The forecasts were carried out using the UK Met Office global model, version 6.0. The horizontal resolution was $0.83^{o}\times0.56^{o}$, or roughly 60 km, and in the vertical there were 38 levels.

3. RESULTS

The two figures presented emphasize some of the results of the study.

Figure 1 shows the impact of the additional observations on the 500 hPa geopotential height in the whole North Atlantic region, the verification areas for each event and the difference between the two as a function of forecast time. In the North Atlantic region the impact of the additional observations grew steadily during the forecasts. In the verification areas, on the other hand, there was a more rapid increase in the impact until a forecast range of about 42 hours. The optimization time for the events varied between 30 and 78 hours but was for most events 42 hours. Therefore, these results indicate that the targeted observations were added in the right location, reaching the verification area at verification time. At 42 hours forecast range, the observational impact in the verification area is about a factor 1.7 larger than the impact in the whole North Atlantic region.

Figure 2 shows the difference in forecast error in the verification area between the Control forecast and the Atarg forecast in sea level pressure, 850, 500 and 200 hPa during the second half of the campaign. The forecast error is measured in terms of root mean square error (RMSE) verifying the forecasts against the ATReC analysis, the analysis using all available data. Positive values indicate a reduction in the RMSE. The figure shows that there is a large case-to-case variation in the forecast improvement and deterioration as well as a vertical variation.

Forecast	**Specification**
Control	Routine observations only
Atarg	Same background field as in Control but A-TReC observations at initial time
ATReC	A-TReC observations both at initial time and in the background field

Table 1. Name convention for forecasts.

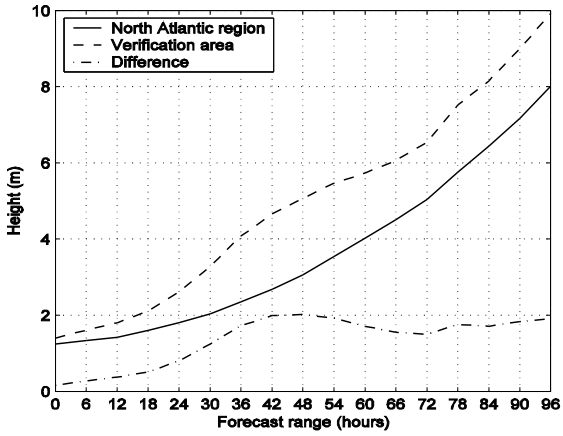

Figure 1. The time evolution of the mean impact of the additional observations on the Atarg forecast of 500 hPa geopotential height (m) in the North Atlantic region (solid) and the verification areas (dashed). The difference field is shown by a dot-dashed line. The impact is averaged over all events.

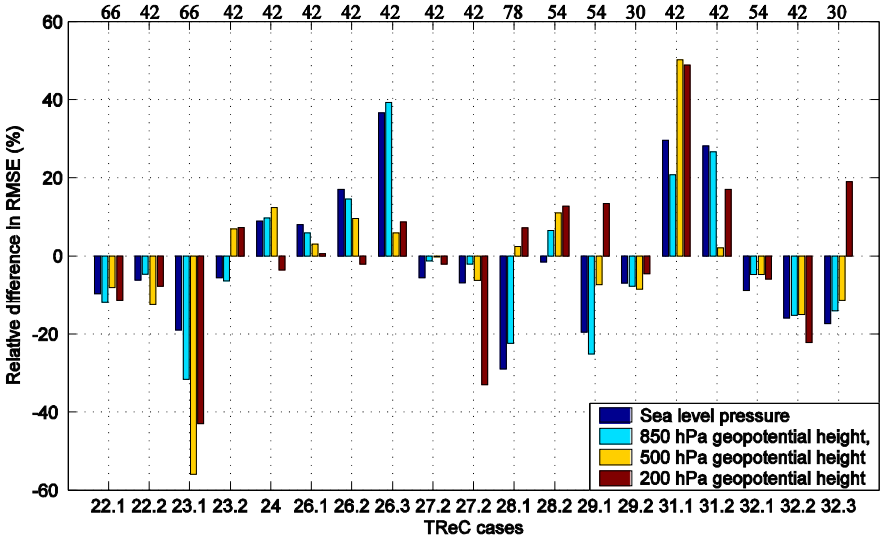

Figure 2. The difference in RMSE between the Control forecast and the Atarg forecast in the verification area at verification time for events from the second half of the campaign. The difference is normalized with the RMSE in the Control forecast and positive values indicate less error in the Atarg forecast than in the Control forecast.

In 32% of the events there was an overall reduction in RMSE. In 53-63% of the events there was an improvement at one level. These results are similar to results from both FASTEX and WSR.

6. CONCLUSION

The current results indicate that the targeted observations were made in the right location to influence the forecasts in the verification area at verification time. However, this did not always result in improved forecasts and there was a large case-to-case as well as vertical variation in the impact. These results are related to small forecast uncertainties during the campaign making small improvements or deterioration likely. This behaviour related to the utilisation and effectiveness of targeted observations by the data assimilation system is an important area for future research. Further results from the study can be found in Petersen and Thorpe (2006).

Acknowledgements: *Richard Dumelow at UK Met Office ran the reanalysis and the forecasts necessary for the study. G. N. Petersen was funded by Vaisala and the UK Met Office through a THORPEX Postdoctoral Research Fellowship.*

REFERENCES

Mansfield, D., D. Richardson and B. Truscott, 2005: An overview of the Atlantic THORPEX Regional Campaign. In Proceedings of the First THORPEX international science symposium, 6-10 December 2004, Montreal, Canada.

Petersen, G. N. and A. J. Thorpe, 2006: The impact on weather forecasts of targeted observations during A-TReC. Q. J. R. Meteorol. Soc. Submitted.

PROSPECTS OF FORECAST IMPROVMENTS BY ASSIMILATING IN THE UNSTABLE SUBSPACE

Anna Trevisan[1], Alberto Carrassi and Francesco Uboldi

[1] ISAC - CNR, Bologna, Italy
E-mail: *A.Trevisan@isac.cnr.it*

Abstract: The status of the work and the recent results of the application of the Assimilation in the Unstable Subspace are reported with special emphasis to the analysis of the stability induced by the assimilation of observations.

1. INTRODUCTION

The essence of the Assimilation in the Unstable Subspace (AUS), one of the novel approaches to data assimilation, is the detection and elimination of the unstable components of the forecast error. Those observations that are able to detect such instabilities maximize the reduction of the error in the state's estimate.
When adaptive observations are available, the efficiency of AUS is enhanced, but fixed observational networks can also be profitably exploited by AUS (work in progress). The robustness of AUS has been tested several models and observational configurations: low order, quasi-geostrophic and primitive equation models of the atmosphere and ocean, with perfect and noisy observations with or without model error. When the errors are kept within sufficiently low bounds the unstable modes are seen to closely match the forecast error structures.
The forecast-analysis cycle is naturally seen as a forced dynamical system where the assimilation of observations acts as a forcing on the free system equations. The theory predicts that the number of unstable modes characterizing the free system determines the number and frequency of observations necessary to stabilize it (Trevisan and Uboldi, 2004). Results confirm the prediction of the theory and suggest the existence of a relation between the analysis error and a non-dimensional parameter obtained by combining the number and values of positive Lyapunov exponents of the free system with the observational frequency (Carrassi *et al.*, 2006).
The next step will be the implementation of AUS in an operational environment: among the most promising application is the use of remote sensing measurements in those regions where observations are needed to reduce the unstable structures of the error that have been detected.

2. RESULTS

The equation describing the linear perturbative dynamics of the complete forecast analysis cycle is:

$$\delta\mathbf{x}^a(t_{k+1}) = (\mathbf{I}-\mathbf{KH})\mathbf{M}\delta\mathbf{x}^a(t_k)$$

where **K** is the gain matrix, **H** and **M** the (linearized) observation operator and model equations respectively while $\delta\mathbf{x}^a$ represents the perturbed analysis state. The term (**I-KH**) is due to the observational forcing introduced at the analysis step and, depending on the properties of **K** and **H,** has a stabilizing effect on the data assimilation system. Such an effect is common to any properly designed assimilation scheme and is particularly evident when the matrix **K** is defined so that the base of the subspace where the analysis increment is confined is given by the unstable directions of the system.
In the Assimilation in the Unstable Subspace (AUS) the unstable directions are estimated by Breeding on the Data Assimilation System (BDAS), that, in contrast to standard breeding (Toth and Kalnay, 1993; 1997), embeds the information on the observational network, the assimilation system and its dynamical instabilities (Trevisan and Uboldi, 2004; Uboldi *et al.*, 2005; Uboldi and Trevisan, 2006; Carrassi *et al.*, 2006).
For the updates to drive the analysis solution towards the true state, the dynamics of the forecast-analysis cycle must be stabler than that of the pure forecast system. If the system is completely stabilized by the updating process, *i.e.* it has no more positive Lyapunov exponents, this will be sufficient for the uniqueness of the solution as well as necessary for its convergence to the truth. Such complete stabilization will drive analysis errors to lower values.
The stabilizing effect of the assimilation is illustrated by results obtained varying the observational frequency and the extension of the model domain. Figure 1 shows that both the increase of the observational frequency and the reduction of the model domain lead to a progressive stabilization of the analysis solution and that in correspondence of the system stabilization (*i.e.* no positive Lyapunov exponents) an abrupt reduction of the analysis error is obtained (Carrassi *et al.*, 2006). We study the properties of the unstable subspace of the assimilation system with those of the free system. To this end, a non-dimensional parameter is constructed by multiplying the number of positive exponents (N^+) by the leading one (λ_{max}) and by the assimilation interval (τ).

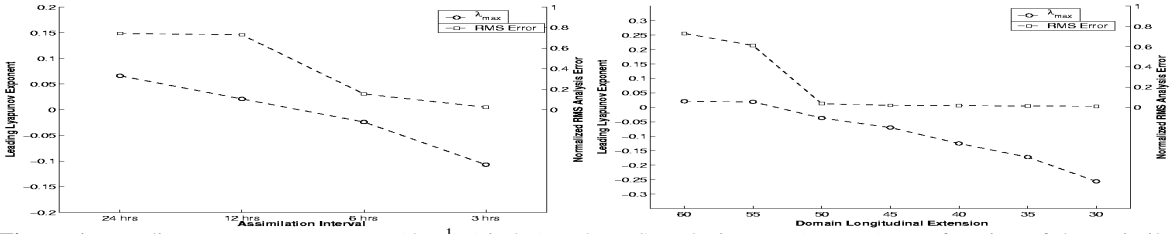

Figure 1. Leading Lyapunov exponent (day^{-1}) (circles) and RMS analysis error (squares) as a function of the assimilation interval (τ) (right panel) and of the domain longitudinal extension (left panel). The error is in potential enstrophy norm and normalized by the natural variability of the system (see Carrassi *et al.*, 2006 for details).

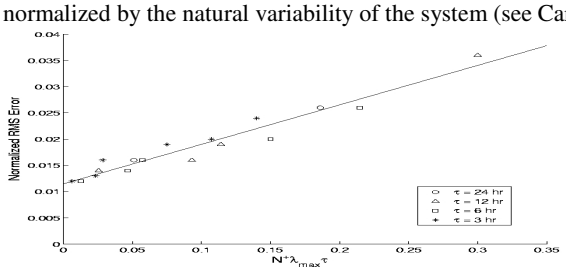

Figure 2. Normalized time and domain analysis error as a function of the non-dimensional parameter $N^{+}\lambda_{max}\tau$ (from Carrassi *et al.*, 2006).

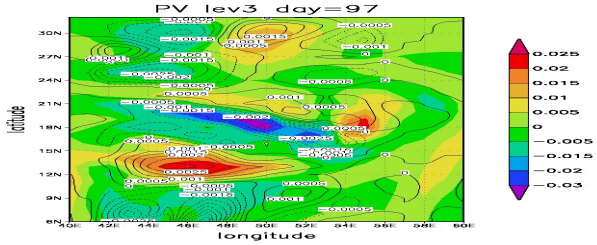

Figure 3. Potential vorticity mid-level actual forecast error (shaded) and forced bred vector (contour) at day 97 (see Carrassi *et al.*, 2006 for details).

Figure 2 shows the average analysis error as a function of this parameter. The error level at which the system stabilizes appears to be a monotonic function of this parameter with an approximate linear dependence. This result supports our claim that the number (frequency) of observations needed to stabilise the system and efficiently reduce the analysis error depends upon the number and growth rate of the unstable directions.
Finally, we show that, when errors in the unstable directions are efficiently reduced, the error becomes smaller and behaves more linearly. In this case, the unstable directions themselves become more representative of the actual error, the unstable structures take a longer time to build up and a smaller number and lower frequency of observations becomes sufficient to control their growth. This point is illustrated by Fig. 3 that depicts the actual forecast error and a forced bred mode at an arbitrary time along the assimilation cycle (Carrassi *et al.*, 2006). This result clearly reveals that bred modes constructed by BDAS share a strong similarity with the actual flow dependent forecast error. Such a good estimate of the forecast error is in turn at the basis of AUS ability to exploit a smaller amount of information by spreading the analysis correction in a dynamically consistent manner.

3. CONCLUSION

A question of some practical importance in weather and ocean prediction concerns the estimate of the efficiency of assimilation systems and observational networks. We have addressed these issues from the standpoint of stability analysis. The stability of the analysis cycle solution is a sufficient condition for its uniqueness and a necessary condition for convergence to the true flow evolution; in turn, the degree of stabilization introduced by the observations may be measured rather precisely by estimating the Lyapunov spectrum of the assimilation system. Furthermore results show that, as predicted by the theory, the observational forcing reduces the dimension of the unstable subspace and stabilises the assimilation system; in particular, the number of observations needed to stabilise the system is related to the instability properties of the free system.

REFERENCES

Carrassi, A., A. Trevisan and F. Uboldi, 2006: Adaptive observations and assimilation in the unstable subspace by breeding on the data assimilation system. In print on *Tellus*.
Toth, Z. and E. Kalnay, 1993: Ensemble forecasting at NMC: the generation of perturbations. *Bull. Amer. Meteorol. Soc.,* **74,** 2317-2330.
Toth, Z. and E. Kalnay, 1997: Ensemble forecasting at NMC: the breeding method. *Mon. Weather Rev.*, **125,** 3297-3318
Trevisan, A. and F. Uboldi, 2004: Assimilation of standard and targeted observations within the unstable subspace of the observation-analysis-forecast cycle system. *J. Atmos. Sci.,* **61,** 103-113.
Uboldi, F., A. Trevisan and A. Carrassi, 2005: Developing a dynamically based assimilation method for targeted and standard observations. *Nonlin. Processes in Geophys.,* **12,** 149-156.
Uboldi, F. and A. Trevisan, 2006: Detecting unstable structures and controlling error growth by assimilation of standard and adaptive observations in a primitive equations ocean model. *Nonlin. Processes in Geophys.,* **13,** 67-81.

THE GERMAN PRIORITY PROGRAM SPP1167 PQP „QUANTITATIVE PRECIPITATION FORECAST": AN OVERVIEW

Andreas Hense[1], Gerhard Adrian[2], Christoph Kottmeier[3], Clemens Simmer[1], Volker Wulfmeyer[4]

[1] Meteorologisches Institut Universtät Bonn, Auf dem Hügel 20, D 53121 Bonn
[2] Deutscher Wetterdienst, Kaiserleistr. 42-44, D 63067 Offenbach
[3]Institut für Meteorologie und Klimaforschung, Universität Karlsruhe, Wolfgang-Gaede-Str.1, 76131 Karlsruhe
[4] Institut für Physik und Meteorologie (IPM), Universität Hohenheim, Garbenstr. 30 D-70599 Stuttgart
e-mail: ahense@uni-bonn.de

Abstract Since April 2004 a coordinated program for improving quantitative precipitation forecasting is running in Germany in a close cooperation between universities, research institutes and the German Weather Service. Besides the extensive measurements campaign COPS as part of the program several more issues of THORPEX related research is addressed e.g. probabilistic forecasting utilizing global and regions ensembles.

1. INTRODUCTION

Since April 2004, a coordinated program (Priority Program SPP 1167-PQP) of more than 20 projects funded by the Deutsche Forschungsgemeinschaft DFG cooperating with the German Weather Service DWD is actively aiming at the improvement of quantitative precipitation forecasts in mid Europe on time scales between 24h and several days. Specifically the goals of this six year planned exercise are:

(1) Identification of physical and chemical processes responsible for the deficiencies in quantitative precipitation forecast
(2) Determination and use of the potentials of existing and new data and process descriptions to improve quantitative precipitation forecast
(3) Determination of the prognosis potential of weather forecast models by statistico-dynamic analyses with respect to quantitative precipitation forecast .

2. OBJECTIVES OF THE PRIORITY PROGRAM

This research program meets the challenges put up by the user groups with respect to quantitative precipitation forecast. It has been initiated by atmospheric scientists at universities and research institutes, who combine the knowledge required to improve quantitative precipitation forecast. Under this priority program, scientists and experts in the following fields cooperate:

- Dynamics of the atmosphere
- Cloud physics and precipitation formation
- Probabilistic treatment of atmospheric processes
- Methods of data assimilation
- Development and application of dynamic simulation models
- Remote sensing of the atmosphere

A priority program combining this expertise accounts for the fact that in view of the high development level of operational weather forecast systems, further improvement of quantitative precipitation forecast can no longer be achieved by isolated efforts of individual groups of researchers. The scope of tasks to be managed simultaneously is so wide that a joint and coordinated effort of university institutes and research institutions is envisaged, with the operational forecast system of the German Weather Service being integrated as a development, testing, and validation instrument.

Although most subprojects work on the forecasting system of DWD: the global model GME and the regional nonhydrostatic forecast model LM but the project is open for tests and applications of other models such as MM5 and WRF. They now concentrate on

- data assimilation and probabilistic forecasts using global as well as regional ensemble simulations with special emphasis on QPF

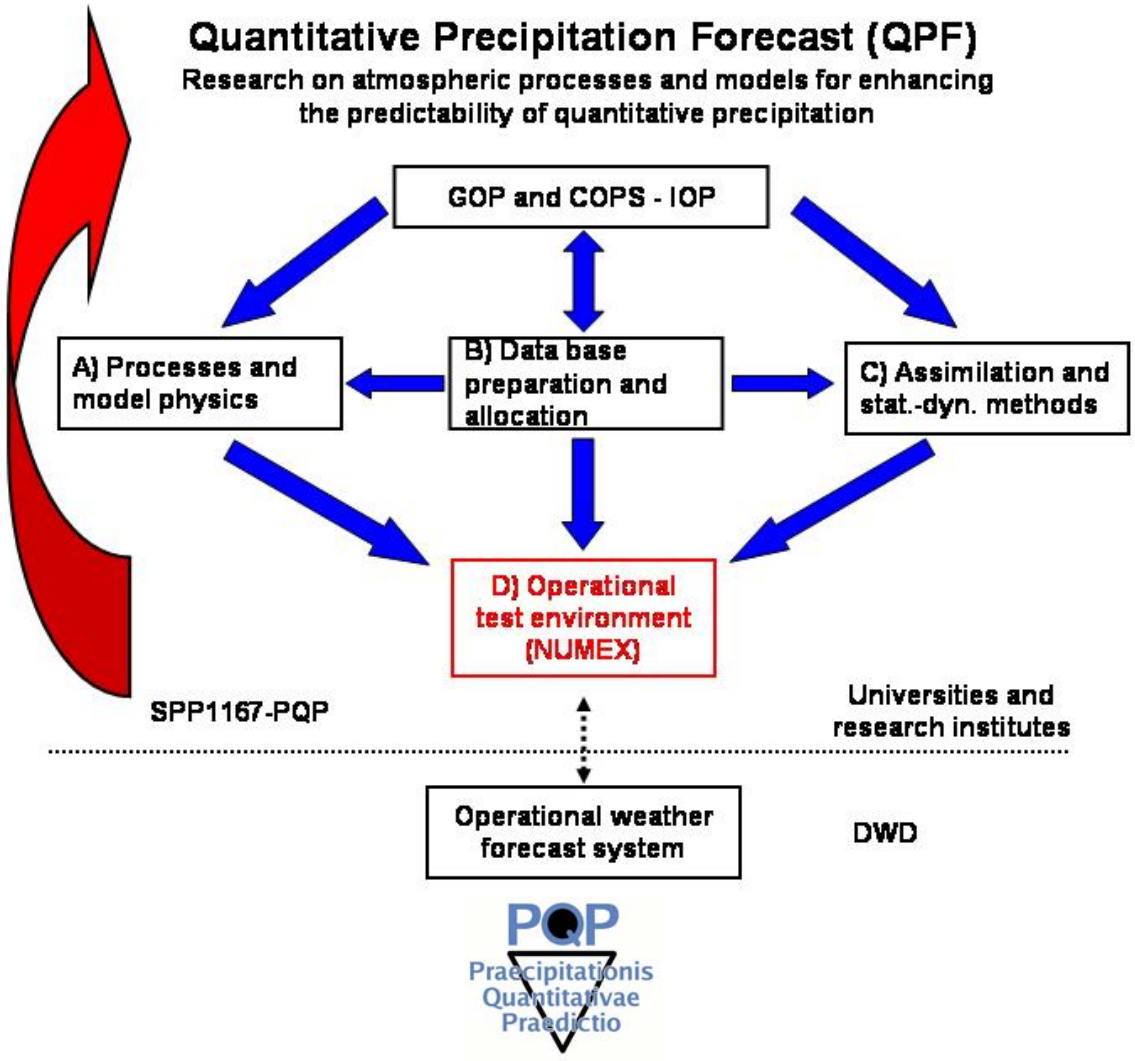

Figure 1: The organisational structure of the Priority Program SPP1167-PQP with respect to the basic goals, the cooperation with the German weather service, universities and research institutes and the observational components of SPP1167 the GOP and the COPS – IOP.

- enhanced and new verification strategies of precipitation and related atmospheric flow structures
- enhancement of existing and development of new process descriptions relevant for precipitation simulations such as advanced cloud microphysics

These efforts are complemented by an extensive measurement campaign in 2007 -- the Convective and Orographically-induced Precipitation Study (COPS) which itself is embedded into a General Observing Period GOP. The overall organisation structure of the program is shown in Fig.1

Besides the fact that the COPS – IOP is a research and development project of the WWRP there are several more SPP1167 projects which deal with THORPEX related research. There are new approaches for global as well as mesoscale ensemble forecasting, the verification of high-resolution mesoscale models especially with respect to precipitation, the verification of probabilistic forecasts and the exploitation of new data sets for mesoscale model initialisation and evaluation.

More details can be found on the web-page http://www.meteo.uni-bonn.de/projekte/SPPMeteo

THE IMPACT OF DROPSONDE OBSERVATIONS AROUND TROPICAL CYCLONES ON THE MEDIUM-RANGE FORECAST FOR EUROPE

Maxi Böttcher[1], Sarah Jones, Sim Aberson

[1]Institut für Meteorologie und Klimaforschung, Universität Karlsruhe/Forschungszentrum Karlsruhe, Germany
Email: *maxi.boettcher@imk.uka.de*

Abstract: The impact of targeted dropsondes designed to improve hurricane track forecasts on the medium-range forecast for Europe is investigated. The operational forecasts from the NCEP global model are compared with forecasts in which all dropsonde data have been removed from the analysis. The forecast error reduction is calculated for 10 cases in 2003, 2004 and 2005. The cases of Bonnie, Charley and Ivan in 2004 are analysed in more detail and the propagation of differences between the forecasts is related to the Eady index.

Keywords *- Targeted observations, tropical cyclones, downstream predictability*

Introduction

The interaction of tropical cyclones with the mid-latitude flow often results in large forecast errors downstream of the tropical cyclone itself. Global models that provide initial conditions for meso-scale and local models can not resolve the inner core of tropical cyclones. The accelerated motion and rapid intensification that can occur as a tropical cyclone interacts with the midlatitude flow are common reasons for a reduction of forecast quality (Jones et al. 2003). The forecast of the spatial and temporal location of the tropical cyclone relative to the mid-latitude planetary waves is especially important for an accurate downstream forecast.

The National Hurricane Center and Hurricane Research Division have been conducting reconnaissance flights around tropical cyclones for a number of years. Measurements from dropsondes released from aircraft are assimilated at operational forecast centers. Targeted observations aimed at improving hurricane track forecasts were made in areas of increased ensemble spread of the deep layer mean wind. For short-range forecasts the additional hurricane data leads to a track forecast error reduction (Aberson 2003).

Data and Approach

Forecasts from the NCEP global model with 1°×1° horizontal resolution and up to 180h lead time are used. Operational forecasts are compared with forecasts in which all dropsonde data of the whole season have been removed from the analyses.

The differences are analysed from a PV perspective, with respect to the main regions of baroclinity based on the Eady index, and in terms of an objective measure of the forecast error reduction. Hurricanes Bonnie, Charley, and Ivan in 2004 are analysed in detail. Each of these tropical cyclones were involved in a cyclogenesis event after interaction with the mid-latitude flow. The forecast error reduction is calculated for a number of other cases also.

Results

Inclusion of the dropsonde data leads to changes in the position and intensity of the tropical cylone in the initial conditions. The forecast differences translate with the system into the mid-latitudes and propagate downstream along areas of enhanced Eady-Index.

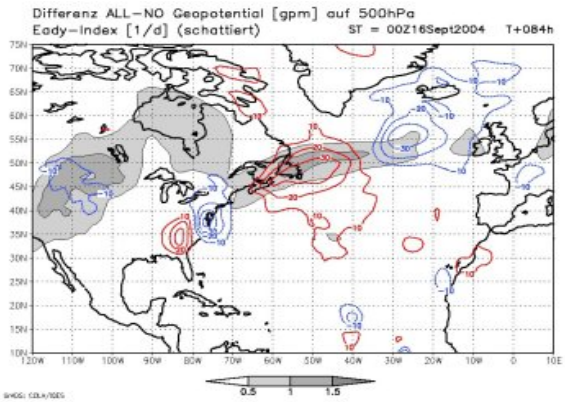

Figure 1. Differences in 500hPa geopotential height between the forecasts with and without dropsonde data from the forecast of 00 UTC 16 September 2004 after 84h, gray shading marks areas of enhanced baroclinity defined by the Eady index.

This is illustrated in Fig. 1, were the dipole to the north of Florida is associated with the different locations of hurricane Ivan in the two forecasts. This feature is strongest at 500hPa and 1000hPa (not shown).
The forecast differences seen along regions of enhanced Eadx index extend to the British Isles and have maximum amplitude at 200hPa. These anomalies appear to be associated with the interaction of Ivan's outflow and the midlatitude tropopause.

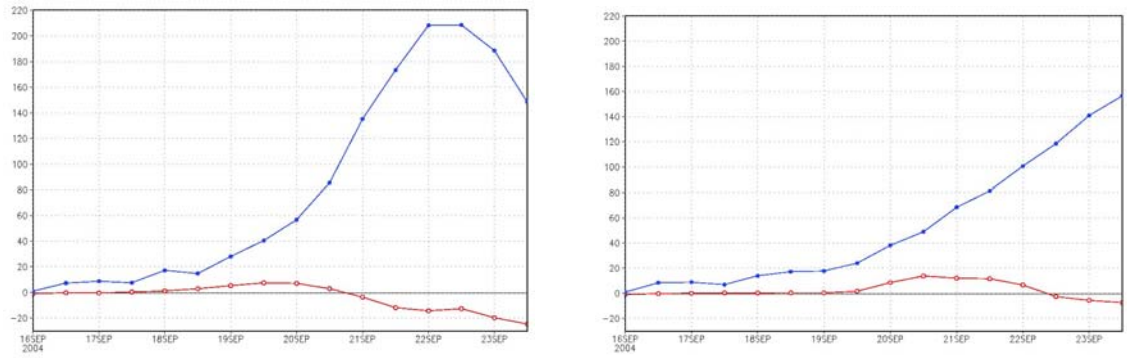

Figure 2. Forecast error reduction of the 500hPa geopotential height caused by the dropsonde data (red) and the forecast error with respect to the analysis (blue) for the Atlantic area (left) and the European area (right) for the forecast of 00 UTC 16 September 2004.

Forecast error reduction was determined by scaling and averaging over selected regions. In the analysed cases the forecast error was reduced temporarily by the inclusion of the dropsondes. The impact on the forecast moves downstream as indicated by the red line in Fig. 2 for the Atlantic area (left) and the European area (right). Averaging over 10 individual forecasts of 2003, 2004 and 2005 does not show a clear advantage of the operational forecast with additional dropsonde data.
Despite individual forecast error reductions of up to 20% the improvement due to the additional dropsonde data is considerably smaller on average than the forecast error itself.
However, in only one of the cases analysed were any data available during an ET event. This was the case of the largest reduction in forecast error. Thus, it would be desirable to repeat this analysis for dropsondes and other observations made during an ET event.

REFERENCES

Aberson, S. D. (2003). Targeted observations to improve operational tropical cyclone track forecast guidance. Monthly Weather Review 131, 1613 1628.

Jones, S. C., P. A. Harr, J. Abraham, L. F. Bosart, P. J. Bowyer, J. L. Evans, D. E. Hanley, B. N. Hanstrum, R. E. Hart, F. Lalaurette, M. R. Sinclair, R. K. Smith und C. Thorncroft (2003). The extratropical transition of tropical cyclones: Forecast challenges, current understanding, and future directions. *Weather and Forecasting 18*, 1052–1092.

ADAPTIVE THINNING OF SATELLITE DATA USING THE ENSEMBLE TRANSFORM KALMAN FILTER (ETKF)

Keir Bovis [1] , Brett Candy [1]

[1] Met Office, Exeter, United Kingdom
E-mail: keir.bovis@metoffice.gov.uk

1. INTRODUCTION

Previous studies have shown that increasing the observation density for satellite observations with uncorrelated error improves the analysis accuracy (Liu and Rabier, 2003). On the other hand, for operational Numerical Weather Prediction (NWP) centres, the cost of processing a dense observation network must also be a consideration.

This paper presents results obtained from a comparative experiment, assessing the utility of assimilating adaptively thinned Advanced Microwave Sounding Unit (AMSU) radiance data with that of an operational global AMSU baseline. Adaptive thinning parameterization is constructed using Sensitive Area Predictions (SAPs) created from the Ensemble Transform Kalman Filter (ETKF) (Bishop et al., 2001) initialized using ECMWF's Ensemble Prediction System (EPS). The SAP is created such that it maximises the reduction in forecast error at a pre-determined forecast range in a pre-defined verification area.

2. EXPERIMENTAL SETUP

To evaluate each AMSU thinning strategy, an Observation System Experiment (OSE) is created using the Met Office's North American mesoscale model. This model generates forecasts out to T+48 at 00UTC and 12UTC of each trial day. At each 00/12 cycle, each OSE is initialized from an identical observation and assimilation background valid at that time. By doing this, the impact of each thinning strategy is apparent and not masked by background departures. Boundary conditions for the regional model are obtained from the Met Office's Global model. The OSE trial period spans 12UTC on 29th August 2005 through to 12UTC on 1st October 2005. Throughout the OSE trial period surface and satellite observations are assimilated.

Adaptive thinning guidance is generated from a configuration of the ETKF initialized using the ECMWF EPS. The length of time between initialisation and SAP generation (the lead time) is 24 hours. Guidance is generated with the aim of improving T+24 forecasts (the optimisation time) in a verification area defined as a bounding box bottom left 35ºN/98ºW top right 45ºN/85ºW. During data assimilation, thinning boxes are constructed in areas that maximise the ETKF signal variance. Boxes are selected until the total area of all boxes contained within a single SAP is approximately 2×10^6 km. Within these boxes, AMSU thinning is carried out at a resolution of 40 km, the effective maximum data usage. Outside of these boxed regions, a thinning resolution of 154 km is used. For every 12-hour cycle during the trial period, the ETKF is run. As a comparison, thinning of AMSU data is undertaken at 40 km across the complete model domain as in the operational model (D40).

3. SUMMARY OF RESULTS

Figure 1 shows the difference in mean forecast Root Mean Squared (RMS) error of T+12, T+24, T+36 and T+48 forecasts. The legend indicates the number of forecast fields in which the ETKF OSE trial gives a smaller mean RMS difference compared with the D40 control. The utility of the adaptive thinning approach can clearly be seen as 15 T+24 fields have a reduced RMS in the ETKF trial compared with the 5 T+24 fields in the control OSE (D40). From Figure 1, consistent improvements in forecast geopotential height at 850, 500 and 250hPa can be seen at all forecast ranges using the adaptive thinning approach. The field with the largest decrease in forecast RMS error is T+24 500hPa relative humidity (R500). By contrast, T+36 forecast 250hPa relative humidity shows the greatest increase in RMS error using the ETKF approach. Verification of surface fields appears mixed and notably T+24 forecast RMS error statistics for Mean Seal Level Pressure (MSLP) are poorer in the ETKF adaptive thinning trial.

Table 1 shows T+24 forecast RMS error for a selection of fields verifying at 25/09/05 12 UTC against surface and radiosonde observations in the verification area. This time coincides with ex-Hurricane Rita approaching the verification region. For this event, the ETKF adaptive thinning approach demonstrates a lower RMS error for MSLP, 500hPa geopotential height (H500) and temperature (T500). In contrast, this approach is inferior in vector wind speed (W500) displaying a higher forecast RMS error than the control OSE (D40).

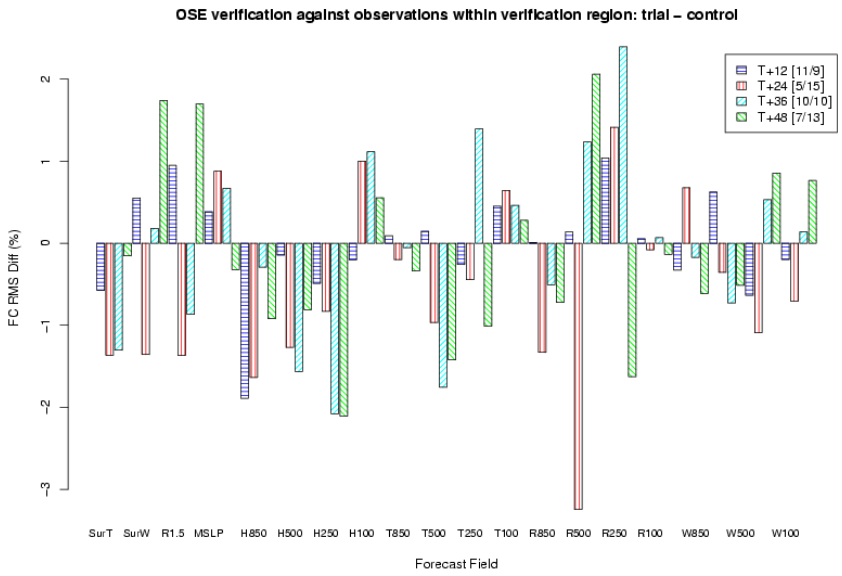

Figure 1. Percentage difference in mean forecast RMS error of T+12, T+24, T+36 and T+48 forecasts. Surface temperature (SurT), vector winds (SurW) and Mean Seal Level Pressure (MSLP) verified against surface observations contained within verification area. Geopotential height (H), temperatures (T), relative humidity (H) and wind vectors (W) verified against radiosonde observations in the verification area.

OSE	T+24 forecast RMS error verifying 25/09/05 12UTC			
	MSLP(hPa)	H500(hPa)	W500(m/s)	T500(K)
D40	303.86	23.29	13.16	1.91
ETKF	289.90	22.64	13.30	1.75

Table 1. Verification of T+24 forecast RMS error for ex-Hurricane Rita at 12UTC on 25/09/05 verified against surface and radiosonde observations within the verification area for control OSE (D40) and trial OSE(ETKF).

4. CONCLUSIONS

This paper has presented the results from a comparative study evaluating the utility of adaptively thinned AMSU radiance data. Thinning guidance has been derived from sensitive areas identified using the ETKF with the aim of improving T+24 forecasts in a pre-defined verification area. Evaluation of this approach has been undertaken by comparing its performance with an operational configuration of the NWP model. Results demonstrate a positive impact for a significant number of forecast fields over a 1-month long trial and in the presence of a notable high-impact weather event. Both OSEs have been evaluated in the presence of an additional control in which thinning of AMSU data is undertaken at 154 km across the complete model domain (D154). Overall skill scores obtained from this comparison, show that control OSE D154 is inferior to D40 and the ETKF approach. This is due to the larger error correlation of AMSU radiance data in the D40 control.

Previous campaigns have considered the targeting of satellite data, for example use of rapid-scan geostationary satellite wind data in the 2003 Atlantic THORPEX Regional Campaign (ATReC). Whilst demonstrating a positive impact, the adaptive thinning of AMSU radiance data is not seen as a candidate for operational implementation. Instead, consideration will be made to its suitability for next generation of sensors such as the Infrared Atmospheric Sounding Interferometer (IASI) that will provide up to 8,500 radiances in each field of view.

REFERENCES

Liu, Z. Q., and F. Rabier, 2003: The Potential of High-Density Observations for Numerical Prediction: A Study With Simulated Observations. Quarterly Journal of the Royal Meteorological Society. **129**(594), 3013-3035.

Bishop, C. H., B. J. Etherton, and S. Majumdar, 2001: Adaptive Sampling with the Ensemble Transform Kalman Filter, Part I: Theoretical Aspects. Monthly Weather Review. **129**(3), 420-436.

OBSERVATION TARGETING USING THE MET OFFICE GLOBAL AND REGIONAL ENSEMBLE PREDICTION SYSTEM

Keir Bovis [1]

[1] Met Office, Exeter, United Kingdom
E-mail: keir.bovis@metoffice.gov.uk

1. INTRODUCTION

Targeted observations collectively obtained from mobile observation platforms have historically formed part of an adaptive observing network. This network is designed to complement the routine observing network used by Numerical Weather Prediction (NWP) models.

This paper presents the results from a series of comparative experiments evaluating the impact of targeting radiosondes using guidance from Sensitive Area Predictions (SAPs). These are created using two configurations of the Ensemble Transform Kalman Filter (ETKF) (Bishop et al., 2001) initialized from the Met Office Global Regional Ensemble Prediction System (MOGREPS). SAPs are created such that they maximise the reduction in forecast error at a pre-determined forecast range in a pre-defined verification area.

2. EXPERIMENTAL SETUP

The MOGREPS ensemble is used to initialise two configurations of the ETKF. Targeting guidance generated from each configuration aims to improve T+24 forecasts (the optimisation time) in a verification area defined as a bounding box bottom left 35ºN/98ºW top right 45ºN/85ºW. The length of time between MOGREPS-initialisation of the ETKF and production of targeting guidance is termed the lead time. One ETKF configuration uses a lead time of 24 hours, *ETKF(24)*, the other 48 hours, *ETKF(48)*. Both will be compared with targeting guidance manually defined from an upstream 500hPa flow analysis (*upstream*). In this paper, the approach used to assess the impact of the different configurations is to generate SAPs and then using these as guidance, deploy and assimilate additional targeted observations by running an Observation System Experiment (OSE). The Met Office's North American mesoscale model is used to evaluate the different configurations of the ETKF. This model generates forecasts out to T+48 at 00UTC and 12UTC of each trial day. At each 00/12 cycle, each OSE is initialized from an identical observation and assimilation background valid at that time. By doing this, the impact of each deployment is apparent and not masked by background departures. Boundary conditions for the regional model are obtained from the Met Office's Global model. The OSE trial period spans 12UTC on 29th August 2005 through to 12UTC on 1st October 2005.

A routine radiosonde network is constructed by subjectively selecting stations from the existing North American network and then thinning them to an approximate resolution of one per 10º latitude/longitude box. Additional adaptive observations may then be added by selecting from those remaining stations. No routine or adaptive observations are deployed within the verification area. Throughout the OSE trial routine surface and satellite observations are also assimilated. For every 12-hour cycle during the trial period, each configuration of the ETKF is run. The ETKF signal variance is interpolated to the locations of the radiosonde stations. Radiosonde observations from the top 10 ranked surface stations maximising the ETKF signal variance are automatically selected for assimilation into the NWP model.

3. SUMMARY OF RESULTS

The overall skill scores calculated for a basket of forecast fields over the complete OSE period are shown in the left-hand side of Table 1. From these results it can be seen that the OSE based on the upstream 500hPa flow analysis (*upstream)* gives the best performance with a skill score of 49.30. The ETKF-based OSE with the longer lead time, *ETKF(48),* out-performs that with the shorter lead time, *ETKF(24)*. The right-hand side of Table 1 shows T+24 forecast RMS error for a selection of fields verifying at 25/09/05 12UTC against surface and radiosonde observation within the verification area. This time coincides with ex-Hurricane Rita approaching the verification region. For this event, both ETKF-based OSEs demonstrate a lower forecast RMS error for Mean Sea Level Pressure (MSLP), 500hPa geopotential height (H500) and vector wind speed (W500). By contrast they are both inferior to the 500hPa temperature (T500) displaying a higher forecast RMS error than the OSE based on a 500hPa flow analysis. The top row of plots in Figure 1, show forecast MSLP and H500 verified against surface and radiosonde observations within the verification region for the OSE pair *ETKF(24)* vs. *upstream*. The bottom row of plots shows the same forecast fields obtained for OSE pair *ETKF(48)* vs. *upstream*.

OSE	Overall skill score
upstream	49.30
ETKF(24)	48.84
ETKF(48)	49.17

OSE	T+24 forecast RMS error verifying 25/09/05 12UTC			
	MSLP(hPa)	H500(hPa)	W500(m/s)	T500(K)
upstream	323.59	25.25	13.32	1.61
ETKF(24)	303.30	24.09	13.10	1.81
ETKF(48)	299.03	24.44	13.19	1.93

Table 1. Verification against surface observations: left: overall skill scores for each OSE; right: T+24 forecast RMS error for ex-Hurricane Rita at 12UTC on 25/09/05 verified against surface and radiosonde observations within the verification area.

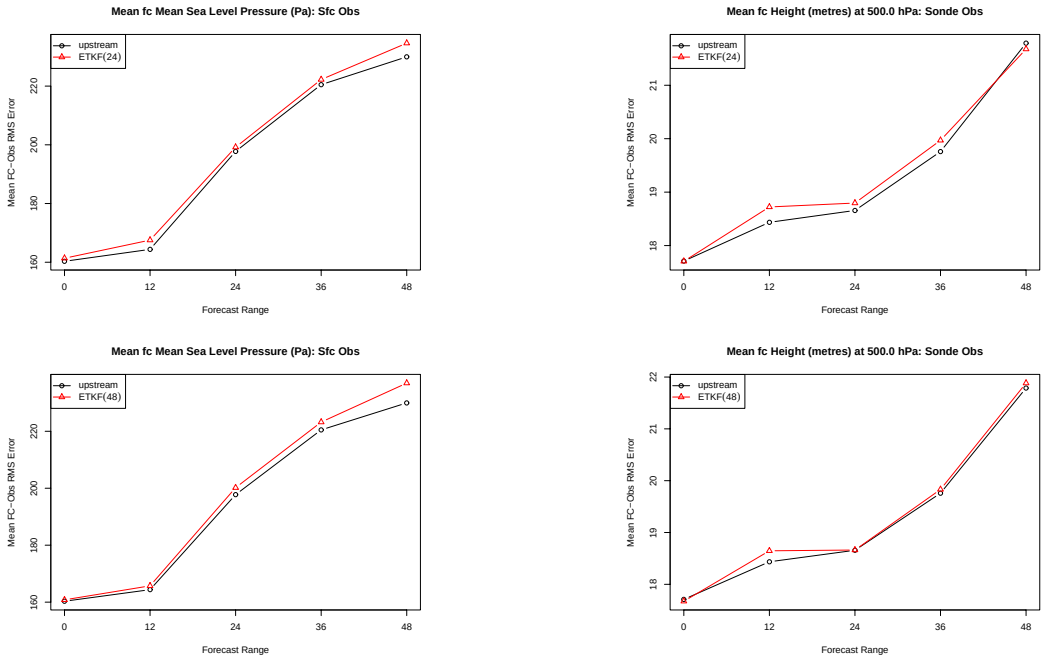

Figure 1. Plots of mean forecast – observation RMS error for: top left: MSLP verified against surface observations for OSEs *ETKF(24)* vs. *upstream*; top right: H500 verified against radiosonde observations for OSEs *ETKF(24)* vs. *upstream*; bottom left: MSLP verified against surface observations for OSEs *ETKF[48]* vs. *upstream*; bottom right: H500 verified against radiosonde observations for OSEs *ETKF(48)* vs. *upstream.*

From the top row of plots in Figure 1, OSE *upstream* clearly out-performs OSE *ETKF(24)* at all forecast ranges for forecast MSLP. This is also true for forecast H500 with the exception at T+48 (top right) in which *upstream* exhibits a greater RMS error at this time. Verification results from the ETKF OSE configured with the longer lead time, *ETKF(48)* is inferior to OSE *upstream* at all forecast ranges but identical for T+24 H500.

4. CONCLUSIONS

The superior performance of assimilating targeted observations using manual guidance is not unexpected as the 500hPa flow analysis is valid at targeting time with an effective zero-length lead time. Verification results presented for both ETKF configurations in the presence of ex-Rita, highlight the potential utility of the method. For these OSEs, the RMS error of key prognostic variables is reduced. Assimilation of targeted observations from ETKF utilising a longer lead time demonstrate improved overall skill scores compared with the shorter lead time. Research is continuing to evaluate the suitability of the ETKF for generating targeting guidance for use in Met Office NWP models.

Acknowledgements: Gareth Dow, Met Office observation monitoring kindly undertook the upstream 500hPa flow analysis.

REFERENCES

Bishop, C. H., B. J. Etherton, and S. Majumdar, 2001: Adaptive Sampling with the Ensemble Transform Kalman Filter, Part I: Theoretical Aspects. Monthly Weather Review. **129**(3) , 420-436.

PRE-EMPTIVE FORECASTS USING AN ENSEMBLE KALMAN FILTER

Brian J. Etherton

Department of Geography and Earth Sciences, University of North Carolina Charlotte, Charlotte, N.C., U.S.A.
E-Mail: *betherto@email.uncc.edu*

Abstract: An Ensemble Kalman Filter (EnKF) estimates the error statistics of a model forecast using ensembles. One use of an EnKF is data assimilation, creating an 'increment' to the first guess field at the observation time. Another use of an EnKF is to propagate error statistics of a model forecast forward in time, as has been done for targeted observations. Combining these two uses of an ensemble Kalman filter, a 'pre-emptive forecast' can be generated. In a pre-emptive forecast, the increment to the first guess field is, using ensembles, propagated to some future time, added to the future control forecast, resulting in a new forecast. This new forecast requires no more time to produce than the time needed to run a data assimilation scheme.

In an OSSE, a barotropic vorticity model was run to produce a 300-day 'nature-run'. The same model, run with a different vorticity forcing scheme, served as the forecast model. The model produced 24-hour and 48-hour forecasts for each of the 300 days. The model was initialized every 24 hours, by assimilating observations of the nature-run using a hybrid Ensemble Kalman Filter / 3D-Var data assimilation scheme. In addition to the control forecast, a 64-member forecast ensemble was generated for each of the 300 days, an EnKF approach was used to create 24-hour pre-emptive forecasts. The pre-emptive forecasts were more accurate than the unmodified, original 48-hour forecasts, though not quite as accurate as the 24-hour forecast. An important result is that the accuracy of the pre-emptive forecasts improved significantly when (a) the ensemble based error statistics used by the EnKF were localized using a Schur product and (b) a model error term was included in the background error covariance matrices.

Keywords – Localization, Schur Product, Kalman Smoother, Ensemble Kalman Filter, Model Error

1. INTRODUCTION

In data assimilation, an EnKF uses ensemble generated error statistics to produce an increment to the first guess field. In targeting, the ETKF (Bishop *et al*., 2001) uses ensemble generated error statistics to estimate the likely impact of observations on future error variance forecasts. Combining these two methodologies, the change to a future forecast resulting from current observations can be calculated using ensemble-based error statistics. In the same manor that adding in increment to the current forecast generates a new analysis, adding a propagated increment to a future forecast results in an updated, or 'pre-emptive' forecast. This technique is not dissimilar from the Kalman Smoother (Evensen and van Leeuwen, 2000), which also uses covariances at more than one time. Just like covariances in space allow observations to update model states that are far from the observation location in space, covariances in time allow observations to update model states that are far from the observation location in time.

The most compelling reason for producing a pre-emptive forecast is speed. Given that the ensemble of forecasts already exists, producing a pre-emptive forecast takes no longer than it takes to run a data assimilation scheme. This is far less time than it would take to run the data assimilation scheme and then integrate the forecast model out to the desired forecast verification time. Assuming that pre-emptive forecasts are of similar skill to the updated model forecasts, pre-emptive forecasts can provide additional time for weather related decision making.

2. METHODS

Five 24-hour model forecasts were made for each day's analysis. These five forecasts were generated from analyses produced by assimilating the 72 observations using one of five methods: (1) a hybrid Ensemble Kalman Filter with no covariance localization, (2) a hybrid Ensemble Kalman Filter *with* covariance localization, (3) a pure Ensemble Kalman Filter, with no covariance localization nor an additive model error term, (4) a pure Ensemble Kalman filter *with* covariance localization, but no additive model error term, and (5) a pure Ensemble Kalman filter with covariance localization and an explicit model error term. These five 24 hour forecasts were compared to the forecast made without assimilating any observations – a 48 hour forecast valid at the same time. These six model integrations are compared with three pre-emptive forecasts. The model used in this OSSE is the same as used in Etherton and Bishop (2004) and Bishop *et al.* (2001).

3. RESULTS

Results, shown in table 1, compare pre-emptive forecasts to forecasts made from analyses produced using an EnKF data assimilation scheme to forecasts made from analyses produced from a hybrid data assimilation scheme. The pre-emptive forecast made using equation (10), which includes localization of the ensemble based covariances and an explicit model error term, had lower average forecast errors (5.906×10^{-5} s^{-1}) than 48-hour forecasts generated from using the hybrid data assimilation scheme (8.718×10^{-5} s^{-1}). The pre-emptive forecast is an adjustment to the 48-hour forecast, rather than a new model integration, and so the forecast improvement resulting from the pre-emptive forecast does not require the model to be run.

In addition, to being better than the 48-hour integrations that they modified, these pre-emptive forecasts were nearly as accurate as the 24-hour forecasts generated from using the hybrid data assimilation scheme (5.906×10^{-5} s^{-1} versus 5.071×10^{-5} s^{-1}). This accuracy of pre-emptive forecasts was only the case when the error statistics were localized and model error was included. With no localization or model error term, the average errors were 9.136×10^{-5} s^{-1}, when localization was applied, 7.343×10^{-5} s^{-1}, and when localization and model error was used, 5.906×10^{-5} s^{-1}. Localization of the background error covariance matrix resulted in a 20% improvement; including model error in the background error covariance matrix produced an additional 20% improvement in forecast accuracy. Note that if neither model error nor covariance localization are included, the pre-emptive forecasts (9.136×10^{-5} s^{-1}) are worse than the 48-hour forecasts (8.718×10^{-5} s^{-1}), implying that the adjustment to the 48-hour forecast was on average a forecast degradation. The rank-deficient background error covariance matrix contains spurious error correlations, and these correlations lead to the forecast degradation if not minimized.

TABLE 1

	Pre-Emptive Forecast (Raw)	Pre-Emptive Forecast (Schur)	Pre-Emptive Forecast (Schur and Model Error)	48 Hour Forecast Hybrid EnKF IC (Raw)
Average Squared Vorticity Error (10^{-5} s^{-1})	9.136	7.343	5.906	8.718

Table 1 - Average daily domain average squared vorticity error for 300 forecasts. Error in units of (10^{-10} s^{-2})

4. CONCLUSIONS

While the 24-hour pre-emptive forecasts are not as accurate as forecasts made by assimilating the data, producing a new analysis, and integrating the forecast model out 24 hours, these results suggest the possibility that a pre-emptive forecast can have value to a forecaster. Pre-emptive forecasts were only 16% less accurate than the baseline 24-hour forecasts, whereas 48-hour forecasts were 59% less accurate. Thus, the pre-emptive forecasts are markedly better than using the 48-hour forecast, and are available sooner than a new 24-hour model integration based on the same set of observational data. Ensembles can be used for much more than providing confidence in official forecasts, and this work represents one way in which a probabilistic approach to data assimilation and forecasting can be leveraged.

5. REFERENCES

Bishop, C. H., B. J. Etherton, and S. J. Majumdar, 2001: Adaptive sampling with the ensemble transform Kalman filter. Part I: Theoretical aspects. *Mon. Wea. Rev.*, **129**, 420–436.

Etherton, B. J., and C. H. Bishop, 2004: Resilience of hybrid ensemble/3D-var analysis schemes to model error and ensemble covariance error. *Mon. Wea. Rev.*,**132**, 1065-1080.

Evensen, G., P.J. van Leeuwen, 2000: An Ensemble Kalman Smoother for nonlinear dynamics. *Mon. Wea. Rev.*, **128**, 1852-1867.

A NEW FLEXIBLE AND PARSIMONIOUS 3-D PHYSICAL-SPACE COVARIANCE MODEL FOR VARIATIONAL ASSIMILATION

M.D.Tsyrulnikov and P.I.Svirenko
Russian Hydrometeorological Center
E-mail: tsyrulnikov@mecom.ru

1 Introduction

The new covariance model is required to have the following properties.

1. The model should be as universal as possible. It is to be applicable to atmospheric, oceanic, and other environmental data assimilation problems on any scale (global, regional, and meso) and in any geometry (plane and spherical).
2. The model should be capable of representing spatially variable flow dependent structures.
3. The implementation of the model in a 3D of 4D-Var type data assimilation system should result in a computationally efficient numerical algorithm.

The 1st of the above requirements implies that the model is to be defined in physical space. To meet the 2nd requirement, the model should be, best, formulated *constructively*. This means that we have to formulate an explicit stochastic model for the underlying (forecast-error) random field, which guarantees that any change in parameters of the stochastic model (e.g. when introducing spatial variability) will result in a valid covariance model.

To obtain computational efficiency (the 3rd requirement) for a physical-space based and constructively defined covariance model, we propose to generalize the well-known in the time series theory (one-dimensional) ARMA (auto-regression and moving average) model to the multi-dimensional (3 or 4-D) case. ARMA models proved to be very efficient in modelling realistic random processes, so that in most situations, the *orders* of both AR and MA digital filters appeared to be very small. Small orders imply small supports of the impulse response functions for the respective filters, hence, both AR and MA operators can be represented by very sparse matrices. If we are able to retain this feature in 3D, we will obtain a fast numerical algorithm for variational assimilation.

2 The basic model

In the most general terms, the proposed spatial ARMA (SARMA) model can be written as

$$S\xi = V\alpha, \tag{1}$$

where ξ is the background-error field, α the driving white noise, S the spatial auto-regression (SAR) filter, and V the spatial moving-average (SMA) filter. Each of the two operators is defined by using discretized integral or differential operators (see below), giving rise to a *sparse* (and thus computationally efficient) matrix formulation.

More specifically, we formulate the spatially continuous univariate 3-D model as

$$\left(\frac{\partial}{\partial\tilde{z}} + T\right)^q \xi = U\alpha, \tag{2}$$

where $\tilde{z}$ is the vertical coordinate, q is an integer, which determines the order of the auto-regression in the vertical, and T and U are horizontal operators.

We define T and U using polynomial or rational approximation, in minus horizontal Laplacian, Δ, in the following way:

$$T = P_T(-\Delta) \qquad \text{and} \qquad U = \frac{P_U(-\Delta)}{Q_U(-\Delta)}, \tag{3}$$

where P_T, P_U, and Q_U are low-order polynomials.

Another way to define U is to use an integral operator:

$$(U \cdot \alpha)(x) = \int u(\rho(x,y))\alpha(y)dy, \tag{4}$$

where x and y are points in the horizontal domain, ρ is the distance between x and y, and $u(\rho)$ is the function that has *small* support. Which of the two above definitions of U (differential or integral) is more suitable depends on the situation.

Note that the definition Eqs.(2)–(4) is based on *operators* and thus is essentially coordinate-free, hence the applicability of the SARMA model on any domain in any geometry. The model produces fully non-separable 3-D correlations.

Spatial variability is easily introduced into model Eq.(2) by specifying spatially variable operators T and U. Other features can be represented with this model, e.g. adding, to T, the term $\mathbf{c}\nabla$ (where $\mathbf{c}$ is a horizontal vector and ∇ the horizontal gradient operator) can describe tilted structures etc. We reiterate that any spatial (in particular, flow-dependent) variability introduced to model Eq.(2) cannot, by construction, violate positive definiteness of the resulting covariance structure.

3 Implementation and first results

The horizontal operators of the above SARMA model are estimated from correlation functions using a spectral approach. 2-D empirical correlations are taken from DWD (Anlauf et al. 2005). In 3D, the covariance model utilizes the 'proportionality of scales' property discussed in (Tsyroulnikov 2001).

A univariate model-space 3D-Var analysis scheme is developed. A sparse linear algebra package is used to solve the analysis equations. The covariance-model set-up is selected as follows: the horizontal resolution is about 100 km, the vertical resolution is 30 levels, the vertical order is $q = 1$, U is defined as the discretized integral operator, Eq.(4), and the order of the P_T polynomial is selected as small as 2. This set-up allows us to reasonably well approximate geopotential correlations. The global analysis takes several minutes on a single Itanium processor. The scheme is tested using generators of pseudo-random fields with the pre-specified SARMA covariance structure.

This study has been supported by the Russian Foundation for Basic Research under grants 04-05-64481, 06-05-08076, and 04-07-90183-v.

REFERENCES

Anlauf H., Wergen W. and Paul G. A study of the flow-dependence of background error covariances based on the NMC method. – Res. Act. Atm. Ocean. Modelling, WMO, 2005, Rep. N 35, pp. 1.1–1.2.

Tsyroulnikov M.D. Proportionality of scales: An isotropy-like property of geophysical fields. – *Q. J. R. Meteorol. Soc.*, 2001,**127**, 2741–2760.

ADJOINT-BASED FORECAST SENSITIVITIES OF TYPHOON RUSA

Hyun Mee Kim[1] and Byoung-Joo Joung[1]

[1] Department of Atmospheric Sciences, Yonsei University, Seoul, Republic of Korea
E-mail: *khm@yonsei.ac.kr*

Abstract: Sensitivities of the forecast to changes in the initial state are evaluated for Typhoon Rusa, which passed through the Korean Peninsula in 2002, to understand the impact of initial condition uncertainties on the forecast and thence to diagnose the sensitive regions for adaptive observations. To assess the forecast sensitivities, adjoint-based sensitivities were used. Sensitive regions are located horizontally in the right half circle of the typhoon, and vertically in the lower and upper troposphere which coincide with the inflow and outflow regions near the typhoon. Forecast error is reduced around 18 % by extracting properly weighted adjoint-based forecast sensitivity perturbations from the initial state, and the correction occurs primarily in the lower to mid-troposphere where the forecast error is the largest. In contrast to the improvement in the overall forecast, the track and intensity forecast are not improved much through the modification of the initial condition by adjoint-based forecast sensitivities.

Keywords – *Typhoon Rusa, Adjoint-based sensitivities, Adaptive observations, Forecast error*

1. INTRODUCTION

Typhoon Rusa landed on the Korean peninsula on 31 August 2002, causing a record-breaking daily rainfall amount of 870.5 mm over the eastern coast of the Korean peninsula. Because of the abnormal precipitation along the typhoon track as it passed through the Korean peninsula (Figure 1), Typhoon Rusa caused many casualties and extensive property damage.

To assess the impact of initial condition uncertainties on the forecast of this event and to detect "sensitive" regions for adaptive (or targeted) observations, adjoint–based forecast sensitivities were applied. Adjoint sensitivity represents the gradient of some forecast aspect with respect to the control variables of the model (i.e., initial conditions, boundary conditions, and parameters) (Errico, 1997) as well as to the observations (Baker and Daley, 2000). Since adjoint sensitivity indicates the sensitivity of specific forecast aspects with respect to the model variables or observations at the initial time, it has been used in adaptive observations (e.g., Bergot, 1999). The goal of adaptive observations is to decrease the forecast error by placing observations in sensitive regions where they might have the most impact. These regions may be considered "sensitive" in the sense that changes to the initial condition in these regions are expected to have a larger effect on a particular measure of forecast skill than changes in other regions.

In this study, adjoint-based forecast sensitivities are used to understand the sensitivity of forecast error with respect to the initial conditions for Typhoon Rusa, and thence to determine the sensitive regions in terms of adaptive observations.

2. EXPERIMENTAL FRAMEWORK

This study uses the Fifth-Generation Pennsylvania State University/National Center for Atmospheric Research (PSU/NCAR) Mesoscale Model (MM5), together with the MM5 adjoint modeling system (Zou et al., 1997), to calculate adjoint sensitivities. The model domain for this study is 100 x 100 horizontal grids (centered at 36˚ N in latitude and 123˚ E in longitude), with a 45 km horizontal resolution and 20 evenly spaced sigma levels in the vertical from the surface to 50 hPa. The model's initial and laternal boundary condition is the National Centers for Environmental Prediction (NCEP) Reanalysis 2 (2.5^o x 2.5^o global grid). The Optimum Interpolation Sea Surface Temperature (OISST) version 2 (Reynolds et al., 2002), produced by the National Oceanic and Atmospheric Administration (NOAA), is used for the lower boundary condition over the ocean. For a more realistic simulation, the Geophysical Fluid Dynamics Laboratory (GFDL) bogussing algorithm (Kwon et al., 2002) is used. Physical parameterizations used in the simulation include the Grell convective scheme, a bulk aerodynamic formulation of the planetary boundary layer, horizontal and vertical diffusion, and dry convective adjustment. Simulations of 36 hours in length, from 1200 UTC 30 August to 0000 UTC 1 September 2002, were performed.

3. SUMMARY

In this study, the adjoint sensitivity of the forecast error to the initial state is evaluated for Typhoon Rusa. Horizontally sensitive regions denoted by the adjoint sensitivities are located mostly in the right half circle of the

typhoon (Figure 2a). Unlike large adjoint sensitivities in the lower troposphere in the case of extratropical cyclones (e.g., Kleist and Morgan, 2005), the sensitive regions of Typhoon Rusa vertically reside in the lower and upper troposphere. While the sensitive regions in the lower troposphere coincide with the inflow regions, those in the upper troposphere are associated with the inflow and outflow regions depending on the horizontal locations of the adjoint sensitivities near the Typhoon. Overall forecast error is reduced around 18 % by extracting properly weighted adjoint-based forecast sensitivity perturbations from the initial state. This correction occurs primarily in the lower to mid-troposphere, where the forecast error is the largest. In contrast, the track and intensity forecast are not improved much by the above adjoint sensitivity-based iterative procedures. The remaining 82 % error might be improved by using better model configurations (i.e., fine resolution, more physics, etc.) and by assimilating adaptive observation data with a more comprehensive data assimilation system. Based on the forecast error reduction by the adjoint sensitivities, we may infer that the adjoint-based forecast sensitivities can serve as an adaptive observing guidance for typhoon forecasts.

Acknowledgements: *This study was supported by the principal project of METRI "Korea Enhanced Observing Period, KEOP" and the Korea Meteorological Administration Research and Development Program under Grant CATER 2006-2102.*

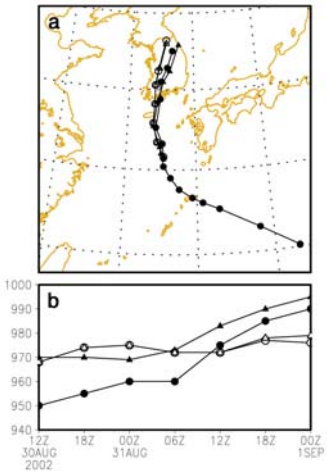

Figure 1. (a) Typhoon tracks and (b) mean sea level pressure at typhoon center from 1200 UTC 30 August to 0000 UTC 1 September: observed (●), simulated (○), modified by adjoint sensitivity-based iterative procedures (▵), and KMA GDAPS analysis (▲). The observed track is from 0000 UTC 28 August to 0000 UTC 1 September.

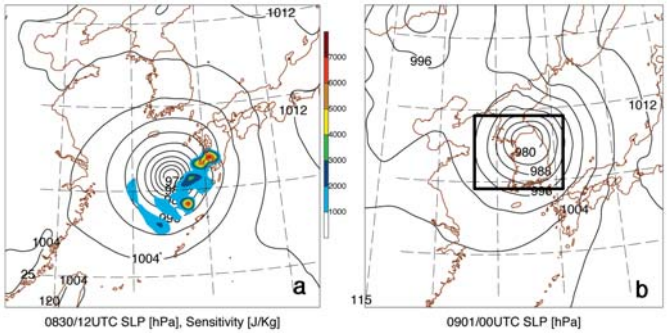

Figure 2. (a) Vertically integrated energy-weighted adjoint sensitivity distributions (JKg^{-1}, shaded) and mean sea level pressure (solid) at 0h (1200 UTC 30 August). (b) Mean sea level pressure of the simulated typhoon at the final time (solid) at 36h (0000 UTC 1 September 2002). The box denotes a geographic region for defining a response function at 36h.

REFERENCES

Baker, N. L., and R. Daley, 2000: Observation and background sensitivity in the adaptive observation-targeting problem, Q. J. R. Meteorol. Soc., 126, 1431-1454.

Bergot, T., 1999: Adaptive observations during FASTEX: A systematic survey of upstream flights, Q. J. R. Meteorol. Soc., 125, 3271-3298.

Errico, R. M., 1997: What is an adjoint model ?, Bull. Amer. Meteor. Soc., 78, 2577-2591.

Kleist, D. T. and M. C. Morgan, 2005: Application of adjoint-derived forecast sensitivities to the 24-25 January 2000 U.S. East Coast snowstorm, Mon. Wea. Rev., 133, 3148-3175.

Kwon, H. J., S.-H. Won, M.-H. Ahn, A.-S. Suh, and H.-S. Chung. 2002: GFDL-type typhoon initialization in MM5, Mon. Wea. Rev., 130, 2966-2974.

Reynolds, R. W., N. A. Rayner, T. M. Smith, D. C. Stokes and W. Wang, 2002: An improved in situ and satellite SST analysis for climate, J. Clim., 15, 1609-1625.

Zou, X., F. Vandenberghe, M. Pondeca, and Y.-H. Kuo, 1997: Introduction to adjoint techniques and the MM5 adjoint modeling system, NCAR Tech. Note NCAR/TN- 435STR, 110 pp.

A COMBINED USE OF METEOSAT WATER VAPOUR IMAGERY AND POTENTIAL VORTICITY INVERSION TO IMPROVE THE NUMERICAL PREDICTION OF THE ALGIERS 2001 SUPERSTORM

S. Argence[1], D. Lambert[1], E. Richard[1], N. Söhne[1], J.-P. Chaboureau[1] and P. Arbogast[2]

[1] Laboratoire d'Aérologie, UMR CNRS/UPS 5560, Toulouse, France
[2] DPrévi/Labo, Météo France, Toulouse, France
E-mail: *sebastien.argence@aero.obs-mip.fr*

Abstract: From 9 to 11 November 2001, an intense cyclone affected North African coasts, causing more than 700 casualties in Algiers and catastrophic damage. In a previous study, it was shown that intensity and distribution of rainfall were highly related to sub-structures of a potential vorticity (PV) anomaly which crossed Western Mediterranean during the event. The present work focus on assessment of initial conditions provided to the numerical model Meso-NH through comparison between PV analysis and METEOSAT water vapour (WV) imagery. It is demonstrated that modifications of the initial PV analysis according to WV observation lead to a substantial improvement of both precipitation and synthetic satellite radiance forecast.

1. INTRODUCTION

In spite of recent improvement in operational forecasting, numerical weather predictions regularly failed to reproduce intensity and distribution of precipitation of heavy rainstorms at the mesoscale. Generally, forecast errors arise from imperfect parameterizations of the numerical model used or errors in the representation of the initial state of the atmosphere. In order to overcome initial conditions problems, several methods have been developed. This study proposes to make use of the close relationship linking METEOSAT WV imagery and PV positive anomalies which allows one to detect significant upper-level dynamical structures associated with synoptic developments. This method which consists in assessing and correcting initial conditions (by PV modifications) provided to numerical models has been successfully used for improvement of extratropical cyclone prediction in some case-studies (Hello and Arbogast 2004; Guerin et al. 2006). The Algiers 2001 superstorm is investigated using this approach coupled with high resolution numerical simulations performed with the French non-hydrostatic Meso-NH model. A brief description of the case-study and PV-correction method is presented in section 2. Section 3 gives an example of analysis modification based on PV-WV comparison. Some conclusions are drawn in section 4.

2. CASE-STUDY AND EXPERIMENTAL DESIGN

The synoptic situation associated with the Algiers 2001 rainstorm is characterized by the presence of an upper-level trough associated with an intense PV anomaly inducing cold air advection over North Africa. In low-levels, a cyclone centred over Algeria leads to warm and moist advection on North Algerian coasts. Large-scale environment promoted convection over Algeria and Morocco and resulted in more than 100 mm of rainfall in many coastal areas with a maximum of about 260 mm on Algiers between 9 and 12 November 2001.

Simulations presented in this study have been performed with the French non-hydrostatic mesoscale model Meso-NH (Lafore et al. 1998) used with three one-way nested domains of 50, 10 and 2 km grid spacing. Preliminary results, based on a 9-members ensemble forecast, highlighted the crucial role played by the upper-level PV anomaly on the distribution and intensity of heavy rainfall which struck North African coasts on 10 November 2001 morning. It was shown that the precipitation pattern was highly related to the low-level cyclone development, itself closely linked to the upper-level trough. Moreover, any of the ensemble members was able to reproduce heavy rainfall of about 130 mm which was recorded at Algiers the 10 November between 6 and 12UTC.

As the precipitation forecast exhibited sensitivity to the upper-level dynamical structures and didn't reproduce large amount of precipitation over Algiers, it was decided to use a correction method of the initial state provided to Meso-NH. Assuming the model perfect, the technique is based on comparison between some derived-PV fields, METEOSAT WV imagery and pseudo WV (PWV) images derived from a radiative transfer code (see Saunders and Brunel 2005 for more information) coupled with the model. In case of mismatch between observations and model analysis, upper-level dynamics may be corrected by local PV modifications (see Chaigne and Arbogast 2000 for more details about the PV inversion tool used) so that PV analysis fits well the WV image.

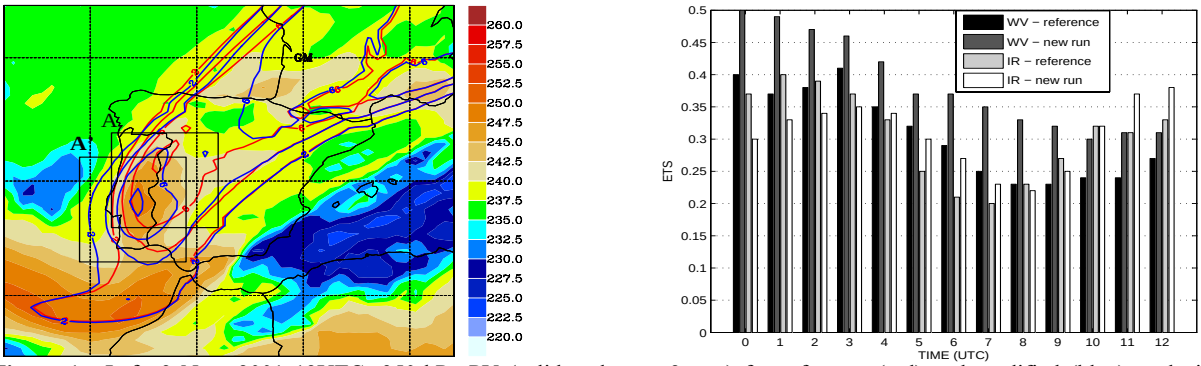

Figure 1. Left: 9 Nov. 2001 12UTC: 350-hPa PV (solid, values > 2 pvu) for reference (red) and modified (blue) analysis superimposed on Meteosat WV BT (colours, K). The positive PV anomaly located in A was moved to A'. Right: 10 Nov. 2001: time evolution of the mean equitable threat score (ETS) computed between observed Meteosat simulated BT (10 km grid).

3. MAIN RESULTS

Operational ARPEGE analysis of 9 November 2001 12UTC was chosen as reference initial state for PV-WV-PWV comparison. Quality of initial conditions was assessed by superimposing PV-fields derived from the analysis on METEOSAT WV brightness temperatures (BT). It revealed a PV maximum shifted to the northeast in respect to WV dark spot (area of high BT). Synthetic BT derived from the analysis showed a good correspondence with those of METEOSAT with a slight northward shift of the main dark spot. Therefore, it was decided to reposition the analysed PV maximum over the observed dark spot (figure 1a). A PV inversion tool was used to make local PV modifications so that the analysis fits better with WV observations. Another Meso-NH run was started from there.

The study focus on the impact of such modifications on the precipitation forecast at 10km-resolution. It is shown that the cyclone trajectory has been modified, resulting in more realistic rainfall over North Morocco and a precipitation pattern closer to the coasts offshore Algiers. Quantitative results based on simulated BT confirmed these results, new run have better scores especially over the critical period of 10 November 2001 morning (figure 1b). Thresholds used for categorical scores were chosen so as to characterize the stratospheric intrusion (WV channel) and high clouds (infrared channel). Thus, it can be concluded that modifications introduced in the initial state lead to a better simulation of convective cloud areas and stratospheric intrusion during 10 November morning.

The same conclusions arise when this correction method is applied to the analysis of 10 November 2001 00UTC. Simulated BT are also better at 10km-resolution and the 2km-forecast starting from modified initial state simulates an heavy rain core of about 120 mm over Algiers the 10 November between 6 and 12UTC (almost as observed).

4. CONCLUSION

Experiments conducted in this work revealed that precipitation pattern, at synoptic- and meso- scale, was strongly related to the upper-level PV anomaly through its interaction with the low-levels cyclone. As any of the simulation performed was able to reproduce intense rainfall over Algiers, it was decided to focus our attention on the initial state provided to Meso-NH using the link existing between METEOSAT WV imagery and positive PV anomalies. Therefore, starting from the ARPEGE analysis of 9 November 2001 12 UTC, a new initial state was built by making PV corrections and served as initial conditions for new Meso-NH run. Qualitative and quantitative evaluations, based on precipitation forecast and model to satellite approach, showed a good improvement of results, mainly due to a better cyclone trajectory prediction. The use of WV imagery to validate initial conditions provided to numerical weather prediction models has proven its utility in this particular case-study. This work also deals with short-term ensemble forecast at the mesoscale. The ability of each method is currently studied in order to determine which one is the more skilful for heavy rainfall prediction in the Mediterranean basin.

REFERENCES

Chaigne, E., and P. Arbogast, 2000: Multiple potential vorticity inversion in two FASTEX cyclones. Quarterly Journal of the Royal Meteorological Society, **126**, 1711-1734.

Guerin, G., G. Desroziers, and P. Arbogast, 2006: 4D-Var analysis of potential vorticity pseudo-observations. Quarterly Journal of the Royal Meteorological Society, **132**, 1283-1298.

Hello, G., and P. Arbogast, 2004: Two different methods to correct the initial conditions applied to the storm of 27 December 1999 over Southern France. Meteorology and Applications, **11**, 41-57.

Lafore, J.-P. et al., 1998: The Meso-NH atmospheric simulation system. Part I: adiabatic formulation and control simulations. Journal of the Atmospheric Sciences, **32**, 320–330.

Saunders, R., and P. Brunel, 2005: RTTOV_8_7 Users Guide, NWP-SAF-MO-UD-008, Version 1.9, EUMETSAT.

THE NEW VERY SHORT RANGE FORECAST MODEL LM-K FOR THE CONVECTION-RESOLVING SCALE

M. Baldauf, K. Stephan, S. Klink, C. Schraff, A. Seifert, J. Förstner, T. Reinhardt, C.-J. Lenz

Deutscher Wetterdienst, Offenbach, Germany
E-mail: Michael.Baldauf@dwd.de

Keywords: Lokal-Modell-Kürzestfrist, convection-resolving modelling

1. INTRODUCTION

The project 'LM-K' ('LM-Kürzestfrist') was established at the Deutscher Wetterdienst (DWD) in the mid of 2003 within the scope of the 'Aktionsprogramm 2003'. The goal of this project is to develop a numeric weather prediction system for the very short forecast range (up to 18 h) and with a resolution on the meso-gamma scale (about 2.8 km). The emphasis of this development lies in the prediction of severe weather events related on the one hand to deep moist convection leading e.g. to super- and multi-cell thunderstorms or squall lines and on the other hand to interactions with fine scale topography which can induce e.g. severe downslope winds or Föhn-storms.
The currently used LM-K-configuration covers the domain of Germany, smaller parts of its neighbouring countries and also a bigger part of the Alpine region with $421 \times 461 \times 50$ gridpoints and a horizontal resolution of 2.8 km. (see figure 1).

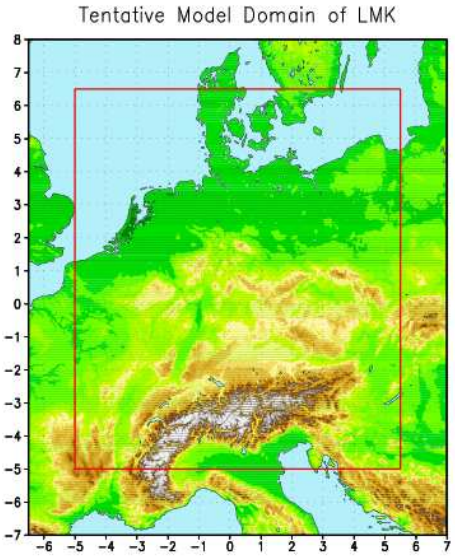

Figure 1. The LM-K model domain (red rectangle)

The developments take place in four subprojects:

1. Supply of quality controlled radar-precipitation data.
2. The installation of an assimilation method for radar reflectivity using latent heat nudging to provide highly resolved initial fields, especially for the initiation of convection.
3. The advancement of the numerical model based on the currently used LM.
4. Finally the accompanying verification and the advancement of verification methods for horizontal model resolutions of about 2.8 km.

2. LATENT HEAT NUDGING

A meso-γ-model has special requirements concerning data assimilation: at this scale highly resolved, rapidly updated data fields are needed, which can in principle be delivered by radar observations. The German radar network has a spatial resolution of radially 1 km and laterally 1° and a temporal resolution of 5 min. for the precipitation scan. The assimilation method should be fast and also relatively easy to implement. The latent heat nudging (LHN) approach fulfills these requirements. It uses the differences between (radar) measured and simulated precipitation rates and interpretes them as a lack or surplus of latent heat along the trajectory of a condensed particle. One basic assumption of the LHN is that this relation is valid in a vertical model column. This basic assumption stands in contradiction to the use of a prognostic precipitation scheme which drifts rain and snow by several grid lengts over several time steps. This leads to some sort of feedback problem, which can

be solved partially by using an undelayed reference precipitation step additionally to the prognostic precipitation step. Another improvement can be obtained by using latent heating increments only in the growth stage of a convective cell. These measurements led to a more realistic assimilation of the precipitation pattern of convective events [Schraff et al., 2006].

3. NUMERICAL MODEL DEVELOPMENT

The dynamical formulation of the LM-K bases on the Lokal Modell (LM) of the German weather service (DWD) [Doms, Schättler, 2002]: it is a non-hydrostatic, fully compressible model in advection form. But there are some differences in the numerical formulation. LM-K now uses a two-timelevel integration scheme based on the Runge-Kutta-method of 3. order for the prediction of the 3 cartesian wind components u, v, w, the pressure perturbation p' from a hydrostatic base state, and the temperature perturbation T'. This allows the use of an upwind advection scheme of 5. order in the horizontal with Courant-numbers up to 1.4. [Förstner, Doms, 2004]. For the 6 humidity variables (mass fractions of moisture, cloud and rain water, cloud ice, snow and graupel) several Courant-number-independent Euler- and Semi-Lagrange-schemes can be used. Idealised tests of this new dynamical core with linear mountain flow and nonlinear density current simulations performed very well.
One of the most farreaching changes from LM is that LM-K will not longer use a deep convection parameterisation. Instead of this, LM-K resolves the bigger parts of convection. For the smaller scales of convection the sligthly modified shallow convection scheme of the Tiedtke Cumulus parameterization scheme is used. This parameterization especially delivers the transport of moisture from the boundary layer to a height of about 3 km and therefore avoids the overestimation of low cloud coverage. Without a deep convection parameterization the need for a faster sedimenting ice phase seems to be necessary. Therefore the former 5-class microphysics scheme was extended by a new precipitation class 'graupel'. This new scheme was tested with the IMPROVE-2 data set and one day of the BAMEX field campeign. In the latter test case, the ability of the LM to resolve deep convection could also be shown. Further improvements of the physics packages are the introduction of 3-dimensional turbulence with full metrics [Baldauf, 2006] and a new 7-level soil model. For the problem of underestimation of precipitation in convective situations, the resolution of 2.8 km is not responsible, as could be shown by comparisons with 1km runs. Instead this problem could be cured by reducing the evaporation of rain below the cloud bottom and by making changes in the boundary layer parameterisation of subgrid scale clouds.

4. OUTLOOK

A pre-operational test phase for LM-K has been started in August 2006. Finally the operational usage is planned for spring 2007.

References

Baldauf, M (2006): Implementation of the 3D-Turbulence Metric Terms in LMK, *COSMO-Newsletter*, 6:44–50.

Doms, G. and U. Schättler (2002): A Description of the Nonhydrostatic Regional Model LM, *Deutscher Wetterdienst*, Nov. 2002.

Förstner, J. and G. Doms. (2004): Runge-Kutta Time Integration and High-Order Spatial Discretization of Advection - a new Dynamical Core for the LMK. *COSMO Newsletter*, 4:168–176.

Schraff, C., K. Stephan, and S. Klink (2006): Revised Latent Heat Nudging to cope with Prognostic Precipitation. *COSMO-Newsletter*, 6:31–37, 2006.

THE DYNAMICS AND PREDICTION OF WEATHER REGIME TRANSITIONS USING STATISTICAL LEARNING AND BRED VECTORS

B. Deremble[1], D. Kondrashov[2], A. Deloncle[3], J. Shen[4], F. D'Andrea[1], R. Berk[4], and M. Ghil[1,2]

[1]Laboratoire de Météorologie Dynamique (CNRS and IPSL), ENS, Paris, France
[2]Department of Atmospheric and Oceanic Sciences, University of California, Los Angeles, USA
[3]LadHyX (CNRS), Ecole Polytechnique, Palaiseau, France
[4]Department of Statistics, University of California, Los Angeles, USA
E-mail: *deremble@lmd.ens.fr*

Abstract: We study weather regimes in an intermediate-complexity model and compare the results of statistical prediction methods with those of a dynamical method based on bred vectors.

Keywords – *dynamical systems, long-range forecasting, low-frequency variability*

1. INTRODUCTION

One view to better understand the evolution of the atmosphere is to see it as a dynamical system governed by a simplified version of the nonlinear Navier-Stokes equations. Lorenz (1963, 1969) has shown such a system to be chaotic and hence unpredictable in detail beyond a few days. Legras & Ghil (1985), however, highlighted the existence of low-frequency atmospheric variability that is characterized by the existence of large-scale, persistent and recurrent flow patterns called *weather regimes*. Kondrashov *et al*. (2004) tried to characterise these regimes, observed in the mid-latitude atmosphere, using the quasi-geostrophic, three-level (QG3) model of Marshall & Molteni (1993). They also highlighted preferential transition paths between the regimes. On the basis of these, Deloncle *et al*. (2006) showed significant skill for two statistical methods to predict the transitions: *k* nearest-neighbours and random forests. To understand the transition mechanism, we first calculated the Bred Vectors (BVs; Toth & Kalnay, 1993, 1997) each day of model integration. Making use of the information contained in these BVs, we could build a simple forecasting model. Finally, we calculated the energy flux in the model atmosphere before and during the transition, in order to explain the physics underlying the transitions, as well as the maintenance of the regimes.

2. THE QG3 MODEL AND THE WEATHER REGIMES

The current study has been carried out using QG3 model simulations. The model is governed by the QG potential vorticity equation on the sphere. We proceed to a Principal Component Analysis (PCA) of a long time series of the stream function at 500 hPa over the Northern Hemisphere. In the phase space of the three leading EOFs, Kondrashov *et al*. (2004) found four distinct zones in which the density of points were high. These clusters of points are also called *weather regimes*. The four regimes are the positive and negative phases of the North Atlantic Oscillation, NAO^+ and NAO^-, and of the Arctic Oscillation, AO^+ and AO^-; see Fig. 1 for details. They also showed the existence of preferential transitions between these regimes.

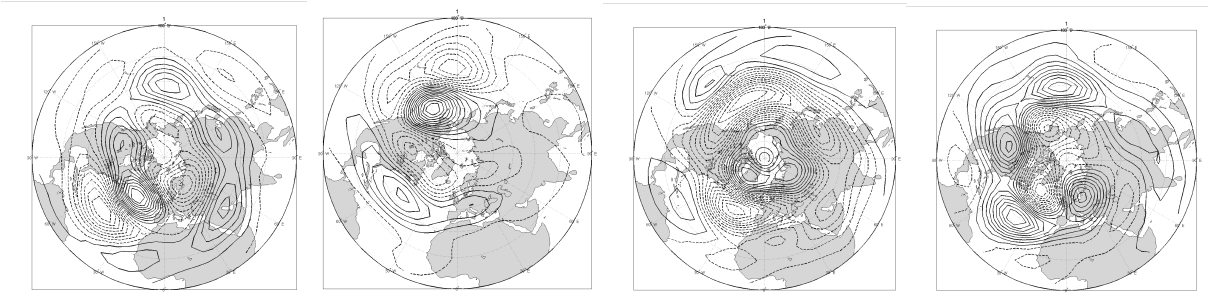

(a) (b) (c) (d)

Figure 1. Stream function anomaly maps at 500 hPa: (a) NAO^-, (b) NAO^+, (c) AO^-, and (d) AO^+ cluster. The contour interval is 8.10^5 m^2 s^{-1} in panels (a,d) and 10^6 m^2 s^{-1} in panels (b,c); negative contours are dashed.

3. PREDICTION USING STATISTICAL LEARNING

Deloncle *et al.* (2006) studied statistical methods to forecast a particularly significant transition, $NAO^- \square NAO^+$. The idea is to look at the position and the velocity in phase space of the points that leave the cluster NAO^- on the following day, and reach NAO^+ as the next cluster some time thereafter. Using these predictors, one classifies all the points of the simulation that do so as *events*, while those that stay in NAO^- or leave, but reach another cluster next, as *non-events*. The actual transitions are compared with three different ways of predicting them in Table 1. Two of these ways are the statistical methods of Deloncle *et al.* (2006); the third one is based on the BVs.

		Forecast		
		No transition	Transition	Model Error (Error/Total)
Observed	No transition	88.1 ‖ **74.4** ‖ *56.5*	1.1 ‖ **15.4** ‖ *15.2*	1.2 ‖ **17.2** ‖ *21.2*
	Transition	7.5 ‖ **1.9** ‖ *12.8*	3.3 ‖ **8.3** ‖ *15.5*	69.4 ‖ **18.3** ‖ *45.2*
	User Error (Error/Total)	7.8 ‖ **2.4** ‖ *18.5*	25 ‖ **64.9** ‖ *49.5*	

Table 1. Results of all three forecast algorithms: contingency table for the transition $NAO^- \square$ NAO+. The observations are in the rows and the forecasts in the columns; the numbers are the percentages of success in each case. The first value is for a k nearest-neighbour method, $k = 9$; the bold value is for the random forests; and the italic for the BV algorithm.

4. THE BREEDING METHOD

The breeding method (Toth & Kalnay, 1993, 1997) consists in making two model integrations: first an unperturbed integration, the control run; in the other run, we let a perturbation grow over a fixed time interval, $\Delta t = n$ time steps, which we rescale before letting it grow again over the next Δt, and so on. For appropriate choices of Δt and rescaling factor, this perturbation yields a set of BVs. The ratio of the norm of the perturbation between two rescaling is called the *growth rate*. We observe that the leading BV, before a transition, points, on average, in the preferred direction of transition, thus providing prior information on a possible transition. We choose therefore, as a predictor, the scalar product between the leading BV and the vector that connects the centres of the two clusters, and set an alarm threshold for the value of this scalar product.

The results for this dynamic forecast method are also shown in Table 1. These results are compared to a random-choice forecast using the Heidke Skill Score (HSS), H. We thus obtain $H = 0.40$, $H = \mathbf{0.41}$ and $H = 0.33$ for the three experiments, respectively.

5. CONCLUSION

Knowing certain characteristics of atmospheric low-frequency variability in the Northern Hemisphere, we implemented three methods, two statistical and one dynamic, in order to study the transitions between various regimes. Both the random-forest and the BV method do show significant skill, but the level of false alarms and misses remains high. This is due, to a large extent, to the fact that the number of transitions remains small. An additional, dynamic approach would be to study the energetics of the transitions. We are currently investigating this behaviour in the QG3 model, and thus try to understand if the preferential instabilities that lead to the transitions are predominantly baroclinic or barotropic.

REFERENCES

Deloncle, A., R. Berk, F. D'Andrea, and M. Ghil, 2006: Weather regime prediction using statistical learning, *J. Atmos. Sci.*, accepted.

Kondrashov, D., K. Ide and M. Ghil, 2004: Weather regimes and preferred transition paths in a three-level quasi-geostrophic model, *J. Atmos. Sci.*, **61,** 568–587.

Toth, Z., E. Kalnay 1993: Ensemble forecasting at NMC: The generation of perturbations. *Bull. Amer. Meteorol. Soc.*, **74**, 2317–2230.

EVALUATION OF OPERATIONAL FORECASTS FOR AMMA

M. NURET[1], O. BOCK[2], F. FAVOT[1], M-N BOUIN[3], E. DOERFLINGER[4] and J.P LAFORE[1]

[1]METEO-FRANCE, CNRM, 42 avenue G. Coriolis, F-31057 Toulouse, France
[2]IPSL/Service d'Aéronomie – Paris, [3]LAREG/IGN - Marne-la-Vallée and [4]LDL - Montpellier
E-mail: *mathieu.nuret@meteo.fr*

Abstract: The AMMA (African Monsoon Multidisciplinary Analysis) is an international project to improve our understanding of the West African Monsoon (WAM) and its variability. A wide range of numerical weather prediction models have been run in an operational mode to provide guidance for the Special Observing Period (SOP) of the AMMA 2006 campaign held in Western Africa this summer (mid May to end September 2006). The contribution of METEO-FRANCE was to provide support at large scale with ARPEGE and ARPEGE-Tropiques (resolution ~50km) and also at meso-scale with ALADIN-AMMA (10km resolution). A very first evaluation of the quality of the forecasts is given here.

Keywords – *THORPEX, WMO, Data assimilation, African monsoon, GPS*

1. INTRODUCTION

The field program of AMMA is organized in three embedded periods: LOP (Long Observing Period)(2001-2010), EOP (Enhanced Observing Period)(2005-2007), SOP (Special Observing Period)(2006).

The aims of the AMMA 2006 Special Observing Period (SOP) was to document the main phases of the West African monsoon cycle which is characterized by:

- an onset stage leading to the northward monsoon jump (end of June)
- a well developed monsoon stage (peak of the rainy season over the Sahel, and little dry season on the coast) from the beginning of July to mid-September
- a period most favourable for the tropical cyclogenesis over the Atlantic Ocean lasting from mid-August to mid-October

In order to achieve these scientific objectives a synergy of observations has been deployed during the 4 months involving up to five research aircrafts (F/ATR-42, F/F-20, D/F-20, UK/Bae146, EEIG/Geophysica), research vessels, various ground and space borne measurements.

To plan the Intensive Observation Periods (IOP) and decision making within the SOP an AMMA Operational Centre (AOC) was set up in Niamey (Niger) with forecasting capabilities, involving African trained forecasters working on shift hours.

2. OPERATIONAL CONSIDERATION

Several models output and real-time AMMA data (such as radar Doppler displays, radio sounding, dropsondes, flights tracks …) were provided to the forecasters of the AOC and made available through a web site (http://www.amma-international.org) in Niamey (Niger) mirrored and updated from Toulouse (France).

The model available were:

- global models: NCEP GFS and NCEP GDAS, ECMWF, UK global (UKMO), ARPEGE and ARPEGE Tropiques (METEO-FRANCE)
- meso-scale models: UK lam (UKMO) NCEP/ETA, ALADIN-NORAF (Morocco), ALADIN-AMMA and Meso-NH (METEO-FRANCE)

3. MODELS CONFIGURATION

ARPEGE and ARPEGE Tropiques are global models initialized by a 4dvar analysis. The main differences between ARPEGE and ARPEGE Tropiques are the mesh which is fixed for ARPEGE Tropiques (uniform 50-km resolution) whereas for ARPEGE a variable mesh is used (maximum 23km, minimum 150km) leading to a slightly better resolution for ARPEGE-Tropiques over Africa and a different cut-off (later for ARPEGE Tropiques).

ALADIN-AMMA is a limited area model, coupled to ARPEGE, whose resolution is 10km. A 3dvar analysis is performed every 6 hours and takes into account the same type of data as ARPEGE 4d-var but with a different sampling as the analysis is performed each 6 hours (3dvar) and not in a time-window (4d-var). The difference lies in the assimilation by the 3dvar of the MSG-8 radiances (two Water Vapour (WV) channels in clear-sky conditions above sea/land and three Infra-Red (IR) channels in clear-sky conditions). This leads to the fact that radiances (and among them MSG radiances) dominate the data flux in the ALADIN 3dvar data assimilation (see

data assimilated for the AMMA 2006 SOP on fig.1). One can also see on the following plot (red bars) the increase of radiosounding data (dropsondes included) due to AMMA "effort" assimilated during the SOP (maximum in August 2006). With respect to previous years AMMA allowed to multiply radiosoundings releases by a factor of ~3.

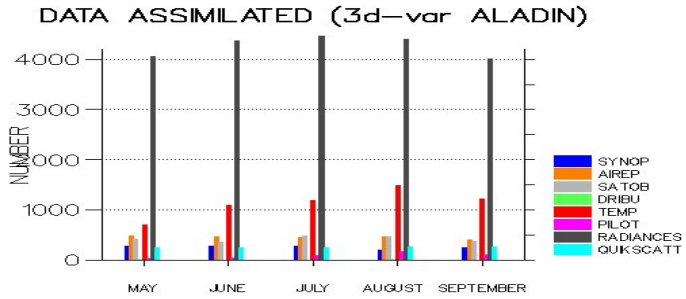

Figure 1. Daily mean number of data assimilated by the ALADIN-AMMA 3dvar analysis (geographical domain is 2°N 20°N, 15°W-20°E).

4. RESULTS

Classical scores are being computed between the forecasts and classical observations (SYNOP – surface stations, and TEMP – upper air station) and will be presented in the poster.

We present here a comparison between the integrated water content (IWC) measured by three GPS stations (among six deployed for AMMA) on a North-South transect (Gao ~ 16°N, Niamey ~ 13°N and Djougou ~ 9°N) and the same quantity computed in the model analysis and forecast. From the plots shown on Fig. 2 one can see that the models have difficulties in handling the diurnal cycle of the IWV (black curves) which shows a maximum around 12 UTC (Gao) or 15UTC (Niamey and Djougou). The bias between observed and forecasted IWV can be partially explained by the difference of altitude between the GPS station and the model elevation. For example the elevation of the GPS station of Gao is 238m, whereas the elevation of the closest gridpoint in ARPEGE is 301m (317m in ARPEGE Tropiques and 233m in ALADIN). The other striking feature which appears when comparing the three plots of Fig.2 is the positive trend with forecast range in the IWV at the northernmost station (Gao) and the negative one at the southernmost station (Djougou) which we believe is a signature of a northern drift of the convection location with increasing forecast range.

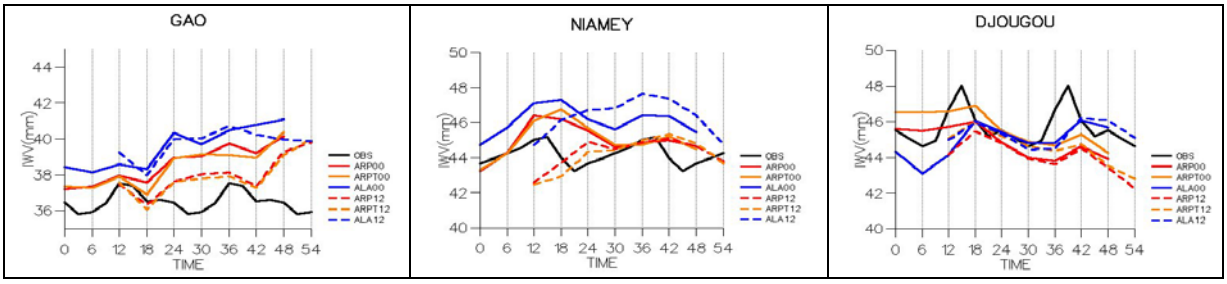

Figure 2. Averaged Integrated water content (IWV in mm) during AMMA2006 SOP observed from AMMA GPS stations in black, and forecasted (red for ARPEGE, orange for ARPEGE Tropiques, blue for ALADIN, straight line for runs initialized at 00UTC, dashed for initialization at 12UTC). GPS station of Gao (left), Niamey (middle) and Djougou (right). Observations available each 3 hours, forecasts each 6 hours (except for ARPEGE Tropiques each 12 hours).

5. CONCLUSION

The AMMA SOP just ended recently and first validation results are presented here. It is felt that GPS data are very valuable for NWP validation and assimilation particularly in the tropics.

Acknowledgements: *WMO and THORPEX-IPO provide financial assistance for the publication of the STISS proceedings volume.*

REFERENCES

O. Bock, C. Keil, E. Richard, C. Flamant, M.N. Bouin, 2005: Validation of precipitable water from ECMWF model analyses with GPS and radiosonde data during the MAP SOP, *Q. J. R. Meteorol. Soc*., **131**, 3013-3036.

EXPERIMENTAL REANALYSIS USING AFES-LETKF AT A T159/L48 RESOLUTION

Takemasa Miyoshi [1], Shozo Yamane [2], and Takeshi Enomoto [3]

[1] Numerical Prediction Division, Japan Meteorological Agency, Tokyo, Japan
E-mail: *miyoshi@naps.kishou.go.jp*
[2] Chiba Institute of Science, and Frontier Research Center for Global Change, JAMSTEC
[3] Earth Simulator Center, JAMSTEC

Abstract: The AFES-LETKF system at a T159/L48 resolution is used to perform an experimental reanalysis from May 2005 to produce a dataset useful for THORPEX-like research in atmospheric predictability. The local ensemble transform Kalman filter (LETKF) is an ensemble Kalman filter (EnKF) method originally developed and tested at the University of Maryland. It was recently applied to AFES (AGCM for the Earth Simulator) at a T159/L48 resolution by Miyoshi and Yamane (2006). Using the AFES-LETKF system, real observations used in the operational global analysis system at the Japan Meteorological Agency except satellite radiances are assimilated to produce experimental reanalysis products from May 2005, which are called "ALERA" standing for AFES-LETKF Experimental ReAnalysis. EnKF is a method ideally considering the analysis errors while taking advantages of bred vectors. ALERA is useful for research in short- to medium-range atmospheric predictability, which is relevant to THORPEX.

Keywords – *Ensemble data assimilation, Local ensemble transform Kalman filter*

1. INTRODUCTION

At the Numerical Prediction Division, Japan Meteorological Agency (NPD/JMA), a four-dimensional local ensemble transform Kalman filter (4D-LETKF or just LETKF hereafter, Hunt et al. 2004; Hunt 2005) is being developed since August 2005. Thus far, we have achieved working LETKF systems with three state-of-the-art models: AFES (AGCM for the Earth Simulator, Ohfuchi et al. 2004), GSM (JMA's operational Global Spectral Model), and NHM (a.k.a. MSM, JMA's operational nonhydrostatic Mesoscale Model).

The AFES-LETKF project is a collaborative project among the NPD/JMA, Chiba Institute of Science (CIS), and Earth Simulator Center (ESC). The NPD/JMA, ESC, and CIS develop the LETKF, AFES, and the experimental system connecting the LETKF data assimilation and AFES forecast, respectively. The model resolution is chosen to be T159/L48, corresponding to the grid of 480x240x48.

The LETKF FORTRAN90 codes are based on the local ensemble Kalman filter (LEKF, Ott et al. 2002; 2004) codes by Miyoshi (2005), with MPI/OpenMP-parallelization and upgrading to LETKF. Miyoshi and Yamane (2006, "MY06" hereafter) described details of the first outcome of the AFES-LETKF, including the code development, perfect model experiments, and experiments with real observations. Based on MY06, real observations are assimilated over a 1-year period after May 2005 to investigate the long-term stability of LETKF and to provide useful products for THORPEX-like research in atmospheric predictability. In this abstract, a brief description of the recent progress of so-called ALERA (AFES-LETKF Experimental ReAnalysis) is outlined.

2. EXPERIMENTAL ENSEMBLE REANALYSIS: ALERA

Based on the successful implementation and preliminary tests by MY06, we have been performing longer-term data assimilation cycle experiments with real observations except satellite radiances; the project is called "ALERA", standing for AFES-LETKF Experimental ReAnalysis. The ensemble size is fixed to be 40, and the experimental period is from May 2005 towards today as long as computational resources are available.

Since in general there is no guarantee that the ensemble Kalman filter (EnKF) is stable for a long period, the primary purpose of ALERA is to investigate the long-term stability of the AFES-LETKF system. Fig. 1 shows time series over 1 year of the analysis ensemble spreads and analysis differences between AFES-LETKF and NCEP/NCAR reanalysis. The AFES-LETKF performs stably for over 1 year. The discontinuity after the initial one month is due to the system upgrade, where we began to apply the vertical localization for surface pressure observations. If the discontinuity is ignored, AFES-LETKF has an about 1-week spin-up period. After the spin-up, the analysis differences are quite stable. We see some seasonal variations: larger analysis differences in winter hemisphere, especially in the NH. However, spreads have smaller seasonal amplitudes.

ALERA contains huge amount of information: 40 analysis members every 6 hours. At an analysis time, Fig. 2 shows the spaghetti diagram of 500 hPa height fields. ALERA contains this kind of map every 6 hours for all variables at all vertical levels. Therefore, it is important to analyze the products more in detail, which is now in progress.

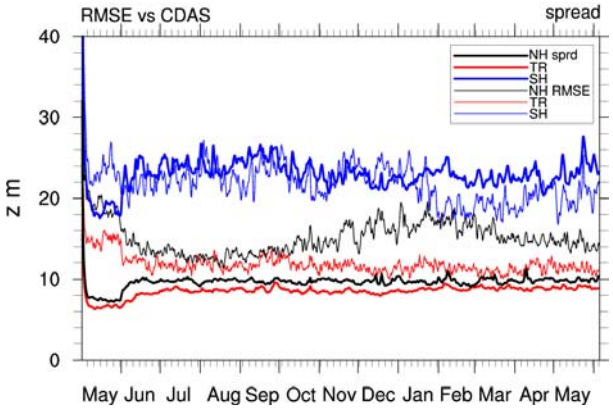

Figure 1. Time series for 13 months from May 2005 of 500 hPa height analysis ensemble spreads and analysis differences between AFES-LETKF and NCEP/NCAR reanalysis (CDAS) in each region.

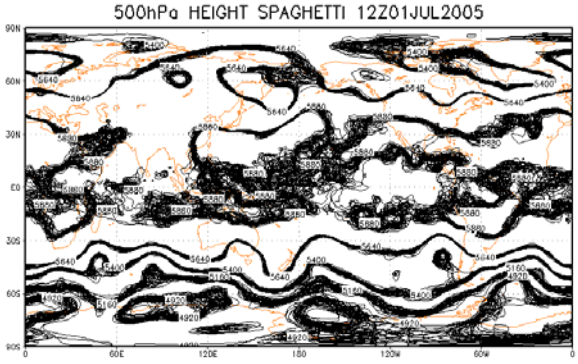

Figure 2. Spaghetti diagram of 500 hPa height (m) for the ALERA analysis ensemble on 12Z July 1, 2005.

3. SUMMARY

ALERA has been performing stably over 1 year, and the computation is continuing towards today as long as computational resources are available. Further verifications and analyses of the products are now in progress.

Acknowledgements: *We thank members of the chaos/weather group of the University of Maryland, especially Prof. Eugenia Kalnay for fruitful discussions. We also thank Dr. Wataru Ohfuchi of ESC and Dr. Tadashi Tsuyuki, Yoshiaki Takeuchi, Yuzo Yotsuya, and Ko Koizumi of NPD/JMA for kind support for the LETKF projects. The AFES-LETKF experiments have been performed on the Earth Simulator under support of JAMSTEC.*

REFERENCES

Hunt, B. R., E. Kalnay, E. J. Kostelich, E. Ott, D. J. Patil, T. Sauer, I. Szunyogh, J. A. Yorke, and A. V. Zimin, 2004: Four-dimensional ensemble Kalman filtering. *Tellus*, **56A**, 273-277.

Hunt, B. R., 2005: Efficient Data Assimilation for Spatiotemporal Chaos: a Local Ensemble Transform Kalman Filter. arXiv:physics/0511236v1, 25pp.

Miyoshi, T., 2005: Ensemble Kalman filter experiments with a primitive-equation global model. Ph.D. dissertation, University of Maryland, 197pp.

Miyoshi, T. and S. Yamane, 2006: Local ensemble transform Kalman filtering with an AGCM at a T159/L48 resolution. *Mon. Wea. Rev.*, submitted.

Ohfuchi, W., H. Nakamura, M. K. Yoshioka, T. Enomoto, K. Takaya, X. Peng, S. Yamane, T. Nishimura, Y. Kurihara, and K. Ninomiya, 2004: 10-km mesh meso-scale resolving simulations of the global atmosphere on the Earth Simulator: Preliminary outcomes of AFES (AGCM for the Earth Simulator). *J. Earth Simulator*, **1**, 8-34.

Ott, E., B. R. Hunt, I. Szunyogh, M. Corazza, E. Kalnay, D. J. Patil, J. A. Yorke, A. V. Zimin, and E. J. Kostelich, 2002: Exploiting Local Low Dimensionality of the Atmospheric Dynamics for Efficient Ensemble Kalman Filtering. arXiv:physics/0203058v3.

Ott, E., B. R. Hunt, I. Szunyogh, A. V. Zimin, E. J. Kostelich, M. Corazza, E. Kalnay, D. J. Patil, and J. A. Yorke, 2004: A local ensemble Kalman filter for atmospheric data assimilation. *Tellus*, **56A**, 415-428.

A LOCAL ENSEMBLE KALMAN FILTER WITH A LIMITED AREA MODEL

Dagmar Merkova[1], G. Gyarmati, E. Kostelich, I. Szunyogh
[1] University of Maryland, College Park, USA
E-mail: medag@glue.umd.edu

Abstract: The main goal of our research is to explore the value that a high resolution limited area data assimilation system can add to the lower resolution global analyses, when both the regional and global analyses are generated with a Local Ensemble Transform Kalman Filter. The model used in this study is the Regional Spectral Model (RSM), which is one of the operational limited area models at NCEP. The RSM is the model that is the most closely related, among all limited area models, to the NCEP Global Forecast System (GFS) model. The RSM is a perturbation model: it simulates the evolution of the atmospheric flow by evolving high-resolution perturbations to the low-resolution global meteorological fields within the limited area. We have tested two approaches for implementation of the LETKF on the NCEP RSM: (i) The first approach cycles only the global analysis and takes only the large-scale initial condition uncertainties into account when estimating the high resolution state within the limited area domain. (ii) The second approach cycles both the global and local analyses, providing a high-resolution estimate of the forecast uncertainty within the limited area. Using simulated observations for the perfect model scenario, we demonstrate that the second approach is far superior to the first one. We also find that adding high resolution details to the low resolution global analysis with the help of the limited area data assimilation system significantly enhances the accuracy of the state estimate within the limited area.

***Keywords**: Data assimilation, Limited area model, LETKF, NCEP RSM*

1. INTRODUCTION

High-resolution limited-area models typically rely on a lower resolution global model to provide the lateral boundary conditions. Recent studies on limited area ensembles (Torn, 2006) demonstrated that proper handling of the boundary conditions is crucial for maintaining the diversity between members of the limited area ensemble. Thus, in an ensemble-based data assimilation and/or forecast system, an efficient strategy is needed to propagate information about uncertainties from the coarse global grid to the high-resolution limited area grid.

The Local Ensemble Transform Kalman Filter (LETKF), introduced by Ott et al. (2002) and Hunt et al. (2006), is one of the two ensemble-based data assimilation schemes that have been successfully tested on the NCEP Global Forecast System model (Szunyogh et al. 2005 and 2006). The other such scheme is the (Local) Square-Root Ensemble Kalman Filter of Whitaker (2006). We note that implementation of the LETKF is more challenging on the limited area model than on the global model due to the role of the lateral boundaries. We believe that the NCEP RSM is the ideal limited area model for an implementation of the LETKF due to its unique compatibility with the NCEP GFS.

The NCEP RSM is a perturbation model: the high resolution forecast it provides is the sum of the larger-scale flow component, as predicted by the NCEP GFS, and a high resolution perturbation component. Unlike most other limited-area models, which are affected by the global fields only through the lateral boundary conditions, the RSM is affected by the global fields throughout the entire limited area (Juang et al., 1994).

2. EXPERIMENTAL DESIGN

We consider two different approaches to implement the LETKF on the NCEP RSM. In the first approach, we cycle only the global analysis that is independent from regional analysis.. The regional analysis is obtained by interpolating of the global ensemble analysis. Both systems are evolved then with the global and the regional model to obtain a global background ensemble and regional background ensemble. Then, the LETKF algorithm is applied to both background ensembles. The limited area ensemble information is utilized to start high resolution ensemble forecasts, but this forecast information is not used at the next analysis time.

In the second approach, both the global and the regional analyses are cycled (Figure 1). Global analysis is independent on the regional again. After application of the LETKF, we form a new analyses. In the following step, information from regional analysis is used to obtain high-resolution perturbation and global analysis supply the base field for limited area model. Such information is processed by the RSM model separately and next regional background ensemble is formed and another analysis cycle is started. Global analysis cycle is not dependent on the regional cycle.

The horizontal resolution of the GFS is T62 (about 150~km), while the resolution of the RSM is 48~km. Both models use the same 28 vertical levels to discretize the meteorological fields in the vertical direction. The limited area is covered by 192 x 139 horizontal grid points at each vertical level. In our initial experiments, we assume that the GFS and RSM models are perfect. Under this assumption, we can generate a time series of true states that have high resolution inside the limited area domain and have coarse resolution elsewhere. This true state is obtained by first generating a time series of coarse resolution global true states by a 60-day integration of the NCEP GFS starting from the operational global analysis of NCEP on 1 January 2000 at 00 UTC. Then, a 60-day integration of the RSM is carried out to add high

resolution features to the true state over the extended North America region.

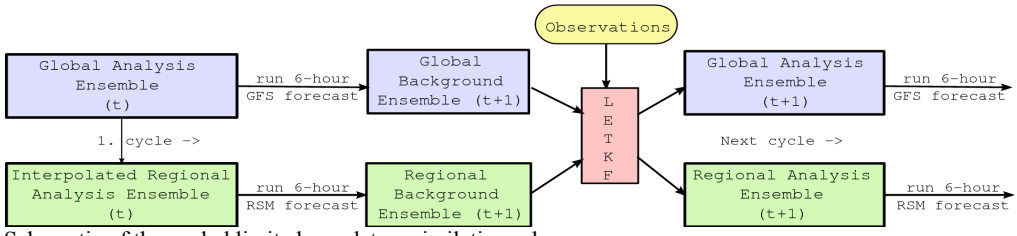

Figure 1: Schematic of the cycled limited one data assimilation scheme.

We generate simulated observations by adding random observational noise to the true state at the location of the observations that were operationally assimilated at NCEP between 1 January 2004 and 29 February 2004. We consider the location of all operationally assimilated observations except for satellite radiances. The random observational noise is generated by assuming that the observations are unbiased and that the observational errors have standard deviations that are identical to those assumed by the operational NCEP data assimilation system.

The data assimilation is carried out by first running a global analysis cycle for 60 days, starting on 1 January 2004 at 0000 UTC. Then a regional analysis cycle is started on 16 January 2000 at 0000 UTC. The beginning of the data assimilation period is started only after 15 days to avoid the propagation of transient effects from the global to the regional assimilation cycle. Figure 1 shows the flowchart for the coupled global-regional data assimilation cycle.

3. RESULTS

The most important free parameters used in the LETKF are the number of ensemble members and the definition of the local volume from which observations are selected to estimate the state at a given grid point. All results shown here are obtained with a 40-member ensemble. The vertical depth of the local volume is a function altitude as in Szunyogh (2005). The horizontal radius of the local volume is about 700--750 km in both the global and the limited area assimilation systems.

Figure 2 presents snapshots of the absolute value of the analysis error in the global, the non-cycled limited area and the cycled limited area analyses for January 21, 2004. The regional analysis obtained without cycling is only slightly, and only in a few local regions, more accurate than the global analysis. The cycled regional analysis, however, is clearly superior to the global analysis over the entire limited area domain. Thus, we will use later approach, cycled regional analysis, for following experiments with the real data set of observations.

REFERENCES

Hunt, B., E. Kostelich, and I. Sunyogh, 2006: Efficient data assimilation for spatiotemporal chaos: a local ensemble transform kalman filter. Physica D, Sub- mitted, http://arxiv.org/abs/physics/0511236

Juang, H. M. H. and M. Kanamitsu, 1994: The NMC nested Regional Spectral Model. Mo. Wea. Rev., 122, 3-26.

Ott, E., B. R. Hunt, I. Szunyogh, M. Corazza, E. Kalnay, D. J. Patil, J. A. Yorke, A. V. Zimin, and E. V. Kostelich, 2002: Exploiting local low dimensionality of the atmospheric dynamics for eficient ensemble Kalman filtering. arXiv:archive/paper 0203058, (http://arxiv.org/abs/physics/0203058).

Ott, E., B. R. Hunt, I. Szunyogh, A. V. Zimin, E. J. Kostelich, M. Corazza, E. Kalnay, D. J. Patil, and J. A. Yorke, 2004: A Local Ensemble Kalman Filter for atmospheric data assimilation. Tellus Ser. A, 56, 415-428.

Szunyogh, I., E. J. Kostelich, G. Gyarmati, E. Kalnay, B. R. Hunt, E. Ott, and J. A. Yorke, 2006: Assessing a Local Ensemble Kalman Filter: Assimilating real observations with the NCEP global model. Tellus, submitted

Szunyogh, I., E. J. Kostelich, G. Gyarmati, D. J. Patil, B. R. Hunt, E. Kalnay, and E. Ott, 2005: Assessing a Local Ensemble Kalman Filter: Perfect model experiments with the NCEP global model. Tellus, 57 A, 528-545.

Torn, R. D., G. J. Hakim, and C. Snyder, 2006: Boundary conditions fro limited- area ensemble Kalman Filters. MWR, 134, 2490-2502.

Whitaker, J. S., T. M. Hamill, X. Wei, Y. Song, and Z. Toth, 2006: Ensemble Data Assimilation with the NCEP Global Forecast System. MWR.

Figure 2: Time series of the spatial average rms error of the surface pressure 01/01/2004-02/29/2004

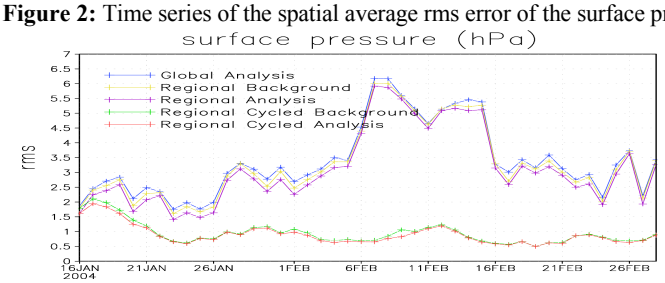

ASSIMILATION OF RADAR DERIVED PRECIPITATION IN THE LM-K

Stefan Klink [1], Klaus Stephan, and Christoph Schraff

[1] Deutscher Wetterdienst, PO Box 10 04 65, 63004 Offenbach am Main, Germany
E-mail: *stefan.klink@dwd.de*

Abstract: A Latent Heat Nudging scheme has been introduced in the nudging-type assimilation scheme of the high-resolution NWP-model LM-K. Due to the changes in the model behaviour caused by the prognostic treatment of precipitation constituents several adaptations to the original approach had to be implemented.

Keywords – *Data assimilation, High-resolution model, Convective scale, Latent Heat Nudging, Radar observations*

1. INTRODUCTION

The main focus of LM-K (Doms and Förstner, 2004), which has been developed as a meso-γ-scale version of the operational non-hydrostatic limited area model LM, is on the very short range prediction of severe weather, which often forms in context with deep moist convection. Thus, in addition to the assimilation of conventional data, as a first step 2D radar derived precipitation data from the German radar network are introduced in the nudging-type analysis of LM-K. Using the Latent Heat Nudging (LHN) technique (Jones and Macpherson 1997) the latent heating of the atmospheric model is scaled by the fraction α of observed to modelled precipitation in order to drive the modelled rain rates towards observed ones.

Past experiments with a purely diagnostic precipitation scheme have shown that precipitation patterns can be assimilated in good agreement with those observed by radar, both in position and amplitude. In order to simulate the horizontal distribution of precipitation in mountainous terrain more realistically, a prognostic treatment of precipitation (Baldauf and Schulz 2004) including advection has been introduced in the model, and is used operationally in the LM-E (LM-Europe). It tends to decorrelate the surface precipitation rate from the vertically integrated latent heat release and thereby violate the basic assumption to the LHN approach. This, and resulting problems have been shown by Klink and Stephan (2005), and they also suggested possible adaptations to the LHN scheme.

2. MAJOR REVISIONS TO THE LHN SCHEME

At horizontal model resolutions of 3 km or less, the prognostic treatment of precipitation allows the model to distinguish between updrafts and downdrafts inside deep convective systems. Compared to using the diagnostic precipitation scheme, it modifies both the 3-D spatial structure and the timing of the latent heating with respect to surface precipitation. Therefore, three revisions have been introduced to the LHN scheme. Two of them address spatial aspects and a third one an important temporal issue:

- In updraft regions at the leading edge of convective cells, very high values of latent heat release occur often where modelled precipitation rates are low. Thus high values of the scaling factor α and of the latent heat nudging temperature increments often occur. To mitigate this, the upper limit for α is reduced to 2 and the lower limit increased accordingly to 0.5. Furthermore, the linear scaling is replaced by a logarithmic scaling, leading to effective limits of 1.7 and 0.3, respectively. This adaptation reduces the simulated precipitation amounts during the LHN.

- In downdraft regions further upstream in convective cells, high precipitation rates occur often where latent heating is weak or even negative in most vertical layers. In order to avoid negative LHN temperature increments and cooling where the precipitation rate should be increased (and vice versa), only the vertical model layers with positive simulated latent heating are used to compute and insert the LHN increments. This modification tends to render the increments more coherent and the scheme more efficient.

- Precipitation produced by the prognostic scheme will take some time to reach the ground where it is compared to the radar-derived surface precipitation rate. Thus, the conventional LHN scheme can notice only with some temporal delay when it has already initiated precipitation aloft. Therefore, a more immediate information on the precipitation rate already initialised is required, i.e. a sort of undelayed 'reference precipitation' which is used merely to replace the delayed prognostic model precipitation in the computation of the scaling factor α. One choice to work reasonably well is found to be the vertically averaged precipitation flux.

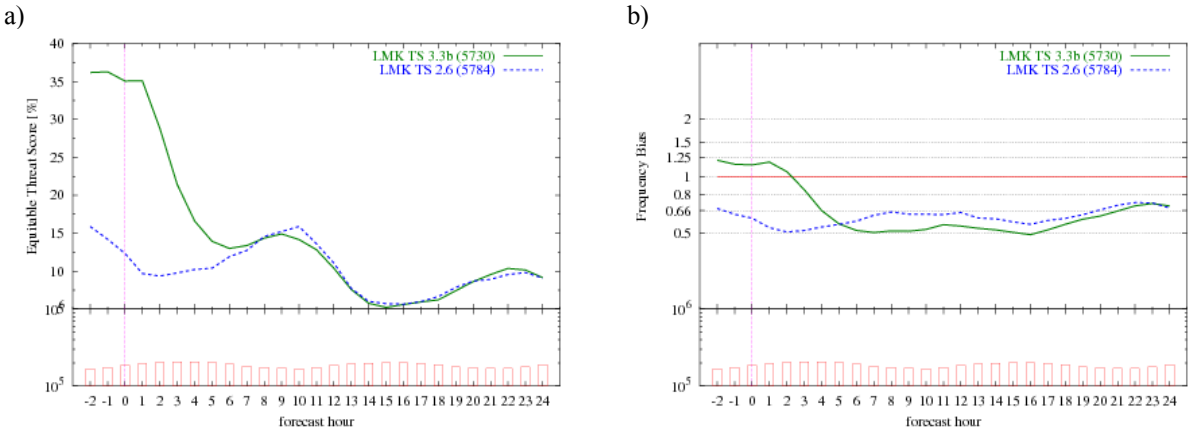

Figure 1. Mean equitable threat score (a) and mean frequency bias (b) for hourly precipitation (threshold 0.1 mm) for the overall (combined 0 and 12 UTC forecast) runs as a function of forecast time. The thin vertical purple lines indicate the starting time of the free forecasts. The "mean" scores were obtained by adding up the contingency table over a 45-day period. Assimilation cycles: nudging without LHN (blue dashed, label "LMK TS 2.6 (5784)") and nudging with LHN (green solid, label "LMK TS 3.3b (5730)"). The red bars at the bottom of the panels show the number of observed precipitation events above the considered threshold value.

3. VERIFICATION OF MODELLED AGAINST RADAR-OBSERVED PRECIPITATION

For an assessment of the overall-performance of the revised LHN during assimilation and especially for an evaluation of LHN's forecast impact, two LM-K experiments have been carried out for a 45-day period in June and July 2006. A LHN experiment, comprising of an LM-K assimilation run with LHN and two daily 24-hour forecasts starting at 0 and 12 UTC, is compared to a control experiment, which has been set up in the same way but does not use LHN during assimilation. The particular comparison measures are "Equitable Threat Score" (ETS) and "Frequency Bias" (FBI) for hourly precipitation.

On average, the positive impact of radar data is visible in the combined 0 and 12 UTC forecasts' ETS for up to 5 hours for a threshold value of 0.1 mm (fig. 1a). This impact time decreases slightly for higher threshold values (not shown). Whether the rapid decrease of ETS is partly due to the double penalty problem inherent to the ETS still needs to be evaluated. The mean FBI curve presented in fig. 1b indicates that LM-K forecasts starting from an assimilation without LHN (blue dashed lines) generally underestimate the precipitation. On the contrary, forecasts starting from an assimilation with LHN (green solid lines) begin with almost ideal values (1.0) of FBI, rapidly drop off towards the graph of the control experiment after 3-4 hours, and afterwards still stay slightly below this one for several hours. It seems that there exists a general model deficiency in generating precipitation, and LHN, however, is only able to help this problem for a short time period directly after the assimilation. More precisely, LHN does not cure the problem but it just rearranges the occurrence of precipitation during the first several hours. A higher FBI during the first four forecast hours is compensated by lower FBI-values for several hours thereafter.

4. CONCLUSION

To conclude, several adaptations to the LHN scheme have been found which enable the model with prognostic precipitation to simulate the rain patterns in good agreement with radar observations during the assimilation. Thus, the problems related to prognostic precipitation appear to be mitigated to a satisfactory degree. However, the rapid decrease of benefit in the forecasts remains a shortcoming.

REFERENCES

Baldauf, M., and J.-P. Schulz, 2004: Prognostic Precipitation in the Lokal Modell (LM) of DWD. COSMO Newsletter, No. 4, 177-180 (available at www.cosmo-model.org).

Doms, G., and J. Förstner, 2004: Development of a Kilometer-Scale NWP-System: LMK. COSMO Newsletter, No. 4, 159-167 (available at www.cosmo-model.org).

Jones, C. D., and B. Macpherson, 1997: A Latent Heat Nudging Scheme for the Assimilation of Precipitation Data into an Operational Mesoscale Model. Meteorol. Appl., 4, 269-277.

Klink, S., and K. Stephan, 2005: Latent heat nudging and prognostic precipitation. COSMO Newsletter, No. 5, 124-131 (available at www.cosmo-model.org).

TOWARDS THE MONITORING OF AN ENSEMBLE PREDICTION SYSTEM

Philippe Arbogast [1], Catherine Piriou and Jean Nicolau

[1] Direction de la Prévision, Météo-France, Toulouse, France
E-mail: *philippe.arbogast@meteo.fr*

Abstract: A technique enabling the assessment of the initial spread of an ensemble is proposed. It is based on a simple diagnosis of the analysis error variance followed by the use of the Ensemble Transform in order to improve the fit between the ensemble spread and the analysis error variances.

Keywords – *Ensemble prediction, Ensemble Transform*

1. INTRODUCTION

Ensemble forecasting is a feasible method to integrate a deterministic forecast with an estimate of the probability distribution of atmospheric states. Assuming that the numerical model for the atmosphere is perfect, the uncertainties of a deterministic forecast are mainly due to the chaotic nature of the atmosphere itself and to uncertainties in the initial conditions. Therefore, it is of primary importance to check if the ensemble at the initial time fits the probability density function of the initial conditions errors of the control run.
The goal of this paper is to discuss the initial and very short range spread in the frame of the Météo-France short-range ensemble with respect to an estimate of the analysis error variance available in the observation space. Finally, the Ensemble Transform (Bishop and Toth, 1999) is applied in observation space to make the ensemble spread closer to the analysis error variance.

2. THE FRENCH SHORT-RANGE ENSEMBLE (PEARP)

An ensemble prediction system is running operationally at Météo-France once a day (at 18UTC) since June 2004. The perturbations used in the ensemble are generated by the singular vectors technique. Nevertheless, vectors are optimized over a 12h interval and over a limited area including the Western Europe and the northern part of the Atlantic Ocean. By this way, perturbations are mainly efficient in the area of interest for the short range forecast over France. Because of heavy computational cost, the ensemble is limited to 11 members (10 perturbed + 1 control). However, it is based on the operational version of the ARPEGE model with a spectral truncation of TL358 and with a stretching coefficient of 2.4 (corresponding to a grid mesh of 23 km over France and 100km over New-Zealand).

3. ANALYSIS ERROR DETERMINATION

The analysis error variance in observation space is computed following Desroziers et al. (2005) and writes: $E\left[\left(\mathrm{y}^{\mathrm{a}}-\mathrm{y}^{\mathrm{b}}\right)\left(\mathrm{y}^{\mathrm{a}}-\mathrm{y}^{\mathrm{o}}\right)\right]=\mathrm{HAH}^{\mathrm{T}}$ where y^{a}, y^{o} and y^{b} stand for the analysis, the observation vector and the background in observation space. The right-hand side of the equation is simply the analysis covariance error matrix in the observation space. Only the diagonal will be considered for the present purpose and will be called P^{a} hereafter. For each observation the expectation of the left-hand side of the equation is computed by averaging over a radius of 350km around each observation. The diagnosis is therefore relevant for the largest scales and the smallest scales resolved by the observation network are filtered out. Each innovation and analysis increment is normalized by the observation error variance so that all the assimilated observations (radiances, temperature, wind…) may be taken into account in one single diagnosis. The equation used for the computation becomes: $\mathrm{R}\,E\left[\left(\mathrm{y}^{\mathrm{a}}-\mathrm{y}^{\mathrm{b}}\right)\left(\mathrm{y}^{\mathrm{a}}-\mathrm{y}^{\mathrm{o}}\right)/\sigma_o^2\right]=\mathrm{HAH}^{\mathrm{T}}$ where R stands for the observation error variance matrix. σ_o^2 is the observation error variance related to the observation y^{o}.

The analysis error variances computed that way are compared with the ensemble spread in the same observation space. However, the projection of each member of the ensemble onto the observation space is computationally expensive especially when satellite data are taken into account. Fig. 1 (two first panels) clearly shows that the ensemble spread at the initial time is weaker than it should be. Moreover, the figure also suggests that the main patterns of ensemble spread do not fit the analysis error variance patterns.

4. THE ENSEMBLE TRANSFORM

The ensemble transform T (k by k matrix) is defined by $\mathrm{T}^{\mathrm{T}}\mathrm{Y}^{\mathrm{T}}\mathrm{P}^{\mathrm{a}\,-1}\mathrm{Y}\,\mathrm{T} = \mathrm{I}$ where Y is the ensemble perturbation matrix in observations space (n rows, k columns where k the size of the ensemble and n the size of the observation vector). Therefore, in particular the diagonal of the covariance of the transformed ensemble $(\mathrm{YT})^{\mathrm{T}}\,\mathrm{Y}\,\mathrm{T}$ is P^{a}. T is exhibited through an eigenvalue problem of small dimension (number of ensemble perturbations, here 10): it is the eigenvector matrix of $\mathrm{Y}^{\mathrm{T}}\mathrm{P}^{\mathrm{a}\,-1}\mathrm{Y}$ where each column is normalized by $\sqrt{1/\lambda_k}$ where λ_k is the corresponding eigenvalue. (YT) is now the transformed ensemble. The prediction at time *t* of the transformed-ensemble spread is now: $\mathrm{P}(t) = (\mathrm{Y}(t)\mathrm{T})^{\mathrm{T}}\,\mathrm{Y}(t)\,\mathrm{T}$. In the example of the figure the mean spread of the transformed ensemble spread is closer to the analysis error variance than the initial ensemble spread although it remains too weak. The comparison of the two last panels shows a clear evidence regarding to the improvement of the space distribution of the variances: As in the analysis error variance field, the transformed ensemble spread is dominated by the pattern located in the central part of the domain (40°- 60°N / 50°W-25°W) and the pattern initially over Ireland becomes secondary.

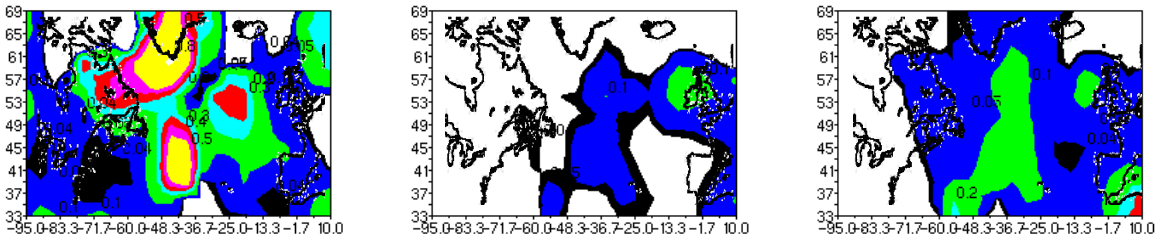

Figure 1. Analysis error variance in observation space computed following section 3 (left-hand panel) and normalized by the observation error and interpolated over a 2° by 2 ° regular grid at 00UTC 13 June 2006. Data below 500hPa are taken into account in the computation (wind, temperature profiles from aircrafts and rawinsondes, GOES and METEOSAT winds, surface data, quickscatt winds). Central panel : initial ensemble spread in observation space also normalized by the observation error and interpolated over the 2° by 2° grid. Right-hand side panel: spread of the transformed ensemble.

7. CONCLUSION

It is common in the forecast practice to use observations in order to reject some model runs when small errors appear at the very short range or in the analysis. A comparable approach is proposed here to assess the spread of an ensemble at the initial time or even at the very short range against an estimation of the analysis error variances in observation space. The rationale is the following: if the initial spread has nothing to do with the initial error variance then the spread of the ensemble has nothing to do with the actual forecast uncertainty. Moreover the authors suggest to follow the same approach in order to build sub-ensemble of TIGGE by re-sampling in order to provide an estimation of the forecast error variance that measures the predictability associated to a NWP system.

REFERENCES

Bishop, C.H. and Z. Toth, 1999: Ensemble transformation and adaptive observations. *J. Atmos. Sci.*, **56**, 1748-1765

Desroziers, G., L. Berre, B. Chapnik and P. Poli, 2005: Diagnosis of observation, background and analysis-error statistics in observation space. *Q. J. R. Meteorol. Soc.* **131** , 3385-3396.

ESTIMATION OF ADJOINT SENSITIVITY GRADIENTS IN OBSERVATION SPACE USING THE DUAL (PSAS) FORMULATION OF THE ENVIRONMENT CANADA OPERATIONAL 4D-VAR.

Josée Morneau[1], Simon Pellerin[2], Stéphane Laroche[2], Monique Tanguay[2]

[1]Meteorological Service of Canada, Environment Canada, Dorval, Canada
[2]Meteorological Reseach Division, Environment Canada, Dorval, Canada
E-mail: *Josee.Morneau@ec.gc.ca*

1. INTRODUCTION

The 3D-Var at Environment Canada (EC) has been re-implemented recently in research mode as a collection of basic transformation operators acting on objects defined in various spaces. This modular approach enabled the development of various assimilation formulations and tools that help diagnose the impact of the different components of our data assimilation system. This study describes and validates an adjoint-based technique, proposed by Langland and Baker (2004), for assessing the value of observations assimilated by 3D-FGAT and 4D-Var algorithms. This represents one application of the 3D/4D-PSAS implementation.

Operational delivery schedule, computational cost of the data assimilation system (DAS) and forecast skill sensitivity with respect to observation's time distribution over the assimilation window are primary parameters to be considered when establishing a "cut-off" time schedule for the reception of observations. The so called "cut-off" problem becomes a particularly challenging issue for operational centers dealing with implementations of expensive four dimensional DASs as shown in Laroche et al. (2006)

The experiments presented in this study aim at understanding the usefulness of observations with respect to their time distribution over the assimilation window and at validating conclusions drawn from adjoint-based observation impact (OI) experiments against those derived from conventional observing system experiments (OSE's).

2. ADJOINT-BASED ESTIMATION OF OBSERVATION IMPACT

The 4D-Var assimilates a large amount of observations of various types every six hours in support of numerical weather prediction. These observations could have significant differences in term of impact on initial conditions and on forecast errors. The method developed by Langland and Baker (2004) makes use of any subset of innovation vector and adjoint sensitivity gradients estimated in observation space to calculate the impact of observations on short-range forecast errors. With this method, it is unnecessary to add or remove observations, like for the OSE method, to assess the impact of a subset of observations on the quality of forecasts.

The differences in short term forecast errors, issued from an analysis $\mathbf{x}^a$ and its background state $\mathbf{x}^b$, can be approximated by

$$\delta e^{f,g} = \left\langle \mathbf{y} - H(\mathbf{x}^b), \mathbf{K}^T \left[\frac{\partial J^f}{\partial \mathbf{x}^a} + \frac{\partial J^g}{\partial \mathbf{x}^b} \right] \right\rangle,$$

where J^f and J^g measure the errors of a forecast initiated from $\mathbf{x}^a$ and $\mathbf{x}^b$ respectively, valid at the same verification time. $\mathbf{y}$ represents the observation vector and $H(\mathbf{x}^b)$ is the non-linear observation operator. The brackets <,> represent a scalar inner product. The sensitivity vectors with respect to the analysis $\partial J^f / \partial x^a$ and to the background $\partial J^g / \partial x^b$ are computed using the adjoint of the forecast model. The transpose of the Kalman gain matrix $\mathbf{K}^T$ can be seen as the adjoint of the data assimilation procedure and must be defined consistently to the later, for instance, using all the observations assimilated by the corresponding analysis procedure. In our implementation of OI estimation, the second term of the inner product above is solved using the dual implementation (PSAS) of our 3D/4D-Var DAS.

3. DESCRIPTION OF EXPERIMENTS

The method described in section 2 was used to compute OI over the month of August 2004 for the operational EC data assimilation system (Gauthier et al., 2006, Laroche et al., 2006). This control cycle, hereafter referred to as 4D[0-6], uses long cut-off times (6-9 hours). The 24h forecast error measure is expressed in terms of dry total energy, globally averaged in the troposphere. $\mathbf{K}^T$ is obtained from a 4D-PSAS with 1 outer loop using simplified physics as in the second outer loop of the operational 4D-Var. In addition to the OI

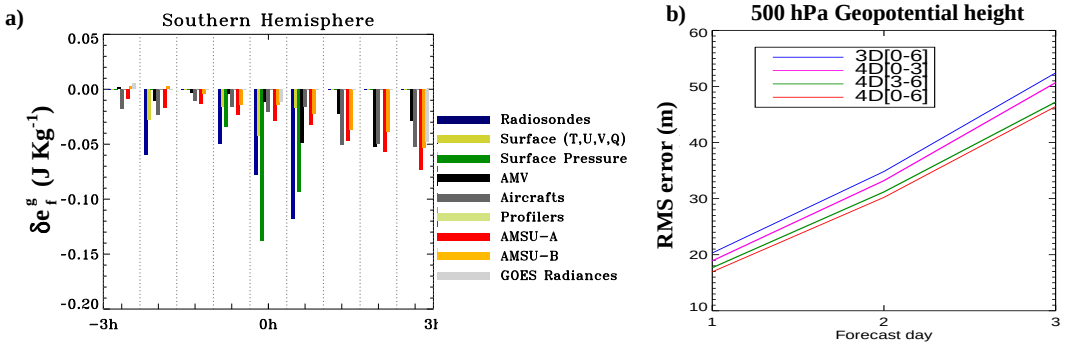

Figure 1. Results from August 2004 DA cycles, for 00z and 12z analysis, over Southern Hemisphere. **a)** Averaged individual OI, discriminated by data type and observation validity over the assimilation window. **b)** Forecast errors from OSE. Refer to section 3 for description. 3D[0-6] (3D-Var cycle) shown for reference only.

calculations, a corresponding OSE was conducted over the same period. The control run for the OSE is the operational 4D-Var DA cycle (4D[0-6]). Two data denial cycles were performed: 1) cycle 4D[3-6]), data valid in the first half of the assimilation window were removed, 2) cycle 4D[0-3], data valid in the second half of the assimilation window were removed. In all experimental cycles, radiosondes and data valid in the central bin were retained.

4. COMPARISON OF OI CALCULATIONS AND OSE

Results will be discussed for Southern Hemisphere since various impacts are more easily discriminated. Figure 1.a) shows that ATOVS (amsu-a and amsu-b) data and, to a lesser extent, aircraft data have a "temporal signature" with increasing OI magnitude as data are valid later in the assimilation window. GOES data, which are used only in the central and the two outer 4D-Var bins, show a similar behavior. AMV's OI also reveal a more important contribution when valid in the second half of the window. This forecast error sensitivity with respect to observation time validity has a significant implication for operational schedule which are constrained by product delivery. At EC, the cut-off time for the 240h forecast is only 3 hours. This early delivery schedule results in a considerable decrease in data volume, particularly for ATOVS data which are virtually absent for the last bins.

Figure 1.b) shows that forecasts from the cycle deprived from data in the second half of the assimilation window, cycle 4D[0-3], suffer from a dramatic degradation. On the other hand, forecasts from cycle 4D[3-6] shows a relatively minor degradation with respect to 4D[0-6]. These results agree well with OI conclusions. Both methods complement each other and allow considering the problem from different perspectives.

5. CONCLUDING REMARKS

Using the adjoint of our operational model and the dual formulation of our operational 4D-Var, we successfully implemented an observation sensitivity computation system that allows the estimation of the impact of arbitrary partitioning of observations on the skill of short term forecast. To address the problem of strong sensitivity of forecast errors to the operational cut-off time of observations assimilated in the EC 4D-Var, a sensitivity study of short-term forecast to time distribution and type of observations over the assimilation window have been shown.

Results from OI computations and the OSE presented in this study are in good agreement. OI based diagnostic allows us to examine the 4D-Var "temporal signature" and clearly shows the increasing impact of observations valid later in the assimilation window. As compared to Northern Hemisphere results (not shown), the "temporal signature" is stronger in the Southern Hemisphere where the assimilation of evenly distributed data dominates the radiosondes OI. The method also reveals unexpectedly strong impact of the AMV observations in the second half of the assimilation window.

REFERENCES

Gauthier, P., M. Tanguay, S. Laroche, S. Pellerin and J. Morneau, 2006: Extension of 3D-Var to 4D-Var: implementation of 4D-Var at the Meteorological Service of Canada. *Mon. Wea. Rev*., (in press)

Langland, R.H., and N.L. Baker, 2004. Estimation of observation impact using the NRL atmospheric variational data assimilation adjoint system. *Tellus*, **56**A, 189-201

Laroche, S., P. Gauthier, M. Tanguay, S. Pellerin and J. Morneau, 2006: Impact of the different components of 4D-Var on the global forecast system of the Meteorological Service of Canada. *Mon. Wea. Rev*., (in press)

EVALUATION OF THE WVSS-II MOISTURE SENSOR USING CO-LOCATED IN-SITU AND REMOTELY SENSED OBSERVATIONS

Ralph Petersen, Sarah Bedka , Wayne Feltz and Erik Olson
Cooperative Institute for Meteorological Satellite Studies, University of Wisconsin – Madison
E-mail: Ralph.Petersen@SSEC.WISC.EDU

BACKGROUND:

A study was conducted in June 2005 to assess the accuracy of WVSS-II humidity data collected from commercial aircraft to determine whether these data could be used as a surrogate for traditional upper-air reports and to fill gaps between conventional observations. Approximately 25 UPS B757 aircraft were equipped with the laser-diode based moisture sensor and provided en-route and profile reports.

The assessment was made using facilities provided by the UW mobile observing system located at Louisville, KY where about 80% of the WVSS-II equipped planes land / take off daily. Intercomparison data sets included 1) an infrared AERI system (providing very high time frequency boundary layer T/q profiles), 2) surface GPS (providing total atmospheric moisture content), 3) standard surface observations (Temp, Wind, Moisture, Ceiling), 4) a portable GPS rawinsonde system, and 5) geostationary and polar satellite data.

TEST PROCEDURES AND CONSTRAINTS:

Approximately 2 weeks of collocated radiosonde and aircraft data were collected, with radiosondes launched 3 times nightly, immediately before, between and after periods of multiple aircraft arrivals/departures. More than 5 co-locations (within 1 hour and 50 km) were obtained daily, including Temperature, Wind Direction / Speed, and Humidity reports.

The WVSS-II assessment focused primarily on water vapor measurement accuracy throughout the troposphere, but was limited by the following constraints.

1 – An occasional design problem was identified which produced erroneous reports in areas of high humidity and clouds, but only in descent. Since the objective of the experiment was to assess the difference in good quality reports made by both the aircraft and rawinsonde, only aircraft ascents were evaluated.

2 – Some of the early WVSS-II units allowed small amounts of moisture to enter the laser sensing unit and thereby biasing the moisture reports upward, especially at extremely low mixing ratio. This problem was addressed by limiting assessments to regions where the observed mixing ratio was greater than 2 g/kg. Both problems have since been addressed.

3 –WVSS-II observations were being truncated before transmission to the ground. Reports of less than 10 g/kg had precision of at least 0.1 g/kg, while reports greater than 10 g/kg had precisions of only 1 g/kg, producing RH reporting errors of 5%. As a result, results were obtained both for the full data set and separately for observations above and below 10 g/kg. An alternative reporting procedure was developed and is being implemented along with the newly modified WVSS-II sensors.

TEST RESULTS:

In addition to testing the engineering aspects of the WVSS-II systems discussed above, statistical evaluations were made of the performance of a variety of factors important for the optimal objective use of the aircraft data in combination with other data sources by assessing:

1) Similarity of reports from the different observing systems and different aircraft,

2) Biases between ascent and descent reports from individual aircraft,

3) Variability between different aircraft (to assess instrument calibration and effects of aging), and

4) Capability to capture sharp moisture gradients accurately, including as aircraft emerge from clouds.

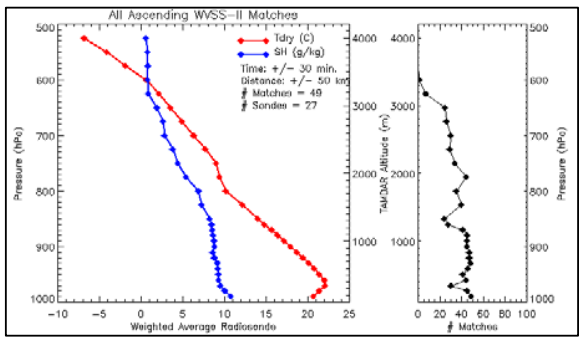

Figure 1 – Mean Temperature (red, more steeply sloped) and Specific Humidity rawinsonde profiles for test period. Data weighted by number of aircraft profiles matching each sonde.

The mean thermodynamic profiles for the test period (Fig. 1) for these night-time reports show generally uniform lapse rates, with two inversions, a shallow one near the surface and a second weaker capping one above 800 hPa. Comparisons of individual observations from different aircraft to rawinsonde data showed generally good agreement Note the close fit of data for the two different aircraft to the rawinsonde report in Fig. 2, including the rapid transition from moist to very dry conditions across the inversion at about 2400m altitude.

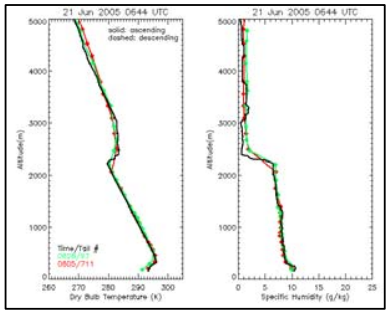

Fig. 2 – Sample comparisons of rawinsonde data (black) and individual aircraft reports of Temperature (left) and Specific Humidity (right) for 21 June 2005.

Overall statistical comparisons in Fig. 3 show very small biases between the two data sets. Root Mean Square (RMS) and Standard Deviation (SD) fits are around 1 g/kg for specific humidity, especially in the more stable areas of the lower troposphere in these night-time comparisons. The full nature of the increased differences above 800 hPa is not fully understood. However, it should be noted that this was both an area of increased atmospheric mixing (above the general trapping inversions present during the tests), lower water vapor content (note more apparent positive biases) and decreased WVSS-II reporting density, as well as where the aircraft-to-rawinsonde separation increased.

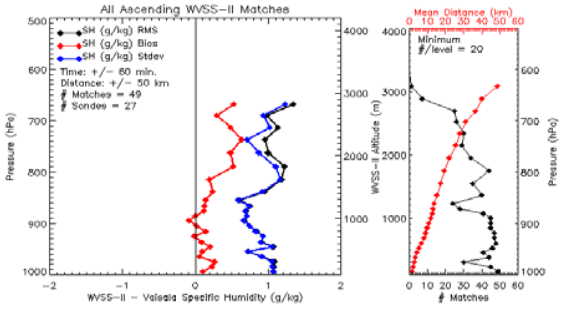

Fig 3 – Statistical comparisons of rawinsonde data with WVSS-II Specific Humidity observations from all ascending aircraft reports for a 2 week period in June 2005.

When the data are divided according to reporting precision, the results for observations below 10 g/kg improve significantly, while data subjected to larger truncations show much more variability. The results in figure 4 clearly show the effects of the reporting truncation differences. For values below 10 g/kg (left panels in Fig. 4), although the low-level bias has become slightly negative, the SD fit for these data approaches 0.5 g/kg in the boundary layer. Comparisons of Relative Humidity (RH) for these data (derived by combining aircraft moisture and raob temperature data, thereby preventing biases in the aircraft temperature reports to affect the RH calculations) show accuracies near 5%, meeting WMO requirements. By comparison, data above 10 g/kg (right panels in Fig. 4) show large positive biases and increased SDs, each ≥ 1 g/kg (the communications truncations limit for these data). It should be noted that this data transmission deficiency affected between 20 and 50% of the data below 800 hPa. Based on these findings, an alternative encoding scheme based on a scaled Mixing Ratio (q) raised to the 0.4 power ($q^{0.4}$) has been developed and is being implemented.

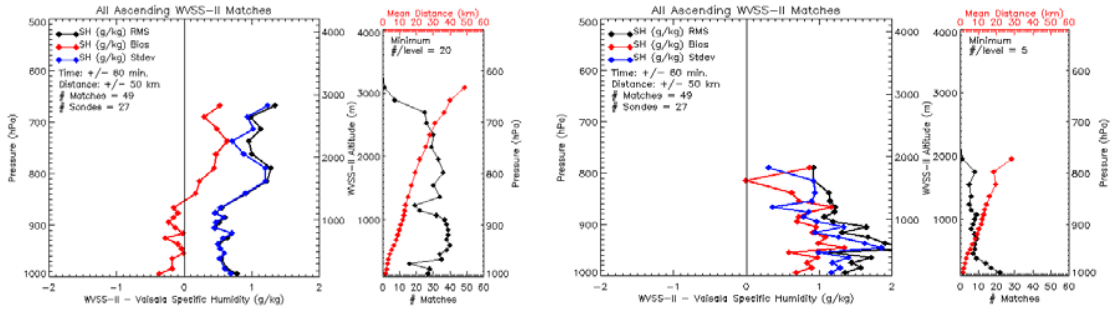

Fig. 4 – Statistical comparisons of rawinsonde data with Specific Humidity observations from ascending aircraft reports for the 2 week test period in June 2005. Left panels for WVSS-II reports < 10 g/kg, right panel for reports >10 g/kg.

SUMMARY:

Comparisons of aircraft based WVSS-II moisture reports to rawinsonde data show agreements as close as 5%, when engineering and processing limitations are restricted. An additional 2-week test is being scheduled this fall to revalidate the results using both ascent and descent data using systems modified to remove the previous engineering and communications deficiencies.

DETERMINING THE ACCURACY AND REPRESENTATIVENESS OF WIND PROFILER DATA

Ralph Petersen, and Kristopher Bedka
Cooperative Institute for Meteorological Satellite Studies, University of Wisconsin – Madison
E-mail: Ralph.Petersen@SSEC.WISC.EDU

INTRODUCTION:

CIMSS has begun to use data from the National Wind Profiler Network (NWPN) to determine the quality of mesoscale cloud motion wind derived from GOES data, as well as other wind data sets. The NWPN data have the potential advantage over all other comparison wind data sets available over the U.S. in that there are many more opportunities for matching the GOES wind data with the frequent wind profiler reports – *especially when the 6-minute data are used for validation.* However, before the 6-minute data could be used as a validation standard, a comprehensive analysis of both the quality and spatial/temporal representativeness of NWPN data was needed. If accurate, they may provide a good data alternative in data sparse areas (both in time and space).

As series of evaluation studies were conducted using a nearly one year long archives of Wind Profiler and high-resolution radiosonde data observed taken at the Lamont, Oklahoma ARM-CART site. The objective of these studies is to determine: 1) additional quality control needed for the 6-minute profile data, 2) spatial variability of wind reports, 3) temporal variability of wind reports, and 4) accuracy of Wind Profiler observations relative to the Radiosonde data. All of these pieces of information will also be essential for the optimal use of any types of wind observations in future mesoscale data assimilation systems and in designing observing system strategies.

QUALITY CONTROL OF 6-MINUTE NWPN REPORTS:

Operational ***hourly*** data from the NWPN are derived as a 'consensus averaging' of at least 4 observations from each "off-vertical" profiler beam which agree most closely during the past hour. Although data are corrected for vertical motion detected by the vertical beam and eliminated if the vertical motion exceeds certain limits, different data can be used in obtaining the averages for each of the two off vertical beams. Little Q/C information is included in the report transmitted to AWIPS or GTS. While the data used may have been observed at any time during the past hour, all *observations are labeled for the beginning of the next hour*, which can result in 'gaps' of as much as 45 minute between actual data averaging and reported observations time and can delay the time the data arrive at the user by up to an hour after the component observations were made.

By contrast, 6-minute data are available immediately on the web with proper time labels. However, only rudimentary quality control is currently used, which compares the most recent report with the previous 10 reports and excluded gross outliers. Detailed investigation of reports taken over individual days showed that while most of the reports showed good temporal consistency, in numerous occasions the wind direction changed scientifically between successive individual reports, then returning to values that were much more consistent with previous observations.

To address this problem, a two-sided quality control (QC) procedure was developed which rejects reports which exceeded limits based on two standard deviations of the ratio for previous reporting periods of the ratio:

$$\frac{(|\Delta V_{(T-(T-6))}| + |\Delta V_{((T+6)-T)}|)}{\sqrt[2]{|(V_{(T-6)} + 2V_T + V_{(T+6)}|}} = \frac{\text{Magnitude of vector change before and after the observation time}}{\text{Square root of mean wind for 3 successive reports}}$$

Using the new Q/C approach, the Vector RMS (VRMS) difference between individual 6 NWPD observation and those 6 minutes earlier and later was reduced by nearly 1 ms^{-1} at low levels, with ~95% of the data falling within 2 Standard Deviations at all levels. Fits between profilers and radiosondes (to be discussed later) were also improved by ~8%. VRMS fits between each observation and those 6 minutes earlier and later were improved by nearly 1 ms^{-1} at low levels, with ~95% of the data falling within 2 Standard Deviations at all levels. Fits between profilers and radiosondes (to be discussed later) were also improved by ~8%.

When applied to the total 10 month observing period, the Q/C technique eliminated a larger percentage of data at all levels when compared with 1-sided QC approach. It is noteworthy that ~60-70% of data were retained between 800 and 550hPa for the 'low-mode' profiler data (see Fig 1) and between 400 and 250 hPa for the 'high-mode' data – leaving a gap in good quality data between

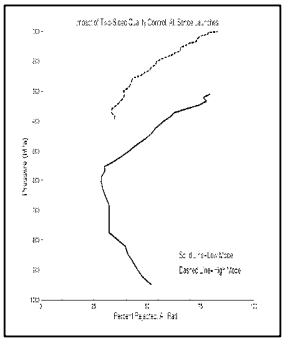

Fig. 1 – Percentage of 6-minute NWPD data rejected by 2-side QC by level.

550 and 400 hPa. Errors for the 6-minute low-mode data increase rapidly above 550 hPa and for high-mode above 250 hPa. On average, more 6-minute data are retained at all levels below 200 hPa than are used in hourly "consensus averaging". The QC results also showed diurnal variability, especially at low levels. Although the 2-sided QC rejects many more daytime data in the boundary layer, the technique rejects more at almost all levels. The largest increases in rejections between night and day are in the upper portion of the low-mode and lower portion of the high-mode data ranges. Explanations of this diurnal behavior are being investigated.

WIND DATA VARIABILITY AND ACCURACY TESTS:

For the wind variability/accuracy tests, six-minute frequency Profiler observations were matched in time and space with data from the radiosonde reports taken four times daily. Spatial variability was determined by creating a series of 10-25 km thick cylindrical 'tubes' around the Wind Profiler site and determining how the vector wind differences change with distance. The results in figure 2 show that the VRMS between reports increases with distance from 2.7 ms^{-1} at 5 km to 3.7 ms^{-1} at 45km for low-mode data and slightly larger values for high mode data within the first 50 km. At larger distances (and in this test higher levels), the VRMS differences increase nearly linearly from 3 ms^{-1} at 12 km to 6 ms^{-1} at 112 km.

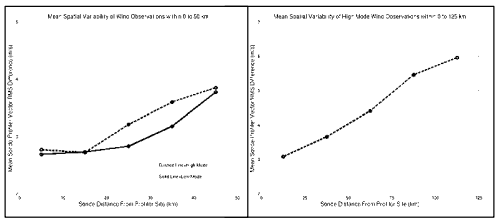

Fig. 2 – Variability of contemporaneous Profiler and GPS rawinsonde data for various observation

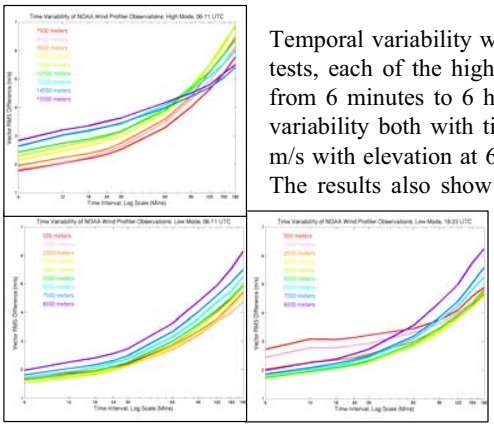

Fig. 3 – Variability by level of Profiler data versus time intervals (high-mode: top, night-time: left).

Temporal variability was determined by from the Wind Profiler data alone. In these tests, each of the high time-resolution Profiler reports is compared with data taken from 6 minutes to 6 hours from that time. The results show increases in temporal variability both with time and elevation, ranging from about 2.5 to greater than 4.5 m/s with elevation at 6 minutes and reaching over 10 m/s at some levels by 6 hours. The results also show significant diurnal variations at low levels, where increased mixing in the boundary layer due to diurnal heating nearly doubles the temporal variability from night to day. These results show that the time 'gap' between consensus averaging and "reported" time of standard hourly observation could add 0.5 to 1.0 ms-1 to the expected errors in the hourly profiler data when compared with correctly labeled 6-minute data, a 30-50% increase in error.

Accuracy tests were made using rawinsonde data located within 25 km of the profiler location and within 6 minutes of the profiler observations. Comparisons show mid-tropospheric VRMS differences of approximately 3 ms^{-1}, with larger differences nearer the earth's surface and farther aloft. The differences are similar for both the "Low Mode" and "High Mode" portions of the Profiler reports, even though the wind bias changes between the two reporting modes. Within the first 25 km, the variability is larger in the planetary boundary layer, but then decreases aloft and remains fairly constant. Above 600 hPa, where radiosonde balloon drift allows comparisons over greater distances, the differences in both the low-mode and high-mode data both show systematic increases in variability with distance at all levels. When the effects of atmospheric variability are removed, the NWPN data should show errors comparable to GPS radiosondes.

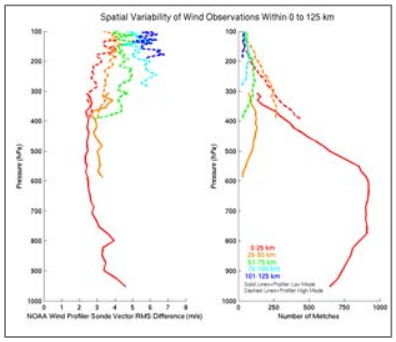

Fig 4 – Level-by-level variability of contemporaneous Profiler and GPS rawinsonde data for various observation separations (left-most line for ≤ 25 km)

SUMMARY:

Six-minute Wind Profiler data from the NWPN: *1)* Are of excellent value, *if* subjected to 2-sided quality control procedures, *2)* Improve upon current hourly NWPN data by removing the time 'lag' in labeling, thereby reduce errors by 0.5 to 1 ms^{-1}, *3)* Show good (and predictable) temporal and spatial continuity, with greater variability in the boundary layer during day, *4)* Agree extremely well with precisely co-located radiosonde data, and 5) Can provide a good option for obtaining data between conventional observations or in otherwise data sparse area.

INSIGHTS INTO THE VERTICAL DISTRIBUTION OF OZONE OVER EASTERN EQUATORIAL AFRICA BASED ON OZONESONDE OBSERVATIONS

William Ayoma[1], Gilbert Levrat[2] and Bertrand Calpini[2]

[1] Kenya Meteorological Department, P.O. Box 30259, Nairobi, Kenya (wayoma@yahoo.com)

[2] MeteoSwiss, Aerological station Payerne, CH-1530 Payerne, Switzerland

Abstract: We present an analysis of 8 years of weekly ozone soundings conducted over Nairobi, Kenya (1˚ 18S, 36˚ 45´E, 1795m asl). The average vertical profile of ozone indicates that the tropopause is located at an altitude range of 14 to 16km asl depending on the seasons of the year, and the maximum ozone values occurs at 26-28km. A statistical analysis of ozone profiles split into 3 layers reveals strong yearly variation in the free troposphere and the tropopause region, while ozone in the stratosphere appears to be relatively constant throughout the year. Total ozone measurements by Dobson and Microtops instruments confirm maximum total ozone content during the short-rains season and a minimum in the warm-dry season, a result in good agreement with TOMS satellite data.

Keywords- Ozonesonde, SHADOZ, Ozone Variability

1. INTRODUCTION

Nairobi is located close to the equator in Eastern Africa, and corresponds to a unique site location for the detection of ozone in tropical region: the Nairobi Ozonesonde Observatory of the Kenyan Meteorological Department (KMD) was put in operation 8 years ago and has since that time operated ozone soundings on a weekly basis. This work is an important contribution to the WMO Global Atmospheric Watch (GAW) programme and SHADOZ ozone sounding network (http://croc.gsfc.nasa.gov/shadoz/).

The vital roles of ozone in the atmosphere have demonstrated the need for precise long-term measurements as well as a quantification of the short-term vertical variability of ozone. The temporal and spatial variability of the vertical profile of ozone from Nairobi, which enhances our understanding of the dynamics of ozone in the atmosphere, has not been conducted so far. This forms the basis of the present study.

2. RESULTS AND DISCUSSION

Figure 1 shows the "seasonally" averaged ozone profile over 8 years of data, for each of the 4 seasons of the year, respectively: the long-rains (March-May), short-rains (October-December), warm-dry (December-February) and cold-dry (July-August) seasons.

In order to highlight the variation of ozone versus altitude, we define somewhat arbitrarily three layers:

- The "free troposphere" (#1) is chosen between 3 and 12km asl. The data between 1795 and 3000m asl are not considered thus avoiding any direct ozone reaction/formation induced by primary pollutants from the city of Nairobi.
- The "tropopause region" (#2) is selected between 12-20km in order to ensure the full coverage of the tropopause height at any time of the year.
- The "stratosphere" region (#3) is selected between 20-32km thus ensuring most of the ozone profile as valid data in the statistical analysis (balloon burst at typ. 35km).

In layer #1, the seasonally averaged vertical ozone profiles show the highest ozone concentration at an altitude of 5 km during the cold-dry season. The magnitude of this relative maximum is related to biomass burning. In layer #3, the lowest ozone concentration is observed during the warm-dry season at an altitude of about 26km. Several studies in the tropics have drawn similar results of ozone vertical distribution (IPCC 1994)

In *figure 2*, we define the *Mean* ozone as the integrated averaged ozone concentration (in nbar) over the entire altitude range of the considered layer, and over 8 years of data. Each data point in *figure 2* corresponds to the relative *monthly* value (in %) by taking the difference between the monthly integrated averaged ozone concentration (typ. 4 profiles per month) and the *Mean*, and dividing by the *Mean*. Thus the results in *figure 2* are given in relative unit (%), with the absolute *Mean* indicated for each layer directly in the figure.

3. CONCLUSION

As a first output of this analysis, the relative ozone variability in the "stratosphere" is weak, thus indicative of small changes in the ozone concentration in the stratosphere over Nairobi during the last 8 years.

On the contrary in the "free troposphere" and "tropopause" regions we observe significant changes: up to 40% of peak to peak variation with a well defined yearly cycle. The lowest ozone monthly values are measured in February during the warm-dry season, and the highest in August-September during the cold-dry to short-rains season. Variability is attributed to biomass burning and turbulent air motions (Ilyas, 1991).

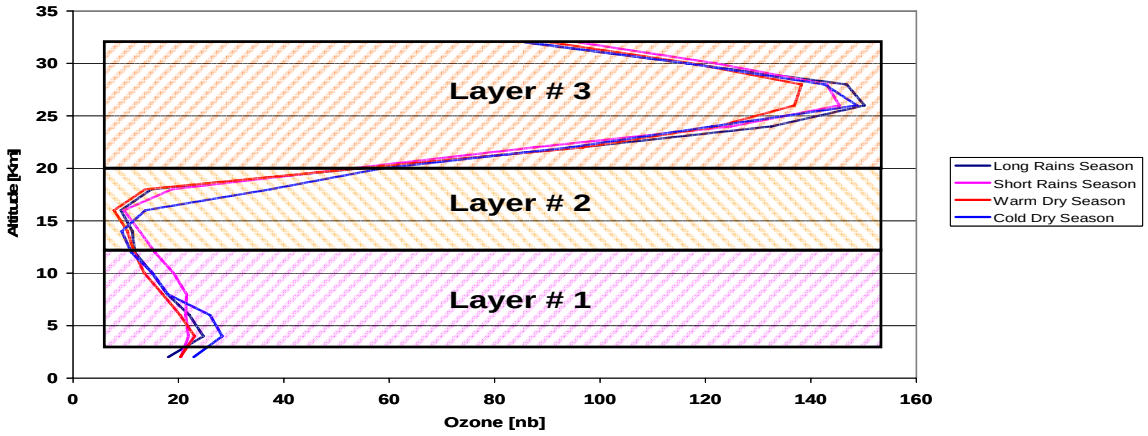

Figure 1*. Mean "Seasonally averaged" ozone profile over Nairobi based on 8 years of ozone sounding, for respectively long-rains, short-rains, warm-dry and cold-dry season.*

Figure 2*: Relative Ozone variability at three different altitude ranges over Nairobi, Kenya (see text for further details)*

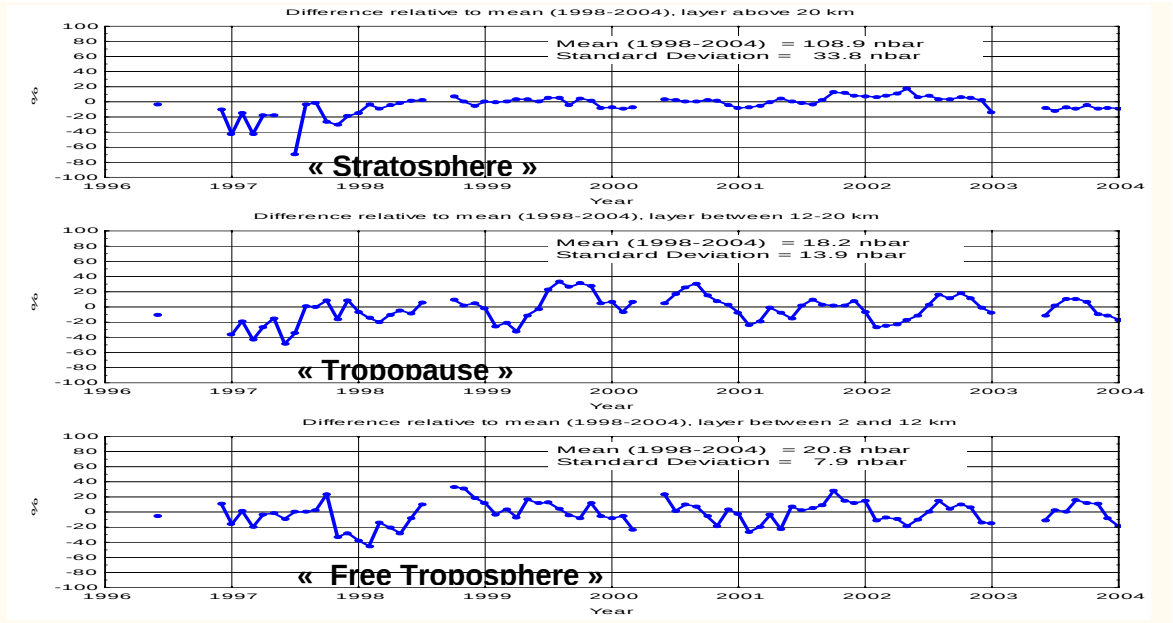

REFERENCES

Ilyas, M., 1991: Ozone depletion. Implications for the tropic. Published by University of Science Malaysia and UNEP, For International Conference on Tropical ozone change, Feb. 20-23, 1990.

IPCC, 1994: Radiative forcing of climate change. The 1994 report of the scientific assessment working group of IPCC.

Thompson, A., 2002. Variability in Tropical Tropospheric ozone: The climate-Dynamical connection observed in SHADOZ ozonesondes. Geophysical Research Abstract.

The added value of prospective spaceborne Doppler wind lidar for extreme weather events

Gert-Jan Marseille[1], Ad Stoffelen, and Jan Barkmeijer

[1] Royal Netherlands Meteorological Institute (KNMI), De Bilt, The Netherlands
E-mail: *Gert-Jan.Marseille@knmi.nl*

Abstract: Lacking an established methodology to test the potential impact of prospective extensions to the meteorological global observing system (GOS) in real atmospheric cases we developed such a method, called Sensitivity Observing System Experiment (SOSE). For example, since the GOS is non uniform it is of interest to investigate complementary observing systems filling its gaps. Unlike full observing system simulation experiments (OSSE), SOSE can be applied to real extreme events that were badly forecast operationally and only requires the simulation of the new instrument. We apply SOSE to the 2nd 1999 Xmas storm "Martin" over Europe and show that an extended GOS by a tandem of spaceborne Doppler wind lidars would have improved the forecast substantially.

Keywords - *SOSE, Doppler wind lidar, Christmas storm*

1. INTRODUCTION

Many resources are spent on new observation types complementing the GOS or its climate equivalent GCOS. This paper presents a new and relative cheap method to assess the added value of additional observations for Numerical Weather Prediction (NWP), named Sensitivity Observing System Simulation Experiment (SOSE). SOSE requires only the simulation of the new instrument and as such it is relatively easy to test various observation strategies culminating in observation requirements for prospective observing systems for instance to sample meteorologically sensitive areas that are otherwise not measured. These sensitive areas are generally associated with atmospheric structures that tend to grow rapidly in time potentially causing forecast failures already on the short term (up to 2 days).

2. SOSE - Sensitivity Observing System Experiment

Impact assessment of prospective observing systems requires a synthetic true atmospheric state for the simulation of the new instrument. This atmospheric state is denoted pseudo-truth and should fulfil the following requirements: (i) it corrects the incorrect analysis, (ii) it improves the 2-day forecast, (iii) it is compatible with observations from existing observing systems and (iv) its spatial structures must be realistic. The pseudo-truth is subsequently used for the simulation of the future observing system under investigation and when the new observing system is capable of (partly) observing the analysis corrections, it will contribute to improve the 2-day forecast. Figure 1 presents a scheme to determine the pseudo-truth based on adjoint first-guess sensitivity structures and fulfilling the stated requirements above.

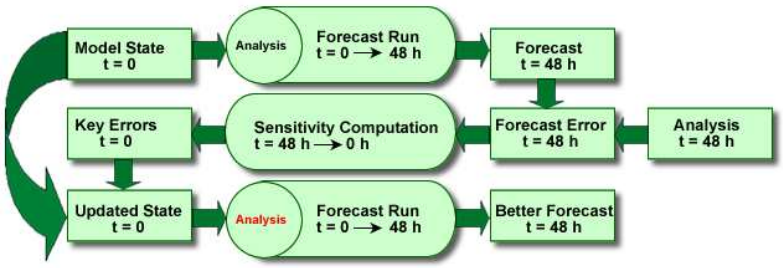

Figure 1: First-guess sensitivity experiment. The updated (red) analysis provides the SOSE pseudo truth.

3. PROSPECTIVE SPACEBORNE DOPPLER WIND LIDAR

The European Space Agency (ESA) is preparing to fly a spaceborne Doppler wind lidar (DWL) for the first time in history within the Atmospheric Dynamics Mission (ADM) named Aeolus (ADM-Aeolus).

The scheduled launch is end of 2008. ADM is a polar orbiting satellite giving a global three-dimensional coverage of single line-of-sight wind components. Anticipating on the success of ADM there is need for wind observation requirements to define an operational network of lidars in the post-ADM era beyond 2011. In a recent study by (Marseille et al., 2006) a number of possible scenarios were considered, including a dual-perspective scenario measuring the full wind vector and a tandem scenario giving double the coverage of ADM, see Fig. 2.

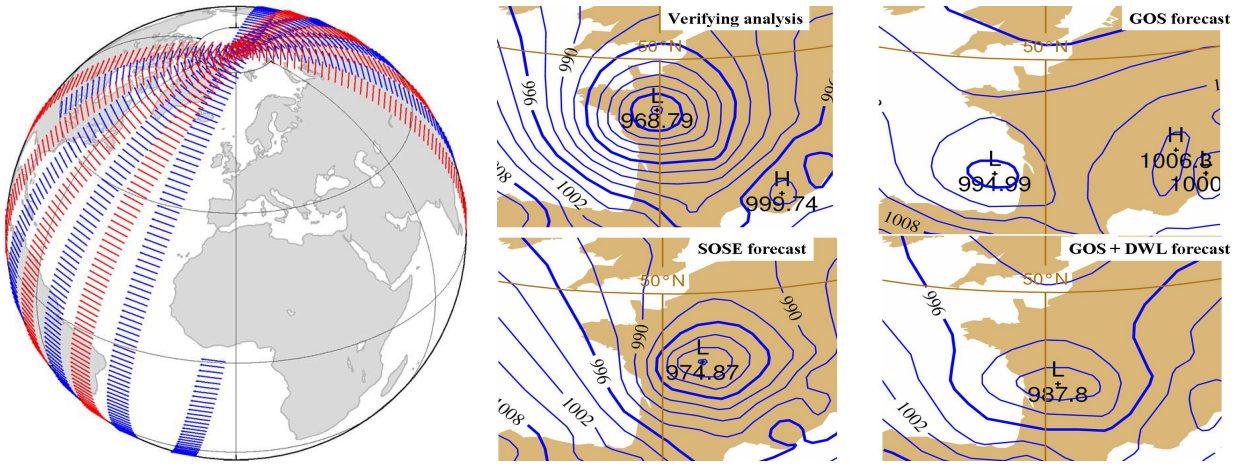

Figure 2: Left, data coverage of a tandem-Aeolus scenario. The arrows show the locations of the measured wind profiles and the direction of the line-of-sight wind components. Blue arrows correspond to ADM, the red arrows show the added coverage in case of flying two Aeolus-type satellites in tandem, separated by half an orbit. Right, ECMWF mean sea level surface pressure at 27/12/1999 18UTC from the verifying analysis (upper left), forecast using the 2003 model version and all available observations (upper right), best achievable forecast from SOSE analysis (lower left), see Fig. 1, and same forecast as upper right panel but now including DWL observations from the tandem-Aeolus scenario (lower right).

4. APPLICATION TO THE XMAS'99 STORM "MARTIN" OVER EUROPE

The SOSE method has been applied to the Xmas'99 storm "Martin" that caused large damage over Europe on 27/28 December 1999. For this purpose, SOSE was run in cycling mode to generate a series of pseudo-truths at 6 hour resolution starting on 23/12 12UTC, i.e. 54 hours before the forecast initiated at 25/12 18UTC. DWL observations were simulated over this 54 hour period and assimilated in the ECMWF operational model in conjunction with real observations from the 1999 operational network. Fig. 2 shows a substantial improvement of the 2-day forecast verifying at 27/12 18UTC by extending the GOS with DWL observations.

Besides a deterministic forecast, an ensemble forecast of 50 members was run for the NoDWL (using the GOS only) and DWL (using GOS+DWL) experiments. For NoDWL 5 out of 50 members included a storm over France against 15 members for DWL, showing a substantial improvement of forecasting the storm in the presence of DWL observations.

5. CONCLUSION

The potential added value of global wind observations from a prospective spaceborne Doppler wind lidar scenario was demonstrated in a Sensitivity Observing System Experiment (SOSE) applied to the Xmas'99 storm "Martin". SOSE is a relatively cheap tool to assess the added value of prospective extensions to the GOS, requiring the simulation of only the new instrument under investigation.

REFERENCES

Marseille, G.J., Stoffelen, A., Barkmeijer, J., 2006: PIEW - Prediction Improvement of Extreme Weather, ESA final report, contact no, 17112/03/NL/MM

EFFORTS TO IMPROVE THE ASSIMILATION AND ANALYSIS OF SATELLITE-DERIVED WINDS

Howard Berger and Christopher Velden

Cooperative Institute for Meteorological Satellite Studies, University of Wisconsin, Madison, WI, USA
E-mail: *howard.berger@ssec.wisc.edu*

1. INTRODUCTION

Atmospheric motion vectors (AMVs) are derived by tracking cloud and water vapor features through a sequence of satellite images (Velden et al. 2005). Most numerical weather prediction (NWP) centers around the globe assimilate AMVs into their models. Although AMVs have shown positive impact on NWP forecasts, quality control and vector height assignment issues remain. The complex nature of AMV observations has made it difficult to accurately assess the true observation error: information that is crucial for data assimilation. To help address this question, we will describe experiments in progress at CIMSS aimed at exploring the application of a new AMV quality indicator.

2. THE "EXPECTED ERROR" AMV QUALITY INDICATOR

The Expected Error (EE) is a new AMV quality identifier that was originally developed by Dr. John LeMarshall whilst at the Bureau of Meteorology in Australia. It is essentially an extension of the currently available Quality Indicator (QI) developed at EUMETSAT, but provides an output in the form of most likely (expected) root-mean square (RMS) error for each vector. To calculate the EE for an AMV, the five vector consistency tests that make up the QI, along with the AMV's speed, pressure, and an NWP model vertical temperature gradient and wind shear surrounding the observation are needed. These values are regressed against co-located AMV – RAOB (regional) vector differences over two-month periods to develop regression coefficients, which are used to calculate real time AMV EEs.

Figure 1 shows a comparison of the actual (measured) AMV – RAOB RMS differences as binned by the new EE (red curve, lower x-axis) and the existing QI (blue curve, upper x-axis) for an AMV dataset spanning a 3-month period in 2006. For example, the red point corresponding to an EE of 5.0 m/s represents all winds that have calculated EEs between 4.5 and 5.5 m/s. The numbers at each point correspond to the number of observations in each bin. As the figure shows, the actual error range for EEs between 3 (high quality) and 7 (lower quality) ms^{-1} varies from about 3.9 to about 6.9 ms^{-1}. For this same AMV dataset, the actual error for QIs ranging from 1.0 (high quality) to 0.5 (lower quality) only varies from 4.5 to about 5.5. This suggests that the EE may be a better measure of AMV quality than the QI. An ideal EE indicator would fall on the dashed 1-1 line shown in the plot.

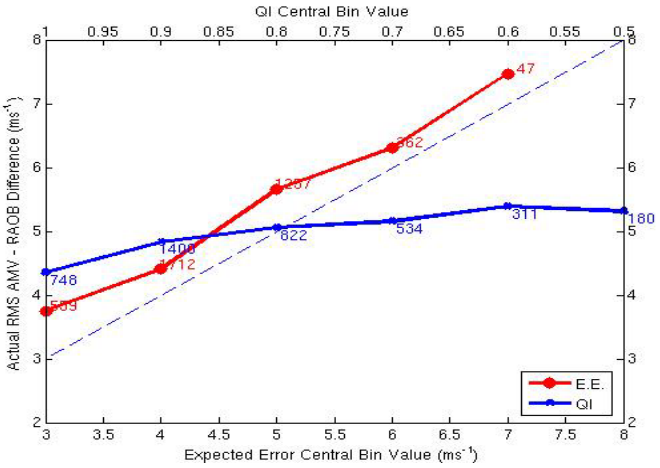

Figure 1. Comparison of the Expected Error (EE, solid red curve) AMV quality identifier with the current operationally employed AMV Quality Indicator (QI, solid blue curve) for operational GOES-E IR AMVs during Aug-Oct 2006. Actual RMS differences between collocated AMV – RAOB matches are used to assess each parameter as a quality indicator. As the curves show, the EE relationship is a better predictor of measured AMV – RAOB differences than the QI. The 1-1 line (dashed blue) is plotted for reference.

3. INITIAL DATA IMPACT EXPERIMENTS

Before testing the impact of the EE as a potential data assimilation aide, it is first worth examining the impact that the operational GOES AMVs have on NWP forecasts. It should be noted that the operational assimilation of GOES AMVs in the NCEP GFS does not currently make use of any AMV quality indicators. This baseline can then be used to compare the impact of any additional AMV data sets, and the EE as a possible data thinning or assimilation aide.

The operational GOES IR and water vapor AMVs were removed from a T126 version of the NCEP's GFS global model for a period from July 28th, 2005 through October 28th, 2005. The results from these NO-AMV experiments are then compared to a control run that include the assimilation of the operational AMVs, and show that although the AMV impact is small, it is positive. Global anomaly correlations from 200hPa u-component winds (not shown) are higher for the CNTRL (AMVs included) run as compared to the NO-AMV runs. These differences, however, are not statistically significant.

The GOES AMVs do, however, significantly improve the GFS model forecasts of Atlantic hurricane tracks. Table 1 shows the track forecast errors (in kilometers) for the two experiments. The CNTRL experiments including the assimilation of GOES AMVs have, on average, lower track error at all forecast times. The forecast times in bold indicate results that are statistically significant at a 99% level. It is reasonable to suspect that the AMVs are better observing the tropical wind fields, particularly over the oceans, thus better capturing the steering currents that determine hurricane tracks. This result is examined in more detail in the poster.

Forecast Time (hrs)	12	24	36	**48**	**60**	**72**	**84**	**96**	108	120
CNTRL (km)	87.6	125.9	162.2	187.3	229.4	264.6	311.4	373.2	467.0	549
NO-AMV (km)	91.0	131.7	167.0	205.4	257.9	312.0	367.7	429.0	520.7	607.9
Number of Cases	89	81	69	65	56	55	50	48	41	39

Table 1. Hurricane track forecast errors (km) as a function of forecast time. The CNTRL (experiment with operational AMVs) has a lower track error than the NO-AMV experiment for all times. The forecast times in bold indicate results that are statistically significant at a 99% level.

4. PLANNED DATA IMPACT EXPERIMENTS

With the baseline experiment described above completed, we can now proceed to test the impact of the AMV EE in the data assimilation process. These tests will be done using GOES Rapid-Scan (RS) AMVs obtained during the 2005 and 2006 North Atlantic tropical cyclone seasons. For the RS AMVs, EEs are produced using static coefficients generated from the operational AMVs as described in the previous section. Two data impact experiments will be carried out during selected time periods. One experiment will assimilate all of the RS AMVs into a GFS NO-AMV analysis. A second will then assimilate the RS AMVs using the EE as a threshold to quality control the data. These experiments will be compared through resulting forecast accuracy, with a particular focus on their performance with tropical cyclone tracks.

5. SUMMARY

This study first shows that the expected error (EE) index can be a useful measure of Atmospheric Motion Vector quality. Through baseline experiments with the GFS model, we have then shown that AMVs do make a positive impact on forecast skill, particularly with tropical cyclone tracks. Our next step will be to examine the impact of high-temporal resolution GOES rapid-scan AMVs using the EE as a measure of observation quality on GFS forecasts. The poster will provide more details about the EE and the baseline data denial experiments. It will also give an update on the progress of our planned data impact experiments.

Acknowledgements: *Thanks to Dr. John LeMarshall for providing the initial EE software. This study is being supported by NOAA Thorpex funding, under the management of John Gaynor and Zoltan Toth (NOAA).*

REFERENCES

Velden *et al.* 2005: Recent Innovations in Deriving Tropospheric Winds from Meteorological Satellites. Bull Amer. Meteorol. Soc. **2** 205-223.

STATISTICAL RELATIONSHIPS BETWEEN SATELLITE-DERIVED ATMOSPHERIC MOTION VECTOR, RAWINSONDE, AND NOAA WIND PROFILER NETWORK OBSERVATIONS

Kristopher M. Bedka[1], Christopher S. Velden[1], Ralph A. Petersen[1], Wayne F. Feltz[1], and John R. Mecikalski[2]

[1] Cooperative Institute for Meteorological Satellite Studies, University of Wisconsin, Madison, WI USA
[2] Atmospheric Science Department, University of Alabama in Huntsville, Huntsville, AL USA

Abstract: Vector difference statistics and height assignment characteristics of NOAA/NESDIS operational (OPER) and experimental mesoscale (MESO) atmospheric motion vectors (AMVs) are evaluated using NOAA Wind Profiler network and rawinsonde observations. OPER AMVs, which have much tighter correspondence to a NWP-based first-guess wind field, exhibit closer agreement with Profiler and sonde than those produced through MESO AMV processing settings. MESO AMV processing requires a greatly reduced dependence on the first-guess, contributing to enhanced flow detail, at the expense of increased noise in the vector field. Evaluation of AMV height assignment reveals that OPER AMVs show better agreement with a layer-mean motion compared to traditional single-level assignment. These findings are quite relevant to the data assimilation community, who treat AMVs as point measurements in space, similar to wind observations by sonde or aircraft.

Keywords – *Satellite-derived winds, AMV, NOAA Wind Profiler, data assimilation, rawinsonde, height assignment*

1. INTRODUCTION

Satellite-derived AMVs are used in a wide variety of meteorological applications such as NWP model data assimilation, tropical cyclone analysis and forecasting, and convective weather nowcasting. Thus, it is important to understand the vector error and height assignment characteristics of the remotely sensed wind estimates, such that they can be effectively understood and properly utilized within these applications.

Within this study, two types of AMVs produced by the UW-CIMSS algorithm (Velden et al. 2005) are compared with NOAA Wind Profiler and rawinsonde observations. Through the combination of these datasets, we can: 1) evaluate the feasibility of using 6-minute resolution Wind Profiler observations as a "truth" standard for wind validation, and 2) understand the speed, direction, and height assignment characteristics of satellite winds over a variety of cloud types and flow regimes. Topic 1 is covered at this meeting by Petersen and Bedka, and topic 2 will be discussed within this paper and poster presentation.

2. DATASETS

GOES-12 OPER and MESO AMVs near the Lamont, OK Wind Profiler site were collected over a one year period from April 2005-2006, providing a database of 15332 MESO and 1132 OPER visible (VIS), water-vapor (WV), and infrared window (IR) channel vectors. MESO AMV processing is designed to depict highly detailed flow regimes through the tracking of smaller cloud and WV features, adjustment of QC settings that were developed to satisfy a coherent AMV field for larger-scale flow regimes, and a reduced impact of a background wind analysis on the resulting AMV field. The primary application of MESO AMVs is the monitoring of cloud growth trends which are used to nowcast convective storm initiation (Bedka and Mecikalski, 2006). 6-minute resolution data from the Lamont, OK 404 MHz NOAA Wind Profiler are compared to GOES AMVs to validate AMV wind speed and direction. The Wind Profiler provides stable, well-calibrated, high temporal resolution observations, which allow for a large sample size of co-located AMV-Profiler data. A detailed evaluation of Wind Profiler error characteristics at the Lamont, OK site is shown within this meeting by Petersen and Bedka.

An expansion of the above study involves a comparison of 3.5 years of OPER AMV data to ARM SGP rawinsonde observations, which are averaged over increasing depths of the atmosphere (10 to 400 hPa in layer thickness) to evaluate whether flow depicted by an AMV best corresponds to a single level or layer-mean motion. This is investigated for the various height assignment techniques (IR window, CO_2 slicing, WV absorption, histogram) that are used within the UW-CIMSS algorithm in clear-sky and cloudy conditions.

3. RESULTS

Figure 1 shows a comparison between Profiler and AMV wind vectors for the one year period described above. OPER AMVs yielded far fewer matches, but exhibit much closer agreement with Profiler wind observations. These results are to be expected, as the OPER AMV processing method incorporates a high degree of vector editing and QC. These post-processing techniques provide more "accurate" wind estimates on average, but do not allow the OPER AMVs to capture the level of detail contained within the MESO fields (see Bedka and Mecikalski, 2006). Positive speed bias indicates that both AMV processing schemes estimate speeds that are faster (< 1 ms^{-1}) than those observed by the Profiler. Higher mean OPER wind speeds reflect that the majority of OPER AMV-Profiler data matches originate from upper-level (< 400 hPa) IR and WV vectors, whereas a high percentage of MESO matches correspond to slower low-level VIS vectors.

AMVs are also separated by wind speed and QC parameters for comparison to Profiler winds. Results show that slow AMVs (< 10 ms^{-1}) exhibit directional RMS differences that are far above average, possibly related to image navigation errors. High speed AMVs exhibit very low directional RMS but higher speed RMS and positive

speed biases (AMV faster than Profiler). AMVs with higher quality indicator (QI) scores exhibit closer AMV-Profiler agreement. In summary, one must decide whether better overall vector accuracy (OPER method) or increased flow detail (MESO method) would better suit his/her AMV application.

Figure 2 shows the results of a "layer of best fit" analysis for GOES-12 OPER AMVs. The minimum vector RMS value along each curve corresponds to the atmospheric depth for which a given set of AMVs exhibits best agreement. The upper-left panel of Fig. 2 shows that motions depicted by GOES-12 low-level IR window AMVs best correspond to a layer of 100 hPa in depth. Layer-mean flow of this depth improves agreement by ~.5 ms^{-1} over AMV-sonde differences found at the single level height assignment (see points along y-axis). Motions depicted by upper-level IR window and cloud WV channel vectors correspond to a much shallower layer of 40-60 hPa in depth. Clear sky WV motions correspond to a far deeper layer, spanning 150 to 225 hPa in depth.

The authors attribute the differences in layer of best fit depth between low and upper-level AMVs to the type and vertical extent of cloud/WV features being tracked, in addition to the vertical wind shear characteristics found within these layers. Cumulus cloud features are often tracked in VIS and shortwave IR channel imagery, whereas cirrus are the dominant cloud type tracked in WV and, to a lesser extent, IR imagery. Cumulus clouds have a greater vertical depth than cirrus, requiring flow over a deeper layer to advect them through an image sequence. Cirrus, on the other hand, are often quite thin and are advected by strongly sheared flow of a shallow layer in the upper-troposphere. Motions observed in the clear-sky WV originate from radiance contributions over a broad atmospheric depth, modulated by the structure of the GOES-12 WV weighting function.

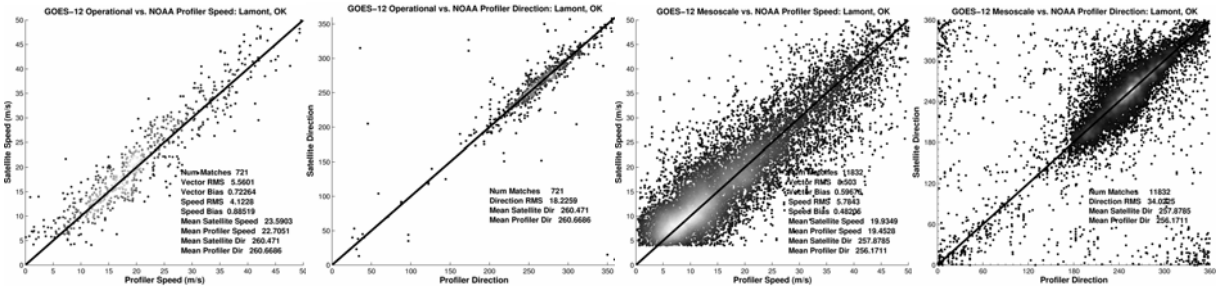

Figure 1. A comparison of OPER AMV wind speed (left), and direction (middle-left), and MESO AMV wind speed (middle-right), and direction (right) to NOAA Wind Profiler observations over the one year study period. Regions of higher scatterpoint density are colored by lighter greyscale tones.

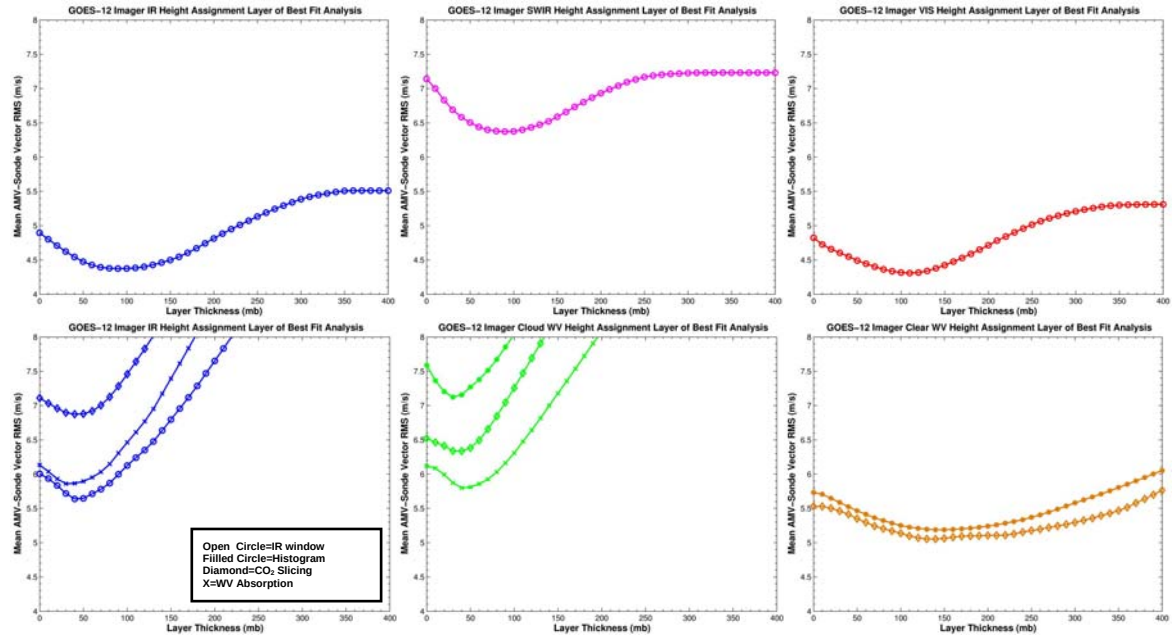

Figure 2. Layer of best fit analysis for GOES-12 (top row) 1000-600 hPa IR window (left), shortwave IR (middle), and VIS (right) AMVs. (Bottom row) 600-100 hPa IR window (left), cloudy WV (middle), and clear-sky WV (right) AMVs. AMV-sonde differences at the single-level AMV height assignment are plotted on the y-axis.

REFERENCES

Bedka, K. M., and J. R. Mecikalski, 2006: Application of satellite-derived atmospheric motion vectors for estimating mesoscale flows. *J. Appl. Meteor.*, **44**, 1761-1772.

Velden C. S.., J. Daniels, D. Stettner, D. Santek, J. Key, J. Dunion, K. Holmlund, G. Dengel, W. Bresky, and P. Menzel, 2005: Recent innovations in deriving tropospheric winds from meteorological satellites. *Bull. Amer. Meteor. Soc.*, **86**, 205-223.

AN OVERVIEW OF THE THORPEX PACIFIC ASIAN REGIONAL CAMPAIGN

Patrick A. Harr [1], David B. Parsons [2], Istvan Szunyogh[3], Tetsuo Nakazawa[4]

[1] Naval Postgraduate School, Monterey, CA USA
E-mail: paharr@nps.edu
[2] National Center for Atmospheric Research, Boulder, CO USA
[3] University of Maryland, College Park, MD USA
[4]Meteorological Research Institute/ Japan Meteorological Agency, Tsukuba, Japan

Abstract: The THORPEX Pacific Asian Regional Campaign (T-PARC) is a major international collaboration focusing on advancing knowledge and improving prediction of i) downstream high-impact weather events over North America, the Arctic and other locations whose dynamical roots and/or forecast errors are driven by aspects of the lifecycle of typhoons and other intense cyclogenesis events over eastern Asian and the western Pacific, and ii) the lifecycle of tropical cyclones over the western Pacific from genesis to extratropical transition/decay.

Keywords – *THORPEX, tropical cyclones, extratropical transition, Rossby waves, predictability*

1. INTRODUCTION

Recent research suggests that the region of the western North Pacific plays an important and unique role in defining many characteristics of the midlatitude circulation of the Northern Hemisphere. Over the western and central North Pacific, baroclinic energy conversion generates a large amount of kinetic energy that is instrumental in maintaining the storm tracks downstream over the eastern North Pacific, North America, and North Atlantic (Chang and Yu 1999; Orlanski and Sheldon 1995). This implies that many of the high-impact weather events that occur over North America have a dynamical origin upstream over the western North Pacific basin. Furthermore, forecasts of downstream developments in the storm track over the eastern North Pacific that impact western North America often contain large errors. Therefore, it is hypothesized that increased understanding of the dynamical linkages between development of high-impact weather events that occur over North America to specific weather systems upstream over the western North Pacific will lead to a significant increase in forecast skill of the downstream events.

2. SCIENCE OBJECTIVES

The scientific framework for PARC addresses the relationships between development of high-impact weather events over North America and upstream sources over the western North Pacific and eastern Asia. While the upper-tropospheric wave packets provide a dynamical link between North America and the western North Pacific, the primary PARC hypotheses address the mechanisms that act to initiate wave packets and their role(s) in downstream predictability. An increase in understanding of the primary upstream forcing mechanisms and their variability will lead to increased predictability via strategies for adaptive control of the observing network and development of data assimilation techniques to best represent the important physical mechanisms. Hakim (2005) demonstrated that upper-tropospheric, eastward-propagating wave packets are a dominant source of forecast errors over the North Pacific. Furthermore, the forecast error patterns move with an eastward group velocity of about 30^{o}-40^{o} per day, which means that the leading edge of increased forecast error can reach western North America in about 3 days and the Great Lakes region in 4-5 days.

Based on the above, a primary objective of T-PARC is improved understanding of the dynamics and factors that limit the regional and downstream predictability of high-impact weather events (e.g., persistent deep convection, typhoons, extratropical transition events, and other intense cyclogenesis events) that occur over the North Pacific and adjacent land areas. Related to this objective is the requirement for increased understanding of forecast error growth and the role of scale interactions in the numerical forecast models that are used for prediction. Forecast error is closely related to initial conditions such that there is a need to develop, advance, and evaluate data assimilation strategies in concert with superior utilization of satellite measurements with the goal of improving prediction of high-impact weather events over the Pacific Rim and downstream locations. Related to this objective and the fact that often errors originate over regions that are void of conventional observations there is the need to quantitatively predict the reduction in forecast error variance due to supplemental/targeted observations and to test new strategies and observational systems for adaptive observing and modeling. The T-

PARC presents a potential for advancing operational forecasting and societal needs, which are addressed as objectives to improving the interpretation and utility of ensemble forecast systems, and increase understanding and improve society's response to weather disasters, including the appropriate use and evaluation of probabilistic information, and estimating the "value" to society that results from improvements in forecast skill.

3. STRATEGY

The general observational framework proposed for the international T-PARC program represents a combination of observational platforms and collaborative experiments that will be utilized to observe the structure and evolution of i) the primary Asian/North Pacific wave guides; ii) high impact events (heavy rainfall, tropical cyclones and extratropical cyclogenesis) that take place over the western North Pacific and East Asian region that interact with these wave guides. Such an ambitious measurement strategy can only be reasonably accomplished with the level of international collaboration envisioned in the late summer of 2008. The experimental design for T-PARC addresses its primary objective for three phenomena: (1) A tropical measurement strategy is designed to examine the large-scale variability in the circulation of the tropical western North Pacific as it relates to enhanced and reduced periods of wide-spread deep convection, tropical cyclone formation and the variations in intensity and track as the systems move to the northwest. Facilities utilized for the tropical component include i) driftsonde systems released from an island (e.g., Wake Island or another suitable site) in the tropical western North Pacific during two periods in May/June and September 2008, and ii) aircraft measurements from dropsondes and radar during September and October 2008. (2) The measurement strategy for the extratropical transition (ET) and downstream impacts is based on the poleward movement of a decaying tropical cyclone and the resulting intense cyclogenesis that results from its interaction with the midlatitude circulation. It will also take place during September and October 2008. The ET process illustrates clearly the need for a tropical-to-extratropical measurement strategies as the predictability of an ET event depends on the intensity and structure of the tropical cyclone, where and when the tropical cyclone arrives in the middle latitude westerlies and the characteristics of the middle latitude wave guide that impact the ET cyclogenesis and the downstream propagation and evolution of the wave packets. Facilities during this phase of T-PARC include i) the NRL P-3 near the interface where the decaying tropical cyclone interacts with the middle latitude flow and ii) the Gulfstream-V High Performance Instrumented Airborne Platform for Environmental Research (HIAPER) aircraft with GPS dropsondes near this interface and in the middle latitude flow where the impacts are observed. An important component of the HIAPER measurement strategy will be the incorporation of the Deutsches Zentrum fur Luft- und Raumfarhrt (DLR) wind lidar. (3) The third measurement strategy focuses on intense extratropical [winter] cyclogenesis in the primary Asian wave guide. Facilities will include driftsonde deployed from Japan for a four week period during November /December 2008.

4. SUMMARY

Observations collected during T-PARC will be used in concert with an unprecedented variety of numerical models, which includes research modeling and assimilation systems together with access to the members of the ensemble forecasts of all the major operational centers through the THORPEX Interactive Global Grand Ensemble (TIGGE). Thus, unlike past weather experiments, T-PARC will be able to readily include the probabilistic nature of the forecast problem, rather than examination of a few deterministic forecasts from research and operational models. TIGGE will provide some insight into the initial condition and model errors, while essentially assuring a strong link between the research and operational communities. An important aspect of TIGGE is that the data set will include both model variables and derived fields of interest to the user community (e.g., potential vorticity, Convective Available Potential Energy, Convective Inhibition, etc) turning the operational data into an even more valuable research data set. An augmented satellite-based observing strategy is also envisioned during T-PARC.

Acknowledgements: *Support from the National Science Foundation, Office of Naval Research, Marine Meteorology Program, and the World Meteorological Organization is gratefully acknowledged. The WMO and THORPEX-IPO provide financial assistance for the publication of the STISS proceedings volume.*

REFERENCES

Chang, E. K. M., and D. B. Yu, 1999: Characteristics of wave packets in the upper troposphere. Part I: Northern Hemisphere winter. *J. Atmos. Sci*., **56**, 1708-1728.

Hakim, G. J., 2005: Vertical structure of midlatitude analysis and forecast errors. *Mon. Wea. Rev*., **133**, 567-575.

Orlanski, I., and J. P. Sheldon, 1995: Stages in the energetics of baroclinic systems. *Tellus,* **47A**, 605-628.

THE IMPACT OF EXTRATROPICAL TRANSITION ON THE DOWNSTREAM FLOW: IDEALISED MODELLING STUDY

Michael Riemer*, Sarah C. Jones, Christopher A. Davis
*Institut für Meteorologie und Klimaforschung,
Universität Karlsruhe / Forschungszentrum Karlsruhe, Germany
Email: michael.riemer@imk.uka.de

1. INTRODUCTION

In addition to its direct impact on the midlatitudes, a tropical cyclone undergoing extratropical transition (ET) (Jones et al. 2003) can excite a Rossby wave train on the midlatitude potential vorticity gradient. This wave train then propagates downstream and alters the midlatitude flow pattern. Thus, ET can initiate severe weather events in a remote region, e.g. an ET event taking place in the western North Atlantic might trigger heavy rainfall in the Mediterranean. Numerical weather forecasts frequently fail to capture this downstream influence and ensemble prediction systems show enhanced uncertainty in the region downstream of ET events.
In an effort to reduce the high complexity of an ET event we conduct numerical experiments with idealised initial conditions to investigate the impact of ET on the midlatitude flow pattern.

2. MODEL

We use the PSU/NCAR MM5 modelling system to perform full physics numerical experiments. Periodic boundaries in the zonal direction allow a channel configuration. A vortex-following two-way nesting renders a higher resolution around the modelled tropical cyclone (TC) possible. The outer domain has a horizontal resolution of 60 km and a zonal and meridional extent of ~17 000 km and ~9 000 km, respectively. The nest has a 20 km horizontal resolution and a domain size of 1 200 km x 1 200 km. The Coriolis parameter varies with the earth's geometry. The 41 vertical levels are irregularly spaced, with a higher resolution in the boundary layer and in the tropopause region. Both domains use the Kain-Fritsch-2 scheme to parameterize convection, the Blackadar scheme to represent boundary layer processes, and the Reisner-5 microphysical scheme. The basic initial conditions consist of a zonally oriented straight jet stream in hydrostatic and thermal wind balance with a baroclinic zone. The jet is centred on 45°N. A TC that was spun up in a quiescent environment on an f-plane is inserted into the domain to the south of the jet.

3. NUMERICAL EXPERIMENTS

The simplest representation of the midlatitude flow pattern is the straight jet stream described above. The TC approaches the jet from the south and the first clear sign of an interaction between the two systems can be seen in the upper troposphere where the outflow impinges on the jet. The subsequent evolution is depicted for selected

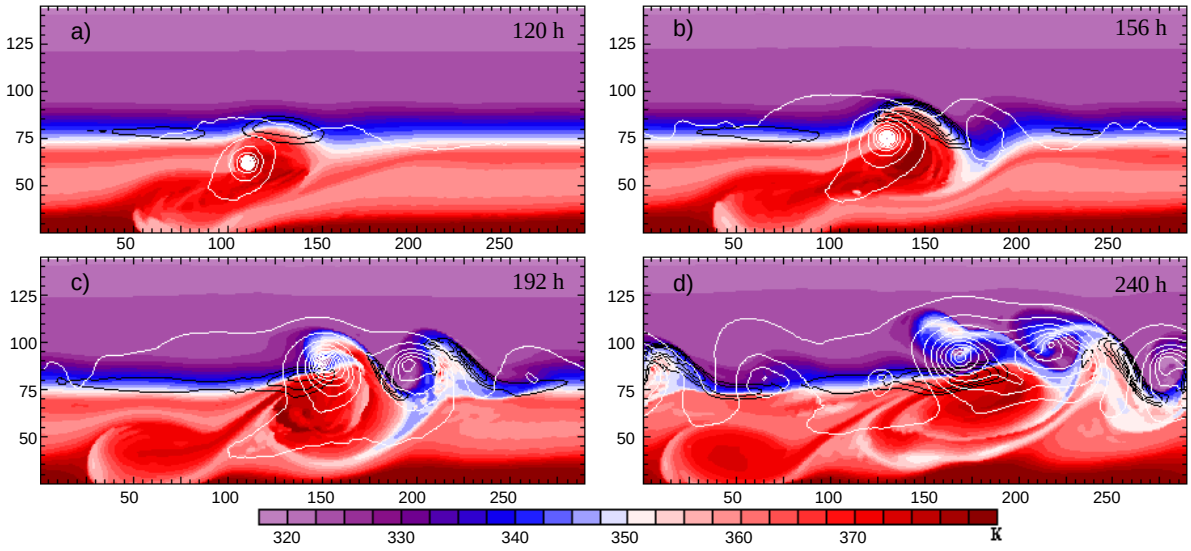

Figure 1: Potential temperature on the dynamic tropopause (PVU=2, colour shaded), surface pressure (white contours, every 5 hPa) and wind speed on 200 hPa exceeding 40 m/s (black contours, every 5 m/s) for times 120 h (a), 156 h (b), 192 h (c), and 240 h (d) into the integration of the straight jet experiment. The scale of the axes is in grid points.

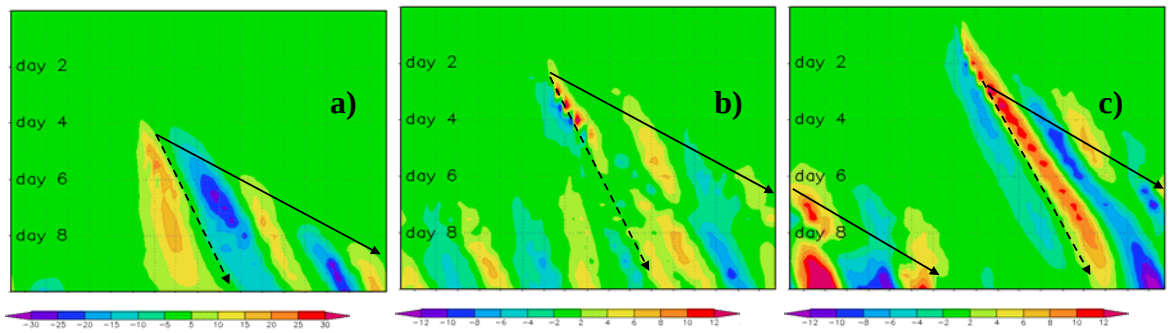

Figure 2: Hovmöller diagram of the 200 hPa meridional wind speed averaged meridionally from grid point 60 to 120 in the domain seen in Fig. 1. a) The experiment depicted in Fig. 1. The stippled arrow denotes the movement of the ET system, the solid arrow the propagation of the RWT. b) Difference between the experiments with mature development, c) as b) but for the developing baroclinic wave. Arrows in b) and c) also indicate the phase and the group speeds. Note the different scale for the wind speed in a) and b) and c). Tick marks every 1000 km.

time steps in Figure 1. At 120 h into the model run a jet streak has formed due to the interaction of the outflow with the jet stream and a ridge-trough couplet is emerging. 36 h later both features are now well pronounced. Beneath the left exit region of the jet streak a surface cyclone starts to develop. In the next 36 h the surface cyclone intensifies rapidly with a pressure drop of about 20 hPa. A further upper-level ridge-trough pattern develops downstream and initiates another surface cyclone. At the end of the simulation the upper-level wave pattern has extended over most of the domain and initiated the development of 3 surface cyclones.

The development at upper levels can be seen as the excitation of a Rossby wave train (RWT) by the ET event. Its propagation can be conveniently depicted in a Hovmoeller plot of the 200 hPa meridional wind speed. The RWT can be identified after day 4. The ET system itself moves only slowly to the east while the Rossby wave energy propagates with a speed of approx. 2 500 km/day to the east (Figure 2a).

Sensitivity experiments reveal that the propagation of the RWT is governed by the jet strength and its amplitude is affected by the strength of the surface development, including moist processes in the midlatitudes. The evolution is therefore best described in terms of 'baroclinic downstream development' (Orlanski and Sheldon 1995). The structure of the TC impacts the timing of the interaction and the evolution of the primary downstream system. A piecewise PV diagnostic shows that in the very early part of the interaction the building of the ridge is attributable to the divergent flow associated with the outflow air and that the cyclonic circulation of the TC becomes an important contributor later on. The balanced flow associated with the outflow contributes significantly to the formation of the downstream trough.

In the next set of experiments we add some complexity but gain a more realistic representation of the midlatitudes and investigate the interaction of the TC with baroclinic waves. The waves can be excited by localised as well as periodic perturbations at different vertical levels. The resulting life-cycles constitute a variety of synoptic patterns for the TC to interact with and for the downstream development to take place.

Here we present a brief summary of the impact of ET on a scenario with mature, periodic baroclinic systems and with an ongoing development excited by a localised upper-level precursor. We use Hovmöller diagrams to depict the differences in the upper-level evolution of the baroclinic life-cycle with and without the TC present. In both cases, ET is in phase with the baroclinic development and the impact is found in a region confined by the phase and group speed lines extending downstream of ET with time (Fig. 2b-c). The differences in the developing-wave scenario are much stronger, i.e. the ET event has a greater influence on this development. In both scenarios the differences that propagate with the phase speed are associated with the ET system itself. In the mature case the ET system is absorbed into the midlatitude cyclone and promotes the zonalisation of the flow. In the developing case the ET acts to amplify the upper-level wave train and accelerates the surface development. These two mechanisms disperse with the group velocity and hence are responsible for the larger scale impact of ET in these experiments.

4. CONCLUSION

In the Hovmöller diagram of a TC interacting with a straight jet the excitation and propagation of an upper-level wave train can be clearly identified. In more complex flow configurations the impact of ET is also found in a plume confined by lines of phase speed and group velocity. Two mechanisms that lead to the downstream propagation of the impact have been identified (so far): enhanced zonalisation of the flow and amplification of the wave train. The impact on the developing wave is greater than on the mature systems.

REFERENCES

Jones, S. C, P. A. Harr, J. Abraham, L. F. Bosart, P. J. Bowyer, J. L. Evans, D. E. Hanley, B. N. Hanstrum, R. E. Hart, F. Lalaurette, M. R. Sinclair, R. K. Smith, and C. Thorncroft, 2003: The Extratropical Transition of Tropical Cyclones: Forecast Challenges, Current Understanding, and Future Directions. *Wea. And Forecasting*, **18**, 1052–1092.

Orlanski, I. and J. P. Sheldon, 1995: Stages in the energetics of baroclinic systems. *Tellus*, **47A**, 605-628

PREDICTABILITY ASSOCIATED WITH THE DOWNSTREAM IMPACTS OF THE EXTRATROPICAL TRANSITION OF TROPICAL CYCLONES

Patrick A. Harr[1], Doris Anwender[2], Sarah Jones[2]

[1] Department of Meteorology, Naval Postgraduate School, Monterey, Ca USA
E-mail: paharr@nps.edu
[2] Institut fur Meteorologie und Klimaforschung, Universitat Karlsruhe / Forschungszentrum Karlsruhe, Karlsruhe, Germany

Abstract: Measures of the relative predictability in global numerical weather forecasts with respect to the downstream impacts of extratropical transition (ET) events are computed based on operational global ensemble prediction systems (EPS). There is evidence that increased variability among ensemble members, which increases downstream of an ET event, is related to decreased forecast accuracy. Variability among EPS members is characterized by a combination of an empirical orthogonal function analysis and a fuzzy cluster analysis applied to potential temperature on the dynamic tropopause. The classification of ensemble members into clusters of preferred forecast development is examined with respect to the deterministic forecasts to identify the preferred evolution of dynamically consistent downstream impacts. Cluster number and size are related to a likelihood associated with each forecast scenario.

Keywords *– THORPEX, extratropical transition, tropical cyclones, cluster analysis, empirical orthogonal function analysis*

1. INTRODUCTION

The poleward movement of a decaying tropical cyclone (TC) often results in a rapidly-moving, explosively-deepening midlatitude cyclone. The re-intensification of the remnant TC as an extratropical cyclone depends on the phasing between the decaying TC and a midlatitude environment that is favorable for midlatitude cyclogenesis (Klein et al. 2002). Furthermore, the export of low potential vorticity air to the midlatitudes from the upper-levels of the poleward-moving TC may result in excitation and dispersion of Rossby waves that have far-reaching impacts on downstream atmospheric conditions (Fig. 1). Therefore, an extratropical transition (ET) of a TC perturbs the midlatitude flow patterns across individual ocean basins with the potential for nearly hemispheric-scale impacts.

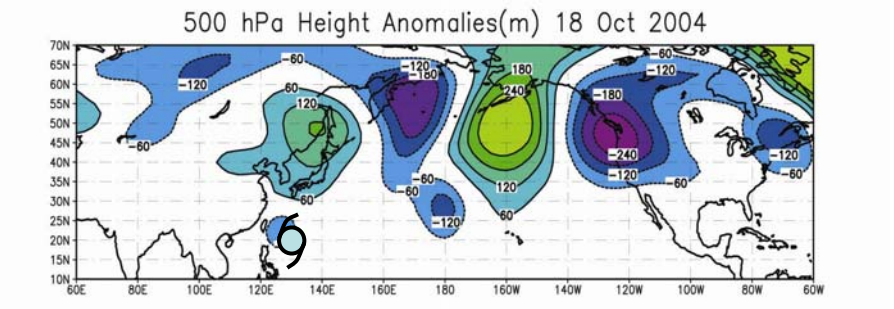

Figure 1. Height anomalies (m) at 500 hPa averaged for 0000 UTC and 1200 UTC 18 October 2004. The location of TY Tokage at 1200 UTC 18 October is defined by the tropical cyclone symbol.

Because of the typical rapid translation speed of the decaying TC, accurate extended-range prediction of the phasing between the remnant tropical circulation and the midlatitude environment into which it is moving is critical. The ET process is extremely sensitive to complex physical and dynamical interactions between the decaying tropical cyclone and the midlatitude circulation into which it is moving (Harr and Elsberry 2000, Harr et al. 2000, Thorncroft and Jones 2000). Although the poleward track of the tropical cyclone may be forecast accurately, the impacts of the ET are often not forecast correctly (Jones et al. 2003). This is especially true at extended forecast ranges. The skill of the 120 h forecasts from the Navy Operational Global Atmospheric Prediction System (NOGAPS) and the Global Forecast System (GFS) global models decreased significantly (Fig. 2) during the ET of TY Nabi between 8-10 September and TY Saola (17W) during 26-28 September. The measure of skill in Fig. 3 is the anomaly correlation at 500 hPa, which represents how well the large-scale pattern has been predicted around the Northern Hemisphere between 20°N-60°N. In this study, measures of the relative predictability in global numerical weather forecasts with respect to the downstream impacts of ET events are computed based on operational (NCEP and ECMWF) global ensemble prediction systems (EPS).

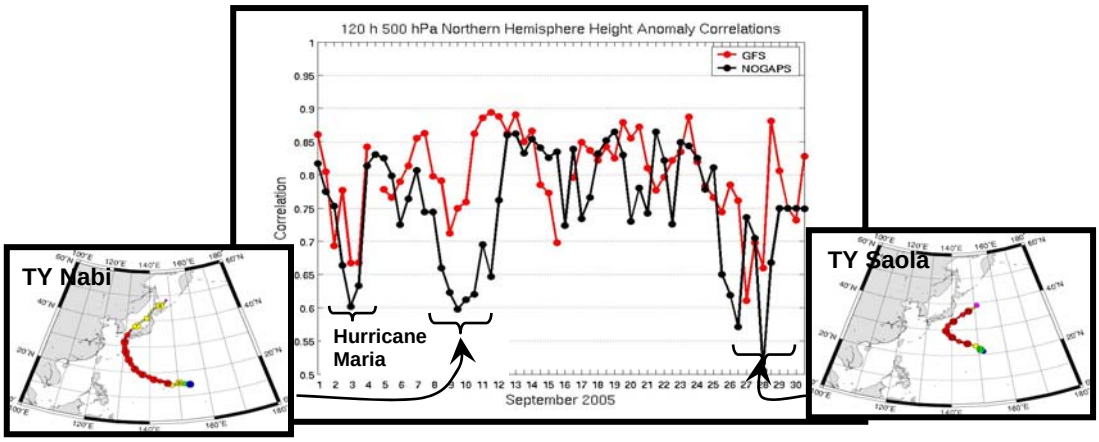

Figure 2. Height anomaly correlations over the Northern Hemisphere for 120-h forecasts from the GFS and NOGAPS models during September 2005. Periods of low correlation values that coincide with the ET of tropical cyclones are labeled. Tropical cyclone track figures courtesy of http://agora.ex.nii.ac.jp/digital-typhoon/.

2. METHOD

Variability among EPS members is characterized by an empirical orthogonal function (EOF) analysis that is applied to potential temperature on the dynamic tropopause. Principal components computed from the EOF analysis are defined based on the projection of individual ensemble members on the EOFs. The principal components provide a framework for a fuzzy cluster analysis, which is applied to identify principal downstream impact scenarios. To identify the temporal change in the variability associated with the forecasts of the ET event and its impacts on the downstream flow patterns, the EOF and cluster analyses are applied successively between 120 h and 24 h prior to the ET time. It is hypothesized that the number of forecast scenarios, which are identified as individual clusters of EPS members, decreases as the uncertainty associated with the downstream impact of the ET is reduced. Furthermore, the EOF and cluster analyses facilitate comparison between ensemble members produced by the NCEP and ECMWF systems.

3. RESULTS

The EOF/cluster methodology is applied to the ensemble forecasts of two cases in 2005, one in the western North pacific and one in the North Atlantic. The characteristics of the development for these cases were very similar in that both systems merged with larger-scale midlatitude cyclones after ET and appeared to have a minor impact on the extratropical development. The deterministic forecast, however, was very different for these cases and exhibited large errors. Before the merger with the midlatitude flow the life-cycles of these two systems were quite different. This may be attributed to the fact that the midlatitude flow during their ET was quite zonal in one case and very non-zonal in the other. The ensemble forecast for these ET events gives insight to the reliability of the deterministic forecast along with other possible dynamically consistent developments of the atmosphere.

Acknowledgements: *Support from the Office of Naval Research, Marine Meteorology Program, and the WMO is gratefully acknowledged. The WMO and THORPEX-IPO provide financial assistance for the publication of the STISS proceedings volume.*

REFERENCES

Harr, P. A., and R. Elsberry, 2000: Extratropical transition of tropical cyclones over the western North Pacific. Part I: Evolution of structural characteristics during the transition process. *Mon. Wea.Rev.*, **128**, 2613-2633.

Harr, P. A., and R. Elsberry, 2000: Extratropical transition of tropical cyclones over the western North Pacific. Part II: The impact of midlatitude circulation characteristics. *Mon. Wea. Rev.*, **128**, 2613-2633.

Jones, S. C., et al., 2003: The extratropical transition of tropical cyclones: Forecast challenges, current understanding, and future directions. *Wea. Forecasting*, **18**, 1052-1092.

Klein, P. M., P. A. Harr, and R. Elsberry, 2002: Extratropical transition of western North Pacific tropical cyclones: Midlatitude and tropical cyclone contributions to reintensification. *Mon. Wea. Rev.*, **130**, 2240-2259.

Thorncroft, C. D., and S. C. Jones, 2000: The extratropical transitions of Hurricanes Felix and Iris in 1995. *Mon. Wea. Rev.*, **128**, 947-972.

NUMERICAL EXPERIMENTS ON THE PREDICTABILITY OF TROPICAL CYCLONE INTENSIFICATION

Sang Van Nguyen[1], Roger K. Smith[1]and M. T. Montgomery[2]
[1]Meteorological Institute, University of Munich, Munich, Germany
[2]Naval Postgraduate School, Monterey, California, USA
E-mail: *roger.smith@physik.uni-muenchen.de*

Abstract: We present numerical model experiments to investigate the predictability of vortex amplification in the prototype problem for tropical-cyclone intensification. The flow that evolves becomes highly asymmetric even though the problem as posed is essentially symmetric. Moreover, the asymmetries that develop are highly sensitive to the surface moisture distribution. When a random moisture perturbation is added in the boundary layer at the initial time with a magnitude that is below the accuracy with which moisture can be measured, the pattern of evolution of the flow asymmetries is dramatically changed and a non-negligible spread in the azimuthally-averaged intensity results. We conclude that: 1) the flow on the convective scales is not deterministic and only those asymmetric features that survive in an ensemble average of many realizations can be regarded as robust; 2) there is an intrinsic uncertainty in the prediction of maximum intensity. There are clear implications for the possibility of deterministic forecasts of the mesoscale structure of tropical cyclones, which may have a large impact on the intensity and on rapid intensity changes.

Keywords – *Tropical cyclones, Asymmetries, Vortical hot towers, Ensemble calculations*

1. INTRODUCTION

The prototype problem for tropical-cyclone intensification considers the evolution of a prescribed, initially cloud-free, axisymmetric vortex on an f-plane in an environment at rest. This problem has been investigated by numerous authors using axisymmetric models. Zhu et al. (2001) used a minimal three-dimensional numerical model and found that asymmetries develop in the flow as the vortex rapidly intensifies, even though the problem posed is symmetric. The asymmetries appeared to be associated with the representation of an axisymmetric flow on a square grid and possibly also with the use of channel boundary conditions in a domain of finite (albeit relatively large) size. In a subsequent paper, Zhu and Smith (2003) showed that the asymmetries are strongly influenced by the choice of vertical grid. In a complementary paper, Montgomery et al. (2006) showed that asymmetries in the form of deep convective vortex cores dominated the development of an initially axisymmetric mesoscale convective vortex.

The evolution of the asymmetries is the main focus of the present study, which uses the Pennsylvania State University/National Center for Atmospheric Research Mesoscale Model (MM5). The calculations are carried out in a large square domain with impervious boundaries with the vortex axis initially at the centre. They are performed on a square horizontal grid. The model resolution (15, 5, 1.67 km in the horizontal and 24 vertical levels) is much larger than used in the foregoing minimal model (20 km and 3 vertical layers). There is no parameterization of cumulus convection: simply when a grid box saturates, latent heat is released and the liquid water is assumed to precipitate out. In addition to the control experiment, where the initial moisture field is uniform, we carry out an ensemble of 10 additional calculations in which a random moisture perturbation is added in the boundary layer at the initial time. The magnitude of these perturbations is below the accuracy with which moisture can be measured. We investigate*, inter alia*, the range of behaviour of the ensemble members.

2. RESULTS

Figure 1 shows time-series of the azimuthally-averaged tangential wind speed for the entire set of calculations. As in previous calculations, the vortex evolution begins with a gestation period during which the vortex slowly decays due to surface friction, but moistens slightly due to evaporation from the underlying sea surface. Subsequently, moist convection begins near the radius of maximum tangential wind speed (initially 135 km) and there ensues a period during which the vortex rapidly intensifies and contracts. At the end of this period, which is typically 48 h, the vortex attains a quasi-steady state in which the vortex exhibits many realistic features of a mature tropical cyclone, with spiral bands of convection surrounding an approximately symmetric eyewall and a central convection-free eye.

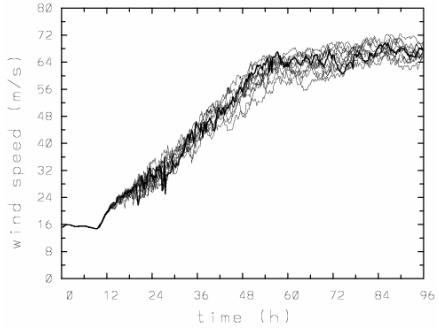

Figure 1. Time series of azimuthally-averaged tangential wind speed in the entire set of calculations showing the spread in intensity between the calculations. The control run is the thick solid line.

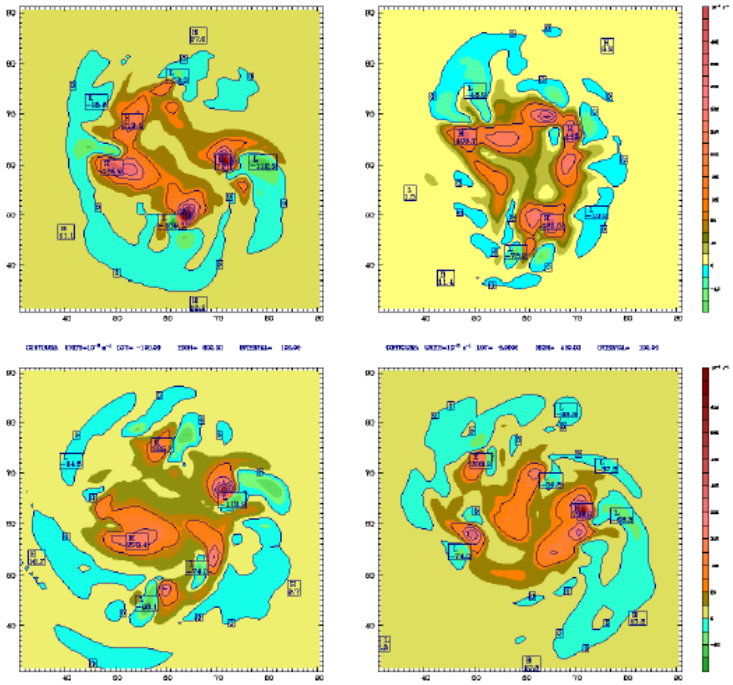

Figure 2. Relative vorticity distribution (10^{-5} s^{-1}) on the 850 mb pressure surface at 24 h in the control calculation (top left) and in three calculations where a random moisture perturbation is added in the boundary layer. Contours interval is 100 × 10^{-5} s^{-1}. Dark red denotes values exceeding 700, pink between approximately 300 and 400; orange between approximately 80 and 300; light brown between 40 and 80; yellow between 0 and 40; light blue between –20 and 0; light green less than –20.

During the gestation period the flow remains close to axisymmetric, but with a weak azimuthal wavenumber-4 asymmetry that necessarily arises from the representation of a circular flow on a square grid. Deep convection is non-existent during this time. For a relatively low horizontal resolution of 15 km, saturation occurs first with a wavenumber-4 pattern, but other wavenumbers quickly emerge, first wavenumber-2 and then other wavenumbers including wavenumber-1. As the mature stage is approached, the flow consolidates into a monopole vortex once again. As the horizontal resolution is increased while keeping the horizontal diffusivity as low as possible, the initial pattern of convection has increasing azimuthal wavenumber: for example with a 5 km grid, the pattern has wavenumber-12, but again other wavenumbers rapidly emerge.

The asymmetries that develop are associated with the development of model deep convection, the cores of which possess intense cyclonic vorticity. These convective structures have been coined “vortical hot towers” (Montgomery et al. 2006). The ensuing evolution of the towers is found to be highly sensitive to the surface moisture distribution. This behaviour is exemplified by the relative vorticity distribution on the 850 mb pressure surface at 24 h shown in Fig. 2. Note that the pattern of evolution of the flow asymmetries is significantly changed when a random moisture perturbation is added.

3. CONCLUSIONS

We conclude that the evolution of the vorticity field in the prototype problem for tropical-cyclone evolution is not deterministic and only those features that survive in an ensemble average of many realizations can be regarded as robust features We believe these results have implications for the possibility of deterministic forecasts of the mesoscale structure of hurricanes, which may have a large impact on the intensity and on rapid intensity changes.

REFERENCES

Zhu, H., R. K. Smith, and W. Ulrich, 2001: A minimal three-dimensional tropical cyclone model. J. Atmos. Sci. **58** , 1924-1944.

Zhu, H. and R. K. Smith, 2003: Effects of vertical differencing in a minimal three-dimensional hurricane model. *Q. J. Roy. Meteorol. Soc.*, **129** , 1051-1069.

Montgomery, M. T., M.E. Nicholls, T. A. Cram, and A. B. Saunders, 2006: A vortical hot tower route to tropical cyclogenesis. *J. Atmos. Sci*. **63** , 355-386.

THE PREDICTION OF RAINFALL DISTRIBUTION DURING SUMMER(JJA) OVER EAST ASIA REGION BASE ON TIME OF SOUTH CHINA SEA SUMMER MONSOON ONSET*

YANG Lin [1,3], WANG Li-ping [2], DING Yi-hui[3]

[1] Fujian Climate Center, Fuzhou 350001,China; [2] National Meteorological Information Center; Beijing 100081, China;
[3] National Climate Center, Beijing 100081, China
E-mail: *yanglin1118@yahoo.com.cn*

Abstract: The time when South China Sea summer monsoon (SCSSM) is onset, which is also a season changing period in Asia-Australia region, it has very important effect on the coming atmospheric circulation changing, vapor translation and the distribution of summer rainfall over East Asia. In this article, the function of the South China Sea summer monsoon set-up time to the distribution of summer rainfall and drought-flood disaster is studied. The out come of the study can provide signal and basis for short climatic predicting in East Asia region in summer.
Keywords *–South China Sea summer monsoon, multiple time scale variations, East Asia region, distribution of summer rainfall, significance of drought-flood predicting*

1. INTRODUCTION

DING Yi-hui[1]and his colleagues have pointed out that since summer monsoon status change significantly from year to year thus the space-time distributions and the rainfall precipitations of main season rain belts are different yearly according to the different break out time, moving speed and scale of the summer monsoon. Those abnormal actions can lead to the break out of drought-flood disaster in China. Because the breaking out, activity, halt and retreat of the monsoon decisively affect the drought/flood disaster distribution in China even in Japan and Korea, meteorological scholars in those countries always pay much attention on the research and prediction of summer monsoon. A lot of research and large scale scientific experiments about monsoon have been conducted, which largely promote the comprehension of the cause of the forming and developing of summer monsoon. Based on that, the prediction of monsoon and its precipitation have been greatly improved.

2. DATA AND DEFINITION OF SCS SUMMER MONSOON SET-UP TIME

East Asia is defined as the continental region of latitude 20-50°N and longitude 110-150°E. Eastern China, Korea, South Korea, most parts of Japan and some parts of Russia and Mongolia are included. 529 stations in this region are selected as the representative stations for our study. The sources of the historical data of this article are: (1) The monthly surface precipitation data from American Global Historical Climate Net (GHCN); (2) The data of South China Sea summer monsoon set-up time in 1951-2005 are defined and analyzed by Beijing Climate Center .

3. VARIETY CHARACTERS OF SCS SUMMER MONSOON IN MULTIPLE TIME SCALE

The following can be observed by cumulate anomalies of the SCS summer monsoon set-up time: In the late 55a, the developing process can be generally divided into two periods. In the first period which lasted for 43 years from 1951 to 1993, the set-up times fluctuated repeatedly between earlier and later. In the second period which lasted for 12 years from 1994 to 2005, the set-up times were obvious early.

earlier event years	time (pentads)	later event years	time (pentads)	normal event years	time (pentads)
1966	25	1970	32	1955	29
1994	25	1973	32	1958	29
1972	26	1987	32	1962	29
1996	26	1991	32	1969	29
1979	27	1954	31	1974	29
1986	27	1956	31	1978	29
1995	27	1971	31	1983	29
2000	27	1981	31	1988	29
2001	27	1982	31	1999	29

Table 1. 9 typical years when SCS Summer Monsoon set-up is earlier,later,normal of three class model

* This research was supported by Natural Science Founation of Fujian Province in 2004 under Grant No.D0410026.

In order to analyze the abnormal characters of the summer precipitation in East Asia, 9 years of each in earlier event years, later event years and normal event years are adopted respectively to even and compose three typical model(Table 1.).

4. RELATIONSHIP BETWEEN THE SCS SUMMER MONSOON SET-UP TIME AND THE DISTRIBUTION OF DROUGHT/FLOOD DISASTERS

The yearly change character of the breaking out and northing of the East Asia summer monsoon and its relationship with the thermal conditions of the Western Pacific has been studied by Huang rong-hui[2] and his colleagues.

By calculating the summer precipitation percentage anomalies in East Asia under the three typical SCS summer monsoon models, the synthesized outcomes fall into the following six kinds of distribution of the summer precipitation and drought/flood disaster (Figure 1.)

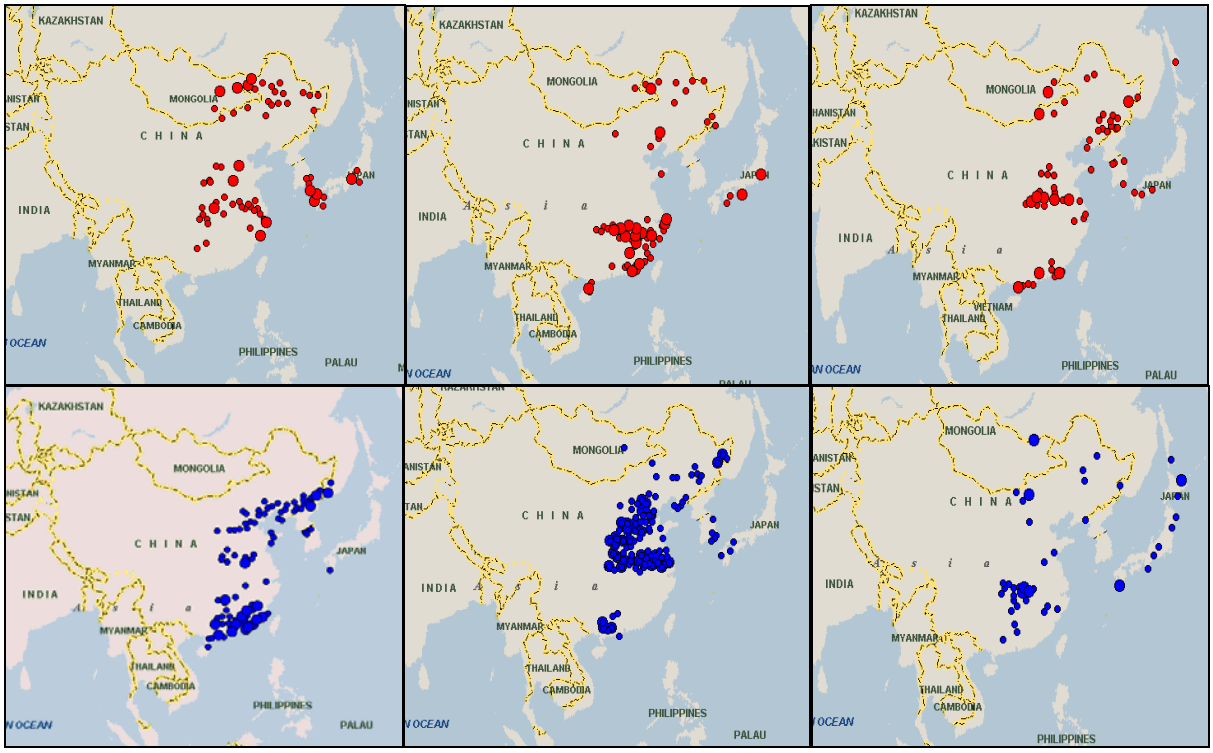

Figure 1. 6 kinds of distribution of the summer precipitation and drought/flood disaster under the three models

5. CONCLUSION

The preliminary results were as follows: (1) In the years when summer monsoon over South China Sea onset early, Yang-Zi river valley, the north part of North-east China, some parts of Hua-bei Plain, the south part of South Korea, the south part of Japan and the east of Mongolia, the summer rainfall was partial little, that easy emergence is drought ; the east part of Hua-Nan region, Huai-He river valley, the north of Bo-Hai gulf, the boundary of both China and Korea and the north of South Korea , summer rainfall was partial more , the easy emergence was flood. (2) In the years when the monsoon onset late, the south of Yang-Zi river, South-east cost, Hainan island, parts of North-east of China and the east of Japan, was partial little, that easy emergence is drought ; the west of Hua-Nan area, Huai-He river basin, most parts of Hua-Bei area, the east part of Nouth-East of China, the south of South Korea and south of Japan, summer rainfall was partial more , the easy emergence was flood. (3) In the years when the monsoon onset in normal time, the south part of Hua-Nan area, Yang-zi & Huai-He river valley, the boundary of both China and Korea, the boundary of both China and Mongolia, some parts of South Korea and the south of Japan, the summer rainfall was partial little, that easy emergence is drought ; But in the same condition, the west part of Jiang-Xi province and most parts of Japan, summer rainfall was partial more , the easy emergence was flood.

REFERENCES

[1] Ding Yihui, Zhang Jin, Xu Ying, Song Yafang, Develop of climatic system and its prediction, Series of the hot topics of global change. Editor in chief: Qin Dahe. China Meteorological Press, 2003, 3 : 75-79

[2] Huang Ronghui, Gu Lei, Xu Yuhong, Zhang Qilong, Wu Shangsen, Cao Jie, Yearly change character of the breaking out and northing of the East Asia summer monsoon and its relationship with the thermal conditions of the Western Pacific. Chinese journal of Atmospheric Sciences, 2005, 29 (1), 20-36.

SINGULAR VECTOR STUDY OF THE EXCITATION OF ROSSBY-WAVE TRAINS

Mark Buehner, Ayrton Zadra and Ahmed Mahidjiba

Meteorological Research Division, Environment Canada, Dorval, Canada
E-mail: *mark.buehner@ec.gc.ca*

Abstract: Singular vectors with appropriate norms and time scales are calculated to identify, at the time of excitation, the mechanisms that control the amplitude of Rossby-wave trains in cases of high-impact weather.

Keywords – *Rossby waves, singular vectors, optimal growth*

1. INTRODUCTION

There is evidence that Rossby wave-trains originating over the Western Pacific may significantly influence the middle- to long-range predictability of high impact weather over North America and beyond (e.g. Shapiro, 2003). These wave trains are an example of the global-scale propagation of local-scale influences on high-impact weather, and their predictability is limited by model errors and errors in initial conditions.

Singular vectors (SV) are the most rapidly growing perturbations over a given time interval, with respect to specified norms. As such, they provide an objective tool to study the optimal excitation of atmospheric waves, and the initial-condition errors that influence the predictability of these waves.

SVs have been used at the Meteorological Service of Canada (MSC) to analyze the influence of physical parametrizations (Zadra et al., 2004) and initial-time norms (Buehner and Zadra, 2005) on the properties of unstable atmospheric disturbances in the Canadian Global Environmental Multiscale (GEM) model. In this study, various events of large-amplitude Rossby-wave train are identified, and SVs calculated using a final-time norm designed to only capture the Rossby wave. These SVs are expected to provide information about the excitation mechanism and the predictability of Rossby-wave trains.

2. METHODOLOGY AND PRELIMINARY RESULTS

Using analysis data on η-levels provided by the Canadian Meteorological Centre (CMC), various events of large-amplitude, long-lasting Rossby-wave trains are selected. The location and duration of these events are then identified using Hovmoeller diagrams of the meridional wind field averaged between $\eta = 0.101$ and $\eta = 0.516$ (i.e. between approximately 110hPa and 520hPa), and between 40°N and 60°N. Wave envelopes are then extracted using the technique of Zimin et al. (2006). Figure 1a shows the wave envelope for one winter case (initial time given by the analysis of 19 Nov 2002, 00Z).

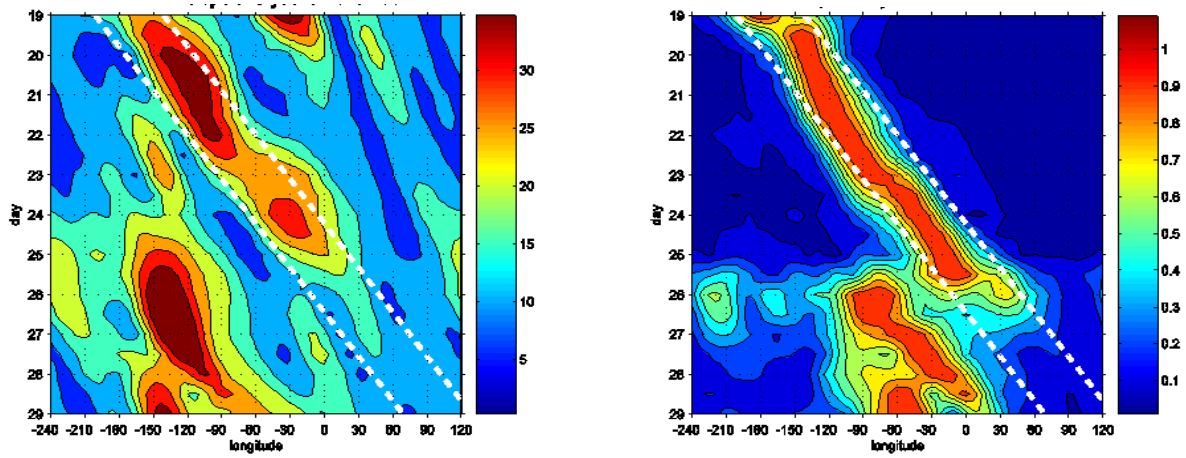

Figure 1. (a) Left: Hovmoeller diagram of the Rossby-wave train envelope derived from operational analyses over the period 19-29 November, 2002, as described in the text. The dashed lines are parallel to the estimated group velocity of the wave train, and indicate the envelope's longitudinal range. (b) Right: same as (a), but for the difference between the original and perturbed forecasts, where the initial perturbation is provided by a linear combination of SVs (Note: In (b), for better visualization, amplitudes are normalized according to daily maximums).

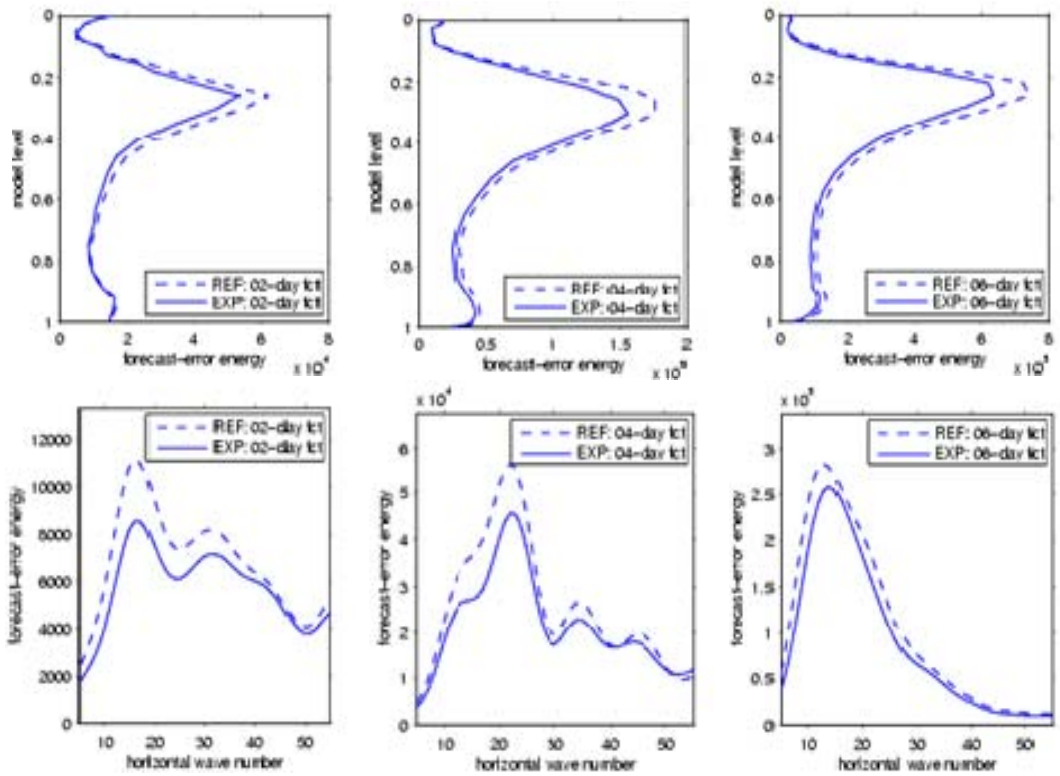

Figure 2. For the case of 19 November, 2002: vertical profiles (top row) and wavenumber spectra (bottom row) of the forecast-error total energy, based on the original analysis (dashed lines) and the analysis perturbed by a linear combination of SVs (solid lines) after 48h (left), 96h (centre) and 144h (right).

For each of several cases, 10 SVs are calculated using an optimization time interval (OTI) of 48h and a complete set of simplified physical parametrizations (Zadra et al., 2004). At initial time, the global total-energy norm is used. The final-time norm is based on the rotational kinetic energy only (to extract vortical modes) and its domain restricted according to the wave envelope extension. In the example shown in Fig.1a, the final-time domain is limited to 35°N < lat < 65°N, 150°W < lon < 90°W and $0.101 < \eta < 0.516$.

In each case, the 10-day forecast and the associated error are considered. To study the relevance of SVs to forecast error growth, the 48-h forecast error is projected on the final-time SVs, to define the linear combination of SVs that best explains the forecast error at that time. The pseudo-inverse of the SV linear combination is then used to perturb the initial conditions, and another (perturbed) forecast produced. The difference between original and perturbed forecasts, which gives the nonlinear propagation of the pseudo-inverse, is then used to produce Hovmoeller diagrams and the corresponding wave envelopes. As shown in Fig. 1b, the nonlinear propagation of the pseudo-inverse seems to follow closely the propagation of the analyzed Rossby-wave train for the case of 19 Nov, 2002. Properties of forecast error of the perturbed analyses are also compared, at various lead times, with those obtained from the original analysis. In the example shown in Fig. 2, the perturbations originally constructed to correct the 48-h forecast, lead to consistent improvements up to day 6.

Other cases are also considered, including cases where Rossby-wave trains are absent. Preliminary results indicate that, in some cases, SVs propagate with the Rossby-wave train and significantly modify its forecast. In those cases, SV-based disturbances of the initial conditions can lead to large consistent improvements to the Rossby-wave train forecasts for many days.

REFERENCES

Buehner, M. and A. Zadra, 2005: Impact of flow-dependent analysis-error covariance norms on extratropical singular vectors. Q. J. R. Meteor. Soc. **132**, 625-646.

Shapiro, M., 2003: A societal/economic impact perspective of Rossby wave-train propagation for the extreme northern-hemispheric weather events of November 2002. EGS - AGU - EUG Joint Assembly, Nice, France, 6 - 11 April 2003.

Zadra, A., M. Buehner, S. Laroche and J.-F. Mahfouf, 2004: Impact of the GEM model simplified physics on extratropical singular vectors. Q. J. R. Meteor. Soc. **130**, 2541-2569.

Zimin, A. V., I. Szunyogh, B. R. Hunt, and E. Ott, 2006: Extracting Envelopes of Nonzonally Propagating Rossby Wave Packets. Mon. Weather Rev. **134**, 1329-1333.

ROSSBY-WAVE PROPAGATION, ROSSBY-WAVE BREAKING AND HEAVY ALPINE PRECIPITATION

Olivia Martius[1], Cornelia Schwierz and Huw C. Davies

[1] Institute for Atmospheric and Climate Science, ETH Zurich, Zürich, Switzerland
E-mail: olivia@env.ethz.ch

Abstract: The focus of this study lies on the local and far-field precursors to a climatological sample (444 members) of heavy precipitation events that occurred along the Alpine south side as identified in a potential vorticity (PV) framework.
The local precursors take the form of PV-streamers (i.e. breaking synoptic-scale Rossby waves) that are located upstream of the precipitation events over France and England. These breaking waves can be preceded by coherent upper-level wave trains that can sometimes be traced back to the eastern Pacific or the waves can form almost in situ over the eastern Atlantic. A strong seasonal variation of the temporal and spatial extension of the upstream wave-precursor exists that is partly linked to the strength and coherence of the PV-wave guide over the Atlantic sector.

1. INTRODUCTION

Upper-level PV-streamers are present over Europe in more than 70% the days with heavy precipitation occurring along the south side of the European Alps (Martius et al. 2006b). These PV-streamers lead to a significant enhancement the precipitation (Massacand et al. 1998). PV-streamers can form during the breaking of synoptic-scale Rossby waves. The upper-level synoptic-scale Rossby wave precursor signals to the heavy precipitation PV streamers are investigated in this study.

The role of synoptic-scale Rossby wave-trains as precursors to heavy precipitation has been discussed in other studies based on single events, for example in the context of the central European floods in summer 2002 (Grazzini and van der Grijn 2002; Blackburn et al. 2003), the flooding over England during October 2000 (Krishnamurti et al. 2003) and torrential rainfall events over central Europe in November 2002 (Shapiro 2004).

2. METHOD

The ERA-40 reanalysis data and an observation-based Alpine precipitation data set that covers the period from 1966 to 1999 (Frei and Schär, 1998) are used for the following analyses.

The identification of days with heavy precipitation along the Alpine south side with a PV-streamer being present concomitantly over Europe is described in detail in Martius et al. (2006b). The identified 444-member sample is not equally distributed among the four seasons. The majority of the events take place in autumn.
A climatology of PV-Hovmöller diagrams showing the meridional velocity (Martius et al. 2006a) is used to compile composite Hovmöller diagrams for the heavy precipitation days. The Hovmöller data up to twelve days prior to the actual rain days is averaged to build a mean heavy precipitation Hovmöller diagram for each season. A Monte Carlo significance test is performed to determine areas of significance within the composite Hovmöller diagrams.

3. RESULTS AND DISCUSSION

Meridional velocity Hovmöller diagram composites for each season (1% percentiles, 98% sig. level) are presented in Fig. 1. The results are discussed for the time (0 – 8 days) prior to the heavy precipitation events. Between day 0 and day 2, a wave signal, associated with the PV-streamer over Western Europe, is identified for all four seasons. The amplitude of this meridional velocity signal is stronger in autumn (Fig. 1c) than in summer (Fig. 1b) despite the fact that the former sample contains significantly more members. A weak downstream wave signal over Eastern Europe is present in the autumn and winter composite (Figs. 1 c and d).

The character of the mean wave precursor signals differs substantially during the four seasons. In winter (Fig. 1d) a coherent wave signal can be identified over the west coast of North America seven days prior to the precipitation. If wave disturbances are triggered in the vicinity of a global wave-guide, they can indeed cover such distances. In the northern hemisphere winter, wave-propagation downstream from the eastern Pacific is observed to seed the Atlantic storm track on a regular basis (Hakim 2003). The composite precursor signal in autumn is similar to that in winter regarding its amplitude, the phase speed and the distance covered.

In spring (Fig. 1a), the in situ wave signal over the eastern Atlantic and Europe is of notable temporal persistence. A wave signal is first observed at day 6 over Europe, but the upstream extension of the precursor signal is shorter in spring than in autumn and winter (reaching back into the western Atlantic only). Of all seasons, the precursor wave is weakest in summer (Fig. 1b), in terms of amplitude as well the temporal and spatial extent. A coherent precursor signal is present only four days prior to the heavy precipitation days in summer, compared with seven days in autumn and winter.

No significant differences are found between the phase velocities, group velocities and the wavelengths of the individual precursor waves to the heavy precipitation events and the climatological distribution of these wave parameters.

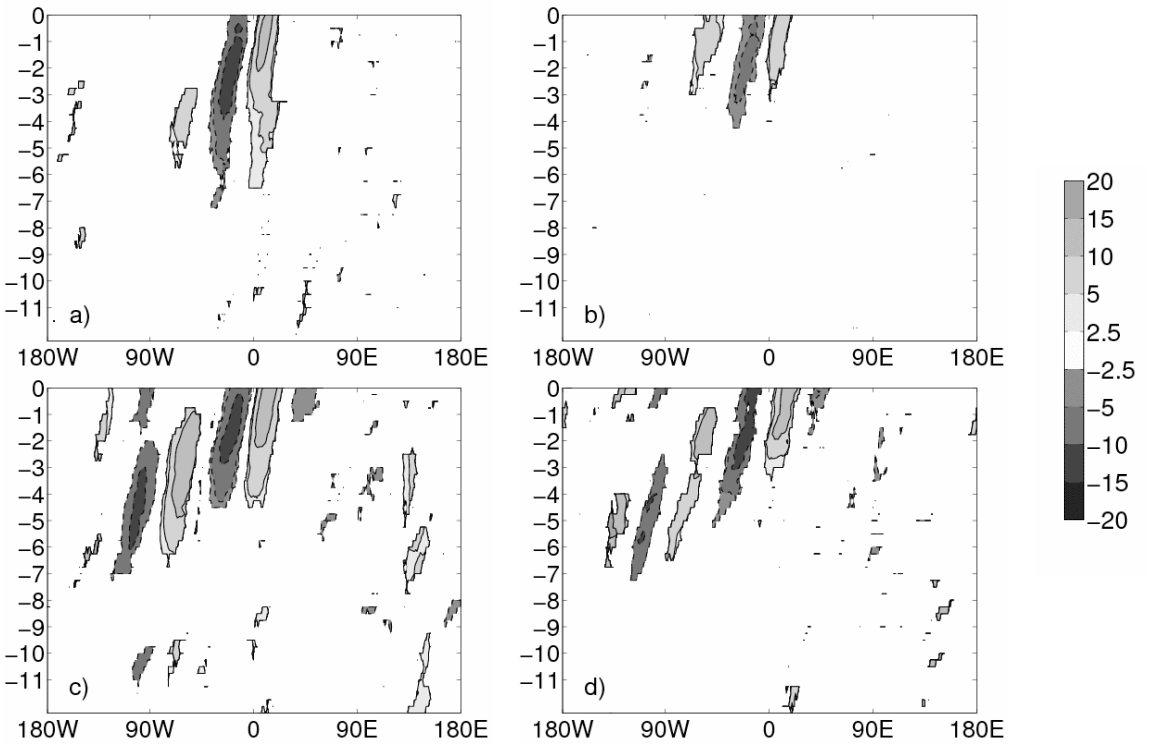

Figure 1: Composite PV-Hovmöller-diagrams of the meridional wind velocity [m/s] in a) spring (99days), b) summer (128 days), c) autumn (177days) and d) winter (40 days). The composites are centered in time at the day of heavy precipitation events in the Alps.

4. SUMMARY AND OUTLOOK

The wave precursor signal to heavy precipitation PV-streamers exhibits significant seasonal variability. In autumn and winter, a wave signal can be traced back to the eastern Pacific up to seven days prior to the precipitation event. In summer the breaking wave seems to form quasi in situ (i.e. over the Atlantic basin). The spring precursor signal is superposition of a more stationary wave located over Europe merging with a faster propagating wave signal emerging from the American east coast.

The reasons for these seasonal differences can be manifold. For example differences in the strength and the spatial coherence of the wave-guides or the processes that trigger the waves can vary (or are differently distributed in space and time) could account for the observed differences.

An analysis of the strength and coherence of the PV-gradients over the Atlantic during the four seasons, shows relatively weak and incoherent gradients in spring and stronger and coherent gradients in summer. In winter and autumn the PV-gradients are very strong and coherent reaching upstream into the Pacific basin (Martius 2005).

REFERENCES

Blackburn, M., B. Hoskins, P. Inness, and J. Slingo, 2003: 2002- a summer of floods and drought. *Planet Earth*, **Summer 2003,** 23.

Grazzini, F. and G. van der Grijn, 2002: Central European Floods during summer 2002. *ECMWF Newsletter***,** 18-28.

Hakim, G. J., 2003: Developing Wave Packets in the North Pacific Storm Track. *Mon. Wea. Rev.*, **131,** 2824-2837.

Krishnamurti, Y., T. S. V. Vijaya Kumar, and K. a. H. Rajendran, A., 2003: Antecedents of the flooding over south-eastern England during October 2000. *Weather*, **58,** 367-370.

Martius, O., 2005: Climatological aspects of wave disturbances on the tropopause and links to extreme weather in Europe, Institute for Atmospheric and Climate Science, PhD-thesis ETH Zürich, 137.

Martius, O., C. Schwierz, and H. C. Davies, 2006a: A refined Hovmöller diagram. *Tellus*, **58A,** 221-226.

——, 2006b: Episodes of Alpine Heavy Precipitation with an Overlying Elongated Stratospheric Intrusion: A Climatology. *International J. Climatol.* , **26,** 1149-1164.

Massacand, A. C., H. Wernli, and H. C. Davies, 1998: Heavy precipitation on the Alpine southside: An upper-level precursor. *Geophysical Research Letters*, **25,** 1435-1438.

Shapiro, M. A., 2004: A societal/economic impact perspective of Rossby wave-train propagation for the extreme northern-hemisphere weather events of November 2002. *84th AMS Annual Meeting*, Seattle, WA, AMS.

A WAVELET REPRESENTATION OF POTENTIAL-VORTICITY COHERENT STRUCTURES

Matthieu Plu[1], Philippe Arbogast and Alain Joly

[1] CNRM/GAME, Météo-France, Toulouse, France
E-mail: *matthieu.plu@meteo.fr*

Abstract: A wavelet-based extraction of synoptic-scale coherent structures is proposed. It relies on the invertibility principle of potential vorticity. It leads to an objective algorithm that defines mathematically and numerically the precursors of extra-tropical cyclones. Moreover, the possibility to extract multipolar configurations of the structure is an improvement compared to a classical monopolar extraction.

Keywords *– potential-vorticity, coherent structure, wavelet basis, feature extraction*

1. INTRODUCTION

The synoptic-scale atmospheric dynamics is driven by the interactions of features at various spatial and temporal scales. Synoptic-scale finite-amplitude vortices, also called anomalies, are one of these features. They may grow in a favorable region, for instance a baroclinic jet-stream in which they follow the well-known paradigm of baroclinic interaction (Petterssen, 1956). The word *anomaly* itself, coming from linear-stability studies, is problematic since it assumes the existence of a stationary part in the flow, which is not proven.

It appears that synoptic-scale dynamics has much more to do with turbulence than with linear modes. As a consequence, it is hypothesized that synoptic-scale vortices may be defined as *coherent structures*. For stratified fluids, potential vorticity is the most appropriate field where to search for these structures thanks to its lagrangian conservative property and the invertibility principle. The capability to determine automatically and in the most objective manner the coherent structures of potential vorticity is a necessary step on the way to a better understanding of the dynamics and of the energetics of synoptic-scale storms, as well as for new tools for predictability issues.

Recent studies in theoretical fluid mechanics (Farge et al., 1999) have been using the discrete wavelet transform (DWT) to separate the coherent and the incoherent part of a turbulent flow. The capability of wavelets to detect the singularities of a signal and its representation of local scales allows to investigate their use to extract coherent structures. The present study aims at applying some similar wavelet methods in order to define and extract the three-dimensional potential-vorticity coherent structures.

2. METHODOLOGY

The orthogonal DWT is applied on bidimensional scalar fields, since theory do not provide compactly-supported orthogonal wavelet on the sphere yet. The resulting wavelet basis enables:

- removing the incoherent part of the original field (Farge et al., 1999) thanks to an adaptive thresholding method;
- a discretization of the field into wavelet modes that have various scales, directions and positions.

However, this transform suffers from a lack of translation-invariance, which is critical to extract the localized coherent structures. As a consequence, the computation of all the translated DWT bases is necessary, which is equivalent to applying the stationary wavelet transform (SWT).

Searching for coherent structures among the SWT modes requires the definition of the optimal DWT basis for each structure. In this local basis, information redundancy is avoided and the modes that compose the structure may be selected. The approach that is proposed, and justified, is to define a maximal scale for the structure, then to select the DWT basis such as a peak of a diagonal mode is colocated with the peak of the coherent structure. The other DWT modes are the ones that are colocated with this first mode, at the other directions and scales, what is called the *cylinder or influence*.

This method is satisfactory for structures that have an aspect ratio not higher than 2. More general techniques for the representation of filamentary structures, which are known to be often present in potential-vorticity dynamics, are currently under investigation.

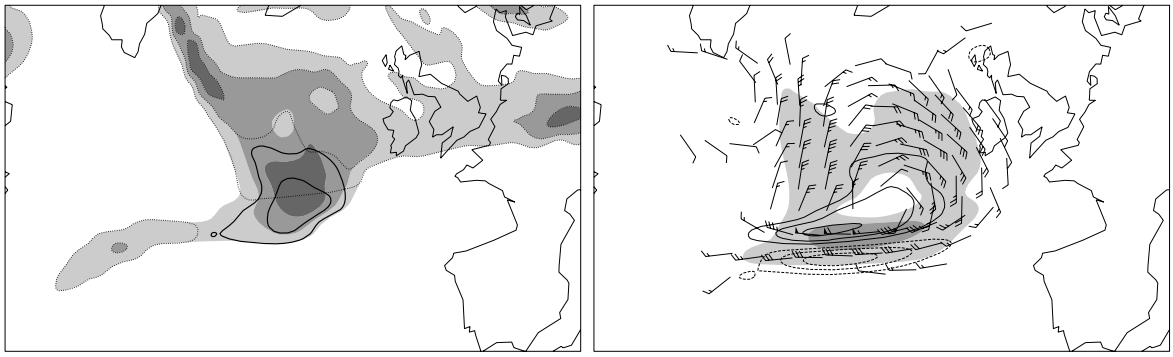

Figure 1. Structure obtained after the wavelet extraction and the inversion of potential vorticity on 27 December 1999 at 06 UTC. Left: direct result of the wavelet extraction on potential vorticity at the 350 hPa level. Grey shadings: the field after adaptive thresholding (contour intervals 1.5 pvu), solid lines: the structure that is extracted (contour intervals 1.5 pvu) and dotted: the field after removal of the extracted structure (contour intervals 1.5 pvu). The potential vorticity unit (pvu) equals 10^{-6} $m^2s^{-1}K$ kg^{-1}. Right: resulting anomaly after the inversions of the three-dimensional potential vorticity distributions, in terms of relative vorticity (black lines, positive solid and negative dashed, contour intervals 5 10^{-5} s^{-1}), wind barbs (minimum speed 5 ms^{-1}), and wind speed (grey shadings, minimum speed 10 ms^{-1}, intervals 10 ms^{-1}).

3. APPLICATION TO A REAL CASE

The mature stage of the second exceptional storm of Christmas 1999 in Europe, called T2 or Martin, was a typical exemple of baroclinic interaction in a strong jet-stream. The upper-level coherent structure has been extracted thanks to the method presented above. The data are the operational 3D-Var analyses from the hydrostatic ARPEGE/IFS model from MÉTÉO-FRANCE at the spherical truncation T199 on a grid with a stretching factor 2.4. Potential-vorticity inversion is performed with an implicit balance condition (Arbogast et al., 2006), given by the dynamics of the model. Thus it is a nonlinear process.

Fig.1 shows the result of the extraction on a single isobaric level and of the inversion of the three-dimensional potential vorticity distribution. The anomaly is defined as the difference between the original field and the inverted field after removal of the extracted structure. The anomaly has the shape of a jet-streak that accelerates the jet up to 25 ms^{-1}. A north-south dipolar configuration may be seen on the field of relative vorticity.

A comparison with a subjectively extracted monopolar structure in the high-frequency field has been performed. Simulations with the ARPEGE/IFS model reveal that the surface cyclone does not show up if the wavelet extracted or the monopolar structure is removed initially. However, this monopolar structure is less coherent in time than the wavelet-extracted one, which is a serious drawback for some applications. These results help to define correctly the concept of coherence in a numerical framework.

4. CONCLUSION

The wavelet-based extraction is proven to work well on the upper-level precursor of a real-case storm. Moreover, it is dynamically more consistent than a classical monopolar extraction, which allows better diagnostics of the storm. The temporal tracking of the extracted anomalies will deserve more attention in the following.

The first application that is foreseeable is to provide the extraction of coherent structures in order to perform an ensemble forecast by perturbing the initial precursors in an operational framework, like Plu and Arbogast (2005) showed in a quasigeostrophic model.

REFERENCES

Arbogast, P., K. Maynard, and F. Crepin, 2006: Ertel potential vorticity inversion under an "implicit balance" condition. *Quart. J. Roy. Meteor. Soc.*, *submitted*.

Farge, M., K. Schneider, and N. Kevlahan, 1999: Non-gaussianity and coherent vortex simulation for two-dimensional turbulence using an adaptive orthogonal wavelet basis. *Phys. Fluids*, **11**(8), 2187–2201.

Petterssen, S. *Weather analysis and forecasting*, I. McGraw-Hill, 1956. 428pp.

Plu, M., and P. Arbogast, 2005: A cyclogenesis evolving into two distinct scenarios and its implications for short-term ensemble forecasting. *Mon. Wea. Rev.*, **133**(7), 2016–2029.

DYNAMICAL ANALYSIS OF THE ECMWF ENSEMBLE PREDICTIONS OF THE EUROPEAN WINTERSTORM "LOTHAR"

Heini Wernli [1], Patricia Kenzelmann [2], Martin Leutbecher [3]

[1] Institute for Atmospheric Physics, University of Mainz, Mainz, Germany
E-mail: wernli@uni-mainz.de
[2] Institute for Atmosphere and Climate Science, ETH Zürich, Zürich, Switzerland
[3] ECMWF, Reading, UK

Abstract: It its early phase, before rapidly intensifying, the European winterstorm "Lothar" (24-26 December 1999) was characterised by a pronounced low-level positive potential vorticity anomaly that rapidly propagated across the North Atlantic. In agreement with the concept of a diabatic Rossby wave (DRW), this vortex was continuously regenerated through condensational diabatic heating. Here, the 50 members from the ECMWF ensemble forecast system are used to investigate the dynamics of the DRW and the relationship between the early DRW phase and the subsequent explosive deepening.

Keywords *– Winterstorm, Diabatic Rossby Waves, Moist Processes, Ensemble Prediction, TIGGE*

1. INTRODUCTION

The European winterstorm "Lothar" (24-26 December 1999) is a recent example of a mid-latitude high-impact weather system that has been very poorly predicted by operational deterministic NWP forecasts. During the 30 hours before the cyclone underwent explosive development close to the coast of France, it propagated rapidly (~30m/s) as a shallow mesoscale system across the Northern Atlantic. The situation was characterized by a zonally oriented, very intense upper-level jet and associated low-level baroclinicity, no clear signature of an upper-level disturbance and a pronounced low-level positive PV anomaly that was sustained through moist diabatic processes (Wernli et al. 2002). This low-level PV anomaly, its diabatic origin and rapid propagation are reminiscent of the concept of diabatic Rossby waves (DRW), introduced by Snyder and Lindzen (1991) and Parker and Thorpe (1995). Recently, Moore and Montgomery (2004, 2005) studied the dynamics of DRWs within an idealized setting. Here, in contrast, the mechanism of DRW propagation is analysed using the 50 ECMWF ensemble forecasts for the "Lothar" storm. This approach on the one hand yields novel insight into the dynamics of DRWs, and on the other hand might serve as a prototype study for dynamical investigations of the TIGGE database.

2. THE "LOTHAR" ENSEMBLE FORECASTS

All members of the operational ECMWF EPS started at 12 UTC 24 December 1999 were initiated with a low-level PV vortex near 50W/40N that in reality developed into winterstorm "Lothar". This low-level PV anomaly is referred to here as the "Lothar"-DRW. About 10 of the 50 members actually captured the explosive development two days later over Central Europe (see Fig. 2.9 in Shapiro and Thorpe 2004). Therefore, these ensemble forecasts can be regarded as a set of dynamically consistent sensitivity experiments to study the evolution of DRWs and the mechanisms that lead to a rapid intensification. A detailed analysis of operational EPS forecasts (- in particular the calculation of PV) is hampered by the fact that their output is only archived on few pressure levels. Therefore, for this study the EPS started at 12 UTC 24 December 1999 has been rerun at ECMWF for 48 hours with the T255L40 model version. Output from the 50 members has been made available with the full vertical resolution and on a horizontal grid with 0.75deg resolution.
In every simulation, the evolution of the low-level PV anomaly that corresponds to the "Lothar"-DRW has been tracked with an algorithm developed by Kenzelmann (2005). Then, the resulting 50 DRW-tracks have been sorted in four categories, depending upon the minimum sea level pressure (SLP) value reached along the track (cat I: no deepening, cat II: weak deepening, cat III: strong deepening, cat IV: exceptional deepening). For every category the temporal evolution of the category-mean values of several parameters has been calculated, in order to identify distinct differences between deepening and non-deepening DRWs.
The statistical analysis shows that after about 12 hours (i.e. at 00 UTC 25 December) clear differences occur between categories I-III: DRWs with stronger low-level PV, lower SLP value, stronger low-level baroclinicity, smaller distance to the upper-level jet and stronger precipitation in the vicinity of the DRW at that time tend to develop into more intense DRWs during the next 30 hours. However, the exceptionally deepening DRWs in category IV show a different behaviour: they are typically weak in the beginning, move rapidly towards the upper-level jet-axis around 06 UTC 25 December and intensify whilst crossing the jet axis. This indicates that a

large amplitude DRW in the early stage is in general beneficial for future intensification, but that the most extreme cases do not show particular characteristics during the early stage of the evolution. This emphasizes the difficulty of forecasting DRWs and their potential explosive development.

3. EXAMPLE DIABATIC ROSSBY WAVES

Figure 1 shows three example DRW evolutions from the ensemble simulations. At 21 UTC 24 December (left panels), they all look fairly similar, with minimum SLP slightly below 1000 hPa and a pronounced low-level PV anomaly about 500 km to the south of the upper-level jet (indicated by the white PV contours). 15 hours later (middle panels), there are already pronounced differences: the second DRW has become rather weak and is no longer associated with a SLP minimum; the two others have similar amplitude, but propagate at different speed. In the third example, the DRW is already close to the upper-level jet and explosive development occurs during the next hours. In contrast, in the first example, intensification and propagation are much slower and in the second example there is hardly any signature in the SLP field at the time when in reality "Lothar" passed over Paris. This illustrates that the slight initial differences amplify to strikingly different storm scenarios.

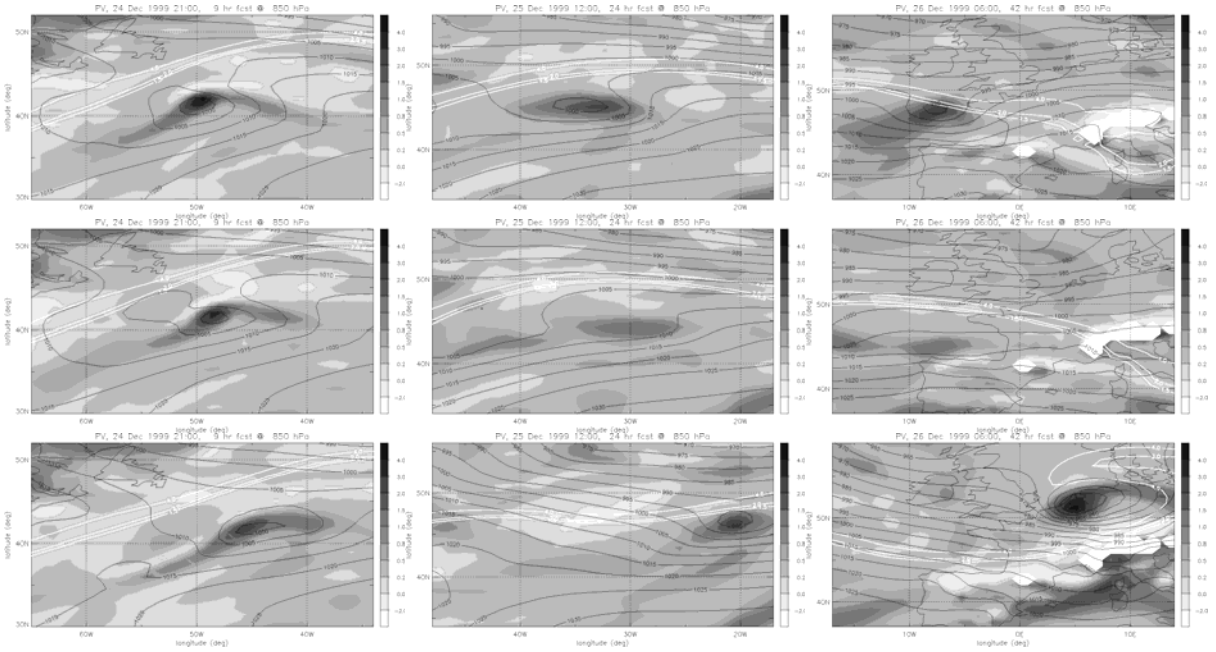

Figure 1. Example DRWs. Top: ensemble member 12 (category III); middle: ensemble member 35 (category I); bottom: ensemble member 43 (category IV). Shown are PV on 850 hPa (grey shading, in pvu), selected PV contours on 250 hPa (white contours for 1.5, 2 and 4 pvu) and SLP (black contours, every 5 hPa) for the time instants 21 UTC 24 December (left), 12 UTC 25 December (middle) and 06 UTC 26 December (right).

Acknowledgements: *We thank the German Weather Service (DWD) and ECMWF for providing access to ECMWF data.*

REFERENCES

Kenzelmann, P., 2005: Dynamik und Klimatologie von diabatischen Rossby Wellen. Diplomarbeit ETH Zürich/Universität Mainz, 90 pp.

Moore, R. W. and M. T. Montgomery, 2004: Reexamining the dynamics of short-scale, diabatic Rossby waves and their role in midlatitude moist cyclogenesis. *J. Atmos. Sci.*, **61,** 754-768.

Moore, R. W. and M. T. Montgomery, 2005: An idealized three-dimensional analysis of the diabatic Rossby vortex: A coherent structure of the moist baroclinic atmosphere. *J. Atmos. Sci.*, **62,** 2703-2725.

Parker, D. J. and A. J. Thorpe, 1995: Conditional convective heating in a baroclinic atmosphere: A model of convective frontogenesis. *J. Atmos. Sci.*, **52,** 1699-1711.

Shapiro, M. A. and A. J. Thorpe, 2004: THORPEX international science plan. Version III. WMO/TD-No. 1246, WWRP/THORPEX No. 2, 51 pp.

Snyder, C. and R. S. Lindzen, 1991: Quasi-geostrophic wave-CISK in an unbounded baroclinic shear. *J. Atmos. Sci.*, **48,** 76-86.

Wernli, H., S. Dirren, M. A. Liniger and M. Zillig, 2002: Dynamical aspects of the life cycle of the winter storm 'Lothar' (24-26 December 1999). *Q. J. R. Meteor. Soc.*, **128,** 405-429.

CONNECTION BETWEEN PV COHERENT STRUCTURES AND CONVECTION OVER WESTERN EUROPE

Karine Maynard[1] and Philippe Arbogast

[1] Direction de la Prévision, Météo-France, Toulouse, France
E-mail : karine.maynard@meteo.fr

Abstract: Since pioneer papers by Petterssen it has been demonstrated that the baroclinic development is a major process for mid-latitudes cyclone development with the presence of upper-level coherent structure with strong PV signatures. It also appears that mesoscale convective systems may also be driven by upper-level features. However the underlying processes are less known in this case. Among others candidates are the destabilization mechanism of the air mass by the thermal structure usually associated to en upper-level disturbance and moisture convergence enabled by the vertical-velocity signature.
Sensitivity studies based on AROME model initialised and forced with boundary conditions provided by different PV distributions thanks to a PV inversion procedure implemented in the frame of ARPEGE-IFS will be shown. The nature of the interaction between mesoscale convective system activity and upper-level features will be addressed.

Keywords – *Potential-Vorticity inversion, mesoscale convective system, AROME, predictability*

1. INTRODUCTION

A major source of uncertainty in Limited-Area Modelling is associated with a deficient knowledge of the initial/lateral coupling conditions, either because of the lack of observations or as a result of using an already imperfect lower-resolution model forecast to construct the initial conditions or both. Another source of errors comes from the incapacity of models to resolve convection explicitly. We will indeed examine the sensitivity of convective simulations to systematic perturbations of the upper-level precursor synoptic-scale trough and the ability of the high resolution model (2.5km) AROME to forecast the quantitative precipitation. An original technique of disturbance of the initial conditions is used: it is based on perturbations of the initial potential vorticity (PV). The present approach is applied to two convective events to generate an ensemble of six mesoscale numerical simulations with perturbed initial intensities or positions of the upper-level PV signature.

2. METHODOLOGY AND NUMERICAL MODELS

The PV inversion method (Arbogast et al. 2007) is coupled to the French global spectral operational model ARPEGE. This tool is used with the following strategy: six ARPEGE simulations of the same case study are compared. These simulations are performed with different initial conditions and by using the same model formulation. The initial condition for the first simulation (reference) is the operational 4DVAR ARPEGE analysis. Initial conditions for the other simulations are obtained from a PV surgery methodology. PV surgery is performed in three steps. First, the ARPEGE analysis is examined to find key PV structures out. Second, these upper-level structures are perturbed in a systematic way in the sense of modifying their location and/or intensifying/weakening their amplitude. Finally the PV inversion tool is used to retrieve modified balanced velocity and temperature fields corresponding to the modified PV fields. This set allows to represent the uncertainty on the large-scale initial state as suggested by Plu and Arbogast (2006). The synoptic-scale forecasts supply then the initial and lateral conditions in the regional model ALADIN (10km resolution). Finally, ALADIN supplies the initial and boundary conditions for AROME: the reached resolution is then of 2.5km. The AROME version is based on the ALADIN-NH dynamics but incorporates the physical package of MESO-NH. It incorporates a shallow precipitation parameterization whereas the deep convection is explicitly solved by the model.

3. RESULTS OF THE PERTURBED SIMULATIONS

Two convective cases have been processed: 6-7 September 2005 (case 1) and 27 June 2006 (case 2). Case 1 is organized in a quasi-stationary convective system over the French southern mountainous areas and Mediterranean sea and case 2 in a convective line propagating rapidly toward northeastern France. The triggering and maintenance of the convection in the first event is linked to the orography but much of the precipitation is not directly orographic since it occurred over lowlands areas. The high-resolution simulation reproduces the convective system pretty well (panel b)). For the other case, the shape of the quantitative precipitation patterns is consistent with convective cells moving towards the North East (panel e)).

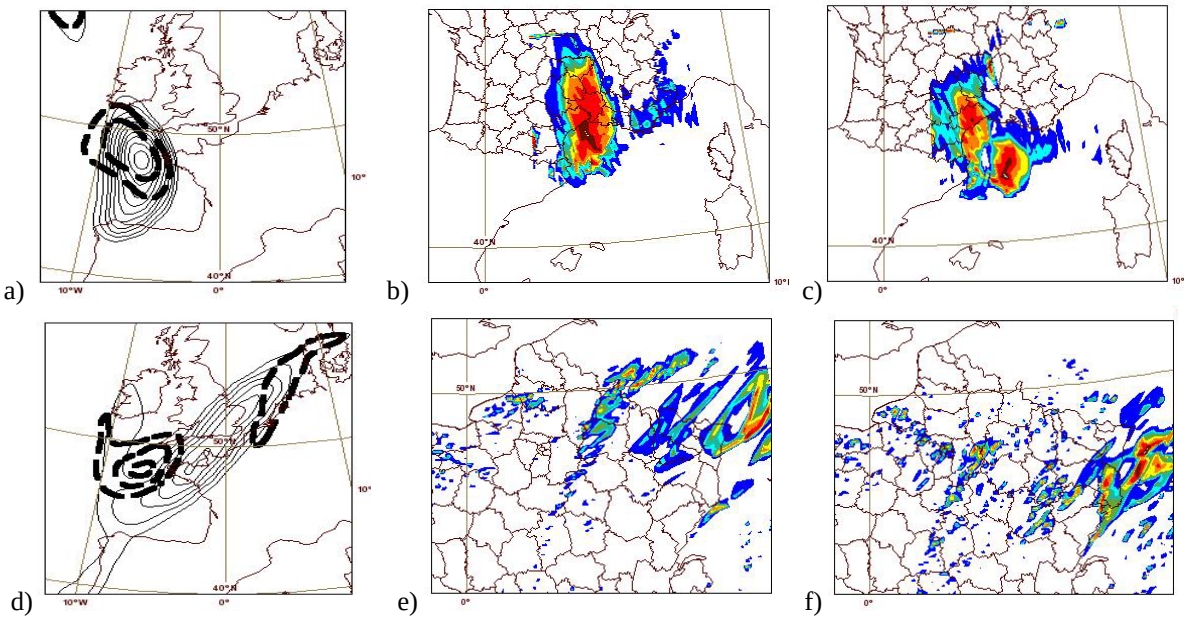

Figure 1: Potential vorticity at 300hPa from ARPEGE for reference simulation (thin solid lines) and a sensitivity experiment (bold shaded contours) in case 1 (a) and in case 2 (d) (initial conditions, contour interval: 1 pvu). AROME forecast in terms of cumulated precipitation over 6h: b) reference simulation, c) sensitivity experiment for case 1 (forecast 18UTC-24UTC, brown=150mm, red=100mm, orange=50mm) and over 3h: e) reference simulation, f) sensitivity experiment for case 2 (forecast 12UTC-15UTC, brown=70mm, red=50mm and orange=30mm).

The comparison of panel b) and c), resp. panel e) and f) shows that initial condition perturbations along upper-level coherent structures may lead to appreciable changes in the spatial and quantitative details of the precipitation field for both cases. Moreover, the spread of the small mesoscale ensemble in terms of precipitation is significantly larger than that obtained with either the small ARPEGE ensemble or the ALADIN ensemble (not shown).
The experiments performed for both cases show other common features: the precipitating activity seems poorly triggered by the upper PV coherent features (panel a) and d)). However, the wind associated to the PV structures contributes significantly to the magnitude of the Jet stream leading to an impact of the initial perturbations in terms of location and/or propagation speed of the main precipitation pattern instead of their magnitude. It should be stressed that in these two intrinsically different cases the ageostrophic wind resulting from baroclinic interaction between the PV structure and its environment does not contribute to the low-level moisture convergence which is one among the precursor of convection.

4. CONCLUSION

Although the magnitude of the PV perturbations is not tuned as the initial perturbations in actual Ensemble Prediction Systems, this study shows that the predictability of precipitating weather systems is affected by the uncertainties on the initial state of synoptic scale.
On the one hand successful mesoscale forecasts require accurate coupling conditions. On the other hand the usefulness of Ensemble Prediction Systems dealing with various resolutions seems obvious.

REFERENCES

P. Arbogast, K. Maynard and F. Crépin: Potential vorticity inversion under implicit balance condition. Submitted to *Q.J.R Meteorol. Soc.*
M. Plu and P. Arbogast, 2005: A cyclogenesis evolving into two distinct scenarios and its implications for short-term Ensemble Forecasting *Mon Wea Rev* Vol 133; pp. 2016-2029

REGENERATION OF SYNOPTIC TRANSIENT EDDIES IN SPECIFIC REGIONS OF THE LARGE-SCALE FLOW

Gwendal Rivière[1] and Alain Joly

[1] CNRM-GAME, CNRS and Météo-France, Toulouse, France
E-mail: *gwendal.riviere@meteo.fr*

Abstract: The aim of our study is to address the question of the preferred regions where synoptic eddies (upper-level disturbances as well as surface cyclones) rapidly intensify. Our methodology consists in decomposing the atmospheric flow into a low- and a high-frequency part for dataset issued from Météo-France or ERA40 (ECMWF) reanalyses. A new measure of the constraint exerted by the large-scale environment on high-frequency disturbances is introduced, called effective deformation, and allows us to localize specific regions where synoptic high-frequency perturbations are likely to be regenerated.

Keywords *– horizontal deformation, barotropic critical region, explosive growth, temporal filter*

1. INTRODUCTION AND METHODOLOGY

It is well-known that weather regimes which are quasi-stationary configurations of the large-scale atmospheric circulation have a strong influence on the life cycle of midlatitude synoptic eddies. However, at the present time, no theory is able to determine for a given weather regime the location of the regions where they will strongly develop. The aim of our study is to address this open question.

In what follows, each atmospheric flow is decomposed into two parts, a high-frequency part (denoted with primes) and a low-frequency part (denoted with subscript m) by applying a temporal filter with a cut-off of around 10 days. The high-frequency part corresponds therefore to the synoptic signal and the low-frequency one to the weather regime.

2. EFFECTIVE DEFORMATION AND BAROTROPIC CRITICAL REGION

Barotropic interaction between the high- and the low-frequency components of the flow can be diagnosed from the so-called barotropic generation rate. It can be expressed as the scalar product $\mathbf{E}.\mathbf{D_m}$ where $\mathbf{E}$ characterizes the anisotropy of the high-frequency eddies and $\mathbf{D_m}$ is the 2D deformation vector whose components are the low-frequency shearing and stretching terms. The barotropic generation rate is generally negative in midlatitudes (Black and Dole, 2000) because of the action of stretching of the large-scale deformation. Synoptic eddies are elongated along dilatation axes and lose therefore their energy. However, this action of stretching is active in specific regions which can be diagnosed with the help of the effective deformation (Rivière and Joly, 2006). This diagnostic is defined as $\Delta_m \equiv \sigma_m^2 - \zeta_m^2$, where σ_m is the low-frequency deformation magnitude ($\sigma_m = |\mathbf{D_m}|$) and ζ_m the low-frequency vorticity. In regions where $\Delta_m > 0$, synoptic eddies are strongly stretched and lose energy whereas in regions where $\Delta_m < 0$, the action of rotation of the large-scale flow is so strong that synoptic eddies cannot be elongated along dilatation axes and barotropic interaction is very weak.

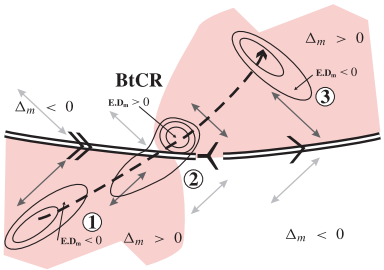

Figure 1. Schematic depicting the large-scale flow configuration making a *barotropic critical region* (BtCR) and the evolution of a perturbation moving through this region. Double solid lines represent the jet core, double arrows are dilatation axes and the color shaded areas indicate zones where $\Delta_m > 0$. The bold solid contours stand for the geopotential of a high-frequency eddy and its evolution during its crossing of the BtCR region is represented in a three step sequence making a trajectory indicated by the bold dashed line.

If a synoptic eddy stays in a region of positive effective deformation where dilatation axes are almost parallel, the perturbation will naturally be stretched and lose energy. It is the case for the eddy in stage 1 of Fig.1. However, the same eddy can be barotropically regenerated if it crosses a barotropic critical region (BtCR) as shown in stage 2. A BtCR is a local area separating two large-scale regions of positive effective deformation where the dilatation axes are almost perpendicular upstream and downstream of

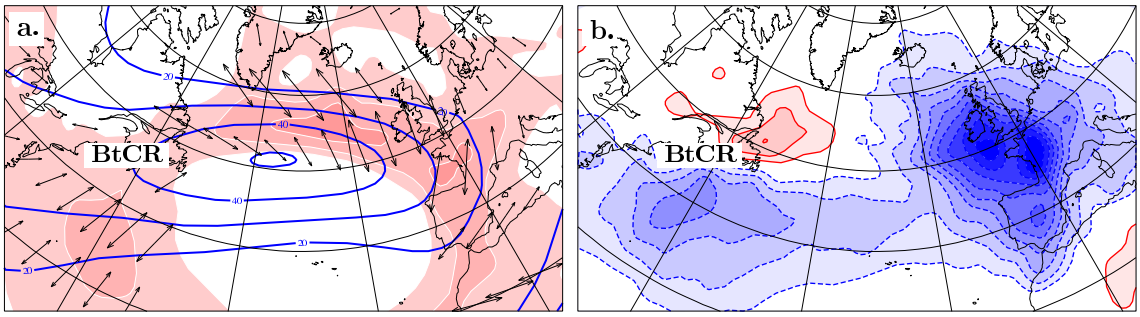

Figure 2. Class of zonal jet presenting a BtCR at its entrance. This class corresponds to 15% of winter zonal regimes over the Atlantic for the ERA40 database (i.e 386 days). a. Positive values of the effective deformation (shaded contours, int: 5.10^{-10} s^{-2}), low-frequency wind modulus (blue solid contours, interval 10 $m.s^{-1}$) and dilatation axes (black arrows) at 300hPa. b. Average of the barotropic generation rate $\mathbf{E.D_m}$ at 300 hPa (blue and red shadings correspond respectively to negative and positive values, int: 1.10^{-2} $m^2.s^{-3}$) for this class of jet.

it. When the eddy crosses the BtCR, it is contracted and temporarily gains kinetic energy. Stage 3 is characterized by an elongation of the eddy along the new dilatation axes. To summarize, the barotropic mechanism around a BtCR is composed of an elongation, a contraction and finally an elongation of the synoptic eddy. The contraction stage (stage 2) is a barotropic regeneration stage for the perturbation.

3. TWO CASE STUDIES

In order to illustrate the mechanism depicted in Fig.1, the evolution of an upper-level tropospheric disturbance around a BtCR will be presented. This eddy is precisely the upper-level precursor leading to the storm Martin that hit France on 27 December 1999.

The second case study is the last growth stage of the FASTEX IOP17 cyclone. This example shows that moving into a BtCR can not only regenerate barotropically the surface cyclone but also can trigger a phase of baroclinic development and lead to an explosive growth phase for the surface cyclone.

4. STATISTICAL RESULTS

ERA40 reanalysis is used to validate statistically our results. Case studies have revealed that two zonal regimes apparently similar can have BtCR regions located at different places and lead therefore to different evolution of the transients. This is the reason why we have classified all the zonal regimes of the ERA40 database into different categories according to their deformation properties. We have applied the cluster algorithm of Michelangeli et al. (1995) to the effective deformation field at 300hPa and 6 clusters have been obtained. One of them is shown in Fig.2. This type of zonal regime has a BtCR at the entrance of the jet. The successive blue-red-blue pattern in Fig.2b corresponds to a loss-gain-loss of kinetic energy for the high-frequency eddies and thus confirms the significant role played by a BtCR in the regeneration of upper-level tropospheric anomalies.

5. CONCLUSION

Our results suggest that local properties of the large-scale circulation play a crucial role in determining regions where synoptic eddies will grow most rapidly. Barotropic critical regions are among these regions as they can favor a barotropic regeneration of synoptic eddies as well as can in some cases indirectly reactivate a phase of baroclinic interaction.

REFERENCES

Black, R., and R. Dole, 2000: Storm-tracks and barotropic deformation in climate models. *J. of Climate*, **13** (15), 2712–2728.

Michelangeli, P.-A., R. Vautard, and B. Legras, 1995: Weather regimes: recurrence and quasi stationarity. *J. Atmos. Sci.*, **52**, 1237–1256.

Rivière, G., and A. Joly, 2006: Role of the low-frequency deformation field on the explosive growth of extratropical cyclones at the jet exit. Part I: barotropic critical region. *J. Atmos. Sci.*, **63**(8), 1965–1981.

DEPENDENCE OF ENSEMBLE SPREAD ON MODEL UNCERTAINTIES FOR EXTRATROPICAL CYCLONE SIMULATIONS

Hongyan Zhu and Alan Thorpe

Because of the difficulty of comparing the difference between different models or measuring the difference between multi-model and varied-model ensemble methods, the model uncertainty is extremely difficult to quantify. Therefore, in this study, we quantify the model uncertainty by varying the model resolution so as to find the dependence of the ensemble forecast spread on the model uncertainty. A model simulation of 90 km grid resolution is taken as the control
experiment, with a larger difference of model grid resolution to 90 km representing a larger model uncertainty. In the simulation, an idealized two-dimensional baroclinic jet is combined with a balanced three-dimensional perturbation to produce a growing baroclinic wave development.

In terms of the central surface pressure, the ensemble spread has three growth phases: an early initial phase of transient growth, exponential growth and a saturation growth phases. The ensemble spread increases with increasing model uncertainty, as does its exponential growth rate. The ensemble spread grows according to a power law when the domain averaged value of surface pressure is taken into account. The forecast spread induced by a larger model uncertainty grows with a larger power. The log of the ensemble spread is in proportional to the square root of the difference in model resolution. Considering the maximum ensemble spread of the surface pressure field, which can be located away from the cyclone centre, the ensemble spread grows in a similar way to that in terms of minimum central surface pressure until 90 h, but instead of decaying after 90 h, the spread continuously increases.

The ensemble spread approximately collocates with the primary cyclone during the development stage, and gradually elongates along the regions with strong gradients as the cyclone matures. There are two coexisting mechanisms accounting for the horizontal ensemble spread distribution described above: amplitude and phase variations. The ensemble spread maximum is located in the center region of the ensemble mean cyclone due to the spread mainly in the amplitude of the cyclone. The ensemble spread induced by the dominating phase variations covers the regions where there are strong gradients. It is clear that during the developing period, the intensity induced spread dominates the forecast spread, and when the cyclone reaches mature stage, the phase spread becomes the main factor on determing the distribution of the ensemble spread.

Forecast spread also grows along with the secondary cyclones. The ensemble spreads of the upstream and downstream cyclones have a similar shape and scale to the pressure distribution of the secondary cyclones. The ensemble spreads associated with the secondary cyclones accompany the development of cyclones themelves with the spread associated with the upstream cyclone appearing and developing earlier compared with that for downstream cyclone. As a result, at 120h the maximum ensemble spread associated with the upstream cyclone is in the region where the strong gradient of ensemble mean upstrem cyclone is, whilst the maximum spread associated with the downstream cyclone is in the region of the downstream cyclone center. The ensemble spreads related to the secondary cyclones increases with increasing model uncertainty for both upstream and downstream cyclones.

Since the four experiments have the same initial condition uncertainties, the different characteristics of the ensemble spread between different ensemble experiments is due to the added model uncertainties. We obtain the qualitatively similar results when the initial condition uncertainty is taken out of each experiment. Without initial condition uncertainty, the ensemble spread is near to zero at the beginning of the integration, and gradually appears in the region of the primary cyclone center, moving towards the region with strong gradients.

To provide a preliminary evaluation as to whether these results are general, we examined cases in which model uncertainty is created by perturbing a physical parameterization scheme. The dependence of the forecast difference on the model uncertainty has similar characteristics to what has been discussed earlier in this paper. This gives us some confidence that the conclusions obtained here using horizontal resolution as a surrogate for model uncertainty are more widely applicable to sources of model uncertainty arising from physical parametrization schemes. Further research is needed to more fully extend our results for other sources of model uncertainty.

FACTORS FOR THE DEVELOPMENT OF EXTREME NORTH ATLANTIC CYCLONES AND THEIR RELATIONSHIP WITH A HIGH FREQUENCY NAO INDEX

G.C. Leckebusch[1], S. Zacharias[2], J.G. Pinto[2], U. Ulbrich[1], A.H. Fink[2]

[1] Institut für Meteorologie, Freie Universität Berlin
Carl-Heinrich-Becker-Weg 6-10, 12165 Berlin, Germany

[2] Institut für Geophysik und Meteorologie, Universität zu Köln
Kerpener Str. 13, 50923 Köln, Germany
E-mail: gcl@met.fu-berlin.de

1. INTRODUCTION

Winter cyclone activity over the North Atlantic and Europe is investigated with respect to factors that influence the growth of cyclones. These are upper-air baroclinicity (300/500 hPa), latent energy (equivalent potential temperature 850 hPa is used as an indicator), horizontal divergence (250 hPa) and jet stream location and strength (250 hPa). Cyclones are identified and tracked using a numerical algorithm, whose results enable a detailed analysis of the life cycle of individual cyclones. Only systems with a minimum lifetime and strength are considered in the subsequent statistics. Additionally, cyclone life cycles must feature a clear strengthening phase (minimum: 0.3 hPa $(\text{deg.lat})^{-2}$ day^{-1}). Based on the maximum strength of the circulation (criterion: laplacian of pressure) reached during a cyclones life cycle, the 10% most intense systems are defined as extreme cyclones. Particular attention is given to such systems which are examined separately from other cyclones. The assignment studies focus on the period of strongest intensification of cyclones and consider the above mentioned growth factors in the vicinity of every individual cyclone. Furthermore, the role of the North Atlantic Oscillation (NAO) phase during the development of extreme cyclones is considered. The NAO pattern is derived from monthly mean data (via Principal Component Analysis of SLP). The daily index is obtained by projecting the pattern on daily data, followed by a 5 day running mean smoothing.

2. DATA

The investigations are based on NCEP Reanalysis data for the period 1958/59-1997/1998. Furthermore, simulations (SRES-scenarios 20C and A1B) of the global climate model ECHAM5/OM1 are used to assess climate change trends. Climate signals refer to the changes between end of the 21st century (2060-2100) and recent climate conditions (1960-2000). For all investigations, the analysis period is the winter half year (ONDJFM).

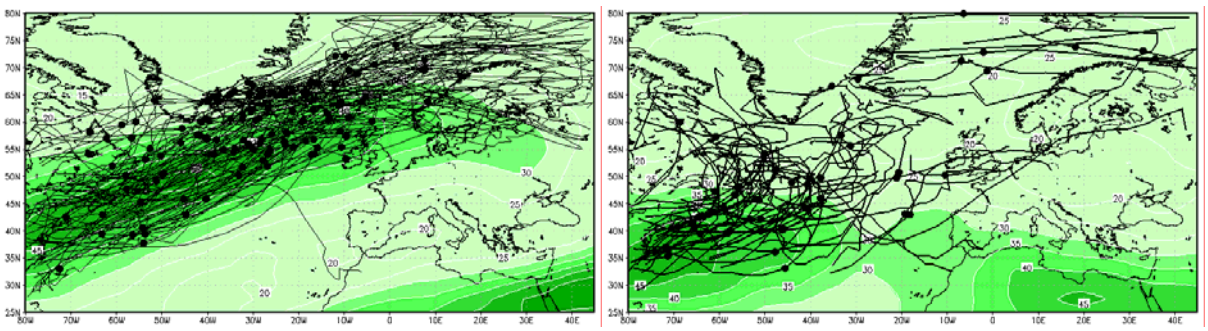

Figure 1. Composites of Jetstream in 250 hPa (interval: 5 ms^{-1}) for extreme cyclones in different phases of the NAO: Left: strong positive NAO phase (NAO++). Right: strong negative NAO phase (NAO--). Black lines represent thr extreme cyclone tracks of the respective NAO phase. Data: NCEP Reanalysis, winter 1958-1998.

3. RESULTS

A strong relationship between the NAO phase and the frequency of extreme systems is identified for the NCEP period: the occurrence of extreme cyclones is enhanced (15,1 % of all cyclones) in strong positive NAO phases (index values above +1,5), while on negative strong NAO phases (index values below -1,5) their occurrence is much less frequent (5,5 % of all cyclones). Moreover, results show that the intensification region and strength are closely coupled with the analyzed growth factors: strong intensification of cyclones is frequently linked to the occurrence of extreme values of e.g. jet stream strength. Additionally, the NAO phase is strongly coupled with the large scale atmospheric circulation, affecting the location of the cyclone tracks (e.g. northeast shift of the storm tracks in positive NAO phases). The growth factors considered during the period of the individual intensification maximum have considerably higher values for the extreme cyclones compared to the non-extreme systems. This result is valid for all NAO phases with very similar values of the considered parameters. The enhanced number of extreme cyclones during the positive NAO phase is thus explained by the larger area with suitable growth conditions.

The same relationships are also detected for cyclones derived from an ECHAM5/OM1 simulation with present climate conditions. The analysis of a simulation following the A1B forcing scenario reveals that the total number of cyclone tracks is decreased by ca. 10% by the end of the 21st century. In terms of extreme cyclones, signals are less homogenous, including both areas with reduced (Northern Scandinavia) and increased activity (British Isles). The signal over the British Isles also includes an average intensification of extreme systems, and is associated to an eastward extension of the jet stream and the barocline zone over the North Atlantic. These changes are observed in all NAO phases. In spite of the changes in cyclone statistics, the relationships between the environment factors and cyclone development derived from present climate conditions remain valid in a future climate.

FORECASTING ACTIVITIES DURING THE SUMMER 2006 SOP OF AMMA PROPOSITION OF A SYNTHETIC ANALYSIS SPECIFIC TO THE WEST AFRICA

J.P. Lafore[1], Z. Mumba[2], P. Chapelet[1], N. Chapelon[1], M. Dufresne[2], R. Agbabu[2], A. Abdoul-Aziz[2], H. Hamidou[3], N. Asencio[1], F. Couvreux[1], M. Nuret[1], A. Garba[4]

[1]METEO-FRANCE, CNRM, 42 avenue G. Coriolis, F-31057 Toulouse, FRANCE
and [2]ACMAD, [3]ASECNA, [4]EAMAC
E-mail: *jean-philippe.lafore@meteo.fr*

Abstract: The AMMA (African Monsoon Multidisciplinary Analysis) is an international project to improve our understanding of the West African Monsoon (WAM) and its variability. A team of African Forecasters have been set up to operationally provide forecasts all during the AMMA 2006 campaign held in Western Africa this summer (1st June to end September 2006). We present here the original forecasting method that has been developed to fulfill the needs of the AMMA Operational Centre in Niamey (Niger).

Keywords *– THORPEX, WMO, African monsoon, Forecasting method*

1. INTRODUCTION

The task of a forecaster involves the analysis of numerous observations and NWP products (both analysis and forecasts) before deciding on the weather forecast for a given location and range. This is a very complex process involving both objective and subjective criteria and where the experience of the forecaster can play an important role on the skill of the final forecast. The difficulty is even stronger for tropical regions where in contrast to midlatitudes the atmospheric flow is weakly balanced resulting in a weaker predictability, especially for convective events. Also this process needs to be performed as quickly as possible.

Our objective is to present a framework aimed at guiding the forecasters task during the Specific Observation Period (SOP) of the AMMA international project focused on the study of the West African monsoon period (JJAS).

2. THE WEST AFRICAN SYNTHETC ANALYSIS/FORECAST

This proposed forecasting approach is based on the preparation of single synthetic maps that summarize all key features of the WAM analyzed or forecasted at a given time. These synthetic maps are named WASA and WASF for West African Synthetic Analysis and Forecast, respectively. The following 10 features are considered as important and figure on the WASA/F (Fig. 1) maps in order to capture the main characteristic of the situation and to forecast the weather.

1. The Intertropical Discontinuity: ITD hereafter.
2. The associated Heat-Low: HL hereafter

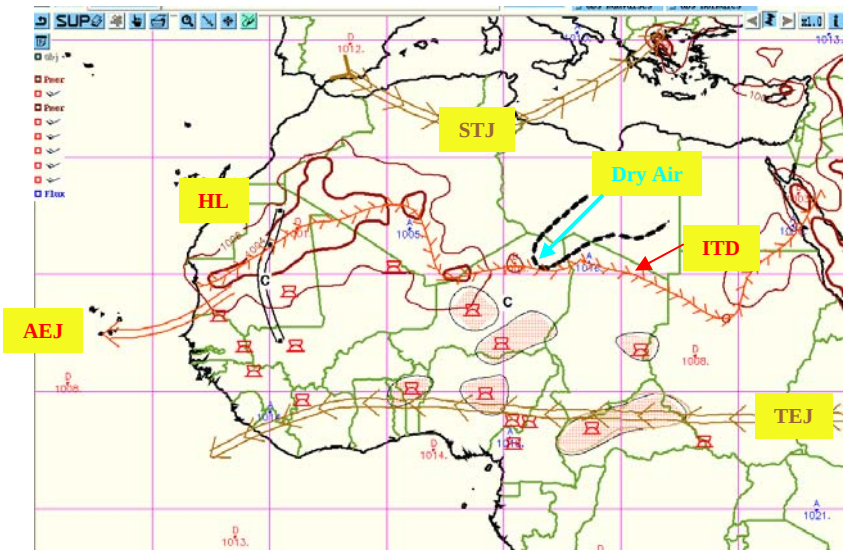

Figure 1. Illustration of the different key features figuring on a WASA/F.

3. SubTrop Jet and eventually the Polar Jet: STJ and PJ hereafter
4. Troughs extending from midlatitudes associated with the STJ or PJ
5. The Tropical Easterly Jet: TEJ hereafter
6. The African Easterly Jet: AEJ hereafter
7. Troughs and cyclonic centres associated with African Easterly Waves: AEW hereafter
8. Midlevel dry intrusions
9. Monsoon layer
10. Convective activity with the distinction between 3 cases:
    a. Suppressed convection areas
    b. Unorganized isolated convective cells
    c. Mesoscale Convective Systems: MCS hereafter and Squall Lines: SL hereafter

The first 9 key features are provided by NWP outputs available at ACMAD (Niger) through the Météo-France forecasting Synergie System (4 PC) fed by the RETIM-Afrique transmission link. They are drawn according to some rules. The model skill to forecast convective activity is poor in such tropical regions, so that the final forecast of MCSs is the result of the combination of all above 9 features, following some rules. For instance active fast moving MCSs need convective instability, high precipitable water, shear (or AEJ), dry air, vicinity of a through and of a vortex at 850 hPa. Figure 2 provide an example of a good forecast of 2 MCSs over West Africa on the 19 of July 2006, up to 2 days in advance.

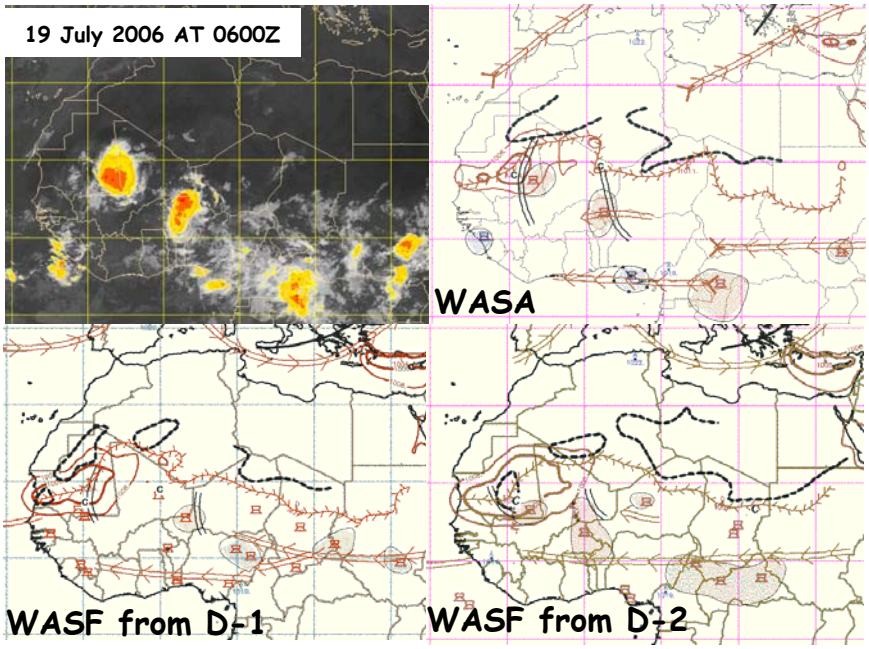

Figure 2. Example of WASA at 0600Z on the 19 of July 2006 as compared with the IR Meteosat image, and corresponding WASFs forecasted 1 and 2 days before.

3. SOME LEARNINGS FROM THE 2006 FORECAST DEMONSTRATION

The AMMA-Forecast team adopted this approach during the 2006 monsoon season, allowing testing it. During the THORPEX conference, we will evaluate the relevance of this approach as used during the 2006 summer demonstration experiment. Further steps will be to objectively evaluate the forecast skill using this approach. Also it appears that the method needs to be improved to define clearer drawing rules based on adequate and objective diagnostics.

We hope that this forecasting demonstration experiment will contribute to the development of a new forecasting method for Africa after its extension to the whole Africa by considering the whole year, not only the West African monsoon season.

Acknowledgements: *WMO and THORPEX-IPO provide financial assistance for the publication of the STISS proceedings volume.*

A HIGH-IMPACT DRY-SEASON PRECIPITATION EVENT OVER WEST AFRICA: EXTRATROPICAL INFLUENCES ON THE HEAT LOW

Peter Knippertz[1], Andreas H. Fink

[1] Institute of Atmospheric Physics, University of Mainz, D-55099 Mainz, Germany
E-mail: *knippertz@uni-mainz.de*

Abstract: This study provides a synoptic and dynamical analysis of a series of unusual weather events affecting large parts of northern Africa in January 2004. These include substantial precipitation in the arid Algerian and Libyan Sahara, the formation of a Saharan cyclone that causes a major dust storm in the eastern Mediterranean region, and widespread and abundant dry-season convection in the tropical Guineo-Sudanian zone. The latter event had substantial impacts on the local hydrology and human activities reaching from rotting harvests to improved grazing conditions. Due to a strong dynamical link to the extratropics the tropical convective precipitation appears to have a comparatively high predictability.

Keywords – *Northern Africa, Heat low, Precipitation, Saharan cyclone, Harmattan, Dust storm, PV inversion*

1. INTRODUCTION

The monsoonal climate of southern West Africa is characterized by a distinct rainy season during the boreal summer half-year. Rainfall during the winter months November to March is usually quite rare and thus long-term January mean precipitation around 10°N ranges between 1 and 5 mm. During this period the strong north–south pressure gradient over northern Africa generates a stable north-easterly flow at low-levels that brings relatively cool, dry and often dusty air from the Sahara into the West African Tropics, called the Harmattan. On average the weak wintertime heat low is located at around 7–8°N, just to the north of the Guinea Coast.

Between 20 and 21 January 2004 large parts of tropical West Africa including the countries of Ivory Coast, Burkina Faso, Ghana, Togo, Benin and Nigeria received significant precipitation amounts, exceeding 40 mm in various places as far north as 10°N, with maxima of up to 100 mm. As a consequence of the unusual precipitation, soil moisture recovered from low dry-season values down to a depth of one meter and it took more than a month until the soil had dried to values close to the time before the event. Pastures in the open tree savannah greened for weeks after the rainfall, a truly unusual sight for the West African dry season. On the other hand the rotting of cotton and other harvests caused substantial economic losses to resident farmers.

2. DRY-SEASON SOUTHWESTERLY MONSOON SURGE

Surface observations on 19 January 2004 reveal unusually hot temperatures (>37°C) over Burkina Faso and neighbouring countries, accompanied by unusually low mean-sea-level pressure and an enhanced cyclonic circulation at low levels. To the southeast of the intensified heat low south-westerly to southerly flow over Ghana, Togo and Benin brings relatively moist air from the Gulf of Guinea far into the continent, similar to typical spring or fall situations. In the afternoon of 20 January 2004 the Intertropical Discontinuity, the sharp boundary between moist tropical and dry Saharan air, reached a very unusual northerly position of 13ºN. In the course of the evening and the following night intense convection spreads across the Guineo-Sudanian zone from south to north (Figure 1, left panel). Convective initiation is most likely related to destabilization by daytime heating and the triggering of new cells is achieved by lifting through northward-progressing convective outflow boundaries, as indicated by observations of strong southerly surface winds ahead of the convection.

3. LINK TO THE EXTRATROPICS

Energy balance investigations suggest that a break in the Harmattan cool air advection was the driving factor for the northward shift and intensification of the heat low. This break is caused by the formation of a surface cyclone over the Algerian Sahara in the course of 19 January (Figure 1, left panel) and the associated reversal of the pressure gradient over parts of the Harmattan region.

A dynamical analysis of this cyclogenesis event based on piecewise inversion of the potential vorticity (PV) field (Davis and Emanuel, 1991) shows a close relation between the lowering of geopotential heights at low levels with the penetration of a pronounced upper-level trough from the extratropics into northern Africa. The penetration of the upper feature to the surface is supported by (a) the low static stability associated with the well mixed boundary layer over the Sahara, (b) the low altitude of the PV anomaly and (c) lee effects of the High Atlas (see Thorncroft and Flocas, 1997).

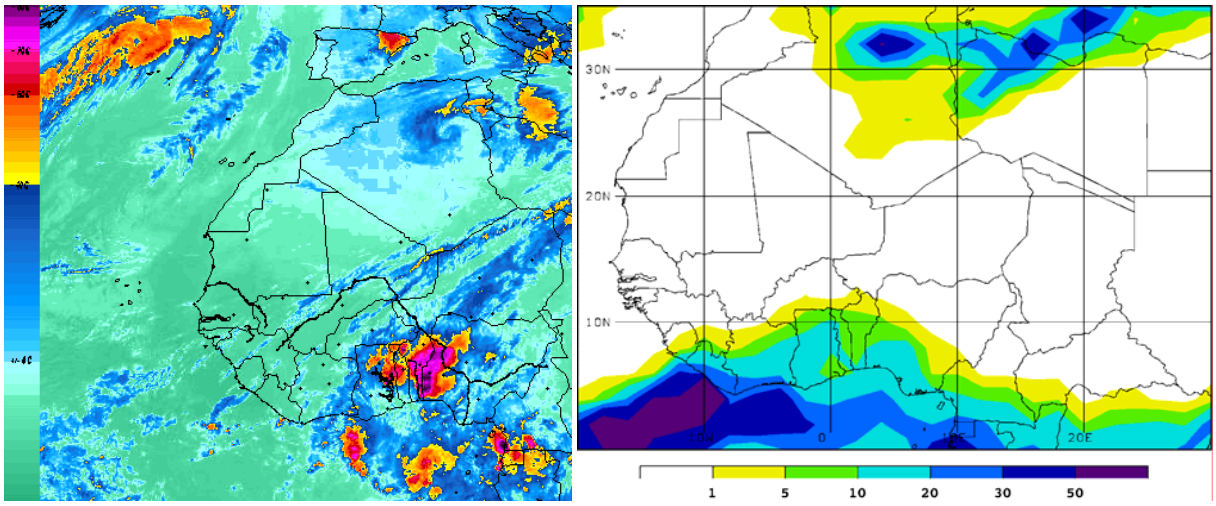

Figure 1. Left panel: Meteosat infrared image over West Africa for 00 UTC 21 January 2004, showing strong convection over Ghana, Togo, Benin and Nigeria, as well as a Saharan cyclone and precipitation over eastern Algeria and Tunisia. Right panel: Total precipitation (in mm) forecast from the ECMWF operational model for the period 00 UTC 19 January – 0600 UTC 22 January 2004.

The unusual nature of this synoptic development is underlined by precipitation in the Algerian and Libyan Sahara on the order of the long-term annual average (Figure 1, left panel) and the development of the Saharan low into an intense eastern Mediterranean cyclone that caused widespread dust storms in Libya, Egypt and parts of the Middle East with visibility down to less than 100 m. The passage of the Saharan low to the east was accompanied by a rapid increase in pressure over western West Africa, a surge in the Harmattan and relatively cool, dry and dusty conditions over the entire Guineo-Sudanian zone (cf. Knippertz and Fink, 2006a).

4. CONCLUSIONS

A synoptic-dynamic analysis of an unusual dry-season precipitation event in tropical West Africa in January 2004 reveals the following causal chain: (1) Penetration of a pronounced upper-level disturbance to subtropical northern Africa, (2) Saharan cyclogenesis, (3) break in the Harmattan cold advection, (4) northward shift and intensification of the weak wintertime heat low, (5) penetration of moist southerlies into the continent and (6) intense convection triggered by daytime heating and near-surface convective outflow. A full-detail description of this analysis is currently under preparation (Knippertz and Fink, 2006b).

These results indicate a close relationship between the tropical rainfall and synoptic-scale processes in the extratropics, which are usually much better forecasted by state-of-the-art numerical weather prediction models than tropical convection on a large range of scales. This leads us to hypothesize a relatively high degree of predictability of the kind of event under study here. In fact operational precipitation forecasts give clear evidence of a northward excursion of the major rain zone into the West African continent more than a day in advance, even though predicted absolute values are much too low (Figure 1, right panel). In our view this forecast of a possible high-impact weather event provides a basis for mitigating actions.

In the future a climatological analysis of wintertime Saharan cyclogenesis should be undertaken to identify typical frequency, structure, duration, location and rainfall patterns. Special attention should be paid to the exact ingredients needed to substantially deform low-level moisture fields in the Tropics. In addition numerical models could be used for sensitivity and predictability studies of dry-season precipitation in West Africa.

Acknowledgements: *The German Science Foundation (DFG; Grant KN 581/2–3) and the IMPETUS project (BMBF Grant 01LW06001A) provided funding to conduct the research presented here.*

REFERENCES

Davis, C. A. and K. A. Emanuel, 1991: Potential vorticity diagnostics of cyclogenesis. Mon. Wea. Rev., **119,** 1929-1953.

Knippertz, P. and A. H. Fink, 2006a: Synoptic and dynamic aspects of an extreme springtime Saharan dust outbreak. Quart. J. Roy. Meteorol. Soc. **132**, 1153-1177.

Knippertz, P. and A. H. Fink, 2006b: An unusual rainfall episode north and south of the Sahara: The influence of an extratropical disturbance on the dry-season heat low. Mon. Wea. Rev., in preparation.

Thorncroft, C. D., and H. A. Flocas, 1997: A case study of Saharan cyclogenesis. Mon. Wea. Rev., **125,** 1147-1165.

EXTRAORDINARY COOL-SEASON PRECIPITATION IN WEST AFRICA AND ITS UPSTREAM DEVELOPMENT: SENSITIVITY EXPERIMENTS WITH THE LOCAL MODEL (LM)

Florian Meier [1], Peter Knippertz

[1] Institute of Atmospheric Physics, University of Mainz, D-55099 Mainz, Germany
E-mail: *meierf@uni-mainz.de*

Abstract: A high-impact heavy precipitation event hit Senegal and Mauretania in January 2002. It was related to a low-latitude upper-level disturbance that is part of a high-amplitude Rossby wave train over the extratropical North Atlantic. Sensitivity experiments with the Local Model (LM) of the German Weather Service show that there is an important impact of latent heating in the extratropics on the wave amplification process.

Keywords – *Tropical-extratropical interactions, Diabatic heating, Rossby wave, Regional model simulations, Sensitivity experiments*

1. INTRODUCTION

On 09–11 January 2002 an extreme precipitation event hit Senegal and the neighbouring West African countries. It caused large damage to the local infrastructure and agriculture, and had other harmful impacts on human lives. With observed precipitation sums of up to 116 mm it was one of the most intense dry-season rainfall events on record (Knippertz and Martin, 2005). In addition to other factors, two upper-level troughs off the West African coast were instrumental for the advection of moisture and the upward motion, which led to the development of a Tropical Plume and initiated the rainfall. The troughs were associated with positive upper-level potential vorticity (PV) anomalies at low latitudes (see Figure 1, left panel, for the first trough). Such PV anomalies protruding from midlatitudes to the subtropics have been shown to be the result of breaking Rossby waves in idealized simulations of dry baroclinic waves (Thorncroft et al., 1993). On the other hand, later studies (Massacand et al., 2001; Knippertz and Martin, 2006) have shown that these events can be connected with massive diabatic heating in the upstream warm conveyor belt regions. Thus considering only dry dynamics might not be sufficient to adequately describe such tropical-extratropical interactions in the real atmosphere.

2. MODEL AND DATA

In a first step the precipitation event was successfully simulated with the Local Model (LM), the nonhydrostatic limited area model of the German Weather Service (DWD) with a horizontal resolution of 0.4° and 40 vertical layers. Analyses of two global models, the Integrated Forecasting System (IFS) of the European Centre for Medium-Range Weather Forecast (ECMWF) and the Global Model (GME) of the DWD, were used as initial and boundary data to drive the LM. Several sensitivity experiments have been conducted to investigate the impact of diabatic processes on the development of the upper-level PV field.

3. RESULTS

In one of the sensitivity experiments diabatic temperature tendencies were set to zero throughout the entire model simulation. Figure 1 (right panel) shows the resulting vertically integrated (500–150 hPa) PV field from the model run with suppressed diabatic heating (right panel) in comparison to the undisturbed full-physics simulation field (left panel) for a 84-hour hindcast. At the time shown in Figure 1 the first trough reaches its southernmost position off the coast of West Africa and initiates moisture transports into the precipitation region (Knippertz and Martin, 2005). The two runs were started at 00 UTC on 2nd January 2002.

The PV structures over North America are very similar in both runs. This is not surprising given the dominant influence of the driving analysis data close to the boundary of the model domain. Over the extratropical North Atlantic a pronounced upper-level wave can easily be recognized in the PV fields of both simulations. However, the PV maximum at about 38°N, 60°W is much more pronounced in the run with suppressed diabatic heating, while the ridge with very low PV values at about 50°N, 30°W over the central North Atlantic is more dominating in the “full physics” run. These differences in the structures of the PV fields are consistent with PV destruction caused by diabatic processes in the warm conveyor belt regions of two extratropical surface cyclones at 42°N, 39°W and 58°N, 37°W. The suppression of diabatic heating also led to a weakening of about 25 hPa of these systems and of the baroclinic zones along their cold fronts (not shown).

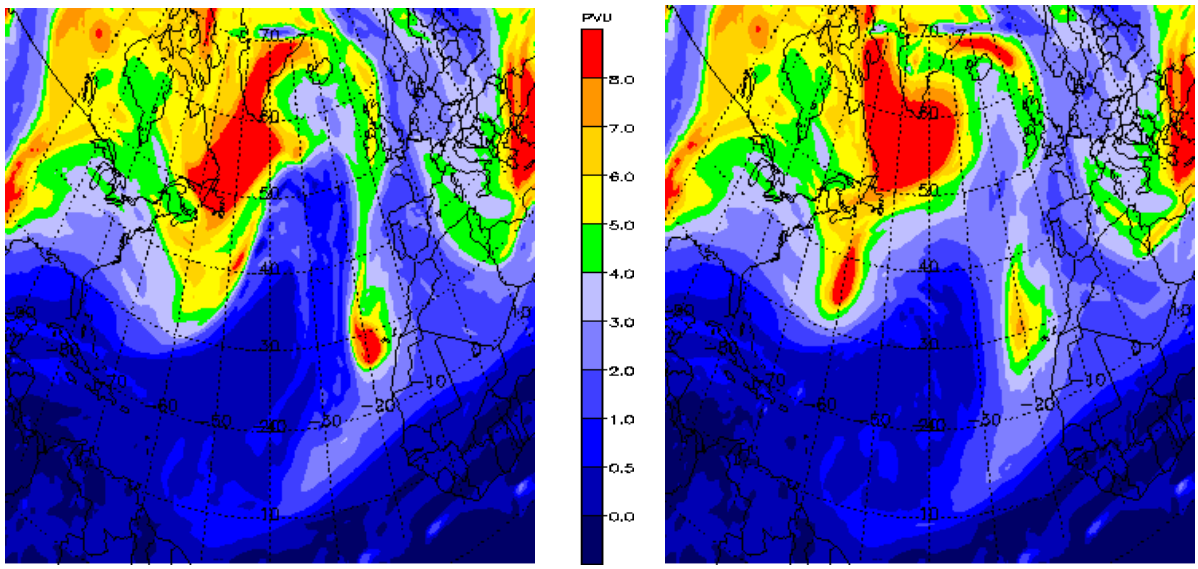

Figure 1: Vertically integrated (500–150hPa layer) potential vorticity fields in PVU (10^{-6} K m^2 kg^{-1} s^{-1}) for 12 UTC on 5th January 2002. The fields are taken from two hindcast simulations with the Local Model (LM) of the German Weather Service started at 00 UTC, 2nd January 2002: model run with "full physics" (left panel) and with suppressed latent heating (right panel). Note the pronounced differences in the development upstream of the precipitation event over West Africa that occurred several days later.

The upper-level PV destruction by diabatic processes was also confirmed by trajectory calculations undertaken with data from the "full physics" run (not shown).

The downstream PV maximum at 28°N, 20°W to the west of the West African coast is clearly stronger in the "full physics" run, most likely a result of the upstream wave amplification just described. This PV pattern initiated a moisture transport from the southwest and south to Senegal, which was crucial to the initiation of the heavy rainfall in the aftermath (Knippertz and Martin, 2005).

4. CONCLUSION

The harmful and extraordinary precipitation event over Senegal and Mauretania in January 2002 and its upstream development have been simulated with the Local Model (LM) of the German Weather Service. In addition to a "full physics" model run a simulation with suppressed latent heating has been conducted. First results show that not only dry dynamic baroclinic wave development and Rossby wave breaking, but also diabatic processes over the upstream extratropical North Atlantic are crucial to generate a strong PV anomaly at almost tropical latitudes. Further sensitivity experiments and the investigation of other similar cases of exceptional precipitation events in West Africa are envisaged.

Acknowledgements: *We would like to thank Jörg Trentmann from the University of Mainz for technical support and very helpful discussions, and the data services of the DWD and ECMWF for providing global model data. Moreover we acknowledge the DWD research and development group for the support to run and modify the LM at the university of Mainz and Michael Sprenger from ETH Zurich for helping us to use the LM with ECMWF boundary data. The German Science Foundation (DFG; Grant KN 581/2–3) provided funding to conduct the research presented here.*

REFERENCES

Massacand, A. C., H. Wernli and H. C. Davis, 2000: Influence of upstream diabatic heating upon an Alpine event of heavy precipitation. Mon. Wea. Rev., **129**, 2822-2828.

Knippertz, P. and J. E. Martin, 2005: Tropical plumes and extreme precipitation in subtropical and tropical West Africa. Quart. J. Roy. Meteorol. Soc., **112**, 2337-2365.

Knippertz, P. and J. E. Martin, 2006: The role of large-scale dynamic and diabatic processes in the generation of cut-off lows over Northwest Africa. Meteorol. Atmos. Phys., in press.

Thorncroft, C. D., B. J. Hoskins and M. E. McIntyre, 1993: Two paradigms of baroclinic-wave life-cycle behavior. Quart. J. Roy. Meteorol. Soc., **119**, 17-55.

A RATIONAL FRAMEWORK FOR IMPROVING THE TREATMENT OF MOIST CONVECTION IN GLOBAL MODELS

David J. Raymond

Physics Department and Geophysical Research Center, New Mexico Tech, Socorro, New Mexico, USA
E-mail: *raymond@kestrel.nmt.edu*

Abstract: A method of comparing cumulus parameterizations with a cumulus ensemble model is outlined and a simple example is presented.
Keywords – *Cumulus parameterization, Cumulus ensemble models.*

1. INTRODUCTION

The problem of the correct treatment of cumulus convection in global models is a tenacious one, at least partially because we lack tools for verifying parameterizations outside of the context of tuning exercises in the model itself.

We propose here the use of a "test cell" in which both cumulus parameterizations and cumulus ensemble models are run on an equal basis, allowing inter-comparisons to be made between the two. Instead of specifying an externally determined vertical velocity in the test cell, as is often done in single column models, the condition of buoyancy equilibrium with the surrounding environment is imposed. This condition is implemented by calculating the vertical velocity needed to counterbalance convective and radiative heating with adiabatic cooling. The moisture advective tendencies associated with this velocity exert a strong control on the humidity field in the test cell. The method used here was originated conceptually by Sobel and Bretherton (2000) and is described in more detail in Raymond and Zeng (2005). (See also Derbyshire et al. 2004.)

Unlike the direct imposition of vertical velocity, this method is causal, at least in tropical regions, since ascent in the tropics is largely produced by the convection itself. The simulated convection is thus placed in a context which does not differ much from the real world, lending confidence to any advances thus made in the parameterization.

As an example of the utility of this method, a cumulus parameterization is tuned to match the sensitivity of precipitation rate to tropospheric saturation fraction seen in a cumulus ensemble model. (Saturation fraction is defined as the ratio of precipitable water to saturated precipitable water.) The effect of this tuning on the resulting behavior of a large-scale circulation model is then explored.

2. METHOD

The cumulus ensemble model is run in two-dimensional mode in a 50 km by 20 km domain. Fixed radiative cooling combined with surface latent and sensible heat fluxes drive the model. The strength of

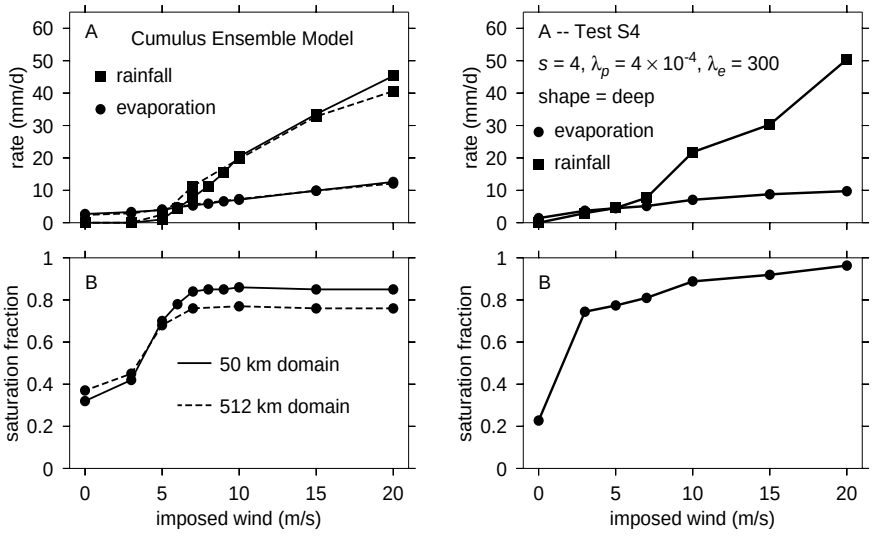

Figure 1: Dependence of rainfall rate, evaporation, and saturation fraction on imposed windspeed in the cumulus ensemble model (left) and the tuned cumulus parameterization (right).

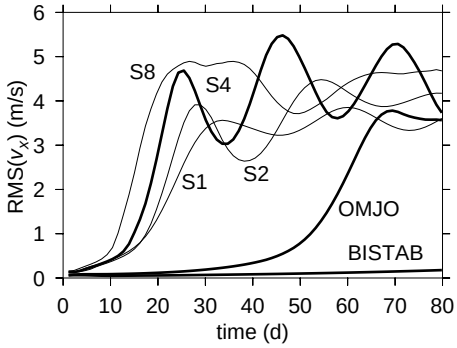

Figure 2: Development of surface zonal wind variance in equatorial beta plane model as a function of cumulus parameterization (see text).

these fluxes is governed primarily by a fixed wind applied normal to the model domain. The reference environment of the model in the test cell is a radiative-convective equilibrium profile obtained using the model itself, with a 5 m s^{-1} imposed wind speed.

A similar calculation is done in which the cumulus ensemble model is replaced with a modified version of the cumulus parameterization of Raymond (2001). The modification consists of altering the sensitivity of the convective rain parameterization to tropospheric relative humidity. The original version of the parameterization had a relatively smooth dependence of rain on humidity. However, the cumulus ensemble model shows a very steep increase of precipitation rate with saturation fraction, and the modification to the parameterization seeks to mimic this dependence.

In order to test the effects of this modification, the equatorial beta plane model of Raymond (2001) was run with the original and modified parameterizations under conditions of uniform sea surface temperature. Disturbances were initiated by random humidity noise.

3. RESULTS

Figure 1 shows how the rainfall rate, surface evaporation rate, and saturation fraction vary as a function of the applied wind for the cumulus ensemble model. Rainfall rate and saturation fraction increase dramatically with wind speed, with the saturation fraction asymptoting to a value near 0.87. For a larger horizontal domain (512 km), the asymptotic saturation fraction is somewhat less but other results are similar.

Figure 1 also shows similar results when the cumulus ensemble model is replaced by the modified version of the cumulus parameterization of Raymond (2001). The crucial aspect of these results is the steepness of the rainfall curve as a function of imposed wind speed.

Figure 2 shows how modifying the cumulus parameterization changes the rate of development of large-scale tropical disturbances in the equatorial beta plane model. OMJO uses the original parameterization of Raymond (2001), which exhibits a weaker dependence of rainfall rate on imposed wind speed than does simulation S4 (see figure 1). The steepness of this curve thus has a major effect on the rate of development of tropical disturbances, and comparison of the behavior of cumulus parameterizations with cumulus ensemble model results in this context should help us improve the parametric treatment of convection in global models.

Acknowledgements: *This work was supported by US National Science Foundation grant ATM-0352639.*

REFERENCES

Derbyshire, S. H., I. Beau, P. Bechtold, J.-Y. Grandpeix, J.-M. Piriou, J.-L. Redelsperger, and P. M. M. Soares, 2004: Sensitivity of moist convection to environmental humidity. *Quart. J. Roy. Meteor. Soc.,* **130,** 3055-3079.

Raymond, D. J., 2001: A new model of the Madden-Julian oscillation. *J. Atmos. Sci.,* **58,** 2807-2819.

Raymond, D. J., and X. Zeng, 2005: Modelling tropical atmospheric convection in the context of the weak temperature gradient approximation. *Quart. J. Roy. Meteor. Soc.,* **131,** 1301-1320.

Sobel, A. H., and C. S. Bretherton, 2000: Modeling tropical precipitation in a single column. *J. Climate,* **13,** 4378-4392.

LOKALMODELL WITH Z-COORDINATES

J. Steppeler [1], H.W. Bitzer , L. Torrisi, Schättler

[1] DWD, Offenbach, Germany
E-mail: *Juergen.steppeler@dwd.de*

Abstract: A version of the Lokalmodell is investigated using terrain intersecting z-co-ordinates based on the finite volume cut cell method adapted from CFD. Advantages of this approach for the circulation caused by mountains are shown.

Keywords – *THORPEX, WMO, Numerics, finite volumes, z-co-ordinates, cut-cell method, nonhydrostatic modelling*

1. INTRODUCTION

A version of the Lokalmodell LM (Steppeler et al. (2003) was developed using the terrain intersecting z-co-ordinate in the vertical with the cut call finite volume method. The cut cell method (Berger and Aftosmos, 1998) was for meteorological applications suggested by Steppeler (2002). It was adapted from CFD (Computational fluid Dynamics), where it is known to produce good results for the flow around obstacles. It is introduced into the version LM-z (Steppeler et. al., 2007), being suitable for realistic atmospheric simulations. In particular it could been shown, that mathematical problems of the step approach, leading to large inaccuracies, were avaided with the cut cell approach.

2. LM-Z

The orography in the LM-Z is represented by a bilinear spline. The grid cells are defined as in the LM (Steppeler et al., 2003) in the case without mountains. Some of these cells are completely above or below mountains. For these the LM discretisation applies. For the cells partly above the bilinear spline representing the mountains the finite volume method is used to derive the discretisation. For the physical parameterisations the grid is refined above the surface in each cell. Therefore even above high mountains a refined grid exists, capable to represent the boundary layer. So this method uses an unstructured and statically adaptive (over mountains) grid. These features are, however, hidden in a structured data format, which is very similar to that of LM. This is achieved by using the points below mountains for dummy calculations. The adaptive feature is equivalent to using two grids, which are connected by transformations.

3. RESULTS

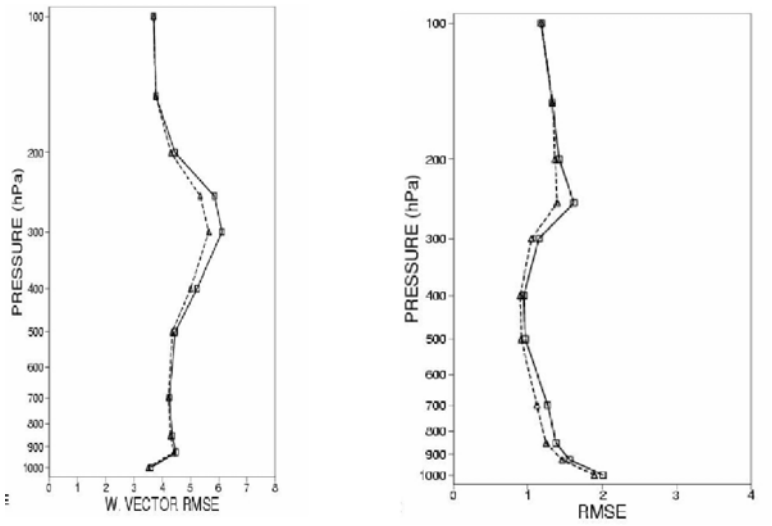

Figure 1.
RMS of winds (left) and temperatures (right) for a set of 35 forecasts; LM: solid; LM-z: dashed.

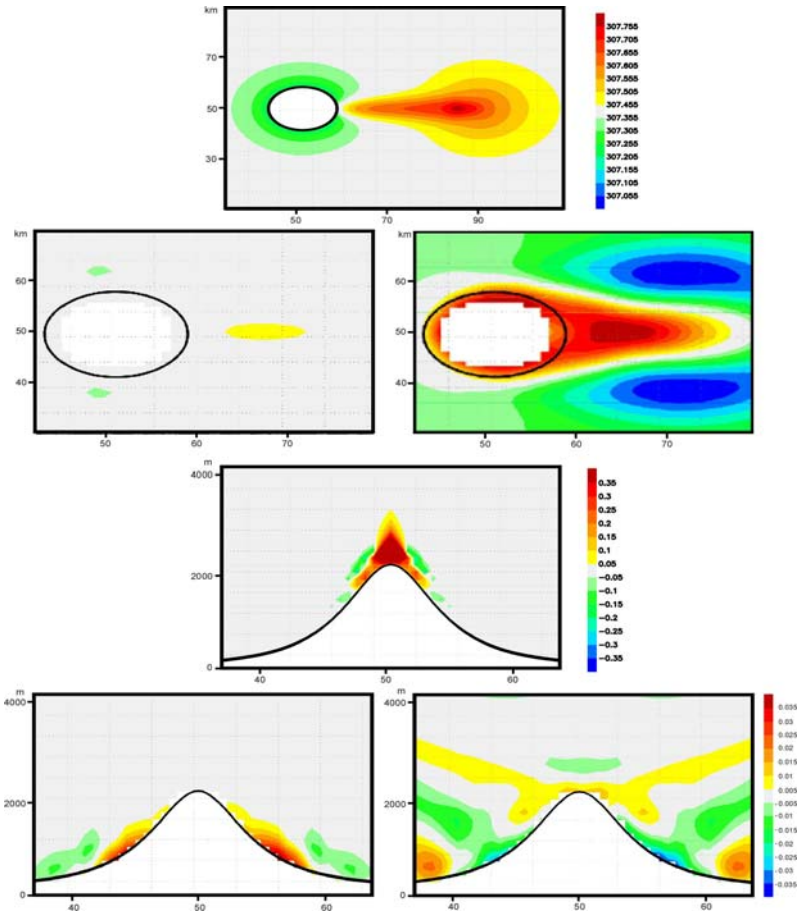

Figure 2. Fig. 2: Flow around a bell shaped mountain, 2 h forecasts. Top: Forecast of the LM-tf with radiation switched off. The temperature field in degrees Kelvin is shown for a horizontal cross section at height 150 m for the flow around a mountain of height 400m. The labels of the x- and y-axes are grid point numbers in a 2 km grid. Second row from top left: as top, for LM-z. Please note the different horizontal scale compared to the diagram above. Second row from top, right: As left, with radiation, corresponding to daytime conditions. Third row from top: Vertical cross section of the vertical wind field in m s^{-1}, 2 h forecast by LM-tf with radiation switched off. The initial values represent an atmosphere at rest and a mountain height is 2300 m. The analytic solution for this case is the atmosphere at rest. Bottom right: As above, using LM-z including radiation for night time conditions. The horizontal and vertical indices are grid point numbers, corresponding to horizontal grid length of 2 km and the vertical coordinate is height in m. Please note that the orographic mask shown is only accurate by half a grid length. Bottom left: as bottom right, for daytime conditions.

4. CONCLUSION

Mesoscale flow around mountains improves with LM.Z, as does RMS against Radiosondes.

REFERENCES

Berger, M., M. J. Aftosmos, 1998: Aspects (and aspect ratios) of cartesian mesh methods, Proceedings of the 16th international conference on numerical methods in fluid dynamics, Lecture note in Physics, Springer Verlag, Heidelberg, Germany

Steppeler,J., H.W. Bitzer, M. Minotte, L. Bonaventura, 2002: Nonhydrostatic atmospheric modelling using a z-coordinate representation. *Mon. Wea. Rev*. **130**, 2143-2149.

Steppeler,J., U. Schättler,H.W. Bitzer, A. Gassmann, U. Damrath and G. Gregoric, 2003: Meso gamma scale forecasts by nonhydrostatic model LM. *Meteor. Atmos. Phys.*, **82,**75-96.

Steppeler, J., H.W. Bitzer, Z. Janjic. U. Schättler, P. Prohl, U. Gjertsen, L. Torrisi, J. Parfinievicz, E. Avgoustoglou, U. Damrath, 2007: Prediction of Clouds and Rain Using a Z-Coordinate Non-Hydrpstatic Model. *Mon. Wea. Rev*. In print.

THE PROPAGATION OF CHANGING SURFACE PRESSURE AND CHANGING GEOPOTENTIAL HEIGHTS: A USEFUL TOOL IN WEATHER FORECASTING ON TIME SCALES OF 1-3 DAYS

Ata Hussain

Pakistan Meteorological Department, Research & Development Division, Islamabad, Pakistan
E-mail: atahussaingill@yahoo.co.in

Abstract: If the Isallobars and Isallohypse charts of different Synoptic hours and days are analyzed and compared & the shift in the highs and lows of the pressure and height are examined and the expected movements in these highs and lows during the next hours or days are calculated by using some suitable techniques, then this can be a very effective tool for the issuance of 1-3 days probabilistic weather forecasts. The probability of the occurrence of forecasted weather can further increase if these analyses are linked with satellite imagery & charts of other atmospheric parameters.

Keywords *–Isallobar, isallohypse, RegCM3*

1. INTRODUCTION

Weather forecasting has always been challenging even for very experienced and seasoned forecasters all over the world, just as the safe landing or taking off of aero planes for the aircraft pilots. Since the beginning of the science of weather prediction, the scientists of the world have been trying their best to explore the possibilities and find the scientific ways not only to predict the future weather conditions but also to make their predictions as accurate as possible. In this paper, the role of changing surface pressures and the changing geopotential heights of various isobaric surfaces has been discussed as a useful tool in issuing weather forecasts on a time scale of 1-3 days.

2. ISALLOBARS AND ISALLOHYPSE CHARTS

Generally, low pressure systems tend to move towards regions of the greatest pressure falls during the preceding hours or days. This is a very useful tool in nowcasting and very short range forecasting. However, if the Isallobars

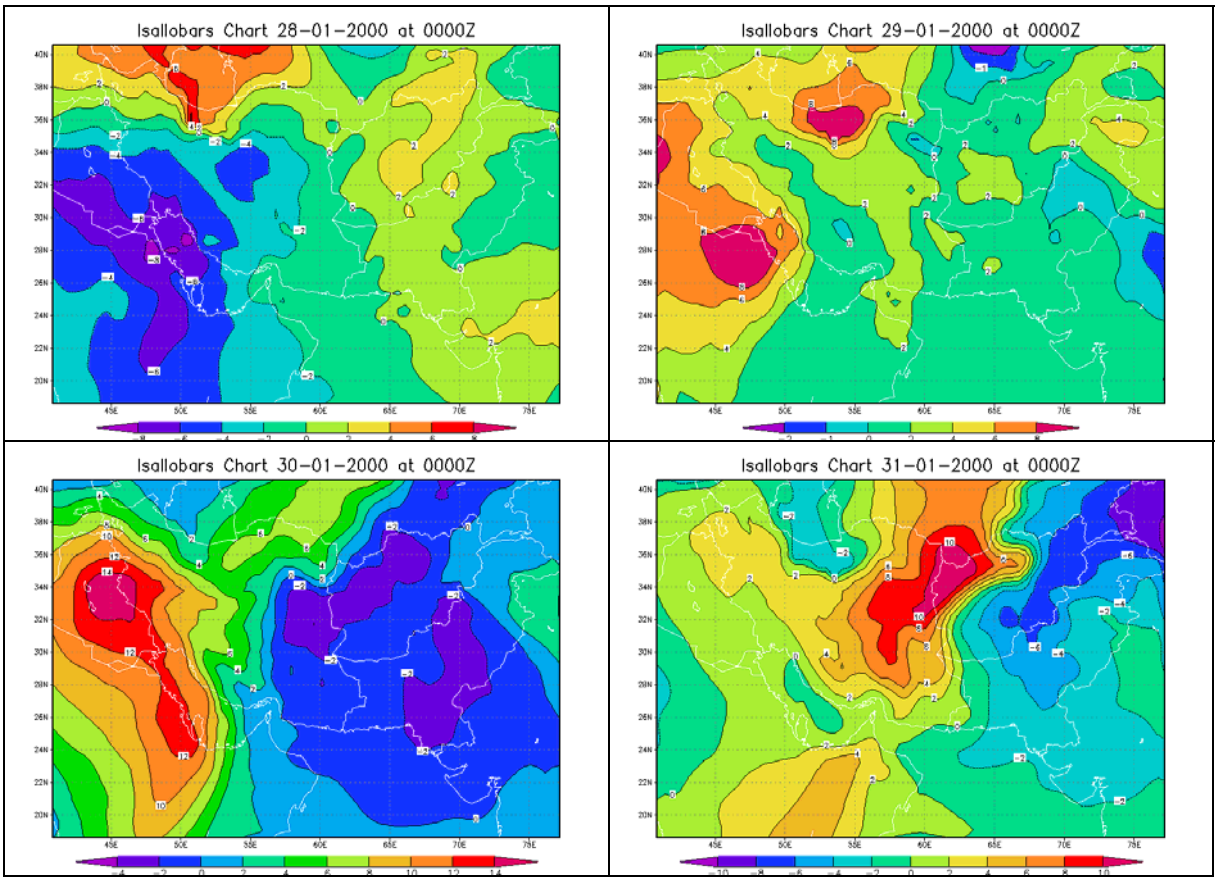

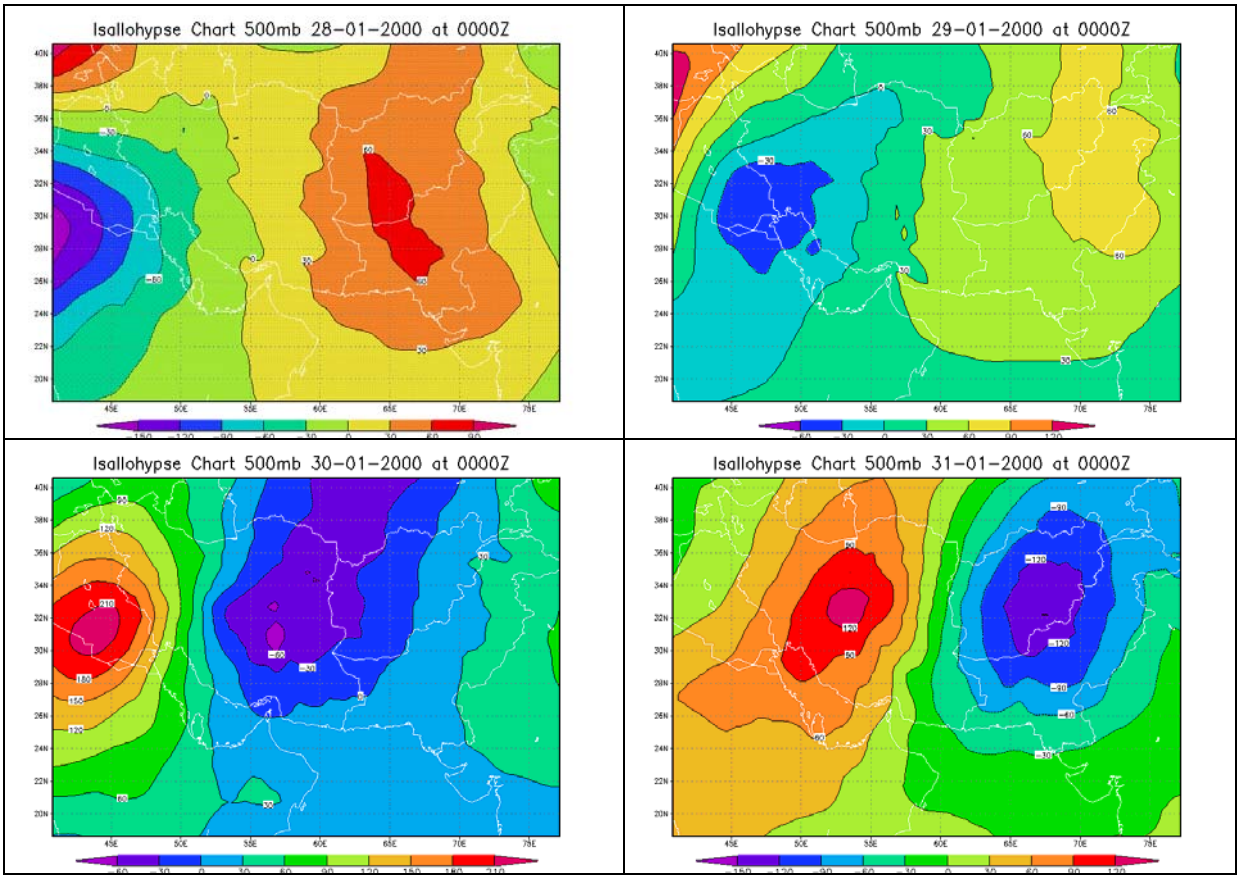

(i.e. pressure change charts) and Isallohypse charts (height-change charts) of 500hpa, 400hpa, 300hpa and 200hpa of different Synoptic hours (e.g. 0000UTC and 1200UTC) or/and days are compared and the shift in the highs (the areas of maximum pressure/height rise) and lows (the areas of maximum pressure/height fall) are examined and the expected movement and reallocation of these highs and lows during the next 12, 24 or 48 hours are calculated by using some suitable techniques (continuity method, displacement formulae and etc. depending upon the past observations, the prevailing conditions, physiography and topography of the region), this can be a very effective tool for the issuance of 1-3 days probabilistic weather forecasts. The probability of the occurrence of forecasted weather can further increase if these analyses of Isallobars charts and Isallohypse charts are linked with satellite imagery & charts of other surface and atmospheric parameters. Even more careful analysis can also lead to the issuance of deterministic forecasts for the period. The figures given above show the isallobars and isallohypse charts from 28 to 31of January, 2000, clearly indication how the changing surface pressure and 500mb heights are propagating towards west across central and south Asia (Iraq, Iran, Afghanistan, Pakistan and etc.) depicting the movement of weather systems over the region. These charts have been generated with the help of the output / simulations of RegCM3 (a sigma-coordinate regional climate model based on NCAR's mesoescale meteorological model, MM4) of ICTP, Italy using ECMWF reanalysis ERA40 datasets.

3. CONCLUSION

For the weather forecasting centers or National Meteorological Services of the world where various models (like MM5, HRM and etc.) are used for weather prediction, the Isallobars and Isallohypse charts can readily be generated and analyzed by making use of the model outputs files and the available prognostic grided surface and atmospheric data and thus the forecasts can timely be issued to the concerned. In many of the developing and most of the least developed countries, the use of Isallohypse charts is not very common. Although it take comparatively more time to generate and analyze these charts manually using conventional techniques, still the benefit of making use of these charts as a useful tool in weather prediction on time scale of 1-3 days can not be ruled out.

4. REFERENCES

Anthes R.A., E.Y Hsie and Y.H Kuo, 1987: Description of the Penn State / NCAR Mesoscale Model Version4 (MM4). NCAR Technical Note, NCAR / TN-282+STR, pp 66

OBJECT-BASED VERIFICATION OF PRECIPITATION FORECASTS FROM DIFFERENT MODELS

Christopher Davis[1], Barbara Brown and Randy Bullock
[1] National Center for Atmospheric Research, Boulder, Colorado, USA
E-mail: *cdavis@ucar.edu*

Abstract: A new method for verifying numerical precipitation forecasts is described and applied to predictions from two real-time forecast models. The method identifies rain areas, regions of contiguous (or nearly so) precipitation that survive a filtering procedure, and computes attributes of these areas (size, orientation, aspect ratio, intensity distribution, etc.). In this paper, we focus on statistical distributions from two models, not considering explicitly the matching of forecast and observed rain areas.

Keywords *– THORPEX, WMO, Verification, Precipitation, WRF model*

1. INTRODUCTION

Measures-based statistics arguably fail to provide useful information about the quality of forecasts of highly intermittent, spatially localized phenomena such as rainfall. Most so-called high-resolution, regularly produced forecasts today (including most operational forecasts) are verified using measures-based approaches.

2. DATA AND MODELS

Forecasts were obtained from a complete set of real-time forecasts by the Eulerian mass-coordinate version of the WRF model (release 2.1, Skamarock et al 2005) and the NCEP Nonhydrostatc Mesoscale Model (NMM, Janjic et al. 2005) during May and early June 2005. The ARW was run on both 4-km and 2-km grids while the NMM grid spacing was 4.5 km. The domains were similar, though not identical, covering a region approximately 2500x2000 km over the Central U.S. Additional details of the models and initialization procedure appear in Kain et al. (2005). Notably, none of the models use an implicit scheme to parameterize deep, moist convection. The observed precipitation was derived from the Stage IV precipitation analyses from NCEP (Baldwin and Mitchell 1997), obtained on a 4-km grid at hourly increments for the entire period. Interpolation was required to map the observations onto the WRF grid.

3. METHOD

The method we adopt is described in more detail in Davis et al. (2006a,b). Herein maximum column reflectivity is used as the variable to be evaluated. Pros and cons of using this variable for verification are discussed in Koch et al. (2005). The first task is to filter the rainfall field and define rain areas. The filtering is done in a two-step process. First, the entire field is convolved with a disk whose radius is closely tied to the minimum scale well resolved by the model or observations. The particular convolution chosen replaces the value of a field at a given point by its average over all grid points within a distance R. In the example shown in Fig. 1, the convolving disk has a radius of eleven grid lengths (44 km). After convolving the raw field, we retain only those points that exceed a threshold T (herein 20 dBZ). Although the original rainfall was smoothed and thresholded to define precipitation areas, we retain the original rainfall values at those points that remain nonzero after filtering. In this way, we can examine statistics of the reflectivity distribution as another object attribute.

4. PRELIMINARY RESULTS

In the present study, matching of forecast and observed objects is not considered. However, the statistics of reflectivity areas can suggest different sources of model error. In the present sample of models, it is clear that rain areas defined from the 2-km and 4-km ARW forecasts are seldom very different. A typical degree of similarity is evident by comparing Figs. 1a and 1b. It is also apparent from Fig. 1 that the differences between different models are generally not as great as the differences between any model and the real atmosphere. This we find is a recurring theme, probably related to the similarity of initial conditions used in these simulations, the relatively short duration of the forecasts in this case and the influence of lateral boundary conditions. Overall, we find that the distributions of object attributes in the three forecasts are broadly similar, and markedly different than distributions (in time and space) obtained from models using parameterized convection (Davis et al. 2003, Davis et al. 2006a).

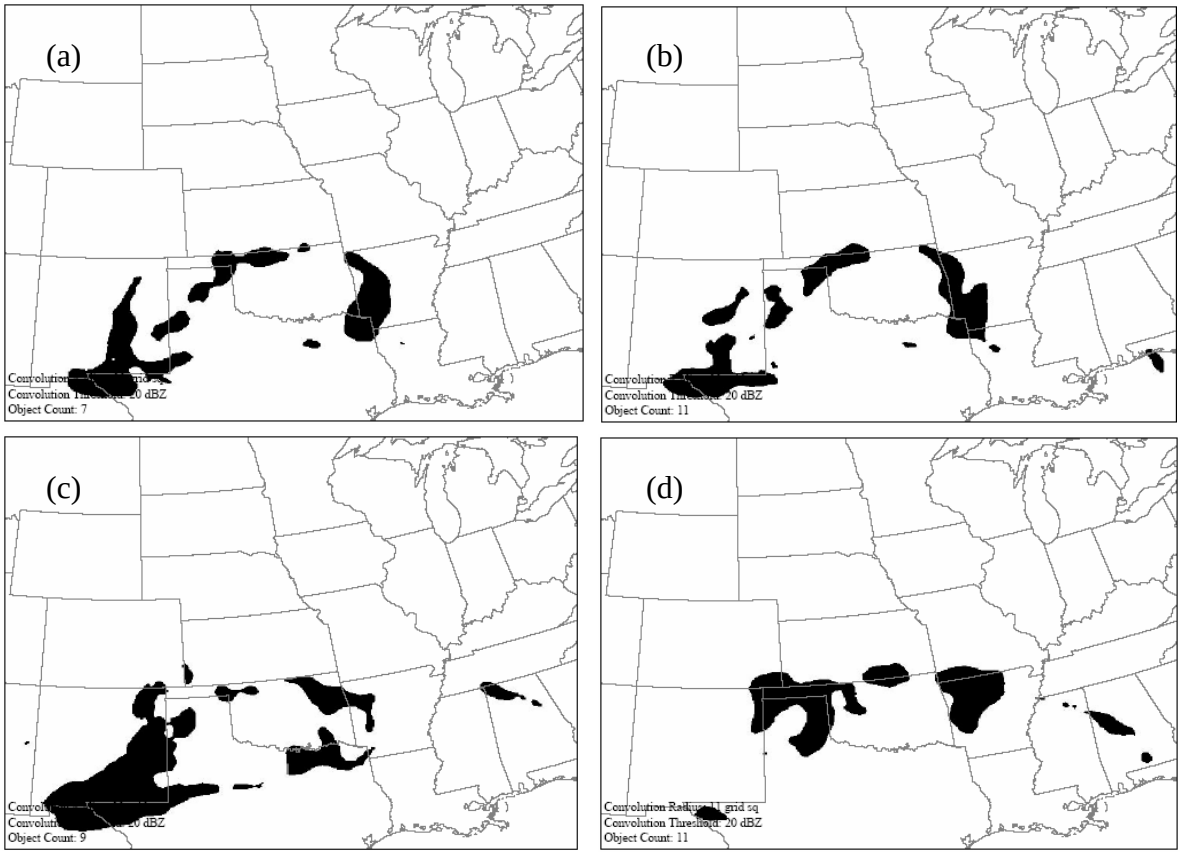

Figure 1. Binary mask (black indicates presence of a reflectivity object) obtained from filtering reflectivity data from (a) 4-km ARW; (b) 2-km ARW; (c) 4.5-km NMM and (d) observations. All times area valid 12 UTC 5 May, 2005, with the model output being a 24-h forecast. The convolution radius was 44 km and the threshold was 20 dBZ. The domains shown are approximately 2500x2000 km. And represent the common analysis domain for all forecasts and observations.

5. DISCUSSION

The purpose of the present forecast comparison is mainly to illustrate the object-oriented methodology. For extended-range forecasts using coarser resolution models, it may be desirable to use slightly different parameters to highlight larger precipitation features. However, the approach is the same. In the THORPEX context, "objects" should more generally be considered "events" wherein the time dimension can be added to define weather systems in forecasts and observations. This approach was followed, albeit in a crude way, in Davis et al. (2006b). Weather systems need not be defined in terms of precipitation. As long as the observations are sufficient to identify a range of temporal or spatial scales, events can be objectively identified. The ultimate advantage of an object-based approach is the ability to link forecast attributes to event-dependent user needs.

REFERENCES

Baldwin, M. E., and K. E. Mitchell, 1997: The NCEP hourly multi-sensor U.S. precipitation analysis for operations and GCIP research. *Preprints, 13th Conf. on Hydrology*, Long Beach, CA, Amer. Meteor. Soc., 54–55.

Davis, C. A., K. W. Manning, R. E. Carbone, J. D. Tuttle, and S. B. Trier, 2003: Coherence of warm season continental rainfall in numerical weather prediction models. *Mon. Wea. Rev.*, **131**, 2667-2679.

Davis, C., B. Brown, and R. Bullock, 2006: Object-based verification of precipitation forecasts, Part I: Methodology and application to mesoscale rain areas. *Mon. Wea. Rev.*, **134**, 1782-1784.

Davis, C., B. Brown, and R. Bullock, 2006: Object-based verification of precipitation forecasts, Part II: Application to convective rain systems. *Mon. Wea. Rev.*, **134**, 1785-1795.

Janjic, Z. I., T. L. Black, M. E. Pyle, H.-Y. Chuang, E. Rogers, and G. J. DiMego, 2005: The NCEP WRF NMM core. Preprints, 2005 WRF/MM5 User's Workshop, 27-30 June 2005, Boulder, CO. CDROM, paper 2.9.

Kain, J. S., S. J. Weiss, M. E. Baldwin, G. W. Carbin, D. Bright, J. J. Levit, and J. A. Hart, 2005: Evaluating high-resolution configurations of the WRF model that are used to forecast severe convective weather: The 2005 SPC/NSSL Spring Experiment. 17th Conference on Numerical Weather Prediction. Americal Meteorological Society, Paper 2A.5.

Koch, S. E., B. S. Ferrier, M. T. Stoelinga, E. J. Szoke, S. J. Weiss, and J. S. Kain, 2005: The use of simulated radar reflectivity fields in the diagnosis of mesoscale phenomena from high-resolution WRF model forecasts. *Preprints, 11th Conf. On Mesoscale Processes*, Albuquerque, NM, American Meteorological Society, paper J4J.7.

Skamarock, W. C., J. B. Klemp, J. Dudhia, D. O. Gill, D. M. Barker, W. Wang and J. G. Powers, 2005: A Description of the Advanced Research WRF Version 2. NCAR Technical Note TN-468+STR. 88 pp.

AN ANALYSIS OF DIFFERENT BIAS-CORRECTION ALGORITHMS IN A SYNTHETIC ENVIRONMENT

Joo-Hyung Son[1], Zoltan Toth[2], Dingchen Hou[3]

[1] Forecaster division, KMA, Seoul, Korea, [2] Environmental Modeling Center NCEP/NWS/NOAA, Campspring, MD, USA, [3] EMC/NCEP/NWS/NOAA and SAIC, Campspring, MD, USA
E-mail: jhson@kma.go.kr, Zoltan.Toth@noaa.gov, Dingchen.Hou@noaa.gov

Abstract: The estimation and correction of systematic errors is an accepted way of improving the performance of numerical weather forecasts. In this study, synthetic model consisted of observation and forecast was generated by ARMA process and then used to investigate the benefits of using larger training data and to compare two bias definitions, the traditional method and Bayesian type method. They were compared by the absolute bias error, RMSE, and CRPS and Bayesian type method had the additional benefits in terms of bias error for EW (equal weight bias correction method) and KF (Kalman Filter bias correction method) and RMSE/CRPS for EW.

1. INTRODUCTION

Most products of numerical weather prediction are subject to systematic error (i.e. bias) and random errors that increase model uncertainty. Therefore, the estimation and correction of systematic errors is an accepted way of improving the performance of numerical weather forecasts. In general, the quality of bias correction depends on how to estimate bias correctly. A range of methods has been proposed and tested on various forecast and corresponding verification data sets to find out the effective and practicable bias estimation methods. (e.g. Geniting et al, 2005; Hamill et al, 2004) However, most forecast data sets to be used for bias estimation are relatively small. Some studies used simple models to investigate bias-correction algorithms with larger training data sets. Another possibility, followed in this study, is the use of synthetically generated observations and forecasts for testing the performance of various bias-correction algorithms. The synthetic set composed of analysis and forecast generated by ARMA model was used for analyzing the characteristics of different bias correction algorithms.

2. GENERATION OF A SYNTHETIC DATA SET

Synthetic observation and forecast were generated with statistics estimated from a series of actual numerical analysis. For an ideal synthetic model that could be general and simple approach, it was assumed that synthetic observation and forecast don't have the annual cycle and they are stationary.

The synthetic observations were generated using an ARMA process with standardized numerical climate analysis. Synthetic forecasts were then produced by adding (a) random forecast errors of various magnitude (to reflect the skill of the forecasts), and (b) a time independent error (to represent systematic error) to the synthetic analyses, where the statistics of the synthetic errors matches that of actual numerical forecasts. This synthetic observations and forecasts were used for comparing bias estimation methods.

3. ALGORITHMS OF BIAS CORRECTION

Two bias estimation definitions were compared as well. The first method uses the traditional bias of the time mean difference between past observations and forecasts. The second method, motivated by the Bayesian theory, defines the bias as the time mean difference between the forecasts and the expected (and not actual) value of the observations, given the forecast value.

Two simple bias-estimation methods were considered to look into properties of bias-correction according to the bias definitions with synthetic analysis and forecast. One is the equal weight method that is commonly used so far and the estimated bias is defined by the average of each bias of each time. Another method is Kalman Filter that is a graded weight method that each bias of each time step has a different weight, the closer bias as a function of time has larger weight.

4. RESULT

Several kinds of error tests were performed to compare the performance of the bias-estimation and definition methods. According to the study, the Bayesian bias definition outperforms the traditional bias definition in both the equal weight and the Kalman Filter methods in terms of time mean error of bias (Figure 1a). It is independent of how much bias error the forecast has. Figure 1b) shows the sample size that the absolute bias error reaches

0.05 and 0.1 according to the correlation between forecast and analysis for the equal weight method. The lower skill forecasts need much lager sample size and the Bayesian method only needs about one-third of traditional method to approach error threshold. In addition, when the training sample size is increased from one season to climatology, the reduction in systematic error is only around 5%. (not shown)

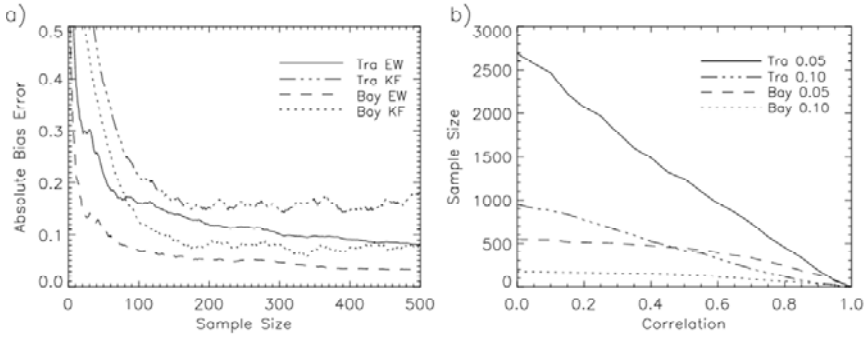

Figure 1. The Relationship between the absolute bias error and the bias correction methods: a) the absolute bias error of each bias correction method as a function of time (sample size) when the correlation between forecasts and analysis is 0.35, b) the sample size that the absolute bias error reaches 0.05 and 0.1 according to the correlation.

RMSE skill score considers random error as well as the systematic error. CRPSS is able to show the effects on ensemble based probabilistic forecast. Most bias correction method outperformed the forecast not to be done any bias correction for both skill scores, as the correlation is low. Figure 2 compares the performance of each method. When the training periods were shorter 200, the traditional bias definition methods showed better performance than the Bayesian methods by contrast with the absolute bias error. However, Bayesian is better than traditional in terms of the equal weight method while the traditional is better than Bayesian in terms of the Kalman Filter method when the training period is larger than around 300 even thought there are no skill above correction 0.5. It is also seen at the CRPSS.

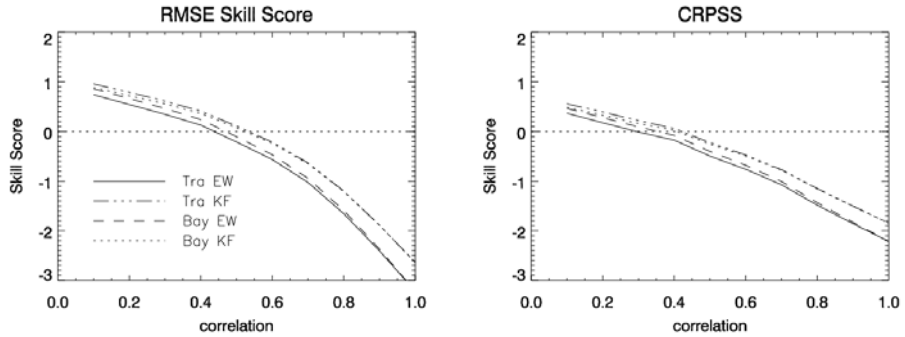

Figure 2. RMSE skill score and CRPSS as a function of correlation between forecasts and analysis when the training period is 400.

5. CONCLUSION

Numerical forecast model is being improved every moment by higher resolution, the observation data of high quality, and data assimilation et al. It's uneconomic to prepare the hind-cast whenever the numerical model is changed. So we need a flexible and effective bias correction method that is available with relatively short training period. Working with synthetic analysis and forecast data sets is useful in the investigation of their performance of various statistical bias correction methods. Bayesian bias estimation method had the additional benefit in terms of the absolute bias error for both correction methods, and RMSE skill score and CRPSS for equal weight method. In addition, it was found that Bayesian definition could save the training sample space a lot. This suggests that the use of large hind-cast datasets generated by frozen systems may be unnecessary.

REFERENCES

Geniting, T., Raftery, A. E., Westveld III, A. H., Goldman, T., 2005: Calibrated Probabilistic Forecasting Using Ensemble Model Output Statistics and Minimum CRPS Estimation. Mon. Wea. Rev. . **133** , 1098-1118.

Hamill, T. M., Whitaker, J. S., Wei, X., 2004: Ensemble Reforecasting: Improving Medium-Range Forecast Skill Using Retrospective Forecast. Mon. Wea. Rev. . **132** , 1434-1447.

QUALITY ASSESSMENT OF MESOSCALE EPS FORECASTS USING SATELLITE AND RADAR DATA

Christian Keil and George C. Craig

Institut für Physik der Atmosphäre, DLR Oberpfaffenhofen, Germany
E-mail: *Christian.Keil@dlr.de*

1. INTRODUCTION

Errors in regional forecasts often take the form of phase errors, where a forecasted weather system is displaced in space or time. For such errors, a direct measure of the displacement is likely to be more valuable than traditional measures. A novel forecast quality measure FQM is applied that is based on image comparison of observed and forecast imagery of cloud or precipitation fields (Keil and Craig, 2006). The objective evaluation is performed using the pyramidal matching algorithm originally developed to detect and track cloud features (e.g. convective clouds, contrails) in satellite imagery (Zinner et al., 2006). The pyramid matching algorithm computes a vector field (optical flow) that deforms, or morphs, an image into a replica of another image by seeking to minimize an amplitude-based quantity at different scales within a fixed search environment. The FQM combines the magnitude of a mean displacement vector and the final mean squared difference of observed and morphed forecast image.

2. MODEL AND OBSERVATIONAL DATA

Mesoscale ensemble forecasts are produced using the COnsortium for Small-scale MOdelling Limited-area Ensemble Prediction System (COSMO-LEPS; Molteni et al. 2001), in which the global ECMWF EPS provides initial and boundary conditions for the mesoscale non-hydrostatic Lokal-Modell (LM, Δx=7km). The LM provides again initial and boundary conditions for a high-resolution LMK ensemble (Δx=2.8km). The generation of model-forecast synthetic satellite (Keil et al., 2006) and radar imagery allows a direct comparison with observed Meteosat-8 IR (i.e. brightness temperature) and Radar Composite (i.e. Radar reflectivity) imagery.

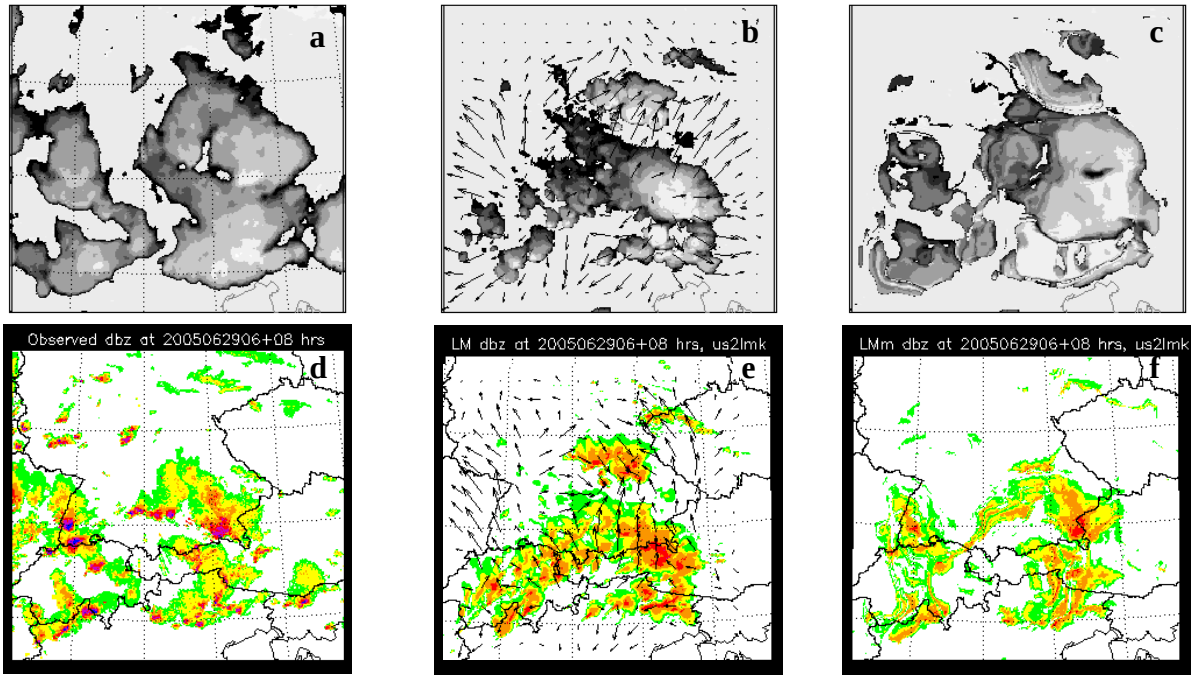

Figure 1. Observed Meteosat-8 infrared image (a) and Radar Composite (d) collocated with LMK forecast synthetic imagery (b,e) on 29 June 2005 14:00 UTC. Superimposed in (b,e) are the displacement vectors computed with the pyramid matching algorithm. The morphed synthetic imagery for satellite and radar is displayed in the last column (c,f).

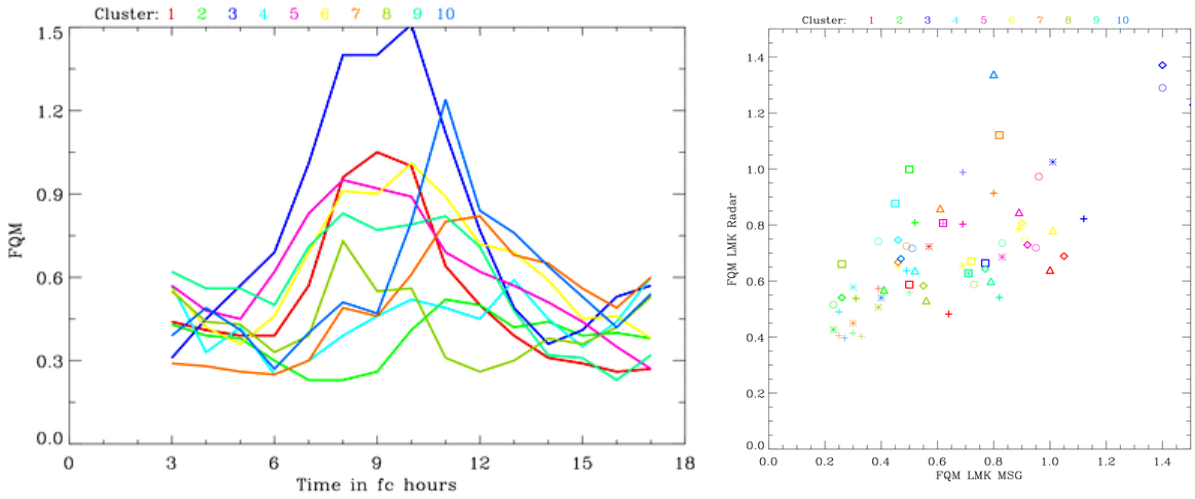

Figure 2. Left: Time series of FQM computed with Meteosat-8 (MSG) data for all ten ensemble members (cluster 1 to 10 displayed in different color code). Right: Scatter diagramme of FQM computed with satellite (MSG) and Radar data (same colors refer to same cluster, different symbols indicate different forecast times).

3. DISCUSSION

Forecast quality of an ensemble of ten high-resolution LMK experiments is assessed using the displacement-based error measure FQM for a domain of 700 x 700 km^2 centred over the European Alps on 29 June 2005. Here, Meteosat-8 IR imagery, used as a proxy to locate precipitating cloud features when applying a threshold brightness temperature of -20°C to mask out the land surface and shallow non-precipitating cloud, and the Radar composite provide corresponding multi-dimensional information to validate the forecasts (Fig. 1a and 1d). Application of the pyramid matching algorithm gives vector fields (Fig. 1b and 1e), which morph the forecast patterns towards observed ones. The normalized mean of the displacement vector field and the normalized mean squared difference of morphed and observed imagery (Fig. 1c vs 1a, and 1f vs 1d, respectively) determine the FQM. For the example depicted, the FQM based on satellite (Radar) data attains 0.3 (0.4) for cluster 2 at 14:00 UTC, i.e. at 8 hours forecast time.

The temporal variation of FQM (w.r.t. satellite data) for the different clusters is shown in Fig.2a, indicating the good quality of cluster 2 (displayed in Fig.1). In contrast, cluster 3 misses the convective evolution giving large FQM values (bad forecast quality). Interestingly, the spread is largest during the convective period starting at 12:00 UTC (+6h forecast) until 18:00 UTC (+12h). Computation of the FQM based on Radar imagery gives similar results, with cluster 2 and 8 performing 'best'. The correlation between FQM based on satellite vs Radar data amounts to 0.73 during the 6 hourly convective period (Fig. 2b).

4. OUTLOOK

A systematic evaluation of the performance of the Regional Ensemble System and the behavior of the novel measure itself is planned during the three month period of the field experiment Convective and Orographically-induced Precipitation Study (COPS) taking place in summer 2007 in a low-mountain area in southwestern Germany/eastern France, which is characterized by high summer thunderstorm activity and particularly low skill of numerical weather prediction models.

REFERENCES

Keil, C. and G. C. Craig, 2006: A displacement-based error measure applied in a regional Ensemble Prediction System. Accepted by *Mon. Wea. Rev.*

Keil, C., A. Tafferner and T. Reinhardt, 2006: Synthetic satellite imagery in the Lokal-Modell. *Atmos. Res.*,**82**, 19-25.

Molteni, F., R. Buizza, C. Marsigli, A. Montani, F. Nerozzi, and T. Paccagnella, 2001: A strategy for high-resolution ensemble prediction. Part I: definition of representative members and global-model experiments. *Quart. J. Roy. Meteor. Soc.*, **127**, 2069-2094.

Zinner, T., H. Mannstein and A. Tafferner: Cb-TRAM: Tracking and monitoring onset, rapid development, and mature severe convection using multi-channel Meteosat-8 SEVERI data. Submitted to *Meteorol. Atmos. Phys.*

COMPARISON OF PROBABILISTIC WIND SPEED FORECASTS PRODUCED FROM ECMWF DETERMINISTIC AND EPS OUTPUTS

Juha Kilpinen

Finnish Meteorological Institute (FMI), Finland

E-mail: *juha.kilpinen@fmi.fi*

1. INTRODUCTION

Probability forecasts have been produced objectively since late 1960ies using different statistical approaches. Among these methods was Model Output Statistics (MOS) which was used in estimating Probability of Precipitation (PoP) e.g. by Glahn and Lowry (1972). Prior to the Ensemble Prediction System (EPS) ECMWF made also tests with a statistical method. However, this system never entered operational phase. The ECMWF EPS forecasts have been used at FMI as guidance almost since the beginning of their operational production. However, the assessment of their local usefulness has not been done. A general verification of EPS wind speed forecasts has been available by Saetra and Bidlot (2004).

EPS forecasts suffer from same kind of bias problems as deterministic forecasts. This holds true especially for near surface parameters like 2 metre temperature and 10 metre wind. The spread of the ensemble is also usually under dispersive. To make EPS forecasts more useful in operational weather the forecasts should be calibrated. EPS guidance should also outperform the guidance provided from deterministic output applying statistical methods.

2. DATA AND METHODS

The data consists of three winters 2002-2003, 2003-2004 and 2004-2005 (October-April). Forecast data was from ECMWF MARS archive and wind observations from 4 stations near southern coasts of Finland. The stations are (WMO number) 02979, 02980, 02981 and 02987 and the number of observations per time incident (00 or 12 UTC) is more than 600. The anemometer height is more than 10 metre and there is a need to reduce the wind speed to make the correspondence between observations and forecasts better. The typical height of the anemometer at these stations is about 30 metres. Tests were made both with original and corrected wind speed. The wind speed was corrected assuming that the wind profile in boundary layer is neutral. This assumption may not be relevant in all cases because during late winter (Feb-March-April) the ice cover of sea may cause that stable conditions occur more often.

The data from MARS was interpolated to 0.5 degree resolution. This may cause some smoothing for wind speed forecasts of at least on one station (02987). The forecast data is not interpolated to station but the nearest grid point is chosen.

Two different methods are used in this study. In first method, probability forecasts of wind speed were produced from ECMWF deterministic (operational) forecasts. The bias of deterministic forecasts is estimated with a recursive algorithm (Young, 1984) and the probabilities are estimated using the posterior (climatologic) error distribution (error dressing method). The estimation of error distribution was also made with a similar recursive method. In second method, EPS wind speed output was calibrated using a similar method as Buizza et al. (2003) but applying the same recursive algorithm as before. Several versions of these methods were tested. These results were then compared to original EPS forecasts.

3. RESULTS

The forecasts are verified against original and corrected wind speed observations. Brier Skill Score (BSS) (see Figure 1) and ROC area were computed besides the traditional deterministic scores. The main interest in this evaluation is in the probability of wind speed exceeding near gale force (>= 14 m/s).

The results indicate that both methods increase the quality of probabilistic output compared to original EPS. The increase of quality against original observations is substantial corresponding to 1 to 2 days in forecast length. The increase of quality was less impressive using corrected observations because correction of observations also reduces part of the bias in forecasts. Not all the increase is due to the calibration because part of increase of quality is just due to correction of the miss match between observations and coarse grid representation. For shorter lead times error dressing of deterministic wind speed forecasts gives better results

while after +84h - +96h forecasts calibrated EPS forecasts perform better. This holds true both with BSS and ROC area (not shown). Test with other thresholds (11 m/s and 17 m/s) give similar results.

Spread skill relation was studied with indirect method by comparing calibrated EPS forecasts and error dressing of EPS mean forecasts. The results show that calibrated EPS guidance with flow dependent spread gives better results after +48h lead times compared to static error dressing indicating the existence of spread skill relation. The added value corresponds to 6-12 hour lengthening of forecast length.

Independent recursive estimation gives almost as good results as dependent batch type estimation (results not shown). This may indicate that at least in continuous variables like wind speed reforecast of historical data is not so important.

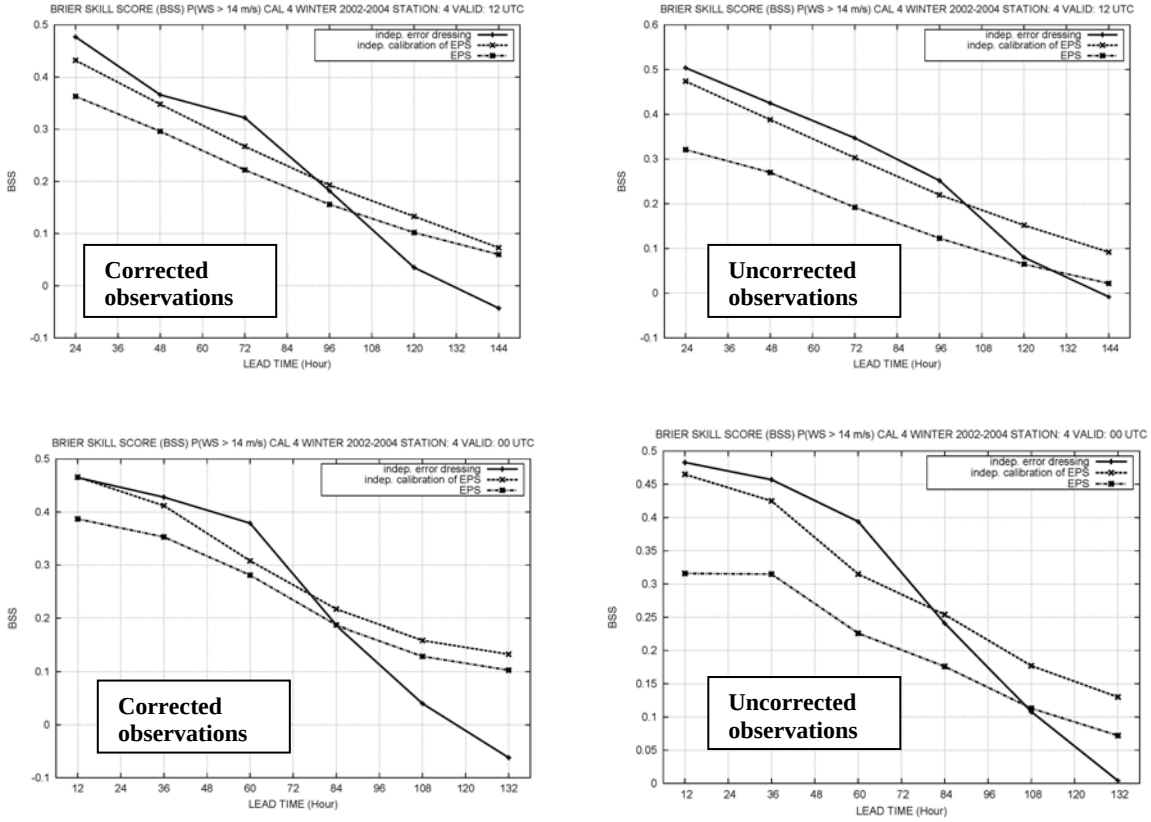

Figure 1: Brier Skill Score against forecast lead time with corrected (right) and uncorrected (left) observations. Calibrated EPS forecasts are compared with original EPS forecasts and forecasts produced with recursive error dressing of deterministic forecasts.

REFERENCES

Buizza R, D.S. Richardson and T.N. Palmer, 2003: Benefits of increased resolution in the ECMWF ensemble system and comparison with poor-man's ensembles, Quart. J. Roy. Meteor. Soc., 129, 1269-1288.

Glahn, H. R. and D. A. Lowry, 1972: The Use of Model Output Statistics (MOS) in Objective Weather Forecasting. J. Appl. Meteor., 111, 1203-1211.

Saetra O. and J.R. Bidlot, 2004: Potential Benefits if Using Probabilistic Forecasts for Waves and Marine Winds Based on the ECMWF Prediction System, Wea. Forecasting, 19, 673-689.

.

Young, P., 1984: Recursive Estimation and Time Series Analysis. An Introduction. Springer Verlag.

EXPLICITLY ACCOUNTING FOR OBSERVATION ERROR IN CATEGORICAL VERIFICATION OF FORECASTS

Neill Bowler

Met Office, Fitzroy Road, Exeter, EX1 3PB, UK
E-mail: *Neill.Bowler@metoffice.gov.uk*

Abstract: Given an accurate representation of errors in observations it is possible to remove the effect of those errors from categorical verification scores, assuming that errors between different observations are independent, and observation errors are independent of the value of the observation. This method can be applied to deterministic verification as well as to measures such as relative operating characteristic (ROC) and Brier skill score. In general the removal of the effect of observation errors improves the apparent performance of a forecasting system.

The method describes the errors in a contingency table based on the probability that an observation error leads to the verification falling into the wrong category (i.e. an event being observed to occur when it did not in reality). This leads to the ability to reconstruct the "true" contingency table based on the values measured against the observations.

Keywords – *ensemble Kalman filter, ETKF, localisation*

1. INTRODUCTION

A major problem in the area of weather forecasting is caused by deficiencies in the observing network, either through the imperfect coverage of the observational network or through errors in the observations themselves. These deficiencies contribute to the initial condition uncertainties that have been the subject of great study. Comparatively little has been written about the effect of observation errors on the verification of forecasts. (Ciach & Krajewski, 1999) introduced an error separation technique for decomposing the mean square error of a forecast into terms involving the error in the observations and the error in the forecast. (Saetra *et al*., 2004) showed how to remove the effect of observation errors from verification using rank histograms. Here the categorical verification of forecasts is addressed, and it is shown how one may attempt to remove the effect of observation errors from such verifications.

2. A DESIRABLE PROPERTY OF VERIFICATION SCORES

An important property of verification scores is that the same score is achieved for a forecast, whatever the quality of the observational network. The importance of this property is seen when one considers a perfect deterministic forecast. Given a perfect observation this forecast would be seen to be perfect. However, any error in the observational network may obscure this fact, leading to the perfect forecast being believed to be in error!

One proposal for dealing with observational error would be to treat the observation as defining a probability density function for the truth and using probabilistic measures (such as the Brier score) to define the forecast quality (Candille and Talagrand, 2004). However, such an approach would penalise a perfect forecast and lead to difficulties when comparing forecasts verified against different observations.

In general the problem of observational errors leads to the same problem as is faced in the verification of probabilistic forecasts - it becomes impossible to state whether a single forecast was "correct". However, by aggregating a number of forecasts, as in categorical verification, it becomes possible once again to recognise the quality of a perfect forecast.

3. ACCOUNTING FOR OBSERVATION ERRORS

In the following a method for performing verification of categorical forecasts is sought which will produce the same results independent of observational errors. If an observation is in error, the event may have been *observed* to have occurred when it did not happen, or vice versa. This means that an event may have been categorised as a hit when it should have been categorised as a false alarm (see table 1). It is therefore natural to define a probability that a false alarm is mis-categorised as a hit

$$p_c = P\left(X = 1 \,|\, Y = 0, F = 1\right) \tag{1}$$

	Event Forecast	Event Not Forecast
Event Occurred	*a* (hit)	*b* (miss)
Event Did Not Occur	*c* (false alarm)	*d* (correct rejection)

Table 1. Contingency table for a categorical forecast. A perfect forecast would have zeroes in the off-diagonal elements.

where X is the observation, Y is the truth, F is the forecast, and 1 (0) defines whether the event threshold has (not) been met. Three other mis-categorisation probabilities may be defined which are

$$\begin{aligned} p_a &= P(X=0 \mid Y=1, F=1) \\ p_b &= P(X=0 \mid Y=1, F=0) \\ p_d &= P(X=1 \mid Y=0, F=0) \end{aligned} \tag{2}$$

If table 1 is taken as the contingency table when the forecast is verified against the truth, then table 2 gives the contingency table which would result when verification is performed against the (noisy) observations. As an example of how table 2 is constructed, one may write the expected number of *observed* hits as

$$\begin{aligned} e &= P(X=1 \mid Y=1, F=1)a + P(X=1 \mid Y=0, F=1)c \\ &= (1-p_a)a + p_c c \end{aligned} \tag{3}$$

From a corrupted contingency table, such as table 2, it is possible to re-construct the true contingency table values by solving the set of four equations for a,b,c and d, provided the probabilities of mis-categorisation are known. Table 3 gives the reconstructed values for a, b, c and d, and it is clear that tables 1, 2 and 3 all give the same values if the mis-categorisation probabilities are zero. So, provided that the probability of an event being mis-categorised is known, then the contingency table which describes the verification against truth can be re-constructed. However, the estimation of these probabilities is not a trivial matter. In (Bowler, 2006) a deconvolution method for reconstructing this contingency table is given, and is illustrated using artificial data.

4. CONCLUSION

The effects of errors in observations on contingency table verification is non-trivial and some account should be taken of these effects. A method of estimating the "true" contingency table values has been outlined based on a mis-categorisation approach. A deconvolution method can also be used to estimate these values.

ACKNOWLEDGEMENTS

The author would like to thank Beth Ebert for the illuminating discussions which lead to this work.

REFERENCES

Bowler, N., 2006: "Explicitly Accounting for Observation Error in Categorical Verification of Forecasts", Monthly Weather Review, **134**, 1600–1606

Candille, G. and O. Talagrand, 2004: "Impact of observational errors on the validation of ensemble prediction systems", Poster at Ensembles Workshop, Exeter.

Ciach, G. J. and W. F. Krajewski, 1999: "On the estimation of radar rainfall error variance", Advances in Water Resources, **22**, 585-595

Saetra, O., H. Hersbach, J-R. Bidlot and D. S. Richardson, 2004: "Effects of observation errors on the statistics for ensemble spread and reliability", Monthly Weather Review, **132**, 1487-1501

	Event Forecast	Event Not Forecast
Event Observed	$e = (1-p_a)a + p_c c$	$g = (1-p_b)b + p_d d$
Event Not Observed	$f = (1-p_c)c + p_a a$	$h = (1-p_d)d + p_b b$

Table 2. The contingency table for forecasts verified against observations, using the mis-categorisation approach.

	Event Forecast	Event Not Forecast
Event Occurred	$\dfrac{(1-p_c)e - p_c f}{(1-p_a)(1-p_c) - p_a p_c}$	$\dfrac{(1-p_d)g - p_d h}{(1-p_b)(1-p_d) - p_b p_d}$
Event Did Not Occur	$\dfrac{(1-p_a)f - p_a e}{(1-p_a)(1-p_c) - p_a p_c}$	$\dfrac{(1-p_b)h - p_b g}{(1-p_b)(1-p_d) - p_b p_d}$

Table 3. Reconstructed contingency table in terms of the measured values and the probabilities of mis-categorisation.

FORECASTING EXTREME PRECIPITATION EVENTS IN TERMS OF QUANTILES

Petra Friederichs and Andreas Hense

Meteorological Institute, University of Bonn, Auf dem Hügel 20, 53121 Bonn, Germany
E-mail: *pfried@uni-bonn.de*

Abstract: We present a forecasting approach for extreme weather events that communicates a probabilistic forecast in terms of quantiles. Furthermore, a new validation score for quantile forecasts, namely the quantile verification skill score, is introduced. It applies to quantile forecasts for continuous as well as mixed discrete-continuous variables (i.e. daily precipitation totals).

Keywords - downscaling, quantile regression, censoring, precipitation, extremes, verification score

1 INTRODUCTION

In order to provide reliable forecasts of the occurrence of extreme weather events, model forecasts have to be calibrated towards local conditions. In general, a model output statistics (MOS) system is employed to re-calibrate a model forecast. However, MOS systems apply to expectation values. In this study, quantile regression (Koenker, 2005) is used to formulate a MOS system that provides calibrated forecasts in terms of conditional quantiles. Furthermore, censored quantile regression provides a tool to estimate forecast quantiles for mixed discrete-continuous variables. The censored quantile verification score (CQVS) enables to validate a forecast with respect to a reference forecast. To instance the forecast approach we present a hindcast for daily precipitation totals at the station Dresden in August 2002 (Elbe flood).

2 THE STATISTICAL DOWNSCALING APPROACH AND DATA

Statistics. Let Y be the univariate response variable (e.g., daily precipitation totals) and X the conditioning multivariate variable (NCEP re-analysis). Then the statistical linear model is

$$Y|\mathbf{X} = \max(0, \beta^T\mathbf{X} + \gamma^T\mathbf{X}u) \qquad u \sim i.i.d \tag{1}$$

where β represent the coefficients of the model, and γ accounts for a denpency of the error variance on the covariate (heteroscedasticity). By taking only values of zero and above the model accounts for the censoring. The estimated conditional quantiles at probability τ are $Q_Y(\tau|\mathbf{X}) = \max(0, \beta^T\mathbf{X})$. The model is solved by minimizing a piecewise linear censored least absolute deviation function $\hat{\beta}_\tau = \arg\min_{\beta_\tau} \sum_{i=1}^{n} \rho_\tau(y_i - \beta_\tau^T\mathbf{x}_i)$, where ρ is the check function $\rho_\tau(u) = \begin{cases} \tau u & \text{if } u \geq 0 \\ (\tau-1)u & \text{if } u < 0 \end{cases}$

The censored quantile regression naturally provides a scoring rule, the censored quantile verification score (CQVS)

$$\mathrm{CQVS}_{for} = \sum_{i=1}^{n} \rho_\tau(y_i - \max(0, \hat{\beta}_\tau^T\mathbf{x}_i)). \tag{2}$$

As the CQVS is a proper scoring rule (Gneiting and Raftery, 2004), one can construct a skill score analogously to the Brier skill score as $\mathrm{CQVSS}(\tau) = 1 - \mathrm{CQVS}_{for}(\tau)/\mathrm{CQVS}_{ref}(\tau)$, which enables to estimate the relative gain of a forecast with respect to a reference forecast (CQVS_{ref}) (here marginal distribution or climatology).

Data: Daily resolution precipitation totals at meteorological stations in Germany from the European Climate Assessment project (ECAD) are used as a forecast target (Klein Tank and Coauthors 2002). The procedure is applied to the cold season, November to March (NDJFM), and warm season, May to September (MJJAS) for the period from 1948 to 2004, seperately. The multivariate covariates are taken from the NCEP re-analysis project (Kalnay et al. 1996). Variables are daily means of relative vorticity and vertical velocity both at the 850 hPa pressure level, and precipitable water. The data are available on a 2.5° x 2.5° grid. We have chosen a sector that covers large parts of Europe (5°W-20°E, 42.5°N-60°N).

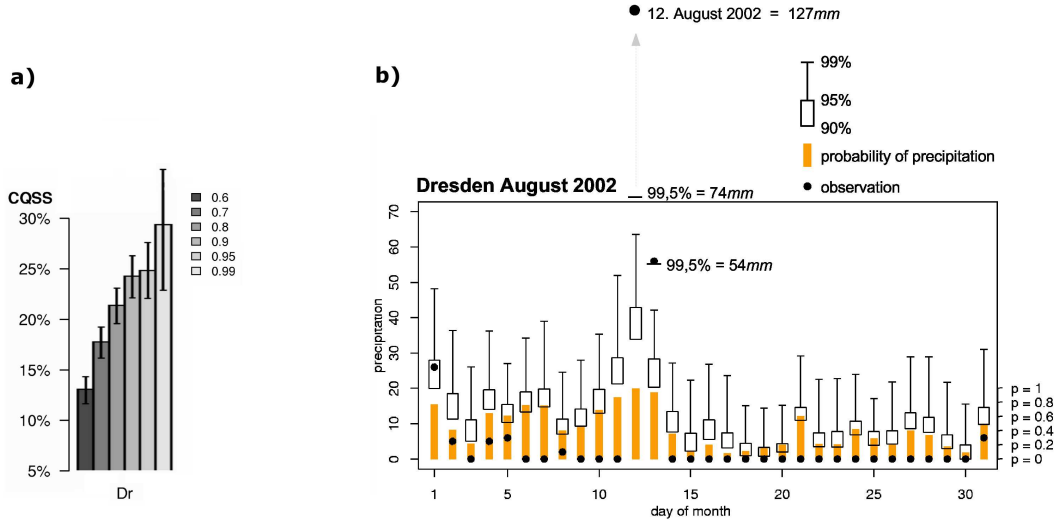

Figure 1: a) CQVSS for summer precipitation at ECAD station Dresden. b) Daily precipitation hindcasts at Dresden in August 2002. Orange bars give the probability of precipitation (right axis), black circles are the observed precipitation totals, and the Box graphs indicate the 90%, 95%, and 99% quantile (left axis in mm).

The degrees of freedom are reduced using principal component analysis (PC). The conditional quantiles are derived using cross-validation. Best scores are obtained with approximately 20 EOFs. For details see Friederichs and Hense (2006).

3 RESULTS

The conditional quantiles are estimated for different probabilities. Fig. 1 shows the CQVSS for summer precipitation at weather station Dresden. The CQVSS varies between 13compared to the reference. Due to the censoring, smaller quantiles show less skill (0.6), while the uncertainty of the skill estimate increases for very large quantiles (0.99). In winter (not shown) the skill scores are higher than in summer.

Fig. 2 shows an example (weather station Dresden in August 2002 Elbe flood) for a hindcast using censored quantile regression. First, censored QR implies an estimate of the probability of censoring, hence the probability of the occurence of precipitation (orange bars) are shown. Furthermore, forecasts for different quantiles are shown in a box plot. On August 12 127mm of rain was observed. The 99% quantile hindcast amounts to 63mm. The QR estimates a probability of 0.005 for an event exceeding 75mm.

4 CONCLUSIONS

We presented a novel statistical downscaling approach for precipitation at a single station given the large scale circulation as represented by the NCEP re-analysis data. The approach uses quantile regression (QR). The first application in a meteorological context was carried out by Bremnes (2004). Two extensions of the QR approach mark this work. (1.) This study shows that a mixed discrete-continuous response variable such as daily precipitation totals can be statistically described by a censored variable. (2.) The censored QR provides a natural basis for a proper scoring rule in order to assesses the relative gain of a quantile forecast compared to a reference forecast.

REFERENCES

Bremnes, J.B., 2004: Probabilistic forecasts of precipitation in terms of quantiles using NWP model output. Mon. Wea. Rev., 132, 338-347.

Friederichs, P. and Hense, A., 2006: Statistical down-scaling of extreme precipitation events using censored quantile regression. Mon. Wea. Rev. (in press, request to pfried@uni-bonn.de).

Gneiting, T. and Raftery, A.E., 2005: Strictly proper scoring rules, prediction, and estimation. University of Washington TechnicalReport, 463R

Kalnay, E., M., et al., 1996: The NCEP/NCAR 40-year reanalysis project. Bull. Amer. Meteor. Soc., 77, 437 471.

Klein Tank, A. M. G., et. al, 2002: Daily dataset of 20th-century surface air temperature and precipitation series for the European climate assessment. Int. J. of Climatol., 22, 1441 1453.

Koenker, R., 2005: Quantile Regression. Econometric Society Monographs. Cambridge, 349p.

VERIFICATION FOR AREMS/973 REAL-TIME PRECIPITATION FORECASTS OVER CHINA REGION DURING FLOOD SEASON IN 2004

Qiu-Xia WU [1], SHI Li, WENG Yong-Hui, YANG Yu-Hua, and NI Yun-Qi

1. State Key Laboratory of Severe Weather, Chinese Academy of Meteorological Sciences, Beijing 100081, China

halen_mona@sohu.com

1. INTRODUCTION

Funded by the national basic research 973 program of China (Research on theories and methods of monitoring and predicting of heavy rainfall in south China), AREMS/973 is a real-time operational system and covers China and the surrounding areas. The system produces real-time 24 h accumulated precipitation predictions and is automatically run twice daily, initialized at 0000 and 1200UTC using the China Meteorological Administration (CMA) MICAPS/9210 operational data interface.

The main structure of the system consists of two parts, which are an advanced regional eta (η) model (AREM) (Yu, 1989) and pre-processing 3-D variation system (GRAPeS-3DVAR) (Xue, 2001). AREM is a meso-scale regional hydrostatic model with eta vertical coordinate, and the model was set up with 37 x 37 km horizontal grid and 35 vertical levels. Its prognostic variables are: potential, horizontal wind components, temperature, and specific humidity; and they are distributed on the Arakawa E-grid. The model predicts grid scale precipitation and sub-grid scale precipitation, a moist saturated condensed scheme is used for the grid scale precipitation and Betts-Miller-Janjic (BMJ) convective scheme for the sub-grid scale precipitation.

In 2004, AREMS/973 became officially operational in China. In this paper, the 24 h real-time accumulated precipitation forecasts for the 2004 summer season based on 0000UTC were verified against the observations, for a comprehensive and objective evaluation that tested the 24 h accumulated precipitation forecast skill of AREMS/973.

2. OBSERVED DATA AND VERIFICATION METHODS

The observed 24h accumulated precipitation is from the CMA MICAPS/9210 operational data interface, AREMS/973 24h accumulated precipitation will be verified against the observed precipitation. The model coverage is about 15°N~55°N, 85°E~135°E and there are about 2310 surface observation stations in this region. Using Cressman interpolation method, the model gridded values will be interpolated to the observed station locations. And then the threat, bias and Heidke skill scores will be calculated, and the spatial and temporal characteristics of the 24 h accumulated precipitation will also be concerned.

3. CONCLUSIONS

The verification areas covered the middle and east China, that is, the mid-lower reaches of the Yangtze river (25°N~35°N, 110°E~123°E), south China (18 °N~25 °N, 105 °E~123 °E), north China (35 °N~45 °N, 110 °E~123 °E), northeast China (40 °N~53 °N, 120 °E~135 °E), and eastern southwest China (20 °N~35 °N, 100 °E~110 °E).

AREMS/973 has shown a surprising skill in forecasting the precipitation of the Chinese flood seasons, and the 24 h accumulated monthly total precipitation forecasts have correctly shown the location, strength and coverage of the main rain belt during the different periods of the flood seasons. At the same time, the model can predict the day-to-day variations of the observed precipitation, although the system cannot produce the details in spatial and temporal variation of the observation. The time series of domain-accumulated daily total

precipitation forecasts, especially over the middle and lower Reaches of the Yangtze River and Northeast China, are in very good agreement with the observations. AREMS/973 usually under-predicted precipitation amounts for the China flood season, except for North China in May and August, eastern Southwest China in May, and the middle and lower reaches of the Yangtze River in May and June. Moreover, above the threshold of 25 mm/d, the model produces forecasts predicting rainfall in more limited areas than observation.

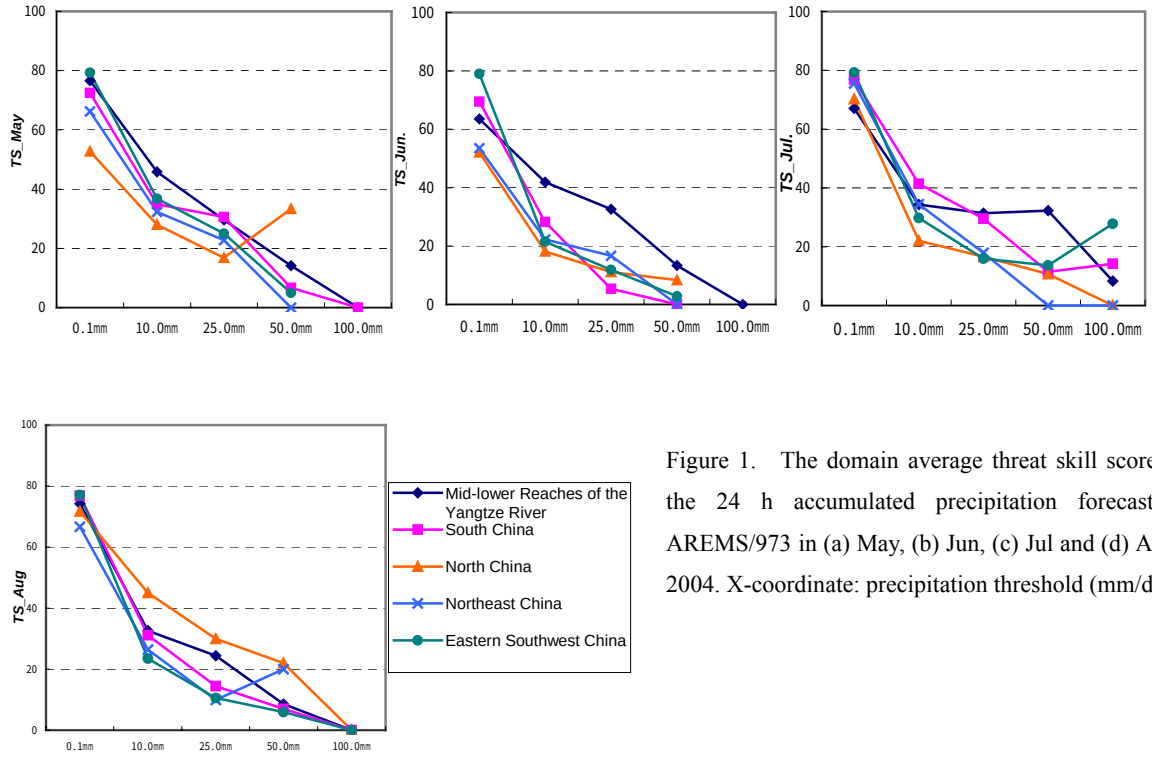

Figure 1. The domain average threat skill scores for the 24 h accumulated precipitation forecasts of AREMS/973 in (a) May, (b) Jun, (c) Jul and (d) Aug of 2004. X-coordinate: precipitation threshold (mm/d).

The forecast skill scores of AREMS/973 usually decrease from the light to the heavy precipitation categories, that is, the more intense the precipitation events are, the poorer the prediction skill is. For the above 50 mm/d precipitation categories, the forecast is similar to the random control.

For May, the precipitation forecast over the middle and lower reaches of the Yangtze River is the best, but there is little difference in comparison with other areas. The second best-forecast area is South China. In June, the China rainfall belt moves to the middle and lower Reaches of the Yangtze and Huai River, where the system's forecast skill is better than other areas. From the end of July through August, the flood season commences over North China. Simultaneously, the best forecast area moves north to North China. In other words, the best-forecast area usually coincides with the area of the China rainfall belt. Explanations for this result are presented within the body of this paper

REFERENCES

Rucong YU, 1989: Design on a regional numerical prediction model with a steep topography. *Chinese Journal of Atmospheric Sciences* (Scientia *Atmospherica Sinica*) (in Chinese), **13**, 139–149.

Jishan XUE, Shiyu ZHUANG, Guofu ZHU et al, 2001: Scientific design scheme of GRAPeS 3D-Var system. Chinese Academy of Meteorological Sciences (in Chinese), Beijing, China, 18pp.

THE EUROPEAN SEVERE WEATHER DATABASE (ESWD): AN INVENTORY OF CONVECTIVE HIGH-IMPACT WEATHER EVENTS FOR FORECAST AND WARNING EVALUATION, CLIMATOLOGY, AND RISK ASSESSMENT

Nikolai Dotzek [1], Thomas Kratzsch [2], Pieter Groenemeijer [3]

[1] Institut für Physik der Atmosphäre, Deutsches Zentrum für Luft- und Raumfahrt, Oberpfaffenhofen, Germany
E-mail: *nikolai.dotzek@dlr.de*
[2] Zentrale Fachleitung, Deutscher Wetterdienst, Offenbach, Germany
E-mail: *thomas.kratzsch@dwd.de*
[3] Institut für Meteorologie und Klimaforschung, Forschungszentrum Karlsruhe, Karlsruhe, Germany
E-mail: *pieter.groenemeijer@imk.fzk.de*

1. INTRODUCTION

The main goal of the ESWD database (**eswd.eu**, Groenemeijer et al., 2004, 2005) is to collect and provide detailed and quality-controlled information on severe convective storm events over Europe using a homogeneous data format and a web-based user-interface where both collaborating national meteorological and hydrological services (NMHS) and the public can contribute and retrieve observations.

ESWD development was motivated by the fact that severe convective weather events strongly depend on micro- and meso-scale atmospheric conditions, and in spite of the threat that they pose for life and property, they usually escape the meshes of existing operational monitoring networks. Besides, such events are often embedded in systems acting on a larger scale, and even if damage is local, severe weather can continue for hours or days and affect more than one European country during its lifespan.

When dealing with severe weather events, researchers and forecasters need to know when and where these events have taken place on a European scale to evaluate numerical and conceptual models or theories, and to verify forecasts, nowcasting and warnings. Moreover, the only way to obtain a robust and homogeneous climatology and risk analysis of severe local storms in Europe is to carry out a systematic collection of observations of severe atmospheric phenomena or of the damage they caused. Here we focus on a preliminary comparison of ESWD reports to DWD forecasts and warnings in a European severe weather episode from 26-31 July 2005.

2. ESWD DATABASE

After two years of test operations, 2006 is the year with a first operational ESWD service, and three NMHS are collaborating: DWD, INM and ZAMG. Currently, the following categories of severe weather are included in the ESWD: Straight-line winds, tornadoes, large hail, heavy precipitation, funnel clouds, gustnadoes, and lesser whirlwinds. Extending both the number of collaborating NMHS and the range of covered phenomena are further ESWD objectives. Fig. 1 provides an overview of the ESWD reports since 1950 (a) and for 2006 alone (b).

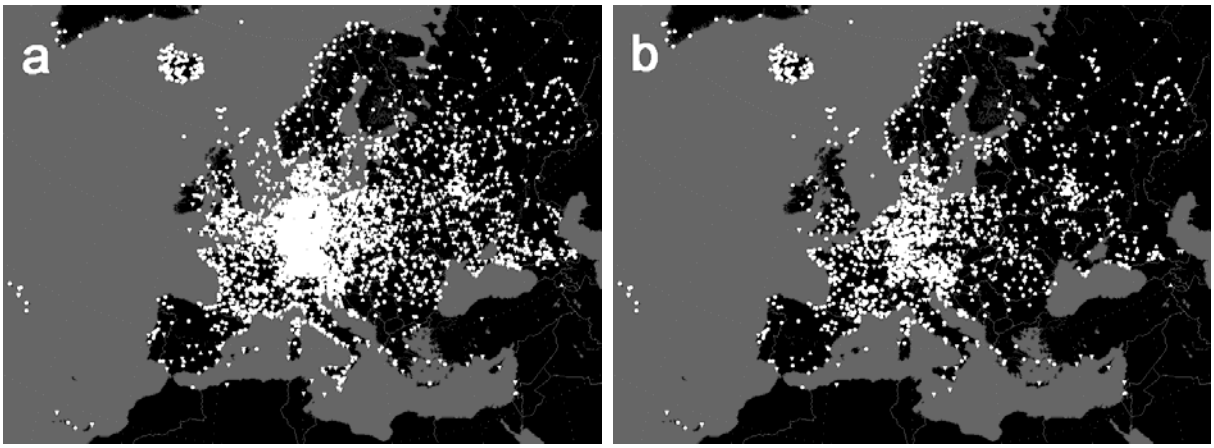

Figure 1. All ESWD reports for (a, *n = 7350*) 1950-2006 and for 2006 alone (b, *n = 2515*, as of 2 Nov 2006). In (a), data density is highest in Germany due to inclusion of the TorDACH reports (tordach.org/de/) which are available until 2005. Panel (b) shows that the ESWD reporting is becoming more and more homogeneous over Europe.

3. ESWD REPORTS RELATED TO DWD FORECASTS / WARNINGS, EPISODE 26-31 JULY 2005

Fig. 2 shows daily ESWD reports from 26-31 July 2005 (still within the ESWD test phase, thus homogeneous completeness of reports all over Europe is not granted). The peak of this severe weather episode was from 27-29 July. On 27 July, mostly damaging winds and a few tornadoes occurred in Germany to the west and north or Frankfurt. On the 28th, damaging winds and heavy precipitation concentrated over northern Germany, while 29 July brought SW-NE-oriented corridors of heavy precipitation from the Benelux to the Baltic Sea, and of damaging winds, hail and some tornadoes from the French and Swiss Jura to western Poland. On this day, also a low-precipitation supercell producing very large hail in the Chemnitz region in eastern Germany was well-documented by storm chasers. A general eastward translation of the ESWD reports over this period is apparent.

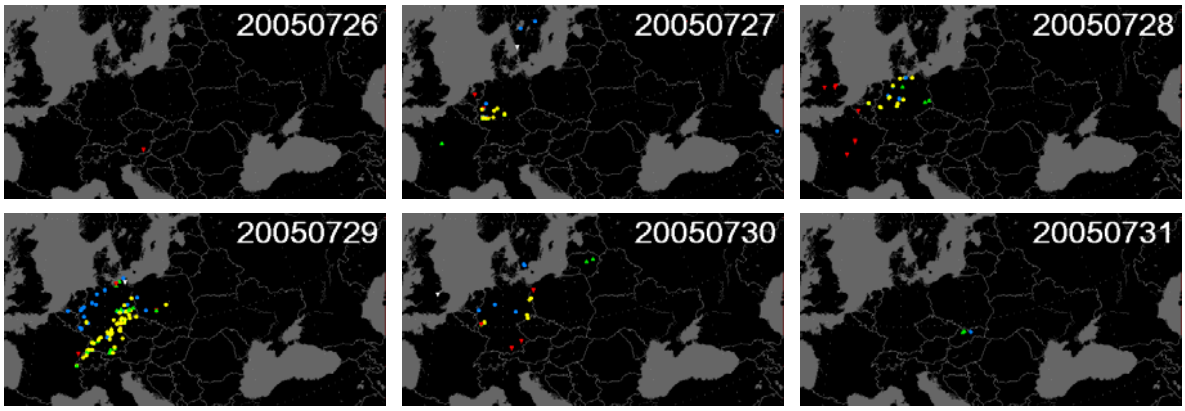

Figure 2. Daily ESWD reports from 26-31 July 2005 (last year of ESWD test phase). Red: tornado, yellow: damaging wind (>25 m/s), green: hail (>2 cm diameter), blue: heavy precipitation, white: funnel cloud (colour version available on the CD).

In a first step of the comparison of DWD severe weather warnings and ESWD reports, DWD's severe weather warnings in Germany generally showed that in most cases of severe convective storm events, a severe thunderstorm warning was prepared, issued, and active. In 2005, DWD did not yet operationally provide dedicated tornado warnings. Instead, any tornado threat was subsumed in the warnings of thunderstorms capable of producing damaging winds, hail or heavy precipitation. For the selected severe weather period, however, a DWD warning of thunderstorms in the affected county existed in all tornado cases reported to the ESWD.

4. CONCLUSIONS

Our first study of the relation between severe weather warnings and actual reports showed:

- The ESWD provides pan-European coverage of severe convective storm reports in a homogeneous data format. The ESWD site is maintained by the European Severe Storms Laboratory, ESSL, currently being established as a non-profit research organisation.
- Since 2006, the NMHSs DWD, INM, and ZAMG are cooperating, and run their local installations of the ESWD software. Additional collaboration of more European NMHSs with the ESWD is highly welcome.
- The collaborating NMHSs perform quality-control (QC) for the ESWD data gathered by them in their countries. For the public severe weather reports entered on the main ESWD site eswd.eu, the ESSL is to perform the ESWD 3-level QC.
- A severe weather episode with good ESWD data coverage in and around Germany in July 2005 showed that ESWD reports can be applied to verify severe weather forecasts, watches or warnings as issued by NMHSs.
- The ESWD data have further been applied for climatological and risk analysis (e. g., Bissolli et al., 2006).

In addition to main site **eswd.eu**, the ESWD development will be documented at **essl.org/projects/ESWD/**.

REFERENCES

Bissolli, P., J. Grieser, N. Dotzek, and M. Welsch, 2006: Tornadoes in Germany 1950-2003 and their relation to particular weather conditions. *Global and Planetary Change*, in press.

Groenemeijer, P., N. Dotzek, F. Stel, H. Brooks, C. Doswell, D. Elsom, D. Giaiotti, A. Gilbert, A. Holzer, T. Meaden, M. Salek, J. Teittinnen, and J. Behrendt, 2004: ESWD - A standardized, flexible data format for severe weather reports. Preprints, *3rd European Conf. on Severe Storms*, Léon, 9.-12. November 2004, 2 pp. [essl.org/projects/ESWD/]

Groenemeijer, P., N. Dotzek, F. Stel, and D. Giaiotti, 2005: First results of the European Severe Weather Database ESWD. Preprints, *5th Ann. Meeting European Meteor. Soc.*, Utrecht, 12.-16. September 2005. [essl.org/projects/ESWD/]

WIND TURBULENCE CHARACTERISTICS AND SEASONAL COMPARISON AT THE COM. FERRAZ ANTARTIC STATION FROM 2003 TO 2004

Luciana Bassi Marinho Pires, Francisco Eliseu Aquino,
Marcelo Romão, Ana Carolina Vasques and Alberto Setzer

Center for Numerical Weather Forecast and Climate Studies - CPTEC,
National Institute for Space Research – INPE, São José dos Campos, SP, Brazil
E-mail: *lubassi@cptec.inpe.br*

Abstract: This study presents the first characterization and a preliminary seasonal comparison of the wind turbulence at the Com. Ferraz Antarctic Station (EACF) from 2003 to 2004. Turbulence was estimated using the wind gust factor and wind turbulence definitions used in applied engineering studies of meteorology. The EACF (62°05'S; 58°23.5';W) is located on the Keller Peninsula, Admiralty Bay, King George Island, northern Antarctic Peninsula.

Keywords – *wind gust factor, wind turbulence, King George Island, Antarctica.*

1. INTRODUCTION

The low pressure belt around Antarctica, between 60ºS e 65ºS, is the most marked one on the Planet. The predominant westerly winds over the Antarctic Peninsula enhance extratropical cyclone activity. This study presents a first characterization and preliminary results on the structure of the atmospheric turbulence employing the seasonal comparison of the turbulence observed at the Brazilian Antarctic scientific station, *Estação Antártica Comandante Ferraz* (EACF), between 2003 and 2004.

2. MATERIALS AND METHODS

The EACF is located, on the east side of the Keller Peninsula (3.8 km x 2.2 km), a ridge with altitudes in the range of 250 to 360 m, on the northern coastline of Admiralty Bay (Figure 1). Set 794 m from the base of Flagstaff Mt., EACF is within a turbulent recirculation zone, were severe regional meteorological conditions are a constant presence.

Turbulence analysis was made according to the definitions normally employed in applied meteorology studies for engineering problems, e.g. as in Plate (1982), Bergstrom (1987), Kristensen et al., (1991) and Young and Kristensen (1992). The analysis of wind gusts is one of the ways to study the structure of turbulence at any place, and where such events can be defined as the sudden increase/decrease of wind speed at very small and continuous cycles.

Figure 1. Map of King George Island, Keller Peninsula (black arrow) and EACF (red dot).

To conduct the comparative seasonal study we used the wind data obtained with a Wind Monitor Sensor R.M.Young Model 05103. This equipment is installed on a 10 m anemometric tower adjacent to EACF, at 20 m msl. Wind speed and direction were stored in a Datalogger Campbell 21X, and where the full hour value registered is the average of the last ten minutes interval, sampled at each second – see http://www.cptec.inpe.br/antartica. The data spanned the period from January/2002 to December/2003. The parameters measured were the 10-minutes average scalar speed (ms^{-1}), 10-minutes average direction (degrees), and the daily maximum gust; the calculated variables were the wind gust factor, gust amplitude (ms^{-1}) and turbulence intensity.

3. RESULTS

Table 1 shows the measured values of speed and maximum speed) and the calculated values of the variables: gust factor $G = V_{max} / V_{mean}$, gust amplitude $A = (V_{max} - V_{mean})$, and turbulence intensity $I = \sigma_{speed} / V_{mean}$.

Season	2003					2004				
	V_m	V_{max}	G	A	I	V_m	V_{max}	G	A	I
DJF	5.0	13.9	3.7	8.9	0.8	4.5	13.0	5.3	8.5	0.7
MAM	5.9	16.4	2.3	10.5	0.7	6.1	16.9	5.9	10.8	0.8
JJA	7.5	20.2	5.7	12.8	0.7	7.1	19.6	4.9	12.5	0.7
SON	6.7	18.3	5.1	11.6	0.7	6.7	18.8	4.4	12.1	0.7

Table 1. Mean values for wind characteristics: mean speed (V_m), maximum speed (V_{max}), wind gust factor (G), gust amplitude (A) and turbulence intensity (I).

The most intense winds occurred in winter (JJA) with a seasonal average of 7 ms^{-1}, and the least intense in summer (DJF), averaging 4.5 ms^{-1}. The maximum sustained wind speed of 20 ms^{-1} occurred in winter of 2003, followed by a value of 18 ms^{-1} in spring. The EACF climatology for the winters of 1986 to 2005 presents the mean wind speed of 6.4 ms^{-1} and the maximum wind gusts of 49 ms^{-1}, in agreement with the results of this study. Turbulence intensity did not present seasonal differences, stabilizing around 0.7. The wind gust factor showed a minimum value of 2.3 ms^{-1} in the fall (MAM) of 2003 and a maximum of 5.9 ms^{-1} in the fall of 2004, therefore varying inversely between the two years. Wind gust amplitude was greater in JJA in both years, with approximate mean values of 13 ms^{-1}, followed by SON.

6. CONCLUSION

In this preliminary characterization of the seasonal structure of atmospheric turbulence, it is evident that the summer season (DJF) is the best period for outdoor and fieldwork activities in the EACF region, due to the smaller values in wind speed maxima (13 ms^{-1}) and wind speed averages (5 ms^{-1}). Wind gust amplitude was also weaker in summer, about 8 ms^{-1}, showing values over 10 ms^{-1} at all other periods. Turbulence intensity did not present any differences among the four seasons, probably due to the complex atmospheric circulation in the fjord structure of Admiralty Bay, together with the frequent regional extratropical cyclonic activity and constant local KGI winds.

Acknowledgements: *PROANTAR (CNPq+SECIRM) and CPTEC/INPE for the financial and logistics, and Heber R. Passos and Marilene A. da Silva for their technical support.*

REFERENCES

Bergstrom, H., 1987: A statistical analysis of gust characteristics. *Boundary Layer Meteorology*, v.39, n.1, p.153-73.

Kristensen, L., Casanova, M., Courtney, M.S., Troen Rise, I, 1991: In search of a gust definition, *Boundary Layer Meteorology*, v.55, n.1, p.91-107.

Plate, E., 1982: Studies in Wind engineering and industrial aerodynamics. *Engineering Meteorology*. Amsterdam, Elsevier, 740p.

Young, G.S., Kristensen, L., 1992: Surface Layer gusts for aircraft operation, *Boundary Layer Meteorology*, v.59, n.2, p.231-242.

ESTIMATION OF LAKE EVAPORATION USING A FLOATING CLIMATOLOGIC STATION DATA IN AN EXPERIMENTAL BASIN OF SEMIARID

Carlos Magno de Souza Barbosa [1], Arthur Mattos (presenting)

[1] LARHISA – Laboratório de Recursos Hídricos e Saneamento Ambiental,
UFRN – Universidade Federal do Rio Grande do Norte, Natal/RN, Brasil
E-mail: *carlosmagno25@hotmail.com*

Abstract: The understanding of the effects of the evaporation in the amount and quality of the available water in reservoirs is important ally for the preservation of the sources of supply in the semi-arid, through the efficient management of their waters To have an estimate of the evaporation in the lake more precise it was used data of a floating climatologic station in an experimental basin of semiarid, located in Serra Negra do Norte, Rio Grande do Norte State, Brazil. This work presents the results of the first eight moths of analysis

Keywords – *Lake evaporation, Floating climatologic station, Semiarid.*

1. INTRODUCTION

The need of a better understanding of the water processes in semiarid area, allied to the fact that the area has been suffering, along the years, serious socioeconomic problems, current of the irregularity of rain distribution, it has been motivating the accomplishment of studies that improve the rationality of the use of the water, and the progress of the scientific knowledge in benefit of the sustainable development in the area.

In such case the studies accomplished with the implantation of experimental basins can be extracted management guidelines for application in places without information and that it doesn't possess financial resources to revert that situation.

The understanding of the effects of the evaporation in the amount and quality of the available water in reservoirs is important ally for the preservation of the sources of supply in the semi-arid, through the efficient management of their waters. However, the evaporation is a complex phenomenon that depends on the atmospheric conditions, of the local water availability and of the characteristics of the surface of the evaporation.

Reliable estimates of evaporation of lakes are essential in the planning and management of water resources and in the studies of environmental impact. Most of the methods esteem the evaporation starting from data observed in meteorological stations installed in the terrestrial ambient, significantly influenced by the characteristics of the soil, therefore no representative of the lake.

Evaporation studies in lakes in micrometeorological scale supply an important comparison in the estimate of the regional evaporation and a great understanding of the terms of evaporation tax. It is right that theoretically evaporation estimates also based in techniques as energy budget are important for the understanding of the effects of long period in the climatic change about the evaporation of the lake.

In this context a floating base was developed to install a climatologic station that stores meteorological data of the own lake. Estimates of evaporation methods that use data observed in the surface of the lake are more precise, because the climatic variables are influenced by the phenomena that happen there. This work presents the estimation of the evaporation of the lake in an experimental basin located in Serra Negra do Norte/RN, representative semiarid area of Brazilian northeast.

2. DATA

The data used in this work were obtained in the experimental basin of Serra Negra do Norte, located in the Ecological Station of Seridó in the geographical coordinates: latitude 6º34'41", longitude 37º15'18" and altitude 249 m, located in the municipal district of Serra Negra do Norte in the Rio Grande do Norte State.

For estimate the evaporation with data of the surface of the lake a fiberglass base was elaborated on which a climatological station is installed equipped with the following ones sensor: Infrared for measurement of the temperature of the surface of the water, to 1, 2, 3 and 4 meters of depth of the water level; relative humidity of the air; solar radiation; Rain; Wind sensor of speed and direction.

The flotation base for the climatological station is made of fiberglass and it possesses the dimensions: 2,0m x 2,20m x 0,50m, being the same fixed by a tube of PVC connected in a concrete bracket in the bottom of the reservoir, making possible only the vertical movement with the stuffing or emptying of the dam.

Figure 1. Floating climatological station installed in the dam Campos in the experimental basin of Serra Negra do Norte/RN.

3. METHODS

The floating climatological station was installed at the end of January 2006, and the data used in this work were from February to September 2006, totaling eight months. The methods used for evaporation estimate were: Penman method, energy balance, Priestley and Taylor method, and Thornthwaite method.

4. CONCLUSIONS

The Figure 2 presents the result of evaporation in millimeters per month for all of the methods mentioned previously.

Two distinct effects in the behavior of the evaporation in Campos dam are: an expressive increase of the evaporation from June (in September, all the models reach the maximum value) and a reduction from March, drawn out until May or June. The values had been minimum in all the models, in the months of May and June.

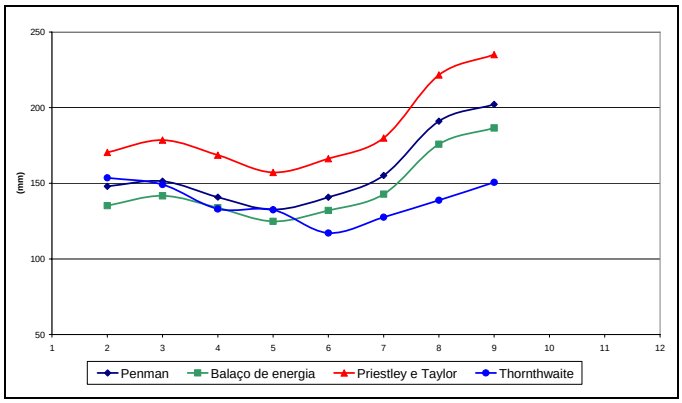

Figure 2. Evaporation values in millimeters per month for all of the methods: Penman, energy balance, Priestley and Taylor, and Thornthwaite.

The analysis of the climatologic data in the floating station shows a variation compared with the data collected in the station installed in the surface, about 200 m of the lake, showing that the alteration in the results of the evaporation models will occur, allowing that determines parameters of correction for the methods of evaluation of evaporation in lakes in the semiarid region of the Rio Grande do Norte State, however this work still been done.

Acknowledgements: *CNPq/CT-Hidro, IBAMA.*

REFERENCES

Fontes, A. S., 2004. Estudo da evaporação em reservatórios situados em região semi-árida: Uso de bacia experimental. Master Dissertation. Universidade Federal da Bahia, Salvador/BA.

Tubelis, A.; Nascimento, F. J. L., 1980. Meteorologia Descritiva: Fundamentos e Aplicações Brasileiras. Ed. Nobel, São Paulo, 374p.

Vianello, R. L.; Alves, A. R. 1991. Meteorologia Básica e Aplicações. Imprensa Universitária. UFV, Viçosa. 449p.

MULTI-USER CONSORTIUM APPROACH TO MULTI-MODEL WEATHER FORECASTING SYSTEM BASED ON INTEGER PROGRAMMING TECHNIQUES

Oleg M. Pokrovsky

Main Geophysical Observatory, St. Petersburg, 194021, Russia
E-mail: *pokrov@main.mgo.rssi.ru*

Abstract: Decision making problem related to multi-model weather forecasting EPS is considered with account to a collective of potential users. User benefit maximization under linear constraints for the minimal model efficiency described individual interest rates of particular users has been developed. An illustrative example concerned to the case of 3 users and 4 meteorological events to be forecasted by EPS system is presented and analysed. Proposed approach creates a background for objective market evaluation of alternative weather forecasting systems.

Keywords – *weather forecasting users, requirements, decision making, optimal design, mathematical economy*

1. INTRODUCTION

Requirements for weather forecast products can vary significantly and are typically oriented to the needs of specific user groups. Nonetheless, in many respects the requirements are rather similar, such as a common need for information on basic variables such as temperature, humidity, and precipitation (mean, maximum, minimum). On other hand, it is hardly to imagine that every user could provide their own forecast product because of substantial costs of both inputs observing data and model development/maintenance. In the case of specified forecast some additional observations might be required to increase prescribed reliability or probability. Therefore, it is more rational to select a set of few forecast models and observing systems, which respond to the right extent to optimal set of requirements generated by multi-user economical and mathematical model. Consortium of multi-user will get benefits of mathematically optimal decisions under minimal costs. User investments in a weather forecast system should be proportional to their expected benefits derived from the early warning of short-term weather fluctuations or extreme events. Under circumstances a consortium of multi-users approach would be more likely to derive benefits from the mathematically optimal decisions for minimum investment. Meteorological community is interested in such approach in order to reduce a number of observing programs and forecasting models. Latter might become a background to increase its efficiency (Pokrovsky, 2005).

2. APPROACH

Mathematical economic techniques (Kantorovich, 1966) are quite appropriate to the solution of such problem. A decision maker rule in a simple system is typically based on classification techniques (discriminate analysis, statistical hypothesis tests and others). Because of its complexity, a multi-user model statement is closer to the formulation of an optimal solution problem in mathematical programming (MP). The MP problems are optimization tasks in which the objective function and the constraints are all linear or non-linear. If the unknown variables are all required to be integers, then the problem is called an integer programming (IP). The "0-1" IP is the special case of integer programming where variables are required to be 0 or 1 (rather than arbitrary integers). IP is a most convenient MP form for decision maker use (Korbut, and Finkelstein, 1969).

3. ELEMENTARY STATEMENT OF PROBLEM

Let us assume that there are *n users* of climate forecasting data with their *n* benefits of early warning: c_i (i=1,.., *n*). These users are interested to forecast *m* specific *meteorological events* numerated as j=1,…*m*. But usefulness of them are various and described by matrix of coefficients A=$\{a_{ij}\}$. Each magnitude a_{ij} can be considered as expenses of *i*-th user with account for *j*-th meteorological event delivered by some forecast model. *Minimum efficiency* for *i*-th user is bounded by value $b_i^{\min}$. Let us introduce *decision maker variable*:

$$x_i = \begin{Bmatrix} 1, if\ \_ i-th\_user\_adopts\_\ forecast\_data \\ 0, otherwise \end{Bmatrix}$$

Now we come to formulation of optimization problem for $\{x_i\}$:

$$\max \sum_{i=1}^{n} c_i x_i \qquad (1)$$

under constraints:

$$\sum_{j=1}^{n} a_{ij} x_j \geq b_i^{\min} \qquad (2)$$

Another interpretation of coefficients and more complex method to derive them is possible. A generalization to the forecast multi-model case is evident.

4. ILLUSTRATIVE EXAMPLE

Let us consider a multi-user decision making to many meteorological events. We used the ECMWF EPS prediction system for T850 anomaly, Europe, Jan-Feb, 1998 (see details in Richardson, 2000) with n=3 (number of users), m=4 (number of meteorological events). Matrix of EPS forecast relative economic values are presented in tabl.1, minimal efficiency for each user – in tabl.2. In the case of equal importance of users we came to the optimal solution x_{opt} for (1) constrained by (2). This solution showed that EPS forecasting system has prior importance for the user 2. Least contribution is related to the user 3. Let us now enhance a priory importance of

Users	Meteorological events:			
	(T<-8K)	(T<-4K)	(T>+4K)	(T>+8K)
1	0.40	0.36	0	0
2	0.32	0.29	0.32	0.19
3	0.22	0.19	0.41	0.46

Table 1. Matrix of constraints - $A = \{a_{ij}\}$

Users	$b_i^{\min}$
1	0.1
2	0.2
3	0.3

Table 2. Constraint vector of minimal efficiencies – b_{min}

Users	x_{opt}
1	2.31
2	5.21
3	0.85

Table 3. Optimal decision "x" in the case of equitable users: c=(1, 1, 1)

Users	x_{opt}
1	2.26
2	0.36
3	1.99

Table 4. Optimal decision "x" in the case of priority user N 3: c=(0.5, 0.5, 1)

the user 3 by changing values of target function (1) from c=(1, 1, 1) to c=(0.5, 0.5, 1). Even in this case the user 3 remains at second place after user 1. It is interesting to note that the output for user 1 is insensitivity one with account to a priory weights.

5. CONCLUSION

Approach based on MP found a wide application area in many branches of economical sciences. It assisted in decision making related to multidimensional target function constrained by many linear cost restrictions. This paper shows that similar problems arisen in meteorology might be efficiently solved by described approach.

REFERENCES

Kantorovich L.V. (ed), 1966: *Mathematical models and methods of optimal economical planning.* Novosibirsk, "Nauka", 256 p. (in Russian).

Korbut, A.A., and Yu.Yu. Finkelstein. 1969: *Discreet programming. Moscow*, "Nauka", 302 p. (in Russian).

Pokrovsky O.M., 2005: Development of integrated "climate forecast-multi-user" model to provide the optimal solutions for environment decision makers. - *Proceedings of the 7 -th International Conference for Oil and Gas Resources Development of the Russian Arctic and CIS Continental Shelf*, St. Petersburg, 13-15 September 2005, Publ. by AMAP, Oslo, Norway, September 2005, p. 661-663.

Richardson, 2000: Skill and relative economic value of the ECMWF Ensemble Prediction System. - *Q. J. Roy. Met. Soc*, **126**, p.649-668.

HOW WELL CAN ICING EPISODES BE PREDICTED BASED ON CURRENT NWP MODELS?

Jón Egill Kristjánsson[1], Bjørn Egil Kringlebotn Nygaard[1], Lasse Makkonen, Erik Berge

[1] Department of Geosciences, University of Oslo, Oslo, Norway
E-mail: *j.e.kristjansson@geo.uio.no*

Abstract: We investigate the potential for predicting episodes of in-cloud icing, which are a major weather hazard at mid- and high-latitudes in winter. For this purpose, simulations of supercooled water content using a state-of-the-art NWP model have been compared to precise measurements at a mountain top in Finland. The results are also compared to a similar study carried out 10 years ago. For all three cases considered, good agreement is found between the simulated and observed supercooled water content, when the most sophisticated condensation scheme is applied and the grid spacing of the innermost domain is 1 km or less. Poorer agreement is found if grid resolution is coarsened or if simpler cloud microphysics schemes are used. A dramatic improvement is found when comparing to the results obtained 10 years ago. The results suggest that simple empirical schemes that are widely used for icing predictions can now be replaced by direct NWP model output of supercooled water. This would be of great value to a variety of applications, such as wind turbines, power lines and telecommunication towers.

1. INTRODUCTION

In-cloud icing on structures is a major weather hazard during winter at mid- and high latitudes. It occurs when liquid cloud droplets are present at temperatures below freezing. If liquid droplets that stay in the air in the liquid phase hit an object, such as a power line or a telecommunication mast, they will immediately freeze. The supercooling occurs at temperatures between 0°C and -35°C, due to the scarcity of ice nuclei (IN) in the atmosphere. On the other hand, supercooled water can be rapidly depleted by precipitation particles falling through the cloud, while turbulence also tends to speed up glaciation in a supercooled cloud.

In-cloud icing can disrupt modern society in several ways: Power lines may be coated by ice, leading to cable galloping, and in severe cases, the lines may collapse. Wind turbines use rotor blades that have a sensitive aerodynamic design. Even a thin (mm) coating of ice may disrupt these aerodynamic properties significantly, leading to a dramatic reduction in efficiency. Furthermore, the ice load may cause the blades to rotate unevenly, resulting in major damage of the equipment.

2. ICING EPISODES AND DATA

The purpose of this study is to investigate the potential for forecasting in-cloud icing events using state-of-the-art numerical weather prediction models, run at high spatial resolution. We will focus on three cases for which accurate validating measurements are available. These measurements have been carried out at the top of Mt. Ylläs (67.6°N, 24.3°E) in northern Finland, having an elevation of 706 m. It is a rounded peak, and is the highest mountain in a large region. At Mt. Ylläs, accurate in-situ measurements of in-cloud icing have been carried out for several years, using a rotating multicylinder instrument (Makkonen, 1992). All three cases are characterized by stable stratification and advection of warm and moist air. Table 1 summarizes the observations.

Date	Time (UTC)	Wind direction	Wind speed ($m\ s^{-1}$)	Temperature (°C)	Liquid Water Content ($g\ m^{-3}$)
14 Feb 1990	06	E	4	-5	0.27
09 Jan 1996	11	SSW	13	-5	0.30
10 Jan 1996	11	SW	20	-5	0.43

Table 1: Measured values at Mt. Ylläs in northern Finland for the three cases considered.

3. MODEL AND EXPERIMENTAL SETUP

The WRF model has been used for our simulations of supercooled water. It is a non-hydrostatic mesoscale NWP model, developed jointly by several institutions in the United States (Skamarock et al., 2005). For each of the three cases, the simulations have been carried out using a two-way nested grid, with grid spacings of 13.2 km, 3.3 km and 0.825 km. Two simulations have been carried out; a Control run using the Thompson scheme for

cloud microphysics, including a prognostic calculation of ice cloud number concentrations (Thompson et al., 2004) and a run with a simpler, more economical cloud microphysics scheme, that we have termed "Simple ice".

4. RESULTS AND INTERPRETATION

Highlights from the two model simulations are shown in Table 2 and Figure 1, below. We note that the simulated cloud water contents are greatly underestimated by the coarsest grid, while good agreement is found for the finest grid, but with some overestimation. When the simpler cloud microphysics scheme is used, a large portion of the condensate is in the form of ice (not shown), and the supercooled liquid water is partly removed by precipitation, resulting in an underestimation of the liquid water content. Table 2 compares these results to those obtained by Vassbø et al. (1998) using the HIRLAM model with a grid spacing of 5.0 km.

Experiment	Control, innermost grid	Simple ice, innermost grid	Control, intermediate grid	Control, outermost grid	Vassbø et al. (1998); innermost grid
14 Feb 1990	1.37	0.80	0.80	0.13	0.00 (0.44)
09 Jan 1996	1.30	0.57	0.83	0.08	0.00 (0.33)
10 Jan 1996	1.19	0.67	0.76	0.08	0.00 (0.23)

Table 2. The ratio of simulated vs. observed supercooled liquid water content (g m^{-3}) for the three grids and the two model simulations described in the text. For Vassbø et al. (1998) the values in parentheses are for the next-to-lowest model level.

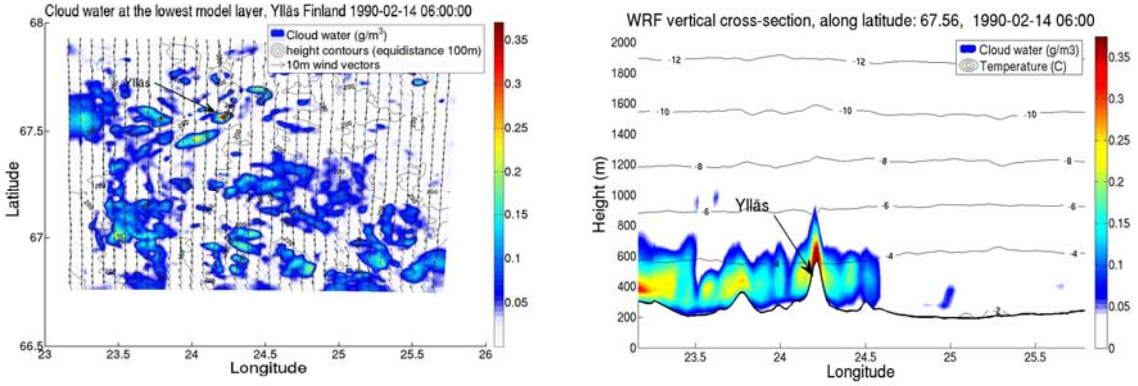

Figure 1. Simulated supercooled liquid water content (SLW) from Control run at 06 UTC on 14 February 1990. The observed supercooled cloud water content at Mt. Ylläs was 0.27 g m^{-3} (see Table 1). Left: SLW from the lowest model level (color shading), displayed as a function of longitude and latitude. Right: SLW (color shading) and temperature (isolines, ºC) in a longitude-height cross section at a latitude of 67.56°N.

5. CONCLUSIONS

The above results suggest that there is a large potential for quantitative forecasts of episodes of in-cloud icing, using current NWP models at high spatial resolution and with sophisticated cloud microphysics parameterizations. The results shown here are for stratified continental air. More testing is needed to investigate how well the model performs in maritime air with fewer CCN, more turbulence and more effective riming.

REFERENCES

Makkonen, L., 1992: Analysis of rotating multicylinder data in measuring cloud-droplet size and liquid water content. J. Atmos. Oceanic Technol., **9**, 258-263.

Skamarock, W. C., J. B. Klemp, J. Dudhia, D. O. Gill, D. M. Barker, W. Wang, and J. G. Power, 2005: *A description of the Advanced Research WRF Version 2*. NCAR Technical Note, NCAR/TN-468+STR.

Vassbø, T., J. E. Kristjánsson, S. Fikke and L. Makkonen, 1998: An investigation of the feasibility of predicting icing episodes using numerical weather prediction model output. In: *Proc. 8th Int. Workshop on Atmospheric Icing on Structures (IWAIS)*, pp. 343-347.

Thompson, G., R. M. Rasmussen, and K. Manning, 2004: Explicit forecasting of winter precipitation using an improved bulk microphysics scheme. Part I: Description and sensitivity analysis. Mon. Wea. Rev., **132**, 519-542.

METEOROLOGICAL AIRPORT BRIEFING IN GERMANY

Björn-R. Beckmann and Jürgen Kubon

German National Meteorological Service (DWD), Department of Aeronautical Meteorology, Kaiserleistr. 42, 63067 Offenbach, Germany
E-mail: *Bjoern-Ruediger.Beckmann@dwd.de*, *Juergen.Kubon@dwd.de*

Abstract: The seven aviation advisory centres of the German National Meteorological Service offer meteorological airport briefings to the German international airports, because the meteorological information exceeds the content of the standard Terminal Area Forecast (TAF) easily. The conception for these briefings is arisen on a request of the three key account customers German Air Navigation Services (DFS), Deutsche Lufthansa (DLH) and Fraport AG. For a better and safer regulation of the overloaded airspace of Rhein/Main region exists demand on a client-specific meteorological airport briefing.

The meteorological airport briefings are offered on a Web-Portal. Different reports and charts with a forecast period up to 12 hours are to find there. Beside the display of information on the portal several telephone briefings take place every day.

The airport operators Frankfurt and Munich are advised in situ if the necessity (severe weather situations) exists. To optimise the meteorological advisory of the airport Frankfurt the displacement of the whole aviation advisory centre Offenbach to the airport Frankfurt is planed for December 2006.

Keywords – *Meteorological airport briefing, Airport Frankfurt, Airport Munich, Model output statistic (MOS).*

1. INTRODUCTION

The seven aviation advisory centres of the German National Meteorological Service offer meteorological airport briefings to the German international airports, because the needed meteorological information exceeds the content of the standard Terminal Area Forecast (TAF) easily. The conception for these briefings is arisen on a request of the three key account customers German Air Navigation Services (DFS), Deutsche Lufthansa (DLH) and Fraport AG. For a better and safer regulation of the overloaded airspace of Rhein/Main region exists demand on a client-specific meteorological airport briefing. A short description of the method of the meteorological airport briefing at the international airport Frankfurt is given below.

2. Meteorological Airport Briefing on the Web-Portal

On a special Web-Portal, which is available for the three key account customers German Air Navigation Services (DFS), Deutsche Lufthansa (DLH) and Fraport AG (Airport operator) of the German National Meteorological Service, several types of meteorological information are provided. The forecast period of the products goes up to 12 hours. A weather report for +12 hours, Radar-, lightning- and SAT-charts, aviation meteorological warnings, a meteogram, an AMDAR-wind profile and a special nowcast report with a forecast period of 6 hours in tabular form are part of the meteorological airport briefing. The NOWCAST is shown in Table 1. For generating this table model output statistics (MOS) in form of categorical and probability forecasts are offered as a first guess guidance to the forecaster. The forecaster has the freedom of modifying the given MOS forecasts and convert the probabilities into categorical declarations respectively. Weather is forecasted only in cases of significant weather. Gusts are given in the table above a threshold of 25 Knots.

Time (UTC)	12	13	14	15	16	17	18
Wind Direct	190	190	190	190	190	180	180
Wind Speed	12 KT	12 KT	12 KT	10 KT	8 KT	8 KT	8 KT
Gusts	-	-	-	-	-	-	-
Tailwind 18	none	none	none	none	none	none	None
Weather	-RA						
TEMPO	RA	-RA	-RA	-RA	-RA	-RA	-
VIS	> 10 km	> 10 km	> 10 km	> 10 km	> 10 km	> 10 km	> 10 km
Variation	5-10 km	5-10 km	-	-	-	-	-
Ceiling	1000-1900 ft	2000-5000 ft	2000-5000 ft	2000-5000 ft	2000-5000 ft	2000-5000 ft	2000-5000 ft
Variation	300-900 ft	1000-1900 ft	1000-1900 ft	-	-	-	-
Wind 5000 ft	230/025			240/025			230/030
Wind 3000 ft	240/025			240/025			220/025
Wind 2000 ft	230/025			220/025			210/030

Table 1: Nowcast forecast up to 6 hours for the airport Frankfurt issued at 12 UTC, 23rd October 2006. This table is part of the meteorological airport briefing.

3. Meteorological Airport Briefing by telephone and in situ

Beside the supply of information by the Web-Portal, supervisors of the Airport, Air Traffic Control Centre (ATC) of the DFS and Deutsche Lufthansa (DLH) take part in two telephone briefings, that take place every day at 04:15 and at 15:00 local time. At demand, that means in cases of severe weather situations, additional telephone briefings take place.

The airports Frankfurt and Munich are advised in situ if the necessity (severe weather situations) is given. During winter time the advisory take place at the airport ramp control centre. The winter time advisory is mainly focussed on steering the winter services of the airport. During summer time the in situ advisory take place at the Air Traffic Control Centres. Thus, weather influenced restrictions to the air traffic can be better minimised.

To optimize the meteorological advisory of the airport Frankfurt the displacement of the whole aviation advisory center Offenbach to the airport Frankfurt is planed for December 2006.

6. CONCLUSION

The customers are very satisfied with the results using the meteorological airport briefing and the in situ advisories. Unnecessary expenses can be saved by working together in situ, because air traffic and operation of an airport could be optimised by this way. Positive feedback to one season of briefing at the places where decisions were made, was the starting for the displacement planning of the whole aviation advisory centres Offenbach and Munich directly to the airports.

A COMPARISON BETWEEN AIRBORNE WIND MEASUREMENTS AND OPERATIONAL ANALYSIS

S. Buss[1], T. P. Bui[2] and H. C. Davies[1]
[1]Institute for Atmospheric and Climate Science, ETH, Zürich, Switzerland
E-mail: sandro.buss@env.ethz.ch
[2]NASA Ames Research Center, Moffett Field CA, USA}

Abstract: Aircraft wind measurements from several flight campaigns conducted in the time span 1995-2006 are juxtaposed with high resolution analyses fields of one major operational centers (ECMWF). This updated inter-comparison reconfirms that peak analyzed winds remain too weak in comparison with in-situ flight measurements. Moreover case studies demonstrate that the analyses can substantially mis-locate, and / or underestimate the strength and sharpness of individual jet streams at tropopause level. Such shortcomings are important since such jets are seminal components of dynamical development and hence reducing the associated biases could contribute importantly to improving weather prediction.

1. INTRODUCTION

Several comparisons of airborne wind observations with meteorological analysis have been published over the last decade (see e.g. Tenenbaum, 1996, Francis, 2002 and Cardinali, 2004). In the present study use is made of data derived from eight separate scientific and commercial measuring campaigns that amount to a total of 420 flights (or flight segments). These eight data sets, here referred to as NOXAR, GTE, CRYSTAL, SPURT, SWISS, MIDCIX, AVE and CRAVE, encompass the period May 1995 to Feb 2006 and were not assimilated into the contemporaneous standard NWP analyses. Thus they serve as independent verification data, and with one minor exception (see Jeker, 2000) have not hitherto been compared with analyzed winds.

In the present study, we address the following questions: How do the NCEP and ECMWF wind analyses compare at tropospheric levels with the fore-mentioned flight measurements, and in particular how well is the correspondence in the neighbourhood of jet streams? How do the "measurement - analysis" differences derived herein compare with those of earlier studies, and also is there evidence of a reduction in these differences over the time period 1995-2006 ?

2. DATA and METHOD

2.1 Airborne wind measurements

Eight different, heterogeneous, independent and non-assimilated data sets of airborne wind observations are utilized in the present study: NOXAR (1995-1996), GTE (Feb-Apr 2001), CRYSTAL (May-Jul 2002), SPURT (2001-2003), SWISS (11th of Mar 2004), MIDCIX (Mar-May 2004), AVE (Oct 2004-Jun 2005) and CRAVE (Jan-Feb 2006).

2.2 Meteorological analysis

The airborne wind measurements are compared to interpolated 4D analyzes of the European Center for Middle Range Weather Forecast (ECMWF). The ECMWF operates a spectral meteorological model and uses a four-dimensional variational data assimilation scheme (4-D var) since November 1997 (Rabier, 1997).

Note that over the time window encompassed by the wind measurements the ECMWF model cum assimilation suite underwent three major changes:- during the NOXAR campaign the suite was the triangular truncation version T213 with 31 levels; the triangular truncation version T511 with 60 vertical levels was introduced in November 2000; and in Feb 2006, the resolution was further increased to T799L91.

2.3 Approach

For the present study the 6 hourly analysis fields were interpolated to the time and location of the in situ wind observations, and comparison of the "measurement-analysis" differences were made for each flight campaign separately. In addition case studies were undertaken of the near-tropopause structure of the wind measurement and ECWMF wind analyses to examine the possible misrepresentation of individual jet streams in terms of their strength and structure including their lateral width and across-jet asymmetry.

3.RESULTS

A sample of the derived results is provided in Fig. 1. It shows the root mean square (RMS) of the "measured - analysed" wind as a function of observed wind for the three campaigns (CRYSTAL, AVE, and CRAVE).

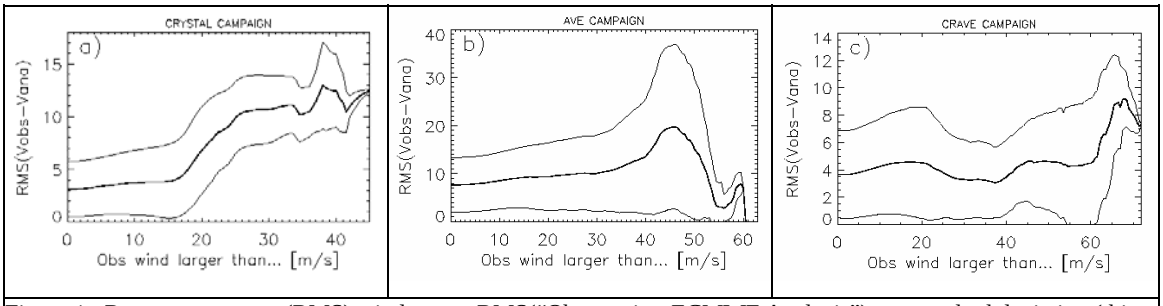

Figure 1: Root mean square (RMS) wind error: RMS("Observation-ECMWF Analysis") ± a standard deviation (thin line) as a function of minimum observed wind velocity for (a) CRYSTAL campaign, (b) AVE campaign and (c) CRAVE campaign.

Such inter-comparison results together with the case studies suggest that strong winds (sic. jets) are often significantly underestimated in the initial conditions of the ECMWF NWP suite with the difference being as large as 15 ms^{-1} for an observed wind of 45 ms^{-1}. This difference prompts concern on two grounds. First jets are an integral and important components of cyclogenesis and their structure should be captured adequately, and second the rationale for ensemble prediction is predicated upon examining the different flow evolutions resulting from "small" changes in the initial conditions. (Some preliminary work also suggest that similar conclusions pertain for the NCEP analysed wind fields).

REFERENCES

Cardinali, C. and Rukhovets, L. and Tenenbaum, J., 2004: Jet stream Analysis and forecast errors using GADS aircraft observations in the DAO, ECMWF, and NCEP models. Mon. Wea. Rev., 132, 765-779.

Francis, J.~A., 2002: Validation of reanalysis upper-level winds in the Arctic with independent rawinsonde data. Geophys. Res. Lett., 29, Art. No. 1315.

Jeker, D. P. and Pfister, L. and Thompson, A. M. and Brunner, D. and Boccippio, D. J. and Pickering, K. E. and Wernli, H. and Kondo, Y. and Staehelin, J., 2000: Measurements of nitrogen oxides at the tropopause: Attribution to convection and correlation with lightning}. J. Geophys. Res., 105, 3679 (1999JD901053)

Rabier, F. and JÃ¤rvinen, H. and Klinker, E. and Nahfouof J.-F. and Simmons, A., 2000: The ECMWF operational implementation of four dimensional variation assimilation. Part I: Experimental results with simplified physics. Quart. J. Roy. Meteor. Soc., 126, 1143-1170.

Tenenbaum, J., 1996: Jet stream winds: Comparison of aircraft observations with analyses. Wea. Forecasting, 11, 188-197.

TURBULENCE: AN IMPORTANT FACTOR FOR FLIGHT OPERATIONS AT ANTARTIC STATION COM. FERRAZ

Francisco Eliseu Aquino, Luciana Bassi Marinho Pires,
Marcelo Romão, Ana Carolina Vasques and Alberto Setzer

Center for Numerical Weather Forecast and Climate Studies - CPTEC,
National Institute for Space Research – INPE, São José dos Campos, SP, Brazil
E-mail: *francisco.aquino@ufrgs.br*

Abstract: This study presents the case of an extreme wind gust event that occurred between the 18th and 19th of January of 2002, in the Brazilian Antarctic Station (EACF) area, where the near-ground air turbulence hindered a helicopter from landing for more than 10 hours, even under favorable general synoptic conditions. The EACF (62°05'S; 58°23,5'W) is located on the Keller Peninsula (3.8 km long, 2.2 km wide), which is a ridge of elevations between 250 e 360 m msl protruding into Admiralty Bay, King George Island, Antarctica. Turbulence was estimated using the wind gust factor and wind turbulence definitions that are normally applied in engineering studies of applied meteorology.

Keywords – *Wind Turbulence, Gust Factor, Flight Operations, King George Island, Antarctica.*

1. INTRODUCTION

The Antarctic Peninsula Region is noted for its intense airborne activity. On King George Island (KGI), in the South Shetland Archipelago, with elevations up to 700 m, aligned in the NE-SW direction, and where wind speeds can easily reach 36 ms^{-1} (70 knots) at least once every month (Romão et al., 2005), it is common for airplanes and helicopters to face local turbulence. Among the many scientific stations at KGI, the Brazilian scientific station *Estação Antártica Comandante Ferraz* (EACF) is located on the Keller Peninsula, deep inside the northern sector of a fjord known as Admiralty Bay, the largest inlet on KGI (Figure 1).

Figure 1. Map of King George Island, Keller Peninsula (black arrow) and EACF (red dot).

During the 18th and 19th of January 2002, a Uruguayan Air Force helicopter (Bell UH-1H) approaching EACF aborted its landing on the helipad many times after facing near-ground air turbulence. At least three air currents occurred at that moment: one, coming down from the local glaciers in the north, another from the sea at south and east, and the third coming down from Flagstaff Mt., the 216 m elevation at west behind the EACF.

The objective of this work is to understand the structure of this atmospheric turbulence that occurred at the EACF helipad.

2. MATERIALS AND METHODS

The EACF helipad (62º05'S; 58º23,5'W) is located on the east side of the Keller Peninsula, approximately 800 m from the base of Flagstaff Mt., situating this station inside a zone of turbulent recirculation, where severe regional meteorological conditions are common. Turbulence analysis was made according to the definitions normally employed in applied meteorology studies for engineering problems, e.g. as in Plate (1982), Bergstrom (1987), Kristensen et al., (1991) and Young and Kristensen (1992). The analysis of wind gusts is one of the ways to study the structure of turbulence at any place, and where such events can be defined as the sudden increase/decrease of wind speed at very small and continuous cycles.

For the purpose of comparison, the event of 2002 was analyzed in relation to two other years, 2001 and 2003, during the period of 15th to the 25th of January in the three years. The wind data was obtained with a Wind Monitor Sensor R.M.Young Model 05103. This equipment is installed on a 10 m anemometric tower adjacent to EACF, at 20 m msl. Wind speed and direction were stored in a Datalogger Campbell 21X, and where the full hour value registered is the average of the last ten minutes interval, sampled at each second – see http://www.cptec.inpe.br/antartica. The parameters measured were the 10-minutes average scalar speed (ms^{-1}),

10-minutes average direction (degrees), and the daily maximum gust; the calculated variables were the wind gust factor, gust amplitude (ms^{-1}) and turbulence intensity.

3. RESULTS

Table 1 shows the measured values of speed and maximum speed) and the calculated values of the variables: gust factor $G = V_{max} / V_{mean}$, gust amplitude $A = (V_{max} - V_{mean})$, and turbulence intensity $I = \sigma_{speed} / V_{mean}$.

At investigating the maximum and minimum average wind speeds, the wind gust factor and turbulence intensity from the 15th to the 25th of January, 2002, we were able to establish that from the 15th on, turbulence conditions occurred with values over the registered mean values for the EACF region. The maximum registered wind speed were approximately 30 ms^{-1} for the 15th, 15 ms^{-1} for the 16th, 22 ms^{-1} for the 17th, 25 ms^{-1} for the 18th and 17 ms^{-1} for the 19th. The landing of any aircraft was possible only on the latter day. Wind gust amplitude values were also high for the same period, varying between 20 and 10 ms^{-1}. The turbulence intensity for the same period stabilized around 0.6. The synoptic conditions during this period showed extra-tropical cyclones located over the eastern side of the Antarctic Peninsula (southeast of the EACF) and occluding on the 18th.

Year	2001					2002					2003				
Day	V_m	V_{max}	G	A	I	V_m	V_{max}	G	A	I	V_m	V_{max}	G	A	I
15	8.3	18.5	2.2	10.2	0.5	9.4	29.6	3.1	20.2	0.6	3.3	11.2	3.4	7.9	0.3
16	4.5	14.7	3.3	10.2	0.4	5.2	14.7	2.8	9.5	0.6	2.3	8.1	3.5	5.8	0.3
17	7.7	17.2	2.3	9.6	0.3	6.2	22.0	3.6	15.8	0.6	2.3	8.2	3.5	5.9	0.4
18	2.3	9.3	4.1	7.1	0.3	7.2	25.1	3.5	17.9	0.5	1.1	5.2	4.6	4.0	0.5
19	3.2	10.1	3.1	6.9	0.5	6.4	17.0	2.7	10.6	0.4	5.5	9.8	1.8	4.3	0.8
20	3.7	11.9	3.3	8.2	0.4	6.7	21.3	3.2	14.6	0.5	8.0	16.2	2.0	8.2	0.3
21	3.6	9.0	2.5	5.3	0.6	4.1	25.3	6.2	21.3	0.4	3.0	9.8	3.3	6.8	0.6
22	4.5	10.5	2.3	6.0	0.6	2.1	8.0	3.8	5.9	0.6	2.3	6.9	3.1	4.7	0.6
23	7.2	23.2	3.2	16.0	0.6	5.5	13.6	2.5	8.1	0.4	2.3	7.6	3.3	5.3	0.4
24	3.8	10.4	2.8	6.7	0.4	4.0	13.0	3.3	9.0	0.4	9.7	18.3	1.9	8.6	0.4
25	3.7	9.1	2.5	5.4	0.7	3.6	10.1	2.8	6.6	0.6	10.0	22.9	2.3	12.8	0.2

Table 1. Mean values for wind characteristics: mean speed (V_m), maximum speed (V_{max}), wind gust factor (G), gust amplitude (A) and turbulence intensity (I).

4. CONCLUSION

Between the 18th and the 19th of January, 2002, the EACF faced adverse wind conditions for helicopter landing, noticed in the average and maximum wind speed, and in the wind gust factor and amplitude. The reason for such results is that this factor is obtained dividing the maximum speed by the average speed. Noteworthy is the fact that the wind gust factor of 2002 is inferior to the compared 2001 and 2003 corresponding periods. Turbulence intensity did not present any distinct behavior when related to the observed wind speed for the period in 2002. This is probably due to the wind circulation complexity deep inside the fjord, and also to persistent regional winds. 2001 and 2003 served as the baseline to compare and analyze the 2002 extreme event, which presented above average climatological values. The occurrence of this event is possibly related to the relatively high average wind intensity (~5 ms^{-1} above average) and predominating southeast winds, that when combined to the KGI topography and the EACF position on Keller Peninsula, result in a near-ground air turbulence and wind gust occurrence zone, making flight operations potentially difficult or even hazardous.

Acknowledgements: *PROANTAR (CNPq+SECIRM) and CPTEC/INPE for the financial and logistics, and Heber R. Passos and Marilene A. da Silva for their technical support.*

REFERENCES

Bergstrom, H., 1987: A statistical analysis of gust characteristics. *Boundary Layer Meteorology*, v.39, n.1, p.153-73.

Kristensen, L., Casanova, M., Courtney, M.S., Troen Rise, I, 1991: In search of a gust definition, *Boundary Layer Meteorology*, v.55, n.1, p.91-107.

Plate, E., 1982: Studies in Wind engineering and industrial aerodynamics. *Engineering Meteorology*. Amsterdam, Elsevier, 740p.

Romão, M., Setzer, A., Aquino, F.E., 2005: Ondas de Montanha e a Segurança nas Operações Aéreas na Antártica. *Boletim SBMET*, nov/05, 59-63.

Young, G.S., Kristensen, L., 1992: Surface Layer gusts for aircraft operation, *Boundary Layer Meteorology*, v.59, n.2, p.231-242.

STATISTICAL EVALUATION OF EXTREME STORM SURGES BASED ON DYNAMICAL DOWNSCALING OF EPS-FORECASTS: THE MUSE PROJECT

Detlev Majewski

Deutscher Wetterdienst, Offenbach, Germany
E-mail: detlev.majewski@dwd.de

Abstract: Extreme water levels during winter storm surges at the German North Sea coast have been calculated by a physically consistent combination of meteorological and storm surge models. The meteorological scenarios have been taken from about 4500 simulations of the global ensemble prediction system of the ECMWF and dynamical downscaling with the Lokal Modell LM of the DWD.

1. INTRODUCTION

Extreme winter storm surges like the famous 1962 "Hamburg" storm, leading to flooding of coastal areas pose a constant thread for the German North Sea coast. To estimate extreme water levels for events of very low occurrence probability in the order of 10^{-3} to 10^{-4} year^{-1}, observational data sets which are recorded for the past 100 to 150 years only are not sufficient. Previous attempts to provide meteorological scenarios for storm surge studies were based on a combination of past events by an experienced forecaster. But these artificial scenarios did not allow to derive the temporal evolution of the storm in a dynamically consistent way. Moreover, the probability of these extreme events could not be estimated.

Therefore, in the framework of the MUSE project (Modelling of extreme storm surges with very low probabilities of transgression in the German North Sea) the three participating institutes, Deutscher Wetterdienst (DWD), Bundesamt für Seeschifffahrt und Hydrographie (BSH) and the Research Centre for Water and Environmental Engineering (FWU) at University of Siegen, choose a different approach to derive meteorological scenarios leading to extreme water levels (Jensen et al., 2006).

2. CONSISTENT SIMULATION OF METEOROLOGICAL SCENARIOS LEADING TO EXTREME STORM SURGES

Storm surges at the North Sea coast are usually caused by strong and steady westerly winds in the winter season piling up the water at the coast. Thus storm surges can be expected if near surface winds exceed BFT 8 (~ 17 m/s) from WSW to NNW about 3 hours before high tide. From empirical studies based on observed events a single parameter, called the effective wind (v_{eff}) which is the average wind speed from 295° (WNW) at 10 m in the German Bight (Figure 1), characterizes the potential of extreme events. For six observed storm surges in 1962, 1967, 1976, 1990, 1994 and 1999 at Cuxhaven the Ensemble Prediction System (EPS) of the European Centre for Medium Range Weather Forecasts (ECMWF) is used to derive potential storm scenarios. Each ensemble run consists of 50 different forecasts (model T_L255L40, i.e. 80 km grid spacing and 40 layers) based on different initial states ("singular vectors") and modified physical parameterizations ("stochastic physics").

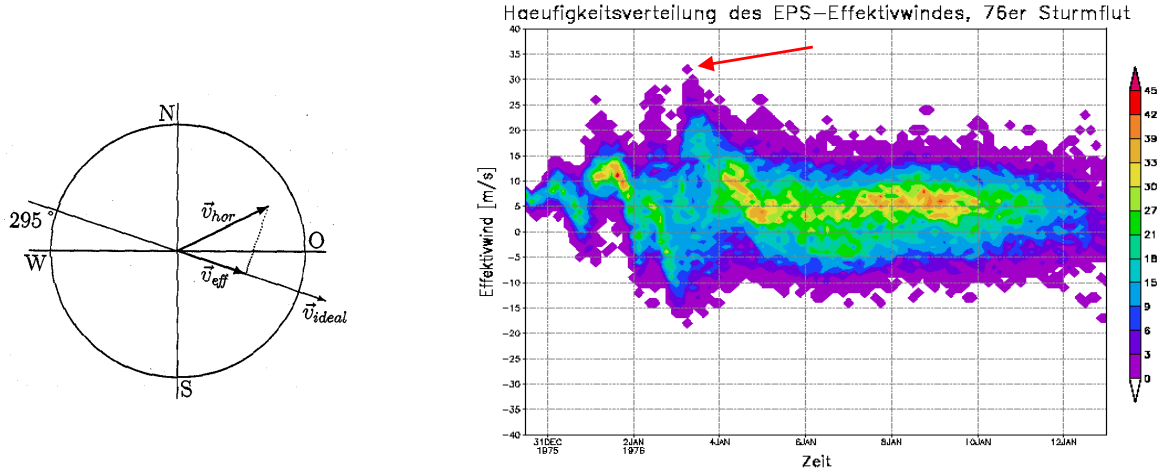

Figure 1. Left: Definition of the effective wind (v_{eff}). Right: Frequency distribution of v_{eff} for the 1976 storm surge. The red arrow points to the maximum wind forecasted by ensemble member #45.

A total of about 4500 forecasts are computed for the six observed storm surges. For each of these forecasts the effective wind (v_{eff}) is calculated.

3. MODELLING SYSTEMS EMPLOYED

The meteorological scenarios for the storm surges are derived by downscaling the forecasts of the global EPS (Buizza, R. et al., 1999) with the Lokal Modell (LM, Doms, G. and U. Schättler, 1997). LM covers Central Europe with a grid spacing of 7 km and 325x325 grid points. Out of 4500 simulations 36 cases yielded v_{eff} in excess of 17 m/s and for 27 cases v_{eff} exceeds even 22 m/s which give rise to extreme water levels.

Based on the high resolution meteorological forecasts of the LM, BSH computed the corresponding water levels at the German North Sea coast. The modelling system at the BSH consists of a 3-D baroclinic model for the North Sea and the Baltic Sea with a grid spacing of 10 km (Dick et al., 2001) and a high resolution (2 km grid) coastal model.

The third project partner (FWU), evaluated the extreme water levels predicted by the BSH models to derive transgression probabilities for nine sites at the German coast.

4. RESULTS

The water levels at nine coastal stations (Table 1) are simulated for all LM forecasts where v_{eff} exceeds 22 m/s. For wind speeds in the range of 3 to 22 m/s, a linear relation between drag coefficient and wind speed is fairly well known by observations. For higher wind speeds some measurements indicate a constant drag coefficient (or even a slight decrease) above about 25 m/s. Therefore, the water levels were calculated with different functional relationships between drag coefficient and wind speed. For one case, EPS member #45 initialized on January 3, 1976 at 00 UTC, water levels exceeding observed extremes by up to 110 cm were predicted.

Station	Extreme water level (cm above MSL); year of event	Maximum simulated water level level (cm above MSL)	Range of water level (cm ab. MSL), depending on drag-wind relation
Emden	517 (1906)	609	570 639
Norderney	410 (1962)	512	475 537
Bremerhaven	535 (1962)	674	629 702
Helgoland	392 (1962)	499	461 521
Cuxhaven	510 (1976)	651	603 672
Husum	566 (1976)	669	609 691
Büsum	514 (1976)	635	585 655
List	404 (1982)	483	442 506
Dagebüll	472 (1982)	555	513 576

Table 1 Observed water levels and maximum water levels simulated for a storm surge on January 3, 1976

Taking the results of the numerical simulation of extreme storm surges into account it is possible to quantify the extreme water levels for events of very low occurrence probability in the order of 10^{-3} to 10^{-4} $year^{-1}$. For nine stations at the North Sea coast the maximum water levels observed so far correspond to an occurrence probability in the order of 10^{-2}. For an occurrence probability in the order of 10^{-4} the water levels may exceed the observed extreme values by about 60 to 110 cm. These results will form the basis of further coastal engineering studies.

Acknowledgements: The Muse project has been funded by the Bundesministerium für Bildung und Forschung (BMBF) under grant 03KIS039.

REFERENCES

Buizza, R., Miller, M., and Palmer, T.N., 1999: Stochastic representation of model uncertainties in the ECMWF Ensemble Prediction System. Quarterly Journal of the Royal Meteorological Society, **125**, 2887-2908.

Dick, S., Kleine, E., Müller-Navarra, S.H., and Komo, H., 2001: The operational circulation model of BSH (BSHcmod) Model description and validation. Berichte des BSH Nr. 29 48 pp.

Doms, G. and U. Schättler, 1997: The nonhydrostatic limited-area model LM (Lokal-Modell) of DWD. Part I: Scientific Documentation. Deutscher Wetterdienst (DWD), Offenbach, March 1997.

Jensen, J., Mudersbach, Ch., Müller-Navarra, S., Bork, I., Koziar, Ch. and Renner, V.: Modellgestützte Untersuchungen zu Sturmfluten mit sehr geringen Eintrittswahrscheinlichkeiten an der Deutschen Nordseeküste, Die Küste, Heft 71, 2006, (in print), Boyens Medien, Heide i. Holstein

INFORMATIONS METEOROLOGIQUES, OUTILS D'AIDE A LA DECISION EN MILIEU RURAL AU MALI

MAIGA Djibrilla Ariaboncana,
Direction Nationale de la Météorologie
Email : dnm@afribone.net.ml djibamaigfr@yahoo.fr

Résumé

Le Mali est un pays sahélien à vocation agro sylvo pastorale caractérisée par de phénomènes climatiques extrêmes notamment des sécheresses récurrentes depuis le début des années 1970 avec des conséquences socio-économiques et environnementales très graves pour les populations les plus exposées notamment celles rurales et les femmes.
La production, la fourniture et l'utilisation d'avis et conseils agro météorologiques, de prévisions saisonnières et météorologiques permettent aux producteurs de minimiser ce risque majeur et contribuent à l'amélioration de la productivité et de la production agricole.

I INTRODUCTION

Le Mali un pays sahélien et continental d'environ 1 241 000 km2 et plus de 10 000 000 d''habitants, l'économie est essentiellement agro-pastoral.
Les cultures vivrières (mil, sorgho, mais et riz) dont la part commercialisée est de seulement 30% de la production totale occupe environ 80% de la population. C'est une agriculture de subsistance essentiellement pluviale avec de faible niveau de mécanisation et d'irrigation et sans utilisation d'engrais dont le cout est exorbitant pour les paysans (6).
Cette activité reste donc largement tributaire des fluctuations climatiques notamment de la variabilité pluviométrique avec des conséquences socio-économiques et environnementales importantes tels que la baisse des rendements des cultures, la modification des systèmes de production et des écosystèmes, la mauvaise croissance du couvert végétal et élimination des espèces les moins résistantes à la sécheresse, l'ensablement et assèchement des fleuves et rivières,le déplacement des ruraux vers les villes augmentant le chômage et la pauvreté, créant des zones d'insalubrité et d'insécurité etc.
Ce papier tente de montrer en quoi une bonne utilisation de l'information météorologique permet de minimiser le risque lié à cet phénomène météorologique extrême comme la sécheresse.

II METHODOLOGIE UTILISEE POUR L'ASSISTANCE METEOROLOGIQUE EN MILIEU RURAL

L'application des informations et avis agro météorologiques en agriculture revêt un caractère pluridisciplinaire et nécessite l'implication effective des organisations paysannes, des services techniques de l'agriculture, des services d'agro-hydro-météorologie, des projets/programmes d'alerte précoce et de sécurité alimentaire, des médias, de la recherche agronomique, de la protection civile et des ONG chargés de transférer sur le terrain le paquet technologique y compris les informations météorologiques.
Ces structures composent le groupe de travail pluridisciplinaire (GTPA) chargé de la collecte, du traitement, de l'élaboration et de la diffusion des informations et avis agro météorologiques.
Dans le cadre de la déconcentration des activités d'assistance météorologique, des groupes locaux d'assistance (GLAM) fonctionnent également.
L' assistance météorologique au monde rural concerne l'alerte précoce pour la sécurité alimentaire et l' amélioration de la productivité et de la production agricole.

III - ALERTE PRECOCE ET SECURITE ALIMENTAIRE

Les produits élaborés concernent essentiellement:

- bulletin agro-hydro-météorologique décadaire sur l'évolution de la campagne agricole;
- Les caractéristiques de la saison pour la détermination des zones à risque pour un suivi rapproché ;
- La prévision saisonnière qui donne une estimation qualitative de la pluviométrie pendant les mois de juillet-août-septembre considérés comme les mois où on recueille les 80% de la pluviométrie annuelle (5).

Les informations élaborées dans le domaine de l'alerte précoce et de sécurité alimentaire sont surtout destinées aux services de planification agricole, aux éleveurs pour la recherche des pâturages et des points d'eau, et aux décideurs, aux organismes nationaux et internationaux chargés d'alerte précoce et de sécurité alimentaire.

IV- AMELIORATION DE LA PRODUCTION AGRICOLE

Deux préoccupations essentielles prises sont à prendre en compte notamment :

- la planification de la saison agricole pour une exploitation rationnelle des ressources à travers le choix des spéculations et de variétés, le choix de sites appropriés etc.

Les informations agro météorologiques utilisées sont :

- la prévision des ressources agro climatiques (pluviométrie, début, fin et longueur moyens de la saison etc.);
- la prévision saisonnière élaborée en avril-mai et mise à jour en juin et juillet,

- l'application opérationnelle concerne la prise de décision pratique sur le terrain par les exploitants agricoles.

Les informations concernent essentiellement :

- le calendrier prévisionnel de semis qui permet de conseiller aux paysans de semer sur la base d'un seuil pluviométrique, et d'une variété de cultures données.

- les prévisions météorologiques quotidiennes qui permettent aux exploitants de mieux conduire d'une manière efficace les activités quotidiennes notamment l'épandage d'engrais, le traitement phytosanitaire, l'entretien des champs (sarclage, démariage etc.), la récolte et leur stockage. Les informations sont directement destinées aux exploitants ruraux pour une prise de décision pratique dans la conduite opérationnelle de leurs activités quotidiennes et de planification et aux femmes pour les activités ménagères et artisanales actuellement dévolues aux femmes rurales et urbaines génératrices de revenus, telles que le séchage de certains produits alimentaires (couscous, sauces, gombo, oignon, etc.), la teinture et dans leurs parcelles.

V- METHODE DE DIFFUSION DES INFORMATIONS

Les avis et conseils agro météorologiques et les prévisions météorologiques quotidiennes sont diffusés dans les différents médias en français et dans les langues nationales.

TYPES INFORMATIONS	UTILISATEURS	CULTURALES	MODE DE DIFFUSION
- Prévision des caractéristiques de la saison - Prévision saisonnière	-Planificateurs -Services techniques	- Choix de variétés culturales - Choix de topo séquence - Système de production	- Réunions ordinaires - Bulletin - Courrier
- Prévisions saisonnières - Prévision de rendement - Prévision décadaire Bulletin de Suivi agricole - Prévisions des zones à risque	-Décideurs -Services d'alerte précoce et de sécurité alimentaire	Prévention et gestion de situation de sécheresse	- FV, Radio -Communication Verbale -Carte -journaux
- Prévisions météorologiques Calendrier personnel de semis - Prévision saisonnière	Exploitants agricoles	- Travaux champêtres - Date optimale de semis - Lutte antiacridienne et traitement phytosanitaire - Récolte et stockage	- Radio, TV - Journaux
Prévision météorologiques quotidiennes	Femmes	Travaux ménagers générateurs de revenu	- Radio, TV

Table 1 .Produits et modes de communication

2.4 - APPLICABILITE DES PREVISIONS EN MILIEU RURAL ET BESOINS EN INFORMATIONS METEOROLOGIQUES

Les avantages socio-économiques de l'application des informations météorologiques dépendent en grande partie de la qualité de l'information élaborée, de sa diffusion en temps réel et de son utilisation correcte par les exploitants agricoles (3).

Au Mali,les informations météorologiques diffusées sous forme d'avis et conseils auprès des paysans a permis une augmentation des rendements de 20-25% des mil/sorgho/maïs et 40 % du coton. Cependant de nouveaux besoins sont apparus :

- les prévisions météorologiques quotidiennes de plus en plus localisées et d'échéances de plus en plus courtes,
- la prévision suffisamment tôt des débuts et fins de saison des pluies,des quantités saisonnières des précipitations et des épisodes de sécheresse pendant la saison des pluies

VII- CONCLUSION

Il apparaît que des informations météorologiques y compris les prévisions climatiques, avis et conseils agrométéorologiques fiables et adaptées constituent un véritable outils d'aide à la décision et contribuer à la réduction de la pauvreté ,à la protection de l'environnement,t et à un développement durable.

Références

1. Djibrilla A. MAIGA- Some elements of climate variability in Mali. In Proceedings of the international CLIVAR conférence, Paris, France,
2-4 décembre 1998.
2. Kaliba KONARE – Applications de la Météorologie et de l'Hydrologie aux problèmes d'environnement et de développement.
3. SIVAKUMAR. M.V.K, Maidoukia.A, STERN. R.D - Agro climatologie de l'Afrique de l'Ouest : le Niger, Bulletin d'information N°51, ICRISAT, Niamey (Niger), 1993.données à long terme ,Dossier n119 septembre 2003.

5. BIRAMA DIARRA- Rationalisation de l'assistance agro météorologique opérationnelle au monde rural travaux de fin d'études à la FUL 1996/1997 Arlon.

ADVANTAGES DE PRÉVISIONS PLUS EFFICACES POUR LA SOCIÉTÉ, L'ÉCONOMIE ET L'ENVIRONNEMENT

Luis Mendes Cherno [1]

[1] Direction Générale de la Météorologie Nationale, Guinée-Bissau
Email : *cherno_lm@yahoo.fr*

1. INTRODUCTION

Depuis en 1997, la Direction du Service de la Météorologie Nationale de la Guinée Bissau (DSGN) en collaboration avec le Centre Africain de l'Application de la Météorologie pour le Développement (ACMAD) et avec l'appui des Centres Mondiaux, tels que: NOOA-OGP, Météo France, UK-Meteo Office, organisent annuellement module de la formation action, destinée aux techniciens climatologistes, pour élaborer la prévision saisonnière par l'Afrique Occidental et Centrale.

Pour l'élaborer cette prévision on tiens compte avec la température de la surface des océans, qui a un aspect sur le climat de la sous région et, consiste l'établissement de la corrélation entre les anomalies des températures des eaux de la mer (SST) et les index de la précipitation (RR).

Les prévisions élaborées sont présentées au forum (PRESAO) que regroupe les Experts régionaux et les Scientifiques des centres mondiaux, pour permettre l'élaboration d'une PREVISION CONCENSSUELLE par la période de Juillet, Août et Septembre (JAS).

Le thème pour cette année est suivant : "**Prévision Climatique, Sécurité Alimentaire et la Réduction de la Vulnérabilité aux Risques naturelles** ".

2. OBJECTIF

Les objectifs du forum consistent :

- Elaborer les questionnaires destinés aux utilisateurs selon leurs besoins pour l'assistance des vies et des biens pour un développement socio-économique ;

- Identifier les membres des services météorologiques qui peuvent intégrer et charger du point focal par la diffusion des questionnaires ;

- La réflexion sur l'ancien travail du forum précédente avec l'objectif d'améliorer et de répondre aux besoins des usagers des produits de la prévision saisonnière, pour permettre la prévention et gestion des catastrophes naturelles ;

3. RESULTAT DE LA PREVISION SAISONNIERE JUILLET, AOUT ET SEPTEMBRE (JAS /2006) POUR LA GUIEE-BISSAU

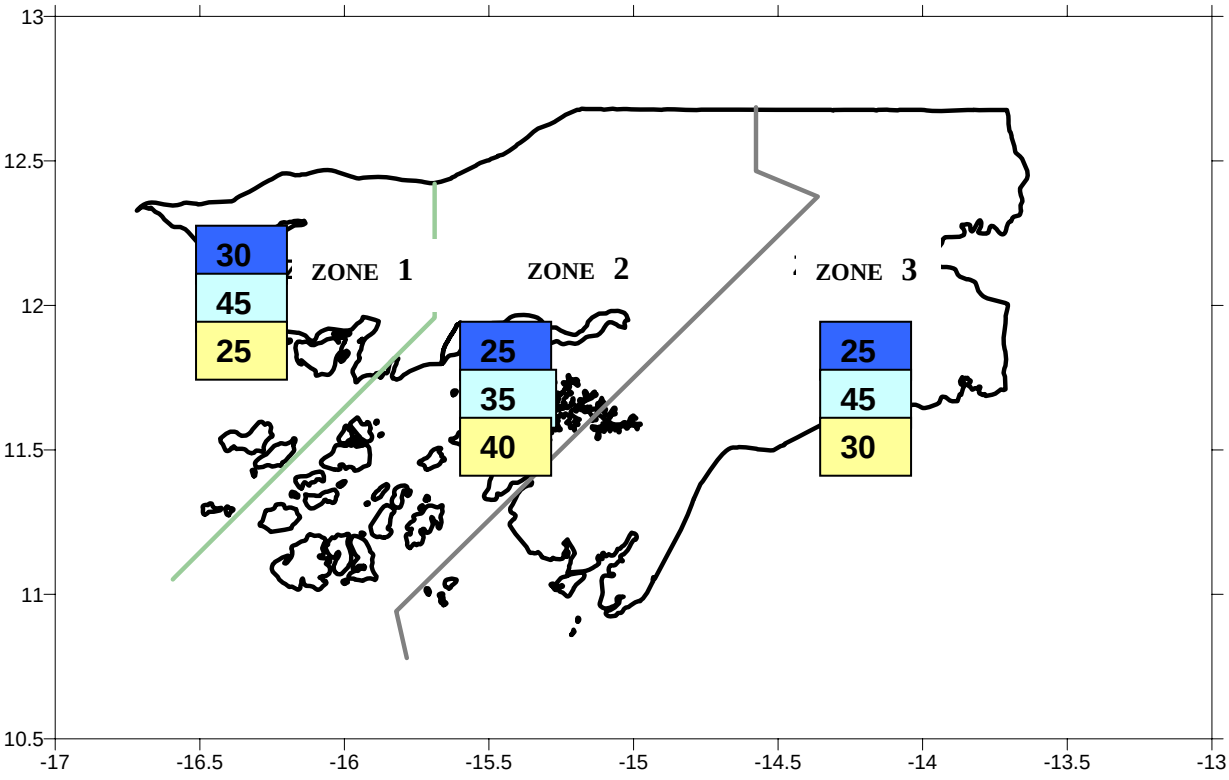

Figure. 1: Résultat de la prévision saisonnière pour la Guinée-Bissau de l'an 2006

4. SELON LA PREVISION SAISONNIERE POUR L'ANNEE 2006, NOUS AVONS COMME LE RESULTAT SUIVANT :

ZONE 1: Normale à la tendance sec
ZONE 2: Humide à la tendance normale
ZONE 3: Normale à la tendance humide

5. CONCLUSION

Selon le résultat de prévision saisonnière de l'année 2006, pour la Guinée-Bissau , une cumule de la précipitation aux mois de Juillet, Août et Septembre (JAS), des valeurs proches de la normale (1961-1991), les conditions qui prévoit un bon résultat de la campagne agricole par rapport à l'année 2005.

L'an 2005 a été observé des épisodes secs de plus de 10 jours dans les localités de **Cacheu, Bula, Ingoré, Farim, Mansôa et Mansabá**.

Dans la même en question a été observé une pause pluviométrique d'environ deux semaines en fin août - début septembre dans la région de **Tombali** (sud du pays). En septembre, l'intensité des pluies a baissé, sans toutefois qu'il n'y ait d'épisodes secs prolongés. Une situation qui a ramené dans cette zone une famine totale, les agriculteurs n'ont pas eu des semences pour la prochaine campagne.

INTEGRATION OF METEOROLOGICAL FORECASTS INTO AGROMETEOROLOGICAL MODELS: AN INNOVATIVE METHODOLOGY FOR EARLY WARNING FOR FOOD SECURITY IN THE SAHEL

Genesio L. [1],Bacci M. [1], Di Vecchia A. [1], Guarnieri F. [2], Pasqui M. [2], Pini G. [1], Tarchiani V. [1]

[1] Institute of Biometeorology, National Research Council, Florence, Italy
[2] Laboratory for the Meteorology and Environmental Modelling (LaMMA), Tuscany Region, Florence, Italy
E-mail: *L.Genesio@ibimet.cnr.it*

Abstract: This paper presents the integration of meteorological forecasts with classical agrometeorological monitoring achieved by ZAR model. Input data are Rainfall Estimate provided by Meteosat Second Generation and forecasts from GFS (Global Operation Forecast) model, Precipitation at ground, at 7 days, downscaled at 8 kilometres. Such integration allows the production of information, as prevision of good conditions for sowing, of crops onset in sowed areas and of crop conditions during the growing period.

Keywords – *Early Warning, Food Security, Sahel, ZAR model, Rainfall estimate, Rainfall forecast, GFS, downscaling.*

1. INTRODUCTION

Food insecurity still represents a major problem in the sahelian region. Since the ‘70s Early Warning Systems have been developed in order to avoid major food crisis. Such systems insist on two levels: prediction and prevention. Considering that food availability mostly depends on rainfed agriculture, agrometeorology is a critical sector for food security monitoring and in this context advises to farmers are a fundamental component. Currently, the production of meteorological forecasts allows early warning systems to provide significant information to farmers and to decision makers, in order to reduce the impact of meteorological related risks.

In this framework, AGRHYMET Regional Center and IBIMET-CNR in collaboration with WMO, have developed a model, called ZAR (Zones A Risque), in order to integrate meteorological forecasts into classical agrometeorological models based on rainfall estimates. This integration allows the production of information such as the prediction of good conditions for sowing, the crops onset in sowed areas and crop conditions during the season.

2. THE STUDY AREA

The Sahel covers the area between the Sahara and the Sudan, laying from Senegal to Chad, and receiving about 250-500 mm summer rainfall or, for other authors, 150-600 mm. In spite of some local exceptions, it is characterized by semi-desert grassland, shrubs and wooded grasslands, in which Acacia species play a dominant role. In this context, the ZAR is operational at regional level and locally in four of the nine CILSS (Comité permanent Inter-Etats de Lutte contre la Sécheresse au Sahel) countries: the Senegal, Mali, Burkina Faso and Niger.

The study area coincides with the agricultural zone: in the north this area is delimited by the isohyet 250 millimetres. Millet and sorghum are the most important food crops, representing respectively 43% and 24% of the total agricultural production (AGRHYMET, 2003).

3. DATA

The model input data are Rainfall Estimate data and Rainfall Forecasts, evapotranspiration, available soil moisture and agronomic data for the crops that ZAR simulates.

The model works with different sources of rainfall estimate (MSG-Ibimet, FEWS, CRA) and with forecasted rainfall from the downscaled GFS (Global Forecasting System) model precipitation. Such downscaling technique, developed originally at Ibimet, increases the resolution at ground from 0.5° to 0.08° using the rainfall spatial distribution coming from the MSG precipitation patterns, observed in the previous 3 days, for the following 180 hours (Guarnieri et al. 2006).

4. MODEL

ZAR model is currently used in operational way by AGRHYMET Regional Centre for regional early warning and by National Meteorological Services of Senegal, Mali, Burkina Faso and Niger for the monitoring of agricultural season.

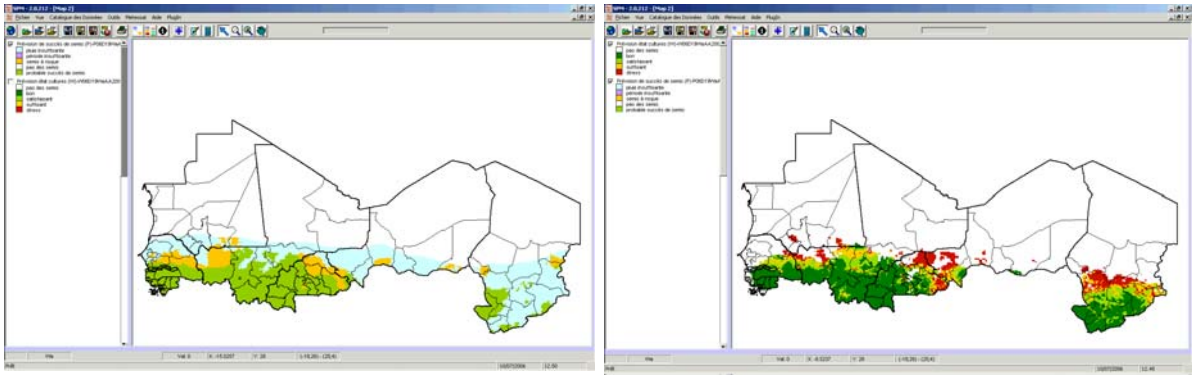

Figure 1. Example of ZAR outputs Left: Installation forecast for the 1st decade of July 2006 (forecast time 1st of July 2006). Right: Crop water needs satisfaction forecast for the 1st decade of July 2006 (forecast time 1st of July 2006)

Starting from the decadal or pentadal rainfall estimates by the MSG images, the ZAR model identifies the zones where the crops have been established later than normally because of the late onset of the rain season or because of the first sowing failure. In these conditions it might happen the crops can not finish the growing cycle. The agronomic consequence is a reduction of the yields that can drive to a complete loss of agricultural production in those areas with a low agricultural suitability (Martini, 1994). During the crop cycle, ZAR assesses the satisfaction of crop water needs showing the stress areas. ZAR allows the user personalizing different parameters such crops and varieties (pearl millet 85 and 130 days; cowpea 75 days; groundnut 100 and 140 days and sorghum 110 days), sowing conditions (rain threshold and period) and geographical extent of analysis area.

Specifically for the forecast, ZAR integrates two modules operating during different periods of the growing season.

1. The sowing condition forecast module produces information to be used by farmers for their sowing activities management. In particular, it can be used to plan of field preparation activities and to identify the best sowing period, aiming at reducing the risks for sowing failure.
2. The forecast of crop conditions module is used during the seasonal monitoring and it aims at forecasting the crops conditions in those areas where stress conditions have been identified.

5. CONCLUSION

Given the absence of a dense rain gauge network in the Sahelian region, the satellite rainfall estimates are a precious source of data for decadal rainfall estimation and spatial distribution patterns. This information is essential to identify the risk zones for agricultural production and to monitor the agricultural campaign.

Rainfall forecasts, produced by the GFS system, were not able to represent all the spatial characteristics of precipitation in the Sahel region. Furthermore their original spatial resolution is too coarse for practical applications. Combining rainfall forecasts with rainfall estimates, adds a new value to agrometeorological modelling. The methodological approach proposed in this paper to detect risk zones for rain-fed crops can be very useful both for the identification of zones with potential production shortage and for the reduction of agrometeorological risk through advises to farmers.

The reliability of rainfall forecast still remain a critical point for the production of agrometeorological forecasts, as shown in Melani et al., but such combined approach reveals an effective improvement respect the original GFS and other rainfall products such as CMORPH. Thus downscaling the original GFS rainfall products allows their utilisation at regional or national scale with effective benefits. Furthermore, even if by extending the temporal range would enable a better advices exploitation, leaving to farmers more time to make decision and to carry out field activities, the comprehensive seven days forecast, now available, allows producing useful advises.

REFERENCES

Guarnieri F., Pasqui M., Genesio L., Melani S. and Vignaroli P., 2006. *Statistical downscaling for GFS precipitation forecast over Sahel region based on Meteosat Second Generation rainfall estimates.* 14th Conference on Satellite Meteorology and Oceanography. Atlanta, USA.

Martini M., 1994. *Méthodologie pour déterminer les zone à risque pour les cultures céréalières pluviales au Sahel. Actes de l'Atelier 'Problèmes de validation des méthodes d'estimation des précipitations par satellite en Afrique intertropicale.* Niamey du 1er au 3 décembre. Pp 151- 161. Ed. Bernard Guillot - ORSTOM.

Melani S., M. Pasqui, A. Antonini, B. Gozzini, F. Guarnieri and A. Ortolani, 2006. *Quantitative analysis of convective MSG - rainfall estimates in the Sahelian area.* 2nd Conference on Quantitative Precipitation Forecast, Boulder, USA.

Vignaroli P., Tarchiani V. and Sorbi V., 2006. *Le Calendrier de Prévision des Crises Alimentaires : Une approche opérationnelle à support des actions de prévention et gestion des crises alimentaires au Sahel.* CILSS-OMM-Cooperation Italienne, Florence, Italy. http://www.ibimet.cnr.it/Case/SVS/

SRNWP-PEPS: SOME RESULTS OF VERIFICATION

Sebastian Trepte, Michael Denhard, Martin Göber, and Bernhard Anger

Deutscher Wetterdienst, Offenbach, Germany
E-mail: *Sebastian.Trepte@dwd.de*

Abstract: The EUMETNET Short-Range Numerical Weather Prediction Programme (SRNWP) has 26 national Meteorological Services to produce their operational forecasts. Using most of these deterministic products the SRNWP-PEPS (Poor man's Ensemble Prediction System) generates operational probability forecasts for Europe. This is done by interpreting the overlapping areas of the single forecasts as members of a local ensemble. An objective and subjective verification found that the system generates stable forecasts and gives useful guidance in situations when single models show great differences. The ensemble reflects the same limitations that fundamentally hold for its members, e.g. bad performance when forecasting convective thunderstorms.

Keywords – *ensemble prediction, multi-model ensemble, forecast verification*

1. INTRODUCTION

One of the most important challenges the operational forecaster is faced with is the effective usage of the existing variety of operational numerical weather forecasts. There is the feeling that joining these operational forecasts in a multi-model ensemble could lead to better results within the forecast and warning process.
Regional Modelling in Europe is organised in 4 Consortia: HIRLAM, ALADIN, COSMO and the UK Met Office, each of them having their own regional model. A reasonable variety of operational forecasts exist, which are produced on different domains with different grid resolutions using different model parameterisations or releases and data assimilation techniques on different computers.
In 2002 at Deutscher Wetterdienst (DWD) the idea was born to start a project which should bring all available high resolution numerical forecasts together in a **P**oor man's **E**nsemble **P**rediction **S**ystem (PEPS). The DWD suggested at the EUMETNET Council to start the project within the SRNWP programme.

2. MODEL

Up to now, 20 Meteorological Services have joined the project providing 23 forecast models. All services deliver an extract of their operational model output containing parameters at surface or rather near surface. As a result of SRNWP-PEPS 40 deterministic and probabilistic forecast products are distributed to the contributing members on an operational basis four times a day.
The single model forecasts are interpreted on a reference grid, the PEPS grid. It has a grid spacing of 0.0625° (~7 km) like the Lokal Modell (LM) of DWD, covering Europe and the North Atlantic Ocean. Since the individual members have different resolutions and integration areas, the ensemble size depends on location. Ensemble mean and exceedance probabilities of certain thresholds are calculated at each PEPS grid point from the ensemble members using a nearest neighbour approach. At the moment all ensemble members are equally weighted and the probability is calculated by counting the corresponding members at each grid point.

3. DATA AND METHOD

A subjective evaluation of the performance of the SRNWP-PEPS is being carried out by the forecasters of DWD. Furthermore, the system is objectively evaluated using a set of deterministic and probabilistic quality indices (verification scores). In order to quantify the added value bring about by an ensemble system, SRNWP-PEPS is compared with the operational deterministic model LM. The comparison is made in terms of 24-hour precipitation against observed data of the DWD station network. For probabilistic investigation the event considered here is precipitation exceeding 20 mm. This threshold indicates an intense precipitation event which has considered in the weather warning process. For verification summer period 2005 and winter period 2005/2006 have been chosen.
To verify this type of forecast we start with a contingency table that shows the frequency of "yes" and "no" forecasts and occurrences. It forms the basis for the calculation of scores and histograms. Typical categorical scores are: (1) POD (probability of detection), which shows what fraction of the observed "yes" events were correctly

forecast, (2) FAR (false alarm ratio), which shows what fraction of the predicted “yes” events actually did not occur, (3) BIAS (frequency bias) which shows how the forecast frequency of “yes” events did compare to the observed frequency of “yes” events and (4) HSS (Heidke skill score), which shows the accuracy of the forecast in predicting the correct category, relative to that of random chance. Scores for SRNWP-PEPS are calculated for

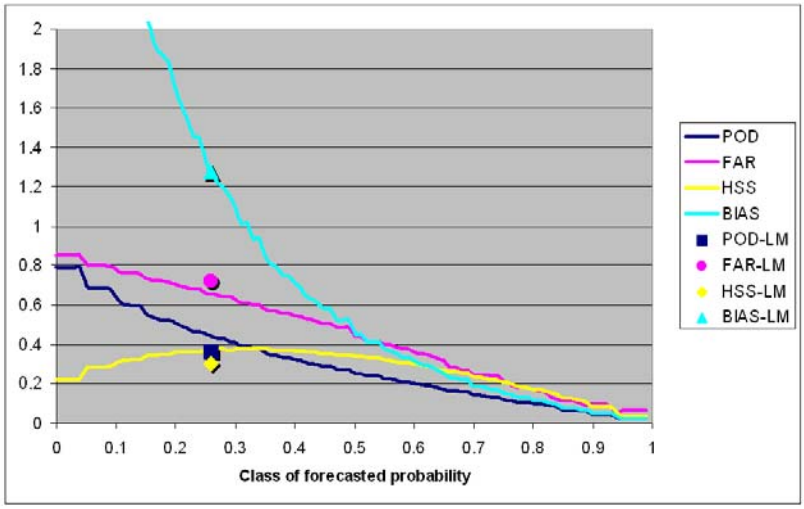

Figure 1. Example for 4 categorical scores of SRNWP-PEPS and LM for predicting a precipitation rate of 20mm/24hours. For verification station data of the DWD network in summer 2005 (April - September) are used.

100 classes of forecasted probabilities between 0 and 1. Since the LM only gives “probability” 0 or 1 for predicting a specific event, the comparability is applied to that PEPS’s class of probability where the biases of both forecasting systems are equal. In the case shown at Figure 1, PEPS outperforms the LM with higher POD and HSS and lower FAR.
Subjective evaluation was done by the operational forecast centre at DWD and a working group in terms of heavy precipitation, snowfall, wind gusts and maximum temperature. In case of precipitation PEPS ensemble median gives more consistent forecast compared to single models but an underestimation in rain amount in convective situations. On wind gusts an underestimation in convective cases and overestimation in non-convective cases was observed.

4. CONCLUSIONS

The main goal of the project has been the evaluation of PEPS to decide whether it provides a significant support and improvement of the warning process. A first verification shows good performance in comparison to the operational model LM of DWD. However, these simple PEPS forecasts are biased and uncalibrated. As a next step we plan the calibration of the ensemble using the Bayesian Model Averaging method by Raftery et al. (2005).

Acknowledgements: *Many thanks go to the director of the EUMETNET SRNWP Programme Jean Quiby*

REFERENCES

Raftery, A., T. Gneiting, F. Balabdaoui, and M. Polakowski, 2005: Using Bayesian Model Averaging to Calibrate Forecast Ensembles. Monthly Weather Review **133** , 1155-1174.

COMBINATION AND CALIBRATION OF AN IDEALIZED MULTI-MODEL ENSEMBLE

Christine Johnson

Met Office, Exeter, UK
E-mail: *christine.johnson@metoffice.gov.uk*

Abstract: Idealized experiments, based on the Lorenz 1963 model with time-dependent errors, are used to evaluate the benefits of a multi-model ensemble. It is shown that bias correction is only successful at correcting errors at short lead times, because flow-dependent errors are dominant at long lead times. A simple combination of forecasts improves the ensemble-resolution and the model-dependent weights give further improvements in the reliability, with all three weight-estimation methods tested here performing equally well.

Keywords – *Bayesian model averaging, bias-correction, multiple-regression, reliability, resolution*

1. INTRODUCTION

The aim of ensemble forecasting is to give a range of the possible outcomes by producing many forecasts based on different initial conditions and different forecast models. In some situations, the forecasts might cluster together, giving high probabilities, whereas in other situations the forecasts might diverge, giving low probabilities. In a typical operational ensemble, the forecasts are produced from perturbed initial conditions with the same forecast model. This often means that the model error is not accounted for properly and hence the ensemble spread is too small at long lead times and the ensemble-mean is biased. These biases can be corrected for using ensemble calibration, where the forecasts are adjusted towards a reference dataset, but a better method would be to use both different forecast models and different analyses to generate the ensemble.

Projects such as the THORPEX Interactive Grand Global Ensemble (TIGGE) have recently allowed access to two-week ensemble forecasts from a variety of operational models. A key question is whether model combination can bring further improvements in comparison to a calibrated single-model ensemble. The Met Office is currently developing a 15-day multi-model ensemble and associated products for research purposes, based on the TIGGE data archive (Swinbank, 2006). In preparation, the question is addressed here using the 3-variable Lorenz 1963 model (Lorenz, 1963). This model exhibits the chaotic behaviour that results in the rapid growth of errors and a dimensional scaling is applied so that the fast timescale is similar to a synoptic timescale of 5 days. Two forecast models are defined by adding seasonal bias terms that have a sinusoidal variation with time. This means that the forecast models exhibit different levels of skill in different seasons. To simulate reality, we produce 8-member, 15-day ensemble forecasts for each model, every 12 hours. A moving-window of forecasts from the previous 50-days is used to define the calibration and combination parameters. For a fair comparison, the multi-model ensembles have the same number of members as the single-model ensembles.

2. CALIBRATION

We first examine the improvement resulting from the calibration of a single-model ensemble. Bias-correction is applied to the ensemble mean using linear-regression, so that the ensemble-mean is closer to the true state over the previous 50 days and the scaling-factor for the ensemble-perturbations is adjusted so that the ensemble-variance is closer to the ensemble-mean root-mean-square-error (RMSE). This calibration is successful in correcting the overall ensemble biases, as shown by the rank histograms. However, it is not always successful in reducing the RMSE of the ensemble-mean.

At short lead times, the bias coefficients show slow variations associated with the sinusoidal seasonal biases applied to the forecast models. This means that the calibration window is able to obtain a good estimate for the bias coefficients and hence is able to reduce the RMSE. At longer lead times, the bias coefficients show rapid fluctuations, resulting from rapid changes in the initial conditions. These fluctuations mean that the calibration window does not give an accurate bias and hence the method is unable to reduce the RMSE.

The RMSE at long lead times can be reduced if the calibration data is based on a moving-window of forecasts that are centred over the calibration time; however, this would not be possible in a real system.

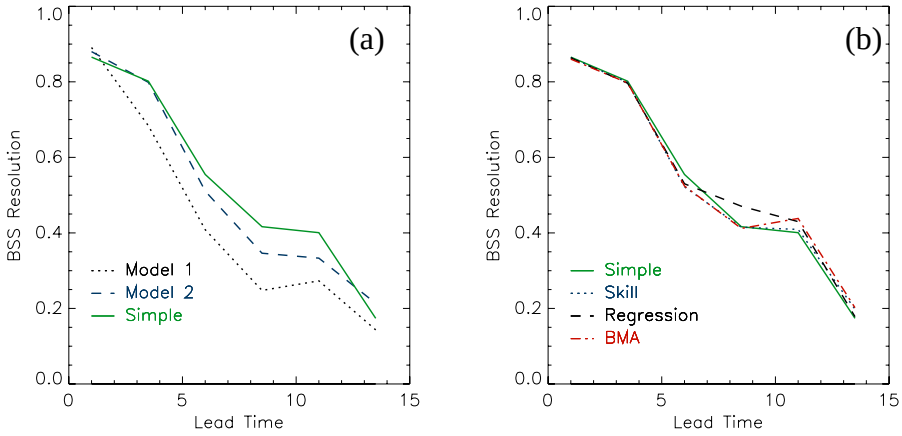

Figure 1. Resolution components of the Brier skill score. In (a) the single model ensembles are compared with a simple multi-model ensemble, and in (b) different weight estimation methods are compared with the simple combination.

3. COMBINATION

We now examine the further improvement brought by the simple combination of the two models, and then by a more complicated combination in which the models are given different weights that are a function of both lead time and verification time.

To combine the ensembles, it is assumed that the multi-model probability distribution function (pdf) is given by a linear combination of the pdfs from the single-models. This means that the multi-model ensemble mean and probabilities are linear combinations of the single-model ensemble means and probabilities respectively. The single-model ensemble means are first bias-corrected, the ensembles are then combined and finally the multi-model ensemble variance is adjusted.

With a simple combination (equal weight is given to each model) there is a decrease in the RMSE and an improvement in the resolution component of the Brier skill score (Fig.1a), with the improvement being mainly at the longer lead times. This improvement in probabilities, gained from averaging ensembles, can be understood as being similar to the improvement in a single-forecast gained from averaging forecasts (i.e. the ensemble-mean compared to a deterministic forecast).

Three different methods are used to calculate the optimal weights. The skill-based method calculates weights based on the ensemble mean RMSE, the multiple-regression methods performs the bias-correction and weight-estimation simultaneously, and the Bayesian model averaging (BMA) method treats the problem as a mixture density problem and finds the maximum likelihood estimate using the EM algorithm.

The results show that there is little change in the RMSE of the ensemble mean, or the ensemble resolution (Fig. 1b). However, there is an improvement in the reliability component of the Brier skill score because the multi-model ensemble draws closer to the most reliable model. The weights estimated by each method are very similar, making it difficult to identify the best weight estimation method. However, the BMA method is the only method to give an improvement in the reliability at all lead times.

4. CONCLUSION

We have shown that although calibration can give some improvements in ensemble forecasts, it is difficult to correct the errors at long lead times because they are dominated by flow-dependent errors. More significant improvements at long lead times can be achieved using a simple combination of ensembles from different forecast models and further slight improvements can be made by using a sophisticated combination of models, by giving the models different weights. The three very different methods to compute the model-dependent weights actually give similar estimates for the weights and hence there does not seem to be much value gained from the more complicated methods.

REFERENCES

Lorenz, E.N., 1963: Deterministic non-periodic flow. J. Atmos. Sci., **20**, 130-141.
Swinbank, R., 2006: Medium-range ensembles at the Met Office, these proceedings.

CAN MULTI-MODEL COMBINATION REALLY ENHANCE PREDICTIVE SKILL OF PROBABILISTIC ENSEMBLE FORECASTS ?

Andreas P. Weigel, Mark A. Liniger and Christof Appenzeller

Federal Office of Meteorology and Climatology (MeteoSwiss), Zurich, Switzerland
Email: andreas.weigel@meteoswiss.ch

Abstract: A simple synthetic probabilistic climate toy model is used to identify the conditions under which multi-model combination can enhance prediction skill. It is found that an improvement of skill through a multi-model approach strongly depends on the reliability of the involved models, in particular on their overconfidence. Results are extended to global seasonal forecast runs using data from the DEMETER project.

Keywords – *DEMETER, Overconfidence, Reliability, Seasonal predictions, Toy model*

1. MOTIVATION

Probabilistic forecasts with ensemble prediction systems have found a wide range of applications in weather and climate risk management, and their importance grows continuously. While "classical" ensembles account for the uncertainties in initial conditions, the uncertainties due to model formulation can be considered in a pragmatic way by combining single model ensembles (SMEs) to a multi-model ensemble (MME). It has been shown that forecasts issued on the basis of such MMEs outperform any single model strategy on average. Multi-model forecasts are even superior to a "best model approach", that is a strategy which for any given forecast context (location, predictand, start time, etc.) always selects the respective best single model available.

Given that a MME contains information of *all* participating models, including the less skillful ones, the question arises as to why, and under which conditions, a multi-model can have higher skill than a best model approach. In this contribution, we seek to resolve this supposed paradox by employing a synthetic toy model. The findings are then substantiated with a real multi-model seasonal forecasting system.

2. THE CLIMATE TOY MODEL

The probabilistic climate toy model is designed as a "forecast-observation pair" generator with following properties:

(i) Artificial "observations" x are randomly sampled from a normally distributed "climate".
(ii) The corresponding N-member "forecast" ensembles $\boldsymbol{f} = (f_1, f_2, ..., f_N)$ are generated such that they follow the same climatology as the verifying observations, i.e. the "model climatology" is perfectly calibrated.
(iii) *Physical predictability* is controlled by a model design parameter α, which is the average correlation coefficient between the forecast ensemble members and the observations.
(iv) The degree of *overconfidence* is controlled by a design parameter β. A value of ß=0 corresponds to perfect ensembles covering the entire range of uncertainty inherent to the system. With increasing β, the forecast ensembles become sharper but are more likely to be centered at the wrong value.

A "forecast generator" fulfilling these conditions is given by

$$\begin{pmatrix} f_1 \\ f_2 \\ \dots \\ f_N \end{pmatrix} = \alpha x + \epsilon_\beta + \begin{pmatrix} \epsilon_1 \\ \epsilon_2 \\ \dots \\ \epsilon_N \end{pmatrix} \quad \text{with} \quad \begin{aligned} x &\sim \mathcal{N}(\mu = 0, \sigma = 1) \\ \epsilon_\beta &\sim \mathcal{N}(\mu = 0, \sigma = \beta) \\ \epsilon_1, \epsilon_2, ..., \epsilon_N &\sim \mathcal{N}(\mu = 0, \sigma = \sqrt{1 - \alpha^2 - \beta^2}) \\ \alpha^2 &\leq 1 \quad , \qquad \beta^2 \leq 1 - \alpha^2 \quad . \end{aligned}$$

3. COMBINATION EXPERIMENTS

Using this toy model, we systematically evaluate how multi-model performance depends on α and ß. The procedure applied is as follows: Firstly, 100,000 observations are randomly sampled. Then the toy model is used to generate 100,000 corresponding SMEs (with ensemble size 9 and given α and ß). This is repeated n times,

representing the *n* independent SMEs that participate in the multi-model. MMEs are obtained by pooling together the sampled SMEs with each ensemble member having equal weight. As a verification measure, the debiased ranked probability skill score $RPSS_D$ (Müller et al. 2005, Weigel et al. 2006,2007) is employed with three equiprobable categories. The skill has then been evaluated for a varying number of models being either overconfident or not (Fig. 1). **Multi-model combination can indeed enhance prediction skill, but only if the SMEs are highly overconfident.** The reason for the improvement is that the $RPSS_D$ penalizes overconfidence (as a probabilistic skill score should). By combining multiple overconfident models, the net overconfidence of the MME decreases, thus reducing the "penalty" and increasing skill.

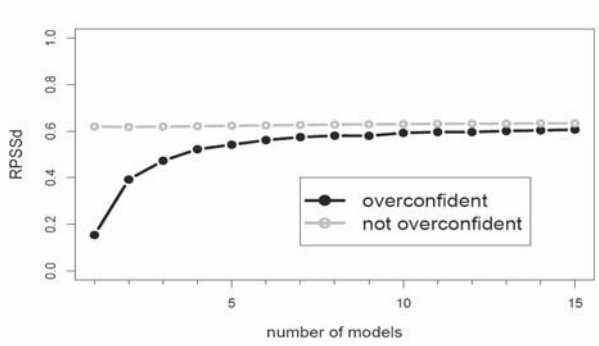

These findings are now compared with results from real dynamical ensemble forecast systems. Mean near surface temperature summer predictions of two seasonal prediction models (ECMWF and Met Office from the DEMETER database, Palmer et al. 2004) are considered, and the parameters α and ß are estimated for both models at each gridpoint. The regions where both models are highly overconfident ($ß \geq 0.7$) correspond quite consistenly to those regions where model-combination (applying the method of Rajagoplan et al. 2002) yields higher skill than any of the participating models alone (Fig. 2). This supports the conclusion drawn above: While multi-model combinations cannot remedy deficiencies in physical skill (i.e. low α), they improve deficiencies in ensemble spread (i.e. overconfidence is reduced).

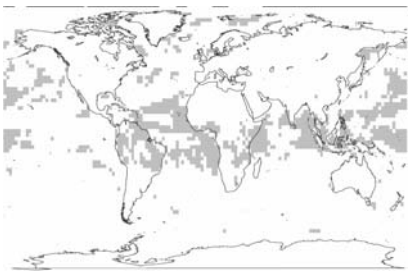

Figure 2: *Combination of two DEMETER models. The grey pixels show (a) where both models are highly overconfident with $ß \geq 0.7$, and (b) where model combination truly enhances skill.*

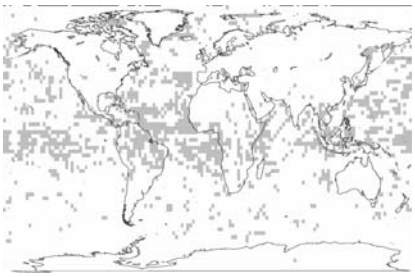

Acknowledgements: *This study was supported by the Swiss National Science Foundation through the National Centre for Competence in Research (NCCR) Climate.*

REFERENCES

Rajagopalan B., U. Lall and S. E. Zebiak, 2002. Categorical climate forecasts through regularization and optimal combination of multiple GCM ensembles. *Mon Wea Rev* **130**, 1792-1811

Müller W.A., C. Appenzeller and C. Schär, 2004. A debiased ranked probability skill score to evaluate probabilistic ensemble forecasts with small ensemble sizes. *J Clim* **18**, 1513-1523

Palmer T.N. and co-authors, 2004. Development of a European multimodel ensemble system for seasonal-to-interannual prediction (DEMETER). *Bull. Americ. Meteor. Soc.,* **85**, 853-872

Weigel A.P., M.A. Liniger and C. Appenzeller, 2006. The discrete Brier and ranked probability skill scores. *Mon Wea Rev* (in press)

Weigel A.P., M.A. Liniger and C. Appenzeller, 2007. Generalization of the discrete Brier and ranked probability skill scores for weighted multi-model ensemble forecasts. *Mon Wea Rev* (accepted)

THE DEVELOPMENT OF FEATURE-BASED DIAGNOSTICS TO ASSESS TIGGE HANDLING OF HIGH-IMPACT EXTRA-TROPICAL CYCLONES

Helen Watkin[1] and Tim Hewson

[1] Met Office, FitzRoy Road, Exeter, EX1 3PB, U.K.
E-mail: *helen.watkin@metoffice.gov.uk*

Abstract: The Cyclone Database uses model fields to objectively identify fronts and cyclonic features, and is ideally suited to analysing output from a multitude of ensemble members, where manual post-processing is too costly in terms of resource and time. Tracking and matching schemes have been implemented, allowing the production of feature-based diagnostics, which are currently being used as a real-time forecasting tool. The handling of high-impact extra-tropical cyclones by each TIGGE model will also be assessed via this method, thereby providing insight into the benefit of the multi-model approach.

Keywords – *THORPEX, TIGGE, high-impact weather, feature-based diagnostics, extra-tropical cyclones*

1. INTRODUCTION

As part of THORPEX, the Met Office is developing high-impact weather diagnostics for use on the multi-model ensemble known as TIGGE (THORPEX Interactive Grand Global Ensemble). The lower resolution of ensemble forecasts means that many types of high-impact weather are not fully resolved. This encourages the use of a feature-based approach, whereby feature development and attributes, after post-processing, can be interpreted in the context of potential high-impact events, alongside the traditional parameter-based diagnostics. This paper describes one such feature-based tool for use with extra-tropical cyclones: the 'Cyclone Database'.

2. CYCLONE DATABASE METHODS AND PRODUCTS

Historically, cyclones have been identified using mean sea level pressure minima or low level vorticity maxima. Unfortunately, using pressure minima, extreme storms of small geographical intent are often recognised very late. Conversely vorticity maxima can often be displaced from the true cyclonic centre. The Cyclone Database uses alternative objective techniques, which replicate synoptic practice and relate closely to conceptual models of cyclone development. Fronts are identified objectively as 'lines, adjacent to a baroclinic zone, across which the magnitude of thermal gradient changes most abruptly'. 'Frontal waves' and 'diminutive waves' are then identified on these fronts using the vorticity of the cross-front wind, to focus on frontal buckling. A third (non-frontal) type, called here a 'barotropic low', completes the cyclonic feature set. See Hewson (1997) for details of the defining equations. Figure 1a provides an example of the identified fronts and features. The other output is the 'database' itself, which contains a wide range of feature-point attributes.

The tracking scheme is based on the Terry and Atlas (1996) algorithm, with several adaptations utilising the cyclone attributes to facilitate more reliable association. A combination of extrapolation and the 500hPa steering wind vector is first used to estimate future position. Then, from all nearby 'candidate centres', the optimum one for each track is selected using a combination of 1) distance from estimated position, 2) feature-typing, and 3) 1000-500hPa thickness. A similar method is used to cross-reference features across members. These developments have facilitated the creation of storm track diagnostics. At shorter forecast ranges, interactive clickable maps allow the user to select a feature, bringing up feature-specific plumes of intensity measures with coincident maps of track locations. At longer forecast ranges, storm track strike probability maps show the number of members predicting a cyclonic feature of a set severity to track within 300km in a certain period.

3. CASE STUDY

Figure 1 illustrates use of the cyclone database products in a high-impact weather case study: the development of a frontal wave (situated off the New England coast at 00Z on 9th Jan 2005). By 00Z on 12th this low had rapidly deepened to 945mb and was just off Northern Scotland, resulting in heavy persistent rain and hurricane force winds over Northern Scotland, causing major disruption. Figure 1a shows the control T+0 image. Clicking, within a browser, on the key frontal wave would bring up plots 1b-e showing how the ECMWF EPS members are predicting it to develop. There is an interesting bifurcation of the tracks and the feature-specific plumes, but there is a cluster of tracks lending good support to the actual outcome (overlain in black), for both track and intensity. The maximum wind strength at 1km within a 300km radius (e) is a proxy for the maximum gust strength likely within the low's circulation, in relatively unstable air. Plumes of 300mb jet speed are also produced (not shown) and can be used to infer, empirically, an approximate maximum achievable surface gust.

As these parameters typically exhibit less bias than 10m wind, they are one way in which the feature-based approach is able to address some of the deficiencies of the lower resolution ensemble models, and provide useful information on the potential of a feature to cause high-impact weather.

The products are now available to Met Office forecasters in real time using input from the new Met Office 15-day ensemble (see Swinbank in this volume). Further studies of how the TIGGE multi-model ensemble and its component models handled recent cases of high-impact extra-topical cyclones are in progress.

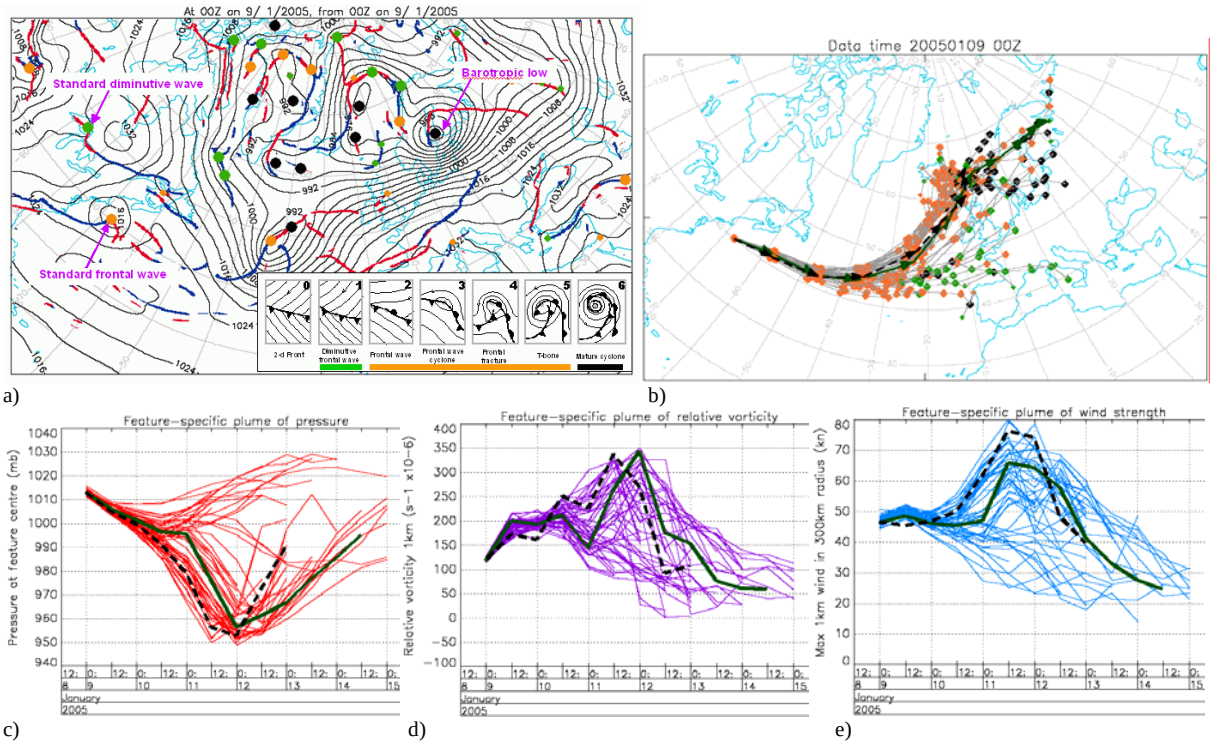

Figure 1. Example case study using the Cyclone Database on ECMWF EPS data from 00Z 09/01/2005: a) Control T+0 image of objectively identified fronts and cyclonic features. The key frontal wave is off the New England coast; b) Forecast tracks from each ensemble member; c/d/e) Associated feature-specific plumes of intensity (control=thick, analysis=dashed).

4. OTHER HIGH-IMPACT WEATHER DIAGNOSTICS

The Met Office are also developing other high-impact weather diagnostics for use on the TIGGE multi-model ensemble. Continuing the feature-based approach, forecast tracks of tropical cyclones are being produced. Additionally, a new diagnostic, intended to highlight changes in synoptic regime, classifies forecast circulation types based on an objective 'Grosswetterlagen' method (James, 2006). Parameter-based products also continue to be developed for use alongside feature-based tools, showing, for example, the risk of persistent wet, dry, hot and cold spells over the 15-day TIGGE forecast range.

5. CONCLUSION

Carefully tailored post-processing is imperative for the successful utilisation of the vast quantities of data involved in the TIGGE multi-model ensemble. The work to develop feature-based diagnostics using ensemble data will add an extra dimension to the evaluation of TIGGE performance for high-impact weather. It is also providing new and valuable forecasting tools. On a wider scale, it is hoped that international collaboration through the THORPEX programme could lead to these techniques becoming widely adopted as tools for forecasting high-impact weather across the globe.

REFERENCES

Hewson, T.D., 1997: Objective identification of frontal wave cyclones. Meteorological Applications, **4**, 311-5

James, P.M., 2006: An objective classification method for Hess and Brezowsky Grosswetterlagen over Europe. Theoretical and Applied Climatology. In print.

Terry, J. and R. Atlas, 1996: Objective cyclone tracking and its applications to ERS-1 scatterometer forecast impact studies. In Proceedings of 15th Conference on Weather Analysis and Forecasting Conference, American Meteorological Society.

EVALUATING THE IMPACT OF MODEL PHYSICS CHANGES ON MET OFFICE THORPEX FORECASTS

Nicholas Savage [1], Sean Milton[1], David Walters[1], Julian Heming[1]

[1] Global Model Development and Diagnostics, Met Office, Exeter, UK
E-mail: *nicholas.savage@metoffice.gov.uk*

Abstract: A set of improvements to the Unified Model physical parameterisations have been tested in a series of 15 day deterministic forecasts. Major improvements are found in Northern Hemisphere winter surface temperatures and tropical circulation, precipitation and humidity.

Keywords – *TIGGE, model evaluation*

1. INTRODUCTION

As part of the THORPEX Interactive Grand Global Ensemble (TIGGE) the Met Office is running the global Unified Model out to 15 days as a 24 member ensemble twice a day. The aim is to provide early warning of high impact weather on the global scale as part of the TIGGE multi-model ensemble. Important properties of a global model for THORPEX is that it maintains a realistic level of variability out to 15 days ahead and that model error growth is minimised. For an overview of medium range ensemble forecasting at the Met Office see Swinbank (2006). In this study we evaluate the systematic (model) error growth in the Met Office THORPEX forecasts for the current configuration. In March 2006 a new physics package was introduced into the operational 5-day global NWP forecasts. This included changes to the convective and boundary layer parameterisations intended to improve tropical performance. The impact of this physics package on the 15-day THORPEX forecasts has been evaluated and results are presented here.

2. UNIFIED MODEL CONFIGURATIONS AND EXPERIMENTS

The model used for this study is the UK Met Office Unified Model (UM) with a non-hydrostatic, fully compressible, deep atmosphere dynamical core with semi-implicit semi-Lagrangian time integration (Davies et al, 2005). All these model runs used a horizontal resolution of N144 (1.25° longitude by 0.83° latitude) with 38 levels in the vertical from the surface to 38 km which is the same as that used by the 15 day Ensemble Prediction System currently being run. The physical formulation used as a control is closely based on the atmospheric part of the coupled climate configuration HadGEM1 (described in Martin et al, 2005) and has only minor differences with the 15 day version of the Met Office Global and Regional Ensemble Prediction System currently being run.

A package of improvements to model physics in the global operational version of the UM were introduced on the 14th March 2005. The principal aims of the package were to improve the tropical performance of the UM and in particular to reduce errors in: sea surface evaporation; precipitation over the sea; boundary layer winds over the sea and the vertical profiles of temperature and humidity. For more details of the changes to model physics and their impact on the short range forecasts see Willett (2006). In addition the new model formulation also had a restructured convection scheme, changes to the CAPE closure formulation and values of sea surface temperature (SST), snow depth, soil moisture content, deep soil temperature and sea ice.

20 deterministic forecasts of 15 days length have been performed with both model versions and the results evaluated against UM operational analysis, surface and sonde data plus Global Precipitation Climatology Project data. The 20 cases were chosen to be non overlapping to give a degree of synoptic independence with 10 Cases from Northern Hemisphere Summer and 10 from NH Winter. The initial analyses used were produced with the operational variational data assimilation system (3D Var before 10/2004 and 4D Var thereafter).

3. RESULTS

Overall the model performance was significantly improved by the revised physics package and the other changes. We find a much reduced NH winter near surface cold bias (the initial runs had a bias of -8K whereas in the new configuration this is close to zero) possibly as a result of increased cloudiness. In the tropics at 250hPa the cold bias is also reduced from -1K to near zero and there are beneficial changes in zonal wind speeds in response to these improvements in the temperatures via thermal wind balance. We also see a reduced dry bias (from over -12% to -8%) in the tropical upper troposphere, and large reduction of errors in tropical circulation due to an improved treatment of convective detrainment. In particular, the anomaly in the Indian Ocean (with a

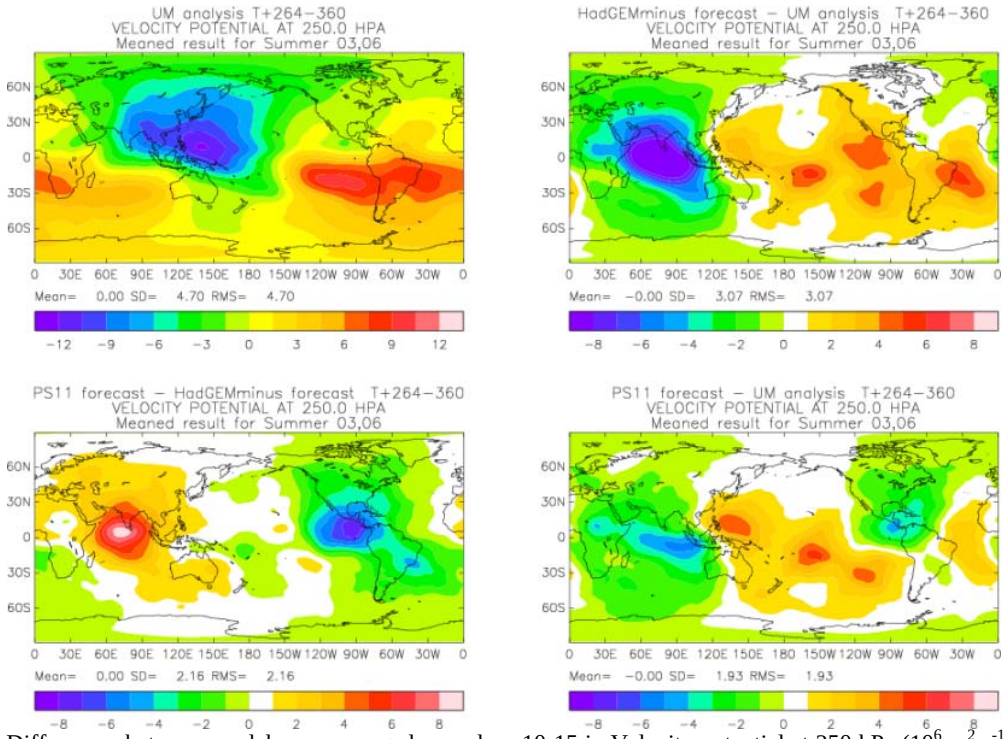

Figure 1. Differences between model runs averaged over days 10-15 in Velocity potential at 250 hPa (10^6 m^2 s^{-1}, divergent winds point from negative to positive velocity potential.) Top left: mean velocity potential in UM analyses from days 10-15 of forecasts. Top right: control (HadGEMminus) forecast minus analysis. Bottom left: new physics forecast (PS11) minus control. Bottom right: new physics minus analysis. The new model configuration shows a large reduction in the divergent anomaly over the Indian Ocean.

low level convergent bias and an upper level divergent anomaly indicating too much ascent in this region) is much reduced (see Figure 1).

Connected with this improved circulation in the Indian Ocean is a reduction in precipitation over the Indian Ocean giving better agreement with GPCP data. Although the revised model still does not do a very good job of representing the precipitation patterns associated with the Madden-Julian Oscillation it does weaken significantly spurious westward propagating disturbances seen in the control. The new physics however does cause some detriments: in particular the summer warm bias over Asia and North American is made worse and a positive precipitation bias over Africa and the north of South America is worsened. Both these issues are also found with the operational model and work is ongoing to resolve them via modifications to cloud cover over land.

4. CONCLUSIONS

We have shown that the physics package introduced to the operational version of the Unified Model in spring 2006 gives significant improvements in model performance in most regions. We now plan to implement these changes in the ensemble prediction system. Work is ongoing to evaluate the stochastic physics used in the 15 day ensemble prediction system and to test potential improvements to model performance from the use of time evolving SSTs and the implementation of a prognostic dust parameterisation. In the longer term we plan to investigate the effects of coupled modelling on the predictability of the MJO and other aspects of intraseasonal variability.

REFERENCES

Davies, T., M.J.P. Cullen, A.J.P. Malcom, M.H.Mawson, A. Staniforth, A.A. White, and N. Wood, 2005, A new dynamical core for the Met Office's global and regional modelling of the atmosphere. Q. J. R. Meteorol. Soc., **131**, 1759 - 1782.

Martin, G.M., M.A. Ringer, V.D. Pope, A. Jones, C. Dearden, and Hinton, T.J., 2005, The physical properties of the atmosphere in the new Hadley Centre Global Environmental Model (HadGEM1). Part I: Model description and global climatology, J. Climate, **19,** 1274-1301.

Swinbank, R., 2006: Medium-range ensemble forecasts at the Met Office, this volume.

Willett M., 2006: Unified Model has improved physics, NWP Gazette, June 2006, http://www.metoffice.gov.uk/research/nwp/publications/nwp_gazette/jun06/um_imp_phys.html.

SHORT-RANGE QPF AND PQPF USING TIME-PHASED MULTI-MODEL ENSEMBLES

Chungu Lu, John McGinley, Paul Schultz, Huiling Yuan, Linda Wharton, and Chris Anderson

NOAA Earth System Research Laboratory, Boulder, CO, USA Email: chungu.lu@noaa.gov

Abstract: A time-phased multi-model ensemble forecast system is investigated for short-range quantitative precipitation forecast (QPF) and probability QPF (PQPF). One of the advantages of such an ensemble forecast system is its low-cost generation of ensemble members. The combined use of this ensemble system and a frequently-cycling data-assimilation system with a diabatic initialization (such as NOAA-LAPS) makes up a particularly appealing approach for the application of the QPF and PQPF.

Keywords- *Short-range QPF, PQPF, ensemble forecasting, LAPS*

1. INTRODUCTION

Short-range (0 –24h) quantitative precipitation forecasting (QPF) is very important to flash flood warning, transportation management (including aviation and highway decision making), and fire weather forecasting. However, hydrological forecasts, such as river flow forecasts, so far, still rely very much on medium-range (3 days-2 weeks), global model QPF and precipitation climatology as the atmospheric inputs.

In this study, a time-phased multi-model ensemble forecast system is proposed for short-range quantitative precipitation forecast (QPF) and probability QPF (PQPF). One of the advantages of such an ensemble forecast system is its low-cost generation of ensemble members. The combined use of this ensemble system and a frequently-cycling data-assimilation system with a diabatic initialization (such as NOAA-LAPS) makes up a particularly appealing approach for the application of the QPF and PQPF.

Through a case study, the usefulness of this ensemble forecast system is demonstrated. In particular, the ensemble PQPF provides a much superior performance over both deterministic forecast and ensemble-mean QPF. Statistical verifications of QPF and PQPF from this ensemble system are conducted with a sample of observational data, which show that the QPF possesses some positive skill, but PQPF has substantial skill in comparison with the deterministic forecasts. This result stresses the importance of constructing PQPF using an ensemble system, because the ensemble mean often poses a too severe filter (over smoothing) for QPF, which provides only marginal gain in precipitation forecast skill.

2. TIME-PHASED MULTI-MODEL ENSEMBLES

The time-phased ensemble forecast system utilizes a frequently-updating data-assimilation/forecast system to generate a family of ensemble forecasts. By post-processing this set of deterministic forecasts generated by the model from initializations at different analysis times, one could obtain both probabilistic and ensemble-mean forecasts. This ensemble forecast system could be considered as an ensemble system with a set of perturbed initial conditions. Whenever the forecast model is run, a forecast for a particular projection time is generated. At the next cycle, a second forecast for this particular time is generated as well, and this process is repeated. Each cycle generates a new forecast. No additional cost is incurred for the generation of ensemble members during this process. Therefore, the time-phasing a set of forecasts provides an efficient and economical way to obtain ensemble samples.

It can be expected that the older the forecast, the larger the error contributed by that member. Therefore, to include forecasts many hours old may bring about a negative impact on the verification of the ensemble forecast. On the other hand, ensemble forecasting needs a set of very diversified model solutions (sometimes with large errors) to help broaden the statistical sample domain to have a better chance of capturing the true solution. In this study, forecasts from 1 to 12 hours old are used as valid candidates. This may limit the number of ensemble members (12 members for an hourly initialization forecast system). However, the time-phased ensemble can be enhanced by including additional models. Such a mixture gives rise to the concept of a time-phased multi-model ensemble system, which not only helps for the increase of ensemble size, but also enhances the diversity of the ensemble members. Figure 1 shows schematically the time-phased ensembles with a combination of the WRF and MM5 models (in practice, there could be more models used for this purpose

3. ENSEMBLE QPF

In Figure 2, the time-phased multi-model ensemble mean QPF was plotted at 1800 UTC, 2100 UTC, 0000 UTC, and 0300 UTC on 10-11 April 2005 (Fig. 2a-d), respectively. To compare these model forecast QPFs with the observed ones, we also plot rainfall distributions from the stage IV dataset side-by-side for the same corresponding times and same domains (Fig. 2e-h). From the figures, one can see that the ensemble-mean QPFs do give approximately the right shapes and areas of precipitation. However, it is also quite clear that the ensemble-mean QPF inflates the precipitation coverage area and at the same time smoothes out the areas with

significant rainfall amounts. Areas with precipitation amounts larger than 6.35 mm (0.25 in) are all absent from the ensemble-mean prediction.

4. ENSEMBLE PQPF

The 24 time-phased multi-model ensemble members provide a good statistical sample for computing the probability of QPF. Shown in Fig. 3a-d is the set of probabilities of precipitation (POP) for the four different thresholds: 0.254, 2.54, 6.35, and 12.70 mm/hr (corresponding to 0.01, 0.1, 0.25, and 0.5 in/hr) at 1800 UTC 11 April 2005

From Figs. 3a-3d, not surprisingly, one can see that for a given precipitation threshold, the rainfall area decreases with the increase of the probability. For example in Fig. 3b, compare the area covered by the 10% contour for 2.54 mm with the 50% contour for the same amount. On the other hand, for a given probability, the coverage area for precipitation decreases with the increase of precipitation threshold, as one goes from Fig. 3a to 3b, 3c, and 3d. In contrast to the ensemble mean QPF, the PQPF does preserve minority members' opinions for a possible high precipitation event. For example, there were two areas in northeast Nebraska with 10% probability (about 2-3 members' forecasts) of potentially very high precipitation (> 12.70 mm/hr), while in the ensemble mean case, these 2-3 members were completely dominated by the other 21-22 members, so that this potential threat area was eliminated (see Fig. 2d: no any area had precipitation > 12.70 mm/hr).

5. CONCLUSIONS

Short-range QPF and PQPF were investigated through an application of the time-phased multi-model ensembles for a precipitation episode associated with a classic synoptic weather system. Both the ensemble-mean QPF and PQPF presented approximately right shape, orientation, and location of the rainfall. However, the ensemble-mean QPF over-forecasted the rainfall coverage areas, and at the same time, smoothed out the higher categories of rainfall amount. On the other hand, the ensemble PQPF had a better handle on the both of these problems.

Acknowledgments: We would like to thank Drs. Alexander MacDonald and Steven Koch for discussions on the subject. This research is funded by the NOAA Office of Oceanic and Atmospheric Research. The views expressed are those of the authors and do not necessarily represent the official policy or position of NOAA.

REFERENCES

Lu, C., J. McGinley, P. Schultz, H. Yuan, B. Jamison, L. Wharton, and C. Anderson, 2006: Short-range forecast using time-lagged ensembles. *J. Hydrometeorology*, in review.

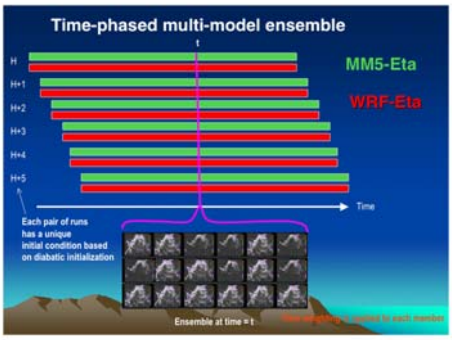

Fig. 1: Conceptual diagram for time-phased multi-model ensemble forecast system.

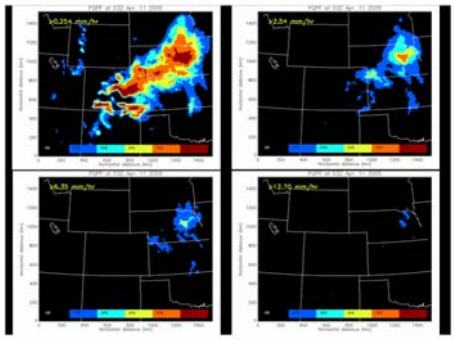

Fig. 3: Ensemble PQPF.

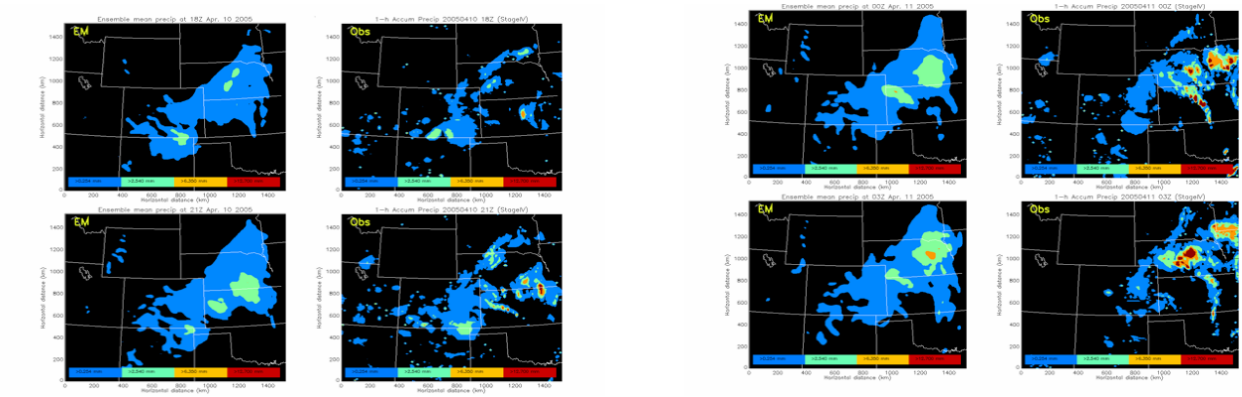

Fig. 2: Ensemble-mean QPF (left column) and Stage IV observations (right column) for a) 1800 UTC, b) 2100 UTC, c) 0000 UTC, and d) 0300 UTC 10-11 April 2005.

ON SOME ASPECTS OF THE DEFINITION OF INITIAL CONDITIONS FOR PROBABILISTIC PREDICTION

Laurent Descamps [1], Olivier Talagrand [1]
[1] Laboratoire de Météorologie Dynamique (IPSL), ENS, Paris, France
E-mail: *descamps@lmd.ens.fr*

Abstract: Various methods for initialization of ensemble forecasts are systematically compared, namely the method of Singular Vectors (SV), the method of Bred Modes (BM), the Ensemble Kalman Filter (EnKF), the Perturbed Observations method (PO) and the Ensemble Transform Kalman Filter (ETKF). The comparison is done on synthetic data with three models of the flow, *viz*. a low-order model introduced by Lorenz, a three-level quasi-geostrophic atmospheric model (for which a perfect and an imperfect model situations are considered) and the operational NWP model ARPEGE of Météo-France. The performance of the various initialization methods is assessed in terms of the statistical reliability and resolution of the ensuing ensemble predictions. The relative performance of the four methods, is in the order EnKF ~ PO > ETKF > BM > SV. In the case of the SV method, the need for obtaining realistic ensemble spread at medium range imposes unrealistic small initial perturbations, which results in significant underdispersion of the ensembles in the growing phase of the singular vectors. The general conclusion is that, if the quality of ensemble predictions is assessed by the degree to which the predicted ensembles statistically sample the uncertainty on the future state of the flow, the best initial ensembles are those that best statistically sample the uncertainty on the present state of the flow.

Keywords – *THORPEX, WMO, predictability, ensemble prediction.*

1. INTRODUCTION

Ensemble prediction, intended at providing probabilistic forecasts, has now become an established part of operational global weather prediction. One aspect of ensemble forecasting that is still actively debated is the best method for generating a set of initial conditions. Most of the works that compare the relative merits of the different approaches have been performed with relatively simple models: Anderson (1997), Hamill *et al*. (2000) (hereafter HM00) and Bowler (2006) globally found that classical 'dynamically constrained' methods (*i.e*. bred modes (BM) and singular vectors (SV)) produce less skillful ensembles than unconstrained methods (*i.e* perturbed observation (PO), ensemble Kalman filter (EnKF), ensemble transform Kalman filter (ETKF)). In a recent comparison of the ensemble forecast systems of ECMWF, MSC and NCEP, Buizza *et al*. (2005) did not conclude as to the relative performance of the different initialization schemes as they could only measure the overall quality of the three systems. The present work is a further comparison of methods for initialization of ensemble forecasts using three different models of the flow: the low-order model of Lorenz (1995), the three-level quasigeostrophic atmospheric model developed by Marshall and Molteni (1993) and the operational NWP model ARPEGE of Météo-France. The compared performance of the different initialization methods is assessed by the quality of the ensuing ensemble predictions. That quality is measured by fundamentally the same scores that are used for the evaluation of operational EPSs.

2. EXPERIMENTAL SETUP

A reference or 'truth run', from which observations to be assimilated are extracted, and in comparison with which the quality of forecasts is assessed, is first produced. Most of experiments are 'perfect model' experiments in which the assimilations and forecasts are performed with the same version of the model used for producing the truth run. The observations to be assimilated are obtained by adding a random noise to values extracted from the truth run. The low-order model defined by Lorenz (1995) is governed by a system of m differential equations with cyclic boundary conditions (here m=40 is used). The quasigeostrophic model (hereafter QG) is spectral, with 3 vertical levels and triangular truncation T21. ARPEGE is a NWP spectral model used here with 41 vertical levels, triangular truncation T149 and the physical parametrisations as in its operational version. For the Lorenz and the QG models, N=30 ensemble members produced by the BM, SV, EnKF and ETKF methods are compared over a 10-day prediction period. For the ARPEGE model, N=15 ensemble members produced by the BM, SV and PO methods are compared over a 5-day prediction period. A number of experiments have been performed with the QG model in which model error is present. This has been achieved by producing the truth run at the higher resolution T81 (and still three levels), while still performing the assimilation and forecast at resolution T21.

3. RESULTS

For the various probabilistic scores used is this study (Brier score, rank histogram, reduced centered variable, ROC curves), unconstrained methods (EnKF, ETKF, PO) globally show better skill than either BM or SV. Figures (a) and (b) respectively show, for the ARPEGE experiments, the time evolution of the Brier score (negatively oriented) and the area under ROC curves (positively oriented) (both scores are computed on the 500-hPa geopotential height for an event that occurs with overall frequency 0.33). For the two scores, the observed advantage for the PO method is always statistically significant (according to a paired t-test (see HM00) at 99% level of confidence level). Other scores also show better results for the unconstrained methods (EnKF and ETKF for the QG and Lorenz models, PO method for ARPEGE), with significant differences mostly for the short and early medium range. It is important to note that results obtained with the ARPEGE model in a 'close to operational context' confirm those obtained with the Lorenz and QG models and the clear superiority of unconstrained approaches. The experiments performed with the with QG model that include 'model error' show that the overall relative performance of the four initialization methods is in the same order as in the case of no model error, but is statistically significant for a shorter period. Concerning the SV method, a set of experiments (with the QG and ARPEGE models) on the relative impact of the choice of the optimization period and of the initial amplitude of the perturbations show that reducing initial perturbations amplitude significantly improves the ensemble skill.

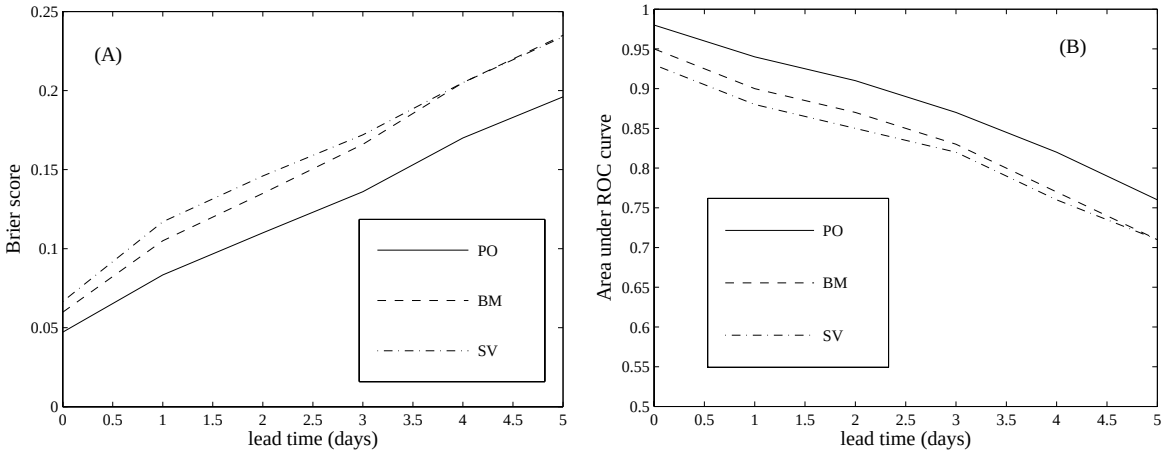

4. CONCLUSION

A systematic comparison has been performed of various methods for initialization of ensemble predictions. Two simple models and an operational NWP model have been used. Special care has been taken in order to make the comparison as clean as possible, so that the differences in the performance of the various predictions result only from differences in the initialization methods. The general conclusion is that if the quality of ensemble forecasts is assessed on the basis of how well the predicted ensembles sample the probability distribution of the future state of the flow, then the best initial ensembles are those that best sample the probability distribution of the initial state of the flow. Consideration of the instabilities that may develop over the forecast period is useless for the definition of the initial ensembles. These results confirm and extend to a more realistic context those that have already been obtained by several authors (Anderson, 1997, H00, Bowler, 2006).

REFERENCES

Anderson, J. L., 1997: Impact of dynamical constraints on the selection of initial conditions for ensemble predictions : low-order perfect model results. Mon. Wea. Rev., 125, 2969-2983.

Bowler, N., 2006: Comparison of error breeding, singular vectors, random perturbations and ensemble Kalman filter perturbation strategies on a simple model. Tellus, 58A, 538-548.

Buizza, R., P. Houtekamer, Z. Toth, G. Pellerin, M. Wei, and Y. Zhu, 2005: A comparison of the ECMWF, MSC, and NCEP global ensemble prediction system. Mon. Wea. Rev., 133, 1076- 1097.

Hamill, T. M., C. Snyder, and R. E. Morss, 2000: A comparison of probabilistic forecasts from bred, singular-vector, and perturbed observation ensembl es. Mon. Wea. Rev., 128, 1835-1851.

Lorenz,1995: Predictability: a problem partly solved. ECMWF Proceeding of workshop on predictability, volume 1, 1-18.

Marshall, J. and F. Molteni, 1993: Toward a dynamical understanding of planetary-scale flow regimes. J. Atmos. Sci., 50, 1792-1818.

ALADIN LIMITED AREA ENSEMBLE FORECASTING (LAEF)

Yong WANG[1], Alexander KANN[1], Xulin MA[2] , Weihong TIAN[2] and Wei WANG[3]

[1]Zentralanstalt für Meteorologie und Geodynamik (ZAMG), Hohe Warte 38, A-1190 Vienna, Austria
[2]CAMS, China Meteorological Adminstration, 46 Zhongguancun Nandajie, Beijing, China
[3]College of Enviromental Science and Engineering, Nankai University, 94 Weijinglu, Tianjing, China

1. Introduction

Scientific and computational limitations prevent us from constructing a perfect NWP model of real systems. Small errors in the initial condition, in the boundary conditions, in the model, e.g. physics and dynamics, can grow exponentially and eventually render a forecast useless. For dealing with those uncertainties, ALADIN regional EPS system LAEF (Limited Area Ensemble Forecasting) has been developed at ZAMG. Works have been focused on the initial condition perturbation, different methods, as Breeding, ETKF/ET (Ensemble Transform Kalman Filter /Ensemble Transform) have been compared. The impact of the uncertainty on the lateral boundary conditions, especially the impact of the inconsistency in the generation of ensemble lateral boundary conditions from global EPS system with the generation of the ensemble initial conditions from the limited area ensemble system itself, has been investigated.

2. ALADIN-LAEF and experiments

The ALADIN model used for LAEF is run in hydrostatic mode, with 18 km horizontal resolution, and 31 levels in the vertical. The model domain covers Europe and a large part of the North Atlantic. For dealing with the diverse uncertainties in the model and analysis, several experiments with LAEF have been carried out.

- *Initial condition perturbation with Breeding, ETKF and ET*

The Breeding method is used for constructing the initial perturbed conditions for LAEF. By Breeding (breeding of growing vectors), the perturbed initial conditions were generated in sets of positive and negative pairs around a control analysis. Our implementation of the breeding method has the following features: *a)* warm start, *b)* 12 hour cycle, *c)* two-side and centering around the control analysis, *d)* wind, temperature, moisture and surface pressure are perturbed at each level and model grid-point, *e)* 5 pairs, *f)* constant rescaling.

Another method ETKF has been also implemented in LAEF for constructing the initial perturbation. The ETKF analysis perturbations are achieved by postmultiplying the short-term ensemble forecast perturbations by a transformation matrix. For ETKF experiment, we used the fixed observation network, ca. 120 observation stations on three levels 850hPa, 500hPa and 250hPa. The interpolated ARPEGE analysis of wind and temperature as the observation, 12h cycle, 10 members. Same as in Breeding method, wind, temperature, moisture and surface pressure are perturbed at each level and grid-point. Since the ETKF analysis perturbation is not centered around the analysis, we applied a spherical simplex transformation for preserving perturbation is around the analysis.

Similar as ETKF, we have also implemented the ET for having the initial perturbation. The ET method has been proposed originally for the target observation studies.

- ***Lateral boundary condition perturbation***

For investigating the impact of the inconsistency in the generation of ensemble lateral boundary conditions from global EPS system with the generation of the ensemble initial conditions from the limited area ensemble system itself, experiments of ALADIN LAEF with perturbations of lateral boundary conditions from different global ensemble systems NCEP (with Breeding) and ARPEGE (with singular vector) superimposed on control lateral boundary conditions, e.g. from ARPEGE, has been done. The method of the initial conditions perturbation in LAEF was Breeding.

3. Results

To investigate the uncertainties in ALADIN, we have chosen a winter month (1-28 Feb. 2006) for all the experiment. 10 ensemble members were chosen for each experiment. In the following we will focus on the spread of the LAEF experiments.

3.1 Comparison: Breeding, ETKF and ET

A preliminary comparison of the spread of 850hPa temperature as a function of forecast time with using Breeding, ETKF and ET has been shown in Fig. 1. Those three methods show very similar performance. This is

likely due to ensemble size (10 members) is not large enough. Differences between the ET/ETKF and breeding are only likely to be significant as the ensemble size exceeds the number of directions in which breeding ensembles maintain variance.

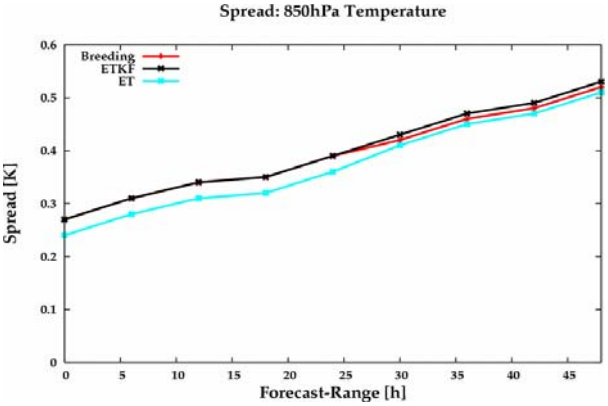

Figure 1. Comparison of the spreads of 850hPa temperature with using Breeding, ETKF and ET. All the experiments are with 10 members.

Based on the theory of ETKF, we expect that ETKF ensemble would maintain error variance in all amplifying normal modes, but the Breeding would only in the direction related to the most rapidly amplifying modes. To demonstrate this, we compute the mean spectra of eigenvalues of ensemble-based 12h forecast covariance matrices normalized by observation error covariance for the 10 member ETKF and the Breeding (not shown). It is found that the spectrum of ETKF eigenvalues is flatter than the norm from Breeding.

3.2 Impact of the inconsistent LBC perturbation with IC perturbation

Concerning the impact of mismatch between LBC perturbation from global EPS system and the IC perturbation from LAM model, we coupled LAEF with ARPEGE EPS system (with Sigular Vector) and NCEP EPS system (with Breeding). In LAEF the analysis perturbation is generated by Breeding. Fig. 2 show the impact of different coupling system. It is very clear that the performance of LAEF strongly depends on the ensemble diversity of the global EPS system. With Breeding in LAEF coupled with Breeding global EPS system brings more benefits to the one with SV EPS system.

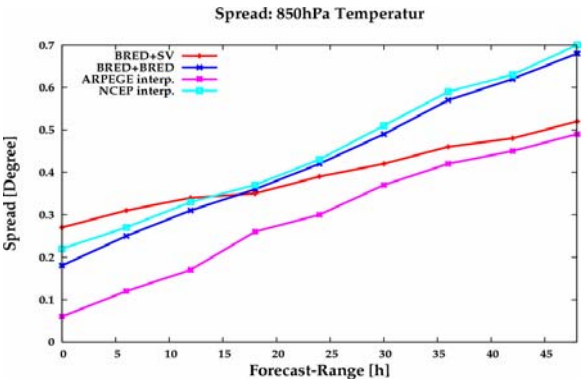

Figure 2. Comparison of the spreads of 850hPa Temperature 500hPa Geopotential, LAEF Breeding coupling with ARPEGE EPS (SV) and NCEP EPS (breeding), and the spread of ARPEGE and NCEP global systems.

4. Conclusions

We have carried out several experiments with our LAEF system, the focus was put on different aspects of the limited area model uncertainties, like initial condition perturbation, impact of the LBC on the performance of the LAM-EPS. All the experiments have been done with a winter month (1-28.02.06). The results can be summarized as follows:

a. ETKF with 10 members has very similar performance to Breeding. It is also true for ET perturbation. The reason is might be due to the small ensemble size.
b. LBC perturbation is very important for keeping diversity growing after 12h. LAMEPS coupling with different global model EPS has much impact on forecast. For the short range probabilistic forecast, it seems that LAMEPS coupling with global Breeding EPS has more benefit than with global SV EPS.

Acknowledgements

We gratefully acknowledge the colleagues E. Bazile, J. Nicolau (Meteo-France), J. Du, Z. Toth, M. Wei (NCEP), C. Bishop (NRL) and X. Wang (NOAA) for the discussions.

STOCHASTIC NATURE OF PHYSICAL PARAMETERIZATIONS IN ENSEMBLE PREDICTION: STOCHASTIC CONVECTION

Joao Teixeira[1,2] and Carolyn A. Reynolds[2]

[1] NATO Undersea Research Centre, La Spezia, Italy, [2] Naval Research Laboratory, Monterey, USA
E-mail: *teixeira@nurc.nato.int*

Abstract: In this paper it is argued that ensemble prediction systems can be devised in which physical parameterizations of sub-grid scale motions should be viewed and utilized in a stochastic manner, rather than in a deterministic way as it is typically done. This can be achieved within the context of current physical parameterization schemes in weather and climate prediction models. Parameterizations are typically used to predict the evolution of grid-mean quantities due to unresolved sub-grid scale processes. However, parameterizations can also provide estimates of higher moments that could be used to constrain the random determination of the future state of a certain variable. A simplified algorithm for a stochastic moist convection parameterization is proposed as a preliminary attempt. Results from the implementation of this stochastic convection scheme in the Navy Operational Global Atmospheric Prediction System (NOGAPS) ensemble are presented. It is shown that this method is able to generate substantial tropical perturbations that grow and "migrate" to the mid-latitudes as forecast time progresses, while moving from the small scales where the perturbations are forced to the larger synoptic scales. This stochastic convection method is able to produce substantial ensemble spread in the tropics when compared to results from ensembles created from initial-condition perturbations. Although smaller, there is still a sizeable impact of the stochastic convection method in terms of ensemble spread in the extra-tropics. Preliminary simulations with initial-condition and stochastic convection perturbations together in the same ensemble system show a promising increase in ensemble spread and decrease in the number of outliers in the tropics.

Keywords – *Stochastic parameterizations, ensemble prediction systems, moist convection*

1. INTRODUCTION

The main point of the present paper is to argue that, in terms of physical parameterizations, ensemble prediction could be viewed as fundamentally different from deterministic prediction. Ensemble systems can be devised in such a way that for each ensemble member there is no *a priori* reason to assume that the physical parameterizations should be providing the evolution of the grid-mean value of a variable. Each ensemble member does not have to represent the evolution of the mean variables and could be providing a probable value of such a variable. These randomly selected values should be constrained by the PDFs that are implicitly associated with a particular physical parameterization. Although a complete knowledge of such distributions is impossible, approximations using only the mean and the variance can often be fairly straightforward to obtain. In this context, the approach that is being proposed differs from previous studies on stochastic parameterizations in the sense that the PDFs that are used to constrain the random determination of the future states of a variable are based on the parameterization schemes themselves.

As a summary, the main rationale behind the methodology being suggested is that: E*nsemble prediction systems can be devised in which parameterizations should be utilized in a stochastic manner, which should be based on PDFs produced by the parameterizations.*

2. RESULTS

In this section results are shown that use the stochastic approach discussed above for the moist convection parameterization within the Navy Operational Global Atmospheric Prediction System (NOGAPS). The ensemble system is used in the following configuration: 32-member ensembles are run for 10 days at a T119L30 resolution, once a day for the month of May 2005. In some experiments, there are no initial-condition perturbations and the ensemble spread is based entirely on the stochastic convection forcing. In other experiments, initial perturbations are introduced based on randomly sampling the analysis error variance estimate produced by the NRL Atmospheric Variational Data Assimilation System.

Figure 1 shows the total energy difference between an ensemble member with stochastic convection and the control simulation with no stochastic convection, as a function of total wave number (out to T119) for the tropics (20 S to 20 N) and the Northern Hemisphere (NH) mid-latitudes (30 N to 70 N) for several forecast time ranges (from 12 to 240 hours), averaged for daily forecasts from May 2005. For the tropical case it appears that the total energy is starting to saturate after a few days on all but the largest scales. In contrast, for the mid-latitudes saturation of the small scales occurs later, while a distinct peak at the synoptic scales develops and continues to grow up to ten days. The reader should be reminded that the stochastic convection perturbations that are being

introduced are uncorrelated in space and time, and as such represent perturbations that occur at small spatial and temporal scales and only when the moist convection parameterization is being triggered. These plots illustrate the significant transfer of perturbation energy to larger scales as the forecasts proceed, especially in the extra-tropics.

One of the more practical motivations for this study, as well as for some of the recent studies on stochastic physics in general, is the general lack of spread in current ensemble prediction systems. In particular, in the tropics the problem seems to be worse than elsewhere in the globe. In order to investigate the impact of the approach proposed here on this issue, a comparison is performed between an ensemble that uses only the stochastic convection method and an ensemble that uses only initial-condition perturbations as described in the beginning of this section.

Fig. 2 shows the ensemble spread for the mean-sea-level (MSL) pressure, the temperature at 850 hPa and the wind at 250 hPa for the tropics and the extra-tropics, averaged for the month of May 2005. In the tropics, Fig. 2a, the simulations with initial condition (IC) perturbations show an initial decay or slow growth of the ensemble spread for the first 3 forecast days and only after this, does the IC spread start to increase. On the other hand, the simulations with the stochastic convection (SC) approach show a continuous increase of the ensemble spread, with the SC spread reaching values comparable to the IC spread after about 72 hours for both the MSL pressure and the wind at 250 hPa. In the extra-tropics (Fig. 2b), although there is, as expected, a smaller ensemble spread for the SC method relative to the IC method,it is still substantial. For the IC ensemble, the spread is rapidly increasing in the beginning but starts leveling-off after about 7 forecast days. The SC ensemble spread, although always less than that of the IC simulations is still far from saturation even after 10 forecast days.

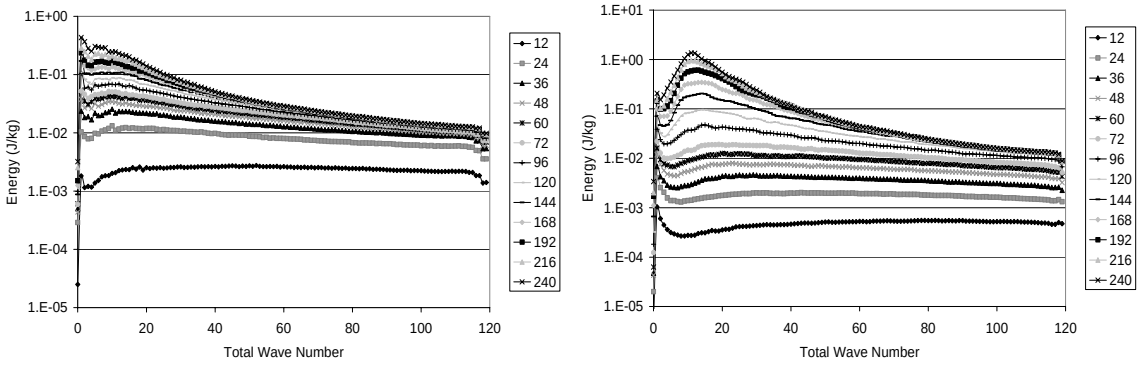

Figure 1. Total energy difference (Jkg^{-1}) between an ensemble member with stochastic convection and the control simulation with no stochastic convection, as a function of total wave number (out to T119) for several forecast ranges (from 12 to 240 hour), for (a) the tropics (20 S to 20 N) and (b) the NH mid-latitudes (30 N to 70 N), averaged for the month of May 2005.

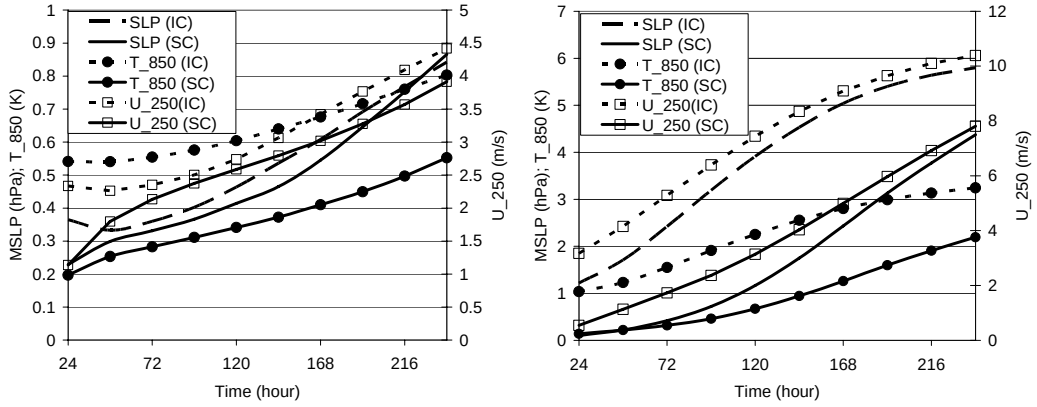

Figure 2. Evolution of the ensemble spread of the mean-sea-level pressure (SLP, in hPa), the temperature at 850 hPa (T_850, in K) and the wind speed at 250 hPa (U_250, in ms^{-1}), averaged for the month of May 2005, for (a) the tropics and (b) the extra-tropics. Two different ensembles are analyzed: one that uses only initial-condition (IC) perturbations and one that uses only stochastic convection (SC) perturbations.

Acknowledgements: *We acknowledge the support of a NOAA cooperative agreement for THORPEX.*

A CANADIAN LIMITED-AREA ENSEMBLE PREDICTION SYSTEM BASED ON MOIST SINGULAR VECTORS AND STOCHASTIC PHYSICS

Martin Charron [1], Xiaoli Li [2], Lubos Spacek [1], and Guillem Candille [1]

[1] Recherche en prévision numérique, Meteorological Research Division, Science and Technology Branch, Environment Canada, Dorval, Québec, Canada
[2] Department of Atmospheric and Oceanic Sciences, McGill University, Montréal, Québec, Canada
E-mail: *Martin.Charron@ec.gc.ca*

Abstract: A Regional Ensemble Prediction System (REPS) with the limited area version of the Canadian Global Environmental Multiscale (GEM) model at 15 km horizontal resolution is developed and tested. The total energy norm singular vectors (SVs) targeted over north-east North America are used for initial and boundary perturbations. Two SV perturbation strategies are tested: dry SVs with dry simplified physics, and moist SVs with simplified physics including stratiform condensation and convective precipitation as well as dry processes. Model physics uncertainties are partly accounted for by stochastically perturbing two parameters: the trigger function in the Kain-Fritsch deep convection scheme and the threshold humidity in the Sundqvist explicit scheme. The perturbations are obtained from first order Markov processes. Short-range ensemble forecasts in summer with 16 members are performed for five different experiments. The experiments employ different perturbation and piloting strategies, and two different surface schemes. Verification focuses on quantitative precipitation forecasts. Results indicate that using moist SVs instead of dry SVs impacts more strongly on precipitation than on dynamical fields. Forecast skill for precipitation is greatly influenced by the dominant synoptic weather systems. For stratiform precipitation caused by strong baroclinic systems, the forecast skill is improved in the moist SV experiments compared to the dry SV experiments.

Keywords *– Regional Ensemble Prediction System, Singular vectors, Limited-area model, Stochastic physics, Markov processes.*

1. INTRODUCTION

Until recently, most of the works using singular vectors (SVs) as initial perturbations in EPSs were still based on a linearized version of the model without representation of subgrid scale moist processes. Some studies showed that the inclusion of moist processes in SV calculations can increase the growth of perturbations and affect baroclinically unstable modes. The usefulness of moist SVs for short range EPSs was also expected by Hoskins and Coutinho (2005) by investigating the predictability of several poorly forecasted European cyclones. Zadra *et al.* (2004) examined the influence on SVs of different components of simplified physics using the Global Environmental Multiscale (GEM) model. This simplified physics includes stratiform and convective (Kuo-type) precipitation processes, which are used to calculate the so-called moist SVs. Two of the goals of the present study are to validate a regional ensemble prediction system (REPS) using a limited-area version of GEM with targeted SVs as initial and boundary perturbations, and also to investigate the impact of moist SVs on precipitation forecasts. Moreover, we consider the stochastic perturbation of physical parameters related to convection and condensation using a method inspired from Lin and Neelin (2000) and based on first order Markov processes.

2. DESCRIPTION OF EXPERIMENTS

Two different sets of initial SV perturbations are considered for the global GEM ensemble piloting the LAMs. The first set is constructed from dry SVs. They are calculated with simplified and linearized dry processes: vertical diffusion and orographic drag schemes. The second set is constructed from moist SVs that include vertical diffusion and orographic drag, but also simplified and linearized stratiform condensation and deep convection in the tangent-linear and adjoint models of GEM. Parameter perturbations are also considered in this paper. In some experiments, the threshold vertical velocity in the Kain-Fritsch scheme and the threshold relative humidity in the Sundqvist condensation scheme for the LAM runs were perturbed by first order Markov processes. The impact of two different surface schemes in the GEM-LAM runs was also tested: the Force-Restore scheme and the Interactions Soil-Biosphere-Atmosphere (ISBA) schemes were tested separately. Moreover, two different updating frequencies by the piloting global runs for GEM-LAM were tested: 6 hours and 3 hours. Table 1 describes the combination of five different GEM-LAM ensemble configurations that have been designed.

Experiment name	Initial and Lateral Boundary Conditions	Surface Scheme	Physics Perturbations
DSVF-P6	Dry SVs, 6h piloting	Force-Restore	No
MSVF-P6	Moist SVs, 6h piloting	Force-Restore	No
MSVF-P3	Moist SVs, 3h piloting	Force-Restore	No
MSVI-P3	Moist SVs, 3h piloting	ISBA	No
MSVI-TH-P3	Moist SVs, 3h piloting	ISBA	Threshold vertical velocity (Kain-Fritsch) and threshold relative humidity (Sundqvist)

Table 1. Main characteristics of the experiments.

3. IMPACT ON SHORT-RANGE PRECIPITATION SCORES

The Brier Skill Scores (BSS) of 24h accumulated precipitation are shown in Fig. 1 for 16 days is summer 2003 over north-east North America. DSVF-P6 shows the lowest BSS for most of the thresholds and is skillful for thresholds less than 20 mm only. MSVF-P6 and MSVF-P3 show very similar BSS behavior except for smaller thresholds. They show skill until the 40 mm threshold. The MSVI-P3 and MSVI+TH-P3 exhibit higher BSS than the other experiments within the threshold range 20-50 mm. MSVI+TH-P3 shows slightly better performance than MSVI-P3 (except for the threshold range 20-30 mm), and has skill up to the 45 mm threshold.

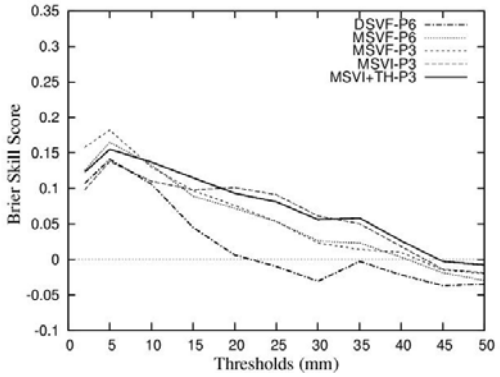

Figure 1. The Brier Skill Scores for 24h accumulated precipitation (from 12h lead time to 36h lead time) as a function of precipitation thresholds. 16 cases in summer 2003 over north-east North America.

4. CONCLUSIONS

The use of moist SVs instead of dry SVs leads to a general skill increase for QPF over a wide range of thresholds, and slightly reduces the wet bias of precipitation forecast. The QPF skill is clearly dependent on the dominating weather regime. Precipitation caused by strong synoptic low pressure systems can be reasonably well forecasted. The quality of the results are also strongly influenced by the following factors: (1) the surface scheme ISBA produces a clear positive impact on stratiform precipitation forecasts for thresholds larger than 15 mm per 24h; (2) increasing the LBC updating frequency can also produce a positive impact on QPF for thresholds larger than 10 mm per 24h; (3) stochastic parameter perturbations tend to mostly enhance the performance of the REPS, especially for the small rainfall rates. On the other hand, poorer results are obtained when precipitation is mainly controlled by weak synoptic forcings favoring convective processes. These results are clearly less sensitive to the different perturbation and piloting strategies that were tested in this study. It shows a clear limitation of this REPS for convective precipitation probabilistic forecasts.

Acknowledgements: Part of this work was funded by the Canadian Foundation for Climate and Atmospheric Sciences (CFCAS).

REFERENCES

Hoskins, B. J., and M. M. Coutinho, 2005: Moist singular vectors and the predictability of some high impact European cyclones. Quart. J. Roy. Meteor. Soc., **131,** 581-601.

Lin, J. W. B., and J. D. Neelin, 2000: Influence of a stochastic moist convective parameterization on tropical climate variability. Geophys. Res. Lett., **27,** 3691-3694.

Zadra, A., M. Buehner, S. Laroche, and J.-F. Mahfouf, 2004: Impact of the GEM model simplified physics on extra-tropical singular vectors. Quart. J. Roy. Meteor. Soc., **130,** 2541-2569.

THE ENSEMBLE TRANSFORM (ET) SCHEME ADAPTED FOR THE GENERATION OF STOCHASTIC PERTURBATIONS

Justin. G. McLay [1], Craig. H. Bishop, Carolyn A. Reynolds

[1] Naval Research Laboratory, Monterey, CA, USA and NRC RAP, Washington, D.C., USA
E-mail: *justin.mclay@nrlmry.navy.mil*

Abstract: Stochastic perturbations obtained from an adaptation of the ensemble transform analysis error sampling scheme are assessed in terms of structure, spatial correlation, balance, and conditioning for growth. Experiments suggest that the perturbations have the potentially desirable property of maintaining or increasing their total energy upon numerical integration.

Keywords – *Ensemble Transform, Stochastic Perturbations, Correlation, Balance, Growth*

1. INTRODUCTION

Numerical weather prediction (nwp) ensembles are subject to sampling inadequacies and imperfect numerical models. As a result, the nwp-ensemble forecast error covariance matrix, $\mathbf{P_f^{ens}}$, does not effectively describe the so-called true forecast error covariance matrix, $\mathbf{P_f^{true}}$, which gives the covariance of forecast errors given the control forecast. That is, $\mathbf{P_f^{true}} - \mathbf{P_f^{ens}} = \mathbf{Q}$, where **Q** is some matrix other than the zero matrix. There is growing interest in simulating **Q** as part of the ensemble prediction process. Existing methods for simulating **Q** seek stochastic perturbations that have properties such as spatial correlation and dynamical balance, but none specifically seek perturbations that grow. Presented here are some results for an approach to simulating **Q** that seeks stochastic perturbations that have a growth or non-decay property. The approach is an adaptation of the ensemble transform (ET) method of analysis perturbation (Bishop and Toth 1999).

2. METHOD

The proposed approach was used to obtain stochastic perturbations that mimic missing 24h-leadtime forecast error variance in a global nwp ensemble. The nwp ensemble was comprised of 32 members generated via the ET technique at 0000UTC for each day in the period 01 January 2006 to 01 March 2006. Ensemble integrations were performed using the Navy Operational Global Atmospheric Prediction System (NOGAPS) primitive equation, spectral model at resolution T119 and with 30 vertical levels (Hogan and Rosmond 1991).

A set of 32 stochastic perturbations was generated. The state vector of each of the 32 perturbations was comprised of horizontal wind, temperature, and terrain pressure perturbations. A specific desire was that the variance of the stochastic perturbations be large only at points in the latitude band of 15^0S to 15^0N where the 24h nwp ensemble on average was sub-variant relative to the observed error variance.

Two experiments were performed using the stochastic perturbations. In the first, each of the 32 stochastic perturbations was added to a different 24h-leadtime perturbed member of the 0000UTC 01 March 2006 NOGAPS ET ensemble. Each of the 32 augmented 24h-leadtime ET members was then integrated an additional 96h. In the second, each stochastic perturbation was added to the 00h-leadtime control forecast of the 01 March 2006 ET ensemble, rather than to one of the 24h-leadtime perturbed members. The resulting 32 different augmented 00h control forecasts were then integrated for 168h.

3. RESULTS

The amplitudes of several of the leading eigenvectors of the stochastic perturbations' sample covariance matrix are shown in Fig. 1a, for the case of meridional wind. Note that the eigenvector amplitude is quite well localized to the tropical latitudes, as per desire. Figure 1b shows a cross-section of the meridional wind component of one of the 32 perturbations. This illustrates the vertical structure and correlation within the perturbation.

Regards the first experiment, Figure 2a shows the ensemble-average domain-integrated perturbation dry total energy within the target 15^0S to 15^0N latitude band between the augmentation leadtime of 24h and the final leadtime of 120h. It is seen that the average total energy of the augmented ensemble substantially exceeds that of the unaugmented ensemble for the entire 4d integration period.

Regards the second experiment, Figure 2b shows the ensemble-average domain-integrated dry total energy of the stochastic perturbations as a function of leadtime for several tropical latitude bands. Within the target latitude band of 15^0S to 15^0N the average total energy of the perturbations is largely preserved during the first

48h of integration. Following the 48h leadtime the average total energy slowly increases within the target latitude band. These results and those of the first experiment suggest that the stochastic perturbations have no propensity for abrupt and significant decay at the outset of integration.

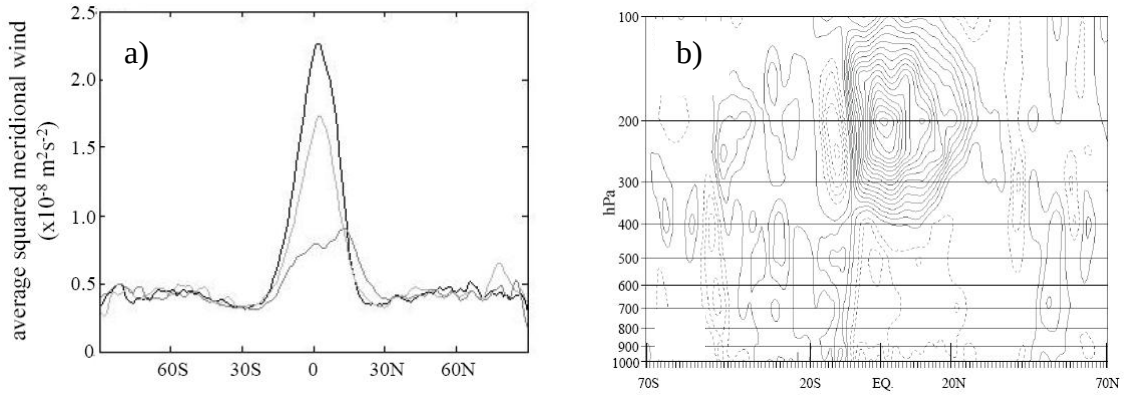

Figure 1. a) Zonally and vertically averaged squared elements of the 1st (black), 2nd (dark grey), and 10th (light grey) eigenvectors of the stochastic perturbations' sample covariance matrix, for the case of meridional wind. b) Cross-section along 50^0E longitude showing the meridional wind component of one of the stochastic perturbations. Positive (negative) values represented by grey solid (dashed) line contours every 1 (-1) m/s beginning at 1 (-1) m/s.

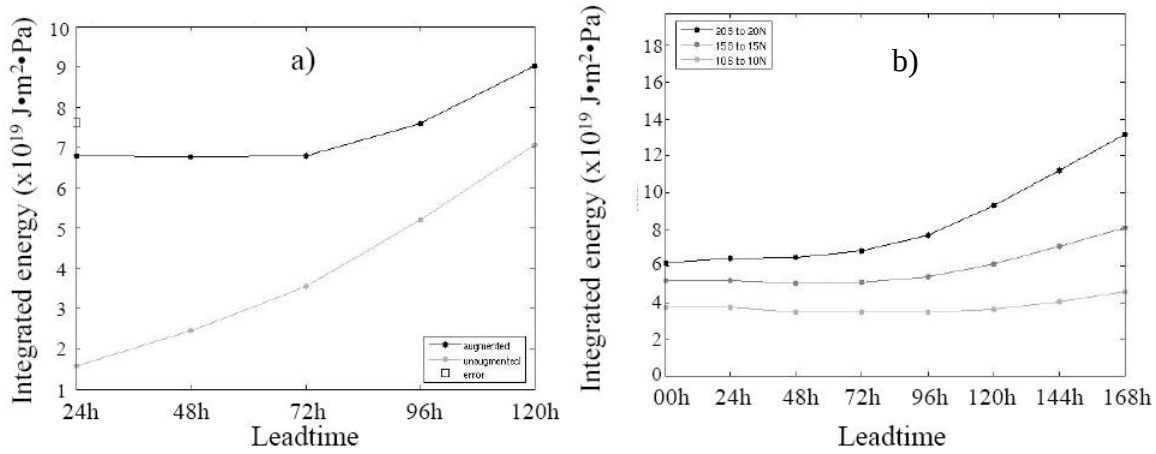

Figure 2. a) Ensemble-average domain-integrated perturbation dry total energy within the 15^0S to 15^0N latitude band for the augmented (black) and unaugmented (light grey) 0000UTC 01 March 2006 32-member NOGAPS ET ensemble. b) Domain-integrated perturbation dry total energy averaged over the 32 stochastic perturbations to the 0000UTC 01 March 2006 NOGAPS ET ensemble control forecast. Results shown for the tropical latitude bands of 20^0S to 20^0N (black), 15^0S to 15^0N (dark grey), and 10^0S to 10^0N (light grey).

6. CONCLUSION

The stochastic perturbations on average maintain or increase their energy in the target latitude band as integration proceeds, and as a result provide a lasting increase in domain-integrated ensemble variance when they are used to augment baseline global ensemble members. These results suggest that the adapted ET method incorporates effective correlation, balance, and growth conditioning into the stochastic perturbations.

Acknowledgements: *This research was sponsored by the Naval Research Laboratory and the Office of Naval Research under program element 0601153N, project number BE-033-03-4M. The DoD High Performance Computing program at NAVO MSRC and at FNMOC provided the computing resources.*

REFERENCES

Bishop, C. H., and Z. Toth, 1999: Ensemble transformation and adaptive observations. *J. Atmos. Sci.*, **56**, 1748-1765.

Hogan, T. F., and T. E. Rosmond, 1991: The description of the Navy Operational Global Atmospheric Prediction System's spectral forecast model. *Mon. Wea. Rev.*, **119**, 1786-1815.

IDEAS AND PLANS FOR AN INTERACTIVE ENSEMBLE GUI IN NINJO

Michael Denhard

Deutscher Wetterdienst, Offenbach, Germany
E-mail: *michael.denhard@dwd.de*

Abstract: What is the role of the forecaster in an ensemble environment ?

Keywords – *Ensemble, Postprocessing, Graphical User Interface*

1. INTRODUCTION

The challenge of today's operational weather forecasting is to handle and interpret a huge amount of numerical weather forecasts. For example the size of the TIGGE ensemble will be in the order of 351 members per day. Today, the forecasters at DWD are confronted with more than a hundred forecasts from the deterministic and limited area models as well as different post processed versions of these models (including an hourly GME-MOS update) and various ensemble Systems (ECMWF-EPS, COSMO-LEPS, SRNWP-PEPS). For sure this number will further increase in the future. To be able to make use of that lot of information an efficient way of analyse, arrange and interpret large ensemble systems is required.

2. THE FORCASTERS BURDEN

Undoubtedly, an automatic post processing is required to be able to understand the behaviour of large ensemble prediction systems at all. The Postprocessing must account for systematic and random errors (bias correction, calibration, ensemble dressing), discover the significant properties of an ensemble system (means, best forecasts, clusters, extremes) and evaluate the ensemble relative to the latest observations (online verification). But what's about the forecaster and his expertise? Is he still needed for issuing weather forecasts or warnings? Wouldn't it be sufficient to use the ensemble mean as a guidance and the predicted probability density (pdf) in conjunction with certain probability thresholds in the case of warnings? As it is shown in figure 1, this in principle depends on the ability of a forecaster to enhance the sharpness of a forecasted ensemble pdf using his expertise and the most recent observations. If he is able to enhance sharpness, would he be able to react in time and change the mean guidance to more extreme and more unlikely predictions from the ensemble? What are the demands on a Graphical User Interface (Ensemble-GUI) in that context?

3. THE FORECASTERS DUTY

It will be at least the forecasters duty to monitor predictions coming from ensemble systems and change the guidance in those situations in which even the ensemble is not able to capture the phenomenon, e.g. due to basic model deficiencies. Moreover, he should be able to choose target areas for clustering, compose on-demand regional ensembles and produce new guidances by selecting a certain ensemble member or subensemble from the primary ensemble. This requires an Ensemble Graphical User Interface (Ensemble-GUI)

4. THE TECHNICAL ENVIRONMENT

An adequate system to implement an Ensemble-GUI is the NinJo meteorological workstation environment developed at Deutscher Wetterdienst (DWD), the German Military Geophysical Service (GMGO), Meteo-Swiss, the Danish Meteorological Institute (DMI) and the Meteorological Service of Canada (MSC). NinJo was developed using Java and does not assume or prescribe any hardware or data infrastructure. The Version 1.2 is now running operationally. Some ideas of an Ensemble-GUI in NinJo are presented incorporating an automatic ensemble post processing along with the interactive component.

.

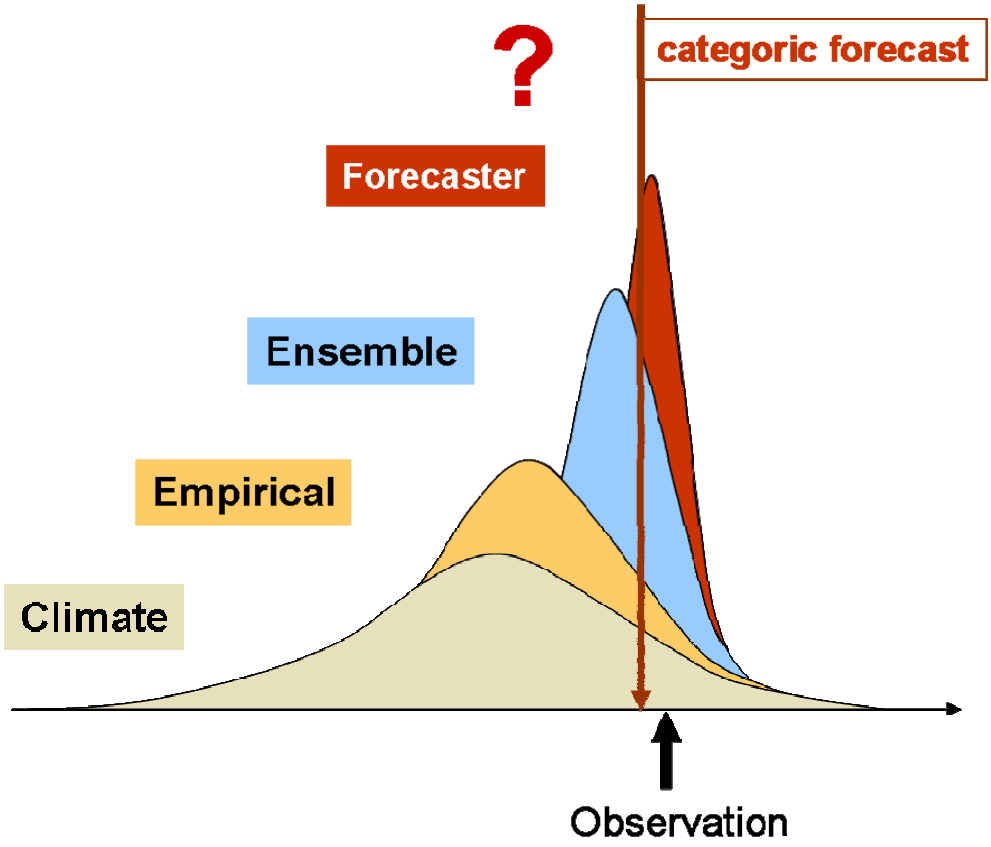

Figure 1. Role of a human forecaster in a probabilistic ensemble prediction environment.

REFERENCES

Paul J., H.-J. Koppert and D. Heizenreder, 2005: Severe Weather Forecasting Tools in the NinJo Workstation, Tech Report, DWD, Offenbach.

Koppert, H.K., 2002: A Java based meteorological workstation, IIPS, AMS.

Koppert, H.K., T.B.Pederson, B. Zuercher and P. Joe, 2004: How to Make an International Workstation Successful, AMS, IIPS, Seattle.

EXTENDED SAMPLE ABSTRACT FOR A STISS-PRESENTATION IN LANDSHUT: A CASE OF INTERACTIVE SOCIETAL IMPACT (ALL CENTERED 12 PT BOLD)

Hans Volkert[1], George Craig, Heini Wernli (10 pt font centred)

[1] Institut für Physik der Atmosphäre, Deutsches Zentrum für Luft- und Raumfahrt, Oberpfaffenhofen, Germany
E-mail: *hans.volkert@dlr.de*

Abstract: This example abstract presents all layout details for an easy production of a two-page account for each oral and poster presentation which was accepted for the Second THORPEX International Science Symposium (STISS) to be held in Landshut, Germany from 4-8 December 2006. It induced a large number of responses. (The abstract section is 9 pt)

Keywords – *THORPEX, WMO, Data assimilation, Group dynamics (9 pt in italics)*

1. INTRODUCTION (headline in CAPITALS, 10 pt, bold)

Conferences are a standard medium for a personal distribution of findings from scientific research. A full week with 4.5 days (Monday morning to Friday noon) is considered to be the maximum duration, which can realistically be managed. A single session format is optimal in the sense that everybody can listen and communicate with everybody and the organisational work is limited.

Presentations are divided into oral talks of 12 minutes each (plus 3 minutes for discussion and the change to the next speaker) and poster displays for an interactive discussion in rooms adjacent to the general venue (cf. Figure 1). Table 1 shows the number of presentations submitted to STISS broken up by session. Authors of both equally important classes of presentations have the possibility to send an extended abstract of two pages to the STISS organisation committee. From these a conference volume will be compiled. It will be distributed to the participants when they register for STISS. In this fashion everybody can select at leisure and with suitable material at hand all the STISS presentations that are of special interest to him.

2. CONTENTS OF EXTENDED ABSTRACTS

The extended abstract ideally resembles a short scientific publication (note) with sections ‘Introduction’, ‘Data’, ‘Model’, ‘Conclusions’. A few references may help the interested reader to find further information. A table or a typical figure, accompanied by an appropriate caption, may be well suited to raise the reader’s curiosity.

Some information about the status of the work, like ‘in progress’, ‘exploratory’ or ‘maturely settled’ may be useful to set the scene for discussions with the audience during the conference.

3. LAYOUT OF EXTENDED ABSTRACTS

The extended abstract should be formatted as this example on two pages in **A4-format** (21.0 cm wide, 29.6 cm high) with margins of 2.5 cm on each side. This results in a printable area of 16.0 cm wide and 24.6 cm high. The best font is ‘Times New Roman’ with the font size in points (pt) as specified at various places of the text.

The text runs in one wide column and is ideally structured in sections and paragraphs. New paragraphs begin indented without an empty line. Pages **must not** be numbered as the pagination will be done for the full volume.

THROPEX working group	Oral-A	Oral-B	Oral-C	Oral-D	Poster-I	Poster-II	Poster-III
DAOS	5	5	4		10	10	9
OS	3	5				6	7
PDP	6	6	7	6	16	15	16
SERA	6	5	5		9	9	11
TIGGE	3	5			9	9	

Table 1. Example for a table: Number of announced oral and poster presentations in the various sessions. Caption underneath and best placed at the bottom of page 1 (or top of page 2); table entries should be in 10 pt font; captions in 9 pt.

Figure 1. Details of the STISS venue during a visit in November 2005: Left: Hall for oral presentations with high screen and balcony around (there will be no tables but only chairs). Right: One of the adjacent rooms where the boards for poster displays will be placed (caption in 9 pt font; figure is preferably placed at bottom of page 1 or top of page 2).

4. STRUCTURE OF EXTENDED ABSTRACT

Each abstract starts with a centred title/subtitle which may take up several lines (in 12 pt and all in CAPITALS). First name and last name of all co-authors follow. The affiliation with postal and email addresses should be only given for the first (i.e. presenting) author. This saves space. These details help the reader to contact an authoring team.

Optional, though useful pieces of short information are **abstract** and ***keywords*** as exemplified above. They may be dropped, especially if space turns out to be short. A few numbered sections can help to structure the text. Subsections should be avoided in favour for equally important ordinary sections as two pages do not provide much room anyway. Acknowledgements are also an optional item to be placed between the text and a short list of references (as e.g. Bougeault et al., 2001; Palmer and Hagedorn, 2006).

5. FORMATTING AND POSTING OF EXTENDED ABSTRACT

The extended abstract should be formatted with MS-Word (as this example) or an equivalent word-processing scheme. The following naming convention helps us to produces the Volume of Extended Abstracts:

STISS-<first-author>-<oral/poster>.doc

This file is consequently called 'STISS-Volkert-poster.doc'. We will convert the doc-file to pdf-format and assemble the entire volume with table of contents and pagination.

Files formatted in pdf-format and named

STISS-<first-author>-<oral/poster>.pdf

are also acceptable, especially from all who use other word processing systems.

Please send your extended abstract by Email to **hans.volkert@dlr.de** at your earliest convenience, but not later than 1 November 2006. Otherwise the STISS-Volume cannot be produced in time.

6. CONCLUSION

Nearly 140 co-authoring teams submitted Extended Abstract, the large majority of them well adhering to the deadline and the example provided. This example is updated and included in proceedings volume to make a bit more explicit how a scientific community, which is quite diverse in many respects, is willing to co-operate on a voluntary basis. A short deadline before the meeting with some flexibility for late comers and the avoidance of an extra charge appear to have contributed significantly to the large number of responses.

Acknowledgements: *WMO and THORPEX-IPO provide financial assistance for the publication of the STISS proceedings volume. Jana Freund (DLR) is commended for having competently compiled and annotated these 300 pages (in 9pt italics).*

REFERENCES (example for journal article and book; in 9 pt; second line indented for better distinction)

Bougeault, P., P. Binder, A. Buzzi, R. Dirks, R. Houze, J. Kuettner, R. B. Smith, R. Steinacker, and H. Volkert, 2001: The MAP Special Observing Period. Bull. Amer. Meteorol. Soc. **82** , 433-462.

Palmer, T. and R. Hagedorn (eds.), 2006: *Predictability of weather and climate.* Cambridge University Press, Cambridge, UK, xv + 702 pp.

LIST OF THORPEX SERIES PUBLICATIONS

1. International Core Steering Committee for THORPEX. Third Session. 16-17 December 2003, Montreal, Canada. Final Report. WMO/TD-No. 1217, WWRP/THORPEX No. 1.

2. M.A. SHAPIRO, A.J. THORPE, 2004: THORPEX International Science Plan Version 3. WMO/TD-No.1246, WWRP/THORPEX No. 2.

3. International Core Steering Committee for THORPEX. Fourth Session. 2-3 December 2004, Montreal, Canada. Final Report. WMO/TD-No. 1257, WWRP/THORPEX No. 3.

4. THORPEX International Research Implementation Plan Version 1. WMO/TD-No. 1258, WWRP/THORPEX No. 4.

5. First Workshop on the THORPEX Interactive Grand Global Ensemble (TIGGE), Reading, United Kingdom, 1-3 March 2005, WMO/TD No. 1273, WWRP/THORPEX No.5

6. Symposium Proceedings - The First THORPEX International Science Symposium, 6-10 December 2004, Montreal, Canada, WMO/TD 1237, WWRP/THORPEX No. 6

7. Programme & Extended Abstracts – The Second THORPEX International Science Symposium, 4-8 December 2006, Landshut, Bavaria, Germany, WMO/TD No. 1355, WWRP/THORPEX No. 7

THORPEX International Programme Office
Atmospheric Research and Environment Programme Department

World Meteorological Organization
Secretariat
7bis, avenue de la Paix
Case postale 2300
CH-1211 Geneva 2
Switzerland
www.wmo.int/thorpex